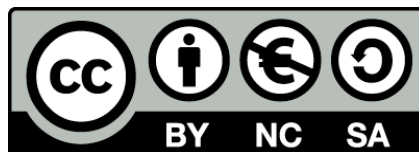




UNIVERSITAT DE
BARCELONA

Combining exome sequencing and functional studies to identify causal genes of ultra-rare neurodevelopmental disorders

Laura Castilla-Vallmanya



Aquesta tesi doctoral està subjecta a la llicència **Reconeixement- NoComercial – CompartirIgual 4.0. Espanya de Creative Commons.**

Esta tesis doctoral está sujeta a la licencia **Reconocimiento - NoComercial – CompartirIgual 4.0. España de Creative Commons.**

This doctoral thesis is licensed under the **Creative Commons Attribution-NonCommercial-ShareAlike 4.0. Spain License.**



UNIVERSITAT DE
BARCELONA

Combining exome sequencing and functional studies to identify causal genes of ultra-rare neurodevelopmental disorders

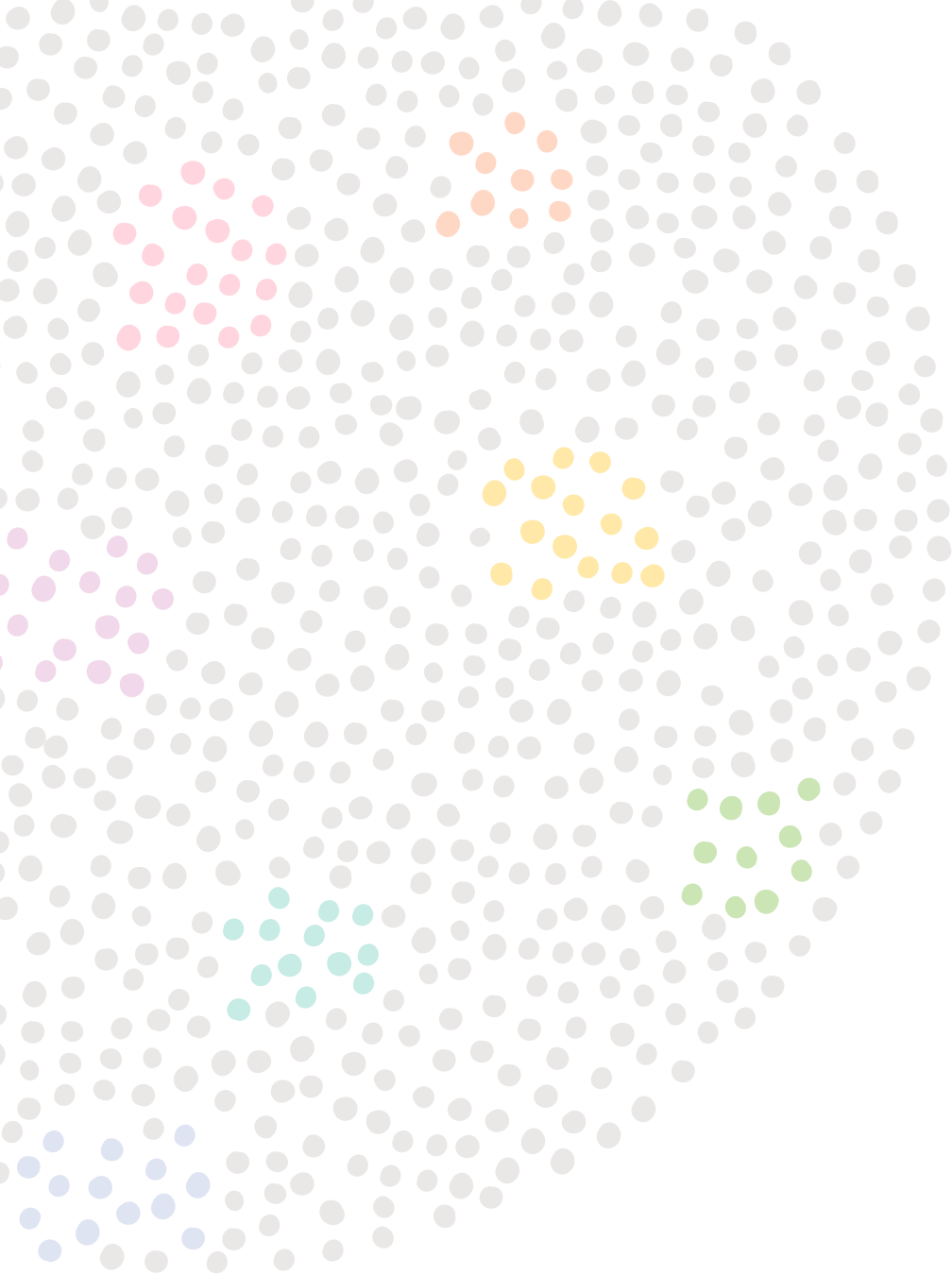
Laura Castilla-Vallmanya



Aquesta tesi doctoral està subjecta a la llicència **Reconeixement- NoComercial – CompartirIgual 4.0. Espanya de Creative Commons.**

Esta tesis doctoral está sujeta a la licencia **Reconocimiento - NoComercial – CompartirIgual 4.0. España de Creative Commons.**

This doctoral thesis is licensed under the **Creative Commons Attribution-NonCommercial-ShareAlike 4.0. Spain License.**



Combining exome sequencing
and functional studies to identify causal genes
of ultra-rare neurodevelopmental disorders

Laura Castilla Vallmanya

2021

Tesi Doctoral

Universitat de Barcelona

Combining exome sequencing and functional studies to identify causal genes of ultra-rare neurodevelopmental disorders

Memòria presentada per

Laura Castilla-Vallmanya

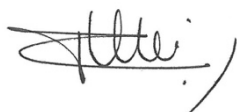
Per optar al grau de

Doctora per la Universitat de Barcelona

Programa de Genètica

Departament de Genètica, Microbiologia i Estadística

Tesi dirigida per la Dra. Roser Urreizti Frexedas (codirectora) i la Dra. Susanna Balcells Comas (codirectora i tutora)



Dra. Roser Urreizti Frexedas
(codirectora)



Dra. Susanna Balcells Comas
(codirectora i tutora)



Laura Castilla-Vallmanya

Barcelona, Juliol del 2021



UNIVERSITAT DE
BARCELONA

L'autora de la tesi doctoral, Laura Castilla Vallmanya, i les seves directores, la Dra. Susanna Balcells Comas i la Dra. Roser Urreizti Frexedas, volen deixar constància de que el present treball ha sigut dirigit també pel Dr. Daniel Grinberg Vaisman, en igualtat de condicions que les altres dues directores. Per raons administratives, el seu nom no ha pogut constar oficialment.

Barcelona, Juliol de 2021



Laura Castilla Vallmanya
(Estudiant)



Dr. Daniel Grinberg Vaisman
(Professor emèrit)



Dra. Susanna Balcells Comas
(Codirectora i tutora)



Dra. Roser Urreizti Frexedas
(Codirectora)

A la meva àvia Margarita

AGRAÏMENTS

Durant aquests anys he intentat imaginar molts cops què sentiria el dia en que escrigués els agraïments de la meva tesi doctoral. Avui, que ha arribat el gran moment, la sensació d'agraïment que sento és tan genuïna i real que no se si seré capaç d'expressar-la amb paraules, deixeu-m'ho intentar... Escric aquestes línies des de la que ha sigut casa meva durant els últims 5 anys, la 3^a planta de l'edifici Prevosti. Un espai que m'ha permès créixer com a científica i com a persona, que m'ha ensenyat que l'única reacció vàlida a les caigudes és aixecar-se i seguir lluitant, que m'ha vist en moments de profund desànim i també de plena felicitat. Però sobretot, que m'ha permès conèixer un munt de persones úniques que han fet que deixés de ser una casa per convertir-se en una llar.

En primer lloc, vull agrair a la **Roser**, la **Susanna** i el **Dani** per haver-me guiat durant la realització d'aquest projecte, però sobretot per tenir sempre la porta del despatx oberta i una paraula amable per donar-me ànims. Gràcies a l'**Isaac**, per acollir-me tant bé al seu laboratori i per tot el que vaig poder aprendre, i al **Salvador**, per ajudar-me a entrar al món de la recerca i fer que m'hi volgués quedar. També vull donar les gràcies a tots els **clínic**s i **investigadors** amb els que hem pogut col·laborar durant aquests anys; en les malalties minoritàries, la unió fa la força i "para muestra, un botón". Gràcies infinites també als **pacients** i a **les famílies** per la vostra col·laboració i per estar sempre al peu del canó, evitant que se'ns oblidí l'objectiu real d'aquest projecte.

Totes les persones amb les que he compartit pòpiata, cerveses i viatges durant aquests anys han sigut personatges claus en aquest capítol de la meva vida. Moltíssimes gràcies a totxs! Malauradament, a més de la possibilitat de quedar-se sense lloc per dinar, el problema de ser un laboratori tant multitudinari és que la probabilitat d'oblidar-me a algú és molt alta, si és així, no m'ho tingueu massa en compte. Primer de tot, gràcies a totes les meravelloses persones que en algun moment han format part del Team Opitz: **Héctor**, quin gust haver compartit les nostres primeres passes com a científics. **Guillem**, **Ari**, **Raúl**, **Miguel**, **Mónica** i **Aina**, espero haver aconseguit ensenyar-vos una mínima part del que vosaltres m'heu fet aprendre a mi. A **Núria**, gracias por ser un pilar dentro y fuera del lab y por todas las risas y lágrimas compartidas, ¡no te vayas de mi lado, cabecita loca! A **Ester**, qué suerte la mía de que hayamos andado este camino en paralelo, ¡por muchas más vueltas, amiga! Gràcies **Edgar** per tots els moments suprems viscuts i pels que ens queden. A la **Noe Vintage**, per ser un referent de dona científica i tenir un cor tan noble. A **María**, gracias por acompañarme en algunas de las etapas más duras del doctorado y por todo lo demás, que no fue poco. Thank you **Maja**, you were also there and I hope you will always be. A la **Neus**, gràcies per escoltar-me sempre, per tots els consells i per les passejades. A

la **Judit**, la **Bàrbara** i la **Laura P**, gràcies per ser unes neuro-companyes de 10. A **Aldo**, gracias por haber hecho que algunos de mis martes fueran mucho menos martes. A **Mónica Cozar** y a **Noelia Benetó**, fue muy guay trabajar las tres, pero aún mejores los desayunitos en mi ordenador. A la **Roser C** i a la **Kelly**, per ser tant bones coordinadores de pràctiques i per pujar-me sempre els ànims. A tota la gent que esteu començant: **Nerea, Juan, Eva, Ainhoa, Estefanía, Irene, Mario...** Estimeu-vos molt i cuideu-me bé el laboratori. La veritat és que de departament tampoc em puc queixar: els sopars de nadal, les calçotades, els PhDDay... Soc incapaç de decidir quin és el meu esdeveniment preferit, sens dubte el millor de tots ells, els **organizers**. Mil gràcies pels nervis i riures compartits!

Tot i que és cert que les hores a l'edifici Prevosti han sigut moltes, sempre he tingut persones fantàstiques a fora disposades a escoltar-me parlar del lab (encara que perdessin una mica el fil) i també a ajudar-me a desconnectar en el moments en que jo sola no era capaç d'aconseguir-ho. Eternament agraïda de tenir dos llocs al món que considero casa meva: Barcelona i Blanes. Moltes gràcies a la **María** i al **Jordi** per ser els millors companys de pis que mai podria haver imaginat, només vosaltres podíeu aconseguir que tingués un boníssim record d'un confinament, ¡por una vida plena de planes geniales! Als **Durfis**, per ser l'inici d'aquesta aventura que és la vida adulta i per seguir aquí tants anys després. A **Cris**, por ser mi mejor consecuencia del máster y por tu apoyo incondicional. A **Jud** y a **Ari**, por todas las veces que se nos ha ido de las manos. Gracias a **Manel, Joaquín** y **Ari**, por esta amistad tan random y tan bonita. A mis **Pexakuxas**, no sé qué tenéis que es juntarnos y se me pasan todos los males, mis salvavidas.

A **Juan**, fue conocerte y mi suerte en Lund empezó a cambiar, me niego a pensar que fue casualidad. Gracias por poner banda sonora a mi vida, espero ansiosa los siguientes temas. A **Virginia**, mi sistah from another mistah, pocas cosas me hacen sentir tan orgullosa como nuestra amistad. Al **team Castilla**, gracias por todas las comidas familiares y los bingos. A la **Pina** i al **Pere**, per ser els meus segons pares i formar part de molts dels meus millors records. A la **Natàlia**, encara em sorprèn com dues persones tan diferents poden entendre's amb només una mirada. Perquè totes les coses difícils, amb tu no ho són tant. Als **meus pares**, pel seu amor, suport i confiança incondicionals, per entendre'm i fer-me sentir tant estimada sempre.

Encara recordo el vestit de flors que portava el primer dia que vaig trepitjar el laboratori feta un manat de nervis. Qui m'anava a dir que 5 anys després escriuria aquestes línies amb l'ànima tant plena d'amor i sentint-me la versió més real de mi mateixa.

Seguim!

ABSTRACT

Neurodevelopmental disorders (NDDs) are a group of chronic diseases in which the development of the central nervous system is impaired, resulting in disability at the neuropsychiatric, motor and/or intellectual level. Some of these disorders are considered syndromic. For instance, intellectual disability (ID) may present comorbidity with other neurological conditions (such as seizures or behavioral problems), dysmorphic features and/or internal organ anomalies. The vast majority of syndromic NDDs have a genetic origin and are considered to be rare, affecting less than 1 in 2000 people. However, globally, these diseases represent a serious social and health issue. Even though the majority of them are monogenic, many of them remain with an unknown molecular basis. Next-generation sequencing technologies have played a critical role in the optimization of the diagnosis of NDDs during the last decades. In this thesis, we have used a combination of whole-exome sequencing (WES) and functional studies to establish the diagnosis of 9 cases tentatively diagnosed as Opitz C, a clinical entity that encompasses patients with very different molecular causes.

We identified the genetic origin of the disorder in the 7 tested families, which happened to be different variants in different genes for each of them. We showed that WES is a powerful approach to identify the molecular basis of ultra-rare NDDs. A significantly higher diagnosis yield was reached compared with other studies, potentially explained by a deep analysis of the sequencing data using *in silico* predictors, followed by the performance of specific functional studies for each case. We identified four different variants putatively affecting splicing patterns of different genes (*ASXL1*, *KAT6A*, *PIGT* and *FOXP1*) and tested them directly using fibroblasts obtained from patients or indirectly using a mini-gene splicing assay. We assessed the effect of variants in *DPH1* in protein function combining a biochemical technique with a protein structural model and we established a correlation between the results of the tests and the severity of the patients' phenotype. We contributed to the delineation of a recently described syndrome caused by germline mutations in *TRAF7* by gathering and describing a cohort of 45 patients. We also performed a transcriptomics analysis on fibroblasts from different patients carrying *TRAF7* mutations, which showed alterations in the expression of different genes that might contribute to the phenotype. Aiming to characterize truncating mutations in *MAGEL2*, which are responsible for Schaaf-Yang syndrome (SYS), we performed different experiments that suggest a potential toxic effect of the produced truncated form of the protein, which lacks its most relevant functional domain. Finally, as a first step to establish a relevant *in vitro* model of SYS, we reprogrammed fibroblasts

from different patients to induced pluripotent stem cells (iPSCs), which can be then differentiated to relevant neural cell types and brain organoids to further study the pathophysiological mechanisms underlying this disease.

TABLE OF CONTENTS

ABBREVIATIONS

INTRODUCTION	1
1. NEURODEVELOPMENTAL DISORDERS	3
2. DIAGNOSIS OF ULTRA-RARE NEURODEVELOPMENTAL DISORDERS	5
2.1 Clinical diagnosis	5
2.2 Genetic diagnosis	8
2.2.2 Variant interpretation	10
2.2.3 Functional validation studies	12
2.2.3.1 Cellular models of disease: iPSCs	14
3. GENES RELATED TO THE OPITZ C CLINICAL ENTITY	16
3.1 <i>ASXL1</i> and Bohring-Opitz syndrome	16
3.2 <i>TRAF7</i> and role in tumorigenesis	18
3.3 <i>MAGEL2</i> and <i>MAGEL2</i> -related disorders	21
3.3.1 Prader-Willi syndrome	22
3.3.2 Schaaf-Yang syndrome	24
3.3.3 <i>In vitro</i> and <i>in vivo</i> models of <i>MAGEL2</i> -related syndromes	25
3.4 Other genes identified in Opitz C patients	27
OBJECTIVES	29

RESULTS

REPORT OF THE SUPERVISORS ON THE CONTRIBUTION OF THE PHD CANDIDATE TO THE ARTICLES INCLUDED IN THIS THESIS	35
CHAPTER 1: IDENTIFICATION OF CAUSAL GENES OF PATIENTS CLINICALLY DIAGNOSED AS OPITZ C SYNDROME AND FUNCTIONAL VALIDATION OF THE IDENTIFIED DISEASE-CAUSING VARIANTS	41
Article 1: Extending the phenotypic spectrum of Bohring-Opitz syndrome: Mild case confirmed by functional studies	41
Article 2: De Novo <i>PORCN</i> and <i>ZIC2</i> Mutations in a Highly Consanguineous Family	49
Article 3: The <i>ASXL1</i> mutation p.Gly646Trpfs*12 found in a Turkish boy with Bohring-Opitz Syndrome	69
Article 4: Five new cases of syndromic intellectual disability due to <i>KAT6A</i> mutations: widening the molecular and clinical spectrum	77
Article 5: Case report of a child bearing a novel deleterious splicing variant in <i>PIGT</i>	95

Article 6: A De Novo <i>FOXP1</i> Truncating Mutation in a Patient Originally Diagnosed as C Syndrome	105
Article 7: DPH1 syndrome: two novel variants and structural and functional analyses of seven missense variants identified in syndromic patients	115
CHAPTER 2: CHARACTERIZATION OF <i>TRAF7</i> GERMLINE VARIANTS AT A PHENOTYPIC AND MOLECULAR LEVEL	145
Article 8: Phenotypic spectrum and transcriptomic profile associated with germline variants in <i>TRAF7</i>	145
CHAPTER 3: FUNCTIONAL CHARACTERIZATION OF <i>MAGEL2</i> TRUNCATING MUTATIONS AND GENERATION OF AN <i>IN VITRO</i> MODEL FOR SCHAAF-YANG SYNDROME	187
Article 9: Advancing in Schaaf-Yang syndrome pathophysiology: from bedside to subcellular analyses of truncated <i>MAGEL2</i> in patients' fibroblasts	187
Article 10: Generation of human iPSC lines from two Schaaf-Yang Syndrome (SYS) patients	221
<u>DISCUSSION</u>	231
1. INTERPRETATION OF THE IDENTIFIED VARIANTS	234
1.1 VUS interpretation and IF reporting	235
1.2 Advantages of using trio-WES	237
1.3 Interpretation of public reference databases	238
1.4 Utility of matchmaking tools	239
1.5 Interpreting phenotypic heterogeneity	241
1.6 Dealing with unsolved cases	243
2. VALIDATION AND FUNCTIONAL CHARACTERIZATION OF THE VARIANTS	245
2.1 Validation of splicing variants	245
2.2 Effects on protein function of <i>DPH1</i> variants	247
2.3 Molecular characterization of <i>TRAF7</i> germline mutations	248
2.4 Functional characterization of <i>MAGEL2</i> truncating variants	250
3. <i>IN VITRO</i> AND <i>IN VIVO</i> DISEASE MODELS	254
4. DEVELOPMENT AND CANCER	258
5. FINAL REMARKS AND FUTURE PERSPECTIVES	260
<u>CONCLUSIONS</u>	263
<u>REFERENCES</u>	267

ABBREVIATIONS

aCGH: Compared Genomic Hybridization Array

ACMG: American College of Medical Genetics

ACTH: Adrenocorticotrophic Hormone

ADH: Antidiuretic Hormone

ADHD: Attention Deficit/Hyperactivity Disorder

ADPR: ADPribosylation

ARTHS: Arboleda-Tham syndrome

ASD: Autism Spectrum Disorder

ASXL1: Additional Sex Combs Like Transcriptional Regulator 1

A β ₁₋₄₀: Amyloid β -protein 1-40

BOS: Bohring-Opitz syndrome

CADD: Combined Annotation Dependent Depletion

CAFDD: Cardiac, facial, and digital anomalies with developmental delay

CCD: Central Core Disease of muscle

CHDFIDD: Congenital heart defects, dysmorphic facial features, and intellectual developmental disorder

CNS: Central Nervous System

CNV: Copy Number Variants

CRISPR: Clustered Regularly Interspaced Short Palindromic Repeats

DD: Developmental Delay

DEDSSH: Developmental Delay with Short stature, Dysmorphic features and Sparse Hair

DEGs: Differentially Expressed Genes

DPSCs: Dental Pulp Stem cells

DSM-5: Diagnostic and Statistical Manual of Mental Disorders

DT: Diphtheria Toxin

EIEE26: Early Infantile Epileptic Encephalopathy 26

ESE: Exonic Splicing Enhancer

ESS: Exonic Splicing Silencer

ExAC: Exome Aggregation Consortium

FHD: Focal dermal hypoplasia

FISH: fluorescent in-situ hybridization

GH: Growth Hormone

gnomAD: Genome Aggregation Database

GoF: Gain-of-Function

GTEx: Genotype-tissue expression

hESCs: human Embryonic Stem Cells

HGMD: Human Gene Mutation Database

HGNC: HUGO Gene Nomenclature Committee

HPE5: Holoprosencephaly 5

HPO: Human Phenotype Ontology

ID: Intellectual Disability

IF: Incidental Finding

iPSC: Induced Pluripotent Stem Cell

IRFs: interferon-regulatory factors

IUGR: Intrauterine Growth Retardation

KO: Knockout

LoF: Loss-of-Function

M6PR: Mannose-6-Phosphate Receptor

MAF: Minor Allele Frequency

MAGEL2: MAGE Family Member L2

MAPKs: mitogen-activated protein kinases

MCAHS3: Multiple Congenital Anomalies-Hypotonia-Seizures syndrome 3

MHD: MAGE Homology Domain

MLPA: multiplex ligation-dependent probe amplification

mUPD: Maternal Uniparental Disomy

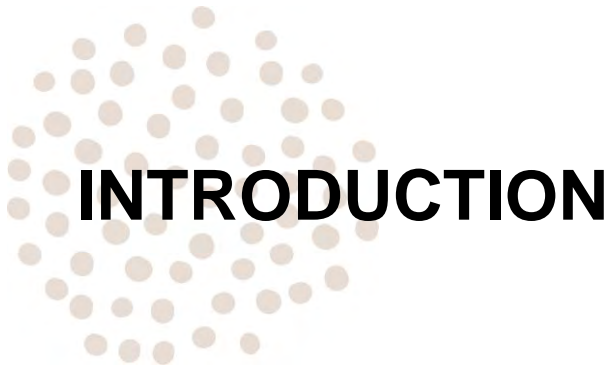
NDD: Neurodevelopmental Disorder

NF- κ Bs: Nuclear Factor- κ Bs

NGS: Next Generation Sequencing

NMD: Nonsense Mediated Decay
OCS: Opitz C Syndrome
OMIM: Online Mendelian Inheritance in Man
ORF: Open Reading Frame
OXT: Oxytocin
PROVEAN: Protein Variation Effect Analyzer
PWS: Prader-Willi Syndrome
PWS-IC: Prader-Willi Syndrome Imprinting Centre
scRNAseq: single-cell RNAseq
SG: Secretory granule
SHRC: WASH Regulatory Complex
SIFT: Sorting Intolerant from Tolerant

SNP: Single Nucleotide Polymorphism
SNV: Single Nucleotide Variant
SYS: Schaaf-Yang Syndrome
TLR2: Toll Like Receptor 2
TNF: Tumour Necrosis Factor
TNF α : Tumour Necrosis Factor-Alpha
TRAF: Tumour Necrosis Factor Receptor-associated factor
TRAF7: TNF Receptor Associated Factor 7
TSH: Thyroid-Stimulating Hormone
VUS: Variant of Unknown Significance
WES: Whole Exome Sequencing
WGS: Whole Genome Sequencing
WT: Wild-Type



INTRODUCTION

1. NEURODEVELOPMENTAL DISORDERS

During the development of the human brain, many different cell types have to proliferate, differentiate into specialized cell types, migrate to specific locations and form connections between them. It is a highly complex and tightly regulated process that will form an organ capable of complex language, cognition and emotion (1).

Neurodevelopmental disorders (NDD) encompass a series of chronic diseases in which the development of the central nervous system (CNS) is perturbed. These disorders, with onset in the developmental period, affect a large and heterogeneous group of patients who may present disability at the neuropsychiatric, motor and/or intellectual level, impairing normal functioning. Many different causes can be the origin of the functional limitations that define NDDs, which can have genetic, metabolic, nutritional, structural and/or immunological origin (2). According to the Diagnostic and Statistical Manual of Mental Disorders (DSM-5), neurodevelopmental disorders include (**Figure 1**): intellectual developmental disorders, communication disorders, autism spectrum disorder (ASD), attention deficit/hyperactivity disorder (ADHD), specific learning disorder, and motor disorders (3). However, NDDs can rarely be treated as independent entities, as the co-occurrence of different neurodevelopmental disorders in one single individual is more frequent than it would be expected by chance (4), making them difficult to diagnose in some cases.

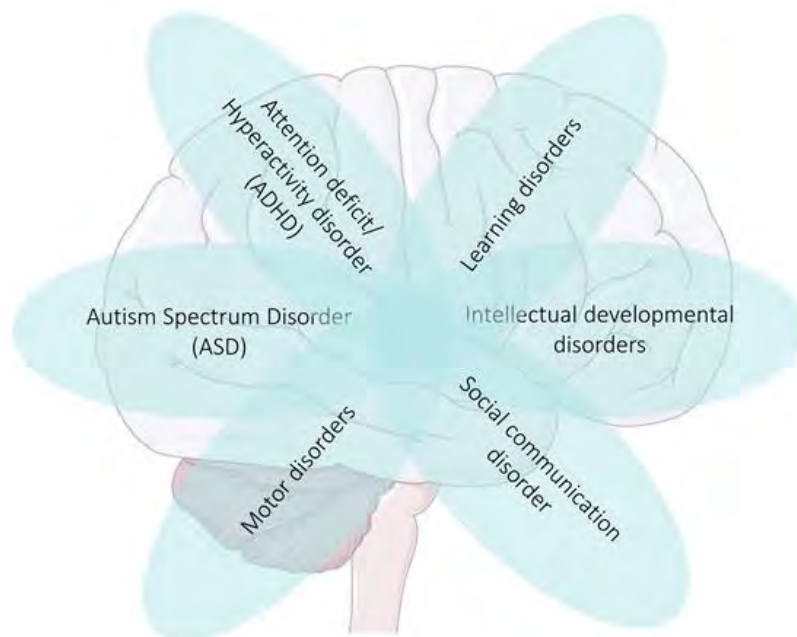


Figure 1. Neurodevelopmental disorders based on Diagnostic and Statistical Manual for Mental Disorders, 5th Edition (DSM-5) (3).

The prevalence of intellectual disability (ID) and developmental delay (DD) in the general population is 1-3% (5) and approximately 50% of the DD/ID cases have a genetic origin (6) (**Figure 2**). ASD phenotypes are present in 0,7% of people (7) while congenital malformations (not always associated with cognitive dysfunction) are observed in 2-3% of the general population (8).

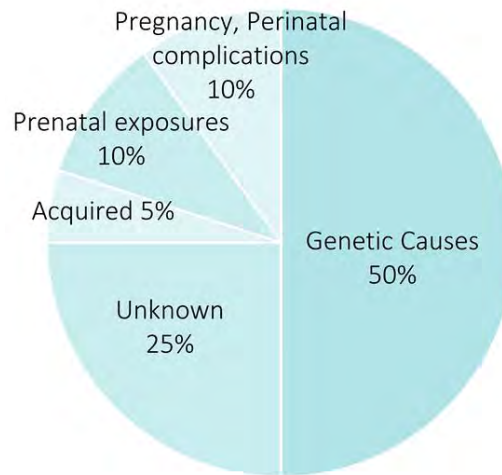


Figure 2. Causes of ID and their respective percentages. [Adapted from Marrus & Hall (6)].

There is a wide range of syndromes that cause ID/DD phenotypes coupled with different kinds of congenital malformations. However, their prevalence in the general population is very low, reason why the majority of them are classified as rare disorders. A certain disorder is considered as rare when it affects less than 1 in 2000 individuals and as ultra-rare if it affects no more than one person in 50000 (9). To date, almost 7000 different rare disorders have been described. Despite the low prevalence of each single disorder, as a group they have a big impact on society, as it is estimated that 6-8% of the EU population are rare disease patients (10). These percentages show how, as a whole, rare diseases represent a serious global issue both at a health and social levels.

Around 80% of rare diseases have a genetic origin (10) and the majority of them are monogenic (11). In 2017 it was estimated that the molecular origin of more than half of the identified rare genetic diseases was still unknown (12), but this percentage has been decreasing over the last years and the same tendency is expected to be maintained in the future (13). Nevertheless, even for those rare genetic diseases which have a clearly identified disease-causing gene, diagnosis and patient management can be very challenging due to the frequently observed phenotypic variability among different mutations (14).

2. DIAGNOSIS OF ULTRA-RARE NEURODEVELOPMENTAL DISORDERS

It is estimated that approximately half of the patients suffering from rare diseases are undiagnosed, while the waiting time for those who have been diagnosed is 5-6 years on average, reaching several decades in some cases of ultra-rare diseases (15). During this time, commonly called “**diagnostic odyssey**”, patients and their families face a long journey, usually full of uncertainty, hope and perseverance. The key to success of the diagnostic odyssey of ultra-rare NDDs is close collaboration of multidisciplinary teams, including clinical, bioinformatic and genetic experts.

2.1 Clinical diagnosis

In clinics, developmental delay is described in patients when two or more features of the developmental process are substantially delayed. These aspects include gross and fine movement, cognitive function, language/speech, social skills and activities of daily life related to personal care. The presence of DD becomes evident when a child fails to reach the developmental milestones associated with his/her specific age group. The concept “developmental delay” is reserved for children under five years old, while “intellectual disability” is used for older patients when IQ can be more accurately tested (16,17).

It is estimated that DD/ID occurs can be classified in four groups depending on its severity: mild, moderate, severe and profound. Approximately 95% of the DD/ID cases account for phenotypes ranging from mild to moderate. These patients require limited assistance and can live independently in an environment providing moderate aid and are normally diagnosed during early educational years due to low academic performance. Severe ID affects about 3.5% of patients, who show obvious delay related to development. They do need daily assistance and supervision but are generally able to learn simple routines and comprehend speech, although their communication skills are usually impaired. Finally, the remaining 1.5% of the cases are considered to present profound ID. They normally present several physical limitations and extremely limited oral communication, which make them completely dependent on a caretaker figure. Both severe and profound ID are identified within the first two years of life and frequently present comorbid conditions (18).

Between 30% and 40% of the ID cases are associated with other conditions that can be syndromic or not. The syndromic DD/ID cases also present with additional neurological

conditions, associated dysmorphic features or both (17,19). A particular feature is considered as dysmorphic when it is present in less than 5% of the population and it has been developed through malformation, deformation or disruption mechanisms. They can be divided into major and minor anomalies depending on the degree of alteration of the physical appearance and normal function. Some of the most frequent major dysmorphic features are orofacial clefts, neural tube defects and limb anomalies. Minor anomalies mostly occur in the head, face and hands. Usually, patients display a distinctive constellation of anomalies that constitutes a specific phenotype that differs from the standard (20). In DD/ID cases it is crucial to perform an exhaustive clinical assessment of these dysmorphic features that should include the description of the following anatomical regions: head shape, eyes, hair, nose, ears, mouth, jaw, neck, trunk area, genitalia and upper and lower limbs. Examination of other internal organ abnormalities, like the heart or the brain, caused by anomalous development should also be performed to develop a complete phenotypic description of the patient (21).

Given the intrinsic phenotypic heterogeneity present in the majority of ultra-rare NDDs, it is essential to try to use standardized terms to describe the observed clinical traits. They help to reduce ambiguity and misinterpretation across the scientific community and improve the implementation of automated analyses and classification, reducing time and errors. With this aim, the Human Phenotype Ontology (HPO) (22) was launched in 2008 and has been actively revised and updated since then. The HPO is a “comprehensive resource that systematically defines and logically organizes human phenotypes” functioning as a translational bridge between genomic data and the disease (**Figure 3**). It has different translational and research applications, such as the interpretation of sequencing data in diagnostics, discovery of novel gene-disease associations and cohort analytics to improve disease phenotypic delineation. Nowadays, the great majority of phenotype-driven genomic diagnostics software use HPO-based computational disease models (22).

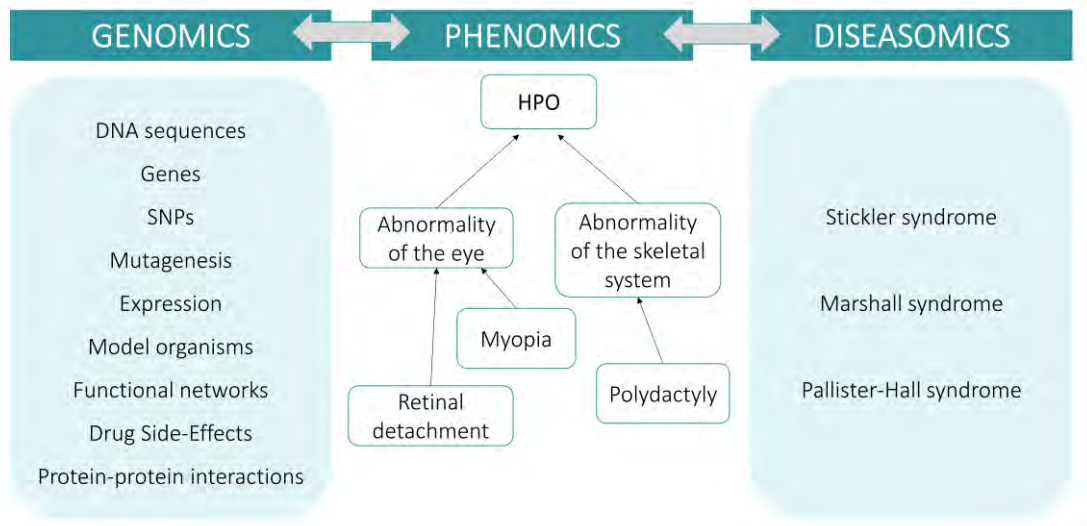


Figure 3. The HPO as a central resource to connect genomic and diseasome data through standardized phenomic descriptions. It facilitates data integration between molecular biology and human disease. [Adapted from Kölher et al. (23)].

While it is essential to perform a deep and systematic clinical phenotyping of the patient, it is important to highlight that the phenotype can be incomplete at the moment of the first clinical evaluation. For this reason, the performance of additional examinations (periodical follow-ups) looking for new traits is highly advisable and might guide the diagnostic process. Also, an exhaustive clinical description can help in a retrospective manner when genetic laboratory results are ambiguous (16).

2.2 Genetic diagnosis

There are cases in which an exhaustive phenotyping leads to a directed clinical suspicion, then the appropriate test according to the associated genetic alteration is performed. In the case that a chromosomal or genomic alteration is suspected, different molecular cytogenetic techniques can be used. Traditionally, the most used one has been the karyotype that allows the detection of large gains or losses of genetic material and large structural reorganizations, present in about 3-5% of DD/ID patients and/or congenital malformations (24). Aiming to improve the diagnosis rates, other techniques have been implemented, for example fluorescent in-situ hybridization (FISH), that allow the precise detection of translocations, and multiplex ligation-dependent probe amplification (MLPA), that allows the detection of microdeletions and microduplications in specific genomic regions (25). Then, the use of whole genome arrays including single nucleotide polymorphisms (SNP) and compared genomic hybridization arrays (aCGH) significantly increased the diagnostic rates of patients with DD/ID, ASD or congenital malformations (26).

If the clinical features can be clearly associated with a specific disease linked to variants in a specific gene, the faster and most cost-effective approach would be performing a screening of the whole candidate gene through Sanger sequencing. This sequencing technique allows the generation of very high quality long reads, however a starting hypothesis is needed as its discovery power is very limited.

When there is not a clear clinical suspicion the strategy to follow usually consists of performing some molecular cytogenetic techniques, such as karyotype and aCGH, to discard the possibility of chromosomal or genomic rearrangements. If the result is negative, an hypothesis-free NGS analysis should be carried out aiming to identify a point mutation or small deletion/insertion.

2.2.1 Next-generation sequencing techniques

Not much more than a decade ago, the diagnostic process of patients suffering from rare NDDs mainly involved many years of documentation of the clinical phenotype and performance of biochemical and imaging tests. In some cases, these investigations led to a suspected particular clinical disorder and different genetic studies were performed using a set of laboratory techniques with low individual efficiency. As could be expected, the success rates were considerably low. The appearance of next generation sequencing

(NGS) technologies represented a before and an after in the NDDs diagnostic field. During their early years they were mostly restricted to particular cases and frequently used by diagnosis research groups due to its low performance and high prices. However, the dramatic technical improvements and cost decrease during the last decade has made their inclusion possible as routine genetics diagnostic tools.

The incorporation of these novel genetic diagnostic tests, together with the improvement of the bioinformatic tools necessary for the analysis of the output data, had led to a significant decrease of the average time needed for rare NDDs patients to get a diagnosis. This has also led to a rapid increase in the identification of novel genes linked to neurodevelopmental disorders. These tools have also shown that, in some particular clinically defined syndromes, there is no common molecular cause. However, in some cases, these clinical entities are still useful as clinical or phenotypical “labels”. The Opitz C syndrome (OCS; OMIM # 211750) is an example of such situations. OCS is an ultra-rare syndromic neurodevelopmental disorder that was first clinically described by Opitz et al in 1969 (27). After deep genetic study, Opitz C syndrome has been redefined as a clinical entity without a common molecular basis, as thoroughly discussed in Urreizti et al. (28).

There are several different NGS platforms ranging from gene panels, which include some key candidate genes, to the sequencing of the whole genome (WGS). In research, the most commonly used strategies are sequencing of the whole exome (WES) and WGS. In the clinical environment, custom **gene panels** for specific groups of disorders are still frequently used, together with the clinical exome. The clinical exome is a gene panel including around 6000 different genes previously associated with disease according to data from different Mendelian disorders databases, such as OMIM (29). Gene panels are an intermediate approach between the screening of one single gene and the analysis of the whole exome. They are still a popular tool in clinics as they present a high sensitivity detecting variants in several candidate genes while reducing the complexity of the analysis and data interpretation. The main limitation of gene panels is that the analysis is restricted to a particular group of genes, meaning that the posterior re-analysis of newly described genes is not possible.

WES is a very powerful approach to identify the disease-causing mutation. Even though the 20000 protein-coding genes contained in the human exome only represent 1-2% of the whole genome, it is estimated that approximately 85% of the described monogenic disorders are associated with variants in coding regions (30). Compared to gene panels, it has the advantage of being a much less restrictive approach, as it is hypothesis-free

and has a much higher discovery potential. Thus, it allows the discovery of variants in genes that have never been associated with disease and the posterior reanalysis of recently described genes in unsolved cases. This advantage is particularly relevant in highly heterogeneous disorders, like NDDs, where new associated genes are frequently identified. However, WES presents disadvantages compared to gene panels as the volume of output data is significantly larger, adding complexity to the processing and interpretation steps. Also, the probability of finding variants with unknown significance (VUS) and incidental findings (IFs) increases, hindering the variant interpretation process (31).

WGS covers the entire genome of an individual. Although the coverage (number of reads of a certain region) is lower than in WES, it is more uniform (32). WGS provides the possibility of detecting deep intronic variants and copy number variants (CNV), overcoming the limitation that WES presents for the detection of large indels or CNVs. It is well known that some deep intronic variants can affect normal splicing patterns and/or interfere with regulatory domains or non-coding RNAs normal function that control the expression patterns of other genes. Like the data obtained from WES, WGS data can also be reanalysed over time. Apart from a relatively higher economic cost compared to WES, the identification of a huge amount of VUS in poorly known genome regions is one of the main limitations of WGS, as it leads to an increase in the time and resources needed for the analysis of the data.

2.2.2 Variant interpretation

A crucial part of the genomic approach to the diagnosis of genetic diseases is the interpretation of the variants identified through NGS. Thousands of variants are identified per exome (33) and millions when performing a WGS (34) (**Figure 4**). The identified single-nucleotide variants (SNVs) and indels are filtered according to different criteria related to mutation type, minor allele frequency in the general population (MAF) and associated clinical phenotype. To systematically prioritize and classify such numbers of variants according to their putative pathogenic consequences, in 2015 the American College of Medical Genetics (ACMG) published the “ACMG Standards and Guidelines” as a resource for clinical geneticists (35) (**Figure 4**).

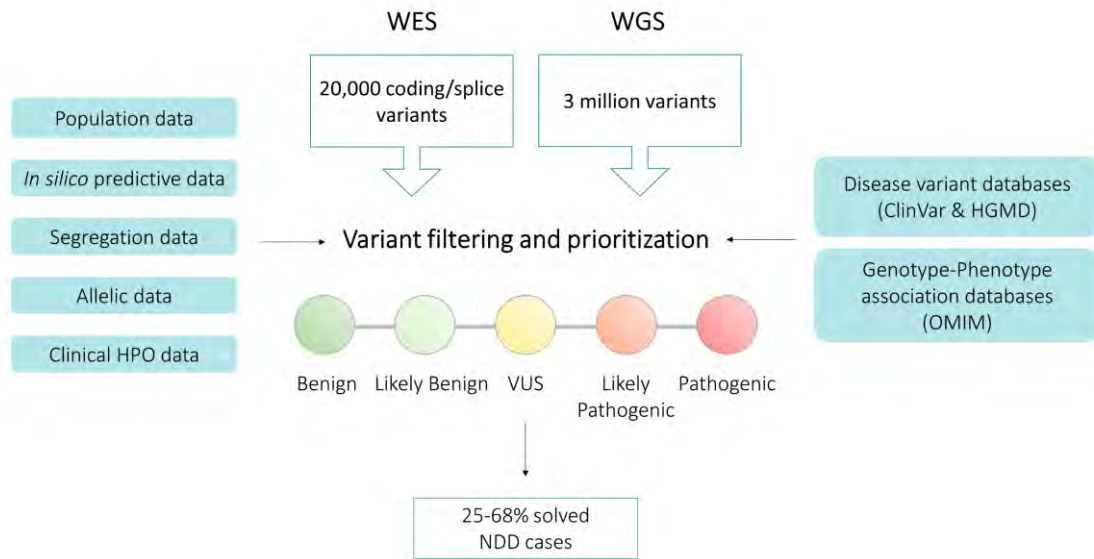


Figure 4. Genomic approach to the diagnosis of rare monogenic neurodevelopmental disorders following the ACMG guidelines. [Adapted from Stenton et al. (36)].

One of the criteria proposed by the ACMG is based on population data, so that the presence of the same variant or other variants with similar consequences in databases such as ClinVar (37), HGMD (38) and OMIM (29), that contain disease-associated mutations, would lean the scale to the pathogenic side. Similarly, its frequency and the number of homozygous individuals in control population databases, such as gnomAD (39), is also considered.

Then, computational and predictive data should also be carefully considered. There are many different *in silico* predictors that allow variant classification according to pathogenicity based on the type of amino acid change, the conservation of the specific residue across different species and possible alterations of the splicing pattern. The ones that are more frequently used are CADD (40), SIFT (41), Mutation Taster (42), PolyPhen-2 (43) and PROVEAN (44). Apart from predictive data, well-established functional studies that show deleterious effects are considered as strong evidence. Unfortunately, strong and robust functional evidence supporting the pathogenicity is not always available. Part of the work presented in this thesis has been carried out aiming to fill this knowledge gap in different particular ultra-rare neurodevelopmental disorders.

Another important evidence is segregation data, which allows the validation of the inheritance pattern of the identified variants. It provides strong evidence in inherited disease cases where the variant cosegregates with the disease in multiple affected family members or, in the case of *de novo* variants, if it is absent in both parents.

Segregation analyses are also key to elucidate if compound heterozygous mutations are in *cis* or in *trans*.

Finally, as mentioned before, adding the clinical description of the patient using HPO terms can reinforce the association of a particular variant, especially when the patient's phenotype is characteristic of mutations in a specific gene.

Consideration of all these criteria recommended by the ACMG guidelines leads to the classification of each variant into one of the following categories: "Benign", "Likely Benign", "VUS", "Likely Pathogenic" and "Pathogenic" (**Figure 4**). It is estimated that the use of NGS techniques coupled with careful variant interpretation lead to the establishment of a clear genetic diagnosis for approximately 25-68% of tested NDD patients (45).

2.2.3 Functional validation studies

The interpretation of the specific contribution that a novel variant may have to the patient's phenotype could be challenging. For instance, nonsense or frameshift variants are usually assumed to be loss-of-function (LoF) alleles as the encoded transcript would lead to the production of a peptide lacking functionally relevant domains or the nonsense-mediated decay (NMD) mechanism could be triggered. Nevertheless, truncating mutations in last exons escape this process and, in some cases, may behave as benign or gain-of-function (GoF) alleles (46). In the case of missense mutations, the complexity is even higher as they can result in many different possible scenarios (e.g., hypomorphic, hypermorphic, neomorphic, antimorphic...). As said before, functional *in silico* predictors can be useful tools to predict the pathogenicity of the identified variants. However, their results should be taken cautiously as they can return incorrect predictions, depending on the algorithms, previous knowledge on the protein structure, function and binding to other partners, etc. (47). These incorrect predictions can lead not to wrong clinical interpretation of variants.

Functional studies constitute essential tools to complement *in silico* predictions, as they provide experimental data that can help to elucidate and understand the effect of a variant at an *in vitro*, *ex vivo* and/or *in vivo* level. These functional validation studies (**Figure 5**) can be performed using a wide range of approaches, such as study of splicing patterns, mutation correction and phenotype rescue, detection of relevant biomarkers levels, generation of knockout (KO) cellular or animal models, etc. It is worth mentioning

that the performance of experiments to check the functionality and pathogenicity of a variant not only benefits that specific patient who will receive an accurate molecular diagnosis, but they may also help to elucidate the molecular mechanisms of the disease, crucial for posterior design and development of therapeutic strategies.

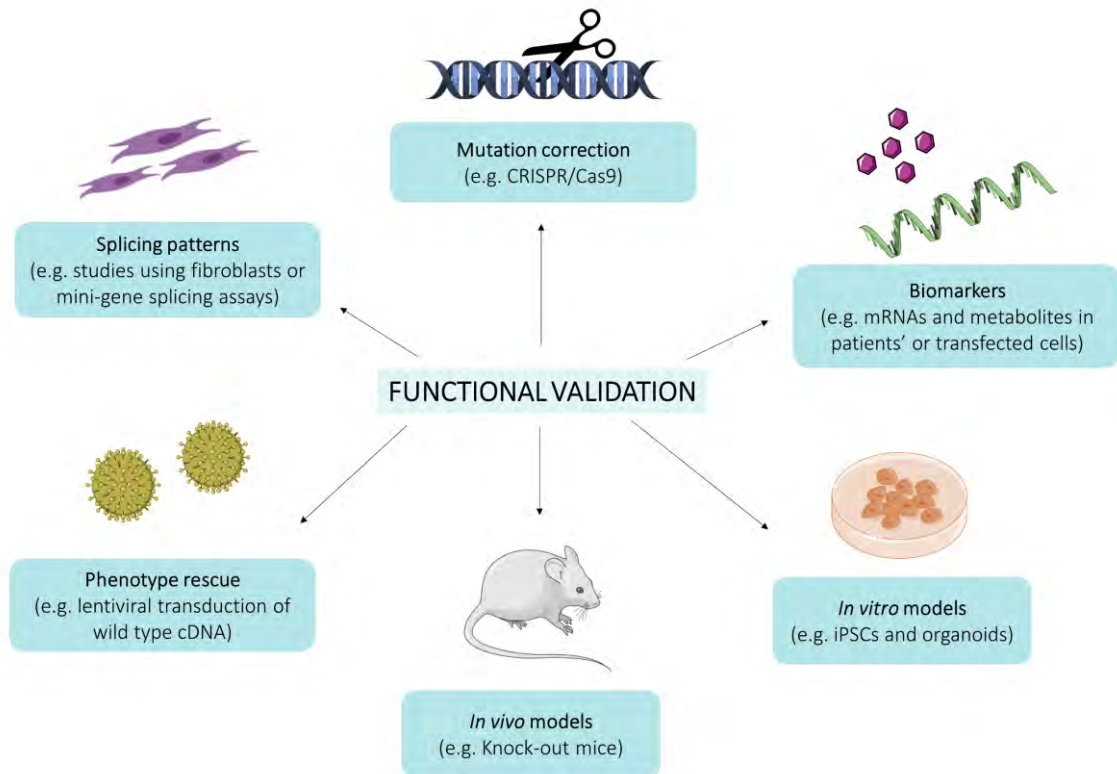


Figure 5. Examples of functional validation approaches frequently used to investigate the pathogenicity of VUS. Image created with Servier Medical Art.

2.2.3.1 Cellular models of disease: iPSCs

Cellular models constitute an effective tool to study the molecular mechanisms of genetic diseases, as well as to perform preliminary tests of different therapeutic strategies. Obviously, they present several limitations, like an incomplete representation of the whole organism reaction to certain compounds. Traditionally, human cell cultures have been limited to immortalized cell lines obtained from tumour biopsies (HeLa, HEK297, SaOs cells, etc) and primary cell lines obtained directly from patients (mainly, but not limited to, lymphoblasts and fibroblasts, due to their accessibility). Despite being useful tools, it is noteworthy that immortalized cell lines may present genetic and epigenetic aberrations and oncogene expression and that it can be difficult to obtain primary cells from patients, especially the relevant cell type for each specific disease (e.g. cells from the CNS in neurodevelopmental disorders).

In 1998, a new and promising path was opened for disease modeling with the derivation of human embryonic stem cells (hESCs) (48). However, this model presented several barriers, including strong ethical concerns regarding the use of hESCs in research. The discovery of methodologies that allow direct reprogramming of somatic cells to induced pluripotent stem cells (iPSCs) (49,50) has reshaped the approach to disease modelling and therapeutic strategy design of many diseases (51), overcoming hESCs limitations. The high potential of iPSCs resides in their capacity to be differentiated to many different cell types (**Figure 6**). Also, iPSCs present the exact same genomic background that the cells they have been differentiated from, usually fibroblasts from patients and controls. In this sense, it is important to consider that different individual iPSC lines may show variability in their potential to differentiate into other cell types, which might be caused by differences in the genetic background and the reprogramming history of each line (52).

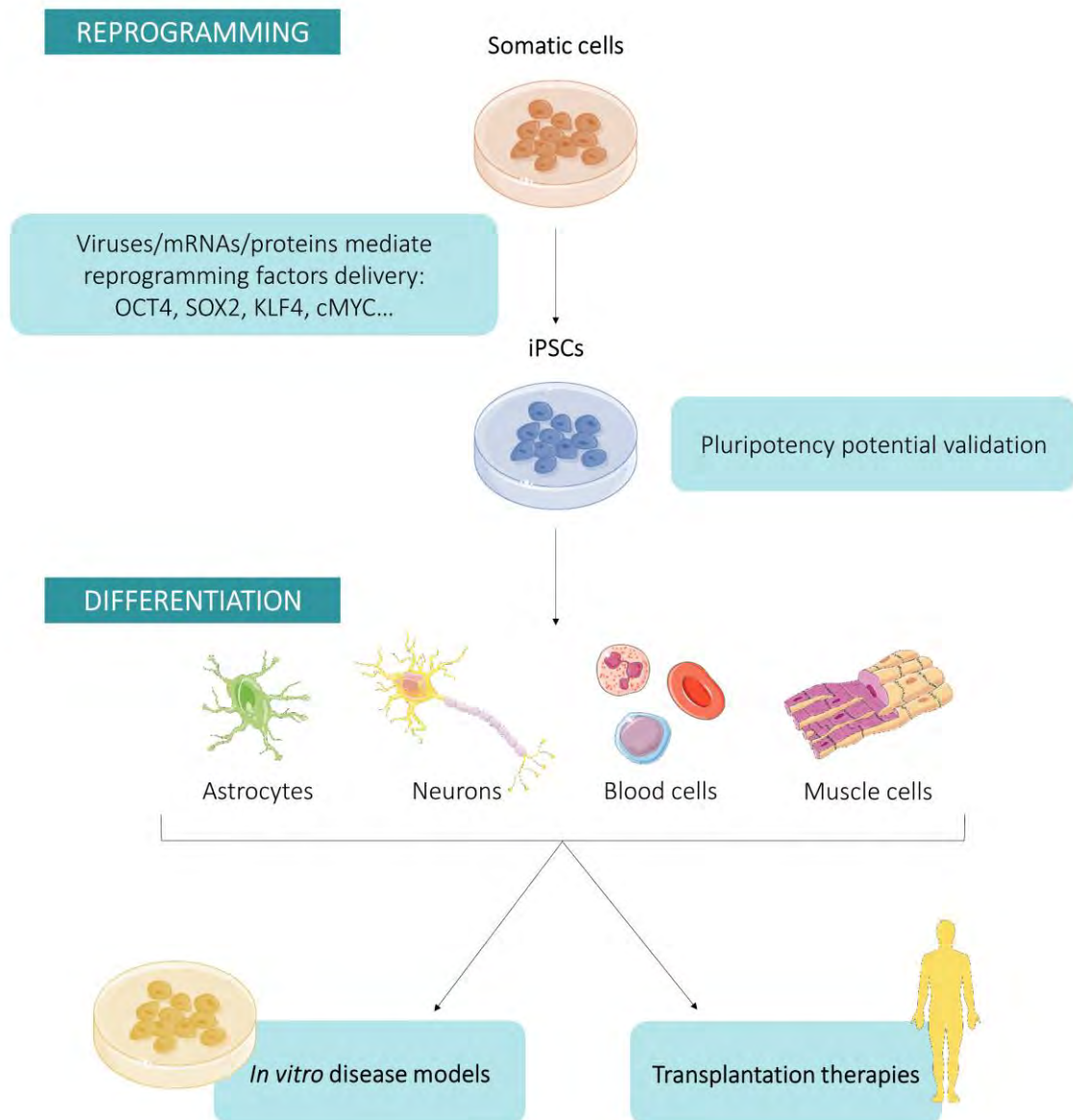


Figure 6. General picture of iPSCs reprogramming and differentiation processes and their main applications: *in vitro* disease modelling and cellular therapy. Image created with Servier Medical Art. [Adapted from Hockemeyer & Jaenisch (52)].

3. GENES RELATED TO THE OPITZ C CLINICAL ENTITY

In this thesis different patients that were clinically diagnosed with Opitz C syndrome were genetically diagnosed using WES aiming to identify the genetic origin of this ultra-rare neurodevelopmental condition. Since its description, more than 60 patients have been diagnosed with OCS, all of them showing highly variable multi-systemic manifestations, including developmental delay, trigonocephaly due to premature fusion of the metopic suture, midline dysmorphologies, hypotonia, seizures, limb malformations and congenital anomalies (53,54). Our group started to gather a cohort of OCS patients in 2011 in collaboration with Dr. G. Neri and Dr. J. Opitz himself, and genetically diagnosed seven of them before the start of the present work in 2017. The identified variants were located in different genes, namely *ASXL1*, *TRAF7*, *MAGEL2*, *KCNB1*, *RYS1* and *CDK13*. Below, the genes that were previously identified and have been more deeply studied at a functional level in this thesis and their preliminar associations with disease are described.

3.1 *ASXL1* and Bohring-Opitz syndrome

The *ASXL1* gene (Additional sex combs like transcriptional regulator 1; OMIM * 612990) is located in the chromosomal region 20q11.21 and belongs to the Enhancer of trithorax and Polycomb gene family. It encodes the ASXL1 protein, which is 1543 amino acids long and plays a crucial role in **chromatin remodelling**, by promoting histone methylation (55) and deubiquitination (56). It acts as a transcriptional activator or repressor depending on the cellular context and regulates *HOX* genes during axial patterning (57). GoF variants have been associated with acute lymphoblastic leukemia (58), myelodysplastic syndromes and chronic myelomonocytic leukemia (59). On the other hand, LoF variants disrupt normal hematopoiesis, but are not associated with tumorigenesis (57).

Germinal mutations in the *ASXL1* gene are the genetic cause of Bohring-Opitz syndrome (BOS, OMIM # 605039). BOS is a severe neurodevelopmental syndrome characterized by intrauterine growth retardation (IUGR), failure to thrive, nevus flammeus, deep psychomotor delay, seizures, severe hypotonia and flexion deformities of the upper limbs. These deformities lead to a clinically recognizable feature known as the “Bohring-Opitz syndrome posture” (60–62). The patients show trigonocephaly, characteristic dysmorphologies and congenital anomalies, resembling other syndromic forms of DD

like the Opitz C syndrome (63,64). In fact, due to the high degree of overlapping, it was proposed that both pathologies were the same syndrome with a very wide severity spectrum, going from mild phenotype (OCS) to a more severe one (BOS) (63).

More than 50 cases of BOS have been reported in the literature and approximately half of them harboured *de novo* mutations in the *ASXL1* gene (62,65–73). The identified germline disease-causing variants are heterozygous nonsense or frameshift mutations and mostly clustered to the centre of the protein (**Figure 7**), however the exact molecular mechanisms underlying these variants are still poorly known.

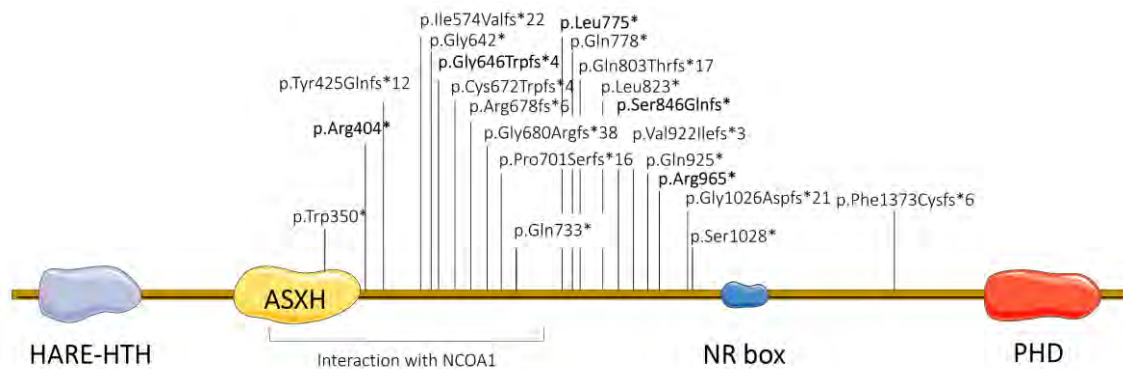


Figure 7. Representation of *ASXL1* with mutations reported in Bohring-Opitz syndrome patients. Mutations in bold have been reported more than once. HARE-HTH: HB1, ASXL, restriction endonuclease HTH domain (aa 11–86); ASXH: ASX homology domain (aa 255–364); NR box: nuclear receptor box (aa 1107–1112); PHD: plant homeodomain (aa 1503–1540). Image created with Servier Medical Art.

Although the BOS phenotype appears to be well-defined, some patients have been clinically diagnosed with BOS but tested negative for *ASXL1* mutations. This situation could be explained by genetic heterogeneity of the syndrome (65), somatic mosaicism or a need to improve the actual clinical diagnostic criteria for BOS (62).

3.2 TRAF7 and role in tumorigenesis

The *TRAF7* gene (TNF receptor associated factor 7; OMIM * 606692) maps to the 16p13.3 chromosomal region, has 21 coding exons and only 1 known protein-coding transcript which translates to the TRAF7 protein (Ensembl data). TRAF7 is one of the seven members of the tumour necrosis factor receptor-associated factor (TRAF) protein family. TRAF proteins act as **signalling adaptors** directly binding to the cytoplasmic domain of receptors of several families. In addition, most of them have E3 ubiquitin ligase activity that can activate downstream signalling events. The signalling pathways in which these proteins participate are involved in a wide range of cellular processes, such as cell survival, proliferation, migration, differentiation, cytokine production and autophagy. Tumour necrosis factor (TNF) family ligands lead to the transduction of these cellular signals through activation of different effectors, such as nuclear factor- κ Bs (NF- κ Bs), mitogen-activated protein kinases (MAPKs), or interferon-regulatory factors (IRFs) (74,75). At a structural level, TRAF proteins share several conserved domains (**Figure 8**). A RING finger domain is present at the N-terminus in all of them, except for TRAF1, and constitutes the core of the ubiquitin ligase catalytic domain. At the C-terminus, there is a TRAF domain, crucial for oligomerization and interaction with their partners (74,75). However, this characteristic TRAF domain is not present in TRAF7; instead, seven repeats of the WD40 domain are found (76).

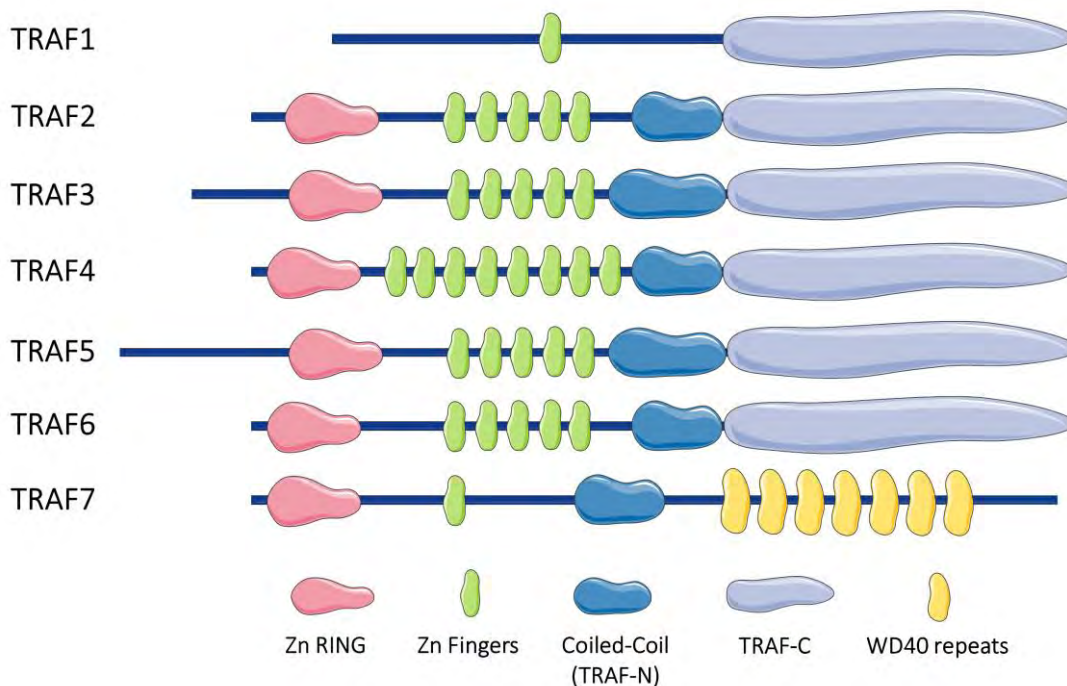


Figure 8. The different members of the TRAF family and their protein domains. Image created with Servier Medical Art.

TRAF7 activation involves homodimerization through its Zn fingers and coiled-coil domains (77). In a Tumour necrosis factor- α (TNF α) induced response (**Figure 9**), the WD40 repeats domain is crucial for the interaction of TRAF7 with MEKK3, which in turn promotes TRAF7 stabilization through phosphorylation and subsequent self-ubiquitination (77). This interaction also promotes the activation of several cellular components such as JNK, p38 and NF- κ B (78,79). Additionally, this domain is essential for the negative regulation of the proto-oncogene c-Myb by sumoylation (80). The Zn RING and Zn fingers domains promote caspase-mediated apoptosis and ubiquitination of NEMO and the NF- κ B subunit p65, leading to lysosomal degradation and a decrease of NF- κ B pathway activity (78). Knocking-down *TRAF7* in primary neuronal cells led to increased active caspase-3 protein levels and a decreased number of apoptotic primary neurons (81). Through the regulation of NEMO, TRAF7 is also involved in MyoD1 regulation, promoting a decrease in myogenesis (82).

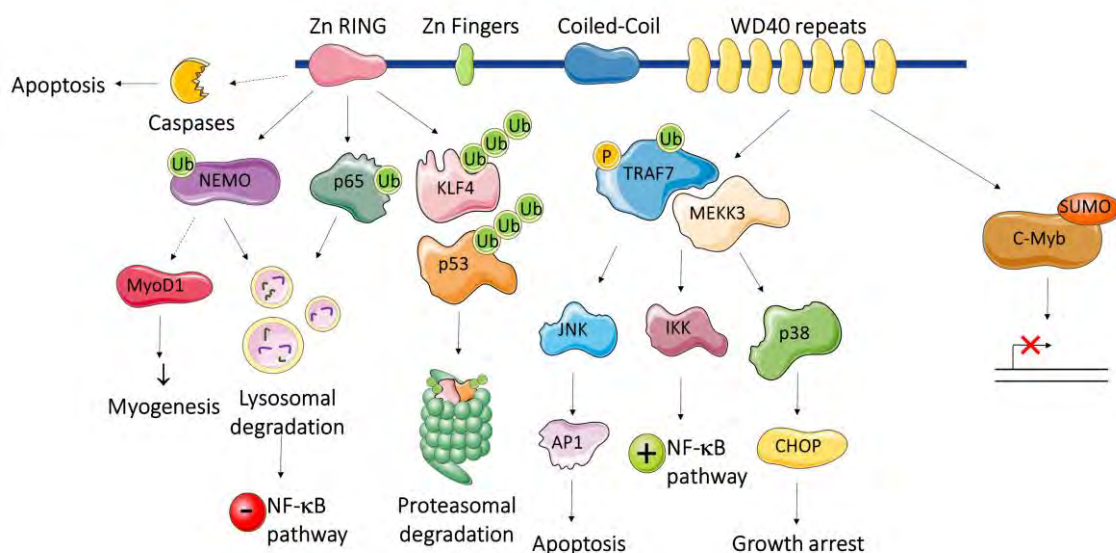


Figure 9. TRAF7 protein roles and functions in TNF α induced response. Image created with Servier Medical Art.

TRAF7 also plays an important role in the Toll Like Receptor 2 (TLR2) signalling pathway. Together with TRAF6, they promote the activation of NF- κ B due to the recognition of pathogen-associated molecular patterns, being of great relevance in innate immunity pathways (83).

Somatic point mutations in *TRAF7* have been linked to the development of different tumour types. So far, more than 70 different mutations have been identified in different types of meningioma (84–88). Mutations in *TRAF7* have been also identified in

intraneural perineuriomas, adenomatoid tumours of the male and female genital tract, well-differentiated papillary mesothelioma of the peritoneum (89–91), diffuse pleural mesothelioma (92) and localized pleural mesothelioma (93). *TRAF7* mutations seem to genetically characterize a group of neoplasms that develop from cells that wrap vital organs such as the brain, the peripheral nerves, the testis, the uterus and the fallopian tube (89). The great majority of the tumour-related mutations in *TRAF7* reported so far are heterozygous, mostly missense and 88% of them are restricted to the WD40 repeats domain at the C-terminus of the protein. The molecular mechanisms by which *TRAF7* somatic missense variants promote tumorigenesis in the different cancer types are nowadays an open research topic. For instance, a recently published study (94) showed that *TRAF7* loss-of-function leads to proteostasis dysregulation and hyperactivation of RAS-related GTPases, causing aberrant actin cytoskeletal organization and promoting oncogenic transformation in meningiomas. This new proposed mechanism put the focus on the function of the WD40 domain as a scaffolding structure important for the interaction with small GTPases (95), instead of the most extensively described one as a modulator of the NF- κ B pathway (96), at least in tumorigenesis.

3.3 *MAGEL2* and *MAGEL2*-related disorders

The *MAGEL2* gene (MAGE family member L2; OMIM * 605283) is a maternally silenced single-exon protein-coding gene contained in the Prader-Willi region (15q11-q13). In adult humans, its expression is mostly restricted to the CNS [according to GTEx data (97)], but it is also present in cells of mesodermal origin, involved in muscle, bone and fat tissues development (98). In adult animal mice, *Mage2* expression is enriched in the hypothalamus and the amygdala, especially enriched in the ventromedial, arcuate, tuberal, lateral, anterior and paraventricular hypothalamic nuclei (99). The *MAGEL2* gene encodes the *MAGEL2* protein, one of the largest proteins of the Type II MAGE protein family.

MAGEL2 has three relevant structural and functional elements (**Figure 10**): a highly proline-rich with an unknown function, a U7BS domain, which is a binding site for USP7 (100,101), and a MAGE Homology Domain (MHD). The MHD is the characteristic domain of the MAGE protein family and it confers high specificity to their protein-protein interactions (102). In particular, *MAGEL2* recognizes and binds to its partners TRIM27 and VPS35 through this domain (103).

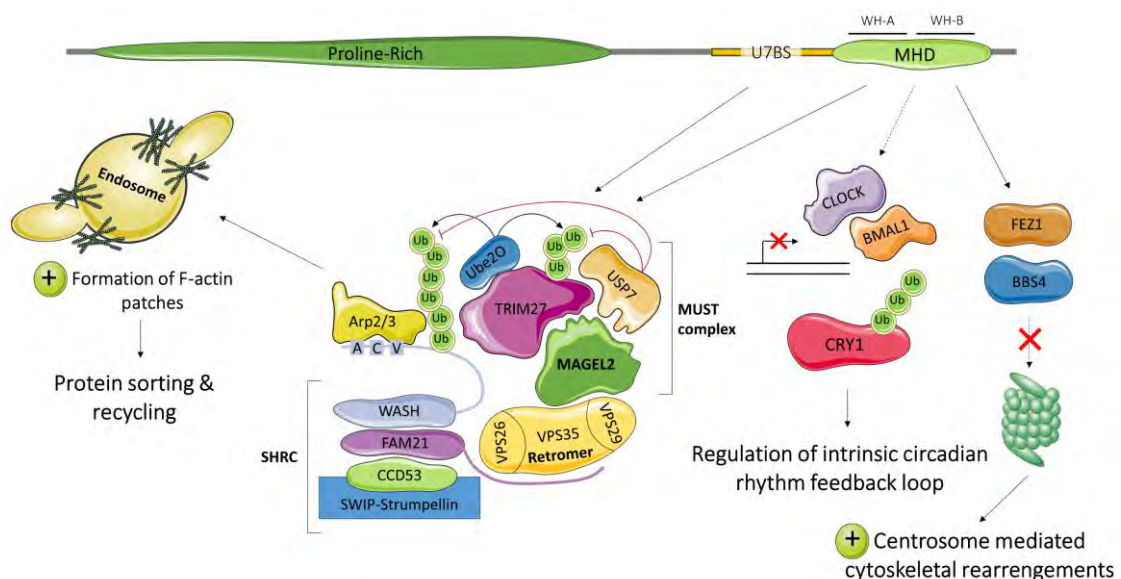


Figure 10. *MAGEL2* protein described roles and functions. Image created with Servier Medical Art.

The role of *MAGEL2* in the retrograde endosomal transport is its most extensively studied cellular function (**Figure 10**). *MAGEL2*, TRIM27 and USP7, form the MUST complex that is recruited to endosomes (100,103), which participate in the sorting of protein cargoes through retrograde and recycling pathways (104). The retromer complex

recruits the MUST complex, via MAGEL2-VPS35 binding, and the WASH regulatory complex (SHRC) to the endosomal membrane. Then, TRIM27 activates the SHRC complex, through WASH polyubiquitination, promoting the formation of endosomal F-actin patches. These localized branched patches are crucial for endosomal protein sorting, as they demarcate discrete domains within the endosome where specific proteins are segregated and sorted to their respective destinations (100,103). A well-coordinated trafficking network is key to ensure an appropriate cell distribution and a correct function of a wide variety of proteins.

It has also been proposed that MAGEL2 is involved in the centrosome-related cytoskeletal rearrangements during neurite outgrowth driven by Fez proteins and BBS4 (**Figure 10**), by protecting them from proteasomal degradation (105).

MAGEL2 shows a highly circadian expression pattern in humans and mice, being one of many clock-controlled genes (106,107). Consistent with *Magel2* expression in the hypothalamus and the role of the suprachiasmatic nucleus of the hypothalamus as a central pacemaker in mammals, *Magel2*-deficient mice showed reduced amplitude of activity and increased daytime activity, together with progressive infertility in males and other endocrine alterations (108). Also, *MAGEL2* contributes to the regulation of the ubiquitination balance of *CRY1*, crucial in the circadian rhythm feedback loop (107) (**Figure 10**).

3.3.1 Prader-Willi syndrome

The Prader-Willi locus is a complex chromosomal region that contains genes that are differentially expressed depending on their parental origin (**Figure 11A**). The PWS region comprises 6Mb on the long arm of chromosome 15, 2.5Mb of which contain five protein-coding genes and more than 80 non-coding RNA genes of exclusive paternal expression and two maternally expressed protein-coding genes (109,110).

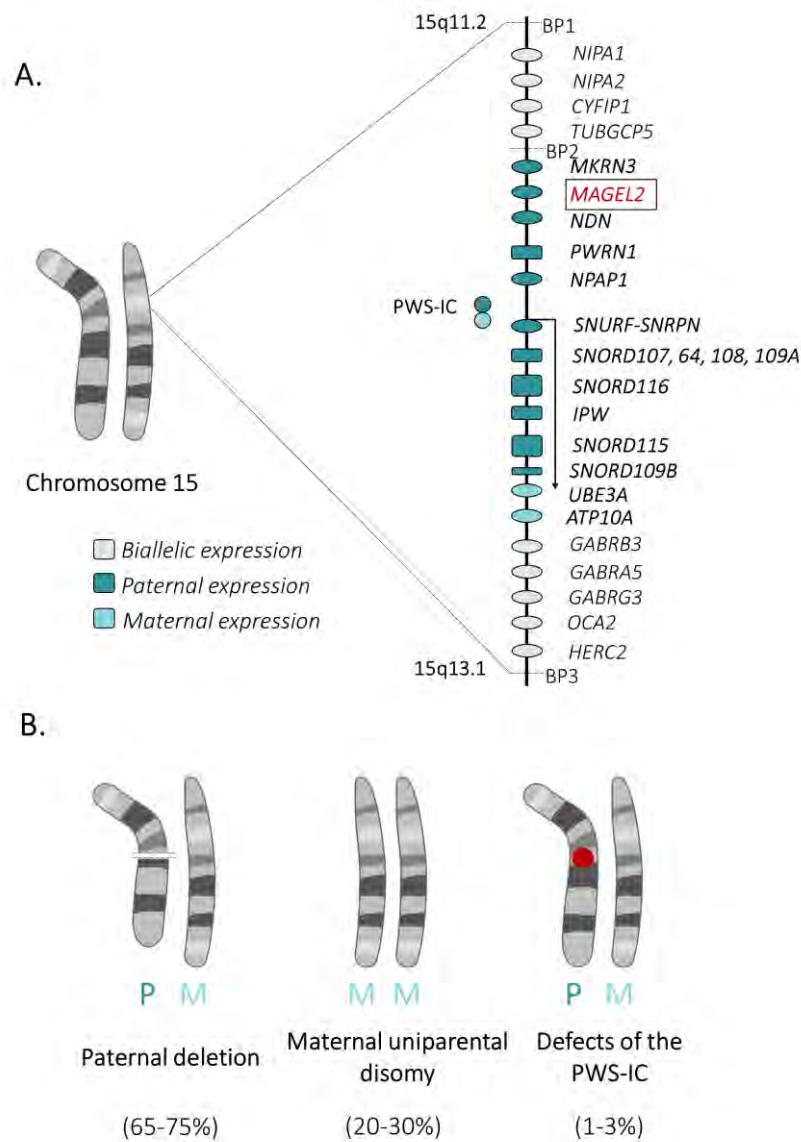


Figure 11. A) Chromosome map of PWS region (15q11-q13). Protein-coding genes are represented as ovals and RNA genes as rectangles. B) Possible genetic causes of Prader-Willi syndrome. In brackets, the frequency in which each phenomenon is observed in PWS patients. Image created with Servier Medical Art.

When the paternal alleles of these maternally silenced genes are not expressed, it causes an haploinsufficiency situation that results in Prader-Willi syndrome (PWS; OMIM # 176270). This lack of expression of the paternal allele can be caused by several molecular causes (**Figure 11B**) with different prevalence: deletion of paternal 15q11-q13 (65-75%), maternal uniparental disomy of chromosome 15 (mUPD) (20-30%) and defects of the PWS-IC (PWS imprinting centre) (1-3%) (111). The individual contribution that the loss of expression of each gene contained in the PWS region has on the typical phenotype observed in patients remains unclear.

Prader-Willi syndrome was described almost 70 years ago, and nowadays, it is still under extensive characterization and study. It is a complex imprinting disorder that causes major alterations in the endocrine, cognitive and neurologic systems, behaviour and metabolism of the affected individuals. PWS is a rare genetic disease that shows a prevalence of 1 in 10,000-30,000 live births, equally affecting both sexes and all ethnic populations (111). Children with PWS show severe hypotonia, feeding difficulties, failure to thrive and developmental delays during early infancy. Older children and adults present other clinical traits such as early-onset obesity, characteristic facial features, hypogonadism, hyperphagia/ obsession with food, obsessive/compulsive behaviour, mild mental retardation, sleep disturbances, high pain threshold, short stature related to growth hormone (GH) deficiency, hypopigmentation and small hands and feet (112). The obesity that these patients tend to develop can become one of the leading life-threatening conditions in this genetic condition (111).

3.3.2 Schaaf-Yang syndrome

Truncating mutations in the paternal allele of *MAGEL2* were first described as disease-causing in four patients with a PWS-like phenotype, but normal methylation patterns at 15q11-q13 (113). The phenotypic differences observed in the patients compared to typical PWS cases led to the delineation of a new disease named Schaaf-Yang syndrome (SYS; OMIM # 615547). Since then, more than 150 cases of SYS carrying more than 50 different variants have been reported in the literature (113–132). These variants are mostly nonsense or frameshift mutations and predominantly located at the C-terminal end of the protein, meaning that there is a partial or a total lack of the MHD, compromising the functions that *MAGEL2* carries out through this domain.

SYS was initially considered a PWS-like phenotype as the patients manifest overlapping clinical phenotypes with PWS patients (**Figure 12**). But there are some characteristics that support that SYS should be considered a differential diagnosis of PWS, especially during the early life period. Overlapping phenotypes include neonatal hypotonia, ID, DD, feeding difficulties, different hormonal disbalances and sleep disorders. However, some of the standardized criteria considered for PWS (e.g., hypopigmentation, characteristic facial dysmorphisms, small hand and feet, hyperphagia, obesity and obsessive-compulsive behaviour) are not frequent in SYS patients. For instance, childhood hyperphagia and increased weight gain present in 67% of PWS patients, are only present in 22% of SYS patients (133). In contrast, SYS cases show more severe ID and DD,

ASD typical behaviours and joint contractures more frequently than PWS patients (110,134,135). In adulthood the differences in the phenotypes of these two syndromes might become less apparent than in childhood, making them more difficult to discern at a clinical level (136).

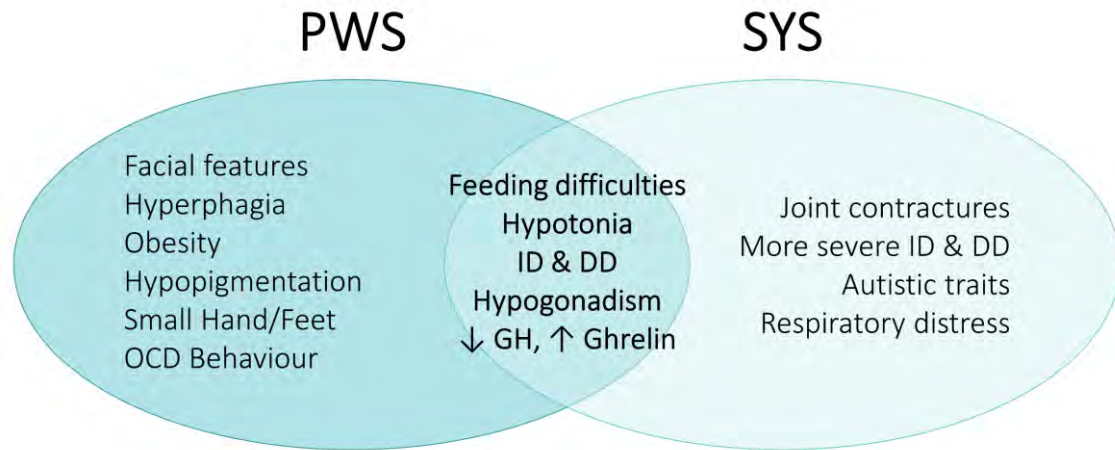


Figure 12. Phenotypic overlap between *MAGEL2*-related syndromes: PWS and SYS.

Endocrine and metabolic alterations in PWS have been widely studied, being hypogonadism and GH deficiency the most prevalent (111). The last one had been reported in more than 300 patients and GH therapy is recommended as an early intervention for PWS (137,138). A review of the literature on endocrine abnormalities in *MAGEL2*-related syndromes has been recently published (133) highlighting GH, thyroid-stimulating hormone (TSH), adrenocorticotrophic hormone (ACTH), antidiuretic hormone (ADH) and gonadotropins as the most common hormonal deficiencies in SYS. These endocrine alterations are thought to be caused by hypothalamic impairment and might lead to hypoglycemia.

An update of the clinical and genetic data of all the published SYS cases have been conducted as part of this thesis in close collaboration with the clinical expert Dr Serrano from Hospital Sant Joan de Déu.

3.3.3 *In vitro* and *in vivo* models of *MAGEL2*-related syndromes

Human *MAGEL2* gene and its murine homologue have a similar genomic organization. The gene in mice is located in chromosome 7, in a syntenic region to the human PWS cluster and it is also expressed only from the paternal allele. Moreover, both *MAGEL2* forms are intronless and contain a CpG island that can be found in its 5'-UTR. The

proteins encoded by the human and the mouse genes have a 77% similarity (139). Two different KO mouse models have been generated to study Magel2 loss.

In the first mouse model, generated by Dr. Wevrick team in 2007, the coding sequence of the gene was replaced by a LacZ reporter leaving the original promoter intact (140). Several publications report extensive phenotyping of this KO mouse (98,108,140–143), the most relevant observed phenotypes are summarized in **Table 1**. Quantitative proteomics of the hypothalamus of these mice showed several components of the dense secretory granules (SG) to be downregulated (99). SG are exocytic organelles involved in the processing and release of hormones and neuropeptides in neuroendocrine cells (144). Decreased SG protein levels were also observed in different PWS *in vitro* models caused by impaired endosomal protein trafficking and subsequent lysosomal degradation, resulting in a reduction of circulating bioactive hypothalamic hormones (99).

Table 1. Relevant phenotypes observed in MAGEL2-related syndromes mouse models.

Phenotype	Magel2 Knock-out		Truncated Magel2
	Wevrick et al	Muscatelli et al	Ieda et al
Neonatal mortality	10%	50%	-
Suckling defects	NA	+	NA
Neonatal failure to thrive and pre-wean growth retardation	+	+	+
Increased leptin plasma levels, reduced leptin sensitivity	+	NA	NA
Weight gain, decreased lean mass with increased adiposity	+	NA	-
Abnormal behaviour in novel environments	+	+	NA
Progressive infertility and decreased olfactory discrimination	+	NA	NA
Decreased locomotor activity, muscle dysfunction and decreases bone mineral content	+	NA	NA
Growth hormone axis impairment	+	+	NA
Decreased oxytocin	+	+	NA
Decreased serotonin	+	NA	NA
Blunted circadian rhythm, decreased orexin levels	+	NA	NA

A second mouse model was generated in 2010 by deleting the promoter and the majority of the coding sequence of *Magel2* (146). This model has not been so deeply characterized as the previously mentioned, a comparison of the observed phenotypes in both models can be found in **Table 1**. Impaired oxytocin (OXT) production in the hypothalamus was one of the highlights of the model, being the prohormone maturation the main issue (146). A daily dosage regimen of subcutaneous injections of OXT for 7 days after birth restored suckling activity, prevented the appearance of abnormal social behaviour and spatial learning deficits and led to partial anatomical and functional restoration of the central OXT system in the animals throughout adulthood (147), suggesting that it should be considered as a potential therapeutic approach for SYS and PWS (148,149). In fact, a phase 2 clinical trial has already been carried out in PWS patients, who after a short course of repeated intranasal OXT administration showed improved oral feeding and social skills (150).

More recently, Ieda et al. (151) generated two additional mouse models to study *Magel2*. In an attempt to model the putative toxic effects of the truncated form of the protein, they generated a transgenic mouse overexpressing the N-terminal region of *Magel2*, including part of the Proline-Rich protein domain. They observed a high rate of fetal and neonatal death, probably caused by the strong ubiquitous overexpression of the truncated form in various organs. They also generated a genome-edited mouse carrying a 234 bp deletion on *Magel2* (c.1690_1924del) that encodes a truncated form of the protein [p.(Glu564Serfs*130)], mimicking an equivalent situation to that observed in SYS patients. They could detect the presence of a shorter transcript in the brain at cDNA levels and maintenance of the normal imprinting pattern. However, the model failed to recapitulate the SYS phenotype (**Table 1**), as no obvious abnormal traits were observed in the *Magel2*^{P:fs} individuals, except for mild neonatal growth retardation.

3.4 Other genes identified in Opitz C patients

Six other genes had been identified as disease-causing in the OCS patients that were diagnosed along this thesis. All of them play crucial roles within the cell and have already been associated with different ultra-rare neurodevelopmental disorders. In principle, all these genes do not belong to the same functional pathway nor present a clear functional connection between them. Making it difficult to find a plausible explanation for the many phenotypic similarities found in those patients that led to their categorization within the same clinical diagnosis.



OBJECTIVES

The main aim of this thesis is to genetically diagnose a group of patients affected by severe syndromic neurodevelopmental disorders and contribute to the elucidation of the underlying pathophysiological molecular mechanisms.

To address this general aim, the following specific objectives were defined:

1) Identification of causal genes of patients clinically diagnosed as Opitz C syndrome and functional validation of some of the identified disease-causing variants.

- To perform whole exome sequencing analysis in eight affected families to identify and validate the molecular cause of the disease.
- To functionally evaluate the effects of the variants predicted to affect splicing in *KAT6A*, *PIGT*, *ASXL1* and *FOXP1* genes, using fibroblasts from patients or mini-gene splicing assays.
- To test the effects on protein activity caused by recessive variants in *DPH1*.

2) Characterization of heterozygous *TRAF7* germline variants at phenotypic and molecular levels.

- To gather a cohort of patients carrying *TRAF7* germline missense mutations to improve the clinical delineation of the novel TRAF7-syndrome.
- To perform an analysis of the transcriptomic profile in TRAF7 patients' fibroblasts to elucidate the pathways that may be affected by the mutations.

3) Functional characterization of *MAGEL2* truncating mutations and generation of an *in vitro* model for SYS.

- To investigate putative changes in transcriptomic and metabolomic profiles and A β ₁₋₄₀ peptide excretion levels that might contribute to the molecular definition of the SYS phenotype in fibroblasts.
- To explore the effects of a truncating MAGEL2 variant in protein stability and subcellular localization.
- To reprogram fibroblasts to iPSCs and characterize its pluripotency as a first step to generate relevant *in vitro* neural models for SYS.



RESULTS

REPORT OF THE SUPERVISORS ON THE CONTRIBUTION OF THE PhD CANDIDATE TO THE ARTICLES INCLUDED IN THIS THESIS

Title of the thesis: “Combining exome sequencing and functional studies to identify causal genes of ultra-rare neurodevelopmental disorders”

Author: Laura Castilla-Vallmanya

Supervisors: Dr Susanna Balcells Comas and Dr Roser Urreizti Frexedas

Susanna Balcells Comas and Roser Urreizti Frexedas acting as PhD supervisors of the thesis entitled “Combining exome sequencing and functional studies to identify causal genes of ultra-rare neurodevelopmental disorders” presented by Laura Castilla-Vallmanya as a compendium of 10 research articles, detail the precise contribution of the PhD candidate to each publication below.

CHAPTER 1: Identification of disease-causing variants in patients clinically diagnosed with Opitz C syndrome and Bohring-Opitz syndrome and functional validation

ARTICLE 1

Title: Extending the phenotypic spectrum of Bohring-Opitz syndrome: Mild case confirmed by functional studies

Authors: Eyby Leon, Jullianne Diaz, Laura Castilla-Vallmanya, Daniel Grinberg, Susanna Balcells & Roser Urreizti

Journal: American Journal of Medical Genetics Part A **Number:** 182A (2020)

Pages: 201-204 **Impact Factor (2020 JCR Science Edition):** 2.802

Contribution of the PhD candidate: The candidate designed and performed the molecular experiments related to the functional validation of the disease-causing variant affecting the normal splicing pattern. She analysed and created the figure related to the molecular results included in the manuscript. She also participated in the drafting of the manuscript and in the revisions after the feed-back from co-authors.

ARTICLE 2

Title: De Novo *PORCN* and *ZIC2* Mutations in a Highly Consanguineous Family

Authors: Laura Castilla-Vallmanya, Semra Gürsoy, Özlem Giray-Bozkaya, Aina Prat-Planas, Gemma Bullich, Leslie Matalonga, Mónica Centeno-Pla, Raquel Rabionet, Daniel Grinberg, Susanna Balcells & Roser Urreizti

Journal: International Journal of Molecular Sciences **Number:** 22 (2021)

Pages: 1549 **Impact Factor (2021 JCR Science Edition):** NA

Contribution of the PhD candidate: Laura Castilla-Vallmanya handled the biological samples and actively participated in the analysis of the WES data, the posterior validation of the identified candidate variants and the interpretation of the obtained results. She participated in the elaboration of the tables included in the main text and as supplementary material. She also actively participated in the drafting of the manuscript and in the implementation of the modifications suggested by co-authors and reviewers.

ARTICLE 3

Title: The *ASXL1* mutation p.Gly646Trpfs*12 found in a Turkish boy with Bohring-Opitz Syndrome

Authors: Roser Urreizti, Semra Gürsoy, Laura Castilla-Vallmanya, Guillem Cunill, Raquel Rabionet, Derya Erçal, Daniel Grinberg & Susana Balcells

Journal: Clinical Case Reports **Number:** 6 (2018) **Pages:** 1452-1456

Impact Factor (2018 JCR Science Edition): NA

Contribution of the PhD candidate: The candidate performed the manual sequencing of the whole *ASXL1* gene and carried out the analysis and interpretation of the obtained chromatograms. After variant identification, she cloned and sequenced the PCR fragment to unequivocally confirm the mutation. She also critically revised the manuscript.

ARTICLE 4

Title: Five new cases of syndromic intellectual disability due to *KAT6A* mutations: widening the molecular and clinical spectrum

Authors: Roser Urreizti, Estrella Lopez-Martin, Antonio Martinez-Monseny, Montse Pujadas, Laura Castilla-Vallmanya, Luis Alberto Pérez-Jurado, Mercedes Serrano, Daniel Natera-de Benito, Beatriz Martínez-Delgado, Manuel Posada-de-la-Paz, Javier Alonso, Purificación Marin-Reina, Mar O'Callaghan, Daniel Grinberg, Eva Bermejo-Sánchez & Susanna Balcells

Journal: Orphanet Journal of Rare Diseases **Number:** 15 (2020) **Pages:** 44
Impact Factor (2020 JCR Science Edition): 4.123

Contribution of the PhD candidate: Laura Castilla-Vallmanya participated in the analysis and validation of the Whole Exome Sequencing data of Patient 1. She participated in the validation and interpretation of the results and in the drafting of the manuscript, contributing to the elaboration of figures and tables and critically revising the manuscript.

ARTICLE 5

Title: Case report of a child bearing a novel deleterious splicing variant in *PIGT*

Authors: Samantha Mason*, Laura Castilla-Vallmanya*, Con James, P. Ian Andrews, Susana Balcells, Daniel Grinberg, Edwin P. Kirk & Roser Urreizti

Journal: Medicine **Number:** 98 (2019) **Pages:** 8
Impact Factor (2019 JCR Science Edition): 1.552

Contribution of the PhD candidate: The candidate handled the biological samples and isolated the DNA from peripheral blood or fibroblasts. She analysed and validated the Whole Exome Sequencing data. She participated in the interpretation of the sequencing results and in the experimental design of the functional validation of the splicing mutation, which she then carried out. She also performed the RT-qPCR analyses. She created the figures related to the analysis of *PIGT* alternative transcripts included in the main text and to the RT-qPCR data included as supplementary material. She also participated in the drafting of the manuscript and its revision.

ARTICLE 6

Title: A De Novo *FOXP1* Truncating Mutation in a Patient Originally Diagnosed as C Syndrome

Authors: Roser Urreizti, Sarah Damanti, Carla Esteve, Héctor Franco-Valls, Laura Castilla-Vallmanya, Raul Tonda, Bru Cormand, Lluïsa Vilageliu, John M. Opitz, Giovanni Neri, Daniel Grinberg & Susana Balcells

Journal: Scientific Reports **Number:** 8 (2018) **Pages:** 694

Impact Factor (2018 JCR Science Edition): 4.011

Contribution of the PhD candidate: Laura Castilla-Vallmanya participated in the analysis and validation of the Whole Exome Sequencing data. She also participated in the elaboration of some of the supplementary material included in the publication and in the drafting and revision of the manuscript.

ARTICLE 7

Title: DPH1 syndrome: two novel variants and structural and functional analyses of seven missense variants identified in syndromic patients

Authors: Roser Urreizti, Klaus Mayer, Gilad D. Evrony, Edith Said, Laura Castilla-Vallmanya, Neal A. L. Cody, Guillem Plasencia, Bruce D. Gelb, Daniel Grinberg, Ulrich Brinkmann, Bryn D. Webb & Susanna Balcells

Journal: European Journal of Human Genetics **Number:** 28 (2020) **Pages:** 64-75

Impact Factor (2020 JCR Science Edition): 4.246

Contribution of the PhD candidate: The candidate participated in the analysis of the Whole Exome Sequencing data of Patient 1 and 2 of the publication, the validation of the identified candidate variants and the interpretation of the results. She also participated in the manuscript writing and revision after co-authors and reviewers' comments.

CHAPTER 2: Characterization of *TRAF7* germline variants at a phenotypic and molecular level

ARTICLE 8

Title: Phenotypic spectrum and transcriptomic profile associated with germline variants in *TRAF7*

Authors: Laura Castilla-Vallmanya, Kaja K. Selmer, Clémantine Dimartino, Raquel Rabionet (...), Susanna Balcells, Stanislas Lyonnet, Daniel Grinberg, Jeanne Amiel, Roser Urreizti & Christopher T. Gordon.

Journal: Genetics in Medicine **Number:** 22 (2020) **Pages:** 1215-1226
Impact Factor (2020 JCR Science Edition): 8.822

Contribution of the PhD candidate: Laura Castilla-Vallmanya prepared the RNA samples from fibroblasts to perform the transcriptomics analysis and performed all the RT-qPCR and cell viability experiments. She analysed the obtained transcriptomics results through the different techniques and actively participated in their biological interpretation. She elaborated all the figures related to molecular data and drafted that part of the manuscript, including the critical discussion of them. Finally, she also participated in the revision and modifications on the final version of the manuscript after the feed-back from co-authors and journal reviewers.

CHAPTER 3: Functional characterization of *MAGEL2* truncating mutations and generation of an *in vitro* model for Schaaf-Yang syndrome

ARTICLE 9

Title: Advancing in Schaaf-Yang syndrome pathophysiology: from bedside to subcellular analyses of truncated *MAGEL2* in patients' fibroblasts

Authors: Laura Castilla-Vallmanya, Mercedes Serrano, Mónica Centeno-Pla, Héctor Franco-Valls, Raúl Martínez-Cabrera, Aina Prat-Planas, Elena Rojano, Pedro Seoane, Miriam Navarro, Clara Oliva, Rafael Artuch, Raquel Rabionet, Daniel Grinberg, Susanna Balcells & Roser Urreizti

Journal: To be submitted to Journal of Medical Genetics

Contribution of the PhD candidate: The candidate actively contributed to the recompilation, revision and interpretation of the previously published genetic and clinical data. She also participated in the experimental design and carried out the experiments related to heterologous expression of the mutated form of the protein and to the measurement of A β ₁₋₄₀ excretion levels. She also prepared the RNA and cellular extract samples for the transcriptomics and metabolomics analyses. She actively participated in data analysis and interpretation of the results of all the molecular experiments, elaborated the tables and figures included in the manuscript and drafted the first version of the manuscript. She also implemented the modifications suggested by the co-authors.

ARTICLE 10

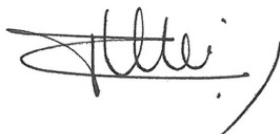
Title: Generation of human iPSC lines from two Schaaf-Yang Syndrome (SYS) patients

Authors: Laura Castilla-Vallmanya, Daniel Grinberg, Susanna Balcells, Roser Urreizti & Isaac Canals

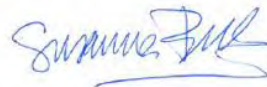
Journal: To be submitted to Stem Cell Research

Contribution of the PhD candidate: Laura Castilla-Vallmanya carried out the reprogramming of the two iPSC lines included in the article. She performed all the characterization experiments to ensure total reprogramming, analysed the results and prepared the results summary figure. She also drafted the first version of the manuscript and carried out the modifications after revision of the rest of the co-authors.

Barcelona,



Roser Urreizti Frexedas



Susanna Balcells Comas

CHAPTER 1: Identification of causal genes of patients clinically diagnosed as Opitz C syndrome and functional validation of the identified disease-causing variants

Article 1: Extending the phenotypic spectrum of Bohring-Opitz syndrome: Mild case confirmed by functional studies

Summary:

Bohring-Opitz syndrome (BOS) has been described as a clinically recognizable genetic syndrome since 1999. Clinical diagnostic criteria were established in 2011 and include microcephaly, trigonocephaly, distinctive craniofacial dysmorphic features, facial nevus flammeus, failure to thrive, and severe developmental delays. The same year, different de novo heterozygous nonsense mutations in the ASXL1 were found in affected individuals. Since then, several cases have been reported confirming the association between this chromatin remodeling gene and BOS. Most affected individuals die in early childhood because of unexplained bradycardia, obstructive apnea, or pulmonary infections. Those that survive usually cannot walk independently and are nonverbal. Some have had success using walkers and braces in late childhood. While few are able to speak, many have been able to express basic needs using communication devices as well as gestures with associated basic vocalizations. In this article, we present a mild case of BOS with a de novo pathogenic mutation c.1720-2A>G (p.I574VfsX22) in ASXL1 detected on whole-exome sequencing and confirmed by functional analysis of the messenger RNA splicing pattern on the patient's fibroblasts. She has typical dysmorphic features and is able to run and walk independently as well as to communicate with basic sign language.

Reference:

Leon E, Diaz J, Castilla-Vallmanya L, Grinberg D, Balcells S, Urreizti R. Extending the phenotypic spectrum of Bohring-Opitz syndrome: Mild case confirmed by functional studies. *Am J Med Genet Part A*. 2020; 182A: 201–204. doi: 10.1002/ajmg.a.61397



Received: 6 May 2019 | Revised: 2 October 2019 | Accepted: 9 October 2019

DOI: 10.1002/ajmg.a.61397

CLINICAL REPORT

AMERICAN JOURNAL OF
medical genetics WILEY

Extending the phenotypic spectrum of Bohring-Opitz syndrome: Mild case confirmed by functional studies

Eyby Leon¹ | Jullianne Diaz¹ | Laura Castilla-Vallmanya² | Daniel Grinberg² | Susanna Balcells² | Roser Urreizti²

¹Rare Disease Institute, Children's National Health System, Washington, District of Columbia

²Department of Genetics, Microbiology and Statistics, Faculty of Biology, IBUB, IRSJD, CIBERER, University of Barcelona, Barcelona, Spain

Correspondence

Eyby Leon, Rare Disease Institute, Children's National Health System, 111 Michigan Avenue NW, Washington, DC 20010.
Email: eleon@childrensnational.org

Funding information

Catalan Government, Grant/Award Number: 2014SGR932; CIBERER, Grant/Award Number: U720; Ministerio de Economía y Competitividad de España, Grant/Award Number: SAF2016-75948-R

Abstract

Bohring-Opitz syndrome (BOS) has been described as a clinically recognizable genetic syndrome since 1999. Clinical diagnostic criteria were established in 2011 and include microcephaly, trigonocephaly, distinctive craniofacial dysmorphic features, facial nevus flammeus, failure to thrive, and severe developmental delays. The same year, different *de novo* heterozygous nonsense mutations in the *ASXL1* were found in affected individuals. Since then, several cases have been reported confirming the association between this chromatin remodeling gene and BOS. Most affected individuals die in early childhood because of unexplained bradycardia, obstructive apnea, or pulmonary infections. Those that survive usually cannot walk independently and are nonverbal. Some have had success using walkers and braces in late childhood. While few are able to speak, many have been able to express basic needs using communication devices as well as gestures with associated basic vocalizations. In this article, we present a mild case of BOS with a *de novo* pathogenic mutation c.1720-2A>G (p. I574VfsX22) in *ASXL1* detected on whole-exome sequencing and confirmed by functional analysis of the messenger RNA splicing pattern on the patient's fibroblasts. She has typical dysmorphic features and is able to run and walk independently as well as to communicate with basic sign language.

KEYWORDS

ASXL1, Bohring-Opitz syndrome, functional studies, mild

1 | INTRODUCTION

Bohring-Opitz syndrome (BOS), also known as Oberklaid-Danks syndrome or C-like syndrome (MIM605039), is a clinically recognizable genetic syndrome described for the first time in Bohring et al. (1999). Twelve years later, in 2011, diagnostic criteria were established by Hastings et al. including microcephaly, trigonocephaly, distinctive craniofacial dysmorphic features, facial nevus flammeus, failure to thrive, and severe developmental delays (Hastings et al., 2011). Craniofacial features include palatal abnormalities, prominent eyes, hypoplastic supraorbital ridges, upslanting palpebral fissures, depressed nasal bridge, anteverted nares, and low-set posteriorly angulated ears. The

same year Hoischen et al. (2011) found the association between mutations in the *ASXL1* gene and BOS after performing whole-exome sequencing (WES) in combination with direct sequencing and found different *de novo* heterozygous nonsense or frameshift mutations.

Congenital anomalies like corpus callosum defects and retinal and optic nerve abnormalities are frequently reported in BOS. Seizures are common as well as truncal hypotonia with hypertonia of the extremities. Affected patients assume a typical posture of the upper limbs including ulnar deviation of the wrists and/or fingers at the metacarpophalangeal joints. Russell et al. (2015) recommended Wilms tumor surveillance every 3 months until age 8 given the link between *ASXL1* and myelodysplastic conditions. Severe feeding problems are

common at the beginning of infancy, and most affected individuals die in early childhood because of unexplained bradycardia, obstructive apnea, or pulmonary infections. The ones who survive usually cannot walk independently and are nonverbal. Some have had success using walkers and braces in late childhood. While few are able to speak, many have been able to express basic needs using augmentative and alternative communication devices as well as gestures with associated basic vocalizations (Russell, Tan, & Graham Jr, 2018).

Additional sex comb-like1 (ASXL1) is known as a chromatin modulator that plays dual functions in transcriptional regulation depending on the cell type. Recent studies using *Asxl1* knockout mice revealed its importance in proliferation and differentiation of hematopoietic progenitor cells, and in the development of organs (An et al., 2019). In this article, we present a mild case of BOS with a de novo pathogenic mutation c.1720-2A>G (p.I574VfsX22) in ASXL1 detected on WES and confirmed by the analysis of the messenger RNA splicing pattern on fibroblasts.

2 | CASE REPORT

Our patient was born full-term via vaginal delivery to a G1, P0, 22-year-old mother and 29-year-old father of Ethiopian descent. Prenatal and family history were unremarkable. Birth parameters included weight 2.83 kg (13th percentile), length 45.7 cm (sixth percentile), and head circumference (HC) 34 cm (eighth percentile). Her newborn course was uncomplicated, and she passed her newborn hearing screen. She was noted to have glabellar nevus flammeus as an infant, which faded with age. She sat up at 7 months, crawled at 11 months, babbled at 12 months, and stood at 14 months. At 14 months, she was found to have a large cup to disc ratio on ophthalmological examination after exotropia was noted. She began to have seizures at 17 months including complex febrile and unprovoked seizures which typically occurred every few months. An electroencephalogram suggested a potential deep seizure focus from the left occipital/posterior quadrant region. Brain MRI demonstrated mild diffuse thinning of the corpus callosum, moderately small optic nerves and chiasm, mildly small pons,

prominence of the left lateral ventricle likely reflecting mild left-sided periventricular white matter volume loss or hypogenesis, and no clear epileptogenic focus. An echocardiogram did not reveal cardiac disease.

She presented to our clinic at 19 months of age with global developmental delay. Her weight was in the 40th percentile, length in the 10th percentile, and HC in the 30th percentile. On physical examination, she was noted to have mild coarsening of the facial features, synophrys, upslanting palpebral fissures, prominent eyes, depressed nasal bridge, anteverted nares, narrow and high arched palate, widely spaced teeth, genu valgum, one hypopigmented macule on the chest, hirsutism, increased sandal gaps on both feet, and mild hypotonia (Figure 1; Figures S1–S4). She walked at 20 months of age and was able to climb the stairs with assistance at 24 months. At age 3, she was pointing and feeding herself with her hands, had balance issues, and had difficulty running. She was diagnosed with autism spectrum disorder at 4 years 3 months. At that time, she was able to respond to her name but had difficulty with eye contact. She had repetitive behaviors including spinning in circles, clapping her hands, and slamming doors.

Growth parameters at the most recent physical examination at age 5 included weight in the 88th percentile, height in the 11th percentile, and HC in the 54th percentile. She is nonverbal but will point and sign for "more." She is hyperactive and has frequent tantrums. She can wave and will pull a parent to what she wants. She needs assistance with dressing and brushing her teeth and is not toilet-trained. She will only scribble with a crayon and does not typically play with toys and will throw them instead. She can go up and down stairs with alternating feet and runs slowly. She is seizure-free on oxcarbazepine and levetiracetam, and her Wilms tumor surveillance has been negative so far. She attends special education preschool and receives speech, occupational, and physical therapies.

3 | MATERIALS AND METHODS

A CMA SNP array (CytoScan[®] Dx) was performed to detect copy-number variants. Gene panels were done by Massively Paralleled



FIGURE 1 (a) Patient at 2 weeks old showing nevus flammeus on forehead, hypoplastic supraorbital ridges, anteverted nares, and prominent eyes. (b) Frontal view at 19 months old not showing the nevus flammeus and mild coarsening of facial features [Color figure can be viewed at wileyonlinelibrary.com]

Sequencing using TruSight One kit (v1.0). WES was performed using the Illumina platform for next-generation sequencing. The exome capture is performed with NimbleGen reagents using a HGSC custom-designed capture reagent called VCROME 2.1. Patient and control's fibroblasts were obtained after signed consent and cultured in Dulbecco's Modified Eagle Medium (DMEM) supplemented with 10% fetal bovine serum (Gibco, Life Technologies) and 1% streptomycin-penicillin (Gibco, Life Technologies, Carlsbad, California) and were maintained at 37°C and 5% of CO₂. Cycloheximide (Sigma-Aldrich) treatment was applied in a concentration of 1 mg/ml in DMEM during 6 h. When confluence was reached, the RNA was extracted with the High Pure RNA Isolation Kit (Roche, Switzerland). RNA was then retrotranscribed using the High-capacity cDNA Reverse Transcription kit (Applied Biosystems, Foster City, California). Amplification of the cDNA region containing the end of exon 12 and the beginning of exon 13 was performed by PCR using specific primers. The different isoforms obtained were cloned to a pGEM[®]T-easy vector (Promega, Madison, Wisconsin) following the manufacturer's instructions. The resulting plasmids were sequenced using the Sanger method by the CCitUB genomic services (Parc Científic, Barcelona). All protocols were approved by the Ethics Committee of the Universitat de Barcelona (IRB00003099), and all methods were performed in accordance with the relevant guidelines and regulations.

4 | RESULTS

Initial genetic testing workup included a negative SNP chromosomal microarray, comprehensive epilepsy panel, and Noonan spectrum disorder panel. WES analysis showed three de novo variants: c.1720-2A>G in *ASXL1* gene (ENST00000375687), c.253G>A in the *STAG1*

gene (ENST00000383202), and c.299_300del in the *BACH1* gene (ENST00000399921) (Table S1). Several other variants of unknown significance were reported in autosomal dominant genes on testing, but all were inherited from an unaffected parent. RNA analysis from fibroblasts and Sanger sequencing of each band showed that the mutant allele led to the full retention of intron 12 (Figure 2). The aberrant transcript generated was not affected by the nonsense mediated decay (NMD) process, as no differences were observed when the culture was performed in the presence of cycloheximide.

5 | DISCUSSION

Variants previously associated with BOS are truncating de novo mutations mainly located in exon 13 (Hoischen et al., 2011; Russell et al., 2018; Urreizti et al., 2016), like the c.1720-2A>G mutation found in our patient. Functional studies on fibroblasts from the patient validated the functional implication of this change. The variant caused a change in the reading frame that would lead to a premature stop codon after 21 residues (p.I574VfsX22). The fact that no exon-exon junction remains downstream of the premature stop codon is consistent with the lack of NMD. This de novo heterozygous intronic mutation in *ASXL1* is affecting the canonical acceptor splice site at intron 12. The resulting protein is predicted to be truncated and will lack the C-terminus part of the protein. For all the reasons stated above, the mutation is considered to be pathogenic.

In many cases, WES will frequently identify several variants of unknown significance including more than one de novo variant, therefore muddling the ability to identify a unifying diagnosis. As with the present case, our patient's medical history alone did not meet strict clinical criteria for BOS and further studies were necessary to confirm

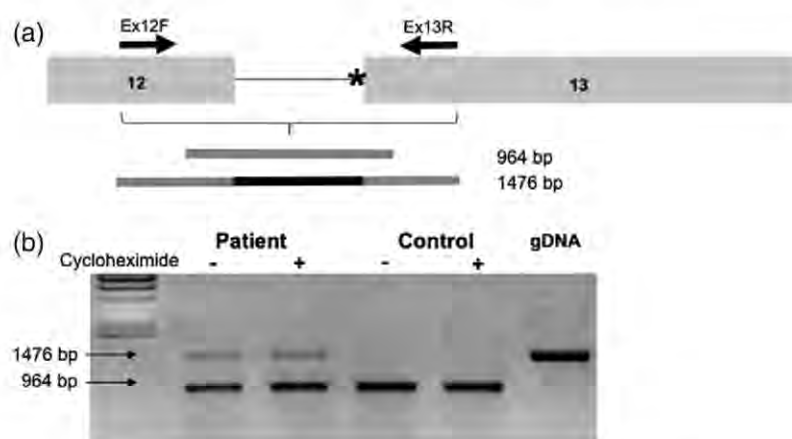


FIGURE 2 Messenger RNA analysis on the splicing pattern of *ASXL1* exons 12 and 13 in the patient compared to a control sample. (a) Schematic representation of the *ASXL1* 3' genomic region. The asterisk marks the position of the c.1720-2A>G mutation, affecting the canonical acceptor site of intron 12. The bars indicate the theoretical Ex12F-Ex12R PCR fragment size with and without retention of intron 12. (b) PCR amplification shows an upper band in the patient's mRNA in the presence and absence of cycloheximide, corresponding in size with the 1,476 band observed in the genomic. The smallest band, also present in the control, corresponds to the correctly spliced transcript. The identity of both bands has been confirmed by Sanger sequencing

her diagnosis. In fact, our patient has been previously reported as "patient 3" in Yuan et al. at the beginning of 2019 in a large cohort of patients with cohesinopathies, as a possible Cornelia De Lange like phenotype (Yuan et al., 2019). This manuscript indicates that the majority of disease-causing mutations described in *STAG1* were loss of function changes and missense mutations mainly affecting specific domains. However, the mutation identified in our patient is far from these domains and predicted to be benign, neutral, or tolerated by PolyPhen 2, SNP and Go, PROVEAN, and SIFT. This prediction is most likely reflecting that valine and isoleucine are similar both in charge and size and suggesting a mild effect of the change on the protein structure and function. While the effect of this mutation of the patient's clinical presentation cannot be ruled out, we consider that this is, at most, a modifier mutation and not the main cause of the disease. Regarding *BACH1*, this gene acts as a transcription factor and plays a role in the regulation of oxidative stress pathway (Tan, Lim, Bennett, Shi, & Harper, 2013). So far, this gene has not been associated with any human disease and the knockout murine model was born at the expected Mendelian ratio and do not show any difference with the wild type (Ota, Brydun, Itoh-Nakadai, Sun, & Igarashi, 2014).

Although there has been at least one mild BOS case reported in the literature (Hoischen et al., 2011), to our knowledge, she is the first genetically confirmed patient with mild BOS who is able to communicate via sign language and walk independently whose mutation has been confirmed by functional studies. While she has typical facial dysmorphic features, she lacks the history of failure to thrive, BOS posture, severe intellectual impairment, microcephaly, and trigonocephaly. The early diagnosis of BOS is important to decrease the mortality rate over time (Russell et al., 2018). However, most reported patients have a severe phenotype including the BOS posture and severe developmental delays, which was not present in our patient. The application of WES in clinically unrecognizable genetic syndromes has not only significantly helped the early diagnosis of rare and new genetic syndromes but has also broadened the clinical spectrum of several known genetic conditions like in our case.

ACKNOWLEDGMENTS

The authors thank the patient and her family for their wholehearted collaboration. Funding was from Catalan Government (2014SGR932), Spanish Ministerio de Economía y Competitividad (SAF2016-75948-R) and from CIBERER (U720).

CONFLICT OF INTEREST

None.

ORCID

Eyby Leon  <https://orcid.org/0000-0002-1852-2849>

REFERENCES

- An, S., Park, U. H., Moon, S., Kang, M., Youn, H., Hwang, J. T., ... Um, S. J. (2019). *Asxl1* ablation in mouse embryonic stem cells impairs neural differentiation without affecting self-renewal. *Biochemical and Biophysical Research Communications*, 508, 907–913.
- Bohring, A., Silengo, M., Lerone, M., Superneau, D. W., Spaich, C., Braddock, S. R., ... Opitz, J. M. (1999). Severe end of Opitz trigonocephaly (C) syndrome or new syndrome? *American Journal of Medical Genetics*, 85, 438–446.
- Hastings, R., Cobben, J. M., Gillissen-Kaesbach, G., Goodship, J., Hove, H., Kjaergaard, S., ... Newbury-Ecob, R. (2011). Bohring-Opitz (Oberklaid-Danks) syndrome: Clinical study, review of the literature, and discussion of possible pathogenesis. *European Journal of Human Genetics*, 19, 513–519.
- Hoischen, A., van Bon, B. W., Rodriguez-Santiago, B., Gilissen, C., Vissers, L. E., de Vries, P., ... de Vries, B. B. A. (2011). De novo nonsense mutations in *ASXL1* cause Bohring-Opitz syndrome. *Nature Genetics*, 43, 729–731.
- Ota, K., Brydun, A., Itoh-Nakadai, A., Sun, J., & Igarashi, K. (2014). *Bach1* deficiency and accompanying overexpression of heme oxygenase-1 do not influence aging or tumorigenesis in mice. *Oxidative Medicine and Cellular Longevity*, 757901, 1–12.
- Russell, B., Johnston, J. J., Biesecker, L. G., Kramer, N., Pickart, A., Rhead, W., ... Graham, J. M., Jr. (2015). Clinical management of patients with *ASXL1* mutations and Bohring-Opitz syndrome, emphasizing the need for Wilms tumor surveillance. *American Journal of Medical Genetics Part A*, 167, 2122–2131.
- Russell, B., Tan, W. H., & Graham, J. M., Jr. (2018). Bohring-Opitz Syndrome. In M. P. Adam, H. H. Ardinger, R. A. Pagon, et al. (Eds.), *GeneReviews*[®] [Internet]. Seattle, WA: University of Washington, Seattle; 1993–2019 <https://www.ncbi.nlm.nih.gov/books/NBK481833/>
- Tan, M. K., Lim, H. J., Bennett, E. J., Shi, Y., & Harper, J. W. (2013). Parallel SCF adaptor capture proteomics reveals a role for SCFFBXL17 in *NRF2* activation via *BACH1* repressor turnover. *Molecular Cell*, 52, 9–24.
- Urreiziti, R., Roca-Ayats, N., Trepast, J., Garcia-Garcia, F., Aleman, A., Orteschi, D., ... Grinberg, D. (2016). Screening of *CD96* and *ASXL1* in 11 patients with Opitz C or Bohring-Opitz syndromes. *American Journal of Medical Genetics, Part A*, 170, 24–31.
- Yuan, B., Neira, J., Pehlivan, D., Santiago-Sim, T., Song, X., Rosenfeld, J., ... Liu, P. (2019). Clinical exome sequencing reveals locus heterogeneity and phenotypic variability of cohesinopathies. *Genetics in Medicine*, 3, 663–675.

SUPPORTING INFORMATION

Additional supporting information may be found online in the Supporting Information section at the end of this article.

How to cite this article: Leon E, Diaz J, Castilla-Vallmanya L, Grinberg D, Balcells S, Urreiziti R. Extending the phenotypic spectrum of Bohring-Opitz syndrome: Mild case confirmed by functional studies. *Am J Med Genet Part A*. 2020;182A:201–204. <https://doi.org/10.1002/ajmg.a.61397>

Supplementary information for:

Extending the phenotypic spectrum of Bohring-Opitz syndrome: Mild case confirmed by functional studies

Eyby Leon, Jullianne Diaz, Laura Castilla-Vallmanya, Daniel Grinberg, Susanna Balcells & Roser Urreizti

Supplemental Figures



Supplemental Figure 1. Lateral view showing posteriorly rotated ears.



Supplemental Figure 2. Hirsutism on back.



Supplemental Figure 3. Increased sandal gap on both feet.



Supplemental Figure 4. Normal hands

Supplemental Table 1: *De novo* variants identified in our patient.

GENE	Position	cDNA	Protein	Pathology¹ (MIM; inh²)	Origin	GnomAD MAF (Hom)	dbSNP	Pathogenicity predictors (PP2/SF)
ASXL1	20:31022233	c.1720-2A>G	p.Ile574Valfs*22	Bohring-Opitz syndrome (#605039; AD)	de novo	-	rs376029425	-/-
STAG1	3:136323195	c.253G>A	p.(Val85Ile)	Mental retardation 47 (#617635; AD)	de novo	-	-	B/T
BACH1	21:30698444_ 30698444delA	c.299_300del	p.(Glu101Argfs*13)	-	de novo	-	-	-/-

¹ Disease associated with mutations in this gene according to OMIM.

² Pattern of inheritance of the associated disease.

inh: Inheritance; **MAF:** Minimum allele Frequency; **PP2:** PolyPhen2; **SF:** SIFT; **B:** Benign; **T:** Tolerated

Article 2: De Novo *PORCN* and *ZIC2* Mutations in a Highly Consanguineous Family

Summary:

We present a Turkish family with two cousins (OC15 and OC15b) affected with syndromic developmental delay, microcephaly, and trigonocephaly but with some phenotypic traits distinct between them. OC15 showed asymmetrical skeletal defects and syndactyly, while OC15b presented with a more severe microcephaly and semilobal holoprosencephaly. All four progenitors were related and OC15 parents were consanguineous. Whole Exome Sequencing (WES) analysis was performed on patient OC15 as a singleton and on the OC15b trio. Selected variants were validated by Sanger sequencing. We did not identify any shared variant that could be associated with the disease. Instead, each patient presented a de novo heterozygous variant in a different gene. OC15 carried a nonsense mutation (p.Arg95*) in *PORCN*, which is a gene responsible for Goltz-Gorlin syndrome, while OC15b carried an indel mutation in *ZIC2* leading to the substitution of three residues by a proline (p.His404_Ser406delinsPro). Autosomal dominant mutations in *ZIC2* have been associated with holoprosencephaly 5. Both variants are absent in the general population and are predicted to be pathogenic. These two de novo heterozygous variants identified in the two patients seem to explain the major phenotypic alterations of each particular case, instead of a homozygous variant that would be expected by the underlying consanguinity.

Reference:

Castilla-Vallmanya, L.; Gürsoy, S.; Giray-Bozkaya, Ö.; Prat-Planas, A.; Bullich, G.; Matalonga, L.; Centeno-Pla, M.; Rabionet, R.; Grinberg, D.; Balcells, S.; et al. De Novo *PORCN* and *ZIC2* Mutations in a Highly Consanguineous Family. *Int. J. Mol. Sci.* 2021; 22:1549. doi: 10.3390/ijms22041549



Case Report

De Novo *PORCN* and *ZIC2* Mutations in a Highly Consanguineous Family

Laura Castilla-Vallmanya ¹, Semra Gürsoy ², Özlem Giray-Bozkaya ³, Aina Prat-Planas ¹, Gemma Bullich ⁴, Leslie Matalonga ⁴, Mónica Centeno-Pla ¹, Raquel Rabionet ¹, Daniel Grinberg ¹, Susanna Balcells ¹ and Roser Urreiziti ^{1,*}

- ¹ IBUB, IRSJD, and CIBERER (ISCIII), Department of Genetics, Microbiology and Statistics, Faculty of Biology, University of Barcelona, 08028 Barcelona, Spain; lcastilla30@gmail.com (L.C.-V.); aina.prat98@gmail.com (A.P.-P.); monicacentpla@hotmail.com (M.C.-P.); kelly.rabionet@ub.edu (R.R.); dgrinberg@ub.edu (D.G.); sbalcells@ub.edu (S.B.)
- ² Department of Pediatric Genetics, Dr. Behcet Uz Children's Hospital, Izmir 35210, Turkey; dr.semra@hotmail.com
- ³ Department of Pediatric Genetics, Faculty of Medicine, Dokuz Eylül University, Izmir 35340, Turkey; ozlemgirayy@gmail.com
- ⁴ CNAG-CRG, Centre for Genomic Regulation (CRG), Barcelona Institute of Science and Technology (BIST), 08028 Barcelona, Spain; gemma.bullich@cnag.crg.eu (G.B.); leslie.matalonga@cnag.crg.eu (L.M.)
- * Correspondence: rurreiziti@fsjd.org
- † Current address: Department of Clinical Biochemistry, Institut de Recerca Sant Joan de Déu and CIBERER, 08950 Barcelona, Spain.



Citation: Castilla-Vallmanya, L.; Gürsoy, S.; Giray-Bozkaya, Ö.; Prat-Planas, A.; Bullich, G.; Matalonga, L.; Centeno-Pla, M.; Rabionet, R.; Grinberg, D.; Balcells, S.; et al. De Novo *PORCN* and *ZIC2* Mutations in a Highly Consanguineous Family. *Int. J. Mol. Sci.* **2021**, *22*, 1549. <https://doi.org/10.3390/ijms22041549>

Received: 8 January 2021
Accepted: 31 January 2021
Published: 4 February 2021

Publisher's Note: MDPI stays neutral with regard to jurisdictional claims in published maps and institutional affiliations.



Copyright: © 2021 by the authors. Licensee MDPI, Basel, Switzerland. This article is an open access article distributed under the terms and conditions of the Creative Commons Attribution (CC BY) license (<https://creativecommons.org/licenses/by/4.0/>).

Abstract: We present a Turkish family with two cousins (OC15 and OC15b) affected with syndromic developmental delay, microcephaly, and trigonocephaly but with some phenotypic traits distinct between them. OC15 showed asymmetrical skeletal defects and syndactyly, while OC15b presented with a more severe microcephaly and semilobal holoprosencephaly. All four progenitors were related and OC15 parents were consanguineous. Whole Exome Sequencing (WES) analysis was performed on patient OC15 as a singleton and on the OC15b trio. Selected variants were validated by Sanger sequencing. We did not identify any shared variant that could be associated with the disease. Instead, each patient presented a de novo heterozygous variant in a different gene. OC15 carried a nonsense mutation (p.Arg95*) in *PORCN*, which is a gene responsible for Goltz-Gorlin syndrome, while OC15b carried an indel mutation in *ZIC2* leading to the substitution of three residues by a proline (p.His404_Ser406delinsPro). Autosomal dominant mutations in *ZIC2* have been associated with holoprosencephaly 5. Both variants are absent in the general population and are predicted to be pathogenic. These two de novo heterozygous variants identified in the two patients seem to explain the major phenotypic alterations of each particular case, instead of a homozygous variant that would be expected by the underlying consanguinity.

Keywords: neurodevelopmental disease; clinical genetics; whole exome sequencing; consanguinity; focal dermal hypoplasia; holoprosencephaly

1. Introduction

Case Description Here, we report two de novo mutations causing severe neurodevelopmental delay in two first degree cousins from a highly consanguineous family of Turkish origin (Figure 1).

Patient 1 was a 10-year-old girl and single child of a healthy, consanguineous couple of Turkish origin. The family had a history of non-syndromic intellectual disability and deafness, with several affected individuals for each trait. Prenatally, the mother was hospitalized for a urinary tract infection. There was no history of polyhydramnios/oligohydramnios or maternal diabetes. Patient 1 was born at term by normal vaginal delivery and the birth was uneventful. Her birth weight and height were 3.1 kg (−0.53 SD) and 48 cm (−0.71 SD),

respectively. Since birth, she presented with failure to thrive and neonatal hypotonia. Additionally, congenital hip dislocation was detected. At the six months follow-up, her weight was 4.5 kg (-4.08 SD), height was 58.5 cm (-3.07 SD), and head circumference was 37.3 cm (-4 SD). She showed several craniofacial dysmorphologies, including severe microcephaly, trigonocephaly (with prominent metopic ridge), facial asymmetry, and other features, such as low hairline, hypoplastic orbital ridges, up-slanting palpebral fissures, strabismus, sparse eyebrows, prominent ears, gingival hyperplasia, and high palate (Figure 2 and Table 1). Ocular examination revealed a minimal bilateral optic disc hypoplasia. Short neck, sometimes with crusting of the skin, was also observed. In addition, she presented with radial head dislocation, hypoplasia of the right clavicle, widely spaced nipples, ulnar deviation of the fingers, and complete cutaneous syndactyly of the right 3rd and 4th fingers with bony fusion of the distal phalanges, overlapping toes on both feet, and spasticity of the lower limbs. She had thickened subcutaneous soft tissue on the proximal phalanges (prominently second finger) of the left hand. The patient had focal dermal hypoplasia in the left region of the neck, axillary region, and the middle region of her right, lower limb. She had also hypo-hyperpigmented lesions in her back, pelvic region, and trunk (not shown). The patient also had hypodontia. Brain magnetic resonance imaging (MRI) revealed periventricular gliotic changes, thin corpus callosum, and moderate cerebellar atrophy. She was severely delayed (no head control at four years) and suffered from epilepsy, which were generally triggered by fever, were amenable to multiple drug regimens. She passed away at the age of 10 due to a respiratory infection. She was considered compatible with Opitz C clinical spectrum. Previous genetic analyses included a normal karyotype and a normal array comparative genomic hybridization (array CGH).

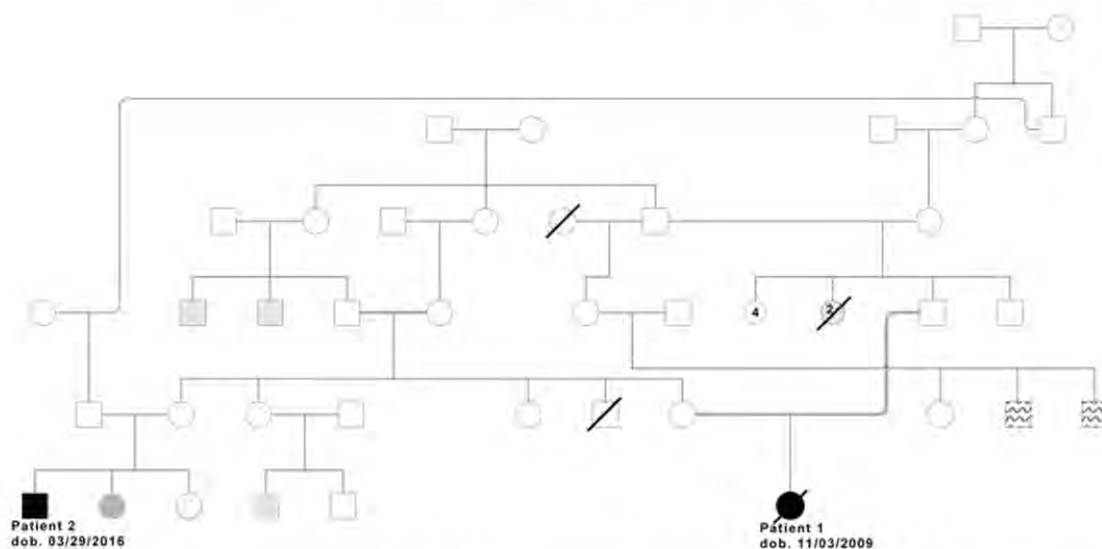


Figure 1. Extended family pedigree showing the relations among all four progenitors, the two mothers being sisters, and the two fathers being cousins once removed. Patient 1's parents are also cousins once removed (connected through a double bond). Patients 1 and 2 in black. Patient 2's microcephalic sister in grey. Squared pattern: congenital deafness. Wavy pattern: intellectual disability.



Figure 2. Pictures of patient 1. (A–D) Face, hand, and foot at age 9. Notice the asymmetry of the face, complete cutaneous syndactyly of the right second and third fingers, and overlapping toes. Thickened subcutaneous soft tissue on the proximal phalanges (prominently second finger) of the left hand (discoloration on the left hand due to traditional ‘red henna’). (E) Radial head dislocation. (F) Right hand radiograph showing distal phalangeal bone fusion of the third and fourth fingers at the age of 6. (G) Patient 1 at 9 years of age. Notice the generalized hypotonia. (H) Patient 1 at 6 years of age. Hyperemic, crusted skin lesions and focal dermal hypoplasia in her neck and axillary region and hypodontia are noticeable.

Table 1. Summary of the clinical features observed in each patient.

Phenotype	HPO Term	Patient 1	Patient 2
Microcephaly	HP:0000252	+	+
Trigonocephaly	HP:0000243	+	+
Protruding ears	HP:0000411	+	+
Upslanted palpebral fissure	HP:0000582	+	+
Neurodevelopmental delay	HP:0012758	+	+
Short stature	HP:0004322	+	+
Muscular hypotonia	HP:0001252	+	+

Table 1. Cont.

Phenotype	HPO Term	Patient 1	Patient 2
Low anterior hairline	HP:0000294	+	—
Facial asymmetry	HP:0000324	+	—
Sparse eyebrows	HP:0045075	+	—
Underdeveloped supraorbital ridges	HP:0009891	+	—
Strabismus	HP:0000486	+	—
High palate	HP:0000218	+	—
Hypodontia	HP:0000668	+	—
Gingival overgrowth	HP:0000212	+	—
Failure to thrive	HP:0001508	+	—
Dislocated radial head	HP:0003083	+	—
Ulnar deviation of finger	HP:0009465	+	—
3-4 finger syndactyly	HP:0006097	+	—
Hip dislocation	HP:0002827	+	—
Hypopigmented skin patches	HP:0001053	+	—
Focal dermal hypoplasia	HP:0007510	+	—
Seizures	HP:0001250	+	—
Semilobar holoprosencephaly	HP:0002507	—	+
Proptosis	HP:0000520	—	+
Retrognathia	HP:0000278	—	+
Tapered fingers (mild)	HP:0001182	—	+

Patient 2 was a first cousin of patient 1, sharing both the paternal and maternal lineages (Figure 3 and Table 1). He was a four-year-old boy and the third child of healthy, non-consanguineous Turkish parents. He was born at term by normal vaginal delivery with a weight of 3.08 kg (−0.72 SD). The mother had had one abortus because of ectopic pregnancy. One older sister (15 years old) presented with microcephaly (head circumference of 50 cm at 13 years, <1st percentile, −3.44 SD), without intellectual disability. The other sister (10 years old) was healthy. Patient's 2 first examination was at 2 months. He was in the normal range for weight (4.8 kg, −0.88 SD) and height (58 cm, 0.04 SD), but he presented with microcephaly (Figure 3) with a head circumference under the first percentile (33 cm, −4.82 SD). At this time, his muscle tone was normal. Follow up at 8.5 months confirmed severe microcephaly (−4.58 SD), with semi-lobar holoprosencephaly and mild trigonocephaly shown by cranial MRI. Additional dysmorphologies included retrognathia, ocular proptosis, up-slanting palpebral fissures, prominent ears, mild tapering fingers, proximal placement of thumb, and short stature (but within the range of his close family). Eye, cardiac, and kidney examination at 8 months were normal. He presented with severe delay in developmental milestones, such as poor head control. Previous genetic analyses included normal karyotype and sequencing of KIF11, which showed no mutations. In spite of some clear differences with his cousin (Table 1), shared phenotypes suggested the presence of one common, major genetic cause for both patients.



Figure 3. Distinctive features of patient 2. (A,B) Frontal view of the face at ages 8 months and 4 years. (C) Lateral view of the head at age 4. Microcephaly, retrognathia, ocular proptosis and upslanting palpebral fissures are appreciable. (D,E) Foot and hands of the patient at age 4.

2. Results and Discussion

Screening for shared pathogenic variants between the two cases was negative. Patient 1 showed large homozygous regions, as revealed by PLINK [1] analysis (55 fragments of more than 1 Mb of homozygosity, with a majority of fragments 2–6 Mb long), indicating consanguinity, while patient 2 showed 20 fragments of more than 1Mb of homozygosity (above average). Assuming an autosomal recessive inheritance pattern, patient 1 displayed variants in 52 selected genes, while patient 2 presented variants in 12 selected genes (Supplementary Tables S1 and S2). None of these homozygous variants was clearly pathogenic. In contrast, each patient harboured a de novo variant in a known ID gene. Patient 1 was heterozygous for a de novo, previously described [2], pathogenic variant in *PORCN* (2)(MIM * 300651), p.Arg95* (X:48369829 C>T; ENST00000326194: c.283C>T), while patient 2 carried a novel de novo heterozygous mutation at the Zinc-finger protein of the cerebellum 2, *ZIC2*, gene (MIM * 603073, mutation p.His404_Ser406delinsPro). Both mutations and their de novo status were confirmed by Sanger sequencing in the patients and their parents (and the respective cousin). WES and the Sanger sequencing results suggest that patient 1 is a mosaic for the *PORCN* p.Arg95* mutation.

The nonsense mutation p.Arg95* in *PORCN* creates a premature STOP codon at position 95 of the 461 residue-long protein-serine O-palmitoleoyltransferase porcupine protein. The mutation lies in exon 2 of 14, which is, therefore, subject to the degradation of the mutated mRNA by nonsense-mediated decay (NMD). In addition, if translated, the truncated protein would lack the majority of functional domains, including the active site. *PORCN* mutations have been associated with Goltz-Gorlin Syndrome (or focal dermal hypoplasia,

FDH, MIM #305600), transmitted as an X-linked dominant trait, and the p.Arg95* mutation found in patient 1 had been identified in a 30 year-old woman also presenting with linear skin lesions, asymmetrical skeletal defects, clinodactyly, dental defects, and microcephaly [2]. However, there is no mention of developmental delay/intellectual disability (DD/ID). Goltz-Gorlin Syndrome is a clinical entity with high phenotypic heterogeneity and developmental delay, although rare, that is described in about 10%–15% of the patients [3–5]. In addition, patient 1 presented with the more frequently reported clinical characteristics, including facial asymmetry, short stature, agenesis of the corpus callosum, or moderate cerebellar atrophy. All this points to p.Arg95* in *PORCN* as a pathogenic mutation and the main cause of the disorder observed in patient 1. *PORCN* is a key regulator of the Wnt signalling pathway mediating the attachment of palmitoleate, a 16-carbon monounsaturated fatty acid, to Wnt proteins. Serine palmitoylation of Wnt proteins is required for efficient binding to frizzled receptors and activation of Wnt signalling [6].

On the other hand, while patient 1 fits well in the FDH phenotypic entity, she has a more severe level of DD than other reported cases. Therefore, we hypothesized that other genetic factors might be contributing to her severe neurological presentation, especially since other family members present with non-syndromic ID (Figure 1). Worthy of interest, three variants were found in homozygosity in relevant genes (Supplementary Table S1): two missense variants in *NCAPD3* [c.3488C>T, p.(Pro1163Leu), rs143158496*] and in *YY1AP1* [c.1858G>A; p.(Ala620Thr)], and a synonymous variant with a putative effect on splicing in *UFC1* (c.246C>T, p.Ile82=). The variant in *NCAPD3*, is present in public databases at a very low frequency, although slightly higher in the Turkish population (gnomAD April 2020: 29 carriers out of 251446 alleles, no homozygotes, higher minor allele frequency (MAF) 0.0009 for East Asian, GME Variome: 1/163, MAF:0.006, Turkish population), which would be consistent with a recessive pattern of inheritance. *NCAPD3* has been previously related to microcephaly with moderate developmental delay [7], and a mouse model for *Ncapd2* (*NCAPD3* partner) shows microcephaly as well. However, only 8 out of 18 in silico predictors consider this change as putatively damaging and, while the *NCAPD3* gene is constrained for loss of function (LoF) variants, it does not show constraint for missense mutations ($o/e = 1.07$ at gnomAD). Therefore, this change is classified as a variant of unknown significance (VUS), according to the American College of Medical Genetics (ACMG) guidelines [8], but we cannot rule out its potential contribution to the severity of the microcephaly and the DD traits of patient 1. Recessive LoF mutations in *YY1AP1* associate with Grange syndrome (GRNG, MIM #602531), whose presentation includes syndactyly and learning difficulties [9–11]. The variant is also present in public databases (gnomAD 18 carriers out of 141388, highest MAF 0.00013, absent in GME Variome). Finally, *UFC1* is associated with “neurodevelopmental disorder with spasticity and poor growth” (MIM #618076) [12] and the variant identified in patient 1 is present in public databases at a very low frequency (gnomAD: 2 alleles out of 251490).

ZIC2 is a transcription factor involved both in activation and repression, which plays a key role in the early stages of the central nervous system (CNS) development [13]. The *ZIC2* mutation detected in patient 2 involves the deletion of 7 bp and the insertion of 1 bp at the cDNA position 1211 [c.1211_1217delACCCCAGinsC (ENST00000376335)], leading to the substitution of the three residues at positions 404 to 406 by a proline (p.His404_Ser406delinsPro). This variant is not found in the general population (gnomAD, Iranome, and GME Variome) and residues 404 to 406 are fully conserved through the 28 species analysed (Supplementary Figure S1). This variant is classified as pathogenic following the ACMG guidelines [8]. The *ZIC* proteins are defined by the presence of a zinc finger domain that consists of five Cys2His2-type zinc fingers and this change is in a mutational hot-spot affecting the fifth C2H2-type Zinc Finger domain of the *ZIC2* protein.

Autosomal Dominant (AD) mutations in *ZIC2* have been associated with holoprosencephaly 5 (HPE5, MIM #609637), characterized by severe neurological impairment, seizures, and characteristic dysmorphic facies. These traits are consistent with the patient’s clinical phenotype, who presented with semi-lobar holoprosencephaly and severe developmental

delay (seizures have not been identified so far). While this specific mutation has not been previously reported, other non-frameshift mutations affecting the same domain have been identified in HPE5 patients [14–17], including the substitution of His 404 by Arg [15]. In conclusion, we have classified the *ZIC2* heterozygous mutation as likely pathogenic, and as the disease-causing mutation responsible for the major phenotypic alterations of the patient.

Other changes that can contribute to the patient's phenotype have also been evaluated (Supplementary Table S2). In particular, the patient and his two sisters are homozygous for mutation p.Tyr1073Cys in *CFTR* (7:117251713 A>G, ENST00000003084: c.3218A>G, p.Tyr1073Cys). This gene encodes an epithelial ion channel that mediates the transport of chloride ions. Autosomal Recessive (AR) mutations in it are associated with cystic fibrosis (CF, MIM #219700), sweat chloride elevation without CF, and congenital bilateral absence of vas deferens (CBAVD, MIM #277180). The same mutation identified in this family had been previously identified in a patient with neonatal hypertrypsinaemia without lung disease and is included in the Cystic Fibrosis Mutation database. This mutation is absent in the common population (gnomAD, Iranome, and GME Variome) and it is predicted to be damaging for the protein performance by most functional prediction algorithms. We have considered this variant to be likely pathogenic, according to the ACMG guidelines [8], and have recommended detailed clinical assessment of the patient and his sisters. In addition to the de novo *ZIC2* mutation, Patient 2 is a homozygote for the *KPNA7* p.Arg217Trp mutation (7:98786174 G>A, ENST00000327442: c.649C>T, Supplementary Table S2), inherited from his parents (both heterozygotes). The healthy sister does not carry the mutant allele, while the sister affected by microcephaly is also homozygous for this change. This variant is rare in the common population (only 27 carriers, no homozygotes, in gnomAD) and algorithms developed to predict the effect of missense changes on protein structure and function (SIFT, PolyPhen2, PROVEAN, or Mutation assessor) do not agree on the potential impact of this missense change. *KPNA7* recessive mutations have been associated with infantile spasms and cerebellar malformation only once in the literature [18]. These authors presented a pair of sibs affected with severe developmental disability, infantile spasms, intractable epilepsy consistent with Lennox–Gastaut syndrome, partial agenesis of the corpus callosum, and cerebellar vermis hypoplasia in which two heterozygous *KPNA7* mutations have been identified by WES. In these patients, microcephaly was not present (with head circumference at the 98th and 50th percentiles). In conclusion, this variant is classified as likely benign and does not seem to be related to the patient's clinical phenotype, but its implication on moderate microcephaly cannot be ruled out without further studies.

Both causal genes that mutated in these cousins (*PORCN* and *ZIC2*) encode proteins that are directly implicated in the Wnt pathway. The mechanistic coincidence on these two factors could explain some of the clinical similarities among these patients, both harbouring mutations in genes that, *prima facie*, seem not to be related. Wnt signalling pathways regulate complex normal biological processes such as cell differentiation, development, tissue homeostasis, and wound healing. However, when the Wnt pathway is aberrantly regulated, it can be associated with bone anomalies, neurodevelopmental disorders, cancer, and cardiovascular diseases, among other diseases [19]. Wnt signalling is a particularly complex pathway that leads to the activation of two main, alternative branches: the canonical and the noncanonical pathway. In the canonical pathway, the binding of Wnt proteins to their receptors (Frizzled and Lrp5/6) triggers the inactivation or disassembly of the destruction complex, which reduces β -catenin phosphorylation and promotes its accumulation and translocation to the nucleus. There, β -catenin forms a complex with Lef/Tcf factors and induces the transcription of specific genes. Activation of the noncanonical pathway does not depend on β -catenin-driven transcription. Instead, it relies on changes that affect cytoskeletal organization and calcium homeostasis [19]. *PORCN* (protein-serine O-palmitoleoyltransferase porcupine) mediates palmitoylation of Wnt proteins, which is an essential modification necessary for their correct secretion and binding to the Frizzled receptors, thus, being a major regulator of Wnt signalling [20–22]. On the other hand, *Zic*

genes are implicated in development of the dorsal neural tube and neural crest as well as the somites and the cerebellum. In addition to the regulation of multiple neural factors, ZIC2 functions as a modulator of Wnt signalling by the direct interaction with TCF4 [23] or by modulating β -catenin accumulation and activity [24].

3. Materials and Methods

Patient 1 was included in the URDCat genetic program and underwent whole exome sequencing (WES) analysis as previously described [25,26] (briefly, sequencing was done at the CNAG facility using the Nimblegen SeqCap EZ MedExome + mtDNA 47Mb capture kit aiming at 90 \times coverage). Patient 2 was analyzed by trio-WES, briefly, (samples from patient 2 and his parents were also sequenced at the CNAG facility). In this case, capture was performed with Agilent SureSelect v5 (Agilent, CA, USA). The samples were sequenced at a coverage of 140 \times . Basic bioinformatic processing of the sequencing data was performed using CNAG's in-house pipeline. Annotation and filtering for both cases was performed with VarAFT [26]. All variants included in Tables S1 and S2 were analysed by Sanger sequencing in the patient, mother, and father, as well as in her affected cousin. Primers and conditions used for PCR amplification and sequencing are available on demand. Sequence alterations are reported according to the Human Genome Variation Society (HGVS) nomenclature guidelines. The gnomAD (v.2.1.1), Iranianome, and Great Middle East Variome databases were accessed on May 2020.

4. Conclusions

Two main considerations arise from this study. In the first place, while in Western countries syndromic and non-syndromic DD and ID are mainly sporadic and caused by de novo mutations [27], in the near and Great Middle East, where there is a high consanguinity rate [28], ID is commonly due to recessive mutations [29]. When presented with highly consanguineous families segregating a disease phenotype, one of the first approaches is to search for pathogenic mutations in homozygosity tracks. In addition, performing WES analysis only on the index case is a common practice, which, in highly consanguineous populations, yields acceptable diagnostic results [30]. While the cost advantage of such an approach is evident, it is important to keep in mind that, even in cases with a very high consanguinity, de novo disease causing mutations may still be present, representing up to 27.8% of the ID mutations identified in these families [29] when trio-WES is performed. It should not be forgotten that these mutations are still one of the major causes of ID. Thus, to avoid misdiagnosis, we strongly recommend trio-WES or, if unavailable, a cautious revision of putative dominant mutations (likely followed by segregation analysis of a higher number of putative candidates) even in these families. In the present study, WES of patient 1 was followed by segregation analysis of up to 16 heterozygous variants, while the trio-WES of patient 2 involved further checking of only six variants. Otherwise, we risk basing our diagnosis solely on putatively pathogenic homozygous variants in the detriment of undetected de novo mutations also present in the patient.

The second important consideration from this study is the co-occurrence of multiple genetic diseases in the same individual, leading to a very complex phenotype. This can be especially likely in families with high levels of consanguinity, potentially segregating various pathogenic mutations [31].

Supplementary Materials: The following are available online at <https://www.mdpi.com/1422-0067/22/4/1549/s1>.

Author Contributions: Conception and design: R.U., S.G., R.R., D.G., and S.B. WES Analysis and validation: R.U., L.C.-V., A.P.-P., and M.C.-P., G.B., and L.M. have analysed the homozygosity data. Clinical evaluation of the patients and generation of the clinical data: S.G. and Ö.G.-B. Table 1: L.C.-V. and S.G. Supplementary Tables S1 and S2 have been prepared by R.U., R.R., L.C.-V., M.C.-P., and A.P.-P. Figures 1–3: R.U., L.C.-V., D.G., S.B., R.R.; S.G., R.U., R.R., S.G., S.B., and D.G. wrote the main manuscript text. All authors critically reviewed the manuscript. All authors have read and agreed to the published version of the manuscript.

Funding: Funding was from the Spanish Ministerio de Ciencia e Innovación (SAF2016-75946R), CIBERER (ACCI2018-15), Associació Síndrome Opitz C. Departament de Salut de la Generalitat de Catalunya, PERIS SLT002/16/00174, URD-Cat (Implementació de la Medicina Personalitzada basada en la Genòmica en Malalties Minoritàries Neurològiques no Diagnosticades), 2017–2019. Funding sources were not involved in the study design, collection, analysis, and interpretation of data, writing of the report, or in the publication of the article.

Institutional Review Board Statement: The study was conducted according to the guidelines of the Declaration of Helsinki, and approved by the Institutional Review Board (or Ethics Committee) of the Universitat de Barcelona (IRB00003099), 20 October 2016, and all methods were performed in accordance with the relevant guidelines and regulations.

Informed Consent Statement: Families have been informed of this publication. They have given signed consent to publish, including pictures of the patients.

Data Availability Statement: The data that support the findings of this study are available on request from the corresponding author. The data are not publicly available due to privacy and ethical restrictions.

Acknowledgments: We thank the patients and their families for their collaboration. We also thank Ariadna Carbonell-Roqué, Raul Martínez-Cabrera, and Mónica Cozar Morillo for their technical support.

Conflicts of Interest: The authors declare no conflict of interest.

References

- Purcell, S.; Neale, B.; Todd-Brown, K.; Thomas, L.; Ferreira, M.A.; Bender, D.; Maller, J.; Sklar, P.; de Bakker, P.I.; Daly, M.J.; et al. PLINK: A tool set for whole-genome association and population-based linkage analyses. *Am. J. Hum. Genet.* **2007**, *81*, 559–575. [[CrossRef](#)] [[PubMed](#)]
- Bornholdt, D.; Oeffner, F.; König, A.; Happel, R.; Alanay, Y.; Ascherman, J.; Benke, P.J.; Boente Mdel, C.; van der Burgt, I.; Chassaing, N.; et al. PORCN mutations in focal dermal hypoplasia: Coping with lethality. *Hum. Mutat.* **2009**, *30*, E618–E628. [[CrossRef](#)] [[PubMed](#)]
- Goltz, R.W. Focal dermal hypoplasia syndrome. An update. *Arch. Dermatol.* **1992**, *128*, 1108–1111. [[CrossRef](#)] [[PubMed](#)]
- Maas, S.M.; Lombardi, M.P.; van Essen, A.J.; Wakeling, E.L.; Castle, B.; Temple, I.K.; Kumar, V.K.; Writzl, K.; Hennekam, R.C. Phenotype and genotype in 17 patients with Goltz-Gorlin syndrome. *J. Med. Genet.* **2009**, *46*, 716–720. [[CrossRef](#)] [[PubMed](#)]
- Yesodharan, D.; Buschenfelde, U.M.Z.; Kutsche, K.; Mohandas Nair, K.; Nampoothiri, S. Goltz-Gorlin Syndrome: Revisiting the Clinical Spectrum. *Indian J. Pediatr.* **2018**, *85*, 1067–1072. [[CrossRef](#)]
- Coombs, G.S.; Yu, J.; Canning, C.A.; Veltri, C.A.; Covey, T.M.; Cheong, J.K.; Utomo, V.; Banerjee, N.; Zhang, Z.H.; Jadulco, R.C.; et al. WLS-dependent secretion of WNT3A requires Ser209 acylation and vacuolar acidification. *J. Cell Sci.* **2010**, *123*, 3357–3367. [[CrossRef](#)]
- Martin, C.A.; Murray, J.E.; Carroll, P.; Leitch, A.; Mackenzie, K.J.; Halachev, M.; Fetit, A.E.; Keith, C.; Bicknell, L.S.; Fluteau, A.; et al. Mutations in genes encoding condensin complex proteins cause microcephaly through decatenation failure at mitosis. *Genes Dev.* **2016**, *30*, 2158–2172. [[CrossRef](#)]
- Richards, S.; Aziz, N.; Bale, S.; Bick, D.; Das, S.; Gastier-Foster, J.; Grody, W.W.; Hegde, M.; Lyon, E.; Spector, E.; et al. Standards and guidelines for the interpretation of sequence variants: A joint consensus recommendation of the American College of Medical Genetics and Genomics and the Association for Molecular Pathology. *Genet. Med.* **2015**, *17*, 405–424. [[CrossRef](#)]
- Guo, D.C.; Duan, X.Y.; Regalado, E.S.; Mellor-Crummey, L.; Kwartler, C.S.; Kim, D.; Lieberman, K.; de Vries, B.B.A.; Pfundt, R.; Schinzel, A.; et al. Loss-of-Function Mutations in YY1AP1 Lead to Grange Syndrome and a Fibromuscular Dysplasia-Like Vascular Disease. *Am. J. Hum. Genet.* **2017**, *100*, 21–30. [[CrossRef](#)]
- Rath, M.; Spiegler, S.; Strom, T.M.; Trenkler, J.; Kroisel, P.M.; Felbor, U. Identification of pathogenic YY1AP1 splice variants in siblings with Grange syndrome by whole exome sequencing. *Am. J. Med. Genet. A* **2019**, *179*, 295–299. [[CrossRef](#)]
- Saida, K.; Kim, C.A.; Ceroni, J.R.M.; Bertola, D.R.; Honjo, R.S.; Mitsuhashi, S.; Takata, A.; Mizuguchi, T.; Miyatake, S.; Miyake, N.; et al. Hemorrhagic stroke and renovascular hypertension with Grange syndrome arising from a novel pathogenic variant in YY1AP1. *J. Hum. Genet.* **2019**, *64*, 885–890. [[CrossRef](#)] [[PubMed](#)]
- Nahorski, M.S.; Maddirevula, S.; Ishimura, R.; Alshahi, S.; Brady, A.F.; Begemann, A.; Mizushima, T.; Guzman-Vega, F.J.; Obata, M.; Ichimura, Y.; et al. Biallelic UFM1 and UFC1 mutations expand the essential role of ufmylation in brain development. *Brain* **2018**, *141*, 1934–1945. [[CrossRef](#)] [[PubMed](#)]
- Nagai, T.; Aruga, J.; Minowa, O.; Sugimoto, T.; Ohno, Y.; Noda, T.; Mikoshiba, K. Zic2 regulates the kinetics of neurulation. *Proc. Natl. Acad. Sci. USA* **2000**, *97*, 1618–1623. [[CrossRef](#)]
- Brown, L.; Paraso, M.; Arkell, R.; Brown, S. In vitro analysis of partial loss-of-function ZIC2 mutations in holoprosencephaly: Alanine tract expansion modulates DNA binding and transactivation. *Hum. Mol. Genet.* **2005**, *14*, 411–420. [[CrossRef](#)] [[PubMed](#)]

15. Roessler, E.; Lachawan, F.; Dubourg, C.; Paulussen, A.; Herbergs, J.; Hehr, U.; Bendavid, C.; Zhou, N.; Ouspenskaia, M.; Bale, S.; et al. The full spectrum of holoprosencephaly-associated mutations within the ZIC2 gene in humans predicts loss-of-function as the predominant disease mechanism. *Hum. Mutat.* **2009**, *30*, E541–E554. [[CrossRef](#)]
16. Solomon, B.D.; Lachawan, F.; Mercier, S.; Clegg, N.J.; Delgado, M.R.; Rosenbaum, K.; Dubourg, C.; David, V.; Olney, A.H.; Wehner, L.E.; et al. Mutations in ZIC2 in human holoprosencephaly: Description of a novel ZIC2 specific phenotype and comprehensive analysis of 157 individuals. *J. Med. Genet.* **2010**, *47*, 513–524. [[CrossRef](#)]
17. Roessler, E.; Hu, P.; Marino, J.; Hong, S.; Hart, R.; Berger, S.; Martinez, A.; Abe, Y.; Kruszka, P.; Thomas, J.W.; et al. Common genetic causes of holoprosencephaly are limited to a small set of evolutionarily conserved driver genes of midline development coordinated by TGF-beta, hedgehog, and FGF signaling. *Hum. Mutat.* **2018**, *39*, 1416–1427. [[CrossRef](#)]
18. Paciorkowski, A.R.; Weisenberg, J.; Kelley, J.B.; Spencer, A.; Tuttle, E.; Ghoneim, D.; Thio, L.L.; Christian, S.L.; Dobyns, W.B.; Paschal, B.M. Autosomal recessive mutations in nuclear transport factor KPNA7 are associated with infantile spasms and cerebellar malformation. *Eur. J. Hum. Genet.* **2014**, *22*, 587–593. [[CrossRef](#)]
19. Sharma, M.; Pruitt, K. Wnt Pathway: An Integral Hub for Developmental and Oncogenic Signaling Networks. *Int. J. Mol. Sci.* **2020**, *21*, 8018. [[CrossRef](#)]
20. Kurayoshi, M.; Yamamoto, H.; Izumi, S.; Kikuchi, A. Post-translational palmitoylation and glycosylation of Wnt-5a are necessary for its signalling. *Biochem. J.* **2007**, *402*, 515–523. [[CrossRef](#)]
21. Chen, B.; Dodge, M.E.; Tang, W.; Lu, J.; Ma, Z.; Fan, C.W.; Wei, S.; Hao, W.; Kilgore, J.; Williams, N.S.; et al. Small molecule-mediated disruption of Wnt-dependent signaling in tissue regeneration and cancer. *Nat. Chem. Biol.* **2009**, *5*, 100–107. [[CrossRef](#)] [[PubMed](#)]
22. Gao, X.; Hannoush, R.N. Single-cell imaging of Wnt palmitoylation by the acyltransferase porcupine. *Nat. Chem. Biol.* **2014**, *10*, 61–68. [[CrossRef](#)] [[PubMed](#)]
23. Pourebahim, R.; Houtmeyers, R.; Ghogomu, S.; Janssens, S.; Thelie, A.; Tran, H.T.; Langenberg, T.; Vleminckx, K.; Bellefroid, E.; Cassiman, J.J.; et al. Transcription factor Zic2 inhibits Wnt/ β -catenin protein signaling. *J. Biol. Chem.* **2011**, *286*, 37732–37740. [[CrossRef](#)] [[PubMed](#)]
24. Morenilla-Palao, C.; López-Cascales, M.T.; López-Atalaya, J.P.; Baeza, D.; Calvo-Díaz, L.; Barco, A.; Herrera, E. A Zic2-regulated switch in a noncanonical Wnt/ β catenin pathway is essential for the formation of bilateral circuits. *Sci. Adv.* **2020**, *6*. [[CrossRef](#)]
25. Study, D.D.D. Prevalence and architecture of de novo mutations in developmental disorders. *Nature* **2017**, *542*, 433–438. [[CrossRef](#)]
26. Scott, E.M.; Halees, A.; Itan, Y.; Spencer, E.G.; He, Y.; Azab, M.A.; Gabriel, S.B.; Belkadi, A.; Boisson, B.; Abel, L.; et al. Characterization of Greater Middle Eastern genetic variation for enhanced disease gene discovery. *Nat. Genet.* **2016**, *48*, 1071–1076. [[CrossRef](#)]
27. Kahrizi, K.; Hu, H.; Hosseini, M.; Kalscheuer, V.M.; Fattahi, Z.; Beheshtian, M.; Suckow, V.; Mohseni, M.; Lipkowitz, B.; Mehvari, S.; et al. Effect of inbreeding on intellectual disability revisited by trio sequencing. *Clin. Genet.* **2019**, *95*, 151–159. [[CrossRef](#)]
28. Monies, D.; Abouelhoda, M.; Assoum, M.; Moghrabi, N.; Rafiullah, R.; Almontashiri, N.; Alowain, M.; Alzaidan, H.; Alsayed, M.; Subhani, S.; et al. Lessons Learned from Large-Scale, First-Tier Clinical Exome Sequencing in a Highly Consanguineous Population. *Am. J. Hum. Genet.* **2019**, *105*, 879. [[CrossRef](#)]
29. Shalev, S.A. Characteristics of genetic diseases in consanguineous populations in the genomic era: Lessons from Arab communities in North Israel. *Clin. Genet.* **2019**, *95*, 3–9. [[CrossRef](#)]
30. Urreiziti, R.; Lopez-Martin, E.; Martinez-Monseny, A.; Pujadas, M.; Castilla-Vallmánya, L.; Perez-Jurado, L.A.; Serrano, M.; Natera-de Benito, D.; Martinez-Delgado, B.; Posada-de-la-Paz, M.; et al. Five new cases of syndromic intellectual disability due to KAT6A mutations: Widening the molecular and clinical spectrum. *Orphanet J. Rare Dis.* **2020**, *15*, 44. [[CrossRef](#)]
31. Desvignes, J.P.; Bartoli, M.; Delague, V.; Krahn, M.; Miltgen, M.; Bérout, C.; Salgado, D. VarAFT: A variant annotation and filtration system for human next generation sequencing data. *Nucleic Acids Res.* **2018**, *46*, W545–W553. [[CrossRef](#)] [[PubMed](#)]

Supplementary information for:

De Novo *PORCN* and *ZIC2* Mutations in a Highly Consanguineous Family

Laura Castilla-Vallmanya, Semra Gürsoy, Özlem Giray-Bozkaya, Aina Prat-Planas, Gemma Bullich, Leslie Matalonga, Mónica Centeno-Pla, Raquel Rabionet, Daniel Grinberg, Susanna Balcells & Roser Urreizti

```

                                404-406
ZIC2_HUMAN 095409-1          PYLCKM--CDKSYTHFSSLRKHKMKVHSSSPQGSSESSPAASSGGYESSTPPGLVSPSAEPQS 449
[Fongo_abelii]              PYLCKM--CDKSYTHFSSLRKHKMKVHSSSPQGSSESSPAASSGGYESSTPPGLVSPSAEPQS 449
[Macaca_mulatta]            PYLCKM--CDKSYTHFSSLRKHKMKVHSSSPQGSSESSPAASSGGYESSTPPGLVSPSAEPQS 449
[Cebus_imitator]            PYLCKM--CDKSYTHFSSLRKHKMKVHSSSPQGSSESSPAASSGGYESSTPPGLVSPSAEPQS 449
[Canis_lupus_dingo]         PYLCKM--CDKSYTHFSSLRKHKMKVHSSSPQGSSESSPAASSGGYESSTPPGLVSPSAEPQS 448
[Ursus_arctos_horribilis]   PYLCKM--CDKSYTHFSSLRKHKMKVHSSSPQGSSESSPAASSGGYESSTPPGLVSPSAEPQS 448
[Rattus_norvegicus]         PYLCKM--CDKSYTHFSSLRKHKMKVHSSSPQGSSESSPAASSGGYESSTPPGLVSPSAEPQS 448
[Mus_musculus]              PYLCKM--CDKSYTHFSSLRKHKMKVHSSSPQGSSESSPAASSGGYESSTPPGLVSPSAEPQS 448
[Felis_catus]               PYLCKM--CDKSYTHFSSLRKHKMKVHSSSPQGSSESSPAASSGGYESSTPPGLVSPSAEPQS 448
[Camelus_ferus]             PYLCKM--CDKSYTHFSSLRKHKMKVHSSSPQGSSESSPAASSGGYESSTPPGLVSPSAEPQS 448
[Sus_scrofa]                PYLCKM--CDKSYTHFSSLRKHKMKVHSSSPQGSSESSPAASSGGYESSTPPGLVSPSAEPQS 448
[Ovis_aries]                PYLCKM--CDKSYTHFSSLRKHKMKVHSSSPQGSSESSPAASSGGYESSTPPGLVSPSAEPQS 448
[Vulpes_vulpes]            PYLCKM--CDKSYTHFSSLRKHKMKVHSSSPQGSSESSPAASSGGYESSTPPGLVSPSAEPQS 426
[Bos_taurus]                PYLCKM--CDKSYTHFSSLRKHKMKVHSSSPQGSSESSPAASSGGYESSTPPGLVSPSAEPQS 448
[Parus_major]               PYLCKM--CDKSYTHFSSLRKHKMKVHSSSPQGSSESSPAASSGGYESSTPPGLVSPSAEPQS 425
[Falco_rusticolus]          PYLCKM--CDKSYTHFSSLRKHKMKVHSSSPQGSSESSPAASSGGYESSTPPGLVSPSAEPQS 425
[Chelonia_mydas]            PYLCKM--CDKSYTHFSSLRKHKMKVHSSSPQGSSESSPAASSGGYESSTPPGLVSPSAEPQS 424
[Gallus_gallus]             PYLCKM--CDKSYTHFSSLRKHKMKVHSSSPQGSSESSPAASSGGYESSTPPGLVSPSAEPQS 423
[Suricata_suricata]         PYLCKM--CDKSYTHFSSLRKHKMKVHSSSPQGSSESSPAASSGGYESSTPPGLVSPSAEPQS 370
[Labeo_roulei]              PYLCKM--CDKSYTHFSSLRKHKMKVHSSSPQGSSESSPAASSGGYESSTPPGLVSPSAEPQS 417
[Denticeps_clupeoides]     PYLCKM--CDKSYTHFSSLRKHKMKVHSSSPQGSSESSPAASSGGYESSTPPGLVSPSAEPQS 417
[Danio_rerio]               PYLCKM--CDKSYTHFSSLRKHKMKVHSSSPQGSSESSPAASSGGYESSTPPGLVSPSAEPQS 474
[Takifugu_rubripes]         PYLCKM--CDKSYTHFSSLRKHKMKVHSSSPQGSSESSPAASSGGYESSTPPGLVSPSAEPQS 455
[Podarcis_muralis]          PYLCKM--CDKSYTHFSSLRKHKMKVHSSSPQGSSESSPAASSGGYESSTPPGLVSPSAEPQS 468
[Xenopus_tropicalis]        PYLCKM--CDKSYTHFSSLRKHKMKVHSSSPQGSSESSPAASSGGYESSTPPGLVSPSAEPQS 468
[Xenopus_laevis]            PYLCKM--CDKSYTHFSSLRKHKMKVHSSSPQGSSESSPAASSGGYESSTPPGLVSPSAEPQS 252
[Caenorhabditis_elegans]    PYNCRINGCDKSYTHFSSLRKHKMKVHSSSPQGSSESSPAASSGGYESSTPPGLVSPSAEPQS 252
[Drosophila_melanogaster]   PYNCRINGCDKSYTHFSSLRKHKMKVHSSSPQGSSESSPAASSGGYESSTPPGLVSPSAEPQS 608
** * * * * *

```

Supplementary Figure 1. Alignment of the region of interest (from the human residue 392 to 449) of ZIC2 proteins in multiple vertebrates, *C. elegans* and *D. melanogaster*. Highlighted in yellow residues 404 to 406, belonging to the 5th C2H2-type Zinc Finger, substituted by proline in Patient 2.

Supplementary Table 1. Variants identified in Patient 1

Chr	Start	Ref	Alt	Genotype	Depth	AAF	Func.refgene	Gene	Gnomad_Exome_AF	Gnomad_Genome_AF	ACMG Classificat	Segregation	DDD
I. Selected variants													
X	48369829	C	T	Heterozygous	148	0.32	exonic	PORCN	.	.	Pathogenic	Patient het (de novo). Absent in parents abd affected cousin.	confirm
1	38053059	T	C	Homozygous	76	1	exonic	GNL2	.	.	VUS	Patient homo; both parents hetero, Patient b wt	.
1	155630257	C	T	Homozygous	181	0.99	exonic	YY1AP1	5.97E-02	9.56E-02	VUS	Patient homo; both parents hetero, Patient b wt	.
2	29462550	G	A	Homozygous	80	1	exonic;splicing	ALK	.	.	LB	Patient and mother homo. Father and and affected cousin hetero.	.
6	159185626	T	G	Homozygous	96	1	exonic	SYTL3	2.78E-02	.	VUS	Patient homo; both parents hetero, Patient b wt	.
7	39991306	C	G	Homozygous	39	0.97	exonic	CDK13	0.0025	0.0022	LB	Patient homo; both parents hetero, Patient b wt	.
11	134037976	G	A	Homozygous	167	0.99	exonic	NCAPD3	0.0001	.	VUS	Patient homo; both parents hetero, Patient b wt	.
15	78290557	C	T	Homozygous	128	1	exonic	TBC1D2B	1.66E-02	.	VUS	patient homo, parents unknown	.
16	56997025	T	G	Homozygous	300	1	exonic	CETP	1.59E-02	.	VUS	Patient homo; both parents hetero, Patient b wt	.
17	4804381	T	G	Homozygous	128	1	exonic	CHRNE	0.0001	.	Benign	Patient, mother and affected cousin homo. Father hetero.	.
19	49963000	C	T	Homozygous	105	1	exonic	ALDH16A1	4.00E-03	.	VUS	Patient homo; both parents hetero, Patient b wt	.
11	125880401	A	G	Heterozygous	136	0.5	exonic	CDON	0.0001	0.000223	Benign	Patient and father hetero. Mother Homo. Affected cousin WT.	confirm

Chr	Start	Ref	Alt	Genotype	Depth	AAF	Func.refgene	Gene	Gnomad_Exome_AF	Gnomad_Genome_AF	Curated ACMG CI	Segregation	DDD
II. Other Variants													
1	2522487	G	A	Heterozygous	87	0.39	exonic	MMEL1	3.44e-05	.	LB	NA	.
1	2541120	A	G	Heterozygous	59	0.58	exonic	MMEL1	.	.	VUS	NA	.
1	156035717	A	G	Homozygous	760	1	exonic	RAB25	0.0049	0.0038	LB	NA	.
1	158988319	C	T	Homozygous	149	1	exonic	IFI16	0.0059	0.0049	VUS	NA	.
1	161127098	C	T	Homozygous	80	1	exonic	UFC1	7.95E-03	.	VUS	NA	.
1	161203076	C	-	Homozygous	551	1	exonic	NR1I3	3.98E-03	.	VUS	NA	possible
1	163039044	G	T	Homozygous	19	1	exonic;splicing	RGS4	0.0003	.	LB	NA	.
1	167096406	A	C	Homozygous	78	1	exonic	DUSP27	.	.	VUS	NA	.
2	71649966	A	G	Homozygous	55	1	exonic	ZNF638	0.0070	0.0069	LB	NA	.
2	75929417	T	C	Homozygous	119	1	exonic	GCF2	7.96E-03	.	VUS	NA	.
2	97317629	G	A	Homozygous	85	1	exonic;splicing	FER1L5	0.0010	6.37E-02	LB	NA	.
2	130832668	C	T	Heterozygous	34	0.62	exonic	POTEF	0.0003	0.000288	VUS	NA	.
2	130877775	C	A	Heterozygous	122	0.36	exonic	POTEF	0.0010	0.00107	LB	NA	.
2	216237085	T	G	Heterozygous	207	0.52	exonic	FN1	4.07e-05	.	LB	NA	problabl
2	240056067	C	T	Heterozygous	400	0.48	exonic	HDAC4	0.0003	.	LB	NA	confirm
3	100170600	-	TCCT	Homozygous	43	1	exonic	LNP1	.	.	VUS	NA	.
4	675797	C	G	Homozygous	177	1	exonic	SLC49A3	3.37E-02	.	VUS	NA	.
4	2877658	C	T	Homozygous	129	1	exonic	ADD1	0.0011	0.0006	LB	Patient 2 is also homozigous	.
4	69870766	A	C	Homozygous	97	1	exonic	UGT2B10	0.0008	0.0007	LB	NA	.
4	70360912	C	A	Homozygous	94	1	exonic	UGT2B4	0.0019	0.0018	LB	NA	.
4	75067064	A	C	Homozygous	54	1	exonic	MTHFD2L	0.0004	0.0005	VUS	NA	.
5	95728961	C	T	Heterozygous	126	0.6	exonic	PCSK1	0.0000239	.	VUS	NA	.
5	95734708	T	G	Heterozygous	109	0.48	exonic	PCSK1	.	.	LP	NA	.
5	150663633	T	A	Heterozygous	113	0.5	exonic	SLC36A3	0.0002	0.0000956	VUS	NA	.
5	150668030	A	T	Heterozygous	88	0.53	exonic;splicing	SLC36A3	.	.	VUS	NA	.
6	44093742	C	T	Heterozygous	123	0.46	exonic	MRPL14	.	0.599	Benign	NA	.
6	44093808	T	G	Heterozygous	114	0.46	exonic	MRPL14	.	0.263	Benign	NA	.
7	69064646	G	A	Heterozygous	75	0.43	exonic	AUTS2	.	.	LB	NA	confirm
8	10467589	T	C	Heterozygous	221	0.52	exonic	RP1L1	.	.	Benign	NA	.
8	10467604	C	A	Heterozygous	225	0.49	exonic	RP1L1	.	0.144	Benign	NA	.
8	61768705	G	C	Heterozygous	155	0.54	exonic	CHD7	0.008592	0.0000318	LB	NA	confirm
8	144732488	A	T	Homozygous	155	1	exonic	ZNF623	0.0042	0.0036	LB	NA	.
9	35906584	CCA	-	Homozygous	17	0.71	exonic	HRCT1	.	.	LB	NA	.
9	98231110	G	A	Heterozygous	139	0.53	exonic	PTCH1	0.0009	0.000701	LB	NA	confirm

Identification of disease-causing variants in patients clinically diagnosed with Opitz C syndrome and Bohring-Opitz syndrome and functional validation

9	138839709	G	A	Homozygous	82	1	exonic	UBAC1	2.00E-02	.	.	VUS	NA	.
9	139749788	C	T	Homozygous	107	1	exonic;splicing	MAMDC4	0.0056	0.0052	.	LB	NA	.
10	101163636	G	A	Homozygous	127	1	splicing	GOT1	0.0049	0.0023	.	LB	NA	.
10	127456139	G	A	Heterozygous	121	0.49	exonic	MMP21	0.0002	0.0000637	.	LP	NA	.
10	127459103	T	C	Heterozygous	157	0.45	exonic	MMP21	.	.	.	LB	NA	confirm
11	22242742	G	A	Heterozygous	193	0.49	exonic	ANOS	0.000024	0.0000638	.	VUS	NA	both DC
11	22281102	T	C	Heterozygous	111	0.49	exonic	ANOS	.	.	.	VUS	NA	both DC
11	67925807	G	T	Heterozygous	150	0.55	exonic	KMT5B	0.00007565	0.00003185	.	LB	NA	confirm
11	76829294	G	A	Homozygous	103	1	exonic	CAPN5	8.36e-05	3.19E-02	.	VUS	NA	.
12	53207583	-	CAC	Homozygous	109	1	exonic	KRT4	.	.	.	LB	NA	.
14	60616070	C	T	Heterozygous	127	0.6	splicing	DHR57	0.0004	0.000127	.	VUS	NA	.
14	60616075	C	T	Heterozygous	134	0.6	exonic	DHR57	0.0004	0.000127	.	VUS	NA	.
15	45445678	GTG,-	-	Heterozygous	64	0.48	splicing	DUOX1	0.0005	0.000225	.	VUS	NA	.
15	45448081	G	A	Heterozygous	64	0.5	exonic	DUOX1	0.0008	0.000796	.	VUS	NA	.
15	75500163	C	T	Homozygous	69	1	exonic	C15orf39	8.09E-03	.	.	VUS	NA	.
15	75650822	T	C	Homozygous	111	0.99	exonic	MAN2C1	0.0004	0.0002	.	VUS	NA	.
15	85788521	G	A	Heterozygous	22	0.86	exonic	GOLGA6L3	.	.	.	VUS	NA	.
15	85788535	A	C	Heterozygous	11	0.64	exonic	GOLGA6L3	.	.	.	VUS	NA	.
15	85788539	T	G	Heterozygous	6	0.33	exonic	GOLGA6L3	.	.	.	VUS	NA	.
16	3592204	-	C	Heterozygous	171	0.54	exonic	NLRC3	.	.	.	VUS	NA	.
16	3594250	G	C	Heterozygous	68	0.63	exonic	NLRC3	.	.	.	VUS	NA	.
16	3599191	G	A	Heterozygous	125	0.47	exonic	NLRC3	0.01471	.	.	VUS	NA	.
16	9857331	A	G	Heterozygous	124	0.47	exonic	GRIN2A	.	.	.	LB	NA	confirm
16	9857331	A	G	Heterozygous	124	0.47	exonic	GRIN2A	.	.	.	LB	NA	confirm
16	9857547	C	T	Heterozygous	75	0.51	exonic	GRIN2A	0.0000239	0.0000319	.	VUS	NA	confirm
16	9857547	C	T	Heterozygous	75	0.51	exonic	GRIN2A	0.0000239	0.0000319	.	VUS	NA	confirm
17	4439595	C	T	Homozygous	127	1	exonic	SPNS2	0.0002	3.19e-05	.	Benign	Patient 2 and his mother are also homozygous	.
17	4542794	C	G	Homozygous	122	1	exonic	ALOX15	0.0059	0.0040	.	LB	Patient 2 also homozygous	.
17	25904590	C	T	Heterozygous	83	0.49	exonic	KSR1	0.0000631	.	.	VUS	NA	.
17	25931750	C	T	Heterozygous	71	0.45	exonic	KSR1	0.0000521	0.0000637	.	VUS	NA	.
17	80788946	G	A	Heterozygous	146	0.52	exonic	ZNF750	0.0000716	0.0000956	.	VUS	NA	probl
19	4511746	A	T	Heterozygous	70	0.33	exonic	PLIN4	.	0.159	.	Benign	NA	.
19	4511955	T	C	Heterozygous	140	0.46	exonic	PLIN4	.	0.898	.	Benign	NA	.
19	21948511	C	G	Heterozygous	104	0.36	exonic	ZNF100	0.0002	0.0001	.	LB	NA	.
19	21948513	G	A	Heterozygous	104	0.36	exonic	ZNF100	0.0002	0.0001	.	LB	NA	.
19	21948524	C	T	Heterozygous	110	0.39	exonic	ZNF100	0.0002	0.0001	.	LB	NA	.
19	39805513	G	A	Homozygous	136	1	exonic	LRFN1	8.82E-02	3.19E-02	.	VUS	NA	.
19	46891882	G	A	Homozygous	125	1	exonic	PPP5C	2.39E-02	.	.	VUS	NA	.
19	49342514	C	T	Homozygous	79	1	exonic	PLEKHA4	0.0004	0.0002	.	VUS	NA	.
19	53410373	A	G	Heterozygous	113	0.49	exonic	ZNF888	.	0.383	.	Benign	NA	.
19	53411166	A	C	Heterozygous	224	0.52	exonic	ZNF888	.	0.378	.	Benign	NA	.
19	54711406	-	TGG	Homozygous	56	1	exonic	RP59	2.00E-05	6.37E-02	.	VUS	NA	.
19	54744358	A	C	Homozygous	17	1	exonic	LILRA6	7.34E-02	0.0003	.	LB	NA	.
19	54744360	A	G	Homozygous	14	1	exonic	LILRA6	2.56E-02	0.0002	.	VUS	NA	.
19	54976343	G	T	Homozygous	87	1	exonic	CDC42EP5	0.0004	0.0002	.	VUS	NA	.
21	45802597	G	T	Heterozygous	162	0.41	splicing	TRPM2	0.000028	.	.	VUS	NA	.
21	45802598	C	T	Heterozygous	165	0.41	splicing	TRPM2	0.000028	.	.	VUS	NA	.
21	47418050	G	A	Heterozygous	125	0.43	exonic	COL6A1	0.0000776	0.0000319	.	LB	NA	confirm

RESULTS: Chapter 1

ExonicFunc.refgene	AAChange.refgene	CADD	GME_AF	Iranome_AF	1000g2015aug_all	avsnp147	Eigen-row	Kaviar	MutationTaster_MutationAssesso	Polyphen2	PROVEAN	SIFT	ClinVar
stopgain	PORCN:NM_203474:exc	37	A
nonsynonymous SNV	GNL2:NM_001323623:e	23.1	0.527	.	D	M	P	D	T
nonsynonymous SNV	YY1AP1:NM_001198899	12.75	.	0.000625	0.000199681	rs142531956	-0.915	3.88e-05	N	L	B	N	T
nonsynonymous SNV	ALK:NM_004304:exon1:	33	0.796	.	D	M	D	D	T
nonsynonymous SNV	SYTL3:NM_001318745:e	8,269	0.001007	.	.	rs759356620	-1,153	2.59e-05	D	L	B	N	D
nonsynonymous SNV	CDK13:NM_003718:exo	9,211	.	0.000642674	0.000998403	rs17537669	-0.523	0.0019146	N	N	B	N	T
nonsynonymous SNV	NCAPD3:NM_015261:ex	20.5	0.000504	0.00125	0.000199681	rs143158496	-0.177	0.0001164	D	M	B	N	T
nonsynonymous SNV	TBC1D2B:NM_144572:e	29.4	.	.	.	rs752725824	0.234	1.94e-05	D	L	D	N	T
stopgain	CETP:NM_000078:exon:	22.6	.	0.000625	.	rs201790757	-0.900	1.29e-05	A
nonsynonymous SNV	CHRNE:NM_000080:exo	29.5	.	.	.	rs145522662	0.452	9.06e-05	D	L	P	N	D
stopgain	ALDH16A1:NM_001145:	35	0.205	.	A
nonsynonymous SNV	CDON:NM_001243597:e	0.097	.	.	0.000199681	rs146002530	-1.4255	0.000103	N	N	B	N	T

ExonicFunc.refgene	AAChange.refgene	CADD	GME_AF	Iranome_AF	1000g2015aug_all	avsnp147	Eigen-row	Kaviar	MutationTaster_MutationAssesso	Polyphen2	PROVEAN	SIFT	ClinVar
nonsynonymous SNV	MMEL1:NM_033467:exi	23.9	0.0005198	.	0.000199681	rs143215062	0.1574	0.0000386	N	M	D	N	D
nonsynonymous SNV	MMEL1:NM_033467:exi	24.6	-0.0073	.	D	L	B	D	D
nonsynonymous SNV	RAB25:NM_020387:exo	32	0.002014	0.00375	0.00359425	rs61751627	0.747	0.0048188	D	L	D	D	D
nonsynonymous SNV	IFI16:NM_001206567:ex	0.331	0.010070	0.008125	0.00199681	rs149606671	-1,181	0.0056338	N	L	B	D	D
synonymous SNV	UFC1:NM_016406:exon	.	0.000504	.	0.000199681	rs529045897	.	1.29e-05
frameshift deletion	NR1I3:NM_001077470:e
nonsynonymous SNV	RGS4:NM_001102445:e	8,073	.	0.00126103	.	rs568489938	-1,228	9.06e-05	N	.	B	N	D
nonsynonymous SNV	DUSP27:NM_00108042f	23.2	0.001007	.	.	.	0.353	.	D	M	D	N	D
nonsynonymous SNV	ZNF638:NM_001014972	1,203	0.004028	0.005	0.00898562	rs61739715	-0.684	0.0058537	D	N	B	N	T
nonsynonymous SNV	GCFC2:NM_001201334:	10.85	.	0.000625	.	.	-0.767	.	D	N	B	D	D
nonsynonymous SNV	FER1L5:NM_001293083	16.23	0.003641	0.004375	0.00139776	rs551147801	0.514	0.0003558	.	L	P	.	.
nonsynonymous SNV	POTEF:NM_001099771:	18.91	0.0005285	.	0.000399361	rs201364219	-0.2668	0.000174	N	M	P	D	D
nonsynonymous SNV	POTEF:NM_001099771:	22.6	.	.	0.00159744	rs534751551	-1.0907	0.000875	N	L	B	D/N	D
nonsynonymous SNV	FN1:NM_001306131:exi	23	.	0.000625	.	rs564795973	0.1892	0.0000579	D	N	D	N	D
nonsynonymous SNV	HDAC4:NM_006037:exc	22.9	0.000506	0.001875	0.000798722	rs144555853	0.05483	0.0002637	D	L	P	N	T
nonframeshift insertion	LNP1:NM_001085451:e	rs71132521	.	6.5e-06
nonsynonymous SNV	SLC49A3:NM_00129434	19.19	.	0.00125	.	rs747165832	-0.621	2.59e-05	D	N	P	N	D
nonsynonymous SNV	ADD1:NM_001119:exon	28.2	0.001010	0.000625	0.00259585	rs2295497	0.385	0.0009767	D	N	D	N	D
nonsynonymous SNV	UGT2B10:NM_0012900f	.	.	.	0.000599042	rs183339797	.	0.0009508
nonsynonymous SNV	UGT2B4:NM_00129761:	6,909	0.000517	.	0.00279553	rs185495830	-1,162	0.0006209	N	L	B	D	T
nonsynonymous SNV	MTHFD2L:NM_0011449	25.1	.	.	.	rs199612978	0.580	0.0003881	D	L	D	D	D
nonsynonymous SNV	PCSK1:NM_000439:exor	19.57	.	.	0.000199681	rs567748971	-0.6746	.	D	N	B	N	T
nonsynonymous SNV	PCSK1:NM_000439:exor	20.4	0.04324	.	D	M	B	D	T
nonsynonymous SNV	SLC36A3:NM_181774:e	28.3	.	.	0.000399361	rs182768240	0.8601	0.0000836	D	M	D	D	D
nonsynonymous SNV	SLC36A3:NM_181774:e	16.64	-0.2738	.	D	L	B	N	T
nonsynonymous SNV	MRPL14:NM_00131877f	.	.	.	0.677716	rs1935611	.	0.595
nonsynonymous SNV	MRPL14:NM_00131877f	.	.	.	0.28135	rs7752653	.	0.227
nonsynonymous SNV	AUTS2:NM_001127231:	26.5	0.2588	.	N	L	P	N	D
nonsynonymous SNV	RP1L1:NM_178857:exor	9,384	0.33887	0.2872	0.441494	rs9657518	-0.7788	0.02215	P	.	P	N	T
nonsynonymous SNV	RP1L1:NM_178857:exor	21.5	.	0.2304	.	rs74366179	-0.6095	0.00749	P	N	D	N	D
nonsynonymous SNV	CHD7:NM_017780:exon	23.5	.	.	.	rs185940313	0.05383	0.0000129	D	L	D	N	T
nonsynonymous SNV	ZNF623:NM_014789:exi	26.2	0.003525	0.00375	0.00179712	rs150073213	0.076	0.0043531	N	M	P	D	D
nonframeshift deletion	HRCT1:NM_001039792:	.	.	0.10498	0.185503	rs143611048	.	0.0001294
nonsynonymous SNV	PTCH1:NM_000264:exo	10.73	0.0126008	0.005	0.00119808	rs149258400	-0.302	0.000855	D	N	B	N	T

Identification of disease-causing variants in patients clinically diagnosed with Opitz C syndrome and Bohring-Opitz syndrome and functional validation

nonsynonymous SNV	UBAC1:NM_016172:exo	23.5	.	.	.	rs749704638	-0.497	6.5e-06	N	L	D	D	D	.
nonsynonymous SNV	MAMDC4:NM_206920:exon6:c.64	0.087	0.003525	0.004375	0.00359425	rs145077934	-1.745	0.0056468	N	N	B	N	T	.
.	NM_002079:exon6:c.64	.	.	0.011335	0.00159744	rs139135226	.	0.0044695
stopgain	MMP21:NM_147191:ex	36	.	.	.	rs145119918	0.2988	0.000186	D	Pathogenic
nonsynonymous SNV	MMP21:NM_147191:ex	0.484	.	.	.	rs764747628	-1.1483	.	N	N	B	N	T	.
nonsynonymous SNV	ANOS:NM_001142649:ε	0.01	.	.	.	rs367731017	-1.7581	0.0000322	N	L	B	N	T	.
nonsynonymous SNV	ANOS:NM_001142649:ε	23.6	-0.0321	.	D	M	B	D	T	.
nonsynonymous SNV	KMT5B:NM_001300908	20.4	0.001007	.	.	rs377489614	-0.0173	0.0000579	N	.	P	N	T	.
nonsynonymous SNV	CAPN5:NM_004055:exo	27	.	.	.	rs782089468	0.479	7.76e-05	D	L	P	N	T	.
nonframeshift insertion	KRT4:NM_002272:exon:	.	.	.	0.878994	rs11267392	.	0.0248444
.	NM_016029:exon6:c.97	29.4	.	0.0025	0.000199681	rs138163363	1.218	0.000315	D
nonsynonymous SNV	DHRS7:NM_001322282:	23.4	0.003021	0.0025	0.000199681	rs143781219	0.346	0.000322	D	M	D	D/N	T	.
.	0.00179712	rs564380796	.	0.000437
nonsynonymous SNV	DUOX1:NM_175940:exc	.	.	0.0025	0.000998403	rs138894830	0.2331	0.000823	D	L	P	N	T	.
nonsynonymous SNV	C15orf39:NM_015492:ε	13.97	.	.	.	rs767559287	-1.171	6.5e-06	N	N	B	N	T	.
nonsynonymous SNV	MAN2C1:NM_0012564ε	27.6	0.006546	0.000625	0.000599042	rs143005170	0.711	0.0003234	D	M	D	D	D	.
nonsynonymous SNV	GOLGA6L3:NM_001310	.	.	0.1011	.	rs202203580	.	0.00102
nonsynonymous SNV	GOLGA6L3:NM_001310	.	.	0.0226	.	rs200324412
nonsynonymous SNV	GOLGA6L3:NM_001310	.	.	0.002841	.	rs879001476
frameshift insertion	NLRC3:NM_178844:exoi
nonsynonymous SNV	NLRC3:NM_178844:exoi	25.8	0.8785	.	D	M	D	.	.	.
stopgain	NLRC3:NM_178844:exoi	36	.	0.000625	.	rs778991379	0.2841	.	A
nonsynonymous SNV	GRIN2A:NM_001134407	25.8	0.8022	.	D	M	D	D	D	.
nonsynonymous SNV	GRIN2A:NM_001134407	25.8	0.8223	.	D	M	D	D	D	.
nonsynonymous SNV	GRIN2A:NM_001134407	10.79	0.0005035	.	.	rs367543132	0.04481	0.0000257	D	N	D	N	T	Uncertain
nonsynonymous SNV	GRIN2A:NM_001134407	10.79	0.0005035	.	.	rs367543132	0.04481	0.0000257	D	N	D	N	T	Uncertain
nonsynonymous SNV	SPN52:NM_001124758:ε	22.5	0.000504	.	.	rs373623953	-0.449	0.0001617	D	N	B	D	T	.
nonsynonymous SNV	ALOX15:NM_001140:ex	23.4	0.006559	0.018125	0.00439297	rs11568142	-0.602	0.0056985	N	M	P	N	D	.
nonsynonymous SNV	KSR1:NM_014238:exonε	34	.	0.00125	.	rs755995795	0.5512	0.000045	D	.	D	.	.	.
nonsynonymous SNV	KSR1:NM_014238:exonε	11.93	.	0.00125	.	rs770696646	-1.447	0.000045	N	.	B	.	.	.
nonsynonymous SNV	ZNF750:NM_024702:exi	0.351	.	0.000625	0.000199681	rs144851291	-1.3336	0.0000643	N	M	B	N	D	.
nonsynonymous SNV	PLIN4:NM_001080400:ε	0.76	.	0.03311	.	rs62115192	-1.2419	0.0119	P	M	P	D	T	.
nonsynonymous SNV	PLIN4:NM_001080400:ε	0.005	0.828629	0.8271	0.879992	rs7260518	-1.5518	0.756	P	N	B	N	T	.
nonsynonymous SNV	ZNF100:NM_00135166ε	0.002	.	0.0025	0.000199681	rs550860903	-1.7219	.	N	N	B	N	T	.
stopgain	ZNF100:NM_00135166ε	23.5	.	0.0025	0.000199681	rs569230674	-0.43	.	A
nonsynonymous SNV	ZNF100:NM_00135166ε	0.002	.	0.0025	0.000199681	rs201163370	-1.6743	0.0000257	N	N	B	N	T	.
nonsynonymous SNV	LRFN1:NM_020862:exoi	16.09	.	0.000625	.	rs201576239	-0.346	9.7e-05	N	L	B	N	T	.
nonsynonymous SNV	PPP5C:NM_001204284:ε	20.3	0.000504	0.000625	.	rs748914520	-0.407	3.88e-05	D	N	B	N	T	.
nonsynonymous SNV	PLEKHA4:NM_020904:ε	10.82	.	.	0.000399361	rs139046967	-1.419	0.0003946	N	N	B	N	T	.
nonsynonymous SNV	ZNF888:NM_001310127	.	.	.	0.409345	rs2870128	.	0.0519
nonsynonymous SNV	ZNF888:NM_001310127	.	.	.	0.425319	rs7255668	.	0.0527
nonframeshift insertion	RPS9:NM_001321705:ε	rs766126457	.	6.5e-06
stopgain	LILRB3:NM_001081450:	32	0.028815	0.0120253	0.0760783	rs1052992	-0.790	0.0030013	A
nonsynonymous SNV	LILRB3:NM_001081450:	0.002	.	0.0126582	.	rs2361802	-1.611	0.0005239	N	N	P	.	.	.
nonsynonymous SNV	CDC42EP5:NM_145057:	19.06	0.002058	.	0.000399361	rs547076131	-0.593	0.0001164	N	L	B	D	D	.
.	NM_001320350:exon9:ε	.	.	.	0.000199681	rs530083183	.	0.0000322
.	NM_001320350:exon9:ε	.	.	.	0.000199681	rs548157020	.	0.0000579
nonsynonymous SNV	COL6A1:NM_001848:ex	23.5	.	.	.	rs760815168	-0.8223	0.0000514	N	N	P	N	D	.

Supplementary Table 2. Variants identified in Patient 2

Chr	Start	Ref	Alt	Genotype	Depth	Frequency	Func.refgene	Gene.ensgene	gnomAD_exome_ALL	gnomAD_genome	ACMG Classification	Segregation
I. Selected variants												
13	100637335	ACCCAG	C	het	119	0.46	exonic	ZIC2	.	.	Pathogenic	de novo and absent in sisters and cousin
7	117251713	A	G	hom	141	1	exonic	CFTR	.	.	LP	Both sisters are homo
Chr	Start	Ref	Alt	Genotype	Depth	Frequency	Func.refgene	Gene.refgene	Gnomad_Exome_AF	Gnomad_Genome_Curated	ACMG Classi	Segregation
II. Other Variants												
1	155721911	C	T	het	37	0.43	exonic	GON4L	0.0057	0.0019	VUS	Maternally inherited
1	155735585	C	T	het	158	0.25	exonic	GON4L	0.0019	0.0085	VUS	Paternally inherited
1	203024757	G	T	het	49	0.53	exonic	PPFIA4	.	.	VUS	Maternally inherited
1	203044784	T	C	het	16	0.56	exonic	PPFIA4	0.0009	0.0009	VUS	Paternally inherited
1	247054333	C	T	hom	75	1	exonic	AHCTF1	0.0002	0.0001	VUS	Absent in Patient 1. Both parents hetero.
2	159526387	A	G	het	53	0.42	exonic	PKP4	0.0000977	.	VUS	de novo (not validated by sanger)
3	4726749	C	T	hom	122	1	splicing	ITPR1	0.00004253	.	VUS	Absent in Patient 1. Both parents hetero.
4	675797	C	G	hom	195	1	exonic	MFSD7	0.0000336	.	VUS	Absent in Patient 1. Both parents hetero.
4	2877658	C	T	hom	130	1	exonic	ADD1	0.0011	0.0006	VUS	Patient 1 is also homozygous.
6	110501788	G	C	het	143	0.57	exonic	CDC40	.	.	VUS	Paternally inherited
6	110536489	C	G	het	92	0.48	exonic;splicing	CDC40	0.007	0.0055	VUS	Maternally inherited
7	98786174	G	A	hom	66	1	exonic	KPNA7	0.0001	0.0004	Benign	One healthy sister is homo
11	540709	C	A	het	156	0.51	exonic	LRRC56	0.0002	0.0002	VUS	Maternally inherited
11	551741	C	T	het	99	0.42	exonic	LRRC56	0.0069	0.0024	VUS	Paternally inherited
11	11373588	G	A	het	136	0.48	exonic	CSNK2A3	0.0035	0.0025	LB	Maternally inherited
11	11374072	C	T	het	162	0.46	exonic	CSNK2A3	0.0004	0.0002	VUS	Paternally inherited
12	52841742	C	T	het	65	0.51	exonic	KRT6B	0.00009745	0.0002	VUS	Maternally inherited
12	52842643	C	T	het	58	0.57	exonic	KRT6B	0.0049	0.0052	VUS	Paternally inherited
13	20279839	T	C	het	13	0.31	exonic	PSPC1	0.0004	0.0000326	VUS	Paternally inherited (CIS)
13	20279879	T	C	het	23	0.3	exonic	PSPC1	0.0005	0.0009	VUS	Paternally inherited (CIS)
14	105415230	G	T	het	72	0.63	exonic	AHNAK2	0.0003	0.0001	VUS	Paternally inherited
14	105415259	C	G	het	72	0.32	exonic	AHNAK2	0.0026	0.0048	LB	Maternally inherited
16	19725706	TTT	-	hom	34	1	exonic	C16orf88	.	.	LB	Absent in Patient 1. Both parents hetero.
17	4439595	C	T	hom	199	1	exonic	SPNS2	0.0002	0.00003237	Benign	Healthy mother and Patient 1 are homo. Father hetero.
17	4542794	C	G	hom	126	1	exonic	ALOX15	0.0059	0.004	LB	Patient 1 is also homozygous.
17	4804381	T	G	hom	108	1	exonic	CHRNE	0.0001	.	Benign	Patient 1 and her mother also homozygous.
19	6387479	C	T	hom	137	1	exonic	GTF2F1	0.00005686	.	VUS	Both parents and Patient 1 are heterozygous.
19	52618471	C	T	het	102	0.5	exonic	ZNF616	0.0049	0.0036	LB	Paternally inherited
19	52619875	C	T	het	161	0.44	exonic	ZNF616	0.00007323	.	LB	Maternally inherited

Identification of disease-causing variants in patients clinically diagnosed with Opitz C syndrome and Bohring-Opitz syndrome and functional validation

DDD	ExonicFunc.refgen	AAChange.refgene	CADD_phred	1000g2015aug_all	avnsnp147	Eigen-raw	GME_AF	Iranome_af	Kaviar	MutationTaster	MutationAssessor	Polyphen2_HDIV	PROVEAN	SIFT
confirmed_monoallelic	Inframe Substituti	ZIC2:NM_007129:c.
.	nonsynonymous S	CFTR:NM_000492:c.26.5	.	.	.	0.8344	.	.	.	D	M	D	N	T
DDD	ExonicFunc.refgen	AAChange.refgene	CADD_phred	1000g2015aug_all	avnsnp147	Eigen-raw	GME_AF	Iranome_AF	Kaviar	MutationTaster	MutationAssessor	Polyphen2_HDIV	PROVEAN	SIFT
possible_biallelic_A	nonsynonymous S	GON4L:NM_00128	23.8	0.00579073	rs201235180	-0.0899	0.0125	0.02125	0.005016	D	L	P	N	T
possible_biallelic_A	nonsynonymous S	GON4L:NM_00128	16.42	0.00878594	rs61748905	-0.3233		0.003125	0.002286	T	M	P	N	T
.	nonsynonymous S	PPFIA4:NM_00130	25.7	.	rs763076240	0.5859	.	.	0.000045	D	M	D	D	T
.	nonsynonymous S	PPFIA4:NM_00130	21.8	0.000599042	rs200298818	-0.2593	0.001014	.	0.000844	D	M	B	D	D
.	nonsynonymous S	AHCTF1:NM_0013	23.1	0.000199681	rs200702767	0.5093	0.001009	0.000625	0.000219	D	M	D	N	D
.	nonsynonymous S	PKP4:NM_0010054	24.3	.	rs764903809	0.5725	.	.	0.000084	D	L	P	N	T
probable_monoallelic	.	NM_002222:exon2	.	.	rs374122245	.	.	0.001875	0.000058
.	nonsynonymous S	SLC49A3:NM_0012	19.19	.	rs747165832	-0.6212	.	0.00125	0.000032	D	N	P	N	D
.	nonsynonymous S	ADD1:NM_001119	28.2	0.00259585	rs2295497	0.3849	0.00101	0.000625	0.000895	D	N	D	N	D
.	nonsynonymous S	CDC40:NM_01589	8103	.	.	-0.6966	.	.	.	N	N	B	N	T
.	nonsynonymous S	CDC40:NM_01589	26.1	0.00439297	rs138462889	0.1069	0.008056	0.0125	0.006691	D	N	P	N	D
possible_Gomez-L	nonsynonymous S	KPNA7:NM_00114	26.6	.	rs746487289	0.4699	.	.	0.000045	D	M	P	D	D
.	nonsynonymous S	LRRCS56:NM_19807	8937	0.000399361	rs142967139	-1.1548	0.001009	0.000625	0.000161	T	L	B	N	T
.	nonsynonymous S	LRRCS56:NM_19807	25.2	0.00878594	rs139348192	0.1108	0.01409869	0.01937	0.006221	T	M	D	N	D
.	nonsynonymous S	CSNK2A3:NM_001	6387	0.00559105	rs201862125	.	.	0.01125	0.002808	D	N	B	.	.
.	nonsynonymous S	CSNK2A3:NM_001	22.1	.	rs750849569	.	.	.	0.000354	D	N	D	.	.
.	nonsynonymous S	KRT6B:NM_00555	26.6	0.000399361	rs200778388	0.1965	.	.	0.000103	D	M	D	D	D
.	nonsynonymous S	KRT6B:NM_00555	25	0.00379393	rs138988810	-0.154	0.01863	0.01312	0.004624	D	M	D	D	D
.	nonsynonymous S	PSPC1:NM_001354	3267	.	rs747690097	-0.3213	0.00738	0.04562	0.000006	D	M	B	N	T
.	nonsynonymous S	PSPC1:NM_001354	1853	.	rs747690097	-0.4521	0.00738	0.04562	0.000006	N	L	B	N	T
.	nonsynonymous S	AHNAK2:NM_0013	0.001	0.000399361	rs377764513	-1.8779	0.003329	0.004397	0.000232	T	L	P	N	T
.	nonsynonymous S	AHNAK2:NM_0013	17.36	0.00359425	rs199967385	-0.5288	0.000557	0.001877	0.000129	T	L	B	N	T
.	nonframeshift dele	KNOP1:NM_00101	D	.
.	nonsynonymous S	SPNS2:NM_00112	22.5	.	rs373623953	-0.4495	0.00050	.	0.000167	D	N	B	D	T
.	nonsynonymous S	ALOX15:NM_0011	23.4	0.00439297	rs11568142	-0.6017	0.006559	0.01812	0.005480	T	M	P	N	D
.	nonsynonymous S	CHRNE:NM_00008	29.5	.	rs145522662	0.4518	.	.	0.000097	D	L	P	N	D
.	nonsynonymous S	GTF2F1:NM_0020	34	.	rs556406656	0.8453	.	.	0.000032	D	M	D	N	D
.	nonsynonymous S	ZNF616:NM_1785	0.112	0.00419329	rs45622033	-1.6337	0.011581	0.01188	0.004540	T	N	B	N	.
.	nonsynonymous S	ZNF616:NM_1785	7527	.	rs747966574	-1.1676	.	0.000625	0.000045	T	M	B	N	.

Article 3: The ASXL1 mutation p.Gly646Trpfs*12 found in a Turkish boy with Bohring-Opitz Syndrome

Summary:

In line with a recent study showing that ASXL1 mutations found in the common population cannot be ruled out as pathogenic, we have identified the ASXL1 p.Gly646Trpfs*12 mutation—present in 132 individuals in ExAC—as a very probable cause of the disease in a Bohring-Opitz syndrome patient.

Reference:

Urreizti R, Gürsoy S, Castilla-Vallmanya L, et al. The ASXL1 mutation p.Gly646Trpfs*12 found in a Turkish boy with Bohring-Opitz Syndrome. *Clin Case Rep.* 2018; 6:1452–1456. doi: 10.1002/ccr3.1603

CASE REPORT

The *ASXL1* mutation p.Gly646Trpfs*12 found in a Turkish boy with Bohring-Opitz Syndrome

Roser Urreizti¹ | Semra Gürsoy² | Laura Castilla-Vallmanya¹ | Guillem Cunill¹ | Raquel Rabionet¹ | Derya Erçal² | Daniel Grinberg¹ | Susana Balcells¹

¹Department of Genetics, Microbiology and Statistics, Faculty of Biology, University of Barcelona, IBUB, IRSJD, CIBERER, Barcelona, Spain

²Department of Pediatric Genetics, Dokuz Eylül University, İzmir, Turkey

Correspondence

Roser Urreizti, Department of Genetics, Microbiology and Statistics, Faculty of Biology, UB. Avda Diagonal, 643, E-08028, Barcelona, Spain. Email: urreizti@ub.edu

Funding information

Associació Síndrome Opitz C, Terrassa, Spain; Agència de Gestió d'Ajuts Universitaris i de Recerca, Grant/Award Number: 2014SGR932; CIBERER, Grant/Award Number: U720; Secretaría de Estado de Investigación, Desarrollo e Innovación, Spanish Ministerio de Economía y Competitividad, Grant/Award Number: SAF2016-75948-R; FECYT; crowdfunding PRECIPITA; Generalitat de Catalunya, Grant/Award Number: PERIS 2016-20

Key Clinical Message

In line with a recent study showing that *ASXL1* mutations found in the common population cannot be ruled out as pathogenic, we have identified the *ASXL1* p.Gly646Trpfs*12 mutation—present in 132 individuals in ExAC—as a very probable cause of the disease in a Bohring-Opitz syndrome patient.

KEYWORDS

ASXL1, Bohring-Opitz syndrome, intellectual disability, mutation prioritization, variants of unknown significance

1 | INTRODUCTION

Bohring-Opitz syndrome (BOS, MIM #605039) is a rare and severe disease characterized mainly by intrauterine growth retardation, feeding difficulties, severe to profound developmental delay, nonspecific brain abnormalities, microcephaly, flexion at the elbows with ulnar deviation and flexion of the wrists and metacarpophalangeal joints (known as BOS posture) and distinctive facial features.¹ Heterozygous *ASXL1* truncating mutations have been identified as the main cause of BOS.^{1,2} A recent publication³ called the attention to the

fact that mutations associated with BOS are also present in the ExAC (Exome Aggregation Consortium) database.⁴ As *ASXL1* is one of the genes most commonly mutated during hematopoietic clonal expansion of cells, the authors hypothesized that the presence of this mutation in public databases could be due to somatic mosaicism, and they could confirm the hypothesis by manual examination of the ExAC WES reads.

We have recently identified a new BOS case, in which Sanger sequencing of *ASXL1* revealed the p.Gly646Trpfs*12 mutation, also present in ExAC.

This is an open access article under the terms of the Creative Commons Attribution-NonCommercial-NoDerivs License, which permits use and distribution in any medium, provided the original work is properly cited, the use is non-commercial and no modifications or adaptations are made.

© 2018 The Authors. *Clinical Case Reports* published by John Wiley & Sons Ltd.

2 | CASE REPORT

The patient is a 4-year-old Turkish boy, only child of a healthy nonconsanguineous couple and born at term via normal vaginal delivery after an uneventful pregnancy. The birthweight was 2.3 kg (1st percentile, -2.4 SD), height was 45 cm (-2.3 SD), and head circumference was 32 cm (4th percentile, -1.7 SD). The patient was referred to the genetics department at the 9th day of life. Physical examination revealed trigonocephaly, microcephaly, nevus simplex (flammeus), dysmorphic features, intrauterine growth retardation, and BOS posture with fixed contractures. In the postnatal period, the patient was intubated due to respiratory problems. As he could not be extubated, at 4 months tracheostomy was performed. He was fed through G tube since the 4th month of life. At 2 months of age, the patient started suffering seizures. Abnormalities were detected by EEG, and antiepileptic treatment with levetiracetam and phenobarbital was initiated. Seizures have been under control thereafter with 3-4 attacks annually of a very short duration.

At 15 months, his weight was 10 kg (24th percentile, -0.69 SD), height was 62 cm (<3 rd percentile, -5.4 SD), and head circumference was 41.5 cm (<1 st percentile, -4.25

SD). At 3.5 years, he had microcephaly (45.5 cm; <3 rd percentile, -2.43 SD), trigonocephaly, up-slanting palpebral fissures, narrow forehead, nevus simplex, hypertrichosis, low-set ears, low frontal hairline, microretrognathia, high palate and delayed teeth eruption (no eruption at 3 years of age; Figure 1A,B). He also had bilateral cryptorchidism and brachydactyly (Figure 1C), as well as hypotonia and spasticity on both his upper and lower extremities. In particular, the patient had contractures of the hands and fingers. Additionally, overlapping toes were detected in the feet (Figure 1D). Cranial magnetic resonance revealed corpus callosum agenesis and atrophy of the optic nerve, and he failed the hearing test bilaterally. The patient also underwent echocardiography, which revealed a small patent ductus arteriosus. Abdominal ultrasound and metabolic tests were normal. The patient's developmental milestones were severely delayed (he was not able to sit, crawl or walk independently and he was not able to speak). His karyotype and aCGH results were normal.

After reviewing the clinical presentation of the patient, Bohring-Opitz syndrome was suspected, and the *ASXL1* gene was manually sequenced. Written informed consent from the patient's family was obtained, and all protocols were approved by the Ethics Committee of the Universitat de Barcelona (IRB00003099). A *de novo* heterozygous



FIGURE 1 Facial, hand and foot phenotypes of the patient at 3 y of age. A and B, Facial dysmorphisms, especially trigonocephaly and nevus simplex (flammeus) is clearly appreciated. C, brachydactyly is appreciable in the patient's hand. D, Foot phenotype with overlapping toes

mutation, c.1934dupG (p.Gly646Trpfs*12), was identified. The PCR amplification and Sanger sequencing were repeated twice, independently and the PCR fragment was cloned and sequenced (see Figure S1) to unequivocally confirm the mutation.

3 | DISCUSSION

While the clinical outcome of the patient clearly pointed to a Bohring-Opitz Syndrome, the fact that he was carrying a mutation (p.Gly646Trpfs*12) present in 132 individuals from the general population hindered taking a final decision on the genetic diagnosis. In this sense, other mutations present in ExAC (among them the p.Arg404Ter described by Carlston et al³) were previously found to be BOS -causing (Table 1). The p.Gly646Trpfs*12 mutation described in our BOS case

is one of the two *ASXL1* loss of function (LoF) changes especially frequent in ExAC, the other being p.Gly645Valfs*58 (found in 118 individuals). Both changes are located in an eight-nucleotide G-homopolymer tract and could be over-represented due to sequencing errors. While these changes were not included in Carlston et al³ analyses, the authors discussed the fact that the p.Gly646Trpfs*12 mutation had been identified in a large series of myeloid malignancies by deep sequencing (confirmed by manual methods in some cases) and had been described as the most common cancer-associated *ASXL1* mutation.⁵ Besides, 66% of the ExAC carriers of the p.Gly646Trpfs*12 mutation belong to the Cancer Genome Atlas (TCGA) population.

This mutation is a truncating mutation affecting the last exons of the *ASXL1* gene, similarly to all the previously described BOS mutations (Figure 2). More recently, the p.Gly-646Trpfs*12 mutation has been filtered from the GnomAD

TABLE 1 BOS-causing *ASXL1* mutations present in ExAC

cDNA mutation	Prot. mutation	Reported phenotype	ExAc	GenomAD	Origen
c.1117C>T	p.Q373*	Focal Epilepsy ^a	no	2/246256	6
c.1129C>T	p.Q377*	ID ^a	no	no	7
c.1210C>T	p.R404*	Bohring-Opitz syndrome	7/121378	4/246248	2, 3, 8, 9
c.1269dupT	p.L424fs	Bohring-Opitz syndrome	no	no	10
c.1272_1273delGT	p.T425Qfs*12	Bohring-Opitz syndrome	no	1/246262	1
c.1544_1545delTG	p.V515Gfs*13	Focal Epilepsy ^a	no	no	6
c.1924 G>T	p.G642*	Bohring-Opitz syndrome	no	no	1
c.1934insG	p.G646Wfs*12	Bohring-Opitz syndrome	132/80804	no ^b	Present study
c.2013_2014 del	p.C672Tfs*4	Bohring-Opitz syndrome	no	no	1
c.2036_2037insG	p.G680Rfs*38	Bohring-Opitz syndrome	no	no	11
c.2100dupT	p.P701Sfs*16	Bohring-Opitz syndrome	no	no	12
c.2197C>T	p.Q733*	Bohring-Opitz syndrome	1/121070 ^c	idem ExAC	2
c.2324 T>G,	p.L775*	Bohring-Opitz syndrome	1/121162	no ^b	1
c.2332C>T	p.Q778*	Bohring-Opitz syndrome	no	no	2
c.2407_2411del15	p.Q803Tfs*17	Bohring-Opitz syndrome	3/120748 ^c	no ^{b,c}	2
c.2468T>G	p.L823*	Bohring-Opitz syndrome	2/120758 ^c	2/244338 ^c	2
c.2535dup	p.S846Qfs*5	Bohring-Opitz syndrome	no	no	1
c.2759_2762dup	p.V922Ifs*3	Bohring-Opitz syndrome	no	no	1
c.2773C>T	p.Q925*	Bohring-Opitz syndrome	no	no	2
c.2893C>T	p.R965*	Bohring-Opitz syndrome	1/121306	3/246200	13
c.3077del	p.G1026Dfs*21	Bohring-Opitz syndrome	no	no	1
c.3083C>A	p.S1028*	Bohring-Opitz syndrome	no	no	2
c.4060 G>T	p.E1354*	Bohring-Opitz syndrome	no	no	14
c.4116_4117del2	p.F1373fs	Bohring-Opitz syndrome ^d	no	no	15

^aClinical history is limited without description of presence or absence of other BOS features.

^bFiltered in GenomAD (failed random forest filters).

^cThese numbers correspond to another mutation affecting the same residue.

^dThe patient is also carrying recessive mutations in the CFTR gene.

Bold type indicates the mutation in the case presented here

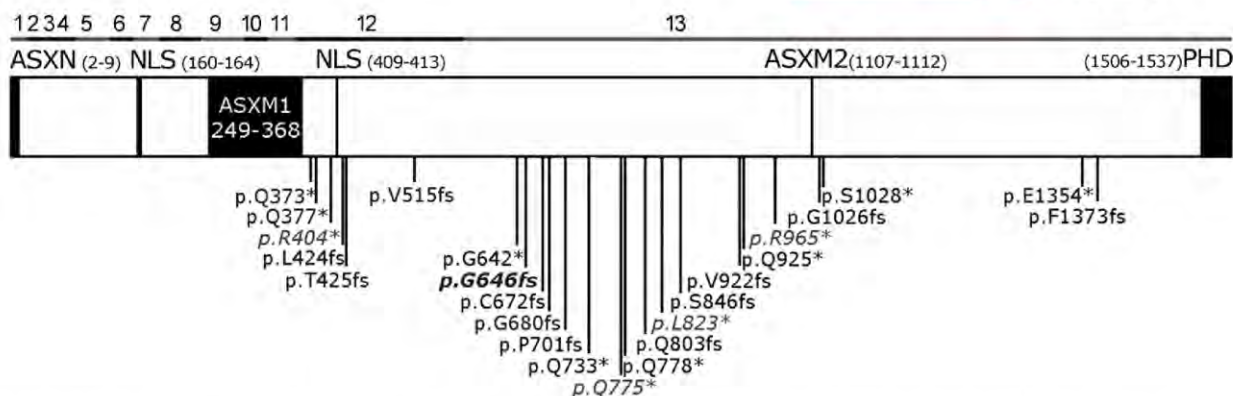


FIGURE 2 ASXL1 protein structure and BOS-causing mutations. In italics, mutations also present in ExAC. ASXL1 coding exons are indicated above. ASXN, ASX N-terminal domain; NLS, Nuclear localization signal; ASXM, ASX middle domains; PHD, plant homeodomain

database as it failed random forest filters. In addition, very recently a new patient with this mutation was reported to ClinVar by GenDX, although the clinical outcome of the patient was not reported.

Taking all this into consideration, we conclude that the p.Gly646Trpfs*12 mutation is a disease-causing mutation responsible for the patient's BOS clinical presentation and that, as Carlston et al³ stated, the assumption that pathogenic variants in genes associated with severe, pediatric-onset, highly penetrant, autosomal dominant conditions have to be absent or extremely rare in public databases has to be taken cautiously.

ACKNOWLEDGMENTS

The authors thank the patient and his family for their wholehearted collaboration. They are also grateful to M. Cozar for technical assistance. Funding was from Associació Síndrome Opitz C, Terrassa, Spain; Spanish Ministerio de Economía y Competitividad (SAF2016-75948-R; FECYT, crowdfunding PRECIPITA), Catalan Government (2014SGR932) and from CIBERER (U720). RR is a postdoctoral fellow under the PERIS 2016-20 program of Generalitat de Catalunya. The authors declare no competing financial interests.

AUTHOR CONTRIBUTION

RU, SG, DG, and SB: contributed to the planning of this work. RU, SG, LCV, GC, RR, DE, DG, and SB: conducted this work. RU, LCV, and GC: performed the sequencing, cloning, and chromatogram analysis. RU and RR: performed the bibliographical, in silico and database analysis of the mutation. SG and DE: clinically evaluated the patient and have generated and written the clinical data. RU, SB, and DG: wrote the main manuscript text. RU and RR: elaborated

Table 1. RU and SG: prepared Figure 1. RU, SB, and DG: prepared Figure 2. RU and GC: prepared Figure S1. All authors reviewed the manuscript.

CONFLICT OF INTEREST

None declared.

ORCID

Roser Urreizti  <http://orcid.org/0000-0003-3617-7134>

REFERENCES

- Russell B, Johnston JJ, Biesecker LG, et al. Clinical management of patients with ASXL1 mutations and Bohring-Opitz syndrome, emphasizing the need for Wilms tumor surveillance. *Am J Med Genet A*. 2015;167A:2122-2131.
- Hoischen A, van Bon BW, Rodríguez-Santiago B, et al. De novo nonsense mutations in ASXL1 cause Bohring-Opitz syndrome. *Nat Genet*. 2011;43:729-731.
- Carlston CM, O'Donnell-Luria AH, Underhill HR, et al. Pathogenic ASXL1 somatic variants in reference databases complicate germline variant interpretation for Bohring-Opitz Syndrome. *Hum Mutat*. 2017;38:517-523.
- Lek M, Karczewski KJ, Minikel EV, et al. Analysis of protein-coding genetic variation in 60,706 humans. *Nature*. 2016;536:285-291.
- Van Ness M, Szankasi P, Frizzell K, Shen W, Kelley TW. Analysis of ASXL1 mutations in a large series of myeloid malignancies. *Mod Pathol*. 2016;29(Suppl. 2):333-388.
- Helbig KL, Farwell Hagman KD, Shinde DN, et al. Diagnostic exome sequencing provides a molecular diagnosis for a significant proportion of patients with epilepsy. *Genet Med*. 2016;18:898-905.
- Grozeva D, Carss K, Spasic-Boskovic O, et al. Targeted next-generation sequencing analysis of 1,000 individuals with intellectual disability. *Hum Mutat*. 2015;36:1197-1204.

8. Asaleh Y. Bohring-Opitz syndrome in Libya. *Libyan J Med Res.* 2014;8:47-49.
9. Zhu X, Petrovski S, Xie P, et al. Whole-exome sequencing in undiagnosed genetic diseases: interpreting 119 trios. *Genet Med.* 2015;17:774-781.
10. Brunelli L, Mao R, Jenkins SM, et al. A rapid gene sequencing panel strategy to facilitate precision neonatal medicine. *Am J Med Genet A.* 2017;173A:1979-1982.
11. Arunachal G, Danda S, Omprakash S, Kumar S. A novel de-novo frameshift mutation of the ASXL1 gene in a classic case of Bohring-Opitz syndrome. *Clin Dysmorphol.* 2016;25:101-105.
12. Urreizti R, Roca-Ayats N, Trepal J, et al. Screening of CD96 and ASXL1 in 11 patients with Opitz C or Bohring-Opitz syndromes. *Am J Med Genet A.* 2016;170A:24-31.
13. Magini P, Della Monica M, Uzielli ML. Two novel patients with Bohring-Opitz syndrome caused by de novo ASXL1 mutations. *Am J Med Genet A.* 2012;158A:917-921.
14. Srivastava S, Cohen JS, Vernon H, et al. Clinical whole exome sequencing in child neurology practice. *Ann Neurol.* 2014;76:473-483.
15. Dangiolo SB, Wilson A, Jobanputra V, Anyane-Yeboah K. Bohring-Opitz syndrome (BOS) with a new ASXL1 pathogenic variant: review of the most prevalent molecular and phenotypic features of the syndrome. *Am J Med Genet A.* 2015;167A:3161-3166.

SUPPORTING INFORMATION

Additional supporting information may be found online in the Supporting Information section at the end of the article.

How to cite this article: Urreizti R, Gürsoy S, Castilla-Vallmanya L, et al. The ASXL1 mutation p.Gly646Trpfs*12 found in a Turkish boy with Bohring-Opitz Syndrome. *Clin Case Rep.* 2018;6: 1452–1456. <https://doi.org/10.1002/ccr3.1603>

Article 4: Five new cases of syndromic intellectual disability due to *KAT6A* mutations: widening the molecular and clinical spectrum

Summary:

Background: Pathogenic variants of the lysine acetyltransferase 6A or *KAT6A* gene are associated with a newly identified neurodevelopmental disorder characterized mainly by intellectual disability of variable severity and speech delay, hypotonia, and heart and eye malformations. Although loss of function (LoF) mutations were initially reported as causing this disorder, missense mutations, to date always involving serine residues, have recently been associated with a form of the disorder without cardiac involvement.

Results: In this study we present five new patients, four with truncating mutations and one with a missense change and the only one not presenting with cardiac anomalies. The missense change [p.(Gly359Ser)], also predicted to affect splicing by in silico tools, was functionally tested in the patient's lymphocyte RNA revealing a splicing effect for this allele that would lead to a frameshift and premature truncation.

Conclusions: An extensive revision of the clinical features of these five patients revealed high concordance with the 80 cases previously reported, including developmental delay with speech delay, feeding difficulties, hypotonia, a high bulbous nose, and recurrent infections. Other features present in some of these five patients, such as cryptorchidism in males, syndactyly, and trigonocephaly, expand the clinical spectrum of this syndrome.

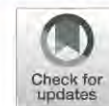
Reference:

Urreizti, R., Lopez-Martin, E., Martinez-Monseny, A. *et al.* Five new cases of syndromic intellectual disability due to *KAT6A* mutations: widening the molecular and clinical spectrum. *Orphanet J Rare Dis* **15**, 44 (2020). doi: 10.1186/s13023-020-1317-9

RESEARCH

Open Access

Five new cases of syndromic intellectual disability due to *KAT6A* mutations: widening the molecular and clinical spectrum



Roser Urreizti^{1,2,3†}, Estrella Lopez-Martin^{2,4†}, Antonio Martinez-Monseny⁵, Montse Pujadas⁶, Laura Castilla-Vallmanya^{1,2}, Luis Alberto Pérez-Jurado^{2,6,7}, Mercedes Serrano^{2,8}, Daniel Natera-de Benito⁸, Beatriz Martínez-Delgado^{2,4}, Manuel Posada-de-la-Paz^{2,4}, Javier Alonso^{2,4}, Purificación Marin-Reina⁹, Mar O'Callaghan⁸, Daniel Grinberg^{1,2†}, Eva Bermejo-Sánchez^{4†} and Susanna Balcells^{1,2†}

Abstract

Background: Pathogenic variants of the lysine acetyltransferase 6A or *KAT6A* gene are associated with a newly identified neurodevelopmental disorder characterized mainly by intellectual disability of variable severity and speech delay, hypotonia, and heart and eye malformations. Although loss of function (LoF) mutations were initially reported as causing this disorder, missense mutations, to date always involving serine residues, have recently been associated with a form of the disorder without cardiac involvement.

Results: In this study we present five new patients, four with truncating mutations and one with a missense change and the only one not presenting with cardiac anomalies. The missense change [p.(Gly359Ser)], also predicted to affect splicing by in silico tools, was functionally tested in the patient's lymphocyte RNA revealing a splicing effect for this allele that would lead to a frameshift and premature truncation.

Conclusions: An extensive revision of the clinical features of these five patients revealed high concordance with the 80 cases previously reported, including developmental delay with speech delay, feeding difficulties, hypotonia, a high bulbous nose, and recurrent infections. Other features present in some of these five patients, such as cryptorchidism in males, syndactyly, and trigonocephaly, expand the clinical spectrum of this syndrome.

Keywords: *KAT6A*, Neurodevelopmental disease, Clinical genetics, Whole exome sequencing, Clinical characterization

Background

The lysine acetyltransferase 6A or *KAT6A* gene (a.k.a. *MYST3* and *MOZ*; MIM #601408) codes for a member of the histone acetyltransferase (HAT) family MYST. This gene was identified at a recurrent break-point of chromosomal translocations associated with acute

myeloid leukaemia (AML) [1]. *KAT6A* acetylates lysine-9 residues in histone H3 (H3K9), playing an essential role in the regulation of transcriptional activity and gene expression. *KAT6A* is also involved in the acetylation and regulation of the tumor suppressor p53, a key factor in essential cell processes such as cell arrest and apoptosis [2]. Moreover, *KAT6A* is able to directly bind and regulate the transcription factors Runx1 and Runx2 through its C-terminal SM (serine and methionine rich) domain [3].

De novo mutations in *KAT6A* have recently been associated with a syndrome mainly characterized by intellectual disability (autosomal dominant mental retardation

* Correspondence: roseruf@yahoo.es

†Roser Urreizti, Estrella Lopez-Martin, Daniel Grinberg, Eva Bermejo-Sánchez and Susanna Balcells contributed equally to this work.

¹Department of Genetics, Microbiology and Statistics, Faculty of Biology, University of Barcelona, IBUB, IRSJD, Barcelona, Spain

²Centro de Investigaciones Biomédicas en Red de Enfermedades Raras (CIBERER), Instituto de Salud Carlos III (ISCIII), Madrid, Spain

Full list of author information is available at the end of the article



© The Author(s). 2020 **Open Access** This article is distributed under the terms of the Creative Commons Attribution 4.0 International License (<http://creativecommons.org/licenses/by/4.0/>), which permits unrestricted use, distribution, and reproduction in any medium, provided you give appropriate credit to the original author(s) and the source, provide a link to the Creative Commons license, and indicate if changes were made. The Creative Commons Public Domain Dedication waiver (<http://creativecommons.org/publicdomain/zero/1.0/>) applies to the data made available in this article, unless otherwise stated.

32; MIM # 616268). To date, a total of 79 patients have been reported [4–15]. All of them present with developmental delay (DD) or intellectual disability (ID) with speech delay. Additionally, low muscle tone, problems with early feeding, and heart and eye defects are frequent [13]. Most of the reported mutations are loss of function (LoF) variants including splicing mutations, stop gain, and frameshift changes. Recently, missense mutations affecting highly conserved residues in relevant functional sites have also been described [12, 13].

The protein KAT6A is part of the MOZ/MORF complex together with ING5, KAT6B, MEAF6, and one of BRPF1–3. Neurodevelopmental syndromes have been associated not only with KAT6A but also with KAT6B and BRPF1. KAT6B mutations are associated with Say-Barber-Biesecker-Young-Simpson syndrome (SBBYSS, MIM # 603736) and Genitopatellar syndrome (MIM # 606170), while BRPF1 mutations associate with IDDDFP (Intellectual developmental disorder with dysmorphic facies and ptosis, MIM # 617333). Like KAT6A syndrome, these two conditions present mainly with DD or ID and speech delay, hypotonia, and midline facial dysmorphic features including a broad nose.

Here, we present five new unrelated cases bearing four truncating mutations and one missense mutation in KAT6A, and we review the existing literature to expand the clinical delineation of KAT6A syndrome.

Results

Clinical description

The detailed phenotypic description of the patients is summarized in Table 1.

Patient 1 (P1)

The patient is a 10-year-old boy from a non-consanguineous and healthy couple. Two younger siblings, a girl aged 5½ years and a boy aged 3, are healthy. During the pregnancy of the proband, intrauterine growth retardation was detected. He was born at 37 weeks by caesarean section with Apgar scores 9/10 at 1 and 5 min, respectively. At birth, weight was 2.04 kg (2nd percentile, –2.04 SD), height 43 cm (<3rd percentile, –2.91 SD), and cranial circumference 30 cm (<3rd percentile, –3.77 SD). The infant presented dysmorphic features such a triangular facies, low-set ears, and short neck, in addition to cryptorchidism. Abdominal and cranial ultrasound studies were performed with no evidence of malformations. Serology for common neonatal infections (toxoplasma, rubella, cytomegalovirus, and herpes simplex) as well as brain computerized tomography (CT) and funduscopy were normal.

At the 5th month of life, a prominent metopic suture was observed. The helical CT confirmed craniosynostosis of the metopic suture and ossification of the anterior

fontanelle. At this follow-up visit developmental delay and limb hypertonia were detected. The subject began to crawl at 4 years of age and made his first unassisted steps at age 5. At 9 years of age absence seizures were clinically suspected and he was treated with valproate, showing good response. At 11 years the treatment was discontinued as the patient did not present seizures anymore and EEG was normal. Brain MRI (magnetic resonance imaging) was always normal. He was also treated with botulinum toxin because of hypersalivation due to dysphagia. The boy was also followed-up for severe myopia and constipation. He had a non-symptomatic large atrial septal defect, ASD (ostium secundum type).

At 10 years of age the dysmorphic traits continued, suggestive of Opitz C syndrome. The patient presented bulging eyes with true proptosis, mild epicanthus, hypoplastic nose, small mouth with normal philtrum and palate, and normal auricles (see detailed description in Table 1 and Fig. 1: a, g and l). From the neurological point of view he presented with spastic tetraparesis, with ulnar deviation of the hands, wide-base gait (increased distance between the tibial malleolus when walking) not in the range of a cerebellar ataxia but denoting clumsiness and a subtle gait disturbance, and flexion of hips and knees. The patient lacks expressive language, but has improved his ability to understand and to establish communication. He does not respond to simple commands and has poor attention span. He is unable to chew and is fed mashed food. He walks with increased lift base and can take some steps alone. Usually, he needs walker support to get around and has no sphincter control. The patient is currently on physiotherapy and speech therapy, and pharmacological treatment with risperidone and methylphenidate due to behavioural disturbances and ADHD (attention deficit-hyperactivity disorder) traits, respectively.

Patient 2 (P2)

The patient is an 11-year-old boy, the first child of healthy non-consanguineous parents. He was born at 38 + 5 weeks via caesarean section due to breech presentation after an uneventful pregnancy. At birth, weight was 2.97 kg (30th percentile, –0.45 SD), length was 49 cm (25th percentile, –0.28 SD), and cranial circumference was 33 cm (10th percentile, –0.61 SD). On neonatal examination, sacral and suprasternal dimples were observed on ultrasound with normal subjacent tissues and reducible bilateral inguinal hernia.

The neonatal period was significant for poor feeding, mild hypertonia of limbs, and delayed gross motor development. He achieved head control at 3 months, sitting at 15 months, and crawling and kneeling later than 24 months; currently he walks only with a walker. His speech was also delayed as he started babbling at 22

Table 1 Deep dysmorphological phenotyping after clinical evaluation of the 5 patients presented here

	Patient 1	Patient 2	Patient 3	Patient 4	Patient 5	Total
Variant's genomic position	8:41792353	8:41792098	8:41792310	8:41834814	8:41791480	
cDNA change	c.3385C > T	c.3640A > T	c.3427_3428insTA	c.1075G > A	c.4254_4257 delTGAG	
Protein change	p.(Arg1129*)	p.(Lys1214*)	p.(Ser1143 Leufs*5)	p.Gly359Ser (p.Pro509 Thrfs*11)	p.(Glu1419 Trpfs*12)	
Exon	17/17	17/17	17/17	7/17	17/17	
Inheritance	De novo	De novo	De novo	De novo	De novo	5 de novo
dbSNP	rs786200960	—	—	—	—	
GnomAD	—	—	—	1/250564	—	
ClinVar	—	—	—	—	Pathogenic	
Current age (years)	16	11	9	8	6	10 av
Gender	Male	Male	Female	Male	Female	2F/3M
Ethnicity (country of origin)	Caucasian (Spain)	Caucasian (Spain)	Caucasian (Spain)	Caucasian (Spain)	Chinese (China)	
Neurological						
Global developmental delay (HP:0001263)/ Intellectual disability (HP:0001249)	+ (severe)	+	+	+	+	5/5
Autistic behaviour (HP:0007229)	NE	+	—	+	+	3/4
Speech delay (HP:0000750)	+	+	+	+	+	5/5
Seizures (HP:0001250)	+	+	—	+	—	3/5
Sleep disturbance (HP:0002360)	—	+	—	+	—	2/5
Hypotonia (HP:0001290)	—	—	—	+	+	2/5
Stereotypy (HP:0000733)	+	+	+	—	+	4/5
Lower limb hypertonia (HP:0006895)	+	+	+	—	—	3/5
Unstable gait (HP:0002141)	+	+	+	+	+	5/5
Craniofacial						
Microcephaly (HP:0000252)	+	+	+	+	+	5/5
Triangular face (HP:0000325)	+	+	+	—	+	4/5
Long face (HP:0000276)	+	—	+	+	+	4/5
Facial asymmetry (HP:0000324)	+	—	—	+	—	2/5
Frontal bossing (HP:0002007)	+	—	—	+	—	2/5
Midface retrusion (HP:0011800)	—	+	+	—	+	3/5
Sparse medial eyebrows (HP:0025325)	+	+	+	+	+	5/5
Arched eyebrows (HP:0002553)	+	+	+	+	+	5/5
Thin eyebrows (HP:0045074)	+	+	+	—	—	3/5
Swollen skin on the upper eyelids (HP:0012724)	—	—	—	+	—	1/5
Epicanthal folds (HP:0000286)	+	—	—	+	+	3/5
Proptosis (HP:0000520)	+	—	+	—	—	2/5
Deep set eyes (HP:0000490)	—	—	+	+	—	2/5
High nasal bridge (HP:0000426)	+	—	—	—	+	2/5
Broad nasal tip (HP:0000455)	+	+	+	—	+	4/5
Bifid nasal tip (HP:0000456)	+	+	+	—	—	3/5
Prominent columella (HP:0009765)	+	—	—	—	—	1/5
Low-set ears (HP:0000369)	+	+	+	—	+	4/5
Anteverted ears (HP:0040080)	—	—	—	+	+	2/5
Prominent antihelix (HP:0000395)	+	+	+	+	+	5/5
Prominent antitragus (HP:0008593)	—	—	+	+	+	3/5
Hypoplastic tragus (HP:0011272)	—	+	—	+	—	2/5

Table 1 Deep dysmorphological phenotyping after clinical evaluation of the 5 patients presented here (*Continued*)

	Patient 1	Patient 2	Patient 3	Patient 4	Patient 5	Total
Small earlobe (HP:0000385)	+	-	+ (mild)	+ (mild)	-	3/5
Short philtrum (HP:0000322)	-	-	±	+ (mild)	-	2/5
Small mouth (HP:0000160)	+	-	-	-	+	2/5
Wide mouth (HP:0000154)	-	-	±	+	-	2/5
Prognathism (HP:0000303)	-	+	±	-	-	2/5
Pointed chin (HP:0000307)	+	+ (mild)	±	-	-	3/5
Ocular						
Convergent strabismus (HP:0000565)	+ (left eye)	+	± (left eye)	-	+	4/5
Astigmatism (HP:0000483)	-	+	±	-	-	2/5
Myopia (HP:0000545)	+	+	-	-	-	2/5
Amblyopia (HP:0000646)	±	-	±	-	-	2/5
Nasolacrimal stenosis (HP:0000579)	±	-	±	-	-	2/5
Conjunctivitis (HP:0000509)	-	-	±	-	-	1/5
Thorax & Abdomen						
Long thorax (HP:0100818)	+	+	±	±	+	5/5
Narrow thorax (HP:0000774)	+	±	±	±	±	5/5
Asymmetric chest (HP:0001555)	pectus excavatum	-	-	-	-	0/5
Wide intermamillary distance (HP:0006610)	±	±	+ (mild)	+ (mild)	±	5/5
Low-set nipples (HP:0002562)	-	±	NE	+ (mild)	±	3/4
Inverted nipple (HP:0003186)	+ (left)	-	NE	-	-	1/4
Bulging abdomen (HP:0001538)	-	-	±	-	±	2/5
Prominent umbilicus (HP:0001544)	-	-	±	-	-	1/5
Limbs						
Skin syndactyly between 3rd and 4th fingers (HP:0011939)	+ (mild)	-	-	-	-	1/5
Upper limb amyotrophy (HP:0009129)	±	±	±	±	-	4/5
Lower limb amyotrophy (HP:0007210)	±	±	±	±	-	4/5
Lower limb asymmetry (HP:0100559)	-	-	±	NE	-	1/4
Genu valgum (HP:0002857)	±	-	+ (mild)	-	-	2/5
Genu varum (HP:0002970)	-	-	-	+ (mild)	-	1/5
Enlargement of the proximal interphalangeal joints (HP:0006185)	±	+ (mild)	-	-	-	2/5
Pes planus (HP:0001763)	±	±	±	±	-	4/5
Deviation of the hallux (HP:0010051)	±	-	±	-	-	2/5
Short halluces (HP:0010109)	-	-	+ (mild)	±	-	2/5
Sandal gap (HP:0001852)	-	-	-	±	-	1/5
Hammertoe (HP:0001765)	-	-	-	±	-	1/5
Other						
Prenatal problems (HP:0001197)	IUGR	-	Mild pyelectasis in left kidney; IUGR	-	-	2/5
Cardiovascular problems (HP:0001626)	±	+ (atrial septal defect)	+ (pulmonary stenosis)	-	+ (atrial septal defect)	4/5
Respiratory problems (HP:0002795)	-	±	-	-	-	1/5
Genitourinary problems (HP:0000119)	Small testis and penis; No sphincter control	-	-	Abnormal sphincter control	-	2/5
Feeding problems (HP:0001968)	±	±	±	±	±	5/5
Freckling (HP:0001480)	Freckles on the thorax	Numerous freckles (face and body)	-	-	-	2/5
Webbed neck (HP:0000465)	-	-	-	-	-	0/5

Av average, IUGR Intrauterine growth retardation, NE Not Evaluable



Fig. 1 Images depicting key phenotypic features of the cases presented here. **a** Patient 1 facies at 16 years of age, **b** and **c** Patient 2 facies at 11 years, **d** Patient 3 facies at 9 years, **e** Patient 4 facies at 8 years, and **f** Patient 5 facies at 6 years. Panels **g** to **k** show the patient's gestalt (at the same age as the facies figure). **l** Patient 1 hand. **m** and **n** Patient 5 ft and hands

months. His fine motor skills have improved with therapy; he is able to grab objects and play with both hands. Recurrent pneumonias were diagnosed with several hospital admissions, and dysphagia to liquids was observed, requiring thickeners. At age 2 years, an echocardiogram showed a 12-mm small ASD, ostium secundum type that was occluded with vascular plug system. Testing for in-born errors of metabolism (with plasma amino acids, acylcarnitine profile, total and free carnitines, and urine organic acids) was negative.

At age 6 years, he presented 2 episodes of loss of consciousness but electroencephalogram (EEG) did not confirm electric seizures. He was treated with valproic acid, currently on withdrawal. Brain MRI showed areas of polymicrogyria on the posterior right insula, delayed myelination, and slight descent of the cerebellar tonsils through the foramen magnum (Arnold-Chiari malformation).

On physical examination at age 11 years (Table 1 and Fig. 1: b, c and h), the patient was found to have a short stature (height 113 cm, <3rd percentile, -4.75 SD), microcephaly (cranial circumference of 49.5 cm, <3rd percentile, -3.74 SD), and dysmorphic facial features such as flat facies, hypertelorism, mildly blue sclera and proptosis, full lower lip and protruding tongue that led to an open mouth expression, and low-set dysplastic ears. Ocular abnormalities included endotropia, astigmatism, and myopia. Additionally, the patient had one right supernumerary nipple, a single palmar crease on the right hand, poor palmar sulcation, and mild fifth finger clinodactyly in both hands. Neurologically, he showed intellectual disability, poor eye contact, generalized hypertonia, the need for a stroller to walk, and absence of comprehensible language, but with babbling. He presents midline manual stereotypies and suffers sleep disturbances with frequent awakenings.

Patient 3 (P3)

The patient is a 9-year-old female, the only child of healthy non-consanguineous parents. Intrauterine growth retardation and mild left pyelectasis were detected during pregnancy. Birth weight was 2.30 kg (1st percentile, -2.25 SD) and cranial circumference was 30.5 cm (<3rd percentile, -3 SD). Screening for congenital disorders of metabolism was negative. Feeding difficulties and oral candidiasis were observed during the perinatal period. The subject achieved head control at 2 months, sat up at 10–12 months, began to crawl at 23 months, and presented unstable gait at age 3. At age 2, she was diagnosed with beta-thalassaemia minor (of paternal inheritance). Mild valvular pulmonary stenosis was also observed, although this problem had disappeared by 6 years of age. EEG was normal at the age of 3 years. Brain MRI, performed at few months of age,

showed unspecific delayed myelination, although repeated imaging was considered normal when the patient was 3 years old.

At 6 years of age, when she was recruited by the SpainUDP (Spanish Undiagnosed Rare Diseases Program, <http://spainudp.isciii.es/>), she had global developmental delay, intellectual disability, language impairment, stereotypies, astigmatism, amblyopia, and recurrent conjunctivitis. Her physical exam showed craniofacial dysmorphisms including microcephaly, midface retraction, mild hypoplasia of the ear lobe, prominent antitragus, sparse medial eyebrows, proptosis, strabismus, broad and bifid nasal tip, short philtrum, prognathism, and big mouth (Table 1 and Fig. 1: d and i). She also had wide intermammillary distance, bulging abdomen, protruding umbilicus placed on a small depression of the abdomen, mild genu valgo, pes planus, and fibular deviation of halluces.

Patient 4 (P4)

The patient is an 8-year-old boy, the only child of non-consanguineous parents. No problems were detected during pregnancy and the neonatal period. He was born at term with a birth weight of 3.7 kg (76th percentile, $+0.70$ SD) and a cranial circumference of 35 cm (34th percentile, -0.42 SD). He achieved head control at 3 months, sat up at 8.5 months, and began to walk independently at 16 months. Microcephaly was detected at 2 months of age and he was diagnosed with atypical absences with eyelid myoclonias at the age of 16 months. He was treated with valproate from 21 months to 5 years with acceptable control of seizures. When the proband was 5 years old, it was withdrawn due to its association with adverse reactions (nauseas, vomiting, and weight loss). A few months later, valproate treatment was administered again since the number and intensity of epileptic crises had increased. In this recurrence of epilepsy, ethosuximide was needed together with valproate to achieve seizure control. Several EEGs carried out starting at age 3 years have disclosed spike-wave anomalies. When he was admitted to SpainUDP, at 6 years of age, the subject showed intellectual disability with altered fine motor coordination, unstable gait with frequent falls, language impairment, and autistic behaviour. He has always had sleep disturbances and hyporexia. Hypotonia with reduced muscle bulk has also been observed. Physical examination (Table 1 and Fig. 1: e and j) showed microcephaly, long face, mid facial asymmetry, frontal central bossing, swollen skin on the upper eyelids, epicanthus, deep set eyes, mildly everted lower eyelid in its external part, and deep horizontal groove under the lower lip. Additional features include a slender appearance, scarce body adiposity, long and narrow thorax, mild genu varo (bilateral), pes planus, short halluces,

sandal gap between the first and second toes, and flexed fifth toes.

Metabolic testing (including urine organic acids and glucose in cerebrospinal fluid) was normal. Brain MRI was normal.

Patient 5 (P5)

The patient is a 6.5-year-old girl, first child of healthy non-consanguineous parents and with a healthy younger sister. The subject was born at term with an uneventful delivery and with a birth weight of 3.14 kg (42nd percentile, -0.2 SD), a cranial circumference of 33 cm (10th percentile, -0.61 SD), and Apgar 9/10 at 1 and 5 min. New-born screening for inborn errors of metabolism was normal. She had feeding problems from the neonatal period. During her hospital admission for dysphagia at 2 months of age, an atrial septal defect (ASD) was detected, which was surgically repaired at 16 months. She had delayed motor skills, with head control at 6 months, sitting up at 13 months, crawling at 16 months, and autonomous although unstable gait developing at age 2.

The subject has received physical, speech, and behavioral therapies and has attended a special school since 6 years of age. She is not able to talk, shows difficulties in adapting to new environments, shows significant behavioral problems with particular impact on the social domain, and has poor eye contact. Physical examination (Table 1 and Fig. 1: f, k, m and n) showed dysmorphic features characterized by midface hypoplasia, almond-shaped eyes, and slightly upslanted palpebral fissures, and absent Cupid's bow. Ears have underdeveloped anti-helix, and are slightly low set, with increased posterior angulation. The hands show a complex palmar dermatoglyphic pattern with abnormal square radial border morphology. Tone, strength, and deep tendon reflexes are normal.

Remarkably, cranial MRI at age 6 revealed prominent cerebellar interfolia space compared with a previous MRI at 2 years of age; this is compatible with progressive cerebellar atrophy. No other significant alterations were detected on MRI. The subject was recruited by the Undiagnosed Rare Disease Program of Catalonia (www.urdc.cat).

Genetic results

Patient 1

A normal karyotype (46, XY) was determined. A trio-based whole exome study (WES) revealed a de novo heterozygous variant NM_006766:c.3385C > T (p.Arg1129*) in the *KAT6A* gene, which was confirmed by Sanger sequencing. This change was previously identified in a child with global developmental delay [5].

Other variants of unknown clinical relevance (VUS) are summarized in Additional file 1: Table S1.

Patient 2

Karyotype, subtelomeric fluorescent in situ hybridization (FISH), kit MLPA panel studying recurrent genomic disorders (SALSA® P245-B1), chromosomal microarray, and testing for fragile X, *MECP2/FOXP1* genes, Angelman syndrome, Pitt-Hopkins syndrome, mucopolysaccharidoses, and congenital disorders of glycosylation, yielded normal results. Clinical exome of the index case revealed a heterozygous de novo variant in *KAT6A* in the proband (NM_006766: c.3640 A > T (p.Lys1214*)]. Other VUS detected in the patient were: heterozygous c.852G > A (p.Leu284Leu) variant and heterozygous c.1467 + 16A > C variant in the *FOXP1* gene (Sup. Table 2).

Patient 3

Prior genetic and metabolic testing included karyotype, FISH at 4p16.3, array-CGH, and 7-dehydrocholesterol testing, all negative. Trio-based WES revealed a heterozygous de novo variant (NM_006766:c.3427_3428insTA) in *KAT6A* in the proband, which was confirmed through Sanger sequencing. This frameshift variant consists of an insertion of two nucleotides at exon 17 and it leads to the premature termination of the protein (p.Ser1143-Leufs*5). The variant has not been previously described in the genomic databases.

Patient 4

Before WES, several genetic tests were carried out, with negative results: karyotype, array-CGH (60 K), Fragile X, Angelman, and diagnostic exome sequencing (DES) for epilepsy (543 genes). Trio-based WES was performed and a de novo *KAT6A* variant was identified in the patient (NM_006766:c.1075G > A), which was confirmed through Sanger sequencing. This variant predicts a replacement of guanine by adenine at codon 359 in exon 7 [p.(Gly359Ser)]. It has been found in only one carrier out of 250,564 alleles in gnomAD. It is predicted to be 'deleterious' or 'putatively pathogenic' by a variety of bioinformatic tools (PolyPhen2, Mutation Taster) and to be 'tolerated' by SIFT (score 0.28); CADD score is 16.9. Altogether, this variant is classified as 'pathogenic' according to the AMCG/AMP 2015 guidelines. In addition, the Human Splicing Finder software (3.1 version; January 10, 2018) predicts a potential alteration of splicing consisting of the generation of a cryptic acceptor site (AGTTCGAACTAGCC) at exon 7 (which was not experimentally observed, see below), and the loss of a predicted ESE (GGCCCTGG) for splicing factor SC35 (starting at c.1075G, which is not present in the mutant allele).

Table 2 Clinical overview of KAT6A syndromic patients

Features	This report		Trinh et al. 2018 [12]	Efthymiou et al. 2018 [15]	Alkhateeb et al. 2019 [14]	Kennedy et al. 2019 [13]			Total			Overall %	
	LT ^a	M ^b	M	LT	LT	ET	LT	M	ET	LT	M		
Protein change	2FS; 2NS	p.G359S	p.N1975S	p.S1113*	p.K1130 fs*	10FS; 7NS; 1del	19FS; 29NS	6MS	10FS; 7NS; 1del	13FS; 38NS	8MS		
Gender (F/M)	2/2	0/1	1/1	0/1	0/1	8/10	25/23	2/4	8/10	27/27	3/6	38/43	
Perinatal features													
Small for gestational age	2/4	0/1	2/2	NR	0/1	2/15	8/44	0/4	2/15	10/49	2/7	14/71	20
Feeding difficulties/failure to thrive	4/4	1/1	1/1	1/1	1/1	10/18	40/46	4/6	10/18	46/52	6/8	62/78	79
Neonatal complications (low Apgar scores, respiratory distress ...)	1/4	0/1	NR	0/1	0/1	0/1	4/5	NR	0/1	5/11	NR	5/12	42
Neurological features													
Global developmental delay/Intellectual disability	4/4	1/1	2/2	1/1	1/1	18/18	44/44	4/4	18/18	50/50	7/7	75/75	100
Speech delay/Absent speech	4/4	1/1	1/2	1/1	1/1	18/18	44/44	5/5	18/18	50/50	7/8	75/76	99
Unstable/abnormal gait	4/4	1/1	0/2	1/1	1/1		1/3	NR	0/0	7/9	1/3	8/12	67
Neonatal hypotonia	2/4	1/1	1/1	1/1	NR	8/18	40/47	5/6	8/18	43/52	7/8	58/78	74
Seizures	2/4	1/1	1/2	1/1	0/1	2/17	2/47	1/6	2/17	5/53	3/9	10/79	13
Sleep disturbance	1/4	1/1	NR	NR	NR	3/16	15/28	2/4	3/16	16/32	3/5	22/53	42
Autistic behavior/behavioral problems	2/3	1/1	NR	NR	NR	4/15	8/18	3/3	4/15	10/21	4/4	18/40	45
Craniofacial features													
Microcephaly	4/4	1/1	2/2	1/1	0/1	1/18	20/45	1/15	1/18	25/51	1/5	27/74	36
Frontal bossing/large forehead	1/4	1/1	NR	1/1	0/1	0/1	1/4	NR	0/1	3/10	1/1	4/12	33
Bitemporal narrowing	1/4	0/1	0/2	1/1	0/1	NR	3/3	NR	NR	5/9	0/3	5/12	42
Ear anomalies (large, low set, rotated, small earlobe ...)	4/4	1/1	NR	1/1	NR	NR	9/11	0/1	NR	14/16	1/2	15/18	83
Palpebral ptosis	1/4	0/1	1/2	0/1	NR	3/18	7/45	0/6	3/18	8/50	1/9	12/77	16
Eye anomalies (proptosis, hypertelorism, deep set)	4/4	1/1	2/2	1/1	1/1	NR	3/8	1/1	0/0	9/14	4/4	13/18	72
Epicanthal folds	2/4	1/1	0/2	NR	0/1	NR	2/7	0/1	0/0	4/12	1/4	5/16	31
Broad/bulbose nasal tip	4/4	0/1	2/2	1/1	0/1	16/18	35/40	3/5	16/18	40/46	5/8	61/72	85
Thin upper lip	0/4	0/1	2/2	0/1	1/1	7/17	28/38	2/4	7/17	29/44	4/7	40/68	59
Micrognathia	0/4	0/1	0/2	0/1	0/1	NR	6/12	0/1	0/0	6/18	0/4	6/22	27
Ocular problems													
Strabismus	4/4	0/1	2/2	NR	NR	9/17	27/47	1/5	9/17	31/51	3/8	43/76	57
Visual defects	4/4	0/1	2/2	NR	NR	9/17	26/38	1/3	9/17	30/42	3/6	42/65	65
Other features													
Congenital heart defect	4/4	0/1	0/2	NR	0/1	5/18	32/46	0/6	5/18	36/51	0/9	41/78	53
Reflux	2/4	0/1	NR	NR	NR	7/18	27/38	3/6	7/18	29/42	3/7	39/67	58
Constipation	1/4	0/1	1/2	NR	NR	4/16	18/28	3/6	4/16	19/32	4/9	27/57	47
Recurrent infections	1/4	0/1	NR	NR	NR	5/16	24/34	1/5	5/16	25/38	1/6	31/60	52

AF Anterior fontanelle, CVI Cortical visual impairment, Del Deletion, ET Early truncating, FS Frameshift, GERD Gastroesophageal reflux disease, LT Late truncating, M Missense, NR not reported, NS nonsense, PDA Patent ductus arteriosus; Features present in more than 60% of the patients are indicated in bold with % of the total

^a Patients 1–3 and 5. ^b Patient 4

Patient 5

The subject has a normal karyotype (46,XX) and molecular karyotype by array-CGH (60 K). Singleton WES was performed followed by trio-based segregation with Sanger sequencing. The analysis showed a heterozygous de novo frameshift deletion of four nucleotides (NM_006766: c.4254_4257delTGAG) in exon 17 of the *KAT6A* gene, already defined as 'pathogenic' in ClinVar and reported by Kennedy et al. [13]. The mutant mRNA is predicted to be translated as a truncated protein with a premature termination 12 amino acids after the frameshift (p. Glu1419Trpfs*12). The variant has not been described in healthy population in the genomic databases.

KAT6A expression analysis

Since pathogenic *KAT6A* mutations are usually truncating, and given that predictors indicate that the c.1075G > A variant identified in patient 4 may be affecting splicing mechanisms, we analysed the *KAT6A* splicing pattern of this patient using mRNA from peripheral blood cells. Expression analysis showed two bands: a normal amplicon of 552 bp and a shorter amplicon of 167 bp (with very low intensity) corresponding to an aberrant splicing (Fig. 2a). Sanger sequencing of this minor fragment revealed the loss of exon 7 (consistent with the predicted loss of an ESE), and of 65 additional bp of exon 6 (indicative of the use of a non-canonical cryptic donor site, Fig. 2b). The putative translation of this aberrant mRNA would involve a frameshift leading to a premature early termination codon (p.Arg330Serfs*13), potentially leading to nonsense mediated decay (NMD). The sequencing of the upper band showed both alleles (wild type and mutant), demonstrating that the allele carrying the missense mutation is mostly correctly spliced (Fig. 2c).

Discussion

Since 2015, around 80 cases of syndromic intellectual disability due to mutations at the *KAT6A* gene have been described in the literature, delineating a new syndrome with variable presentation (Table 2 and Fig. 3) [4–15]. Here, we present 5 patients with de novo variants at *KAT6A*, four 'late truncating' and one missense variant, and we describe their clinical presentations, adding further clinical and molecular delineation to the *KAT6A* syndrome. The four late truncating mutations (in patients P1–3, and 5) are in the last exons and are thus predicted to escape NMD. The phenotypes of these patients are similar to those with late truncating mutations described by Kennedy et al. [13].

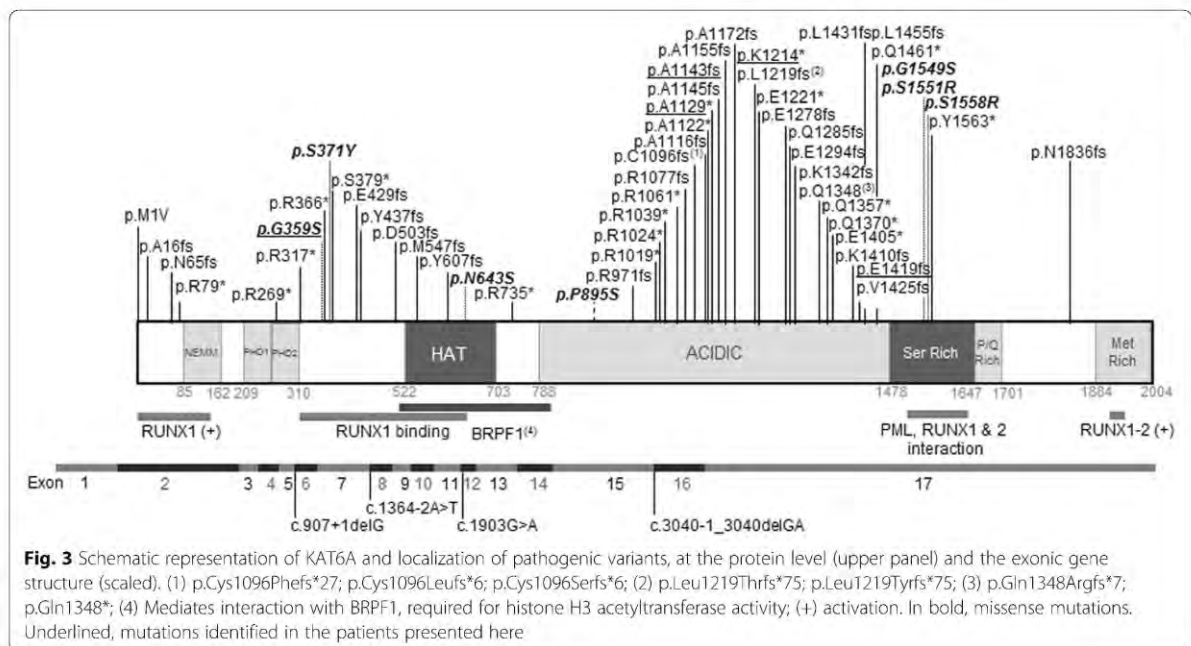
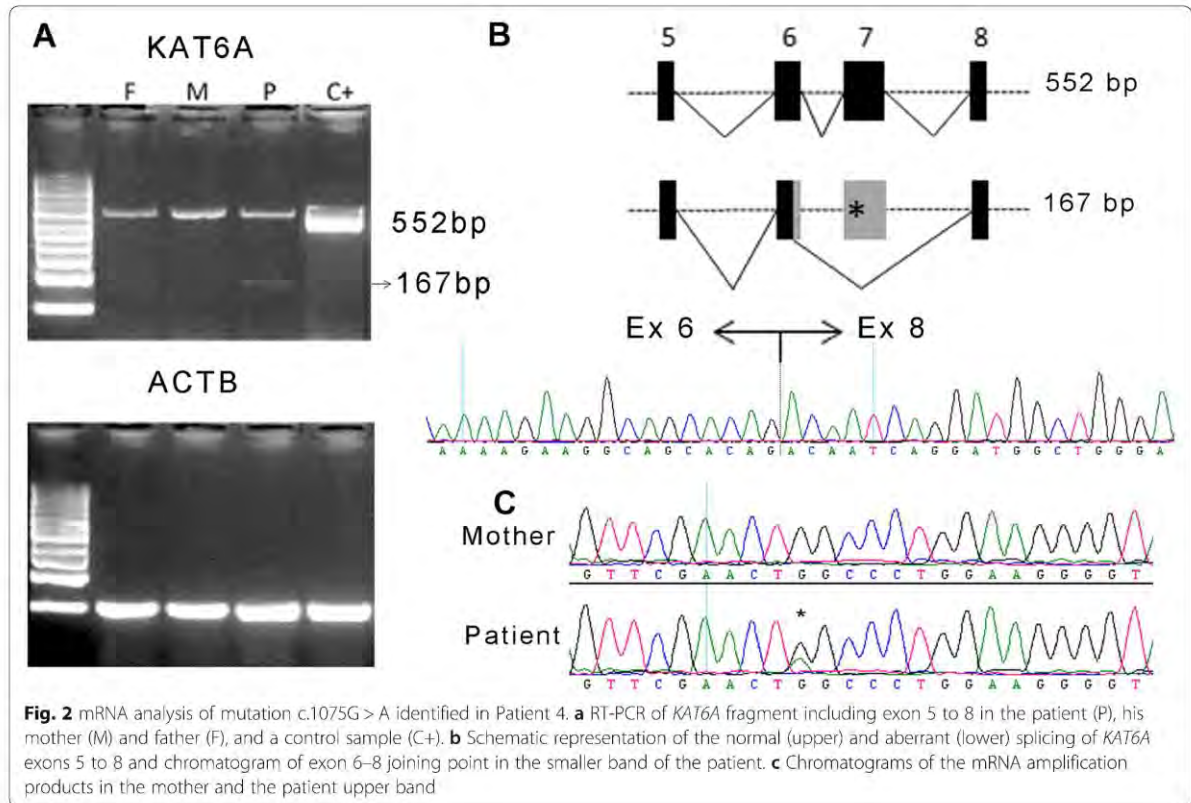
The main characteristic feature of this syndrome is neurological involvement. All five patients presented with moderate or severe developmental delay or intellectual disability with severe involvement of speech and

expressive language being more affected than comprehension, as in nearly all *KAT6A* syndrome patients [13]. Also, all patients described here presented with motor delay, and two of them showed similar manual stereotypies (hand flapping or fluttering), a feature that has not been highlighted in previous reports. This finding combined with the poor eye contact and language impairment could represent part of the autistic spectrum behaviour, one of the most frequent and significant neurological symptoms. In addition, 3 out of the 5 patients presented here suffered epilepsy, a manifestation reported in only 13% of the previously described series.

While craniofacial dysmorphic features are present in all the patients, some of them are very unspecific and some patients present very mild alterations [12, 14], which renders clinical identification of this syndrome very challenging. Nevertheless, some facial similarities can be identified in several patients (such as P2 and P3). All five patients presented with microcephaly. Microcephaly has been reported in 36% of all patients, and nearly in half of the patients with late truncating mutations, but it is less frequent in patients bearing missense or early truncating mutations (Table 2). Also, patient 1 presented with trigonocephaly due to synostosis of the metopic suture. Different kinds of craniosynostoses have been previously reported [4], including sagittal synostosis [8, 13] and scaphocephaly [10]. Frontal bossing and/or bitemporal narrowing is reported in 30–40% of patients. In general, a broad/bulbous nasal tip is present in the majority of patients (86%) together with ocular anomalies (such as hypertelorism, proptosis or deep set eyes and downslanting palpebral fissures [6, 9, 12]), mouth anomalies (down-turned corners of the mouth [9] or protruding tongue [6, 7]) and ear anomalies (large, low set, rotated ...), present in all five patients reported here. Joint hypermobility, a frequent finding in these five patients, has also been previously reported [9]. Other clinical findings previously reported are supernumerary nipple [6], cryptorchidism [6], and syndactyly [6].

Interestingly, all the present patients except for patient 4 (bearing a missense mutation) presented with congenital heart defects. Cardiac defects have been reported in around 70% of patients bearing late truncating mutations, but not hitherto in patients with missense mutations. Brain abnormalities, found in three of our patients (Patients 2, 3 and 5), have been frequently reported, including delayed myelination [13] and benign enlargement of the pericerebral areas [9], with the lack of the olfactory bulb [6] and pituitary abnormalities [11] being the two most consistent and noteworthy midline neuroimaging findings.

All five patients presented with feeding difficulties or failure to thrive, and patients 2, 4, and 5 also presented with neonatal hypotonia, traits reported in more than



70% of the *KAT6A* patients. Severe food allergies have been previously reported in 3 patients [8] and cow's milk intolerance was noted in patient 42 in Kennedy et al. [13], although it is not clear if this is associated with mutations in *KAT6A*. None of the patients reported here presented with food intolerances or allergies.

Recurrent infections, observed in two patients of our cohort with late truncating variants, have been reported in nearly half of the previously published patients and in 71% of patients bearing late truncating variants [13]. This observation is in agreement with the improper B cell differentiation reported in the conditional KO murine model [16] and with the role of *KAT6A* as an essential factor for long-term repopulation of hematopoietic stem cells [17].

While the majority of *KAT6A* syndromic mutations are truncating, missense mutations have recently been described [12, 13]. Here we present a case with clinical characteristics similar to the rest of *KAT6A* patients, bearing the de novo missense mutation p.Gly359Ser. While *KAT6A* is clearly constrained against LoF variants (with a pLI = 1 and oe = 0.02, gnomAD accessed June 2019), it is not constrained for missense mutations, with an oe = 0.83, clearly above the recommended CI < 0.35. All the previous missense mutations associated with pathogenicity affect highly conserved residues in critical functional regions of the protein [13]. In addition, it is of note that all these changes involve serine residues, either eliminating an existing Ser or introducing a new one, as in the case of p.Gly359Ser, reported in patient 4. *KAT6A* C-terminal domain contains a serine- and methionine-rich domain that is essential for its binding to the transcription factor Runx2 [3]. As the hydroxyl group of serine is highly reactive and is able to form hydrogen bonds with a variety of polar substrates, the alteration of their number and position seems to be especially critical in *KAT6A*, otherwise tolerant of missense substitutions. In addition, we have verified that this variant can affect normal processing of pre-mRNA by producing an aberrant splicing consisting of the loss of exon 7 and 65 bp of exon 6. This mutation leads to early truncation and is assumed to be affected by the NMD process, reducing total *KAT6A* mRNA. It should be noted that this alteration seems to have a minor impact. It is likely that the pathological consequences of this variant are mainly due to the amino-acid substitution, leading to a deficit of functional *KAT6A*. Concordantly, the patient did not present with cardiac alterations, similar to the majority of patients bearing missense mutations.

Conclusions

With this study, we have expanded the clinical delineation of *KAT6A* syndrome, an emerging and distinctive entity which is potentially clinically diagnosable. Given

the severity of its clinical features and its reproductive implications, it is important to make an early diagnosis of this condition, including identification of those patients bearing missense mutations.

Material and methods

Biological samples

Genomic DNA of the patients and their parents was obtained from peripheral blood at the respective institutions (Hospital La Fe, Valencia, for P1, Hospital Sant Joan de Deu, Barcelona, for P2, Instituto de Salud Carlos III, Madrid, for P3 and P4, and Hospital del Mar, Barcelona, for P5). Signed informed consent was obtained from each patient's parents. All protocols were approved by the ethics committee of each of the institutions and all methods were performed in accordance with the relevant guidelines and regulations.

Whole exome sequencing and molecular analyses

Patient 1

Whole exome sequencing of the proband and his parents was performed in the National Centre of Genomic Analysis (CNAG; Barcelona, Spain) using the Illumina HiSeq-2000 platform. Exome capture was performed with Agilent SureSelect v5 (Agilent, CA, USA). The samples were sequenced at a coverage of 140x. The data were analyzed as described elsewhere [18]. Annotation, filtering, and prioritization of variants were carried out using VarAFT software [19]. The results were then filtered under de novo dominance and recessive hypotheses. Variants with a minimum allele frequency (MAF) above 0.001 for AD filtering and above 0.01 for AR filtering in the common population (according to gnomAD) were excluded. Variants in genes included in DDG2P (The Development Disorder Genotype-Phenotype Database [15, 20]), and covered by at least 10 reads, were prioritized for validation (it should be noted that those who carried out the original DECIPHER analysis and collection of the data bear no responsibility for the further analysis or interpretation of it).

The mean coverage was of 153.43, 174.29, and 160.829 reads for the patient, father and mother respectively, and 97.2–97.9% of the target region was covered with at least 10 reads (C10). A total of 5 variants in 4 genes were selected for validation by Sanger sequencing. Primer sequences and PCR conditions are available on request. PCR reaction, purification, and sequencing were performed as described previously [20].

Patient 2

Whole exome sequencing of the index case was carried out with the platform Illumina NextSeq500, using the Agilent SureSelect v6 QXT capture kit. For the analysis, several bioinformatics tools were used. The exome

design covered approximately 95% of the coding regions of the analysed genes. The sequences used as reference can be found at the RefSeq database. The estimated frequencies were calculated from the 1000 genomes, Complete Genomics and NHLBI Exome Sequencing Project databases. The nomenclature of mutations was based on the recommendations of the Human Genome Variation Society. The analysis was carried out according to the recommendations of the American College of Medical Genetics. The results were then filtered under *de novo* dominance and recessive hypotheses. Variants with a minimum allele frequency (MAF) above 0.001 for AD filtering and above 0.01 for AR filtering in the common population (according to GnomAD) were excluded. Variants in genes included in DDG2P (The Development Disorder Genotype-Phenotype Database [21, 22]), and covered by at least 10 reads, were prioritized for validation (it should be noted that those who carried out the original DECIPHER analysis and collection of the data bear no responsibility for the further analysis or interpretation of it).

Patient 3

After exhaustive revision of clinical information of patient 3, she was admitted to the Spanish Undiagnosed Rare Diseases Program (SpainUDP) [23]. Also, this patient and her unaffected biological parents were enrolled in the FP7-funded '2016 BBMRI-LPC WES Call' (Eurobiobank website, accessed on 19th July 2018) to carry out the research shown in this article.

Trio-based whole exome sequencing (WES) for this project was conducted at the Centro Nacional de Análisis Genómico (CNAG-CRG, Spain). SureSelect Human All Exon V5 (Agilent Technologies) was used to perform whole exome enrichment following the manufacturer's instructions. The captured libraries were sequenced using TruSeq SBS Kit v3-HS (Illumina, Inc), in paired-end mode with a read length of 2x100bp. On average, 92x median coverage for each sample was generated in a fraction of a sequencing lane on HiSeq2000 following the manufacturer's protocol. Images analysis, base calling, and quality scoring of the run were processed using the manufacturer's software Real Time Analysis (RTA 1.13.48, HCS 1.5.15.1) and followed by generation of FASTQ sequence files by CASAVA. High-quality reads were aligned to the decoy version of the GRCh37 reference genome used by the 1000 Genomes Project (hs37d5) using BWA-MEM (version 0.7.8), and variants were identified following GATK Best Practices [24] using HaplotypeCaller (version 3.6). All variants with a minimum coverage of 8 reads and minimum genotype quality (GQ) of 20 were uploaded to the Genome-Phenome Analysis Platform (RD-Connect GPAP) [25, 26] for variant filtration and prioritization. Additionally,

phenotypic terms were extracted from clinical documents stored in the patient registry by a member of SpainUDP, mapped to HPO (Human Phenotype Ontology) [27] terms, and uploaded to PhenoTips [28], a software tool available in the RD-Connect GPAP. This platform allows filtering and refining of the results by mode of inheritance, population frequencies, *in silico* pathogenicity prediction tools, and HPO codes [25, 26]. This filtering process was carried out by two independent researchers of SpainUDP with common criteria, and the results were compared in order to reach a consensus on selection of the candidate variants, which were confirmed by Sanger sequencing in all family members. Finally, various sources of information were consulted to build a report with a detailed review of the scientific evidence supporting the correlation between the detected causative variant and the proband's phenotype.

Patient 4

Patient 4 was admitted to the SpainUDP and underwent phenotypic analysis following the standard criteria established by this program [23]. After peripheral blood genomic DNA isolation of patient 4 and his biological parents (see case 3 for details), trio-based WES and selection of candidate variants were performed as described by López et al. [23]. Variants assessed as pathogenic and possibly contributing to the proband's phenotype were validated by Sanger sequencing in the full trio.

Patient 5

Patient 5 was admitted to the URDCat Program after deep phenotyping. Patient's whole exome sequencing from extracted DNA from peripheral blood was carried out at the National Centre of Genomic Analysis (CNAG; Barcelona, Spain) using the Illumina HiSeq-2000 platform. Exome capture was performed with Nimblegen SeqCap EZ MedExome + mtDNA 47 Mb and the samples were sequenced at coverage of 90x. Sequencing data were analysed according to the project's established pipeline, and afterwards SNV, indel, CNV, and mosaicism analysis was performed using the RDCat Genomic Analysis Platform. Variants assessed as pathogenic and possibly contributing to the proband's phenotype were validated by Sanger sequencing in the trio.

Gene expression analysis

In the case of patient 4, gene expression of *KAT6A* transcripts was evaluated in peripheral blood cells obtained from the proband and his progenitors. RNA was extracted from cells using RNeasy Mini Kit (Qiagen), and then reverse transcribed by Moloney Murine Leukemia Virus Reverse Transcriptase (M-MLV RT) (Promega), with 0.5 µg random hexamers (ThermoFisher) and 1 µg

total RNA. Reactions were incubated for 60 min at 37 °C in a thermocycler. Primer sequences for expression analysis were designed at exons 5 and 8, as follows: KAT6A_E5F: 5'-CCGAGGTTTTCACATGGAGT-3' and KAT6A_E8R: 5'-CGCTCCTCATTCTTGT TTGC-3'. The ACTB gene was used as reference.

Supplementary information

Supplementary information accompanies this paper at <https://doi.org/10.1186/s13023-020-1317-9>.

Additional file 1: Table S1. Variants of Unknown significance identified in Patient 1. **Table S2.** Variants of Unknown significance identified in Patient 2. **Table S3.** Variants of Unknown significance identified in Patient 3. **Table S4.** Variants of Unknown significance identified in Patient 4. **Table S5.** Variants of Unknown significance identified in Patient 5.

Acknowledgements

The authors thank the patients and their families for their wholehearted collaboration. They are also grateful to Dr. A. Perez Aytés for providing access to patient 1 and M. Cozar for technical assistance. L. Castilla-Vallmanya is recipient of an APiF fellowship from the Universitat de Barcelona. M. Serrano is supported by the Generalitat de Catalunya (PERIS SLT008/18/00194) and National Grant P117/00101. We would like to thank the CNAG-CRG for technical assistance with analysis of samples from patients 3 and 4 through the RD-Connect Genome Phenome Analysis platform. The authors appreciate the support of the UDNI for international data sharing.

Authors' contributions

RU, ELM, MPP, MP, DG and SB were responsible for the conception and design of this work. RU, ELM, AMM, MP, LCV, LAPJ, JA, and BMD analysed and validated the Whole Exome Sequencing data and/or mRNA analyses. AMM, LAPJ, MS, DNB, PMR, MO, MPP, and EBS clinically evaluated the patients and generated the clinical data, including the preparation of Table 1. Table 2 was prepared by RU with contributions by ELM, AMM, MS, DNB and EBS. RU, ELM, AMM, MP, MS, PMR and EBS prepared Fig. 1. Figure 2 was prepared by BMD with the help of ELM. Figure 3 was prepared by RU, ELM, AMM, MS, MP, DG and SB prepared Additional file 1: Table S1, S2, S3, S4 and S5. RU, ELM, DG, SB, AMM, MS and EBS wrote the main manuscript. All authors critically reviewed the manuscript. All authors read and approved the final manuscript.

Funding

Funding was from Associació Síndrome Opitz C, Terrassa, Spain; Spanish Ministerio de Economía y Competitividad (SAF2016-75948-R) and from CIBERER (U720). SpainUDP is an initiative funded by the Instituto de Salud Carlos III. Also, the whole exome sequencing of patient 3 was funded through 2016 BBMRI-LPC Call (FP7/2007-2013, grant agreement n° 313010) and patient 5 was sequenced thanks to the PERIS-URDCat program, funded by the Departament de Salut de la Generalitat de Catalunya (PERIS_SLT002_16_00174).

Funding sources were not involved in the study design, collection, analysis and interpretation of data, writing of the report, or publication of the article.

Availability of data and materials

The data that support the findings of this study are available on request from the corresponding author. The data are not publicly available due to privacy and ethical restrictions.

Ethics approval and consent to participate

All protocols were approved by the ethics committee of each of the institutions (namely Universitat de Barcelona, Hospital Sant Joan de Deu and Instituto de Salud Carlos III) and all methods were performed in accordance with the relevant guidelines and regulations. Signed informed consent was obtained from each patient's parents.

Consent for publication

Families have been informed of this publication. They have given signed consent to publish, including pictures of the patients.

Competing interests

The authors declare no conflict of interest.

Author details

¹Department of Genetics, Microbiology and Statistics, Faculty of Biology, University of Barcelona, IBUB, IRSJD, Barcelona, Spain. ²Centro de Investigaciones Biomédicas en Red de Enfermedades Raras (CIBERER), Instituto de Salud Carlos III (ISCIII), Madrid, Spain. ³Present address: Neurometabolic Unit, Hospital Sant Joan de Déu, Barcelona, Spain. ⁴Institute of Rare Diseases Research (IER), Instituto de Salud Carlos III (ISCIII), Madrid, Spain. ⁵Department of Genetic and Molecular Medicine and Pediatric Rare Diseases Institute (IPER), Institut de Recerca Sant Joan de Déu (IRSJD), Hospital Sant Joan de Déu, Barcelona, Spain. ⁶Genetics Unit, University Pompeu Fabra, Hospital del Mar Research Institute IMIM, Barcelona, Spain. ⁷Women's and Children's Hospital, South Australian Health and Medical Research Institute and The University of Adelaide, Adelaide, Australia. ⁸Department of Neurology, Hospital Sant Joan de Déu, Barcelona, Spain. ⁹Dysmorphology and Clinical Genetics, Division of Neonatology, Neonatal Research Unit, Hospital Universitario y Politécnico La Fe, Valencia, Spain.

Received: 18 October 2019 Accepted: 28 January 2020

Published online: 10 February 2020

References

- Rozman M, Camos M, Colomer D, Villamor N, Esteve J, Costa D, et al. Type I MOZ/CBP (MYST3/CREBBP) is the most common chimeric transcript in acute myeloid leukemia with t(8;16)(p11;p13) translocation. *Genes Chromosomes Cancer*. 2004;40(2):140–5.
- Rokudai S, Laptenko O, Arnal SM, Taya Y, Kitabayashi I, Prives C. MOZ increases p53 acetylation and premature senescence through its complex formation with PML. *PNAS*. 2013;110(10):3895–900.
- Pelletier N, Champagne N, Stifani S, Yang XJ. MOZ and MORF histone acetyltransferases interact with the runt-domain transcription factor Runx2. *Oncogene*. 2002;21(17):2729–40.
- Tham E, Lindstrand A, Santani A, Malmgren H, Nesbitt A, Dubbs HA, et al. Dominant mutations in KAT6A cause intellectual disability with recognizable syndromic features. *Am J Hum Genet*. 2015;96(3):507–13.
- Arboleda VA, Lee H, Dorraní N, Zadeh N, Willis M, Macmurdo CF, et al. De novo nonsense mutations in KAT6A, a lysine acetyl-transferase gene, cause a syndrome including microcephaly and global developmental delay. *Am J Hum Genet*. 2015;96(3):498–506.
- Millan F, Cho MT, Retterer K, Monaghan KG, Bai R, Vitazka P, et al. Whole exome sequencing reveals de novo pathogenic variants in KAT6A as a cause of a neurodevelopmental disorder. *Am J Med Genet A*. 2016;170(7):1791–8.
- Murray CR, Abel SN, McClure MB, Foster J 2nd, Walke MI, Jayakar P, et al. Novel causative variants in DYRK1A, KARS, and KAT6A associated with intellectual disability and additional phenotypic features. *J Pediatr Genet*. 2017;6(2):77–83.
- Elenius V, Lahdesmaki T, Hietala M, Jartti T. Food allergy in a child with de novo KAT6A mutation. *Clin Transl Allergy*. 2017;7:19.
- Gauthier-Vasserot A, Thauvin-Robinet C, Bruel AL, Duffourd Y, St-Onge J, Jouan T, et al. Application of whole-exome sequencing to unravel the molecular basis of undiagnosed syndromic congenital neutropenia with intellectual disability. *Am J Med Genet A*. 2017;173(1):62–71.
- Satoh C, Maekawa R, Kinoshita A, Mishima H, Doi M, Miyazaki M, et al. Three brothers with a nonsense mutation in KAT6A caused by parental germline mosaicism. *Hum Gen Var*. 2017;4:17045.
- Zwaveling-Soonawala N, Maas SM, Alders M, Majoie CB, Fliers E, van Trotsenburg ASP, et al. Variants in KAT6A and pituitary anomalies. *Am J Med Genet A*. 2017;173(9):2562–5.
- Trinh J, Huning I, Yuksel Z, Baalmann N, Imhoff S, Klein C, et al. A KAT6A variant in a family with autosomal dominantly inherited microcephaly and developmental delay. *J Hum Genet*. 2018;63(9):997–1001.
- Kennedy J, Goudie D, Blair E, Chandler K, Joss S, McKay V, et al. KAT6A syndrome: genotype-phenotype correlation in 76 patients with pathogenic KAT6A variants. *Genet Med*. 2019;21(4):850–60.

14. Alkhateeb A, Alazaizeh W. A novel de novo frameshift mutation in KAT6A identified by whole exome sequencing. *J Pediatr Genet.* 2019;8(1):10–4.
15. Efthymiou S, Salpietro V, Bettencourt B and Houlden H. Paroxysmal movement disorder and epilepsy caused by a de novo truncating mutation in KAT6A. *J Pediatr Genet.* 2018;7(3):114–116.
16. Good-Jacobson KL, Chen Y, Voss AK, Smyth GK, Thomas T, Tarlinton D. Regulation of germinal center responses and B-cell memory by the chromatin modifier MOZ. *PNAS.* 2014;111(26):9585–90.
17. Katsumoto T, Aikawa Y, Iwama A, Ueda S, Ichikawa H, Ochiya T, et al. MOZ is essential for maintenance of hematopoietic stem cells. *Genes Dev.* 2006;20(10):1321–30.
18. Sanz-Pamplona R, Lopez-Doriga A, Pare-Brunet L, Lazaro K, Bellido F, Alonso MH, et al. Exome sequencing reveals AMER1 as a frequently mutated gene in colorectal cancer. *Clin Cancer Res.* 2015;21(20):4709–18.
19. Desvignes JP, Bartoli M, Delague V, Krahn M, Miltgen M, Beroud C, et al. VarAFT: a variant annotation and filtration system for human next generation sequencing data. *Nucleic Acids Res.* 2018;46(W1):W545–53.
20. Urreizti R, Cueto-Gonzalez AM, Franco-Valls H, Mort-Farre S, Roca-Ayats N, Ponomarenko J, et al. A de novo nonsense mutation in MAGEL2 in a patient initially diagnosed as Opitz-C: similarities between Schaaf-Yang and Opitz-C syndromes. *Sci Rep.* 2017;7:44138.
21. Firth HV, Richards SM, Bevan AP, Clayton S, Corpas M, Rajan D, et al. DECIPHER: database of chromosomal imbalance and phenotype in humans using ensembl resources. *Am J Hum Genet.* 2009;84(4):524–33.
22. Samocha KE, Robinson EB, Sanders SJ, Stevens C, Sabo A, McGrath LM, et al. A framework for the interpretation of de novo mutation in human disease. *Nat Genet.* 2014;46(9):944–50.
23. Lopez-Martin E, Martinez-Delgado B, Bermejo-Sanchez E, Alonso J, SpainUDP network and Posada M. SpainUDP: The Spanish Undiagnosed Rare Diseases Program. *Int J Environ Res Public Health.* 2018;15(8).
24. DePristo MA, Banks E, Poplin R, Garimella KV, Maguire JR, Hartl C, et al. A framework for variation discovery and genotyping using next-generation DNA sequencing data. *Nat Genet.* 2011;43(5):491–8.
25. Lochmuller H, Badowska DM, Thompson R, Knoers NV, Aartsma-Rus A, Gut I, et al. RD-connect, NeurOmics and EURenOmics: collaborative European initiative for rare diseases. *Eur J Hum Genet.* 2018;26(6):778–85.
26. Thompson R, Johnston L, Taruscio D, Monaco L, Beroud C, Gut IG, et al. RD-connect: an integrated platform connecting databases, registries, biobanks and clinical bioinformatics for rare disease research. *J Gen Intern Med.* 2014;29(Suppl 3):S780–7.
27. Kohler S, Vasilevsky NA, Engelstad M, Foster E, McMurry J, Ayme S, et al. The human phenotype ontology in 2017. *Nucleic Acids Res.* 2017;45(D1):D865–76.
28. Girdea M, Dumitriu S, Fiume M, Bowdin S, Boycott KM, Chenier S, et al. PhenoTips: patient phenotyping software for clinical and research use. *Hum Mutat.* 2013;34(8):1057–65.

Publisher's Note

Springer Nature remains neutral with regard to jurisdictional claims in published maps and institutional affiliations.

Ready to submit your research? Choose BMC and benefit from:

- fast, convenient online submission
- thorough peer review by experienced researchers in your field
- rapid publication on acceptance
- support for research data, including large and complex data types
- gold Open Access which fosters wider collaboration and increased citations
- maximum visibility for your research: over 100M website views per year

At BMC, research is always in progress.

Learn more biomedcentral.com/submissions



Supplementary information for:

Five new cases of syndromic intellectual disability due to KAT6A mutations: widening the molecular and clinical spectrum

Roser Urreizti, Estrella Lopez-Martin, Antonio Martinez-Monseny, Montse Pujadas, Laura Castilla-Vallmanya, Luis Alberto Pérez-Jurado, Mercedes Serrano, Daniel Natera-de Benito, Beatriz Martínez-Delgado, Manuel Posada-de-la-Paz, Javier Alonso, Purificación Marin-Reina, Mar O'Callaghan, Daniel Grinberg, Eva Bermejo-Sánchez & Susanna Balcells

Supplementary Table 1. Variants of Unknown significance identified in Patient 1.

Gene	cDNA	Protein	Zig	Disease ¹ (MIM; Inh)	Origin	gnomAD MAF (Hom)	dbSNP	Effect (CADD/SIFT/PP2)	Clin Var	Class ² (ACMG)
<i>ENPP1</i>	c.350T>C	p.Phe117Ser	het	Cole disease (615522; AD)	De novo	-	-	24.8/T/D	-	Likely benign
<i>APOB</i>	c.3337G>C	p.Asp1113His	hom	Hypobetalipoproteinemia (615558; AR)	Both parents	0.0069 (23)	rs12713844	24.1/D/D	Conflicting: B (7); LB(4); P(1); US(1)	Benign
<i>RNF213</i>	c.12817G>A	p.Asp4273Asn	het	<i>Susceptibility to Moyamoya disease 2</i> (607151)	Pat	0.00027 (2)	rs141329059	29.5/T/D	-	Likely benign
	c.14030G>T	p.Trp4677Leu	het		Mat	0.0104 (29)	rs61741961	28/D/D	-	Likely benign

Zig: homozygosity/heterozygosity; het: heterozygote; hom: homozygotes (number of homozygotes in GnomAD database); Inh: inheritance; Pat: paternal; Mat: maternal; SIFT (D - Damaging; T - Tolerated); PP2: Polyphen2 (D - Probably damaging; P - Possibly damaging; B - Benign).

1. Pathologies previously associated with mutations in these genes. In brackets MIM number of the associated disease and its inheritance (according to OMIM).

2. According with the ACMG/AMP 2015 guideline

Supplementary Table 2. Variants of Unknown significance identified in Patient 2.

Gene	c.DNA	Protein	Zig	Disease1 (MIM; Inh)	gnomAD MAF	dbSNP	Effect (CADD/SIFT/PP2)	Class ² (ACMG)
MYOC	c.767C>T	p.Thr256Met	het	Glaucoma 1A, primary open angle (137750, AD)	0.000083	rs200072086	19,07/D/PD	LB
ITGA8	c.2445G>T	p.Glu815Asp	het	Renal hypodysplasia/aplasia 1 (191830, AR)	0.00048	rs112914197	10,95/T/B	LB
C2CD3	c.6833A>G	p.Asn2278Ser	het	Orofaciodigital syndrome XIV (615948, AR)	0.00038	rs199993353	23,2/D/B	US
UROC1	c.883C>T	p.Arg295Cys	het	Uncertain. Urocanase deficiency (276880, AR)	0.000134	rs372290750	33/D/PD	US
ARID1B	c.4234T>G	p.Ser1412Ala	het	Coffin-Siris syndrome 1 (135900, AD)	0.00012	rs145516400	8,831/T/B	LB
KCNQ3	c.2146G>C	p.Asp716His	het	Seizures, benign neonatal, 2 (121201, AD)	0.000055	rs149324120	16,04/T/B	LB

Zig: homozygosity/heterozygosity; het: heterozygote; Inh: inheritance; Pat: paternal; Mat: maternal; CADD (Phred-SCALED CADD score, indicating level of deleteriousness); SIFT (D - Damaging; T - Tolerated); PP2: Polyphen2 (D - Probably damaging; P - Possibly damaging; B - Benign); LB: Likely Benign; US: Uncertain Significance

1. Pathologies previously associated with mutations in these genes. In brackets MIM number of the associated disease and its inheritance (according to OMIM). (*) Filtered variant in gnomAD

2. According with the ACMG/AMP 2015 guideline.

Note: none of these changes was found in ClinVar.

Supplementary Table 3. Variants of Unknown significance identified in Patient 3.

Gene	cDNA	Protein	Zig	Disease ¹ (MIM; Inh)	Origin	gnomAD MAF	db SNP	Effect (CADD/SIFT/PP2)
<i>TMPO</i>	c.610G>T	p.Gly204Cys	het	-	De novo	-	-	21.4/D/D
<i>APOBEC3F</i>	c.340A>C	p.Thr114Pro	het	-	De novo	0.000164	rs753023597	20.8/D/D
<i>PTPN22</i>	c.2198C>A	p.Thr733Lys	het	Susceptibility to diabetes type 1 (222100; AR) & Susceptibility to rheumatoid arthritis (180300)	Pat	-	-	25.4/D/D
	c.1366C>G	p.Gln456Glu	het		Mat	0.001773	rs72650672	21.1/D/D
<i>ERO1LB</i>	c.278A>G	p.Lys93Arg	het	none	Mat	0.001224 (1)	rs147983087	< 20/T/B
	c.189A>C	p.Lys63Asn	het		Pat	0.002091 (4)	rs35648587	< 20/D/D
<i>SYCP2L</i>	c.177T>A	p.Asn59Lys	het	none	Pat	0.000004	rs1052522642	23.0/D/P
	c.212A>C	p.Asn71Thr	het		Pat	0.000004	rs780214095	< 20/T/P
	c.1100T>C	p.Ile367Thr	het		Mat	0.002272 (1)	rs148762988	23.2/D/D

Zig: homozygosity/heterozygosity; het: heterozygote; Inh: inheritance; Pat: paternal; Mat: maternal; CADD (Phred-SCALED CADD score, indicating level of deleteriousness); SIFT (D - Damaging; T - Tolerated); PP2: Polyphen2 (D - Probably damaging; P - Possibly damaging; B - Benign).

1. Pathologies previously associated with mutations in these genes. In brackets MIM number of the associated disease and its inheritance (according to OMIM).

Note: none of these changes was found in ClinVar.

Supplementary Table 4. Variants of Unknown significance identified in Patient 4.

Gene	cDNA	Protein	Zig	Disease ¹ (MIM; Inh)	Origin	gnomAD MAF	dbSNP	Effect (CADD/SIFT/PP2)	ClinVar classification
<i>LRRC8D</i>	c.1902G>A	p.Met634Ile	het	-	De novo	-	-	23.5/D/P	-
<i>SLC4A8</i>	c.1499C>G ⁷	p.Ala500Gly	het	-	De novo	-	-	< 20/T/B	-
<i>LTBP3</i>	c.2856_2857 delCC	p.Asp952Glufs*41	het	Geleophysic dysplasia 3 (617809; AD)	De novo	-	-	-	-
<i>SCFD2</i>	c.848G>T	p.Gly283Val	hom	-	Pat/Mat	0.007204 (13)	rs79025139	28.7/D/D	-
<i>GPR98</i>	c.746G>A	p.Arg249Lys	het	Usher syndrome, type 2C (605472; AR)	Mat	0.006381 (15)	rs41303344	< 20/T/B	Conflicting: B(3);LB (2);LP (1)
	c.5830G>A	p.Asp1944Asn	het		Pat	0.004284 (6)	rs41302834	25.0/D/D	Benign/Likely benign

Zig: homozygosity/heterozygosity; het: heterozygote; hom: homozygote; Inh: inheritance; Pat: paternal; Mat: maternal; CADD (Phred-SCALED CADD score, indicating level of deleteriousness); SIFT (D - Damaging; T - Tolerated); PP2: Polyphen2 (D - Probably damaging; P - Possibly damaging; B - Benign).

1. Pathologies previously associated with mutations in these genes. In brackets MIM number of the associated disease and its inheritance (according to OMIM).

Supplementary Table 5. Variants of Unknown significance identified in Patient 5.

Gene	cDNA	Protein	Zig	Disease ¹ (MIM; Inh)	Origin	gnomAD MAF	db SNP	Effect (CADD)
<i>PC</i>	c.2491G>A	p.Val831Met	het	Pyruvate carboxylase deficiency; (608786; AR)	NA	0.0000039	rs762323318	25.9
<i>ATP1A2</i>	c.1285G>A	p.Ala429Thr	het	Alternating hemiplegia of childhood; (104290; AD)	NA	0.00004 (5)	rs77608625	26.7
<i>RENBP</i>	c.1091A>C	p.Glu364Ala	het	-	NA	0.000006	-	26.8
<i>PMPCA</i>	c.1263+84delG	intron variant	het	Spinocerebellar ataxia, autosomal recessive 2 (213200; AR)	NA	0.000004	rs773313604	<20

Zig: homozygosity/heterozygosity; het: heterozygote; Inh: inheritance; CADD (Phred-SCALED CADD score, indicating level of deleteriousness). NA: Not Analyzed.

1. Pathologies previously associated with mutations in these genes. In brackets MIM number of the associated disease and its inheritance (according to OMIM)

Note: none of these changes was found in ClinVar.

Article 5: Case report of a child bearing a novel deleterious splicing variant in *PIGT*

Summary:

Rationale: Trio family-based whole exome sequencing (WES) is a powerful tool in the diagnosis of rare neurodevelopmental diseases, even in patients with the unclear diagnosis. There have been previous reports of variants in the phosphatidylinositol glycan anchor biosynthesis class T (*PIGT*) gene associated with multiple congenital anomalies, with a total of 14 affected individuals across 8 families.

Patient concerns: An 18-month-old boy of Greek ancestry presented with global developmental delay, generalized tonic clonic seizures, hypotonia, renal cysts, esotropia, bilateral undescended testes, bilateral vesicoureteric reflux, marked cardiac dextroposition, bilateral talipes equinovarus, and dysmorphic features.

Diagnosis: WES revealed 2 compound heterozygous variants in the *PIGT* gene, c.[494-2A>G]; [547A>C]/p.[Asp122Glyfs*35]; [Thr183Pro]. The splicing mutation was demonstrated to lead to the skipping of exon 4.

Interventions: Seizures, infections, and other main symptoms were treated.

Outcomes: The patient died at 2 years of age before the molecular diagnosis was achieved. Genetic counseling has been offered to the family.

Lessons: Most of the clinical features of the patient are in agreement with the previously described *PIGT* cases corroborating the usefulness of WES as a diagnostic tool.

Reference:

Mason, Samantha; Castilla-Vallmanya, Laura; James, Con; Andrews, P. Ian; Balcells, Susana; Grinberg, Daniel; Kirk, Edwin P.; Urreizti, Roser. Case report of a child bearing a novel deleterious splicing variant in *PIGT*, *Medicine* 2019, 98(8):14524. doi: 10.1097/MD.00000000000014524

informed consent to participate in this study, including explicit permission to share clinical and identifying information, even in online open-access journals. Institutional ethics committee approval was granted by the Prince of Wales Hospital Campus Human Research Ethics Committee, Sydney, Australia (HREC ref no 13/094) and the Ethics Committee of the Universitat de Barcelona (IRB00003099) and all methods were performed in accordance with the relevant guidelines and regulations.

Genomic DNA was obtained from the parents' peripheral blood and the proband's fibroblasts.

2.2. WES and molecular analyses

WES of the proband and his parents were performed in the National Centre of Genomic Analysis (CNAG; Barcelona, Spain) using the Illumina HiSeq-2000 platform. Exome capture was performed with Agilent SureSelect v5 (Agilent, CA). The samples were sequenced at coverage of 140×. The data were analyzed as described elsewhere.¹¹³¹ The results were then filtered under de novo dominance and recessive hypotheses. Variants with a minimum allele frequency above 0.001 (under the dominant) and above 0.01 (for recessive) in the common population (according to ExAC and 1000 genomes) were excluded. Variants in genes included in DDG2P (the development disorder genotype-phenotype database^{114,151}), and covered by at least 10 reads, were prioritized for validation (it should be noted that those who carried out the original DECIPHER analysis and collection of the data bear no responsibility for the further analysis or interpretation of it).

The mean coverage was of 142.49, 179.29, and 166.43 reads for the patient, father, and mother, respectively, and 91.7% to 97.7% of the target region was covered with at least 10 reads (C10). A total of 4 variants were selected for validation by Sanger sequencing. Primer sequences and polymerase chain reaction (PCR) conditions are available on request. PCR reaction, purification, and sequencing were performed as described previously.¹¹⁶¹

2.3. Cell culture

Patient's fibroblasts and those of 6 controls were cultured in DMEM supplemented with 10% fetal bovine serum (Gibco, Life Technologies, Carlsbad, CA) and 1% streptomycin-penicillin (Gibco, Life Technologies) and were maintained at 37°C and 5% of CO₂. Cycloheximide (Sigma-Aldrich, St. Louis, MO) treatment was applied in a concentration of 1 mg/ml in DMEM during 6 hours.

2.4. PIGT transcript analysis

RNA was extracted from confluent fibroblasts plates with the High Pure RNA Isolation Kit (Roche, Basel, Switzerland). Integrity and purity of the RNA were tested using a 1% agarose gel and 260/230 and 260/280 absorbance ratios using an ND-1000 Spectrophotometer (Nanodrop Technologies Inc; Thermo Fisher Scientific, Waltham, MA). The High-capacity complementary DNA (cDNA) Reverse Transcription kit (Applied Biosystems, Thermo Fisher Scientific, Waltham, MA) was used to retrotranscribe up to 2 µg of RNA. Primers cPIGT-spl-F (5'-GCTGGGTAGGCCGAAGTAG-3') and cPIGT-spl-R (5'-TGGTAGCTGGTGTGGAACAA-3') were used to amplify the spliced region. The PCR fragments were separated by 2% agarose gel electrophoresis. The illustra GFX PCR DNA and Gel Band Purification kit (GE Healthcare Life Sciences, Chicago, IL)

was used to isolate each specific band, the obtained purified product was manually sequenced.

2.5. Real-time PCRs

Real-time PCRs were performed in triplicate using Universal Probes Library probes (Roche), gene-specific primers and Universal Probes Mastermix (Roche), with the exception of PPIA assay (Applied Biosystems) (Supplemental Table S2, <http://links.lww.com/MD/C825>). The qPCR reactions were performed on a final volume of 15 µl with 10 ng of cDNA. The amplification was done using the thermocycler LightCycler 480 (Roche). Expression levels of 6 putative reference genes were tested in control and the patient's fibroblast and *GAPDH* and *PPIA* were chosen as they were the genes with the lowest coefficient of variation (<0.3% CV). The relative transcription level was calculated with the crossing point cycle (Cp) calculation using the LightCycler 480 Software (release 1.5.0) (Roche). For every assay, the efficiency (E) of the reaction was calculated from a 6 points standard curve. The intra-assay CV of all the assays at the working conditions used was lower than 1% and Cp standard deviation was smaller than 0.3.

3. Case report

3.1. Clinical report

The patient is the first child to nonconsanguineous, healthy parents of Greek ancestry. At the time of the patient's birth his mother was 27 years of age, and his father 35. The patient was first noted to have a possible bladder outlet obstruction at a 20-week antenatal morphology scan, and the pregnancy was then further complicated by polyhydramnios and the finding of shortened long bones from week 30. At 34 weeks of gestation, he was noted to have left hydronephrosis, and an amniocentesis was performed at this time. Array comparative genomic hybridization showed a normal male pattern. The patient was born via elective Caesarean section at 38 + 3 weeks of gestation. At birth, his length was 43 cm (below 3rd percentile), weight 3.21 kg (25th percentile), and head circumference 36 cm (25th percentile). Postnatal ultrasound confirmed obstructive nephropathy with renal impairment.

The patient was transferred to intensive care unit on day 4 of life with acute bladder outlet obstruction, bilateral hydronephrosis, and evidence of increasing creatinine. During this period, a head ultrasound was normal, and a spinal ultrasound revealed a tethered cord. Spinal and brain magnetic resonance imaging (MRI) were normal at 2 weeks and 5 months of age. Echocardiogram was normal apart from patent foramen ovale.

Multifocal seizures developed at 5 months, often progressing to bilateral convulsive seizures. Dysmorphic features (Fig. 1 and Table 1), global developmental delay, hypotonia, esotropia, delayed visual maturation, hypermetropia, undescended testes, bilateral talipes equinovarus, and bilateral inguinal hernias were also noted. Repeat MRI of the brain and spine were normal and renal ultrasound showed bilateral grade 5 vesicoureteric reflux, and bilateral renal cysts.

He was feeding poorly and had slow growth. Developmentally, he made some early gains but had regression from 3 months followed by a period of developmental stagnation, and some possible further regression from the age of 1 year and 9 months.

On examination, the patient had a high palate with lateral palatine ridging, plagiocephaly was open-mouthed at rest, and had low-set, posteriorly rotated ears (Fig. 1). He had pectus



Figure 1. Most relevant features of the current patient. (A) Facies at 6 days of life. (B and C) Facies at 18 mo old. Note cupid's bow lips, full lower lip, posteriorly rotated ears, and a prominent premaxilla. (D) Deep plantar creases. (E) Small feet, third toes proximally inserted and bilateral 2-3 toe syndactyly. (F) Hand, with broad fingers and relatively large palms.

excavatum, posterior right shoulder dimple and elbow dimples, right single transverse palmar crease, broad fingers, and relatively large palms. The patient presented with bilateral 2-3 toe syndactyly and rhizomelic upper limb shortening, however, his father also had these features, suggesting that they may be unrelated to the *PIGT* variants. The patient's feet were small with the third toes proximally inserted, and he had pudgy soles with deep longitudinal creases bilaterally. Alkaline phosphatase levels were normal.

Seizures were frequent, often prolonged and intractable. He made minimal developmental progress, only achieving the ability to reach, roll, coo, and laugh. He frequently suffered aspiration pneumonia. He died aged 2 years and 3 months of respiratory failure following an adenovirus infection.

3.2. Molecular findings

We performed whole-exome sequencing on the patient and parents' genomic DNA and found 2 heterozygous mutations in the *PIGT* gene (OMIM *610272; ENSG00000124155): the c.547A>C (p.Thr183Pro), inherited from his father and the c.494-2A>G, affecting the canonical splice acceptor site of intron 3, of maternal origin. The p.Thr183Pro was previously identified in a Turkish family^[6] while the c.494-2A>G was novel. The effect of this mutation was studied in the patient's fibroblasts and the skipping of *PIGT* exon 4 was verified by Sanger sequencing (Fig. 2). In control fibroblasts, 2 major *PIGT* RNA isoforms were detected, 1 including all exons (ENST00000279036) and the

other lacking exons 2 and 3 (ENST00000279035). A third minor band corresponding to the isoform lacking exon 3 (ENST00000543458) was also observed. In the patient's fibroblasts, these 3 isoforms were detected, together with 3 additional ones, lacking exon 4. The mutant isoforms were moderately affected by nonsense-mediated decay, as observed in the cycloheximide-treated cells, in which the bands corresponding to the fragments without exon 4 were more intense (band 2 and 4, in Fig. 2).

To further characterize the effect of the *PIGT* variants, we analyzed *FOXC2* expression levels, previously reported to be positively correlated with those of *PIGT*.^[12] In the patient's fibroblasts, we observed an increase in the expression of the *FOXC2* gene when compared with the average of the fibroblasts of 6 control individuals (Supplemental Fig. 1, <http://links.lww.com/MD/C825>), although the results were not conclusive.

In the WES analysis we also identified a de novo variant in the *FBN2* gene and 2 missense mutations in the *ATP10A* gene (Supplemental Table 1, <http://links.lww.com/MD/C825>). These changes have been interpreted as variants of unknown significance.

4. Discussion

There is an emerging syndrome associated with variants in *PIGT*. Besides global developmental delay, seizures, hypotonia, plagiocephaly, strabismus/nystagmus, which are present in all the cases for which data are available,^[1,5-9] over half of the reported

Table 1
Description of clinical features observed in patients with PIGT variations.

Features	Kvarnung 2013 ⁵		Nakashima 2014 ⁷		Lam 2015 ¹		Skauli 2016 ⁸		Pagnamenta 2017 ⁵		Kohashi 2018 ⁹		Yang 2018 ¹⁰		Current patient		
	V-1	V-2	V-3	V-4	1	Sib 1	Sib 2	Sib 1	Sib 2	1	2a	2b	1	1	1	%	
Sex	F	F	F	F	F	M	M	M	M	M	M	M	M	M	M	7F: 8M	88%
Consanguinity	+	+	+	+	+	+	+	+	+	+	+	+	+	+	+	+	100%
Neurological	+	+	+	+	+	+	+	+	+	+	+	+	+	+	+	+	100%
Global developmental delay/intellectual disability	+	+	+	+	+	+	+	+	+	+	+	+	+	+	+	+	87%
Seizures	+	+	+	+	+	+	+	+	+	+	+	+	+	+	+	+	100%
Cortical/cerebellar atrophy	+	+	+	+	+	+	+	+	+	+	+	+	+	+	+	+	20%
Hypotonia	+	+	+	+	+	+	+	+	+	+	+	+	+	+	+	+	67%
Hearing loss	+	+	+	+	+	+	+	+	+	+	+	+	+	+	+	+	21%
Cortical visual impairment	+	+	+	+	+	+	+	+	+	+	+	+	+	+	+	+	14%
Head	+	+	+	+	+	+	+	+	+	+	+	+	+	+	+	+	40%
Macrocephaly	+	+	+	+	+	+	+	+	+	+	+	+	+	+	+	+	100%
Microcephaly	+	+	+	+	+	+	+	+	+	+	+	+	+	+	+	+	45%
Craniosynostosis	+	+	+	+	+	+	+	+	+	+	+	+	+	+	+	+	80%
Plagiocephaly	+	+	+	+	+	+	+	+	+	+	+	+	+	+	+	+	79%
Strabismus/nystagmus	+	+	+	+	+	+	+	+	+	+	+	+	+	+	+	+	60%
Tooth abnormalities	+	+	+	+	+	+	+	+	+	+	+	+	+	+	+	+	55%
Dysmorphic facial features	+	+	+	+	+	+	+	+	+	+	+	+	+	+	+	+	73%
Depressed nasal bridge	+	+	+	+	+	+	+	+	+	+	+	+	+	+	+	+	67%
Broad nasal root	+	+	+	+	+	+	+	+	+	+	+	+	+	+	+	+	20%
Inverted nipples	+	+	+	+	+	+	+	+	+	+	+	+	+	+	+	+	36%
Abnormal lung anatomy	+	+	+	+	+	+	+	+	+	+	+	+	+	+	+	+	40%
Musculo-skeletal	+	+	+	+	+	+	+	+	+	+	+	+	+	+	+	+	100%
Skeletal abnormalities (clinodactyly, syndactyly...)	+	+	+	+	+	+	+	+	+	+	+	+	+	+	+	+	75%
Scoliosis	+	+	+	+	+	+	+	+	+	+	+	+	+	+	+	+	42%
Osteopenia/delayed bone age	+	+	+	+	+	+	+	+	+	+	+	+	+	+	+	+	73%
Slender long bones	+	+	+	+	+	+	+	+	+	+	+	+	+	+	+	+	75%
Short limbs	+	+	+	+	+	+	+	+	+	+	+	+	+	+	+	+	56%
Congenital talipes equinovarus	+	+	+	+	+	+	+	+	+	+	+	+	+	+	+	+	20%
Urologic	+	+	+	+	+	+	+	+	+	+	+	+	+	+	+	+	40%
Nephrocalcinosis	+	+	+	+	+	+	+	+	+	+	+	+	+	+	+	+	50%
Ureteric dilatation	+	+	+	+	+	+	+	+	+	+	+	+	+	+	+	+	20%
Renal cysts and dysplasia	+	+	+	+	+	+	+	+	+	+	+	+	+	+	+	+	55%
Other	+	+	+	+	+	+	+	+	+	+	+	+	+	+	+	+	36%
Endocrine	+	+	+	+	+	+	+	+	+	+	+	+	+	+	+	+	40%
High plasma calcium	+	+	+	+	+	+	+	+	+	+	+	+	+	+	+	+	47%
High urine calcium	+	+	+	+	+	+	+	+	+	+	+	+	+	+	+	+	67%
Low alkaline phosphatase	+	+	+	+	+	+	+	+	+	+	+	+	+	+	+	+	58%
Other	+	+	+	+	+	+	+	+	+	+	+	+	+	+	+	+	67%
Gastroesophageal reflux	+	+	+	+	+	+	+	+	+	+	+	+	+	+	+	+	58%
Congenital heart defects	+	+	+	+	+	+	+	+	+	+	+	+	+	+	+	+	58%

The 'Overall' column refers to the total of patients presenting each feature over all the patients in which this feature has been assessed. This data is also expressed in percentage of the total (%). NA: Not available or not assessed. (1) primitive Sylvian fissures, indicating a possible neuronal migration disorder; (2) urolithiasis; (3) at the lower end of the normal range; (6) he has prominent meiotic suture but craniosynostosis has not been demonstrated; (7) undescended testis.

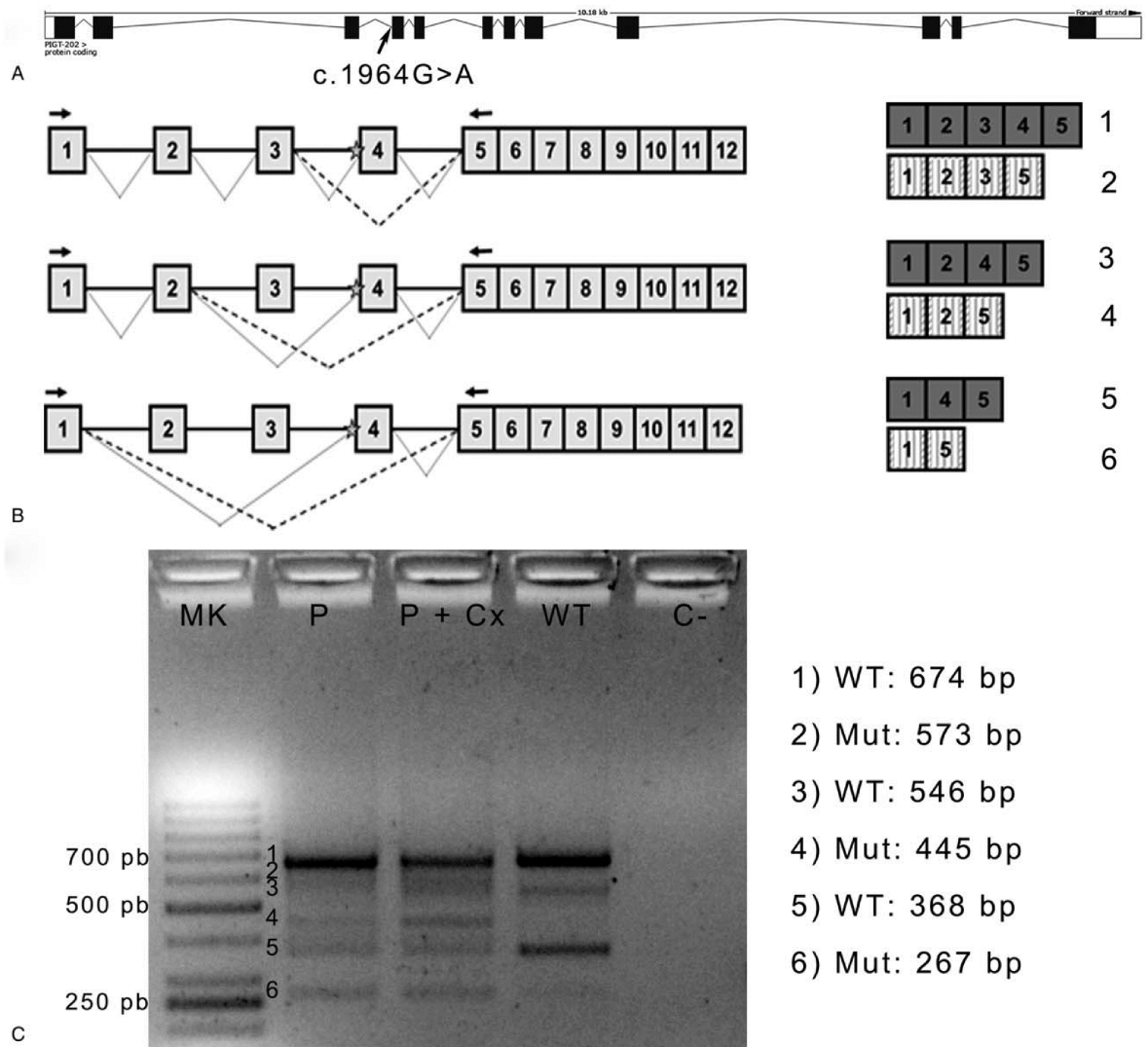


Figure 2. (A) *PIGT* gene representation (ENSG00000124155). The black arrow marks the position of the mutation (at exon 4 splicing acceptor site). (B) Schematic representation of the *PIGT* alternative transcripts and putative splicing events. (C) PCR amplification of the cDNA of the patient cells (P), the patient cells treated with Cycloheximide (P + Cx) and the control cells (WT). Mk: 100 pb molecular weight marker, (C-) PCR negative control. cDNA = complementary DNA, PCR = polymerase chain reaction, *PIGT* = phosphatidylinositol glycan anchor biosynthesis class T.

patients presented with cortical/cerebellar atrophy, cortical visual impairment, osteopenia, skeletal abnormalities, low alkaline phosphatase levels, anteverted nose, a high forehead, and congenital heart defects (Table 1).

At birth, most of the patients with variants in *PIGT* have been noted to feed poorly and have hypotonia (Table 1). All have gone on to develop seizures before 2 years of age, with most having their first seizure before 1 year of age. Initial presentation in most has been with generalized tonic-clonic seizures, often triggered by febrile illness.^[1,5-8,10] Timing of seizures and progression to generalized tonic-clonic seizures in our patient is consistent with previous reports. Severe developmental delay and profound intellectual disability have also been reported in all of the currently known patients with *PIGT* variations (Table 1), with the exception of patient 258,094 at Pagnamenta et al,^[5] presenting with a much milder phenotype. Strabismus and nystagmus have also been reported in all the assessed cases, often

in conjunction with cortical visual impairment (Table 1).^[1,5-8,10] In addition, the majority of these patients presented characteristic craniofacial abnormalities with plagiocephaly, high forehead and bitemporal narrowing, depressed nasal bridge and an arched palate. Cupid bow lips, long philtrum, and low set ears are also observed in around half of the patients.

Skeletal abnormalities, together with osteopenia, slender long bones or delayed bone age are common traits in the “*PIGT* syndrome” patients. While mineralization and ossification problems are common in these patients, low serum alkaline phosphatase level has been observed in 47% of the patients, suggesting that this is not the only reason for the ossification problems.

Our reported patient is similar to the 14 patients previously described in the literature, who had either compound heterozygous or homozygous variants in the *PIGT* gene resulting in an MCAHS3 phenotype.^[1,5-9] Undescended testes, seen in this case, has not been previously reported.

Functional tests performed by us and others reinforce the pathogenic implication of the 2 *PIGT* variants described here. The missense mutation p.Thr183Pro was previously tested in a zebrafish model and was demonstrated to derogate the ability of *PIGT* mRNA to recover the gastrulation defects of *pigt*-depleted zebrafish.^[6] Regarding the c.494-2A>G mutation, we have shown that it alters the normal *PIGT* splicing pattern, leading to the skipping of exon 4. The mutant protein is predicted to have a new reading frame from position 165 and a premature stop codon after 34 residues (p.Asp165Glyfs*34).

Previous studies in breast carcinoma showed that *PIGT* regulates *FOXC2* expression levels in 2 breast cancer cell lines.^[12] We have studied *FOXC2* levels in the patient's fibroblasts but no clear results were obtained.

The patient was also found to bear a de novo heterozygous variant in the *FBN2* gene (c.733C>T; p.Arg245Trp). This gene has been associated with Congenital Contractural Arachnoidactyly (MIM #121050) a rare, autosomal dominant connective tissue disorder. This mutation is reported in ClinVar as a “variant of uncertain significance.” While the *FBN2* variant does not seem to be responsible for the main clinical characteristics of the patient, with the information available at this time we cannot rule out that this change may have some effect and may be modifying the patient's clinical presentation.

MCAHS3 (or *PIGT* syndrome) represents an emerging and distinctive entity, which is potentially clinically diagnosable. Given the severity of its clinical features and its reproductive implications, it is important to make the diagnosis of this condition.

Acknowledgments

The authors thank the patient and his family for wholehearted collaboration. They are also grateful to M. Cozar for technical assistance, and to CNAG for exome sequencing within the “300 exomes to elucidate rare diseases” program. Funding was from Associació Síndrome Opitz C, Terrassa, Spain; Spanish Ministerio de Economía y Competitividad (SAF2014-56562-R; SAF2016-75948-R, FECYT, crowdfunding PRECIPITA); ISCIII Ministerio de Economía y Competitividad (PT13/0001/0044), Catalan Government (2014SGR932), and from CIBERER (U720).

Author contributions

Conceptualization: Susana Balcells, Daniel Grinberg, Edwin P. Kirk, Roser Urreizti.

Data curation: Laura Castilla-Vallmanya, Con James, P. Ian Andrews, Edwin P. Kirk, Roser Urreizti.

Formal analysis: Susana Balcells, Daniel Grinberg.

Funding acquisition: Susana Balcells, Daniel Grinberg, Roser Urreizti.

Investigation: Laura Castilla-Vallmanya, Con James, Susana Balcells, Daniel Grinberg, Edwin P. Kirk, Roser Urreizti.

Methodology: Laura Castilla-Vallmanya, Susana Balcells, Daniel Grinberg, Roser Urreizti.

Project administration: Samantha Mason, Susana Balcells, Daniel Grinberg, Roser Urreizti.

Resources: P. Ian Andrews, Edwin P. Kirk.

Supervision: Susana Balcells, Daniel Grinberg.

Writing – original draft: Samantha Mason, Roser Urreizti.

Writing – review and editing: Susana Balcells, Daniel Grinberg, Edwin P. Kirk, Roser Urreizti.

Laura Castilla-Vallmanya orcid: 0000-0002-2260-9664.

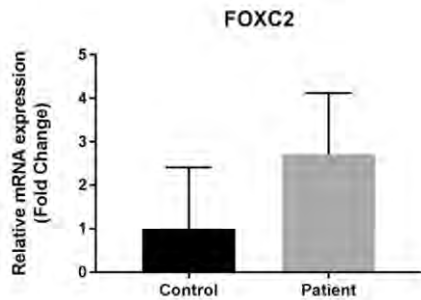
References

- [1] Lam C, Golas GA, Davids M, et al. Expanding the clinical and molecular characteristics of *PIGT*-CDG, a disorder of glycosylphosphatidylinositol anchors. *Mol Genet Metab* 2015;115:128–40.
- [2] Ng BG, Freeze HH. Human genetic disorders involving glycosylphosphatidylinositol (GPI) anchors and glycosphingolipids (GSL). *J Inher Metab Dis* 2015;38:171–8.
- [3] Kinoshita T, Fujita M, Maeda Y. Biosynthesis, remodelling and functions of mammalian GPI-anchored proteins: recent progress. *J Biochem* 2008;144:287–94.
- [4] Nguyen TTM, Murakami Y, Sheridan E, et al. Mutations in *GPAA1*, encoding a GPI transamidase complex protein, cause developmental delay, epilepsy, cerebellar atrophy, and osteopenia. *Am J Hum Genet* 2017;101:856–65.
- [5] Pagnamenta AT, Murakami Y, Taylor JM, et al. Analysis of exome data for 4293 trios suggests GPI-anchor biogenesis defects are a rare cause of developmental disorders. *Eur J Hum Genet* 2017;25:669–79.
- [6] Kvarnung M, Nilsson D, Lindstrand A, et al. A novel intellectual disability syndrome caused by GPI anchor deficiency due to homozygous mutations in *PIGT*. *J Med Genet* 2013;50:521–8.
- [7] Nakashima M, Kashii H, Murakami Y, et al. Novel compound heterozygous *PIGT* mutations caused multiple congenital anomalies-hypotonia-seizures syndrome 3. *Neurogenetics* 2014;15:193–200.
- [8] Skauli N, Wallace S, Chiang SC, et al. Novel *PIGT* variant in two brothers: expansion of the multiple congenital anomalies-hypotonia seizures syndrome 3 phenotype. *Genes* 2016;7:pil: E108.
- [9] Kohashi K, Ishiyama A, Yuasa S, et al. Epileptic apnea in a patient with inherited glycosylphosphatidylinositol anchor deficiency and *PIGT* mutations. *Brain Dev* 2018;40:53–7.
- [10] Yang L, Peng J, Yin XM, et al. Homozygous *PIGT* mutation lead to multiple congenital anomalies-hypotonia seizures syndrome 3. *Front Genet* 2018;9:153.
- [11] Maio N, Rouault TA. Iron-sulfur cluster biogenesis in mammalian cells: new insights into the molecular mechanisms of cluster delivery. *Biochim Biophys Acta* 2015;1853:1493–512.
- [12] Zhao P, Nairn AV, Hester S, et al. Proteomic identification of glycosylphosphatidylinositol anchor-dependent membrane proteins elevated in breast carcinoma. *J Biol Chem* 2012;287:25230–40.
- [13] Sanz-Pamplona R, Lopez-Doriga A, Pare-Brunet L, et al. Exome sequencing reveals *AMER1* as a frequently mutated gene in colorectal cancer. *Clin Cancer Res* 2015;21:4709–18.
- [14] Firth HV, Richards SM, Bevan AP, et al. DECIPHER: database of chromosomal imbalance and phenotype in humans using ensembl resources. *Am J Hum Genet* 2009;84:524–33.
- [15] Samocha KE, Robinson EB, Sanders SJ, et al. A framework for the interpretation of de novo mutation in human disease. *Nat Genet* 2014;46:944–50.
- [16] Urreizti R, Cueto-Gonzalez AM, Franco-Valls H, et al. A de novo nonsense mutation in *MAGEL2* in a patient initially diagnosed as opitz-C: similarities between Schaaf-Yang and Opitz-C syndromes. *Sci Rep* 2017;7:44138.

Supplementary information for:

Case report of a child bearing a novel deleterious splicing variant in *PIGT*

Samantha Mason*, Laura Castilla-Vallmanya*, Con James, P. Ian Andrews, Susana Balcells, Daniel Grinberg, Edwin P. Kirk & Roser Urreizti



Supplemental Figure 1: Real time PCR quantification of *FOXC2* mRNA levels in fibroblasts. The average expression levels in 6 different controls is set as the reference value. The data are represented as means \pm S.D. *GAPDH* was used as normalizer (the results were comparable when normalized with *PPIA*). Results from 3 independent experiments.

Supplemental Table S1: Variants of unknown significance (VUS) identified in the present study

Gene	cDNA	Protein	Origin	Classification	Inher Pattern	Associated Disease	MIM #	Validation	rs	ExAC (homoz)	PolyPhen-2	PROVEAN	SIFT
<i>FBN2</i>	c.733C>T	p.R245W	de novo	VUS	AD	DA9; EOMD	121050; 616118	Sanger	rs146941428	0,000024 (0)	Damaging	Deleterious	Deleterious
<i>ATP10A</i>	c.3850G>A	p.A1284T	paternal	VUS_ putative polymorphism	AR	none	none	IGV	rs116641809	0.006179 (2)	Benign	Neutral	Tolerant
<i>ATP10A</i>	c.3562A>G	p.I1188V	maternal	VUS_ putative polymorphism	AR			IGV	rs2076745	0.003559 (2)	Benign	Neutral	Tolerant

DA9: Distal Arthrogyposis, Type 9; EOMD: Early-Onset Macular Degeneration

Supplemental Table S2: qPCR assays

Gene	Reference	Primer Sequence (5'→3')
<i>FOXC2</i>	UPL probe #23	F: GCACGAAATACTGACGTGTCC R: CCCCTTAATTGTCTGGTTGG
<i>GAPDH</i>	UPL Probe #60	F: AGCCACATCGCTCAGACAC R: GCCCAATACGACCAAATCC
<i>PPIA</i>	Hs99999904_m1 assay	

Article 6: A De Novo *FOXP1* Truncating Mutation in a Patient Originally Diagnosed as C Syndrome

Summary:

De novo *FOXP1* mutations have been associated with intellectual disability (ID), motor delay, autistic features and a wide spectrum of speech difficulties. C syndrome (Opitz C trigonocephaly syndrome) is a rare and genetically heterogeneous condition, characterized by trigonocephaly, craniofacial anomalies and ID. Several different chromosome deletions and point mutations in distinct genes have been associated with the disease in patients originally diagnosed as Opitz C. By whole exome sequencing we identified a de novo splicing mutation in *FOXP1* in a patient, initially diagnosed as C syndrome, who suffers from syndromic intellectual disability with trigonocephaly. The mutation (c.1428 + 1 G > A) promotes the skipping of exon 16, a frameshift and a premature STOP codon (p.Ala450GLyfs*13), as assessed by a minigene strategy. The patient reported here shares speech difficulties, intellectual disability and autistic features with other *FOXP1* syndrome patients, and thus the diagnosis for this patient should be changed. Finally, since trigonocephaly has not been previously reported in *FOXP1* syndrome, it remains to be proved whether it may be associated with the *FOXP1* mutation.

Reference:

Urreizti, R., Damanti, S., Esteve, C. *et al.* A De Novo *FOXP1* Truncating Mutation in a Patient Originally Diagnosed as C Syndrome. *Sci Rep.* 2018; 8: 694 (2018). doi: 10.1038/s41598-017-19109-9

SCIENTIFIC REPORTS

OPEN

A *De Novo* FOXP1 Truncating Mutation in a Patient Originally Diagnosed as C Syndrome

Roser Urreizti¹, Sarah Damanti^{2,3}, Carla Esteve¹, Héctor Franco-Valls¹, Laura Castilla-Vallmanyà¹, Raul Tonda^{4,5}, Bru Cormand¹, Lluïsa Vilageliu¹, John M. Opitz⁶, Giovanni Neri⁷, Daniel Grinberg¹ & Susana Balcells¹

Received: 31 July 2017

Accepted: 21 December 2017

Published online: 12 January 2018

De novo FOXP1 mutations have been associated with intellectual disability (ID), motor delay, autistic features and a wide spectrum of speech difficulties. C syndrome (Opitz C trigonocephaly syndrome) is a rare and genetically heterogeneous condition, characterized by trigonocephaly, craniofacial anomalies and ID. Several different chromosome deletions and point mutations in distinct genes have been associated with the disease in patients originally diagnosed as Opitz C. By whole exome sequencing we identified a *de novo* splicing mutation in FOXP1 in a patient, initially diagnosed as C syndrome, who suffers from syndromic intellectual disability with trigonocephaly. The mutation (c.1428 + 1 G > A) promotes the skipping of exon 16, a frameshift and a premature STOP codon (p.Ala450Glyfs*13), as assessed by a minigene strategy. The patient reported here shares speech difficulties, intellectual disability and autistic features with other FOXP1 syndrome patients, and thus the diagnosis for this patient should be changed. Finally, since trigonocephaly has not been previously reported in FOXP1 syndrome, it remains to be proved whether it may be associated with the FOXP1 mutation.

Severe neurodevelopmental disorders (NDD) affect more than 3% of children and are due to a genetic defect in more than 80% of the cases¹. Until recently, the main diagnostic tools include a great variety of molecular tests (karyotype, array CGH and Sanger sequencing of putative candidate genes) together with multiple clinical evaluations by highly specialized physicians and a variety of complementary tests, some of them invasive, such as neuroimaging, metabolic evaluation or cerebrospinal fluid examination¹. After this “diagnostic odyssey” more than a half of the patients are still miss- or undiagnosed² and this situation is worsened in patients suffering from rare diseases clinically and genetically heterogeneous or with unclear or atypical presentations^{2,3}. Next-generation sequencing (NGS) has revolutionized the field of clinical genetics by highly improving the diagnostic yield of rare diseases, and facilitating the identification novel causative genes³, achieving a molecular diagnosis in 25–68% of the cases⁴.

FOXP1 is one of the genes recently found mutated in a Mendelian developmental disorder. Heterozygous sequence variants have been linked to intellectual disability (ID) with language delay, with or without autistic features (MIM #613670). The FOXP1 (forkhead-box protein P1; MIM 605515) protein is a member of the forkhead-box family of transcription factors characterized by a highly conserved forkhead DNA-binding domain (FOX) and with crucial roles in embryonic development^{5,6}. The FOXP1 protein, as other members of the FOXP family, includes 4 main functional domains: a N-terminal glutamine (Gln) rich region, zinc finger and leucine zipper domains and a C-terminal FOX domain (Fig. 1).

FOXP1 is important in neural development⁷, monocyte differentiation and macrophage function⁵. It has also been described as an oncogene in hepatocellular carcinoma, pancreatic cancer, and various types of B-cell non-Hodgkin lymphomas⁸, being yet another example of the tight connection between cancer-related genes and

¹Department of Genetics, Microbiology and Statistics, Faculty of Biology, University of Barcelona, IBUB, IRSJD, CIBERER, Barcelona, Spain. ²Geriatric Unit, Fondazione Ca'Granda, IRCCS Ospedale Maggiore Policlinico, Milan, Italy. ³Nutritional Sciences, University of Milan, Milan, Italy. ⁴CNAG-CRG, Centre for Genomic Regulation (CRG), Barcelona Institute of Science and Technology (BIST), Barcelona, Spain. ⁵Universitat Pompeu Fabra (UPF), Barcelona, Spain. ⁶Pediatrics Medical Genetics, University of Utah School of Medicine, Salt Lake City, Utah, USA. ⁷Istituto di Medicina Genomica, Università Cattolica Sacro Cuore, Policlinico A. Gemelli, Rome, Italy. Daniel Grinberg and Susana Balcells contributed equally to this work. Correspondence and requests for materials should be addressed to R.U. (email: urreizti@ub.edu)

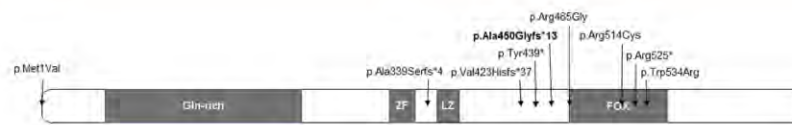


Figure 1. FOXP1 domain organization (for UniProt Q9H334). Point mutations associated with intellectual disability (ID) with language delay, with or without autistic features are shown. In bold, the mutation found in the patient described here.

developmental defects⁹. Most FOX proteins bind to their target DNA sequences as monomers, except members of the FOXP subfamily, which include FOXP1–4. FOXP1 is able to form both homo and heterodimers (with its paralogous FOXP2) via the leucine zipper domain^{10,11}. In mouse, *Foxp1* and *Foxp2* have been shown to be co-expressed in several brain regions¹² as well as in perichondrial skeletal progenitors and proliferating chondrocytes during endochondral ossification and they act as coordinators of osteogenesis and chondrocyte hypertrophy in the developing long bones¹³. In humans, FOXP2 is involved in a rare form of speech and language disorder with developmental verbal dyspraxia (childhood apraxia of speech or CAS, MIM #602081).

Here we present an adult patient with developmental delay, trigonocephaly, speech impairment and ID who was diagnosed as Opitz C syndrome early in life, in whom we have identified by WES a novel splicing mutation in the *FOXP1* gene and provide a detailed clinical description, in comparison to so far reported patients identified carrying deleterious *FOXP1* mutations.

Results and Discussion

The patient described here (Patient 2 in Urreizti *et al.*¹⁴) is a 23-year-old man, second child of non-consanguineous Italian parents. Pregnancy was complicated by threatened abortion. The delivery was vaginal at 40 weeks. Birth weight was 3100 g (25th centile) and length 50 cm (25th centile). Apgar scores were 9 and 10, at 1 and 5 minutes, respectively. Patient's karyotype was normal (46,XY), and so were array CGH (at an average resolution of 75Kb) and *FMR1* sequencing.

He presented with mild macrocephaly (44.5 cm at 4 months and 55 cm at 8 years, which correspond to +1.74 and +2.0 SD, respectively), peculiar facial appearance (Fig. 2) and premature closure of the metopic suture with trigonocephaly (Fig. 2A,B), marked hypertelorism, convergent strabismus, downslanted palpebral fissures, epicanthus, blepharophimosis (since the first months of life), prominent nasal root and anteverted nostrils (Fig. 2C,D), hyperconvolute helix, low-set and posteriorly angulated ears (Fig. 2E), hypoplasia of the malar region, micrognathia, highly arched palate and hypertrophy of the alveolar ridges (Fig. 2F). The patient also had large hands and long fingers, horseshoe kidney, bilateral cryptorchidism, slight deformity of the forefoot with flat-footedness in metatarsal level and clinodactyly of the fifth toes (Fig. 2G,H). He also presented with astigmatism and hypermetropia and had a tendency to form cutaneous keloids. The patient had marked oral and lingual dyspraxia and a reduced facial mimicry. As a child, he manifested enuresis and hyperphagia. He underwent: skull remodeling with bilateral frontal advancement and re-alignment of the orbital bar, correction of strabismus and cryptorchidism and adeno-tonsillectomy for snoring. He is relatively short (158 cm whereas his father's height is 185 cm).

He was able to sit at 11 months, did not crawl and maintained orthostatism at 14 months, with instability and frequent falls. Thereafter, there was an improvement in static and dynamic balance, albeit with an underlying state of hypertonicity, postural oddities and serious coordination deficits of fine and large movements. He was able to walk autonomously at 3 years, but up to 5 years he was unable to protect himself from falls. From 9 to 12 years he was treated with botulinum intra-muscular injections, with only partial and transient benefit. While growing, the hypertonic state gradually resolved, but mobility remained clumsy, with toe-walking and an altered dynamic equilibrium (use of the trunk movement to maintain balance).

The patient displayed a marked developmental delay in all intellectual milestones. First words were at 2 years and complete language was reached at 5 years. During childhood, he had a tendency to repetition and echolalia; over time this improved, but the patient had repetitive speech around the same questions. Expressive language was affected to a greater degree than receptive language. Furthermore, a substantial disorder of attention and cognitive rigidity prevented adequate learning at school. He manifested features of autism spectrum disorders (ASD), such as aggression, hyperactivity, repetitive manipulation of the objects and tendency to explore the environment in a purposeless way. He rejected proposals that did not immediately satisfy his own needs, had reduced social interaction with a childlike and self-interested attitude and a tendency to search for attention and reassurance. ID was of severe degree (IQ 33), with concrete thinking and partial temporal orientation.

The patient was initially diagnosed as C Syndrome (CS, Opitz C trigonocephaly, MIM #211750), a rare condition whose etiology is still poorly understood and whose diagnosis is still only clinical. CS was initially proposed because of trigonocephaly, epicanthus, strabismus, micrognathia, ear anomalies, renal anomalies and severe ID. On the other hand, some of the patient's characteristics did not fit into the C syndrome¹⁵: hypertelorism (whereas in CS hypotelorism is typical), macrocephaly (instead of microcephaly), downslanted palpebral fissures (instead of upslanted) and hypertone (instead of hypotone). After a clinical evaluation at 20 years of age, the patient's diagnosis was changed to "unknown".

We performed whole-exome sequencing on the patient's genomic DNA after obtaining written informed consent and the approval of the protocol by the Ethics Committee of the Universitat de Barcelona. We found a novel *de novo* truncating mutation in the *FOXP1* gene (c.1428 + 1 G > A) in heterozygosis. In addition, we found several variants of unknown significance (VUS) in other genes (reported and commented in Table S1). All these variants were inherited



Figure 2. Main features of the patient. (A–B) Neonatal CT scan. Trigonocephaly is clearly appreciated. For a control CT scan, see Khanna *et al.*³² (C–E) Facial dysmorphism at 2 and 23 years of age. Hypertelorism, convergent strabismus, down slanted palpebral fissures, epicanthus, prominent nasal root and ante-verted nostrils and (F) arched palate and hypertrophy of the alveolar processes are appreciated. (G–H) Foot phenotype with metatarsal flat-footedness and clinodactyly. All images are shared by the family with explicit permission to publish.

from either one of his healthy parents and none seems related to the major clinical outcomes of the patient. Of note, the patient is homozygous for the missense mutation p.Ala632Thr (rs72468667) at the *ASXL1* gene. Truncating mutations in this gene are the main cause of Bohring-Opitz syndrome (BOS, MIM #605039), characterized by intellectual disability and trigonocephaly (present in the patient reported here), together with intrauterine growth retardation, feeding difficulties and failure to thrive, and a typical posture (BOS posture), none of which are present in our patient. So far, no missense mutations have been found associated with BOS. In addition, mutation p.Ala632Thr has been found in the general population in 415 out of 277,188 individuals, including one homozygous individual (data from GenomeAD). Whether this missense mutation might contribute to the trigonocephaly of the patient remains an open question.

The *FOXP1* mutation found in the patient consists on a c.1428 + 1 G > A transition at the donor splice site of intron 16. By means of a minigene strategy, we demonstrated that this change leads to the skipping of exon 16 and to a new reading frame starting at alanine 450 and a premature STOP codon after 13 residues (p.Ala450Glyfs*13). This truncated protein would lack 214 residues at the C-terminus, including the FOX domain (Fig. 1). Functional studies performed on similar truncating mutations (also lacking the terminal FOX domain of the protein) showed that they were retained in the cytoplasm^{16,17} and were unable to repress transcription, as demonstrated by luciferase reported assays. Also, as the majority of the truncating mutations retain the leucine zipper domain, necessary for homo- and heterodimerization (see Fig. 1), they bind the wt FOXP1 and FOXP2 proteins, sequestering them in the cytoplasm. This interaction could lead to a dominant negative effect. On the other hand, Sollis *et al.*¹⁷ found that two truncating mutations (p.Ala339Serfs*4 and p.Arg525*) and the missense mutation p.Trp534Arg were unable to interact with wt FOXP1 or FOXP2 and the nuclear localization of the wt FOXP1 and FOXP2 proteins was unperturbed, ruling out dominant negative effects for these mutations. Additionally, it has been described that some of the alleles bearing truncating mutations are degraded by the nonsense-mediated mRNA

Symptoms	Palumbo 2013	Le Fevre 2013	Shrivastava 2014	Song 2015	Lozano 2015	Blanco-Sánchez 2015	Sollis 2016	Current Patient	Total
De novo mutation	+	9/9	+	+	+	+	3/3	+	18/18
Low birthweight	–	0/2	nd	+	nd	nd	nd	+	2/5
FTT or small for age	–	1/5	nd	–	nd	nd	nd	+	2/8
Obesity	–	2/5	nd	–	nd	nd	nd	–	2/8
Prominent forehead	+	4/7	nd	+	–	+	2/3	+(¹)	10/15
Macrocephaly	–	nd	+	nd	+	–	1/3	mild	4/8
Hypertelorism	–	nd	nd	nd	–	nd	2/3	+	3/6
Down slanted palpebral fissures	+	3/7	nd	–	+	+	1/3	+	8/15
Short nose with broad tip	nd	4/7	nd	+	–	+	2/3	+	9/14
Frontal hair upsweep	nd	2/7	nd	+	–	+	nd	–	4/11
Prominent digit pads	nd	2/7	nd	–	nd	nd	nd	–	2/9
Single palmar creases	nd	1/7	nd	–	nd	nd	nd	–	1/9
Clinodactyly	nd	1/7	nd	–	nd	nd	nd	+	2/9
Congenital anomalies ⁽²⁾	nd	3/8	nd	+	nd	nd	nd	+	5/10
Global delay	+	9/9	nd	+	+	+	3/3	+	17/17
Regression	nd	1/2	nd	–	nd	nd	nd	–	1/4
Intellectual delay	+	8/8	+	+	+	+	3/3	+	17/17
Motor delay	+	8/8	nd	+	+	+	3/3	+	16/16
Speech and language delay	+	9/9	nd	+	+	+	3/3	+	17/17
Expressive language more severely affected than receptive language	nd	7/7	nd	+	+	+	nd	+	11/11
Articulation problems	+	5/5	nd	–	+	nd	3/3	+	11/12
Poor grammar	nd	4/4	nd	–	+	nd	nd	+	6/7
ASD/PDD-NOS	+	3/4	nd	–	+	nd	3/3	+	9/11
Autism	+	2/4	nd	–	+	nd	0/3	–	4/11
Behavioral problems	+	4/5	nd	–	+	nd	3/3	+	10/12
ADHD and/or sensory processing disorders	+	nd	nd	–	+	nd	2/3	+	5/7
Hypertonia	nd	1/2 ⁽³⁾	nd	–	–	nd	0/3	+	2/8
Hypotonia	+	1/2 ⁽³⁾	+	nd	+	nd	3/3	–	7/9
Reflexes	nd	1/2	nd	–	nd	nd	nd	+	2/4
Seizures	nd	2/6	nd	–	nd	nd	nd	–	2/8

Table 1. Clinical revision of FOXP1 patients. FTT: Failure to Thrive; ASD: Autistic Spectrum Disorders; PDD-NOS: Pervasive Developmental Disorder Not Otherwise Specified; ADHD: Attention Deficit Hyperactivity Disorder; nd = no data. ⁽¹⁾The patient presented with trigonocephaly. ⁽²⁾Including: contractures, spina bifida, Chiari I malformation, jejunal and ileal atresia, bilateral inguinal hernia²⁵, bilateral cryptorchidism, horseshoe kidney (current patient) and hyperextension of the joints²⁶. ⁽³⁾One patient in Carr *et al.*²¹ presented with decreased axial tone and increased peripheral tone.

decay (NMD)^{16,18}. Finally, several cases have been described with deletions or balanced translocations affecting just the *FOXP1* gene^{19–23}. A mechanism of loss of function and haploinsufficiency seems to be the common feature of all mutations associated with *FOXP1* disorders, including the one described in our patient.

Table 1 summarizes the main clinical features of FOXP1 patients with published clinical data. It includes point mutations (Fig. 1) or small deletions affecting only the *FOXP1* gene. In agreement with these patients, the patient reported here presented with speech and language impairment (with expressive language more severely affected than receptive language) as well as ID and delay in all motor milestones. He also presented with mild macrocephaly and hypertelorism, a trait commonly observed in these patients. Autism was diagnosed in 3 of 8 patients. However, autistic features and/or behavioral problems were observed in all but one of the reported patients, including the present one who presented with impulsivity, stereotypic behaviors and reduced social interest, among other autistic traits. This is in agreement with the reduced exploratory attitudes and increased evasion of social contact, not due to anxiety, observed in mice with a conditional deletion of *Foxp1* in brain²⁴. Other features shared by the present patient and some of the other FOXP1 cases include relatively short stature, strabismus, high-arched palate and enuresis^{16,17,25,26}.

The patient presented here developed blepharophimosis at an early age, same as in the patient described by Pariani *et al.*²⁷, who bears a deletion of the 3p14.1p13 region including the *FOXP1*, *EIF4E3*, *PROK2* and *GPR27* genes. Our patient also shares epicanthal folds and hypermetropia with the one in Pariani *et al.*, but did not display ptosis of the eyelids. In both patients, hypertone was more severe distally and was not associated with muscular spasm or distal contractions of the fingers. However, in our case hypertone was not equally distributed

at 4 limbs but was predominant at the legs, and there were neither distal contractures (present in Pariani *et al.*²⁷ patient) nor neuropathy.

To our knowledge, this is the first case of *FOXP1* mutation associated with trigonocephaly, although other craniofacial anomalies such as prominent forehead are common in *FOXP1* patients. Interestingly, *FOXP1* negatively regulates the expression of *Runx2*¹³, a master transcription factor essential for bone development, whose haploinsufficiency produces cleidocranial dysplasia, which includes as main features patent sutures and fontanelles. On the other hand, trigonocephaly is a relatively prevalent condition in the general population, and it might be due to an independent concomitant cause in this patient.

In conclusion, we describe a patient presenting with mental retardation, speech and language delay and minor craniofacial dysmorphic features, in whom the genetic cause of the disease, a *de novo* truncating mutation in *FOXP1*, could be identified, putting an end to 23 years of diagnostic uncertainty. To our knowledge, it is the first case of *FOXP1* syndrome presenting with true trigonocephaly due to metopic synostosis, expanding the clinical spectrum of this syndrome.

Material and Methods

Biological samples. Genomic DNA from the patient and his parents was obtained from Istituto di Medicina Genomica, Università Cattolica Sacro Cuore, Rome. The signed informed consent was obtained from the patient's mother, including explicit permission to share clinical and identifying information, including in on-line open-access journals. All protocols were approved by the Ethics Committee of the Universitat de Barcelona and all methods were performed in accordance with the relevant guidelines and regulations.

Whole exome sequencing and molecular analyses. Whole exome sequencing of the proband was performed in the National Center of Genomic Analysis (CNAG; Barcelona, Spain), using the Illumina HiSeq-2000 platform. Exome capture was performed with Nimblegen SeqCap 64Mb v3 (Roche; Mannheim; Germany). The samples were sequenced at a coverage of 50X. The data were analyzed as described elsewhere²⁸. The results were then filtered under *de novo* dominance and recessive hypotheses. Variants with a MAF above 0.001 (under the dominant) and above 0.01 (for recessive) in the common population (according to ExAC and 1000 genomes) were excluded. Variants in genes included in selected databases [The Development Disorder Genotype - Phenotype Database (DDG2P)]^{29,30} and covered by at least 10 reads were prioritized for validation (it should be noted that those who carried out the original DECIPHER analysis and collection of the data bear no responsibility for the further analysis or interpretation of it). In parallel, variant effects were classified as high, moderate or low according to SnpEff³¹ and mutations with a high putative effect and at least 10 reads were also prioritized for validation by Sanger sequencing.

On average, the mean coverage for the patient was of 69 reads, and 93% of the target region was covered by at least 10 reads (C10). A total of 19 variants were selected for validation by Sanger sequencing. Primer sequences and PCR conditions are available on request. PCR reactions, purification and sequencing were performed as described previously¹⁴.

Minigene transcript analysis. In order to study the putative effect of the *FOXP1* mutation on splicing, a minigene was constructed, including the genomic region (ENST00000475937) that encompasses exons 15, 16 and 17 (1800pb). This region was PCR-amplified from the patient's DNA using primers: *FOXP1*-MG-F (5'-CTCGAGTCCCAACTGGTGTACCTAA-3') and *FOXP1*-MG-R (5'-GGATCCGAGCATTCAACCACAATGG-3'). These primers include restriction sites for *XhoI* and *BamHI*, respectively (underlined). The wild-type and mutant PCR fragments were cloned into the pSPL3 vector (Addgene). Splicing was assessed 24 h after transfection in HeLa cells. RNA was extracted using the High Pure RNA isolation kit (Roche) and retro-transcribed using the High-Capacity cDNA Reverse Transcription kit (Thermo Fisher Scientific). Primers SD6 and SA2, specific for the pSPL3 vector, were used to amplify the spliced region. The PCR fragments were separated by agarose gel electrophoresis, purified and Sanger sequenced.

References

1. Thevenon, J. *et al.* Diagnostic odyssey in severe neurodevelopmental disorders: toward clinical whole-exome sequencing as a first-line diagnostic test. *Clin Genet* **89**, 700–707 (2016).
2. Soden, S. E. *et al.* Effectiveness of exome and genome sequencing guided by acuity of illness for diagnosis of neurodevelopmental disorders. *Sci Transl Med* **6**, 265ra168 (2014).
3. Tetreault, M., Bareke, E., Nadaf, J., Alirezaie, N. & Majewski, J. Whole-exome sequencing as a diagnostic tool: current challenges and future opportunities. *Expert Rev Mol Diagn* **15**, 749–760 (2015).
4. Evers, C. *et al.* Impact of clinical exomes in neurodevelopmental and neurometabolic disorders. *Mol Genet Metab* **121**, 297–307 (2017).
5. Shi, C. *et al.* Down-regulation of the forkhead transcription factor *Foxp1* is required for monocyte differentiation and macrophage function. *Blood* **112**, 4699–4711 (2008).
6. Benayoun, B. A., Caburet, S. & Veitia, R. A. Forkhead transcription factors: key players in health and disease. *Trends Genet* **27**, 224–232 (2011).
7. Rouso, D. L., Gaber, Z. B., Wellik, D., Morrisey, E. E. & Novitsch, B. G. Coordinated actions of the forkhead protein *Foxp1* and *Hox* proteins in the columnar organization of spinal motor neurons. *Neuron* **59**, 226–240 (2008).
8. Banham, A. H. *et al.* Expression of the *FOXP1* transcription factor is strongly associated with inferior survival in patients with diffuse large B-cell lymphoma. *Clin Cancer Res* **11**, 1065–1072 (2005).
9. Bellacosa, A. Developmental disease and cancer: biological and clinical overlaps. *Am J Med Genet A* **161A**, 2788–2796 (2013).
10. Wang, B., Lin, D., Li, C. & Tucker, P. Multiple domains define the expression and regulatory properties of *Foxp1* forkhead transcriptional repressors. *J Biol Chem* **278**, 24259–24268 (2003).
11. Li, S., Weidenfeld, J. & Morrisey, E. E. Transcriptional and DNA binding activity of the *Foxp1/2/4* family is modulated by heterotypic and homotypic protein interactions. *Mol Cell Biol* **24**, 809–822 (2004).
12. Ferland, R. J., Cherry, T. J., Preware, P. O., Morrisey, E. E. & Walsh, C. A. Characterization of *Foxp2* and *Foxp1* mRNA and protein in the developing and mature brain. *J Comp Neurol* **460**, 266–279 (2003).

13. Zhao, H. *et al.* Foxp1/2/4 regulate endochondral ossification as a suppresser complex. *Dev Biol* **398**, 242–254 (2015).
14. Urreizti, R. *et al.* Screening of CD96 and ASXL1 in 11 patients with Opitz C or Bohring-Opitz syndromes. *Am J Med Genet A* **170A**, 24–31 (2016).
15. Opitz, J. M. *et al.* Mortality and pathological findings in C (Opitz trigonocephaly) syndrome. *Fetal Pediatr Pathol* **25**, 211–231 (2006).
16. Lozano, R., Vano, A., Lozano, C., Fisher, S. E. & Deriziotis, P. A de novo FOXP1 variant in a patient with autism, intellectual disability and severe speech and language impairment. *Eur J Hum Genet* **23**, 1702–1707 (2015).
17. Sollis, E. *et al.* Identification and functional characterization of de novo FOXP1 variants provides novel insights into the etiology of neurodevelopmental disorder. *Hum Mol Genet* **25**, 546–557 (2016).
18. O’Roak, B. J. *et al.* Exome sequencing in sporadic autism spectrum disorders identifies severe de novo mutations. *Nat Genet* **43**, 585–589 (2011).
19. Horn, D. *et al.* Identification of FOXP1 deletions in three unrelated patients with mental retardation and significant speech and language deficits. *Hum Mutat* **31**, E1851–1860 (2010).
20. Hamdan, F. F. *et al.* De novo mutations in FOXP1 in cases with intellectual disability, autism, and language impairment. *Am J Hum Genet* **87**, 671–678 (2010).
21. Carr, C. W. *et al.* Chiari I malformation, delayed gross motor skills, severe speech delay, and epileptiform discharges in a child with FOXP1 haploinsufficiency. *Eur J Hum Genet* **18**, 1216–1220 (2010).
22. Talkowski, M. E. *et al.* Sequencing chromosomal abnormalities reveals neurodevelopmental loci that confer risk across diagnostic boundaries. *Cell* **149**, 525–537 (2012).
23. Chen, C. M. & Behringer, R. R. Ovocal regulates cell proliferation, embryonic development, and tumorigenesis. *Genes Dev* **18**, 320–332 (2004).
24. Bacon, C. *et al.* Brain-specific Foxp1 deletion impairs neuronal development and causes autistic-like behaviour. *Mol Psychiatry* **20**, 632–639 (2015).
25. Le Fevre, A. K. *et al.* FOXP1 mutations cause intellectual disability and a recognizable phenotype. *Am J Med Genet A* **161A**, 3166–3175 (2013).
26. Song, H., Makino, Y., Noguchi, E. & Arinami, T. A case report of de novo missense FOXP1 mutation in a non-Caucasian patient with global developmental delay and severe speech impairment. *Clin Case Rep* **3**, 110–113 (2015).
27. Pariani, M. J., Spencer, A., Graham, J. M. Jr & Rimoin, D. L. A 785kb deletion of 3p14.1p13, including the FOXP1 gene, associated with speech delay, contractures, hypertonia and blepharophimosis. *Eur J Med Genet* **52**, 123–127 (2009).
28. Sanz-Pamplona, R. *et al.* Exome Sequencing Reveals AMER1 as a Frequently Mutated Gene in Colorectal Cancer. *Clin Cancer Res* **21**, 4709–4718 (2015).
29. Firth, H. V. *et al.* DECIPHER: Database of Chromosomal Imbalance and Phenotype in Humans Using Ensembl Resources. *Am J Hum Genet* **84**, 524–533 (2009).
30. Samocha, K. E. *et al.* A framework for the interpretation of de novo mutation in human disease. *Nat Genet* **46**, 944–950 (2014).
31. Cingolani, P. *et al.* A program for annotating and predicting the effects of single nucleotide polymorphisms, SnpEff: SNPs in the genome of *Drosophila melanogaster* strainw1118; iso-2; iso-3. *Fly (Austin)* **6**, 80–92 (2012).
32. Khanna, P. C., Thapa, M. M., Iyer, R. S. & Prasad, S. S. Pictorial essay: The many faces of craniosynostosis. *Indian J Radiol Imaging* **21**, 49–56 (2011).

Acknowledgements

The authors thank the patient and his family for wholehearted collaboration. They are also grateful to M. Cozar for technical assistance, and to CNAG for exome sequencing within the “300 exomes to elucidate rare diseases” program. Funding was from Associació Síndrome Opitz C, Terrassa, Spain; Spanish Ministerio de Economía y Competitividad (SAF2014-56562-R; SAF2016-75948-R, FECYT, crowdfunding PRECIPITA); ISCIII Ministerio de Economía y Competitividad (PT13/0001/0044), Catalan Government (2014SGR932) and from CIBERER (U720).

Author Contributions

R.U., B.C., L.V., S.B. and D.G. have contributed to the planning of this work. R.U., S.D., C.E., H.F., L.C., R.T., D.G., S.B. have conducted this work. R.U., R.T., C.E., L.C. and H.F. have analyzed and validated the Whole Exome Sequencing data. R.U., H.F. and C.E. have performed the minigene splicing analysis. S.D., J.O. and G.N. have clinically evaluated the patient and have generated and written the clinical data. R.U., S.B., D.G. wrote the main manuscript text. R.U., S.D., G.N. elaborated Table 1. R.U. elaborated Figure 1. R.U. and S.D. prepared Figure 2. C.E., H.F., L.C. elaborated Supplementary Figure S1. R.U., S.B. and D.G. have elaborated Supplementary Table S1. All authors reviewed the manuscript

Additional Information

Supplementary information accompanies this paper at <https://doi.org/10.1038/s41598-017-19109-9>.

Competing Interests: The authors declare that they have no competing interests.

Publisher’s note: Springer Nature remains neutral with regard to jurisdictional claims in published maps and institutional affiliations.



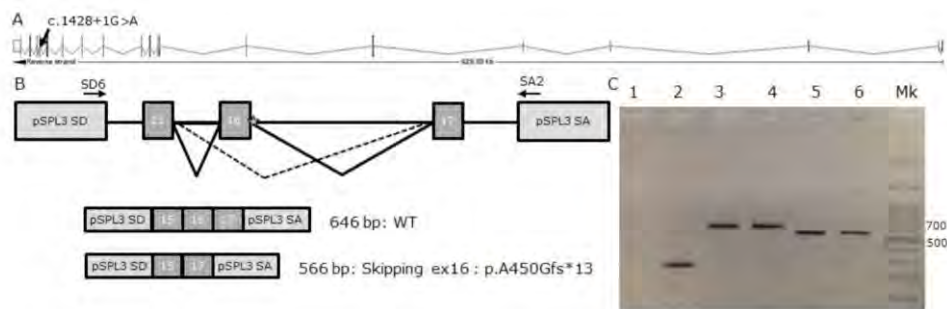
Open Access This article is licensed under a Creative Commons Attribution 4.0 International License, which permits use, sharing, adaptation, distribution and reproduction in any medium or format, as long as you give appropriate credit to the original author(s) and the source, provide a link to the Creative Commons license, and indicate if changes were made. The images or other third party material in this article are included in the article’s Creative Commons license, unless indicated otherwise in a credit line to the material. If material is not included in the article’s Creative Commons license and your intended use is not permitted by statutory regulation or exceeds the permitted use, you will need to obtain permission directly from the copyright holder. To view a copy of this license, visit <http://creativecommons.org/licenses/by/4.0/>.

© The Author(s) 2018

Supplementary information for:

A De Novo *FOXP1* Truncating Mutation in a Patient Originally Diagnosed as C Syndrome

Roser Urreizti, Sarah Damanti, Carla Esteve, Héctor Franco-Valls, Laura Castilla-Vallmánya, Raul Tonda, Bru Cormand, Lluïsa Vilageliu, John M. Opitz, Giovanni Neri, Daniel Grinberg & Susana Balcells



Supplementary Figure S1. (A) *FOXP1* gene representation (ENST00000318789.4). The black arrow marks the position of the mutation (at exon 16 splicing donor site). (B) Schematic representation of the pSPL3 minigene construct and putative splicing events. (C) PCR amplification of the (2) empty vector, the vector containing the minigene with the wt allele (3 and 4) and with the c.1428+1G>A mutation (5 and 6). Mk: 100pb molecular weight marker, (1) negative control.

Supplementary Table S1:

GENE	Change	cDNA	Protein	Inheritance	Disease ¹	MIM number	PT ²	Provean/SIFT/ PolyPhen2	ExAC MAF (homoz.)	Constrained ³	Comments
<i>SLC17A5</i>	C>T	c.567G>A	p.Trp189*	Patient htz; father htz	Salla disease Sialic acid storage disorder, infantile	604369	AR	NA/NA/NA	-	no	Only one putatively pathogenic allele detected in the patient, inherited from an unaffected parent.
						269920	AR				
<i>POLH</i>	->AA	c.117insAA	p.Ser40Asnfs*8	Patient htz; mother htz	Xeroderma pigmentosum	278750	AR	NA/NA/NA	-	no	Only one putatively pathogenic allele detected in the patient, inherited from an unaffected parent.
<i>TRPC5</i>	G/T	c.279C>A	p.Ser93Arg	Patient hemiz; mother htz	none			N/T/B	0.00001 (0)	yes (missense and LoF)	rs779715044. Only one putatively pathogenic allele detected in the patient, inherited from an unaffected parent.
<i>MAP4K2</i>	G>A	c.439C>T	p.Gln147*	Patient htz; father htz	none			NA/NA/NA	0.000008 (0)	no	Only one putatively pathogenic allele detected in the patient, inherited from an unaffected parent.
<i>DMD</i>	C>G	c.2971G>C	p.Glu99I Asn	Patient hemiz; mother htz	Becker muscular dystrophy Cardiomyopathy, dilated, 3B Duchenne muscular dystrophy	300376	XLR	N/T/D	0.0015 (60)	yes (LoF)	rs72468667: described in hemizyosity in 60 healthy individuals. Inherited from an unaffected parent.
						302045	XL				
						310200	XLR				
<i>MAGEL2</i>	C>T	c.1894G>A	p.Ala632Thr	Patient htz; mother htz	Schaaf-Yang syndrome (SHFYNG)	615547	AD	NA/NA/NA	0.00003 (0)	Yes (LoF)	<i>MAGEL2</i> gene is maternally silenced. The mutation is in the inactive copy of the gene. All mutations previously associated with SHFYNG are truncating.
<i>ASXLI</i>	A>G	c.2957A>G	p.Asn986Ser	Patient hom; both parents are htz	Bohring-Opitz Syndrome (BOS)	605039	AD	N/T/B	0.0012 (0)	no	rs145132837: present in 153 healthy individuals, no homozygous individuals reported. All mutations previously associated with BOS are <i>de novo</i> truncating mutations.

HTZ: Heterozygous; Hom: Homozygous; Hemiz: hemizygous, AR: Autosomal Recessive; XLR: X-linked Recessive; XL: X-linked; AD: Autosomal Dominant; NA: Not Available; N: Neutral; T: Tolerated; B: Benign; D: Damaging; LoF: Loss of Function

¹ disease/s associated with mutations in this gene

² PT: pattern of inheritance of the associated disease.

³ Genes "constrained" by evolution according to ExAC database. These genes presented less mutations than expected by chance, suggesting an important function for the gene.

Article 7: DPH1 syndrome: two novel variants and structural and functional analyses of seven missense variants identified in syndromic patients

Summary:

DPH1 variants have been associated with an ultra-rare and severe neurodevelopmental disorder, mainly characterized by variable developmental delay, short stature, dysmorphic features, and sparse hair. We have identified four new patients (from two different families) carrying novel variants in *DPH1*, enriching the clinical delineation of the DPH1 syndrome. Using a diphtheria toxin ADP-ribosylation assay, we have analyzed the activity of seven identified variants and demonstrated compromised function for five of them [p.(Leu234Pro); p.(Ala411Argfs*91); p.(Leu164Pro); p.(Leu125Pro); and p.(Tyr112Cys)]. We have built a homology model of the human DPH1–DPH2 heterodimer and have performed molecular dynamics simulations to study the effect of these variants on the catalytic sites as well as on the interactions between subunits of the heterodimer. The results show correlation between loss of activity, reduced size of the opening to the catalytic site, and changes in the size of the catalytic site with clinical severity. This is the first report of functional tests of *DPH1* variants associated with the DPH1 syndrome. We demonstrate that the in vitro assay for DPH1 protein activity, together with structural modeling, are useful tools for assessing the effect of the variants on DPH1 function and may be used for predicting patient outcomes and prognoses.

Reference:

Urreizti R, Mayer K, Evrony GD, Said E, Castilla-Vallmanya L, Cody NAL, Plasencia G, Gelb BD, Grinberg D, Brinkmann U, Webb BD, Balcells S. DPH1 syndrome: two novel variants and structural and functional analyses of seven missense variants identified in syndromic patients. *Eur J Hum Genet.* 2020; 28(1):64-75. doi: 10.1038/s41431-019-0374-9.



DPH1 syndrome: two novel variants and structural and functional analyses of seven missense variants identified in syndromic patients

Roser Urreizti¹ · Klaus Mayer² · Gilad D. Evrony³ · Edith Said^{4,5} · Laura Castilla-Vallmanya¹ · Neal A. L. Cody^{6,7} · Guillem Plasencia⁸ · Bruce D. Gelb^{6,9,10} · Daniel Grinberg^{5,1} · Ulrich Brinkmann² · Bryn D. Webb^{6,9,10} · Susanna Balcells¹

Received: 23 October 2018 / Revised: 21 February 2019 / Accepted: 1 March 2019 / Published online: 15 March 2019
© European Society of Human Genetics 2019

Abstract

DPH1 variants have been associated with an ultra-rare and severe neurodevelopmental disorder, mainly characterized by variable developmental delay, short stature, dysmorphic features, and sparse hair. We have identified four new patients (from two different families) carrying novel variants in *DPH1*, enriching the clinical delineation of the DPH1 syndrome. Using a diphtheria toxin ADP-ribosylation assay, we have analyzed the activity of seven identified variants and demonstrated compromised function for five of them [p.(Leu234Pro); p.(Ala411Argfs*91); p.(Leu164Pro); p.(Leu125Pro); and p.(Tyr112Cys)]. We have built a homology model of the human DPH1–DPH2 heterodimer and have performed molecular dynamics simulations to study the effect of these variants on the catalytic sites as well as on the interactions between subunits of the heterodimer. The results show correlation between loss of activity, reduced size of the opening to the catalytic site, and changes in the size of the catalytic site with clinical severity. This is the first report of functional tests of *DPH1* variants associated with the DPH1 syndrome. We demonstrate that the in vitro assay for DPH1 protein activity, together with structural modeling, are useful tools for assessing the effect of the variants on DPH1 function and may be used for predicting patient outcomes and prognoses.

These authors contributed equally: Roser Urreizti, Klaus Mayer, Gilad D. Evrony

These authors contributed equally: Ulrich Brinkmann, Bryn D. Webb, Susanna Balcells

Supplementary information The online version of this article (<https://doi.org/10.1038/s41431-019-0374-9>) contains supplementary material, which is available to authorized users.

✉ Roser Urreizti
roseref@yahoo.es

¹ Department of Genetics, Microbiology and Statistics, Faculty of Biology, University of Barcelona, IBUB, IRSJD, CIBERER, Barcelona, Spain

² Roche Pharma Research and Early Development, Large Molecule Research, Roche Innovation Center, Munich, Nonnenwald 2, 82377 Penzberg, Germany

³ Center for Human Genetics & Genomics, New York University Langone Health, New York, NY, USA

⁴ Section of Medical Genetics, Mater dei Hospital, Msida, Malta

Introduction

Diphthamide is a unique post-translationally modified histidine residue found only in eukaryotic and archaeal translation elongation factor 2 (EF2). Diphthamide is conserved across all eukaryotes, and notably, is the target of diphtheria toxin (DT). DT catalyzes the transfer of ADP-ribose from nicotinamide adenine dinucleotide (NAD⁺) to diphthamide, thereby inhibiting protein synthesis and leading to cell death [1].

⁵ Department of Anatomy and Cell Biology, University of Malta, Msida, Malta

⁶ Department of Genetics and Genomic Sciences, Icahn School of Medicine at Mount Sinai, New York, NY, USA

⁷ Sema4, Stamford, CT, USA

⁸ Lead Molecular Design, S.L. Sant Cugat del Vallés, Spain

⁹ Mindich Child Health and Development Institute, Icahn School of Medicine at Mount Sinai, New York, NY, USA

¹⁰ Department of Pediatrics, Icahn School of Medicine at Mount Sinai, New York, NY, USA

Table 1 Clinical features observed in patients with *DPH1* mutations

Reference	Alazami et al. [4]	Loucks et al. [5]	Riazuddin et al. [6]	Sekiguchi et al. [8]	Nakajima et al. [7]	Present study	Present study	Total (%)
Geographical origin	Saudi Arabia	North America	Pakistan	Iran	Japan	Malta	Yemen	
Mutation (at protein level)	p.(Leu234Pro)	p.(Met6Lys)	p.(Pro382Ser)	p.(Ala411Argfs*91)	p.(Glu97Lysfs*8)/ p.(Leu164Pro)	p.(Leu125Pro)	p.(Tyr112Cys)	
Mutation (at cDNA level)	c.701T>C	c.171T>A	c.1144C>T	c.1227delG	c.289delG/c.491T>C	c.374T>C	c.335A>G	
rs SNP ID	rs730882250	rs749267261	rs765677788	–	–	rs200530055	rs772969956	
Allele count (freq.) in gnomAD	1 (0.000004)	1 (0.000004)	4 (0.00001)	–	–	79 (0.00028)	2 (0.000008)	
In vitro enzyme activity	Reduced	as wt	as wt	Reduced	Reduced (for p. Leu164Pro)	Reduced	Reduced	
Number of patients	4	4	2	2	1	2	2	17
Developmental delay/intellectual disability	4/4	4/4	2/2 ⁽³⁾	2/2	1/1	2/2	2/2	17/17 (100)
CNS malformations	4/4	0/2	NA	2/2	1/1	1/1	1/1	9/11 (81.8)
Hypotonia	4/4	0/4	1/2	0/2	0/1	2/2	2/2	9/17 (52.9)
Epilepsy	NA	1/1	NA	1/2	0/1	2/2	1/2	5/8 (62.5)
Short stature	4/4	3/4	NA	2/2	1/1	2/2	2/2	14/15 (93.3)
Abnormal head circumference	NA	macro. 1/4	NA	NA	microc.	microc.	Relative macroc.	6/9 (66.7)
Unusual skull shape	4/4	4/4	NA	2/2	1/1	2/2	2/2	15/15 (100)
Craniofacial dysmorphic features	4/4	4/4	2/2	2/2	1/1	2/2	2/2	17/17 (100)
Dental abnormalities	NA	1/4	NA	2/2	NA	2/2	2/2	7/10 (70)
Sparse hair on scalp, eye lashes, or eyebrows	4/4	4/4	NA	2/2	1/1	2/2	2/2	15/15 (100)
Hand/foot anomalies	4/4 ⁽²⁾	2/2	NA	2/2 ⁽⁴⁾	NA	2/2	2/2	12/12 (100)
Abnormal toe nails	NA	3/4	NA	NA	NA	2/2	1/2	6/8 (75)

Table 1 (continued)

Reference	Alazami et al. [4]	Loueks et al. [5]	Riazuddin et al. [6]	Sekiguchi et al. [8]	Nakajima et al. [7]	Present study	Present study	Total (%)
Heart malformation/abnormality ⁽¹⁾	3/4	0/4	NA	1/2	0/1	1/2	2/2	7/15 (46.7)
Renal disease	3/4	1/4	NA	0/2	0/1	NA	0/2	4/13 (30.8)
Genitalia anomalies	2/4	NA	NA	NA	1/1	1/2	1/2	5/9 (55.6)
Early lethality	3/4	0/4	0/2	0/2 ⁽⁵⁾	0/1	1/2	0/2	4/17 (23.5)
Other features (in all the patients if not specified otherwise)	Bifid uvula, hypotonia	Visual impairment (2/4), sleep apnea (1/4), bilateral inguinal hernia (1/4), ADHD (1/4), anxiety (1/4), failure to thrive (1/4)	Autism, motor weakness	Cleft palate, widely spaced teeth, scleral pigmentation, bilateral single transverse palmar crease, kyphoscoliosis (1/2), ADHD and anxiety (1/2) birth	Bilateral single transverse palmar creases, IUGR, required mechanical ventilation at birth	Bilateral hernia (1/2), keratoconus, hypothyroidism (1/2)	Anxiety (1/2); unilateral single transverse palmar crease (1/2)	

CNS Central nervous System, NA Not assessed or no information available, *macro*: macrocephaly, *micro*: microcephaly, *ADHD*: attention-deficit hyperactivity disorder, *IGUR*: intrauterine growth restriction, (1) Ventricular septal defect, dilated cardiomyopathy, aortic stenosis, atrial septal defect, tetralogy of Fallot... (2) camptodactyly; (3) mild. Both patients with autism; (4) flat foot; (5) an older brother died at 6 month of sudden infant death but the *DPH1* mutation has not been assessed

DPH1 (diphthamide biosynthesis 1, OMIM *603527) encodes the enzyme [2-(3-amino-3-carboxypentyl) histidine synthase subunit 1; EC 2.5.1.108], which is required for the first step in the synthesis of diphthamide and, therefore, is essential for generating the diphthamide modification of eukaryotic EF2 (eEF2). *DPH1* is also a tumor-suppressor gene with a crucial role in the regulation of cell proliferation, embryonic development, and tumorigenesis [2, 3].

Recently, autosomal recessive variants in *DPH1* have been associated with a rare neurodevelopmental disorder, known as DEDSSH (Developmental delay with short stature, dysmorphic features, and sparse hair; MIM #616901), with clinical features, including intellectual disability, short stature, and craniofacial and ectodermal anomalies. So far, five independent groups of DEDSSH patients have been published: one family with four affected members of Saudi Arabian origin [4], a group of four patients from three consanguineous families from an American genetic isolate [5], a Pakistani family with two affected patients [6], a Japanese patient [7], and two siblings from a consanguineous Iranian family [8]. All but one of the *DPH1* variants identified in these patients were missense (Table 1).

Because the functionality of *DPH1* directly affects diphthamide synthesis and consequently the ADP-ribosylation (ADPR) by DT of eEF2's diphthamide residue [9], ADPR assays can be used to probe the presence or absence of diphthamide and thereby indirectly test the functionality of *DPH1* [10]. Here, using whole-exome sequencing (WES), we have identified two novel homozygous missense variants in *DPH1* in two unrelated families with DEDSSH. We applied the ADPR assay to functionally validate and confirm the pathogenicity of these variants as well as all *DPH1* variants previously published. Next, we built a homology model of the *DPH1*-*DPH2* heterodimer to elucidate possible mechanisms by which the variants disrupt protein function. Finally, we established genotype-phenotype correlations for this rare disease, which we propose to rename as *DPH1* syndrome.

Results

Clinical report

Family 1

Patient 1 The patient is a 31-year-old man born in the USA, who was initially clinically diagnosed with Opitz C syndrome. He is the first son of a Maltese couple and was born at 38 weeks gestation by vaginal delivery with a birth weight of 2.35 Kg (-2.5 SD Z-score). He suffered from neonatal seizures and was nursed in the neonatal unit for

2 months because of feeding difficulties and multiple congenital anomalies. He had a high and broad forehead with pronounced metopic suture and trigonocephaly and an open posterior fontanelle. There were capillary hemangiomas on the face, his ears were reportedly low-set and protruding, and the palate was highly arched. Also noted were short digits and clinodactyly of the 5th fingers. He was congenitally hypotonic and did not sit until 17 months. Severe psychomotor delay and failure to thrive were noted from early childhood. He also required treatment for hypothyroidism. As an infant, he developed keratoconus. Orchidopexy and bilateral inguinal hernia repair were performed at 1 year of age. Other anomalies included two fused vertebrae, bony defects of hands and feet, and a horseshoe-shaped kidney. A brain MRI performed when he was 11-year-old showed dilated ventricles and cavum septi pellucidi.

During development, his growth curves for weight and height were below the fifth centile and he suffered from repeated respiratory infections, none of which required hospitalization. He has been tube-fed throughout most of his life. At 18 years of age, he had an episode of congestive heart failure and his echocardiogram showed dilated cardiomyopathy.

On examination at 21 years of age, the patient was severely developmentally delayed, non-ambulatory, with no speech and no sphincter control. He was hypotonic with cortical spasticity. He had short stature (-8.4 SD Z-score), low weight (-13.6 SD Z-score), and low BMI (-2.8 SD Z-score). He was severely microcephalic with an occipital frontal circumference (OFC) of 46.1 cm (-6.1 SD Z-score). The shape of the skull was trigonocephalic with prominent metopic and sagittal sutures, sparse hair and soft left side of the posterior end of the sagittal suture with no hair and temporal prominence. He had a high, broad, triangular forehead with bitemporal prominence and supraorbital ridges. The face was characterized by marked ocular telecanthus (inner canthal distance 3.5 cm; interpupillary distance 7 cm, outer canthal distance 11 cm), bilateral epicanthic folds, downslanting palpebral fissures, keratoconus, ocular proptosis, short nose with depressed nasal bridge, and a small mouth that could not be fully opened. He had a short neck, broad thorax with increased inter-nipple distance, venous reticulum, abnormal fat distribution in trunk and no axillary hair. The hands were small with short tapered fingers. He had loose skin on the back, right hand with a single transverse palmar crease, and cutaneous syndactyly at second, third, and fourth ray. The feet were described to have hallux valgus with hypoplastic, overriding toes. He had a micropenis, hypoplastic scrotum, undescended testes, and a lack of pubic hair. The patient also presented with webbing at the knees and neurological muscle wasting in lower limbs.

Patient 2 She was the younger sister of Patient 1 and died at the age of 20 years after a hospitalization for a severe respiratory tract infection. She was born by elective caesarian section for breech presentation. Apgar scores were 2 and 9, at 1 and 5 min, respectively. At birth, dysmorphic facial features similar to her brother were noted, and it was evident that she had the same syndrome. CT-scan showed leukomalacia, cavum septum pellucidum, ventricular dilatation, synostosis of metopic suture, agenesis of the corpus callosum, and leukodystrophy. Her EEG was abnormal, with very frequent runs of slow generalized spikes and slow wave discharge. At 7 years of age, her bone age was advanced (9 years).

When examined at 10 years of age, she had profound intellectual disability and growth delay, was wheelchair-bound, and had no sphincter control. She presented with microcephaly (OFC -6.2 SD Z-score), short stature (105 cm; -5 SD Z-score), and low BMD (-5 SD Z-score) with a weight of 12 kg (-7.6 SD Z-score). The dysmorphic features were more marked than her brother's. She presented with trigonocephaly and dolichocephaly with prominent sagittal suture, proptosis, downslanting palpebral fissures, telecanthus, a small nose and mouth. Her ears were prominent with low-set auricles, simpler than her brother's. She also had pectus excavatum, venous reticulum, hypoplasia of the nipples, increased inter-nipple distance, and fat in the breast areas. Her hands and feet were similar to her brother's and her knee joints were hyperextensible. She had normal genitalia. Neurologically, she had central hypotonia with brisk tendon reflexes and clonus of the feet.

Family 2

Patient 3 The patient is a 20-month-old male of Yemeni (Bedouin) ancestry born to healthy parents who are first cousins. Prenatal history was notable for a diagnosis of tetralogy of Fallot made by fetal echocardiogram at 20 weeks of gestation. The patient was born at 38 weeks gestation by vaginal delivery with a birth weight of 2.99 kg (-0.94 SD Z-score), length of 41.5 cm (-3.12 SD Z-score), and head circumference of 34 cm (-0.89 SD Z-score). Dysmorphic features were noted at birth, including frontal bossing, epicanthal folds, a depressed nasal bridge, and a short nose with an upturned nasal tip. Echocardiogram performed after delivery confirmed tetralogy of Fallot and a closed patent ductus arteriosus. Renal sonogram was normal. Surgical repair of tetralogy of Fallot was performed at 4 months of age. vEEG completed at 4 months of age due to decreased responsiveness after surgery was notable for diffuse cerebral dysfunction, but no seizure activity. Head CT was significant for mild diffuse generalized cerebral and cerebellar volume loss. At 5 months of age, the patient

received a G-tube due to poor feeding. Head ultrasound at 6 months revealed moderate pan-ventricular dilatation. His MRI completed at 6 months revealed diffuse prominence of the ventricular system and extra-axial fluid spaces, likely secondary to underlying parenchymal volume loss (Supplementary Figure 1). At 17 months of age, the patient presented with fever and a fixed right eye gaze deviation lasting ~30 min, suggesting a febrile seizure. An EEG completed shortly after this event was negative. He was recently diagnosed with obstructive sleep apnea.

On examination at 20 months of age, head circumference was at the 0.65 SD Z-score, weight was at -0.787 SD Z-score, and height was short at -2.4 SD Z-score. The patient appeared macrocephalic with prominent frontal bossing, broad forehead, and high anterior hairline. Sparse, thin, and coarse hair was noted along with sparse eyebrows and absent eye lashes. Eyes appeared hyperteloritic with down-slanting palpebral fissures and epicanthal folds. Ears had overfolded helices bilaterally and micrognathia was noted. He had small peg-shaped teeth, normal palmar creases, short tapered digits, and pes planus. Nails were normal. He had significant hypotonia and gross motor delay, but was able to sit unsupported and support weight on his legs when held. He had loose skin over his hands and feet.

Chromosome analysis was normal. Chromosomal microarray did not reveal any pathogenic CNVs, but was notable for 223 Mb of absence of heterozygosity (AOH) (~7.8% of autosomal genome), consistent with the history of consanguinity (Supplementary Table 1).

Patient 4 The patient is the 7-year-old brother of Patient 3. Prenatal history was unremarkable. The patient was born at 37 weeks gestation by normal spontaneous vaginal delivery. He required 2 days in the neonatal intensive care unit for respiratory support with supplemental oxygen. At 3 months of age, the patient was diagnosed with obstructive sleep apnea and required supplemental oxygen at night for several years. He had a hydrocele, which resolved by 1 year of age. An echocardiogram completed at 5 years of age was notable for a moderately dilated left ventricle with eccentric left ventricular hypertrophy. He has recently had multiple seizures, and EEG revealed suboptimal organization, mild generalized slowing, and occasional bilateral, independent hemispheric spikes. Developmental delays were noted from a young age.

On examination, at 7 years of age, head circumference was at 0.31 SD Z-score, weight was low at -2.8 SD Z-score, and short stature was present with height at -4.0 SD Z-score. Dysmorphic features included frontal bossing, broad forehead, high anterior hairline, low-set and posteriorly rotated ears, short philtrum, and small, peg-shaped teeth. Sparse, thin, and coarse hair was noted with sparse eyebrows and absent eye lashes. His right hand had a single

transverse palmar crease. He had tapered digits, pes planus, and dysplastic toe nails. He had a micropenis. He was nonverbal and had significant hypotonia and gross motor delay, but was able to sit unsupported.

Genetic investigations

Family 1

WES was performed on both affected sibs and parents (four individuals) and revealed six candidate variants in five genes (Supplementary Table 2). In particular, one homozygous variant was identified as “disease causing” in both affected siblings: *DPH1* c.374 T>C; p.(Leu125Pro) (NM_001383.4), inherited from both heterozygous parents. This variant has been submitted to the Leiden Open Variation Database (<http://lovd.nl/3.0/>). The remaining variants were classified as likely benign changes or variants of unknown significance (VUS).

Family 2

WES was performed for the proband and the father. Variants called by WES were filtered for call quality, low frequency in the population, and predicted deleteriousness, yielding 103 variants in 76 genes (Supplementary Table 3). An additional biological context filter identifying variants in genes known or predicted to cause “Tetralogy of Fallot” or “Developmental Delay” yielded a single variant: *DPH1* c.335 A>G; p.(Tyr112Cys). This variant was homozygous in the proband and heterozygous in the father. The variant was confirmed by Sanger sequencing in the proband and father. Additionally, Sanger sequencing confirmed that the older affected brother is also homozygous for this variant. This variant has been submitted to the Leiden Open Variation Database (<http://lovd.nl/3.0/>).

Protein alignments

In order to assess the conservation of the residues affected by the missense variants identified in our patients and those described in the literature (listed in Table 1), the *DPH1* protein sequences from 80 different eukaryotic species were aligned for comparison. In general, the central part of the protein (positions 80 to 310 of the human *DPH1*) was highly conserved, while the N- and C-termini displayed less conservation. Human *DPH1* Met6 corresponds to the initiation codon in most other mammals, while in bonobos (*Pan paniscus*), two sequences with different initiation codon are described (see Supplementary Figure 3). Tyr at position 112 is conserved among all the analyzed species up to and including fungi, while Leu125, Leu164, and Leu234 are conserved in nearly all of them. Finally, Pro382, at the

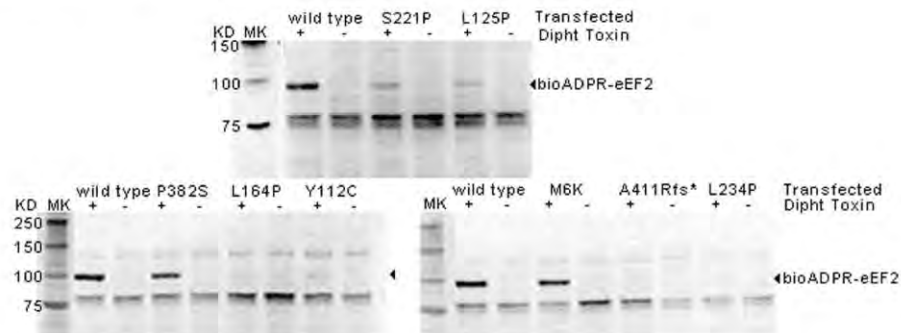
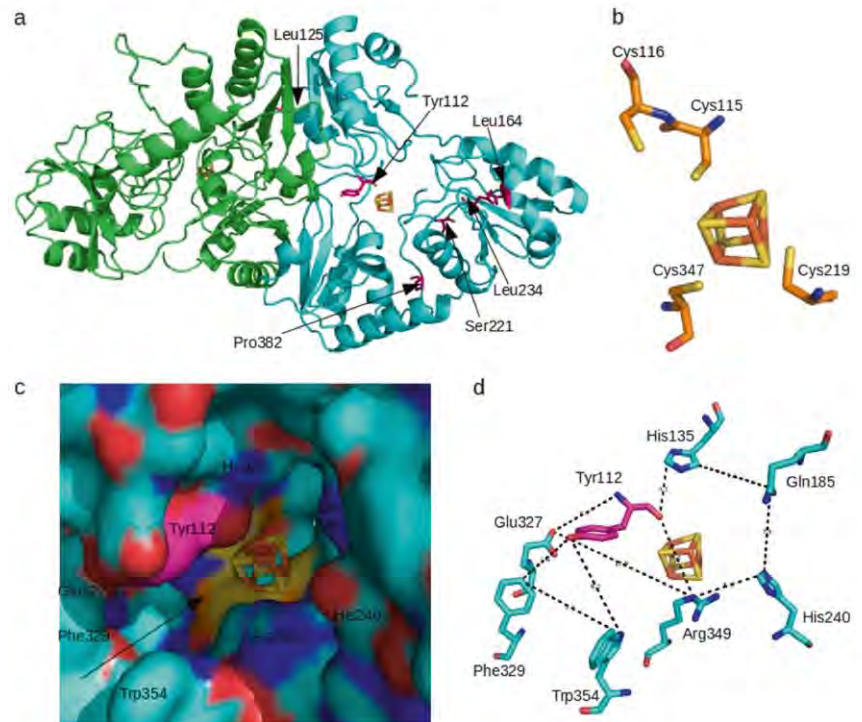


Fig. 1 Assay for diphthamide deficiency and DPH1 function in DPH1-knockout (DPH1ko) cells. Extracts of DPH1ko cells transfected with wild-type or mutant DPH1 variants were subjected to diphtheria toxin (DT)-mediated biotin-ADP-ribosylation of diphthamide. Assay activity was then detected by probing membrane blots with enzyme-

conjugated streptavidin. eEF2 protein is sized 100 kDa. Extracts of DPH1ko cells expressing plasmid-encoded wild-type DPH1 were included as positive controls. Reactions with no DT served as specificity controls. Background bands are biotinylated cellular proteins that provide controls for equal loading of protein

Fig. 2 Homology model of human DPH1-DPH2 heterodimer. Upper panels: **a** Human DPH1-DPH2 model, with DPH2 subunit on the left (in green) and DPH1 subunit on the right (in blue) with a cube-shaped [4Fe-4S] cluster to the right. Arrows show the positions of Tyr112, Leu125, Leu164, Ser221, Leu234, and Pro382. **b** DPH1 subunit Cys116, Cys115, Cys219, and Cys347 form a plane around the [4Fe-4S] cluster (its position in the figure, not optimized, is shown here for reference). Lower panels: **c** Potential iron-sulfur cluster entry points in DPH1 model. Gate A, shown with an arrow in the lower left side of the image, and gate B in the center of the image. **d** Residues forming gate A and gate B potential entry points



less conserved C-terminus of the protein, is present in all the analyzed mammals, *Xenopus*, most birds and insects.

Biochemical investigation of all DPH1 missense variants identified so far in the DPH1 syndrome

We applied an ADP-ribosylation (ADPR) assay to test the functional impact of all previously identified DPH1 missense variants. Diphtheria toxin catalyzes the transfer of ADP-ribose from NAD⁺ to the diphthamide residue on eEF2. In this assay, biotinylated NAD is used, which can

also function as a toxin substrate, such that in cell extracts exposed to DT and biotinylated NAD, biotin-ADP is transferred to diphthamide-eEF2. eEF2 without diphthamide does not become ADP-ribosylated, and hence, is not labeled with biotin.

The degree to which diphthamide is present on eEF2 can thereby be visualized. Figure 1 shows the results of these ADPR assays. Extracts of MCF7 cells with inactivated DPH1 genes (DPH1ko cells with both alleles inactivated [11]) were transfected with plasmids that encode either wild-type DPH1 or DPH1 variants. Those variants included

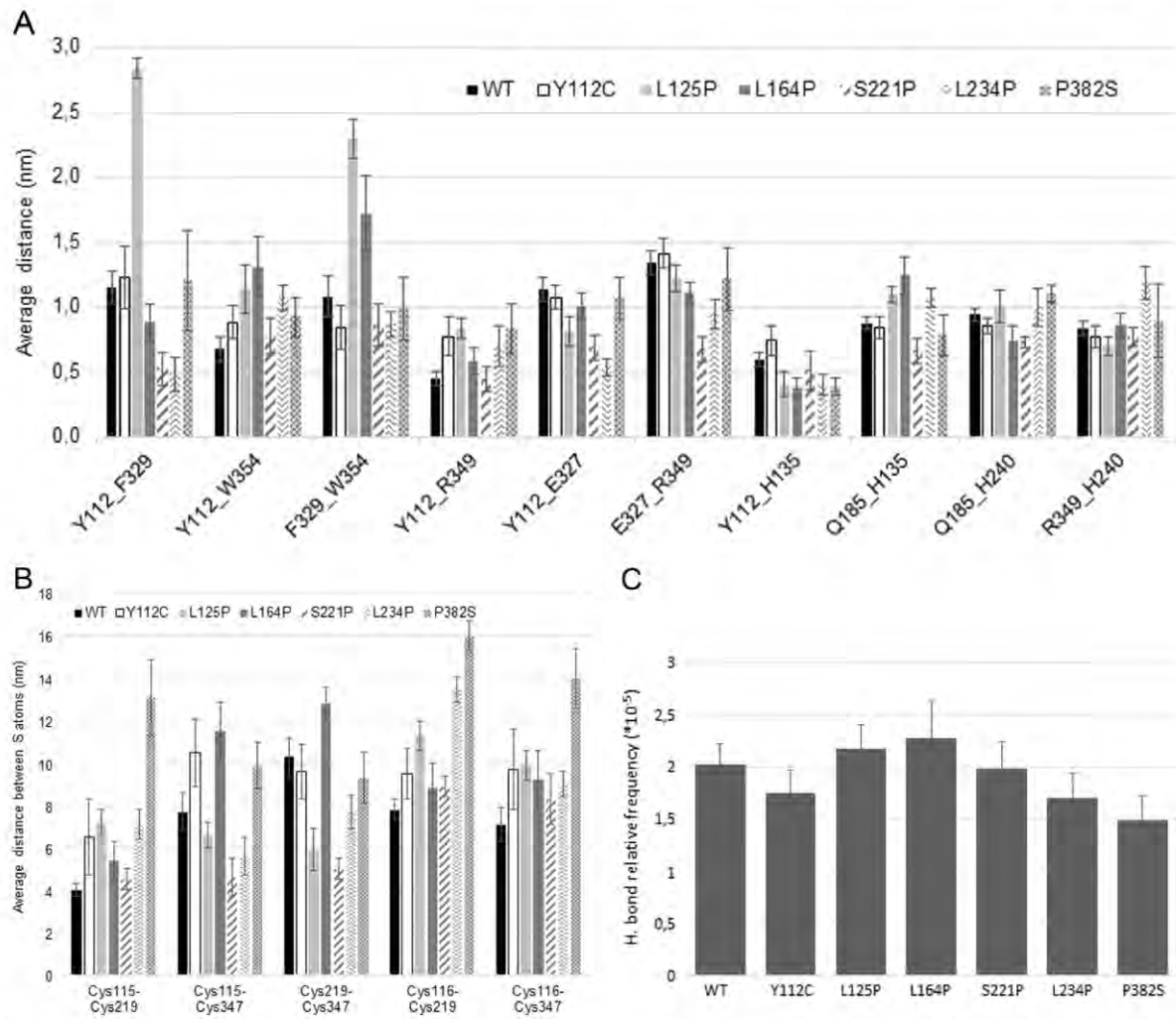


Fig. 3 Distance analysis of human DPH1 model binding site. **a** Average distance in nanometers between atoms that form potential entry points for the iron-sulfur cluster into DPH1 (error bars represent the standard deviation). **b** Average distance in nanometers (error bars show the standard deviation) between side chain sulfur atoms of

cysteine residues potentially involved in binding iron-sulfur cluster in human DPH1. **c** Average relative number of hydrogen bonds between DPH1 and DPH2 (out of all possible hydrogen bonds) along each simulation, (error bars show the standard deviation)

a p.(Ser221Pro) variant that was originally present in the catalogue of somatic variants in cancer (as COSM 1381407, <https://cancer.sanger.ac.uk/cosmic/>) labeled as SNP. We have previously observed that this variant has reduced functionality [10] and have therefore applied it as a control in our assays. The other DPH1 variants that we applied to our assay are those that were identified in the patients described above (Table 1). Compared with cells transfected with wild-type DPH1, cells expressing the variants p.(Tyr112Cys), p.(Leu125Pro), p.(Leu164Pro), p.(Leu234Pro), and p.(Ala411Argfs*91) contained reduced amounts of ADP-ribosylated eEF2. This reflects reduced presence of diphthamide on eEF2, and therefore reduced DPH1 functionality compared with wild-type DPH1. The reduction in

functionality of these variants is similar to or even more pronounced than that observed for the previously tested p.(Ser221Pro) variant [10]. In contrast, no difference in ADP-ribosylation of eEF2 was observed for cells expressing the variants p.(Met6Lys) and p.(Pro382Ser), indicating that these variants do not significantly affect DPH1 function.

Homology models of *Homo sapiens* DPH1-DPH2

Human DPH1-DPH2 heterodimers were modeled using the *Pyrococcus horikoshii* DPH2-DPH2 homodimer structure [12] (PDBID: 3LZD) as a template (Supplementary Figure 3). Our heterodimeric models contained wild-type DPH2 and either the wild-type DPH1, the p.(Ser221Pro)

variant previously described [10], or mutants identified in DPH1 syndrome patients, namely p.(Tyr112Cys), p.(Leu125Pro), p.(Leu164Pro), p.(Leu234Pro), or p.(Pro382Ser) (Fig. 2a). Leu125 is located in the DPH1–DPH2 interface, close to DPH2 residues Thr290, Gln295, Arg297, and Ala318, and we hypothesize that mutant p.(Leu125Pro) may affect the DPH1–DPH2 interaction. DPH1 residues Tyr112, Leu164, Ser221, Leu234, and Pro382 are located far from the DPH1–DPH2 interface, and we propose that the effect of the variants described at these residues is through structural changes that may interfere with functionality.

DPH1 belongs to a superfamily of enzymes that contain a cysteine-bound [4Fe–4S] cluster and can generate radicals of S-adenosylmethionine [13]. Two hybrid and coimmunoprecipitation experiments with yeast and mouse DPH1 suggest that it forms a catalytic complex with DPH2 [14], a highly homologous protein also containing a [4Fe–4S] cluster that forms homodimers. The crystal structure of the functional DPH2 homodimer of *Pyrococcus horikoshii*, an archaeal microorganism, shows each monomer bound to a [4Fe–4S] cluster through the sulfur atoms of three conserved cysteine residues separated by more than 100 residues [12]. The three cysteine residues involved in binding the [4Fe–4S] iron–sulfur cluster in *P. horikoshii* DPH2 homodimer, Cys59, Cys163, and Cys287, were aligned to Cys115, Cys219, and Cys347 residues of human DPH1 (Fig. 2b).

In mammals, the iron–sulfur cluster biogenesis is a complex multistep process, whereby the iron–sulfur cluster is synthesized and transferred to its recipient target [15]. In our models, DPH1 has only one suitable opening for the insertion of the iron–sulfur cluster into the cavity close to the conserved cysteine residues (Fig. 2c). This opening contains two regions, which we name gates A and B. Gate A is a table-shaped tunnel defined by five residues: Phe329 and Trp354 on the outer side, and Glu327 and Arg349 on the inner side, that form the four pillars, and Tyr112, located on top of these four residues. Gate B is a hole with boundaries defined by residues Tyr112, Arg349, His135, Gln185, and His240 (Fig. 2d). Thus, variant Tyr112Cys could hinder the insertion of the iron–sulfur cluster to its final destination.

A proposed reaction mechanism for these types of enzymes involves one iron atom of the cluster, whereas the remaining three iron atoms are bonded to three SH groups of cysteine residues [16]. In *Eukaryota* and *Archaea* organisms, these three cysteine residues are farther away in the sequence of DPH1 than in other members of the radical SAM superfamily, which display a characteristic CX3CX2C motif [13]. We propose that the DPH1 variants p.(Leu164Pro), p.(Ser221Pro), p.(Leu234Pro), and p.(Pro382Ser) might introduce conformational changes that

separate Cys115, Cys219, and Cys347 and prevent or impair their binding to the iron–sulfur cluster.

Molecular dynamics simulations

To further investigate the effect of the studied variants on DPH1 structure, molecular dynamics simulations of human DPH1–DPH2 models containing variants p.(Tyr112Cys), p.(Leu125Pro), p.(Leu164Pro), p.(Ser221Pro), p.(Leu234Pro), and p.(Pro382Ser) were compared with simulations of the wild-type DPH1–DPH2 model. The iron–sulfur cluster was removed from all the models prior to the simulation to allow unrestrained movement of cysteine residues putatively involved in its binding.

First, we measured if the variants reduced the dimensions of gates A and B (Fig. 3a). While no statistical analysis can be performed, large alterations can be observed for variants p.(Ser221Pro) and p.(Leu234Pro), showing a reduced distance between Tyr112 and Phe329, Tyr112 and Glu327, and between Glu327 and Arg349. p.(Ser221Pro) also showed a slightly reduced distance between gate B residues Gln185 and His135. All these results suggest that gate A could be smaller in p.(Leu234Pro) and p.(Ser221Pro) mutant proteins, and might impair the entry of the cube-shaped iron cluster, which has diagonal length of ~4 Å.

On the other hand, p.(Leu125Pro) showed increased distances for gate A residues (for Tyr112–Phe329 and Phe329–Trp354) and p.(Leu164Pro) showed an increased distance for Phe329–Trp354 residues. These increased distances could be hampering the retention of the iron–cluster at the catalytic site. The precise distances between residues are listed in Supplementary Table 4.

The crystallographic structure of *P. horikoshii* DPH2–DPH2 homodimer [12] and the proposed reaction mechanism [16] suggest that only three DPH1 cysteine residues (amongst 115, 116, 219, and 347) are covalently bound to the three iron atoms of the iron–sulfur cluster through their side chain sulfur. The distance between all possible pairs of S atoms of Cys115, Cys116, Cys219, and Cys347 was measured in simulations of *P. horikoshii* and human monomeric DPH1. The distances involving Cys115 were closer to the distances observed between *P. horikoshii* template cysteine residues (Cys59, Cys163, and Cys287) than those involving Cys116, suggesting that Cys115 is better located than Cys116 to bind the iron–sulfur cluster (Supplementary Table 4b).

Next, we analyzed the effect of the variants on the inter-cysteine distances on human DPH1–DPH2 heterodimeric complexes (Fig. 3b), which could hinder the binding of the iron–sulfur cluster in the catalytic site. Variants p.(Leu125Pro), p.(Ser221Pro), and p.(Leu234Pro) showed a reduction in Cys115–Cys347 and Cys219–Cys347 distances. On the other hand, p.(Leu234Pro) showed an

increased Cys116–Cys219 distance and p.(Pro382Ser) showed large distance increases for the Cys115–Cys219, Cys116–Cys219, and Cys116–Cys347 pairs.

To investigate the effect on the strength of DPH1–DPH2 interaction of these variants, the total number of hydrogen bonds between atoms of each subunit was measured in our simulations, relative to the total number of potential hydrogen bonds (Fig. 3c). Variant p.(Pro382Ser) showed the highest reduction in the number of hydrogen bonds between both subunits, whereas p.(Leu234Pro) and p.(Tyr112Cys) showed a slight decrease and all other variants including p.(Leu125Pro), located on the interphase between DPH1 and DPH2, were similar to the wild-type.

In general, all five missense variants analyzed by molecular dynamics simulations displayed some structural alteration compared with the wild-type or affected a residue located in a critical position for the iron–sulfur cluster insertion.

Discussion

To date, a total of 16 patients have been published with homozygous or compound heterozygous variants in *DPH1*, including the ones presented here [4–8]. An emerging DPH1 syndrome phenotype is being delineated, which is characterized mainly by variable developmental delay or intellectual disability, unusual skull shape with or without craniosynostosis (most often with a broad forehead), sparse hair, and a variety of dysmorphic features (Table 1). Most patients also have short stature. Central nervous system malformations are present in nearly all the assessed patients with the exception of two cases [5]. Also, a variety of cardiac defects have been observed in 7 out of 15 of the assessed patients [4, 8], including one of the patients in Family 1 and two patients in Family 2 described here. Abnormal toe nails, observed in Family 1 and one of the affected siblings in Family 2, have also been described for three of the four North American patients [5]. Hypotonia observed in both of siblings of Family 1 has also been previously reported in the patients bearing the p.(Leu234Pro) variant [4]. Moreover, motor weakness is mentioned in one of the two patients with the p.(Pro382Ser) variant [6]. Surprisingly, both micro- and macrocephaly have been observed previously [5, 7]. In addition, abnormal genitalia, micropenis (as observed in one sibling in Family 2), and hypospadias (as observed in the male patient of Family 1), have been previously reported [4, 7].

In order to better understand the effect of each variant and to try to establish genotype–phenotype correlations, we assayed the function of each of the previously described missense variants, together with the variants identified in the patients presented here and the frameshift

p.(Ala411Argfs*91) variant that is allegedly not affected by the NMD degradation process, since it generates a stop codon in the last exon further downstream from the wild-type stop codon. This is the first time in which *DPH1* variants associated with the DPH1 syndrome have been functionally and bioinformatically assessed. Generally, the DPH1 activity measured for each variant by our assay correlated with the severity of the corresponding patients' clinical presentation.

In the four cases bearing the p.(Met6Lys) variant, the intellectual disability was often referred to as mild or moderate [5], with no mention to the heart or CNS malformations. Interestingly, in our assay, the p.(Met6Lys) variant as well as the p.(Pro382Ser) variant, showed similar activity compared with wild-type DPH1. The protein alignment shows that Met6 is the translation initiation codon in a majority of species, including primates. In humans, Met6 could be acting as an alternative initiation codon and its loss could reduce overall DPH1 protein levels *in vivo*, which may not be reflected in our functional assay that uses an exogenous expression construct. In this sense, as stated in Uniprot [17] (Q9BZG8; accessed June 2018), it is uncertain whether Met1 or Met6 is the initiator. A variety of bioinformatic tools predict both Met1 and Met6 as putative initiation codons, with Met1 having the highest scores [18, 19]. Together, these data support the pathogenicity of the p.(Met6Lys) variant and its association with a milder presentation, and future characterization of it could be conducted by analyzing the amount of DPH1 protein in the p.(Met6Lys) homozygous patients' fibroblasts. The clinical information regarding the patients bearing the p.(Pro382Ser) is scarce, but the mention of autism in one patient and “good learner” in the other (while intellectual disability is mentioned for both), and the absence of any reference to CNS or heart conditions, suggests a milder phenotype. This variant retains its activity *in vitro* at levels comparable with wild-type, but as mentioned above, small *in vitro* activity reductions may not be detectable in this system. Our *in silico* models suggest that p.(Pro382Ser) decreases the interaction between DPH1 and DPH2 and increases the distances between the cysteine residues involved in binding the iron–sulfur cluster, which might be causing mild alterations in the protein functionality, not reflected in the *in vitro* assay. While the *in silico* data support the pathogenicity of these two changes and both are associated with mild phenotypes, we cannot rule out these variants being non-pathogenic, and further characterization of them would be necessary.

The remaining five DPH1 variants showed a significantly greater reduction in DPH1 activity, correlating with these patients' more severe clinical presentations. The patients described by Alazami et al. [4] are homozygous for the missense variant p.(Leu234Pro), and three out of four

patients suffered an early death, with heart, renal, and CNS malformations (Table 1) and represent the most severely affected DPH1 syndrome patients. Our modeling studies suggest that this variant could shrink the entry site of the iron–sulfur cluster, and that it might decrease the distance between the cysteine residues involved in binding the iron–sulfur cluster.

The variant p.(Ala411Argfs*91) is expected to produce a longer protein and the functional studies confirm the reduction on its activity, in agreement with the severe presentation of the two siblings homozygous for this variant [8].

The variant p.(Leu164Pro) was identified in compound heterozygosity with the frameshift variant c.289delG [p.(Glu97Lysfs*8)] in two severely affected siblings [7]. The frameshift variant is located at the third exon and is predicted to be affected by the NMD process. In the *in silico* analyses, p.(Leu164Pro) variant shows an increase in the size of gate A and a slight distance increase between cysteines involved in binding of the iron–sulfur cluster.

The patients from Family 1 are homozygous for the p.(Leu125Pro) variant. Our *in silico* models suggest a strong effect of this change on protein structure and function. Similarly to p.(Leu234Pro), p.(Leu125Pro) decreases the distances among cysteines and reduces the entry site for the iron–sulfur cluster. Accordingly, the patients of Family 1 are among the most severely affected, including the premature death of one of them.

Finally, the patients from Family 2 are homozygous for the p.(Tyr112Cys) variant, whose activity is also clearly reduced in our assay. Residue Tyr112 is located in a central position of the entry gate of the iron–sulfur cluster, and while p.(Tyr112Cys) variant does not seem to be causing any dramatic alteration on the size of the gates, it could be affecting the iron–sulfur cluster insertion [15].

In conclusion, the four patients presented here display clinical signs compatible with the previously described patients with *DPH1* recessive variants, clearly delineating a *DPH1* syndrome. We have been able to establish a good correlation between the loss of activity of various *DPH1* variants in our *in vitro* ADPR assay, the *in silico* modeling, and the severity of the clinical manifestations of the patients. Thus, we demonstrate that an *in vitro* assay for *DPH1* protein activity together with structural modeling may be useful tools for assessing *DPH1* variants and predicting patients' outcomes and prognoses.

Materials and methods

All protocols were approved by the Ethics Committee of the Universitat de Barcelona (IRB00003099) (Family 1) or the Icahn School of Medicine at Mount Sinai (Family 2), and

all methods were performed in accordance with the relevant guidelines and regulations. Informed consent was obtained from the patients' parents.

Whole-exome sequencing and molecular analyses

For Family 1, genomic DNA was obtained from the parents' peripheral blood and the patients' fibroblasts. Whole-exome sequencing of both patients and their parents were performed in the National Centre of Genomic Analysis (CNAG; Barcelona, Spain) using the Illumina HiSeq-2000 platform. Exome capture was performed with Agilent SureSelect v5 (Agilent, CA, USA). The filtering criteria were as in Urreiziti et al. [20]. Sequencing data are available on demand.

The mean coverage was 156.84, 151.36, 217.18, and 143.30 reads for patient 1, patient 2, father, and mother, respectively, and a minimum of 99.2% of the target region was covered with at least 10 reads (C10). Six variants were selected for validation by Sanger sequencing (Supplementary Table 2). Primer sequences and PCR conditions are available on request. PCR reaction, purification, and sequencing were performed as described previously [20].

For Family 2, genomic DNA was obtained from peripheral blood. Whole-exome sequencing was performed on the proband (Patient 3) and the proband's father at Genewiz (South Plainfield, NJ, USA). An Agilent SureSelect Exome kit (v6) was used for library preparation, and sequencing was performed on an Illumina HiSeq 2500 instrument (Illumina, San Diego, CA, USA) with 100-bp, paired-end reads. Alignment and variant calling was completed with an in-house GATK-based pipeline. A total of 122,433,475 reads were generated for the proband's sample and 117,272,439 reads were generated for the father's sample. 93.2% and 94.3% of the target had $\geq 30\times$ coverage for the proband's and father's samples, respectively. Variants were filtered with Ingenuity Variant Analysis (Qiagen, Redwood City) based on confidence (call quality ≥ 20), frequency (variants excluded if frequency was at least 0.5% in the 1000 Genomes Project, NHLBI ESP exomes, ExAC, or gnomAD databases), predicted deleteriousness (frameshift, in-frame indel, or start/stop codon change, missense change, splice site loss up to six bases into intron or as predicted by MaxEntScan, CADD score > 15 , disease-associated variant according to computed ACMG guidelines classification criteria of pathogenic or likely pathogenic, or listed in HGMD or ClinVar included). The identified *DPH1* variant was confirmed by PCR and Sanger sequencing.

Determination of *DPH1* functionality

*DPH1*ko cells are MCF7 derivatives that have all chromosomal *DPH1* gene copies inactivated [11]. The cells lack

DPH1 enzyme activity, are diphthamide-deficient, and are resistant to diphtheria toxin. For recombinant expression of DPH1 protein and variants, DPH1ko cells were grown in RPMI/10% FCS at 37 °C in humidified 5% CO₂ and transfected with plasmids containing expression cassettes for CMV-promoter-driven transient DPH1 expression. RIPA extracts (on ice with protease inhibitor addition) were prepared 24 h thereafter. ADP-ribosylation (ADPR) of diphthamide eEF2 was evaluated in RIPA extracts of transfected DPH1ko cells as previously described [10]. Western blots of extracts +/− BioNAD–DT blocked in 5% BSA were incubated with anti-β-actin (mouse monoclonal Ab AC-74, Sigma, cat. no. A2228 1:1500) followed by washing and incubation with anti-mouse goat polyclonal (HRP Dako, cat. no. P0447 1:1500). After additional washing and blocking in 5% BSA, streptavidin–POD was added for 1 h, the blot was washed again and developed with the HRP substrate.

Bioinformatic analyses

DPH1 protein sequences from different species were identified by BLAST using the human DPH1 protein sequence (Q9BZG8) as a query. The selected 85 protein sequences were aligned with Clustal Omega (1.2.4 version). The selection of proteins includes: 40 mammals, 9 birds, 4 reptilia, 1 amphibian (*Xenopus*), 7 fishes, 8 insects, 1 nematoda and 1 ascidia, 10 fungi, and 4 plants. Details of the selected proteins can be found in Supplementary Figure 2.

Homology models of variants and molecular dynamics simulations

Homology models of human DPH1–DPH2 heterodimers, with wild-type DPH2 and wild-type, p.(Tyr112Cys), p.(Leu125Pro), p.(Leu164Pro), p.(Pro221Ser), p.(Leu234Pro), or p.(Pro382Ser) mutants of DPH1 were built using SWISSMODEL [21] using *Pyrococcus horikoshii* DPH2 homodimer structure (PDB ID: 3LZD) as a template. Human DPH1 protein was modeled from residues Glu61 to Ser389. Quality of the models was assessed with Procheck [22], with > 99% residues in allowed areas, and none of the mutated residues in disallowed regions of Ramachandran plot. In order to analyze the geometry of complex, one molecular dynamics simulation of at least 12 ns for each of our models and of the homodimeric *Pyrococcus horikoshii* DPH2–DPH2 template in water was run with Gromacs [23] using OPLS-AA force field [24]. Plots of root mean-squared deviation of the backbone versus time were used to select a time, after the initial equilibration, were backbone movements were bounded and reliable measures could be made.

Several measures were performed in these areas of the simulations: distance between S atoms of Cys115, Cys116, Cys219, and Cys347; number of hydrogen bonds between residues of DPH1 and DPH2; distances between side chain O atom of Tyr112 and CZ atom of Phe329 or NE1 of Trp354; N atom of Tyr112 and OE2 of Glu327; backbone O of Tyr112 and CE1 of His135; CD2 of His135 and CD of Gln185; CD of Gln185 and NE2 of His240, and NE2 of His240 and NE of Arg349.

Acknowledgements The authors thank the families for their participation in our research studies. We are also grateful to M. Cozar for technical assistance, and to CNAG for exome sequencing. Funding was from Associació Síndrome Opitz C, Terrassa, Spain; Spanish Ministerio de Economía y Competitividad (SAF2016-75948-R, FECYT, crowdfunding PRECIPITA), Catalan Government (2014SGR932) and from CIBERER (U720), the Mindich Child Health and Development Institute (MCHDI) at the Icahn School of Medicine at Mount Sinai, and the Genetic Disease Foundation (New York, NY).

Compliance with ethical standards

Conflict of interest RU, GDE, ES, LCV, BDG, DG, BDW, and SB declare no conflict of interest. KM and UB are employees of Roche. Roche is interested in identifying novel targets and approaches for disease diagnosis and therapy. NC is an employee of Sema4, a for-profit genetic testing laboratory. GP is employed by Lead Molecular Design, SL, a company that develops software and offers modeling services for pharmaceutical industries, but has no competing interests on the results of this article.

Publisher's note: Springer Nature remains neutral with regard to jurisdictional claims in published maps and institutional affiliations.

References

1. Collier RJ. Understanding the mode of action of diphtheria toxin: a perspective on progress during the 20th century. *Toxicon*. 2001;39:1793–803.
2. Chen CM, Behringer RR. *Ovca1* regulates cell proliferation, embryonic development, and tumorigenesis. *Genes Dev*. 2004;18:320–32.
3. Yu YR, You LR, Yan YT, Chen CM. Role of *OVCA1/DPH1* in craniofacial abnormalities of Miller-Dieker syndrome. *Hum Mol Genet*. 2014;23:5579–96.
4. Alazami AM, Patel N, Shamseldin HE, Anazi S, Al-Dosari MS, Alzahrani F, et al. Accelerating novel candidate gene discovery in neurogenetic disorders via whole-exome sequencing of pre-screened multiplex consanguineous families. *Cell Rep*. 2015;10:148–61.
5. Loucks CM, Parboosingh JS, Shaheen R, Bernier FP, McLeod DR, Seidahmed MZ, et al. Matching two independent cohorts validates *DPH1* as a gene responsible for autosomal recessive intellectual disability with short stature, craniofacial, and ectodermal anomalies. *Hum Mutat*. 2015;36:1015–9.
6. Riazuddin S, Hussain M, Razzaq A, Iqbal Z, Shahzad M, Polla DL, et al. Exome sequencing of Pakistani consanguineous families identifies 30 novel candidate genes for recessive intellectual disability. *Mol Psychiatry*. 2017;22:1604–14.
7. Nakajima J, Oana S, Sakaguchi T, Nakashima M, Numabe H, Kawashima H, et al. Novel compound heterozygous *DPH1*

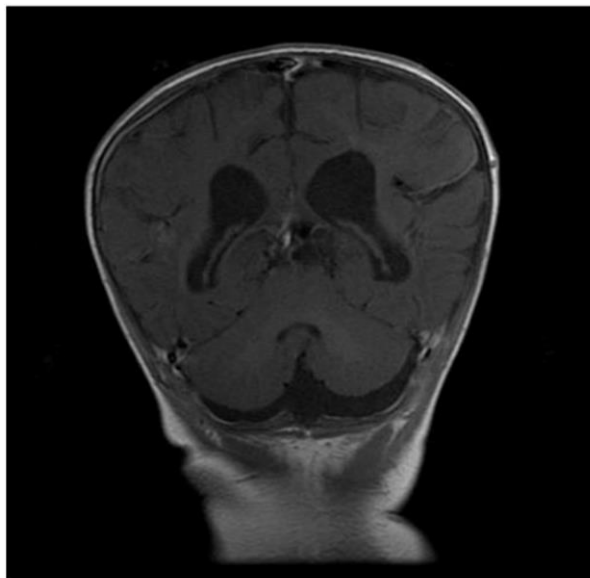
- mutations in a patient with the unique clinical features of airway obstruction and external genital abnormalities. *J Hum Genet.* 2018;63:529–32.
8. Sekiguchi F, Nasiri J, Sedghi M, Salehi M, Hosseinzadeh M, Okamoto N, et al. A novel homozygous DPH1 mutation causes intellectual disability and unique craniofacial features. *J Hum Genet.* 2018;63:487–91.
 9. Stahl S, Mueller F, Pastan I, Brinkmann U. Factors that determine sensitivity and resistances of tumor cells towards antibody-targeted protein toxins. In: Verma R, Bonavida B. (eds.). *Resistance to Immunotoxins in Cancer Therapy. Resistance to Targeted Anti-Cancer Therapeutics 6.* Cham: Springer; 2015. p. 57–73.
 10. Mayer K, Schroder A, Schnitger J, Stahl S, Brinkmann U. Influence of DPH1 and DPH5 protein variants on the synthesis of Diphthamide, the target of ADPRibosylating toxins. *Toxins.* 2017;9:78.
 11. Stahl S, da Silva Mateus Seidl AR, Ducret A, Kux van Geijtenbeek S, Michel S, Racek T, et al. Loss of diphthamide pre-activates NF-kappaB and death receptor pathways and renders MCF7 cells hypersensitive to tumor necrosis factor. *Proc Natl Acad Sci USA.* 2015;112:10732–7.
 12. Zhang Y, Zhu X, Torelli AT, Lee M, Dzikovski B, Koralewski RM, et al. Diphthamide biosynthesis requires an organic radical generated by an iron-sulphur enzyme. *Nature.* 2010;465:891–6.
 13. Broderick JB, Duffus BR, Duschene KS, Shepard EM. Radical S-adenosylmethionine enzymes. *Chem Rev.* 2014;114:4229–317.
 14. Liu S, Milne GT, Kuremsky JG, Fink GR, Leppla SH. Identification of the proteins required for biosynthesis of diphthamide, the target of bacterial ADP-ribosylating toxins on translation elongation factor 2. *Mol Cell Biol.* 2004;24:9487–97.
 15. Maió N, Rouault TA. Iron-sulfur cluster biogenesis in mammalian cells: new insights into the molecular mechanisms of cluster delivery. *Biochim Biophys Acta.* 2015;1853:1493–512.
 16. Dong M, Kathiresan V, Fenwick MK, Torelli AT, Zhang Y, Caranto JD, et al. Organometallic and radical intermediates reveal mechanism of diphthamide biosynthesis. *Science.* 2018;359:1247–50.
 17. Uniprot Consortium, T. UniProt: the universal protein knowledgebase. *Nucleic Acids Res.* 2017;45:D158–D169.
 18. Salamov AA, Nishikawa T, Swindells MB. Assessing protein coding region integrity in cDNA sequencing projects. *Bioinformatics.* 1998;14:384–90.
 19. Wernersson R. Virtual Ribosome—a comprehensive DNA translation tool with support for integration of sequence feature annotation. *Nucleic Acids Res.* 2006;34:W385–8.
 20. Urreiziti R, Cueto-Gonzalez AM, Franco-Valls H, Mort-Farre S, Roca-Ayats N, Ponomarenko J, et al. A De novo nonsense mutation in MAGEL2 in a patient initially diagnosed as Opitz-C: similarities between Schaaf-Yang and Opitz-C syndromes. *Sci Rep.* 2017;7:44138.
 21. Biasini M, Bienert S, Waterhouse A, Arnold K, Studer G, Schmidt T, et al. SWISS-MODEL: modelling protein tertiary and quaternary structure using evolutionary information. *Nucleic Acids Res.* 2014;42:W252–8.
 22. Morris AL, MacArthur MW, Hutchinson EG, Thornton JM. Stereochemical quality of protein structure coordinates. *Proteins.* 1992;12:345–64.
 23. Abraham MJ, Murtola T, Schulz, Páll S, Smith JC, Hess B, et al. GROMACS: high performance molecular simulations through multi-level parallelism from laptops to supercomputers. *SoftwareX.* 2015;1-2:19–25.
 24. Jorgensen WL, Maxwell DS, Tirado-Rives J. Development and testing of the OPLS all-atom force field on conformational energetics and properties of organic liquids. *J Am Chem Soc.* 1996;118:11225–36.

Supplementary information for:

DPH1 syndrome: two novel variants and structural and functional analyses of seven missense variants identified in syndromic patients

Roser Urreizti, Klaus Mayer, Gilad D. Evrony, Edith Said, Laura Castilla-Vallmanya, Neal A. L. Cody, Guillem Plasencia, Bruce D. Gelb, Daniel Grinberg, Ulrich Brinkmann, Bryn D. Webb & Susanna Balcells

Supplementary Figures 1, 2 and 3.



Supplementary Figure 1: MR T1-weighted coronal image revealing prominence of the ventricular system and extra-axial spaces in Patient 3. MRI completed at 6 months of age

NP_001374.3[Homo_sapiens]Primate		0
XP_003816906.1[Pan_paniscus]Primate		0
XP_008968211.1[Pan_paniscus]Primate		0
XP_018668753.1[Gorilla_gorilla]Primate		0
XP_002826867.1[Pongo_abelii]Primate		0
XP_012356920.1[Nomascus_leucogenys]Primate		0
XP_011842657.1[Mandrillus_leucophaeus]Primate		0
XP_008061609.1[Carlito_syrichta]Primate		0
XP_001504395.3[Equus_caballus]mammal_Eu		0
XP_010859626.1[Bison_bison]mammal_Eu		0
NP_001070367.1[Bos_taurus]mammal		0
XP_019837435.1[Bos_indicus]mammal		0
XP_012006497.1[Ovis_aries]mammal		0
XP_017919893.1[Capra_hircus]mammal		0
XP_003131871.3[Sus_scrofa]mammal		0
XP_015103509.1[Vicugna_pacos]mammal		0
XP_008269143.1[Oryctolagus_cuniculus]mammal_Eu		0
XP_016042474.1[Erinaceus_europaeus]mammal_Eu		0
NP_001099279.1[Rattus_norvegicus]mammal_Eu		0
XP_004633594.1[Octodon_degus]mammal_Eu		0
XP_003469582.2[Cavia_porcellus]mammal		0
XP_010640444.1[Fukomys_damarensis]mammal	MS	ASSAIFQNCLEFV
XP_005402655.1[Chinchilla_lanigera]mammal		0
NP_652762.2[Mus_musculus]mammal		0
XP_003507319.1[Cricetulus_griseus]mammal		0
XP_006977441.1[Peromyscus_maniculatus]mammal		0
XP_004667842.1[Jaculus_jaculus]mammal		0
XP_004605318.1[Sorex_saraneus]mammal_Eu		0
XP_006891160.1[Elephantulus_edwardii]mammal_Eu		0
XP_019611088.1[Rhinolophus_sinicus]mammal_Eu		0
XP_011358164.1[Pteropus_vampyrus]mammal_Eu		0
XP_019672915.1[Felis_catus]mammal_eu		0
XP_007076184.2[Panthera_tigris_altaica]mammal_eu	MS	ELSAFFSRCLFD
XP_013972316.1[Canis_lupus_familiaris]mammal_eu		0
XP_007177531.1[Balaenoptera_austrorestrata]mammal_Eu		0
XP_004267102.1[Orinusorca]mammal_Eu		0
XP_010594790.1[Loxodonta_africana]mammal_Eu		0
XP_017507098.1[Manis_javanica]mammal_Eu	MS	ALSAFLWCCLSG
XP_012405311.1[Sarcophilus_harrisii]mammal_marsupial		0
XP_007485825.1[Monodelphis_domestica]mammal_Me		0
XP_011579991.1[Aquila_chrysaetos]Aves		0
XP_015501861.1[Parus_major]Aves		0
XP_017687952.1[Lepidochrix_coronata]Aves		0
XP_005439865.1[Falco_cherrug]Aves		0
XP_008493349.1[Calypte_anna]Aves	MS	NRQTQASIPVLI
NP_001025887.2[Gallus_gallus]Aves		0
XP_018736460.1[Coturnix_japonica]Aves		0
XP_010720021.1[Meleagris_gallopavo]Aves		0
XP_005502175.1[Columba_livia]Aves		0
XP_019400888.1[Crocodylus_potosus]Sauropsida	MD-ARR-LCLGKQKERRAGLQGEST#SGFGPCVLAASLILLGAAVIGQDSTQELWQASPE	36
XP_014379797.1[Alligator_sinensis]Sauropsida		0
XP_015277363.1[Gekko_japonicus]reptilia		0
XP_003230257.2[Anolis_carolinensis]reptilia		0
XP_012812029.1[Xenopus_tropicalis]Amphibia		0
XP_014018522.1[Salmo_salar]Actinopterygii	MS	EMAEKPPVGL
XP_016336999.1[Sinocyclocheilus_anshuiensis]Actinopterygii		0
XP_017550402.1[Pygocentrus_nattereri]Actinopterygii		0
XP_005804152.1[Xiphophorus_maculatus]Actinopterygii		0
XP_019729898.1[Hippocampus_comes]Actinopterygii		0
XP_005157639.1[Danio_rerio]Actinopterygii		0
XP_011606823.1[Takifugu_rubripes]Actinopterygii		0
XP_016836589.1[Nasonia_vitripennis]Insecta	MS	DVSVTVNGAQVCCNCKEESVQD
XP_011866406.1[Volienhovia_emoryi]Insecta		0
XP_015520716.1[Neodiprion_icecontei]Insecta		0
XP_011154130.1[Harpegnathos_saltator]Insecta		0
XP_017957296.1[Drosophila_navojoa]Insecta		0
NP_001261722.1[Drosophila_melanogaster]Insecta		0
XP_013146150.1[Papilio_polytes]Insecta		0
XP_002423182.1[Fedcula_humana]Insecta		0
NP_497750.1[Caenorhabditis_elegans]Secernentea		0
XP_018668637.1[Ciona_intestinalis]Ascidiacea		0
XP_638680.1[Dictyostelium_discoideum]Dictyostelia	MSDSNN-EE-DNVVINTITNTDNTDTFTTDTNTES	41
XP_011316328.1[Fusarium_graminearum]Sordariomycetes	NEEDRQKTDLGTAA--DIEEAQLAQAQSPPAIENETESAAG	52
XP_018742809.1[Fusarium_verticillioides]Sordariomycetes	NEEDRQKTDLGTAA--DIEEAQLAQAQSPPAIENETESAAG	45
XP_018150409.1[Pochonia_chlamydosporia]Sordariomycetes	NEEDRQKTDLGTAA--DIEEAQLAQAQSPPAIENETESAAG	43
XP_018656688.1[Trichoderma_gamsii]Sordariomycetes	NEEDRQKTDLGTAA--DIEEAQLAQAQSPPAIENETESAAG	43
XP_001208548.1[Aspergillus_terreus]Eurotiomycetes	NEEDRQKTDLGTAA--DIEEAQLAQAQSPPAIENETESAAG	15
XP_002379550.1[Aspergillus_flavus]Eurotiomycetes	NEEDRQKTDLGTAA--DIEEAQLAQAQSPPAIENETESAAG	20
XP_002563943.1[Penicillium_rubens]Eurotiomycetes	NEEDRQKTDLGTAA--DIEEAQLAQAQSPPAIENETESAAG	25
XP_015467246.1[Debaryomyces_fabryi]Saccharomycetes	NEEDRQKTDLGTAA--DIEEAQLAQAQSPPAIENETESAAG	16
KZV10512.1 DPRI[S_cerevisiae]Saccharomycetes	NEEDRQKTDLGTAA--DIEEAQLAQAQSPPAIENETESAAG	13
XP_006827105[Amborelia_trichopoda]Plant		0
XP_002454772.1[Sorghum_bicolor]Plant		0
XP_020865862.1[Arabidopsis_lyrata]Plant		0
XP_008643787[Zea_mays]Plant		0

Identification of disease-causing variants in patients clinically diagnosed with Opitz C syndrome and Bohring-Opitz syndrome and functional validation

Accession	Species	Met 6	Position
NP_001374.3	[Homo sapiens]Primate	MRQVMAALVSGAAE	31
XP_003816906.1	[Pan paniscus]Primate	MRQVMAALVSGAAE	31
XP_008968211.1	[Pan paniscus]Primate	MAALVSGAAE	26
XP_018868753.1	[Gorilla gorilla gorilla]Primate	MAALVSGAAE	26
XP_002824667.1	[Pongo abelii]Primate	MAALVSGAAE	26
XP_012356920.1	[Nomascus leucogenys]Primate	MAALVSGAAE	26
XP_011842657.1	[Mandrill]Lus leucophaeus]Primate	MAALVSGAAE	26
XP_008061609.1	[Carliro_oryzicta]Primate	MAALVSEAAE	26
XP_001504395.3	[Equus caballus]mammal_Eu	MAALVSEVAE	26
XP_010859626.1	[Bison bison bison]mammal_Eu	MAALVAEAAE	26
NP_001070367.1	[Bos taurus]mammal	MAALVAEAAE	26
XP_019837435.1	[Bos indicus]mammal	MAALVAEAAE	26
XP_012006497.1	[Ovis aries musimon]mammal	MAALVAEAAE	26
XP_017919893.1	[Capra hircus]mammal	MAALVAEAAE	26
XP_003131871.3	[Sus scrofa]mammal	MAALVAEAAE	27
XP_015103509.1	[Vicugna pacos]mammal	MAALVAEAAE	26
XP_008269143.1	[Oryctolagus cuniculus]mammal_Eu	MAALVSEAAE	26
XP_016042474.1	[Erinaceus europaeus]mammal_Eu	MAALVTEVAE	26
NP_001099279.1	[Rattus norvegicus]mammal_Eu	MAALVTEVAE	26
XP_004635394.1	[Octodon degus]mammal_Eu	MAALVSEAAE	26
XP_003469582.2	[Cavia porcellus]mammal	MAALVSEAAE	26
XP_010640444.1	[Fukomys damarensis]mammal	PRVGRQMAALVVAEAAE	47
XP_005402655.1	[Chinchilla lanigera]mammal	MAALVVAEAAE	26
NP_652762.2	[Mus musculus]mammal	MAALVSEAAE	26
XP_003507319.1	[Cricetulus griseus]mammal	MAALVSEAAE	26
XP_00697444.1	[Peromyscus maniculatus]mammal	MAALVSEAAE	26
XP_004667842.1	[Jaculus jaculus]mammal	MAALVSEAAE	26
XP_004605318.1	[Sorex araneus]mammal_Eu	MAALVSEAAE	26
XP_006891160.1	[Elephantulus edwardi]mammal_Eu	MAALVSEAAE	26
XP_019611098.1	[Rhinolophus sinicus]mammal_Eu	MAALVSEAAE	26
XP_011388164.1	[Pteropus vampyrus]mammal_Eu	MGRAYMAALVSEAAE	31
XP_019672915.1	[Felis catus]mammal_Eu	MAALVSEAAE	26
XP_007076184.2	[Panthera tigris altaica]mammal_Eu	LHVGRVMAALVSEAAE	47
XP_013972316.1	[Canis lupus familiaris]mammal_Eu	MAALVAEAAE	26
XP_007177531.1	[Balaenoptera acutorostrata]mammal_Eu	MAALVAEAAE	26
XP_004267102.1	[Orcinus orca]mammal_Eu	MAALVVAEAAE	26
XP_010394790.1	[Loxodonta africana]mammal_Eu	MAALVSEAAE	26
XP_017507098.1	[Manis javanica]mammal_Eu	LHVGRVMAALVSEAAE	47
XP_012405311.1	[Sarcophilus harrisii]mammal_marsupial	MAALAEFAEAG	23
XP_007485825.1	[Monodelphis domestica]mammal_Me	MAALAEFAEAG	23
XP_011579991.1	[Aquila chrysaetos]Aves	MAA	27
XP_015501861.1	[Parus major]Aves	MAG	27
XP_017687952.1	[Lepidothrix coronata]Aves	MAA	22
XP_005439966.1	[Falco cherrug]Aves	IT	24
XP_008493491.1	[Calypte anna]Aves	MEVEAV	16
NP_001025887.2	[Gallus gallus]Aves	MAA	24
XP_015736460.1	[Coturnix japonica]Aves	MAA	24
XP_010720021.1	[Meleagris gallopavo]Aves	M	19
XP_005502175.1	[Columba livia]Aves	MAA	22
XP_019400888.1	[Crocodylus porosus]Sauropsida	LT	24
XP_014379797.1	[Alligator sinensis]Sauropsida	MEVSAV	24
XP_015277363.1	[Gekko japonicus]reptilia	MEVEAV	16
XP_003230257.2	[Anolis carolinensis]reptilia	TD	48
XP_012812029.1	[Xenopus tropicalis]Amphibia	POIGMMPA	48
XP_014018522.1	[Salmo salar]Actinopterygii	MAAFVETQVPAKKA-T-VGFR	22
XP_016336999.1	[Sinocyclocheilus anshuiensis]Actinopterygii	MAAFVETQVPAKKA-T-VGFR	22
XP_017550402.1	[Epiplatys nattereri]Actinopterygii	MAAFVETQVPAKKA-T-VGFR	22
XP_005804152.1	[Xiphophorus maculatus]Actinopterygii	MAAFVETQVPAKKA-T-VGFR	22
XP_019729898.1	[Hippocampus comes]Actinopterygii	MAAFVETQVPAKKA-T-VGFR	22
XP_005157638.1	[Danio rerio]Actinopterygii	MENACTEPALV	37
XP_011606823.1	[Takifugu rubripes]Actinopterygii	MENACTEPALV	37
XP_016836589.1	[Nasonia vitripennis]Insecta	LTMK-GVATVSDSQSEKVDKSELVNSSEQMKENRDELDLVVVVAKP-V-RKVFAPK	68
XP_011866406.1	[Volienhovia emeryi]Insecta	MAFVTVVVAAP-V-RKVFAPK	21
XP_015502716.1	[Neodiprion lecontei]Insecta	MSEGESVTVVVAAP-V-RKVFAPK	25
XP_011154130.1	[Harpegnathos saltator]Insecta	MTESESVTVVVAAP-V-RKVFAPK	24
XP_017957296.1	[Drosophila nvojoa]Insecta	ML-DIVQPIDHLNENNNNSDVIIVRAFP--RKVEKPKA	34
NP_001261722.1	[Drosophila melanogaster]Insecta	ML-DIVQPIDHLNENNNNSDVIIVRAFP--RKVEKPKA	34
XP_013145150.1	[Papilio polytes]Insecta	MED-LALNPGVVVVAAPKPEQ-RKTFKPAI	28
XP_002423182.1	[Pediculus humanus]Insecta	MVILQVQCS-KTVVTKTCQIVQAKP-D-RKVFAPK	35
NP_497750.1	[Caenorhabditis elegans]Secernentea	MAA	5
XP_018668637.1	[Clona intestinalis]Ascidiacea	MEPTAE	27
XP_638680.1	[Dictyostelium discoideum]Dictyostelia	RFVGRKRAAQQQQENI-DNVTTTITTTTTT-TTTPFDKIVTTEKVVVVGGLA	98
XP_011316328.1	[Fusarium graminearum]Sordariomycetes	S-GATCES	87
XP_018748209.1	[Fusarium verticillioides]Sordariomycetes	S-ASCES	81
XP_018150409.1	[Fochonia chlamydosporia]Sordariomycetes	STDCES	78
XP_018658688.1	[Trichoderma gamsii]Sordariomycetes	TEEGGS	78
XP_001208548.1	[Aspergillus terreus]Eurotiomycetes	A-QDVES	51
XP_002379550.1	[Aspergillus flavus]Eurotiomycetes	S-QDVES	57
XP_002563943.1	[Penicillium rubens]Eurotiomycetes	S-QDVES	61
XP_015457246.1	[Debaryomyces fabryi]Saccharomycetes	TS	43
KZ101512.1	[DPH1 (S. cerevisiae)]Saccharomycetes	TS	43
XP_006827105	[Amborella trichopoda]Plant	AGALCGETL	26
XP_002454772.1	[Sorghum bicolor]Plant	DAGDASTSL	35
XP_020865862.1	[Arabidopsis lyrata]Plant	MKLS	20
XP_008643787	[Zea mays]Plant	DAGDASTAL	35

NP_001374.3[Homo sapiens]Primate	RVANQTPPEILNPNQIQ-AIRVLPSSNYNFEIPKTIWRIQQAQAKKVALQMPGEGLLIFAC	90
XP_003816906.1[Fan paniscus]Primate	RVANQTPPEILNPNQIQ-AMRVLPSSNYNFEIPKTIWRIQQAQAKKVALQMPGEGLLIFAC	90
XP_008968211.1[Fan paniscus]Primate	RVANQTPPEILNPNQIQ-AMRVLPSSNYNFEIPKTIWRIQQAQAKKVALQMPGEGLLIFAC	89
XP_018868753.1[Gorilla gorilla gorilla]Primate	RVANQTPPEILNPNQIQ-AIQVLPSSNYNFEIPKTIWRIQQAQAKKVALQMPGEGLLIFAC	85
XP_002826667.1[Pongo abelii]Primate	RVANQTPPEILNPNQIQ-AIQVLPSSNYNFEIPKTIWRIQQAQAKKVALQMPGEGLLIFAC	85
XP_012356920.1[Nomascus leucogenys]Primate	RVANQTPPEILNPNQIQ-AVVALEPSNYNFEIPKTIWRIQQAQAKKVALQMPGEGLLIFAC	83
XP_011842657.1[MandrillLula leucophaea]Primate	RVANQTPPEILNPNQIQ-AIQVLPSSNYNFEIPKTIWRIQQAQAKKVALQMPGEGLLIFAC	85
XP_008061609.1[Carollia gyrichta]Primate	RLANQVPEEILNPNQIQ-AIQVLPSSNYNFEIPKTIWRIQQAQAKKVALQMPGEGLLIFAC	85
XP_001504395.3[Equus caballus]mammal_Eu	RLANQVPEEILNPNQIQ-AIRVLPSSNYNFEIPKTIWRIQQAQAKKVALQMPGEGLLIFAC	85
XP_010859626.1[Bison bison bison]mammal_Eu	RLANQVPEEILNPNQIQ-AIQVLPSSNYNFEIPKTIWRIQQAQAKKVALQMPGEGLLIFAC	85
NP_001070367.1[Bos taurus]mammal	RLANQVPEEILNPNQIQ-AIQVLPSSNYNFEIPKTIWRIQQAQAKKVALQMPGEGLLIFAC	86
XP_019837435.1[Bos indicus]mammal	RLANQVPEEILNPNQIQ-AIQVLPSSNYNFEIPKTIWRIQQAQAKKVALQMPGEGLLIFAC	85
XP_012006497.1[Ovis aries musimon]mammal	RLANQVPEEILNPNQIQ-AIQVLPSSNYNFEIPKTIWRIQQAQAKKVALQMPGEGLLIFAC	85
XP_017919893.1[Capra hircus]mammal	RLANQVPEEILNPNQIQ-AIQVLPSSNYNFEIPKTIWRIQQAQAKKVALQMPGEGLLIFAC	85
XP_003131871.3[Sus scrofa]mammal	RLANQVPEEILNPNQIQ-AIQVLPSSNYNFEIPKTIWRIQQAQAKKVALQMPGEGLLIFAC	86
XP_015103509.1[Vicuugna pacos]mammal	RLANQVPEEILNPNQIQ-AIQVLPSSNYNFEIPKTIWRIQQAQAKKVALQMPGEGLLIFAC	85
XP_008269143.1[Oryctolagus cuniculus]mammal_Eu	RLANQVPEEILNPNQIQ-AIQVLPSSNYNFEIPKTIWRIQQAQAKKVALQMPGEGLLIFAC	85
XP_016042474.1[Erinaceus europaeus]mammal_Eu	RLANQVPEEILNPNQIQ-AIQVLPSSNYNFEIPKTIWRIQQAQAKKVALQMPGEGLLIFAC	85
NP_001099279.1[Rattus norvegicus]mammal_Eu	RLANQVPEEILNPNQIQ-AIQVLPSSNYNFEIPKTIWRIQQAQAKKVALQMPGEGLLIFAC	85
XP_004635394.1[Octodon degus]mammal_Eu	RLANQVPEEILNPNQIQ-AIQVLPSSNYNFEIPKTIWRIQQAQAKKVALQMPGEGLLIFAC	85
XP_003469582.2[Cavia porcellus]mammal	RLANQVPEEILNPNQIQ-AIQVLPSSNYNFEIPKTIWRIQQAQAKKVALQMPGEGLLIFAC	85
XP_010640444.1[Fukomys damarensis]mammal	RLANQVPEEILNPNQIQ-AIQVLPSSNYNFEIPKTIWRIQQAQAKKVALQMPGEGLLIFAC	106
XP_005402655.1[Chinchilla lanigera]mammal	RLANQVPEEILNPNQIQ-AIQVLPSSNYNFEIPKTIWRIQQAQAKKVALQMPGEGLLIFAC	85
NP_652762.2[Mus musculus]mammal	RLANQVPEEILNPNQIQ-AIQVLPSSNYNFEIPKTIWRIQQAQAKKVALQMPGEGLLIFAC	85
XP_003507319.1[Cricetulus griseus]mammal	RLANQVPEEILNPNQIQ-AIQVLPSSNYNFEIPKTIWRIQQAQAKKVALQMPGEGLLIFAC	85
XP_006977441.1[Peromyscus maniculatus]mammal	RLANQVPEEILNPNQIQ-AIQVLPSSNYNFEIPKTIWRIQQAQAKKVALQMPGEGLLIFAC	85
XP_004667842.1[Jaculus jaculus]mammal	RLANQVPEEILNPNQIQ-AIQVLPSSNYNFEIPKTIWRIQQAQAKKVALQMPGEGLLIFAC	85
XP_004605318.1[Sorex araneus]mammal_Eu	RLANQVPEEILNPNQIQ-AIQVLPSSNYNFEIPKTIWRIQQAQAKKVALQMPGEGLLIFAC	85
XP_006891160.1[Elephantulus edwardi]mammal_Eu	RLANQVPEEILNPNQIQ-AIQVLPSSNYNFEIPKTIWRIQQAQAKKVALQMPGEGLLIFAC	85
XP_019611098.1[Rhinolophus jintus]mammal_Eu	RVANQTPPEILNPNQIQ-AIQVLPSSNYNFEIPKTIWRIQQAQAKKVALQMPGEGLLIFAC	85
XP_011388164.1[Pteropus vampyrus]mammal_Eu	RLANQVPEEILNPNQIQ-AIQVLPSSNYNFEIPKTIWRIQQAQAKKVALQMPGEGLLIFAC	90
XP_019672915.1[Felis catus]mammal_Eu	RLANQVPEEILNPNQIQ-AIQVLPSSNYNFEIPKTIWRIQQAQAKKVALQMPGEGLLIFAC	85
XP_007076184.2[Panthera tigris altaica]mammal_Eu	RLANQVPEEILNPNQIQ-AIQVLPSSNYNFEIPKTIWRIQQAQAKKVALQMPGEGLLIFAC	106
XP_013972316.1[Canis lupus familiaris]mammal_Eu	RLANQVPEEILNPNQIQ-AIQVLPSSNYNFEIPKTIWRIQQAQAKKVALQMPGEGLLIFAC	86
XP_007177531.1[Balaenoptera acutorostrata]mammal_Eu	RLANQVPEEILNPNQIQ-AIQVLPSSNYNFEIPKTIWRIQQAQAKKVALQMPGEGLLIFAC	85
XP_004267102.1[Orccinus orca]mammal_Eu	RLANQVPEEILNPNQIQ-AIQVLPSSNYNFEIPKTIWRIQQAQAKKVALQMPGEGLLIFAC	85
XP_010594790.1[Loxodonta africana]mammal_Eu	RLANQVPEEILNPNQIQ-AIQVLPSSNYNFEIPKTIWRIQQAQAKKVALQMPGEGLLIFAC	85
XP_017507098.1[Manis javanica]mammal_Eu	RFANQVPEEILNPNQIQ-AIQVLPSSNYNFEIPKTIWRIQQAQAKKVALQMPGEGLLIFAC	106
XP_012405311.1[Sarcophilus harrisii]mammal_marsupial	RLANQVPEEILNPNQIQ-AIQVLPSSNYNFEIPKTIWRIQQAQAKKVALQMPGEGLLIFAC	82
XP_007485825.1[Monodelphis domestica]mammal_Me	RLANQVPEEILNPNQIQ-AIQVLPSSNYNFEIPKTIWRIQQAQAKKVALQMPGEGLLIFAC	86
XP_011579991.1[Aquila chrysaetos]Aves	RAAQVPEEILNPNQIQ-AIQVLPSSNYNFEIPKTIWRIQQAQAKKVALQMPGEGLLIFAC	81
XP_015501861.1[Parus major]Aves	LVAAQVPEEILNPNQIQ-AIQVLPSSNYNFEIPKTIWRIQQAQAKKVALQMPGEGLLIFAC	79
XP_017687952.1[Lepidotrichus coronata]Aves	HVAQVPEEILNPNQIQ-AIQVLPSSNYNFEIPKTIWRIQQAQAKKVALQMPGEGLLIFAC	81
XP_005439966.1[Falco cherrug]Aves	RVANQTPPEILNPNQIQ-AIQVLPSSNYNFEIPKTIWRIQQAQAKKVALQMPGEGLLIFAC	106
XP_008493491.1[Colaptes auratus]Aves	RVANQTPPEILNPNQIQ-AIQVLPSSNYNFEIPKTIWRIQQAQAKKVALQMPGEGLLIFAC	84
NP_001025887.2[Gallus gallus]Aves	RTAQVPEEILNPNQIQ-AIQVLPSSNYNFEIPKTIWRIQQAQAKKVALQMPGEGLLIFAC	83
XP_015736460.1[Coturnix japonica]Aves	RTAQVPEEILNPNQIQ-AIQVLPSSNYNFEIPKTIWRIQQAQAKKVALQMPGEGLLIFAC	83
XP_010720021.1[Meleagris gallopavo]Aves	RTAQVPEEILNPNQIQ-AIQVLPSSNYNFEIPKTIWRIQQAQAKKVALQMPGEGLLIFAC	78
XP_005502175.1[Columba livia]Aves	RAAQVPEEILNPNQIQ-AIQVLPSSNYNFEIPKTIWRIQQAQAKKVALQMPGEGLLIFAC	81
XP_019400888.1[Crocodylus porosus]Sauropsida	RAAQVPEEILNPNQIQ-AIQVLPSSNYNFEIPKTIWRIQQAQAKKVALQMPGEGLLIFAC	154
XP_014379797.1[Alligator sinensis]Sauropsida	RVANQTPPEILNPNQIQ-AIQVLPSSNYNFEIPKTIWRIQQAQAKKVALQMPGEGLLIFAC	10
XP_015277363.1[Gecko japonicus]reptilia	QVAVQVPEEILNPNQIQ-AIQVLPSSNYNFEIPKTIWRIQQAQAKKVALQMPGEGLLIFAC	83
XP_003230257.2[Anolis carolinensis]reptilia	HVAQVPEEILNPNQIQ-AIQVLPSSNYNFEIPKTIWRIQQAQAKKVALQMPGEGLLIFAC	77
XP_012812029.1[Xenopus tropicalis]Amphibia	RVANQTPPEILNPNQIQ-AIQVLPSSNYNFEIPKTIWRIQQAQAKKVALQMPGEGLLIFAC	107
XP_014018522.1[Salmo salar]Actinopterygii	RVANQTPPEILNPNQIQ-AIQVLPSSNYNFEIPKTIWRIQQAQAKKVALQMPGEGLLIFAC	81
XP_016336999.1[Sinocyclocheilus anshuensis]Actinopterygii	RVANQTPPEILNPNQIQ-AIQVLPSSNYNFEIPKTIWRIQQAQAKKVALQMPGEGLLIFAC	81
XP_017550402.1[Epiplatys nattereri]Actinopterygii	RVANQTPPEILNPNQIQ-AIQVLPSSNYNFEIPKTIWRIQQAQAKKVALQMPGEGLLIFAC	80
XP_005804152.1[Xiphophorus maculatus]Actinopterygii	RVANQTPPEILNPNQIQ-AIQVLPSSNYNFEIPKTIWRIQQAQAKKVALQMPGEGLLIFAC	81
XP_019729898.1[Hippocampus comes]Actinopterygii	RVANQTPPEILNPNQIQ-AIQVLPSSNYNFEIPKTIWRIQQAQAKKVALQMPGEGLLIFAC	82
XP_005157638.1[Danio rerio]Actinopterygii	RVANQTPPEILNPNQIQ-AIQVLPSSNYNFEIPKTIWRIQQAQAKKVALQMPGEGLLIFAC	96
XP_011606823.1[Takifugu rubripes]Actinopterygii	RVANQTPPEILNPNQIQ-AIQVLPSSNYNFEIPKTIWRIQQAQAKKVALQMPGEGLLIFAC	81
XP_016836589.1[Nasonia vitripennis]Insecta	RVANQTPPEILNPNQIQ-AIQVLPSSNYNFEIPKTIWRIQQAQAKKVALQMPGEGLLIFAC	146
XP_011866406.1[Vollenhovia emeryi]Insecta	RVANQTPPEILNPNQIQ-AIQVLPSSNYNFEIPKTIWRIQQAQAKKVALQMPGEGLLIFAC	79
XP_015502716.1[Neodiprion lecontei]Insecta	RVANQTPPEILNPNQIQ-AIQVLPSSNYNFEIPKTIWRIQQAQAKKVALQMPGEGLLIFAC	83
XP_011154130.1[Harpagynia saltator]Insecta	RVANQTPPEILNPNQIQ-AIQVLPSSNYNFEIPKTIWRIQQAQAKKVALQMPGEGLLIFAC	82
XP_017957296.1[Drosophila nvojoa]Insecta	RVANQTPPEILNPNQIQ-AIQVLPSSNYNFEIPKTIWRIQQAQAKKVALQMPGEGLLIFAC	96
NP_001261722.1[Drosophila melanogaster]Insecta	RVANQTPPEILNPNQIQ-AIQVLPSSNYNFEIPKTIWRIQQAQAKKVALQMPGEGLLIFAC	92
XP_013145150.1[Papilio polytes]Insecta	RVANQTPPEILNPNQIQ-AIQVLPSSNYNFEIPKTIWRIQQAQAKKVALQMPGEGLLIFAC	87
XP_002423182.1[Pediculus humanus]Insecta	RVANQTPPEILNPNQIQ-AIQVLPSSNYNFEIPKTIWRIQQAQAKKVALQMPGEGLLIFAC	93
NP_497750.1[Caenorhabditis elegans]Secernentea	TQISTVPEEILNPNQIQ-AIQVLPSSNYNFEIPKTIWRIQQAQAKKVALQMPGEGLLIFAC	64
XP_018668637.1[Ciona intestinalis]Ascidiacea	NTPNQPPEILNPNQIQ-AIQVLPSSNYNFEIPKTIWRIQQAQAKKVALQMPGEGLLIFAC	86
XP_638680.1[Dityostelium discoideum]Dityostelia	RVANQTPPEILNPNQIQ-AIQVLPSSNYNFEIPKTIWRIQQAQAKKVALQMPGEGLLIFAC	157
XP_01134328.1[Fusarium graminearum]Sordariomycetes	RLANQVPEEILNPNQIQ-AIQVLPSSNYNFEIPKTIWRIQQAQAKKVALQMPGEGLLIFAC	147
XP_018748209.1[Fusarium verticillioides]Sordariomycetes	RLANQVPEEILNPNQIQ-AIQVLPSSNYNFEIPKTIWRIQQAQAKKVALQMPGEGLLIFAC	140
XP_018150409.1[Pochochia hamydosporia]Sordariomycetes	RLANQVPEEILNPNQIQ-AIQVLPSSNYNFEIPKTIWRIQQAQAKKVALQMPGEGLLIFAC	137
XP_018658688.1[Trichoderma gamsii]Sordariomycetes	RLANQVPEEILNPNQIQ-AIQVLPSSNYNFEIPKTIWRIQQAQAKKVALQMPGEGLLIFAC	137
XP_001208548.1[Aspergillus terreus]Eurotiomycetes	RLANQVPEEILNPNQIQ-AIQVLPSSNYNFEIPKTIWRIQQAQAKKVALQMPGEGLLIFAC	110
XP_002379550.1[Aspergillus flavus]Eurotiomycetes	RLANQVPEEILNPNQIQ-AIQVLPSSNYNFEIPKTIWRIQQAQAKKVALQMPGEGLLIFAC	116
XP_002563943.1[Penicillium rubens]Eurotiomycetes	RLANQVPEEILNPNQIQ-AIQVLPSSNYNFEIPKTIWRIQQAQAKKVALQMPGEGLLIFAC	120
XP_015457246.1[Debaryomyces fabryi]Saccharomycetes	RVANQTPPEILNPNQIQ-AIQVLPSSNYNFEIPKTIWRIQQAQAKKVALQMPGEGLLIFAC	108
KZ010512.1[DPH1 (S. cerevisiae)]Saccharomycetes	RVANQTPPEILNPNQIQ-AIQVLPSSNYNFEIPKTIWRIQQAQAKKVALQMPGEGLLIFAC	106
XP_006827105[Amborella trichopoda]Plant	RVANQTPPEILNPNQIQ-AIQVLPSSNYNFEIPKTIWRIQQAQAKKVALQMPGEGLLIFAC	85
XP_002454772.1[Sorghum bicolor]Plant	RVANQTPPEILNPNQIQ-AIQVLPSSNYNFEIPKTIWRIQQAQAKKVALQMPGEGLLIFAC	98
XP_020865862.1[Arabidopsis lyrata]Plant	RVANQTPPEILNPNQIQ-AIQVLPSSNYNFEIPKTIWRIQQAQAKKVALQMPGEGLLIFAC	79
XP_008643787[Zea mays]Plant	RVANQTPPEILNPNQIQ-AIQVLPSSNYNFEIPKTIWRIQQAQAKKVALQMPGEGLLIFAC	95

Identification of disease-causing variants in patients clinically diagnosed with Opitz C syndrome and Bohring-Opitz syndrome and functional validation

	Leu234	
NP_001374.3[<i>Homo sapiens</i>]Primate	-Y-RVSVFQCKPLSPGELIGCTSPRLSK-----EVEAVVYDGGRFHLESVMIANFN	250
XP_003816906.1[<i>Pan paniscus</i>]Primate	-Y-RVSVFQCKPLSPGELIGCTSPRLSK-----EVEAVVYDGGRFHLESVMIANFN	250
XP_008968211.1[<i>Pan paniscus</i>]Primate	-Y-RVSVFQCKPLSPGELIGCTSPRLSK-----EVEAVVYDGGRFHLESVMIANFN	234
XP_018868753.1[<i>Gorilla gorilla gorilla</i>]Primate	-Y-RVSVFQCKPLSPGELIGCTSPRLSK-----EVEAVVYDGGRFHLESVMIANFN	245
XP_002826867.1[<i>Pongo abelii</i>]Primate	-Y-RVSVFQCKPLSPGELIGCTSPRLSK-----EVEAVVYDGGRFHLESVMIANFN	245
XP_012356920.1[<i>Nomascus leucogenys</i>]Primate	-Y-RVSVFQCKPLSPGELIGCTSPRLSK-----EVEAVVYDGGRFHLESVMIANFN	245
XP_011842657.1[<i>MandrillLus leucophaeus</i>]Primate	-Y-RVSVFQCKPLSPGELIGCTSPRLSK-----EVEAVVYDGGRFHLESVMIANFN	245
XP_008061609.1[<i>Carollia yrichta</i>]Primate	-Y-RVSVFQCKPLSPGELIGCTSPRLSK-----EVEAVVYDGGRFHLESVMIANFN	245
XP_001504395.3[<i>Equus caballus</i>]mammal_Eu	-Y-RVSVFQCKPLSPGELIGCTSPRLSK-----EVEAVVYDGGRFHLESVMIANFN	248
XP_010859626.1[<i>Bison bison bison</i>]mammal_Eu	-Y-RVSVFQCKPLSPGELIGCTSPRLSK-----EVEAVVYDGGRFHLESVMIANFN	245
NP_001070367.1[<i>Bos taurus</i>]mammal	-Y-RVSVFQCKPLSPGELIGCTSPRLSK-----EVEAVVYDGGRFHLESVMIANFN	246
XP_019837435.1[<i>Bos indicus</i>]mammal	-Y-RVSVFQCKPLSPGELIGCTSPRLSK-----EVEAVVYDGGRFHLESVMIANFN	248
XP_012006497.1[<i>Ovis aries musimon</i>]mammal	-Y-RVSVFQCKPLSPGELIGCTSPRLSK-----EVEAVVYDGGRFHLESVMIANFN	245
XP_017919893.1[<i>Capra hircus</i>]mammal	-Y-RVSVFQCKPLSPGELIGCTSPRLSK-----EVEAVVYDGGRFHLESVMIANFN	245
XP_003131871.3[<i>Sus scrofa</i>]mammal	-Y-RVSVFQCKPLSPGELIGCTSPRLSK-----EVEAVVYDGGRFHLESVMIANFN	246
XP_015103509.1[<i>Vicuña pacos</i>]mammal	-Y-RVSVFQCKPLSPGELIGCTSPRLSK-----EVEAVVYDGGRFHLESVMIANFN	245
XP_008269143.1[<i>Oryctolagus cuniculus</i>]mammal_Eu	-Y-RVSVFQCKPLSPGELIGCTSPRLSK-----EVEAVVYDGGRFHLESVMIANFN	248
XP_016042474.1[<i>Erinaceus europaeus</i>]mammal_Eu	-Y-RVSVFQCKPLSPGELIGCTSPRLSK-----EVEAVVYDGGRFHLESVMIANFN	245
NP_001099279.1[<i>Rattus norvegicus</i>]mammal_Eu	-Y-RVSVFQCKPLSPGELIGCTSPRLSK-----EVEAVVYDGGRFHLESVMIANFN	245
XP_004635594.1[<i>Octodon degus</i>]mammal_Eu	-Y-RVSVFQCKPLSPGELIGCTSPRLSK-----EVEAVVYDGGRFHLESVMIANFN	245
XP_003469582.2[<i>Cavia porcellus</i>]mammal	-Y-RVSVFQCKPLSPGELIGCTSPRLSK-----EVEAVVYDGGRFHLESVMIANFN	245
XP_010640444.1[<i>Fukomys damarensis</i>]mammal	-Y-RVSVFQCKPLSPGELIGCTSPRLSK-----EVEAVVYDGGRFHLESVMIANFN	256
XP_005402655.1[<i>Chinchilla lanigera</i>]mammal	-Y-RVSVFQCKPLSPGELIGCTSPRLSK-----EVEAVVYDGGRFHLESVMIANFN	245
NP_652762.2[<i>Mus musculus</i>]mammal	-Y-RVSVFQCKPLSPGELIGCTSPRLSK-----EVEAVVYDGGRFHLESVMIANFN	245
XP_003507319.1[<i>Cricetulus griseus</i>]mammal	-Y-RVSVFQCKPLSPGELIGCTSPRLSK-----EVEAVVYDGGRFHLESVMIANFN	245
XP_006977441.1[<i>Peromyscus maniculatus</i>]mammal	-Y-RVSVFQCKPLSPGELIGCTSPRLSK-----EVEAVVYDGGRFHLESVMIANFN	245
XP_004667842.1[<i>Jaculus jaculus</i>]mammal	-Y-RVSVFQCKPLSPGELIGCTSPRLSK-----EVEAVVYDGGRFHLESVMIANFN	245
XP_004605318.1[<i>Sorex araneus</i>]mammal_Eu	-Y-RVSVFQCKPLSPGELIGCTSPRLSK-----EVEAVVYDGGRFHLESVMIANFN	245
XP_006801601.1[<i>Elephantulus edwardii</i>]mammal_Eu	-Y-RVSVFQCKPLSPGELIGCTSPRLSK-----EVEAVVYDGGRFHLESVMIANFN	245
XP_019611098.1[<i>Rhinolophus sinicus</i>]mammal_Eu	-Y-RVSVFQCKPLSPGELIGCTSPRLSK-----EVEAVVYDGGRFHLESVMIANFN	245
XP_011381641.1[<i>Pteropus vampyrus</i>]mammal_Eu	-Y-RVSVFQCKPLSPGELIGCTSPRLSK-----EVEAVVYDGGRFHLESVMIANFN	250
XP_019672915.1[<i>Felis catus</i>]mammal_Eu	-Y-RVSVFQCKPLSPGELIGCTSPRLSK-----EVEAVVYDGGRFHLESVMIANFN	245
XP_007076184.2[<i>Panthera tigris altaica</i>]mammal_Eu	-Y-RVSVFQCKPLSPGELIGCTSPRLSK-----EVEAVVYDGGRFHLESVMIANFN	246
XP_013972316.1[<i>Canis lupus familiaris</i>]mammal_Eu	-Y-RVSVFQCKPLSPGELIGCTSPRLSK-----EVEAVVYDGGRFHLESVMIANFN	246
XP_007177531.1[<i>Balaenoptera acutorostrata</i>]mammal_Eu	-Y-RVSVFQCKPLSPGELIGCTSPRLSK-----EVEAVVYDGGRFHLESVMIANFN	245
XP_004267102.1[<i>Orcinus orca</i>]mammal_Eu	-Y-RVSVFQCKPLSPGELIGCTSPRLSK-----EVEAVVYDGGRFHLESVMIANFN	245
XP_010594790.1[<i>Loxodonta africana</i>]mammal_Eu	-Y-RVSVFQCKPLSPGELIGCTSPRLSK-----EVEAVVYDGGRFHLESVMIANFN	245
XP_017507098.1[<i>Manis javanica</i>]mammal_Eu	-Y-RVSVFQCKPLSPGELIGCTSPRLSK-----EVEAVVYDGGRFHLESVMIANFN	266
XP_012405311.1[<i>Sarcophilus harrisii</i>]mammal_marsupial	-Y-RVSVFQCKPLSPGELIGCTSPRLSK-----EVEAVVYDGGRFHLESVMIANFN	242
XP_007485825.1[<i>Monodelphis domestica</i>]mammal_Me	-Y-RVSVFQCKPLSPGELIGCTSPRLSK-----EVEAVVYDGGRFHLESVMIANFN	246
XP_011579991.1[<i>Aquila chrysaetos</i>]Aves	-Y-RVSVFQCKPLSPGELIGCTSPRLSK-----EVEAVVYDGGRFHLESVMIANFN	240
XP_015501861.1[<i>Parus major</i>]Aves	-Y-RVSVFQCKPLSPGELIGCTSPRLSK-----EVEAVVYDGGRFHLESVMIANFN	246
XP_017687952.1[<i>Lepidodirix coronata</i>]Aves	-Y-RVSVFQCKPLSPGELIGCTSPRLSK-----EVEAVVYDGGRFHLESVMIANFN	246
XP_005439966.1[<i>Falco cherrug</i>]Aves	-Y-RVSVFQCKPLSPGELIGCTSPRLSK-----EVEAVVYDGGRFHLESVMIANFN	267
XP_008493491.1[<i>Calyptra anna</i>]Aves	-Y-RVSVFQCKPLSPGELIGCTSPRLSK-----EVEAVVYDGGRFHLESVMIANFN	243
NP_001025887.2[<i>Gallus gallus</i>]Aves	-Y-RVSVFQCKPLSPGELIGCTSPRLSK-----EVEAVVYDGGRFHLESVMIANFN	242
XP_015736460.1[<i>Coturnix japonica</i>]Aves	-Y-RVSVFQCKPLSPGELIGCTSPRLSK-----EVEAVVYDGGRFHLESVMIANFN	242
XP_010720021.1[<i>Meleagris gallopavo</i>]Aves	-Y-RVSVFQCKPLSPGELIGCTSPRLSK-----EVEAVVYDGGRFHLESVMIANFN	237
XP_005502175.1[<i>Columba livia</i>]Aves	-Y-RVSVFQCKPLSPGELIGCTSPRLSK-----EVEAVVYDGGRFHLESVMIANFN	240
XP_019400888.1[<i>Crocodylus porosus</i>]Sauropsida	-Y-EVCFVQCKPLSPGELIGCTSPRLAQ-----DTDAVYDGGRFHLESIMIANFG	313
XP_014379797.1[<i>Alligator sinensis</i>]Sauropsida	-Y-EVCFVQCKPLSPGELIGCTSPRLAQ-----DTDAVYDGGRFHLESIMIANFG	169
XP_015277363.1[<i>Gekko japonicus</i>]reptilia	-Y-TVCTFQCKPLSPGELIGCTSPRLAR-----DTDAVYDGGRFHLESIMIANFG	242
XP_003230257.2[<i>Anolis carolinensis</i>]reptilia	-Y-CVLIQCKPLSPGELIGCTSPRLPS-----DTDAVYDGGRFHLESIMIANFG	236
XP_012812029.1[<i>Xenopus tropicalis</i>]Amphibia	-Y-RVTVFQCKPLSPGELIGCTSPRLDK-----SDAVVYDGGRFHLESIMIANFG	266
XP_014018522.1[<i>Salmo salar</i>]Actinopterygii	-Y-EVTVFQCKPLSPGELIGCTSPRLDR-----NNAVLYDGGRFHLESIMIANFG	240
XP_016336999.1[<i>Sinycylocheilus anshuiensis</i>]Actinopterygii	-Y-EVTVFQCKPLSPGELIGCTSPRLDK-----HVNALYDGGRFHLESIMIANFG	240
XP_015750402.1[<i>Epiplatys nattereri</i>]Actinopterygii	-Y-EVTVFQCKPLSPGELIGCTSPRLDK-----HVNALYDGGRFHLESIMIANFG	239
XP_005804152.1[<i>Xiphophorus maculatus</i>]Actinopterygii	-Y-DVTVFQCKPLSPGELIGCTSPRLDC-----HVDALYDGGRFHLESIMIANFG	240
XP_019729898.1[<i>Hippocampus comes</i>]Actinopterygii	-Y-DVTVFQCKPLSPGELIGCTSPRLDR-----HVNALYDGGRFHLESIMIANFG	241
XP_005157638.1[<i>Danio rerio</i>]Actinopterygii	-Y-EVTVFQCKPLSPGELIGCTSPRLDK-----HVNALYDGGRFHLESIMIANFG	255
XP_011606823.1[<i>Takifugu rubripes</i>]Actinopterygii	-Y-DVTVFQCKPLSPGELIGCTSPRLDR-----HVDALYDGGRFHLESIMIANFG	240
XP_016836589.1[<i>Masonia vitripennis</i>]Insecta	GY-SVTVFQCKPLSPGELIGCTAPQLND-----VDLVYDGGRFHLESAMIANFK	305
XP_011866406.1[<i>Volienhovia emeryi</i>]Insecta	GY-EVTVFQCKPLSPGELIGCTAPQVRC-----ADAVVYDGGRFHLESAMIANFK	238
XP_015520716.1[<i>Neodiprion lecontei</i>]Insecta	GY-EVTVFQCKPLSPGELIGCTAPQVRC-----ADAVVYDGGRFHLESAMIANFK	242
XP_01154130.1[<i>Harpagathous saltator</i>]Insecta	GY-EVTVFQCKPLSPGELIGCTAPQVRC-----ADAVVYDGGRFHLESAMIANFK	241
XP_017957296.1[<i>Drosophila navajoa</i>]Insecta	GY-DVTVFQCKPLSPGELIGCTSPQLPE-----TTVMILYDGGRFHLESAMIANFL	253
NP_001261722.1[<i>Drosophila melanogaster</i>]Insecta	GY-DVTVFQCKPLSPGELIGCTSPQLPE-----TTVMILYDGGRFHLESAMIANFL	267
XP_013145150.1[<i>Papilio polytes</i>]Insecta	DY-IVTVFQCKPLSPGELIGCTAPQLQ-----SDVILYDGGRFHLESAMIANFS	245
XP_002423182.1[<i>Pedicularis humanus</i>]Insecta	GY-SVTVFQCKPLSPGELIGCTAPQVRC-----VDVYDGGRFHLESAMIANFT	282
NP_497750.1[<i>Caserochabditis elegans</i>]Secernentea	SI-RIDFQCKPLSPGELIGCTSPFLDA-----SKYDALVYDGGRFHLESIMIANFG	326
XP_018686837.1[<i>Ciona intestinalis</i>]Ascidiacea	GI-EVTVFQCKPLSPGELIGCTSPRLGE-----TKADALVYDGGRFHLESIMIANFG	247
XP_638680.1[<i>Dictyostelium discoideum</i>]Dictyostelia	F8-NIFIQCKPLSPGELIGCTSPRLKTS-----PDGDEENNEVLVYDGGRFHLESIMIANFG	324
XP_011316328.1[<i>Fusarium graminearum</i>]Sordariomycetes	GF-RVLVFPQAPLSPGELIGCTSPRLTE-----DDKLDLILVYDGGRFHLESIMIANFG	309
XP_018742809.1[<i>Fusarium verticillioides</i>]Sordariomycetes	GF-RVLVFPQAPLSPGELIGCTSPRLTD-----DDNLDLILVYDGGRFHLESIMIANFG	302
XP_018150409.1[<i>Frochonia chlamydosporia</i>]Sordariomycetes	GF-RVLVFPQAPLSPGELIGCTSPRLAD-----EDAVVYDGGRFHLESIMIANFS	299
XP_018658688.1[<i>Trichoderma gamsii</i>]Sordariomycetes	GF-SVVVFPQAPLSPGELIGCTSPRLGD-----EDGLDLILVYDGGRFHLESIMIANFS	299
XP_001208548.1[<i>Aspergillus terreus</i>]Eurotiomycetes	GF-RVTVFQCKPLSPGELIGCTSPQLSS-----EEDLILVYDGGRFHLESAMIANFS	270
XP_002379550.1[<i>Aspergillus flavus</i>]Eurotiomycetes	GF-RVTVFQCKPLSPGELIGCTSPQLSS-----EEDLILVYDGGRFHLESAMIANFS	277
XP_002563943.1[<i>Penicillium rubens</i>]Eurotiomycetes	GF-RVTVFQCKPLSPGELIGCTSPQLSE-----TEIDALVYDGGRFHLESAMIANFS	281
XP_015467246.1[<i>Debaryomyces fabryi</i>]Saccharomycetes	TM-VLITFQCKPLSPGELIGCTSPRLNK-----EQLSALVYDGGRFHLESAMIANFS	265
KZV10512.1_DPH1[<i>S. cerevisiae</i>]Saccharomycetes	ML-VLITFQCKPLSPGELIGCTSPRLNK-----EQLSALVYDGGRFHLESAMIANFS	271
XP_006827105[<i>Amborella trichopoda</i>]Plant	FP-SVAVFQCKPLSPGELIGCTSPRLPL-----KGAADVYDGGRFHLESAMIANFG	246
XP_002454772.1[<i>Sorghum bicolor</i>]Plant	GYKDIVVQCKPLSPGELIGCTAPLTKK-----SBE-VGAVVYDGGRFHLESAMIANFG	264
XP_020865862.1[<i>Arabidopsis lyrata</i>]Plant	GF-NVMTFQCKPLSPGELIGCTAPLTKK-----VEDGRDQVLPVYDGGRFHLESAMIANFK	244
XP_008643787[<i>Zea mays</i>]Plant	GYHDIIVQCKPLSPGELIGCTAPLTKK-----SBE-VGAVVYDGGRFHLESAMIANFG	264

NP_001374.3[Homo sapiens]Primate	VPAYRYDPSYKVLSEHYDHRMQAARQEAIAATARSASWGLILGTLGRQGSFWLLEHLE	310
XP_003816906.1[Fan paniscus]Primate	VPAYRYDPSYKVLSEHYDHRMQAARQEAIAATARSASWGLILGTLGRQGSFWLLEHLE	310
XP_008968211.1[Fan paniscus]Primate	VPAYRYDPSYKVLSEHYDHRMQAARQEAIAATARSASWGLILGTLGRQGSFWLLEHLE	294
XP_018868753.1[Gorilla gorilla gorilla]Primate	VPAYRYDPSYKVLSEHYDHRMQAARQEAIAATARSASWGLILGTLGRQGSFWLLEHLE	305
XP_002826867.1[Pongo abelii]Primate	VPAYRYDPSYKVLSEHYDHRMQAARQEAIAATARSASWGLILGTLGRQGSFWLLEHLE	305
XP_012356920.1[Nomascus leucogenys]Primate	VPAYRYDPSYKVLSEHYDHRMQAARQEAIAATARSASWGLILGTLGRQGSFWLLEHLE	305
XP_011842657.1[MandrillLula leucophaea]Primate	VPAYRYDPSYKVLSEHYDHRMQAARQEAIAATARSASWGLILGTLGRQGSFWLLEHLE	305
XP_008061609.1[Carollia gyrichta]Primate	VPAYRYDPSYKVLSEHYDHRMQAARQEAIAATARSASWGLILGTLGRQGSFWLLEHLE	305
XP_001504395.3[Equus caballus]mammal_Eu	VPAYRYDPSYKVLSEHYDHRMQAARQEAIAATARSASWGLILGTLGRQGSFWLLEHLE	305
XP_010859626.1[Bison bison bison]mammal_Eu	VPAYRYDPSYKVLSEHYDHRMQAARQEAIAATARSASWGLILGTLGRQGSFWLLEHLE	305
NP_001070367.1[Bos taurus]mammal	VPAYRYDPSYKVLSEHYDHRMQAARQEAIAATARSASWGLILGTLGRQGSFWLLEHLE	305
XP_019837435.1[Bos indicus]mammal	VPAYRYDPSYKVLSEHYDHRMQAARQEAIAATARSASWGLILGTLGRQGSFWLLEHLE	305
XP_012006497.1[Ovis aries musimon]mammal	VPAYRYDPSYKVLSEHYDHRMQAARQEAIAATARSASWGLILGTLGRQGSFWLLEHLE	305
XP_017919893.1[Capra hircus]mammal	VPAYRYDPSYKVLSEHYDHRMQAARQEAIAATARSASWGLILGTLGRQGSFWLLEHLE	305
XP_003131871.3[Sus scrofa]mammal	VPAYRYDPSYKVLSEHYDHRMQAARQEAIAATARSASWGLILGTLGRQGSFWLLEHLE	305
XP_015103509.1[Vicugna pacos]mammal	VPAYRYDPSYKVLSEHYDHRMQAARQEAIAATARSASWGLILGTLGRQGSFWLLEHLE	305
XP_008269143.1[Oryctolagus cuniculus]mammal_Eu	VPAYRYDPSYKVLSEHYDHRMQAARQEAIAATARSASWGLILGTLGRQGSFWLLEHLE	305
XP_016042474.1[Erinaceus europaeus]mammal_Eu	VPAYRYDPSYKVLSEHYDHRMQAARQEAIAATARSASWGLILGTLGRQGSFWLLEHLE	305
NP_001099279.1[Rattus norvegicus]mammal_Eu	VPAYRYDPSYKVLSEHYDHRMQAARQEAIAATARSASWGLILGTLGRQGSFWLLEHLE	305
XP_004635594.1[Octodon degus]mammal_Eu	VPAYRYDPSYKVLSEHYDHRMQAARQEAIAATARSASWGLILGTLGRQGSFWLLEHLE	305
XP_003469582.2[Cavia porcellus]mammal	VPAYRYDPSYKVLSEHYDHRMQAARQEAIAATARSASWGLILGTLGRQGSFWLLEHLE	305
XP_010640444.1[Fukomys damarensis]mammal	VPAYRYDPSYKVLSEHYDHRMQAARQEAIAATARSASWGLILGTLGRQGSFWLLEHLE	326
XP_005402655.1[Chinchilla lanigera]mammal	VPAYRYDPSYKVLSEHYDHRMQAARQEAIAATARSASWGLILGTLGRQGSFWLLEHLE	305
NP_652762.2[Mus musculus]mammal	VPAYRYDPSYKVLSEHYDHRMQAARQEAIAATARSASWGLILGTLGRQGSFWLLEHLE	305
XP_003507319.1[Cricetulus griseus]mammal	VPAYRYDPSYKVLSEHYDHRMQAARQEAIAATARSASWGLILGTLGRQGSFWLLEHLE	305
XP_006697441.1[Peromyscus maniculatus]mammal	VPAYRYDPSYKVLSEHYDHRMQAARQEAIAATARSASWGLILGTLGRQGSFWLLEHLE	305
XP_004667842.1[Jaculus jaculus]mammal	VPAYRYDPSYKVLSEHYDHRMQAARQEAIAATARSASWGLILGTLGRQGSFWLLEHLE	305
XP_004605518.1[Sorex araneus]mammal_Eu	VPAYRYDPSYKVLSEHYDHRMQAARQEAIAATARSASWGLILGTLGRQGSFWLLEHLE	305
XP_006891160.1[Lephantulus edwardi]mammal_Eu	VPAYRYDPSYKVLSEHYDHRMQAARQEAIAATARSASWGLILGTLGRQGSFWLLEHLE	305
XP_019611098.1[Rhinolophus sinicus]mammal_Eu	VPAYRYDPSYKVLSEHYDHRMQAARQEAIAATARSASWGLILGTLGRQGSFWLLEHLE	305
XP_011358164.1[Pteropus vampyrus]mammal_Eu	VPAYRYDPSYKVLSEHYDHRMQAARQEAIAATARSASWGLILGTLGRQGSFWLLEHLE	310
XP_019672915.1[Felis catus]mammal_Eu	VPAYRYDPSYKVLSEHYDHRMQAARQEAIAATARSASWGLILGTLGRQGSFWLLEHLE	305
XP_007076184.2[Panthera tigris altaica]mammal_Eu	VPAYRYDPSYKVLSEHYDHRMQAARQEAIAATARSASWGLILGTLGRQGSFWLLEHLE	326
XP_013972316.1[Canis lupus familiaris]mammal_Eu	VPAYRYDPSYKVLSEHYDHRMQAARQEAIAATARSASWGLILGTLGRQGSFWLLEHLE	306
XP_007177531.1[Balaenoptera acutorostrata]mammal_Eu	VPAYRYDPSYKVLSEHYDHRMQAARQEAIAATARSASWGLILGTLGRQGSFWLLEHLE	305
XP_004267102.1[Orccinus orca]mammal_Eu	VPAYRYDPSYKVLSEHYDHRMQAARQEAIAATARSASWGLILGTLGRQGSFWLLEHLE	305
XP_010594790.1[Loxodonta africana]mammal_Eu	VPAYRYDPSYKVLSEHYDHRMQAARQEAIAATARSASWGLILGTLGRQGSFWLLEHLE	305
XP_017507098.1[Manis javanica]mammal_Eu	VPAYRYDPSYKVLSEHYDHRMQAARQEAIAATARSASWGLILGTLGRQGSFWLLEHLE	326
XP_012405011.1[Sarcophilus harrisii]mammal_marsupial	VPAYRYDPSYKVLSEHYDHRMQAARQEAIAATARSASWGLILGTLGRQGSFWLLEHLE	302
XP_007485825.1[Monodelphis domestica]mammal_Me	VPAYRYDPSYKVLSEHYDHRMQAARQEAIAATARSASWGLILGTLGRQGSFWLLEHLE	306
XP_011579991.1[Aquila chrysaetos]Aves	VPAYRYDPSYKVLSEHYDHRMQAARQEAIAATARSASWGLILGTLGRQGSFWLLEHLE	300
XP_015501861.1[Parus major]Aves	VPAYRYDPSYKVLSEHYDHRMQAARQEAIAATARSASWGLILGTLGRQGSFWLLEHLE	296
XP_017687952.1[Lepidodhrax coronata]Aves	VPAYRYDPSYKVLSEHYDHRMQAARQEAIAATARSASWGLILGTLGRQGSFWLLEHLE	300
XP_005439966.1[Falco cherrug]Aves	VPAYRYDPSYKVLSEHYDHRMQAARQEAIAATARSASWGLILGTLGRQGSFWLLEHLE	327
XP_008493491.1[Calypte anna]Aves	VPAYRYDPSYKVLSEHYDHRMQAARQEAIAATARSASWGLILGTLGRQGSFWLLEHLE	303
NP_001025887.2[Gallus gallus]Aves	VPAYRYDPSYKVLSEHYDHRMQAARQEAIAATARSASWGLILGTLGRQGSFWLLEHLE	302
XP_015736460.1[Coturnix japonica]Aves	VPAYRYDPSYKVLSEHYDHRMQAARQEAIAATARSASWGLILGTLGRQGSFWLLEHLE	302
XP_010720021.1[Meleagris gallopavo]Aves	VPAYRYDPSYKVLSEHYDHRMQAARQEAIAATARSASWGLILGTLGRQGSFWLLEHLE	297
XP_005502175.1[Columba livia]Aves	VPAYRYDPSYKVLSEHYDHRMQAARQEAIAATARSASWGLILGTLGRQGSFWLLEHLE	300
XP_019400888.1[Crocodylus porosus]Sauropsida	VPAYRYDPSYKVLSEHYDHRMQAARQEAIAATARSASWGLILGTLGRQGSFWLLEHLE	313
XP_014379797.1[Alligator sinensis]Sauropsida	VPAYRYDPSYKVLSEHYDHRMQAARQEAIAATARSASWGLILGTLGRQGSFWLLEHLE	229
XP_015277363.1[Gekko japonicus]reptilia	VPAYRYDPSYKVLSEHYDHRMQAARQEAIAATARSASWGLILGTLGRQGSFWLLEHLE	302
XP_003230257.2[Anolis carolinensis]reptilia	VPAYRYDPSYKVLSEHYDHRMQAARQEAIAATARSASWGLILGTLGRQGSFWLLEHLE	296
XP_012812029.1[Xenopus tropicalis]Amphibia	VPAYRYDPSYKVLSEHYDHRMQAARQEAIAATARSASWGLILGTLGRQGSFWLLEHLE	326
XP_014018522.1[Salmo salar]Actinopterygii	VPAYRYDPSYKVLSEHYDHRMQAARQEAIAATARSASWGLILGTLGRQGSFWLLEHLE	300
XP_016336999.1[Sinocyclocheilus anshuensis]Actinopterygii	VPAYRYDPSYKVLSEHYDHRMQAARQEAIAATARSASWGLILGTLGRQGSFWLLEHLE	300
XP_015750402.1[Egocentrus nattereri]Actinopterygii	VPAYRYDPSYKVLSEHYDHRMQAARQEAIAATARSASWGLILGTLGRQGSFWLLEHLE	299
XP_005804152.1[Xiphophorus maculatus]Actinopterygii	VPAYRYDPSYKVLSEHYDHRMQAARQEAIAATARSASWGLILGTLGRQGSFWLLEHLE	300
XP_019729898.1[Hippocampus comes]Actinopterygii	VPAYRYDPSYKVLSEHYDHRMQAARQEAIAATARSASWGLILGTLGRQGSFWLLEHLE	301
XP_00167638.1[Danio rerio]Actinopterygii	VPAYRYDPSYKVLSEHYDHRMQAARQEAIAATARSASWGLILGTLGRQGSFWLLEHLE	315
XP_011606823.1[Takifugu rubripes]Actinopterygii	VPAYRYDPSYKVLSEHYDHRMQAARQEAIAATARSASWGLILGTLGRQGSFWLLEHLE	300
XP_016836589.1[Masonia vitripennis]Insecta	VPAYRYDPSYKVLSEHYDHRMQAARQEAIAATARSASWGLILGTLGRQGSFWLLEHLE	365
XP_011866406.1[Volienhovia emeryi]Insecta	VPAYRYDPSYKVLSEHYDHRMQAARQEAIAATARSASWGLILGTLGRQGSFWLLEHLE	299
XP_015520716.1[Neodiprion lecontei]Insecta	VPAYRYDPSYKVLSEHYDHRMQAARQEAIAATARSASWGLILGTLGRQGSFWLLEHLE	302
XP_01154130.1[Harpagathoa saltator]Insecta	VPAYRYDPSYKVLSEHYDHRMQAARQEAIAATARSASWGLILGTLGRQGSFWLLEHLE	301
XP_017957296.1[Drosophila melanogaster]Insecta	VPAYRYDPSYKVLSEHYDHRMQAARQEAIAATARSASWGLILGTLGRQGSFWLLEHLE	317
NP_001261722.1[Drosophila melanogaster]Insecta	VPAYRYDPSYKVLSEHYDHRMQAARQEAIAATARSASWGLILGTLGRQGSFWLLEHLE	313
XP_013149150.1[Papilio polytes]Insecta	VPAYRYDPSYKVLSEHYDHRMQAARQEAIAATARSASWGLILGTLGRQGSFWLLEHLE	305
XP_002423182.1[Fedicalius hageni]Insecta	VPAYRYDPSYKVLSEHYDHRMQAARQEAIAATARSASWGLILGTLGRQGSFWLLEHLE	312
NP_497750.1[Caenorhabditis elegans]Secernentea	VPAYRYDPSYKVLSEHYDHRMQAARQEAIAATARSASWGLILGTLGRQGSFWLLEHLE	316
XP_01868637.1[Ciona intestinalis]Ascidiacea	VPAYRYDPSYKVLSEHYDHRMQAARQEAIAATARSASWGLILGTLGRQGSFWLLEHLE	307
XP_638680.1[Dictyostelium discoideum]Dictyostelia	VPAYRYDPSYKVLSEHYDHRMQAARQEAIAATARSASWGLILGTLGRQGSFWLLEHLE	384
XP_011316328.1[Fusarium graminearum]Sordariomycetes	VPAYRYDPSYKVLSEHYDHRMQAARQEAIAATARSASWGLILGTLGRQGSFWLLEHLE	369
XP_018742809.1[Fusarium verticillioides]Sordariomycetes	VPAYRYDPSYKVLSEHYDHRMQAARQEAIAATARSASWGLILGTLGRQGSFWLLEHLE	362
XP_018150409.1[Foichonia chlamydosporia]Sordariomycetes	VPAYRYDPSYKVLSEHYDHRMQAARQEAIAATARSASWGLILGTLGRQGSFWLLEHLE	359
XP_018658688.1[Trichoderma gamsii]Sordariomycetes	VPAYRYDPSYKVLSEHYDHRMQAARQEAIAATARSASWGLILGTLGRQGSFWLLEHLE	359
XP_001208548.1[Aspergillus terreus]Eurotiomycetes	VPAYRYDPSYKVLSEHYDHRMQAARQEAIAATARSASWGLILGTLGRQGSFWLLEHLE	330
XP_002379550.1[Aspergillus flavus]Eurotiomycetes	VPAYRYDPSYKVLSEHYDHRMQAARQEAIAATARSASWGLILGTLGRQGSFWLLEHLE	337
XP_002563943.1[Penicillium rubens]Eurotiomycetes	VPAYRYDPSYKVLSEHYDHRMQAARQEAIAATARSASWGLILGTLGRQGSFWLLEHLE	344
XP_015467246.1[Debaryomyces fabryi]Saccharomycetes	VPAYRYDPSYKVLSEHYDHRMQAARQEAIAATARSASWGLILGTLGRQGSFWLLEHLE	325
KZ110512.1_DP1[S. cerevisiae]Saccharomycetes	VPAYRYDPSYKVLSEHYDHRMQAARQEAIAATARSASWGLILGTLGRQGSFWLLEHLE	331
XP_006827105[Amborella trichopoda]Plant	VPAYRYDPSYKVLSEHYDHRMQAARQEAIAATARSASWGLILGTLGRQGSFWLLEHLE	306
XP_002454772.1[Sorghum bicolor]Plant	VPAYRYDPSYKVLSEHYDHRMQAARQEAIAATARSASWGLILGTLGRQGSFWLLEHLE	324
XP_020865862.1[Arabidopsis lyrata]Plant	VPAYRYDPSYKVLSEHYDHRMQAARQEAIAATARSASWGLILGTLGRQGSFWLLEHLE	304
XP_008643787[Zea mays]Plant	VPAYRYDPSYKVLSEHYDHRMQAARQEAIAATARSASWGLILGTLGRQGSFWLLEHLE	324

Identification of disease-causing variants in patients clinically diagnosed with Opitz C syndrome and Bohring-Opitz syndrome and functional validation

NP_001374.3[<i>Homo sapiens</i>]Primate	SLRALGLSFVRLLSLSEIPFSKLSLLEF-VDDVVQVACPRLSIDWGTAFKPLLPFYEA	369
XP_003816906.1[<i>Pan paniscus</i>]Primate	SQRLALGLSFVRLLSLSEIPFSKLSLLEF-VDDVVQVACPRLSIDWGTAFKPLLPFYEA	369
XP_008968221.1[<i>Pan paniscus</i>]Primate	SQRLALGLSFVRLLSLSEIPFSKLSLLEF-VDDVVQVACPRLSIDWGTAFKPLLPFYEA	369
XP_018868753.1[<i>Gorilla gorilla gorilla</i>]Primate	SLRALGLSFVRLLSLSEIPFSKLSLLEF-VDDVVQVACPRLSIDWGTAFKPLLPFYEA	364
XP_002826867.1[<i>Pongo abelii</i>]Primate	SLRALGLSFVRLLSLSEIPFSKLSLLEF-VDDVVQVACPRLSIDWGTAFKPLLPFYEA	364
XP_012356920.1[<i>Nomascus leucogenys</i>]Primate	SLRALGLSFVRLLSLSEIPFSKLSLLEF-VDDVVQVACPRLSIDWGTAFKPLLPFYEA	364
XP_011842657.1[<i>Mandrill</i>]Mammal	SLRALGLSFVRLLSLSEIPFSKLSLLEF-VDDVVQVACPRLSIDWGTAFKPLLPFYEA	364
XP_008061609.1[<i>Carollia yrichta</i>]Primate	SLRALGLSFVRLLSLSEIPFSKLSLLEF-VDDVVQVACPRLSIDWGTAFKPLLPFYEA	364
XP_001504395.3[<i>Equus caballus</i>]mammal_Eu	SLRALGLSFVRLLSLSEIPFSKLSLLEF-VDDVVQVACPRLSIDWGTAFKPLLPFYEA	364
XP_010859626.1[<i>Bison bison bison</i>]mammal_Eu	SLRALGLSFVRLLSLSEIPFSKLSLLEF-VDDVVQVACPRLSIDWGTAFKPLLPFYEA	364
NP_001070367.1[<i>Bos taurus</i>]mammal	SLRALGLSFVRLLSLSEIPFSKLSLLEF-VDDVVQVACPRLSIDWGTAFKPLLPFYEA	364
XP_019837435.1[<i>Bos indicus</i>]mammal	SLRALGLSFVRLLSLSEIPFSKLSLLEF-VDDVVQVACPRLSIDWGTAFKPLLPFYEA	364
XP_012006497.1[<i>Ovis aries musimon</i>]mammal	SLRALGLSFVRLLSLSEIPFSKLSLLEF-VDDVVQVACPRLSIDWGTAFKPLLPFYEA	364
XP_017919893.1[<i>Capra hircus</i>]mammal	SLRALGLSFVRLLSLSEIPFSKLSLLEF-VDDVVQVACPRLSIDWGTAFKPLLPFYEA	364
XP_003131871.3[<i>Sus scrofa</i>]mammal	SLRALGLSFVRLLSLSEIPFSKLSLLEF-VDDVVQVACPRLSIDWGTAFKPLLPFYEA	365
XP_015103509.1[<i>Vicuña pacos</i>]mammal	SLRALGLSFVRLLSLSEIPFSKLSLLEF-VDDVVQVACPRLSIDWGTAFKPLLPFYEA	364
XP_008269143.1[<i>Oryctolagus cuniculus</i>]mammal_Eu	SLRALGLSFVRLLSLSEIPFSKLSLLEF-VDDVVQVACPRLSIDWGTAFKPLLPFYEA	364
XP_016042474.1[<i>Erinaceus europaeus</i>]mammal_Eu	SLRALGLSFVRLLSLSEIPFSKLSLLEF-VDDVVQVACPRLSIDWGTAFKPLLPFYEA	364
NP_001099279.1[<i>Rattus norvegicus</i>]mammal_Eu	SLRALGLSFVRLLSLSEIPFSKLSLLEF-VDDVVQVACPRLSIDWGTAFKPLLPFYEA	364
XP_004635394.1[<i>Octodon degus</i>]mammal_Eu	SLRALGLSFVRLLSLSEIPFSKLSLLEF-VDDVVQVACPRLSIDWGTAFKPLLPFYEA	364
XP_003469582.2[<i>Cavia porcellus</i>]mammal	SLRALGLSFVRLLSLSEIPFSKLSLLEF-VDDVVQVACPRLSIDWGTAFKPLLPFYEA	364
XP_010640444.1[<i>Fukomys damarensis</i>]mammal	SLRALGLSFVRLLSLSEIPFSKLSLLEF-VDDVVQVACPRLSIDWGTAFKPLLPFYEA	365
XP_005402655.1[<i>Chinchilla lanigera</i>]mammal	SLRALGLSFVRLLSLSEIPFSKLSLLEF-VDDVVQVACPRLSIDWGTAFKPLLPFYEA	364
NP_652762.2[<i>Mus musculus</i>]mammal	SLRALGLSFVRLLSLSEIPFSKLSLLEF-VDDVVQVACPRLSIDWGTAFKPLLPFYEA	364
XP_003507319.1[<i>Cricetulus griseus</i>]mammal	SLRALGLSFVRLLSLSEIPFSKLSLLEF-VDDVVQVACPRLSIDWGTAFKPLLPFYEA	364
XP_006977441.1[<i>Peromyscus maniculatus</i>]mammal	SLRALGLSFVRLLSLSEIPFSKLSLLEF-VDDVVQVACPRLSIDWGTAFKPLLPFYEA	364
XP_004667842.1[<i>Jaculus jaculus</i>]mammal	SLRALGLSFVRLLSLSEIPFSKLSLLEF-VDDVVQVACPRLSIDWGTAFKPLLPFYEA	364
XP_004605318.1[<i>Sorex araneus</i>]mammal_Eu	SLRALGLSFVRLLSLSEIPFSKLSLLEF-VDDVVQVACPRLSIDWGTAFKPLLPFYEA	364
XP_006801160.1[<i>Elephantulus edwardi</i>]mammal_Eu	SLRALGLSFVRLLSLSEIPFSKLSLLEF-VDDVVQVACPRLSIDWGTAFKPLLPFYEA	364
XP_019611098.1[<i>Rhinolophus sinicus</i>]mammal_Eu	SLRALGLSFVRLLSLSEIPFSKLSLLEF-VDDVVQVACPRLSIDWGTAFKPLLPFYEA	364
XP_011358164.1[<i>Pteropus vampyrus</i>]mammal_Eu	SLRALGLSFVRLLSLSEIPFSKLSLLEF-VDDVVQVACPRLSIDWGTAFKPLLPFYEA	364
XP_019672915.1[<i>Felis catus</i>]mammal_Eu	SLRALGLSFVRLLSLSEIPFSKLSLLEF-VDDVVQVACPRLSIDWGTAFKPLLPFYEA	364
XP_007076184.2[<i>Panthera tigris altaica</i>]mammal_Eu	SLRALGLSFVRLLSLSEIPFSKLSLLEF-VDDVVQVACPRLSIDWGTAFKPLLPFYEA	365
XP_013972316.1[<i>Canis lupus familiaris</i>]mammal_Eu	SLRALGLSFVRLLSLSEIPFSKLSLLEF-VDDVVQVACPRLSIDWGTAFKPLLPFYEA	365
XP_007177531.1[<i>Balaenoptera acutorostrata</i>]mammal_Eu	SLRALGLSFVRLLSLSEIPFSKLSLLEF-VDDVVQVACPRLSIDWGTAFKPLLPFYEA	364
XP_004267102.1[<i>Orcinus orca</i>]mammal_Eu	SLRALGLSFVRLLSLSEIPFSKLSLLEF-VDDVVQVACPRLSIDWGTAFKPLLPFYEA	364
XP_010594790.1[<i>Loxodonta africana</i>]mammal_Eu	SLRALGLSFVRLLSLSEIPFSKLSLLEF-VDDVVQVACPRLSIDWGTAFKPLLPFYEA	364
XP_017507098.1[<i>Manis javanica</i>]mammal_Eu	SLRALGLSFVRLLSLSEIPFSKLSLLEF-VDDVVQVACPRLSIDWGTAFKPLLPFYEA	365
XP_012405311.1[<i>Sarcophilus harrisii</i>]mammal_marsupial	SLRALGLSFVRLLSLSEIPFSKLSLLEF-VDDVVQVACPRLSIDWGTAFKPLLPFYEA	361
XP_007485825.1[<i>Monodelphis domestica</i>]mammal_Me	SLRALGLSFVRLLSLSEIPFSKLSLLEF-VDDVVQVACPRLSIDWGTAFKPLLPFYEA	369
XP_011579991.1[<i>Aquila chrysaetos</i>]Aves	SLRALGLSFVRLLSLSEIPFSKLSLLEF-VDDVVQVACPRLSIDWGTAFKPLLPFYEA	359
XP_015501861.1[<i>Parus major</i>]Aves	SLRALGLSFVRLLSLSEIPFSKLSLLEF-VDDVVQVACPRLSIDWGTAFKPLLPFYEA	377
XP_017687952.1[<i>Lepidodirix coronata</i>]Aves	SLRALGLSFVRLLSLSEIPFSKLSLLEF-VDDVVQVACPRLSIDWGTAFKPLLPFYEA	359
XP_005439966.1[<i>Falco cherrug</i>]Aves	SLRALGLSFVRLLSLSEIPFSKLSLLEF-VDDVVQVACPRLSIDWGTAFKPLLPFYEA	386
XP_008493491.1[<i>Calypte anna</i>]Aves	SLRALGLSFVRLLSLSEIPFSKLSLLEF-VDDVVQVACPRLSIDWGTAFKPLLPFYEA	362
NP_001025887.2[<i>Gallus gallus</i>]Aves	SLRALGLSFVRLLSLSEIPFSKLSLLEF-VDDVVQVACPRLSIDWGTAFKPLLPFYEA	361
XP_015736460.1[<i>Coturnix japonica</i>]Aves	SLRALGLSFVRLLSLSEIPFSKLSLLEF-VDDVVQVACPRLSIDWGTAFKPLLPFYEA	361
XP_010720021.1[<i>Meleagris gallopavo</i>]Aves	SLRALGLSFVRLLSLSEIPFSKLSLLEF-VDDVVQVACPRLSIDWGTAFKPLLPFYEA	356
XP_005502175.1[<i>Columba livia</i>]Aves	SLRALGLSFVRLLSLSEIPFSKLSLLEF-VDDVVQVACPRLSIDWGTAFKPLLPFYEA	359
XP_019400888.1[<i>Crocodylus porosus</i>]Sauropsida	SLRALGLSFVRLLSLSEIPFSKLSLLEF-VDDVVQVACPRLSIDWGTAFKPLLPFYEA	432
XP_014379797.1[<i>Alligator sinensis</i>]Sauropsida	SLRALGLSFVRLLSLSEIPFSKLSLLEF-VDDVVQVACPRLSIDWGTAFKPLLPFYEA	288
XP_015277363.1[<i>Gekko japonicus</i>]reptilia	SLRALGLSFVRLLSLSEIPFSKLSLLEF-VDDVVQVACPRLSIDWGTAFKPLLPFYEA	361
XP_003230257.2[<i>Anolis carolinensis</i>]reptilia	SLRALGLSFVRLLSLSEIPFSKLSLLEF-VDDVVQVACPRLSIDWGTAFKPLLPFYEA	355
XP_012812029.1[<i>Xenopus tropicalis</i>]Amphibia	SLRALGLSFVRLLSLSEIPFSKLSLLEF-VDDVVQVACPRLSIDWGTAFKPLLPFYEA	385
XP_014018522.1[<i>Salmo salar</i>]Actinopterygii	SLRALGLSFVRLLSLSEIPFSKLSLLEF-VDDVVQVACPRLSIDWGTAFKPLLPFYEA	359
XP_016336999.1[<i>Sinocyclocheilus anshuiensis</i>]Actinopterygii	SLRALGLSFVRLLSLSEIPFSKLSLLEF-VDDVVQVACPRLSIDWGTAFKPLLPFYEA	359
XP_015904021.1[<i>Epiplatys nattereri</i>]Actinopterygii	SLRALGLSFVRLLSLSEIPFSKLSLLEF-VDDVVQVACPRLSIDWGTAFKPLLPFYEA	359
XP_005804152.1[<i>Xiphophorus maculatus</i>]Actinopterygii	SLRALGLSFVRLLSLSEIPFSKLSLLEF-VDDVVQVACPRLSIDWGTAFKPLLPFYEA	356
XP_019729898.1[<i>Hippocampus comes</i>]Actinopterygii	SLRALGLSFVRLLSLSEIPFSKLSLLEF-VDDVVQVACPRLSIDWGTAFKPLLPFYEA	370
XP_005157638.1[<i>Danio rerio</i>]Actinopterygii	SLRALGLSFVRLLSLSEIPFSKLSLLEF-VDDVVQVACPRLSIDWGTAFKPLLPFYEA	364
XP_011606823.1[<i>Takifugu rubripes</i>]Actinopterygii	SLRALGLSFVRLLSLSEIPFSKLSLLEF-VDDVVQVACPRLSIDWGTAFKPLLPFYEA	359
XP_016836589.1[<i>Masonia vitripennis</i>]Insecta	SLRALGLSFVRLLSLSEIPFSKLSLLEF-VDDVVQVACPRLSIDWGTAFKPLLPFYEA	424
XP_011866406.1[<i>Volienhovia emeryi</i>]Insecta	SLRALGLSFVRLLSLSEIPFSKLSLLEF-VDDVVQVACPRLSIDWGTAFKPLLPFYEA	357
XP_015520716.1[<i>Neodiprion lecontei</i>]Insecta	SLRALGLSFVRLLSLSEIPFSKLSLLEF-VDDVVQVACPRLSIDWGTAFKPLLPFYEA	361
XP_01154130.1[<i>Harpagathous saltator</i>]Insecta	SLRALGLSFVRLLSLSEIPFSKLSLLEF-VDDVVQVACPRLSIDWGTAFKPLLPFYEA	360
XP_017957296.1[<i>Drosophila melanogaster</i>]Insecta	SLRALGLSFVRLLSLSEIPFSKLSLLEF-VDDVVQVACPRLSIDWGTAFKPLLPFYEA	376
NP_001261722.1[<i>Drosophila melanogaster</i>]Insecta	SLRALGLSFVRLLSLSEIPFSKLSLLEF-VDDVVQVACPRLSIDWGTAFKPLLPFYEA	372
XP_013145150.1[<i>Papilio polytes</i>]Insecta	SLRALGLSFVRLLSLSEIPFSKLSLLEF-VDDVVQVACPRLSIDWGTAFKPLLPFYEA	363
XP_002423182.1[<i>Pedicularis hians</i>]Insecta	SLRALGLSFVRLLSLSEIPFSKLSLLEF-VDDVVQVACPRLSIDWGTAFKPLLPFYEA	371
NP_497750.1[<i>Ctenochabditis elegans</i>]Secernentea	SLRALGLSFVRLLSLSEIPFSKLSLLEF-VDDVVQVACPRLSIDWGTAFKPLLPFYEA	348
XP_018668637.1[<i>Ciona intestinalis</i>]Ascidiacea	SLRALGLSFVRLLSLSEIPFSKLSLLEF-VDDVVQVACPRLSIDWGTAFKPLLPFYEA	366
XP_0368680.1[<i>Dictyostelium discoideum</i>]Dictyostelia	SLRALGLSFVRLLSLSEIPFSKLSLLEF-VDDVVQVACPRLSIDWGTAFKPLLPFYEA	443
XP_011316328.1[<i>Fusarium graminearum</i>]Sordariomycetes	SLRALGLSFVRLLSLSEIPFSKLSLLEF-VDDVVQVACPRLSIDWGTAFKPLLPFYEA	428
XP_018742809.1[<i>Fusarium verticillioides</i>]Sordariomycetes	SLRALGLSFVRLLSLSEIPFSKLSLLEF-VDDVVQVACPRLSIDWGTAFKPLLPFYEA	426
XP_018150409.1[<i>Foichonia chlamydosporia</i>]Sordariomycetes	SLRALGLSFVRLLSLSEIPFSKLSLLEF-VDDVVQVACPRLSIDWGTAFKPLLPFYEA	418
XP_018658688.1[<i>Trichoderma gamsii</i>]Sordariomycetes	SLRALGLSFVRLLSLSEIPFSKLSLLEF-VDDVVQVACPRLSIDWGTAFKPLLPFYEA	418
XP_001208548.1[<i>Aspergillus terreus</i>]Eurotiomycetes	SLRALGLSFVRLLSLSEIPFSKLSLLEF-VDDVVQVACPRLSIDWGTAFKPLLPFYEA	389
XP_002379550.1[<i>Aspergillus flavus</i>]Eurotiomycetes	SLRALGLSFVRLLSLSEIPFSKLSLLEF-VDDVVQVACPRLSIDWGTAFKPLLPFYEA	396
XP_002563943.1[<i>Penicillium rubens</i>]Eurotiomycetes	SLRALGLSFVRLLSLSEIPFSKLSLLEF-VDDVVQVACPRLSIDWGTAFKPLLPFYEA	400
XP_015467246.1[<i>Debaryomyces fabryi</i>]Saccharomycetes	SLRALGLSFVRLLSLSEIPFSKLSLLEF-VDDVVQVACPRLSIDWGTAFKPLLPFYEA	384
KZV0512.1_DPH1[<i>S. cerevisiae</i>]Saccharomycetes	SLRALGLSFVRLLSLSEIPFSKLSLLEF-VDDVVQVACPRLSIDWGTAFKPLLPFYEA	390
XP_006827105[<i>Amborella trichopoda</i>]Plant	SLRALGLSFVRLLSLSEIPFSKLSLLEF-VDDVVQVACPRLSIDWGTAFKPLLPFYEA	366
XP_002454772.1[<i>Sorghum bicolor</i>]Plant	SLRALGLSFVRLLSLSEIPFSKLSLLEF-VDDVVQVACPRLSIDWGTAFKPLLPFYEA	384
XP_020865862.1[<i>Arabidopsis lyrata</i>]Plant	SLRALGLSFVRLLSLSEIPFSKLSLLEF-VDDVVQVACPRLSIDWGTAFKPLLPFYEA	384
XP_008643787[<i>Zea mays</i>]Plant	SLRALGLSFVRLLSLSEIPFSKLSLLEF-VDDVVQVACPRLSIDWGTAFKPLLPFYEA	384

Identification of disease-causing variants in patients clinically diagnosed with Opitz C syndrome and Bohring-Opitz syndrome and functional validation

	Pro382	Ala411fs	
NP_001374.3[Homo sapiens]Primate	QQPYMDFYAGSSLGWTVNHRGQDRRPHAFGRFARGKV	-----	415
XP_003816906.1[Fan paniscus]Primate	QQPYMDFYAGSSLGWTVNHRGQDRRPHAFGRFARGKV	-----	415
XP_008968211.1[Fan paniscus]Primate	QQPYMDFYAGSSLGWTVNHRGQDRRPHAFGRFARGKV	-----	399
XP_018868753.1[Gorilla gorilla gorilla]Primate	QQPYMDFYAGSSLGWTVNHRGQDRRPHAFGRFARGKV	-----	410
XP_002826867.1[Pongo abelii]Primate	QQPYMDFYAGSSLGWTVNHRGQDRRPHAFGRFARGKV	-----	410
XP_012356920.1[Nomascus leucogenys]Primate	QQPYMDFYAGSSLGWTVNHRGQDRRPHAFGRFARGKV	-----	410
XP_011842657.1[Mandrill]Lus leucophaeus]Primate	QQPYMDFYAGSSLGWTVNHRGQDRRPHAFGRFARGKV	-----	410
XP_008061609.1[Carlioto_ grichta]Primate	QQPYMDFYAGSSLGWTVNHRGQDRRPHAFGRFARGKV	-----	410
XP_001504395.3[Equus caballus]mammal_Eu	QQPYMDFYAGSSLGWTVNHRGQDRRPHAFGRFARGKV	-----	410
XP_010859626.1[Bison bison bison]mammal_Eu	QQPYMDFYAGSSLGWTVNHRGQDRRPHAFGRFARGKV	-----	410
NP_001070367.1[Bos taurus]mammal	QQPYMDFYAGSSLGWTVNHRGQDRRPHAFGRFARGKV	-----	410
XP_019837435.1[Bos indicus]mammal	QQPYMDFYAGSSLGWTVNHRGQDRRPHAFGRFARGKV	-----	410
XP_012006497.1[Ovis aries musimon]mammal	QQPYMDFYAGSSLGWTVNHRGQDRRPHAFGRFARGKV	-----	410
XP_017919893.1[Capra hircus]mammal	QQPYMDFYAGSSLGWTVNHRGQDRRPHAFGRFARGKV	-----	410
XP_003131871.3[Sus scrofa]mammal	QQPYMDFYAGSSLGWTVNHRGQDRRPHAFGRFARGKV	-----	411
XP_015103509.1[Vicugna pacos]mammal	QQPYMDFYAGSSLGWTVNHRGQDRRPHAFGRFARGKV	-----	410
XP_008269143.1[Oryctolagus cuniculus]mammal_Eu	QQPYMDFYAGSSLGWTVNHRGQDRRPHAFGRFARGKV	-----	410
XP_016042474.1[Erinaceus europaeus]mammal_Eu	QQPYMDFYAGSSLGWTVNHRGQDRRPHAFGRFARGKV	-----	409
NP_001099279.1[Rattus norvegicus]mammal_Eu	QQPYMDFYAGSSLGWTVNHRGQDRRPHAFGRFARGKV	-----	404
XP_004635394.1[Octodon degus]mammal_Eu	QQPYMDFYAGSSLGWTVNHRGQDRRPHAFGRFARGKV	-----	407
XP_003469582.2[Cavia porcellus]mammal	QQPYMDFYAGSSLGWTVNHRGQDRRPHAFGRFARGKV	-----	407
XP_010640444.1[Fukomys damarensis]mammal	QQPYMDFYAGSSLGWTVNHRGQDRRPHAFGRFARGKV	-----	430
XP_005402655.1[Chinchilla lanigera]mammal	QQPYMDFYAGSSLGWTVNHRGQDRRPHAFGRFARGKV	-----	407
NP_652762.2[Mus musculus]mammal	QQPYMDFYAGSSLGWTVNHRGQDRRPHAFGRFARGKV	-----	404
XP_003507319.1[Cricetulus griseus]mammal	QQPYMDFYAGSSLGWTVNHRGQDRRPHAFGRFARGKV	-----	404
XP_006977441.1[Peromyscus maniculatus]mammal	QQPYMDFYAGSSLGWTVNHRGQDRRPHAFGRFARGKV	-----	406
XP_004667842.1[Jaculus jaculus]mammal	QQPYMDFYAGSSLGWTVNHRGQDRRPHAFGRFARGKV	-----	430
XP_004605318.1[Sorex araneus]mammal_Eu	QQPYMDFYAGSSLGWTVNHRGQDRRPHAFGRFARGKV	-----	410
XP_006891160.1[Elephantulus edwardi]mammal_Eu	QQPYMDFYAGSSLGWTVNHRGQDRRPHAFGRFARGKV	-----	410
XP_019611098.1[Rhinolophus sinicus]mammal_Eu	QQPYMDFYAGSSLGWTVNHRGQDRRPHAFGRFARGKV	-----	409
XP_011358164.1[Pteropus vampyrus]mammal_Eu	QQPYMDFYAGSSLGWTVNHRGQDRRPHAFGRFARGKV	-----	411
XP_019672915.1[Felis catus]mammal_eu	QQPYMDFYAGSSLGWTVNHRGQDRRPHAFGRFARGKV	-----	411
XP_007076184.2[Panthera tigris altaica]mammal_eu	QQPYMDFYAGSSLGWTVNHRGQDRRPHAFGRFARGKV	-----	432
XP_013972316.1[Canis lupus familiaris]mammal_eu	QQPYMDFYAGSSLGWTVNHRGQDRRPHAFGRFARGKV	-----	411
XP_007177531.1[Balaenoptera acutorostrata]mammal_Eu	QQPYMDFYAGSSLGWTVNHRGQDRRPHAFGRFARGKV	-----	410
XP_004267102.1[Orcinus orca]mammal_Eu	QQPYMDFYAGSSLGWTVNHRGQDRRPHAFGRFARGKV	-----	410
XP_010594790.1[Loxodonta africana]mammal_Eu	QQPYMDFYAGSSLGWTVNHRGQDRRPHAFGRFARGKV	-----	410
XP_017507098.1[Manis javanica]mammal_Eu	QQPYMDFYAGSSLGWTVNHRGQDRRPHAFGRFARGKV	-----	432
XP_012405311.1[Sarcophilus harrisii]mammal_marsupial	SRRLDSFPTTSLPCSSSGFPFCALPLDPSPEESR	GWWFSEPEAAVF	432
XP_007485825.1[Monodelphis domestica]mammal_Me	QQPYMDFYAGSSLGWTVNHRGQDRRPHAFGRFARGKV	-----	412
XP_011579991.1[Aquila chrysaetos]Aves	QQPYMDFYAGSSLGWTVNHRGQDRRPHAFGRFARGKV	-----	402
XP_015501861.1[Parus major]Aves	QQPYMDFYAGSSLGWTVNHRGQDRRPHAFGRFARGKV	-----	400
XP_017687952.1[Lepidotrix coronata]Aves	QQPYMDFYAGSSLGWTVNHRGQDRRPHAFGRFARGKV	-----	402
XP_005439966.1[Falco cherrug]Aves	QQPYMDFYAGSSLGWTVNHRGQDRRPHAFGRFARGKV	-----	432
XP_008493491.1[Colaptes auratus]Aves	QQPYMDFYAGSSLGWTVNHRGQDRRPHAFGRFARGKV	-----	421
NP_001025887.2[Gallus gallus]Aves	QQPYMDFYAGSSLGWTVNHRGQDRRPHAFGRFARGKV	-----	408
XP_015736460.1[Coturnix japonica]Aves	QQPYMDFYAGSSLGWTVNHRGQDRRPHAFGRFARGKV	-----	406
XP_010720021.1[Meleagris gallopavo]Aves	QQPYMDFYAGSSLGWTVNHRGQDRRPHAFGRFARGKV	-----	403
XP_005502175.1[Columba livia]Aves	DS-----	-----	374
XP_019400888.1[Crocodylus porosus]Sauropsida	QQTYMDFYANQSLGWTNPHASHQDRRPHAFGRFARGKV	-----	480
XP_014379797.1[Alligator sinensis]Sauropsida	QQTYMDFYANQSLGWTNPHASHQDRRPHAFGRFARGKV	-----	336
XP_015277363.1[Gekko japonicus]reptilia	QETTYMDFYANQSLGWTNPHASHQDRRPHAFGRFARGKV	-----	408
XP_003230257.2[Ranolis carolinensis]reptilia	QQTYMDFYANQSLGWTNPHASHQDRRPHAFGRFARGKV	-----	405
XP_012812029.1[Xenopus tropicalis]Amphibia	QQTYMDFYANQSLGWTNPHASHQDRRPHAFGRFARGKV	-----	434
XP_014018522.1[Salmo salar]Actinopterygii	QEVYMDYFNSQSLGWTNPHASHQDRRPHAFGRFARGKV	-----	408
XP_016336999.1[Sinicyclocheilus anshuiensis]Actinopterygii	QEVYMDYFNSQSLGWTNPHASHQDRRPHAFGRFARGKV	-----	407
XP_017530402.1[Egocentrus nattereri]Actinopterygii	QEVYMDYFNSQSLGWTNPHASHQDRRPHAFGRFARGKV	-----	407
XP_005804152.1[Xiphophorus maculatus]Actinopterygii	QEVYMDYFNSQSLGWTNPHASHQDRRPHAFGRFARGKV	-----	408
XP_019729898.1[Hippocampus comes]Actinopterygii	QEVYMDYFNSQSLGWTNPHASHQDRRPHAFGRFARGKV	-----	409
XP_005157638.1[Danio rerio]Actinopterygii	QEVYMDYFNSQSLGWTNPHASHQDRRPHAFGRFARGKV	-----	419
XP_011606823.1[Takifugu rubripes]Actinopterygii	QEVYMDYFNSQSLGWTNPHASHQDRRPHAFGRFARGKV	-----	406
XP_016836589.1[Masonia vitripennis]Insecta	TIQYMDYFASASLGWTVNHRGQDRRPHAFGRFARGKV	-----	435
XP_011866406.1[Volienhovia emeryi]Insecta	QEVYMDYFASASLGWTVNHRGQDRRPHAFGRFARGKV	-----	407
XP_015520716.1[Neodiprion tecontei]Insecta	DRFYMDYFASASLGWTVNHRGQDRRPHAFGRFARGKV	-----	412
XP_011154130.1[Harpegnathos saltator]Insecta	ERFYMDYFATVYSLGWTNPHASHQDRRPHAFGRFARGKV	-----	410
XP_017957296.1[Drosophila navajo]Insecta	TNAYMDYFASASLGWTVNHRGQDRRPHAFGRFARGKV	-----	440
NP_001261722.1[Drosophila melanogaster]Insecta	NNAYMDYFASASLGWTVNHRGQDRRPHAFGRFARGKV	-----	436
XP_013145150.1[Papilio polytes]Insecta	DQTYMDFYNSDLSGWTNPHASHQDRRPHAFGRFARGKV	-----	416
XP_002423182.1[Fedicalius humanus]Insecta	DVEYMDYFANNSLGWTVNHRGQDRRPHAFGRFARGKV	-----	410
NP_497750.1[Caenorhabditis elegans]Secernentea	SDHMDYFNSDLSGWTNPHASHQDRRPHAFGRFARGKV	-----	394
XP_01868637.1[Ciona intestinalis]Ascidiacea	RKTYMDFYANDSSGWTNPHASHQDRRPHAFGRFARGKV	-----	420
XP_638680.1[Dictyostelium discoideum]Dictyostelia	QSVYMDYFNSRE-GGWTNPHASHQDRRPHAFGRFARGKV	-----	472
XP_011316328.1[Fusarium graminearum]Sordariomycetes	DGVYMDYFNSKDGSLGWTNPHASHQDRRPHAFGRFARGKV	-----	462
XP_018742809.1[Fusarium verticillioides]Sordariomycetes	BGVYMDYFNSKDGSLGWTNPHASHQDRRPHAFGRFARGKV	-----	454
XP_018150409.1[Foehonia chlamydosporia]Sordariomycetes	RGVYMDYFNSKDGSLGWTNPHASHQDRRPHAFGRFARGKV	-----	452
XP_018658688.1[Trichoderma gamsii]Sordariomycetes	DGTYMDFYNSDLSGWTNPHASHQDRRPHAFGRFARGKV	-----	458
XP_001208548.1[Aspergillus terreus]Eurotiomycetes	QGLTYMDFYANQSLGWTNPHASHQDRRPHAFGRFARGKV	-----	448
XP_002379550.1[Aspergillus flavus]Eurotiomycetes	KGVYMDYFANQSLGWTNPHASHQDRRPHAFGRFARGKV	-----	436
XP_002563943.1[Penicillium rubens]Eurotiomycetes	KGVYMDYFANQSLGWTNPHASHQDRRPHAFGRFARGKV	-----	436
XP_015467246.1[Debaryomyces fabryi]Saccharomycetes	QGVYMDYFNSKDGSLGWTNPHASHQDRRPHAFGRFARGKV	-----	420
KZV10512.1_DPH1[S. cerevisiae]Saccharomycetes	EKYMDYFANQSLGWTNPHASHQDRRPHAFGRFARGKV	-----	425
XP_006827105[Amborella trichopoda]Plant	EMDYMDYFANQSLGWTNPHASHQDRRPHAFGRFARGKV	-----	464
XP_002454772.1[Sorghum bicolor]Plant	GDYMDYFANQSLGWTNPHASHQDRRPHAFGRFARGKV	-----	472
XP_020865862.1[Arabidopsis lyrata]Plant	DQDYMDYFANQSLGWTNPHASHQDRRPHAFGRFARGKV	-----	453
XP_008643787[Zea mays]Plant	GGDYMDYFANQSLGWTNPHASHQDRRPHAFGRFARGKV	-----	438

Identification of disease-causing variants in patients clinically diagnosed with Opitz C syndrome and Bohring-Opitz syndrome and functional validation

NP_001374.3[Homo sapiens]Primate	LAP	443
XP_003816906.1[Fan paniscus]Primate	LAP	443
XP_008968211.1[Fan paniscus]Primate	LAP	427
XP_018868753.1[Gorilla gorilla gorilla]Primate	LAP	438
XP_002826867.1[Pongo abelii]Primate	LAP	438
XP_012356920.1[Nomascus leucogenys]Primate	LAP	438
XP_011842657.1[Mandrillus leucophaeus]Primate	LAP	418
XP_008061609.1[Carollia syrichta]Primate	LVPGDAP	442
XP_001504395.3[Equus caballus]mammal_Eu	PAP	439
XP_010859626.1[Bison bison bison]mammal_Eu	LAD	438
NP_001070367.1[Bos taurus]mammal	LAD	438
XP_019837435.1[Bos indicus]mammal	LAD	438
XP_012006497.1[Ovis aries musimon]mammal	LAP	438
XP_017919893.1[Capra hircus]mammal	LAP	438
XP_003131871.3[Sus scrofa]mammal	LAP	439
XP_015103509.1[Vicugna pacos]mammal	LAF	438
XP_008269143.1[Oryctolagus cuniculus]mammal_Eu	PAP	438
XP_016042474.1[Erinaceus europaeus]mammal_Eu	FLAELLRAPKTPFSGGAT	453
NP_001099279.1[Rattus norvegicus]mammal_Eu	PAP	438
XP_004635394.1[Octodon degus]mammal_Eu	LAP	438
XP_003469582.2[Cavia porcellus]mammal	SAP	438
XP_010640444.1[Fukomys damarensis]mammal	PAP	461
XP_005402655.1[Chinchilla lanigera]mammal	PAP	438
NP_652762.2[Mus musculus]mammal	PAP	438
XP_003507319.1[Cricetulus griseus]mammal	PAS	438
XP_006977441.1[Peromyscus maniculatus]mammal	PAP	440
XP_004667842.1[Jaculus jaculus]mammal	SAP	464
XP_004605318.1[Sorex araneus]mammal_Eu	PPAL	439
XP_006891160.1[Elephantulus edwardi]mammal_Eu	LAP	438
XP_019611088.1[Rhinolophus sinicus]mammal_Eu	LTP	437
XP_011358164.1[Pteropus vampyrus]mammal_Eu	LVS	440
XP_019672915.1[Felis catus]mammal_eu	LTP	440
XP_007076184.2[Panthera tigris altaica]mammal_eu	LTP	461
XP_013972316.1[Canis lupus familiaris]mammal_eu	RAO	457
XP_007177531.1[Balaenoptera acutorostrata]mammal_Eu	PAP	438
XP_004267102.1[Orcinus orca]mammal_Eu	LAP	438
XP_010394790.1[Loxodonta africana]mammal_Eu	LAP	438
XP_017507098.1[Manis javanica]mammal_Eu	PAP	458
XP_012405311.1[Sarcophilus harrisi]mammal_marsupial	FVILISGFRRGPRALSPFLQAPLSPLSHVVGSTDRVIFPAQESLELAGCFPGAVTLISHP	552
XP_007485825.1[Monodelphis domestica]mammal_Me	PAP	443
XP_011579991.1[Aquila chrysaetos]Aves		426
XP_015501861.1[Parus major]Aves	GEENLSTGDPAAAS	423
XP_017687952.1[Lepidothrix coronata]Aves	AGEQNTGDPAAAS	423
XP_005439966.1[Falco cherrug]Aves	GGNPFSTGDPAAAS	423
XP_008493491.1[Colaptes auratus]Aves	GDAVAVIAAPLSLELAQHFVFPVVLTHP	467
NP_001025887.2[Gallus gallus]Aves	SEELSTGDPGAS	433
XP_015736460.1[Coturnix japonica]Aves	EGSRSAHPFEDTATS	424
XP_010720021.1[Meleagris gallopavo]Aves	EGSRSAHPFEDTATS	422
XP_005502175.1[Columba livia]Aves	EGSRSAHPFEDTTS	419
		374
XP_019400888.1[Crocodylus porosus]Sauropsida	B	720
XP_014379797.1[Alligator sinensis]Sauropsida	H	776
XP_015277363.1[Gekko japonicus]reptilia	Q	481
XP_003230257.2[Anolis carolinensis]reptilia	H	480
XP_012812029.1[Xenopus tropicalis]Amphibia	Q	458
XP_014018522.1[Salmo salar]Actinopterygii	F	434
XP_016336999.1[Sinocyclocheilus anshuiensis]Actinopterygii		457
XP_017550402.1[Epiplatys nattereri]Actinopterygii		487
XP_005804152.1[Xiphophorus maculatus]Actinopterygii		437
XP_019729898.1[Hippocampus comes]Actinopterygii		431
XP_005157638.1[Danio rerio]Actinopterygii		439
XP_011604623.1[Takifugu rubripes]Actinopterygii		476
XP_016836589.1[Masonia vitripennis]Insecta		482
XP_011866406.1[Volienhovia emeryi]Insecta		482
XP_015520716.1[Neodiprion lecontei]Insecta		413
XP_01154130.1[Harpegnathos saltator]Insecta		410
XP_017957296.1[Drosophila navajo]Insecta		468
NP_001261722.1[Drosophila melanogaster]Insecta		654
XP_013145150.1[Papilio polytes]Insecta		416
XP_002423182.1[Fedicalius humanus]Insecta		610
NP_497750.1[Caenorhabditis elegans]Secernentea		394
XP_018668637.1[Ciona intestinalis]Ascidiacea		420
XP_638680.1[Dictyostelium discoideum]Dictyostelia		473
XP_011316328.1[Fusarium graminearum]Sordariomycetes		462
XP_018742809.1[Fusarium verticillioides]Sordariomycetes		454
XP_018150409.1[Phanerochaete chlamydosporia]Sordariomycetes		462
XP_018658688.1[Trichoderma reesei]Sordariomycetes		456
XP_001208548.1[Aspergillus terreus]Eurotiomycetes		434
XP_002379550.1[Aspergillus flavus]Eurotiomycetes		436
XP_002563943.1[Penicillium rubens]Eurotiomycetes		435
XP_015467246.1[Debaryomyces fabryi]Saccharomycetes		420
KZV10512.1 [DPH1] [S. cerevisiae] Saccharomycetes		425
XP_006827105 [Amborella trichopoda] Plant		464
XP_002454772.1 [Sorghum bicolor] Plant		487
XP_020865862.1 [Arabidopsis lyrata] Plant		453
XP_008643787 [Zea mays] Plant		418

NP_001374.3[Homo sapiens]Primate	-----	448
XP_003816906.1[Pan paniscus]Primate	-----	440
XP_008968211.1[Pan paniscus]Primate	-----	427
XP_018868753.1[Gorilla gorilla gorilla]Primate	-----	466
XP_002826667.1[Pongo abelii]Primate	-----	438
XP_012356920.1[Nomascus leucogenys]Primate	-----	428
XP_011842657.1[Mandrillus leucophaeus]Primate	-----	439
XP_008061609.1[Callithrix jacchus]Primate	-----	442
XP_001504395.3[Equus caballus]mammal_Eu	-----	439
XP_010859626.1[Bison bison bison]mammal_Eu	-----	438
NP_001070367.1[Bos taurus]mammal	-----	438
XP_019837435.1[Bos indicus]mammal	-----	439
XP_012006497.1[Ovis aries musimon]mammal	-----	438
XP_017919893.1[Capra hircus]mammal	-----	438
XP_003131871.3[Sus scrofa]mammal	-----	439
XP_015103509.1[Vicuugna pacos]mammal	-----	438
XP_008269143.1[Oryctolagus cuniculus]mammal_Eu	-----	438
XP_016042474.1[Erinaceus europaeus]mammal_Eu	-----	453
NP_001099279.1[Rattus norvegicus]mammal_Eu	-----	438
XP_004635394.1[Octodon degus]mammal_Eu	-----	428
XP_003469582.2[Cavia porcellus]mammal	-----	458
XP_010640444.1[Fukomys damarensis]mammal	-----	461
XP_005402655.1[Chinchilla lanigera]mammal	-----	438
NP_652762.2[Mus musculus]mammal	-----	439
XP_003507319.1[Cricetulus griseus]mammal	-----	438
XP_006977441.1[Peromyscus maniculatus]mammal	-----	440
XP_004667842.1[Jaculus jaculus]mammal	-----	464
XP_004605318.1[Sorex araneus]mammal_Eu	-----	439
XP_006891160.1[Elephantulus edwardi]mammal_Eu	-----	458
XP_019611088.1[Rhinolophus finticus]mammal_Eu	-----	437
XP_011358164.1[Pteropus vampyrus]mammal_Eu	-----	440
XP_019672915.1[Felis catus]mammal_eu	-----	440
XP_007076184.2[Panthera tigris altaica]mammal_eu	-----	461
XP_013972316.1[Canis lupus familiaris]mammal_eu	-----	457
XP_007177531.1[Balaenoptera acutorostrata]mammal_Eu	-----	439
XP_004267102.1[Orcinus orca]mammal_Eu	-----	439
XP_010394790.1[Loxodonta africana]mammal_Eu	-----	448
XP_017507098.1[Manis javanica]mammal_Eu	-----	458
XP_012405311.1[Sarcophilus harrisi]mammal_narupial	GGHFLPAAAFQFQAYLGLDQFTK	576
XP_007485825.1[Monodelphis domestica]mammal_Me	-----	442
XP_011579991.1[Aquila chrysaetos]Aves	-----	429
XP_015501861.1[Parus major]Aves	-----	427
XP_017687952.1[Lepidothrix coronata]Aves	-----	425
XP_005439966.1[Falco cherrug]Aves	GGHFVFAAAEQFPAKLDLDSFRESGGQTEPTGTGV	504
XP_008493491.1[Colaptes auratus]Aves	-----	435
NP_001025887.2[Gallus gallus]Aves	-----	424
XP_015736460.1[Coturnix japonica]Aves	-----	422
XP_010720021.1[Meleagris gallopavo]Aves	-----	419
XP_005502175.1[Columba livia]Aves	-----	419
XP_019400888.1[Crocodylus porosus]Sauropsida	-----	428
XP_014379797.1[Alligator sinensis]Sauropsida	GTNCEGTNSE-----ARGARVE	401
XP_015277363.1[Gekko japonicus]reptilia	GPKCTGTNSE-----DACTGKSLVAVVE	331
XP_003230257.2[Diosaurus carolinensis]reptilia	-----	402
XP_012813029.1[Xenopus tropicalis]Amphibia	-----	468
XP_014018522.1[Salmo salar]Actinopterygii	-----	414
XP_016336999.1[Stenocyclocheilus anshuensis]Actinopterygii	-----	467
XP_017550402.1[Pygocentrus nattereri]Actinopterygii	-----	463
XP_005804152.1[Xiphophorus maculatus]Actinopterygii	-----	459
XP_019729898.1[Hippocampus comes]Actinopterygii	-----	422
XP_005157638.1[Danio rerio]Actinopterygii	-----	439
XP_011604623.1[Takifugu rubripes]Actinopterygii	-----	416
XP_016836589.1[Masonia vitripennis]Insecta	-----	482
XP_011866406.1[Volienhovia emeryi]Insecta	-----	487
XP_015520716.1[Neodiprion lecontei]Insecta	-----	415
XP_011154130.1[Harpegnathos saltator]Insecta	-----	410
XP_017957296.1[Drosophila navejoa]Insecta	-----	458
NP_001261722.1[Drosophila melanogaster]Insecta	-----	454
XP_013145150.1[Papilio polytes]Insecta	-----	416
XP_002423182.1[Pediculus humanus]Insecta	-----	410
NP_497750.1[Caenorhabditis elegans]Secernentes	-----	298
XP_018668637.1[Ciona intestinalis]Ascidacea	-----	429
XP_638680.1[Dictyostelium discoideum]Dictyostelia	-----	417
XP_011316328.1[Fusarium graminearum]Sordariomycetes	-----	446
XP_018742809.1[Fusarium verticillioides]Sordariomycetes	-----	454
XP_018150409.1[Fochonia chlamydsoporia]Sordariomycetes	-----	452
XP_018659688.1[Trichoderma gamsii]Sordariomycetes	-----	468
XP_00120848.1[Aspergillus terreus]Eurotiomycetes	-----	418
XP_002379550.1[Aspergillus flavus]Eurotiomycetes	-----	426
XP_002563943.1[Penicillium rubens]Eurotiomycetes	-----	426
XP_015467246.1[Debaryomyces fabryi]Saccharomycetes	-----	420
KZV10512.1 DPH1[S. cerevisiae]Saccharomycetes	-----	425
XP_006827105[Amborella trichopoda]Plant	-----	464
XP_002454772.1[Sorghum bicolor]Plant	-----	487
XP_020865862.1[Arabidopsis lyrata]Plant	-----	452
XP_008643787[Zea mays]Plant	-----	438

Supplementary Figure 2: DPH1 protein alignment from 80 different eukaryotic species.

Identification of disease-causing variants in patients clinically diagnosed with Opitz C syndrome and Bohring-Opitz syndrome and functional validation

```

Target      MRRQVMAALVVSAAEQGGRDGPRGRAPRGRVANQIPPEILKNPQLQAAIRVLPNSYNF-----EIPKT--IWRIQ
3lzd.1.B   -----MLHEIPKSEILKELK

Target      QQAQAKKVALQMPEGLLLFACTIVDILERFTEAEVMVMGDVTGACCVDDFTARAAGADFLVHYGHSCL-IPMDTSAQDFR
3lzd.1.B   RIGAKRVLIQSPEGLRREAEELAGFLEE-NNIEVFLHGEINYGACDPADREAKLVGCDALIHIGHSYMKLPLEVP-----

Target      VLVVFDIRIDTTHL-DSLRLTFPPATALALVSTIQFVSTLQAAAQELKAE-YRVSVPQ--CKPLSPGEILGCTPRLS
3lzd.1.B   TIFVPAPARVSVVEALKENIGEIKKLGKRIIVTTTAQHIIHQLKEAKFLESEGFVSVIGRSDSRISWPGQVLGNYSVAK

Target      KEVEAVVYSDGRFHLESVMIANPNVPAYRYDPYSKVLREHYDHRMQAARQEAIAATARSAKSWGLILGTLGRQGSFKI
3lzd.1.B   VRGEGILFFIGSGIFHPLGLAVATRK-KVLAI DPYTKAFS--WIDPERFIRKRWAQIAKAMDAKFGVIVSI--KKGQLRL

Target      LE--HLESRIRALGLSFVRLLLSIEFPSKLSLLPEVDVWVQVACPRLSTDWGTAFPKPLLTPYEAAVALRDISWQOPYM
3lzd.1.B   AEAKRIVKLLKKHGREARLIVMNDVNYHKLEGFP-FEAYVVVAQPRVPLDDYGAWRKEPVLTPKEVEILL---GLREYEF

Target      DFYAGSSLGPWTVNHGQDRRFHAPGRFARGKVQEGSARPPSAVACEDCSRDEKVAFLAP
3lzd.1.B   DEILGG-----
    
```

Supplementary Figure 3. Target human DPH1 alignment to *Pyrococcus horikoshii* DPH2 chain B (PDBID: 3LZD). Highlighted in blue the three cysteine residues of *Pyrococcus horikoshii* involved in binding [4Fe-4S] cluster. Shown highlighted in red the Human DPH1 mutants included in our models.

CHAPTER 2: Characterization of *TRAF7* germline variants at a phenotypic and molecular level

Article 8: Phenotypic spectrum and transcriptomic profile associated with germline variants in *TRAF7*

Summary:

Purpose: Somatic variants in tumor necrosis factor receptor–associated factor 7 (TRAF7) cause meningioma, while germline variants have recently been identified in seven patients with developmental delay and cardiac, facial, and digital anomalies. We aimed to define the clinical and mutational spectrum associated with TRAF7 germline variants in a large series of patients, and to determine the molecular effects of the variants through transcriptomic analysis of patient fibroblasts.

Methods: We performed exome, targeted capture, and Sanger sequencing of patients with undiagnosed developmental disorders, in multiple independent diagnostic or research centers. Phenotypic and mutational comparisons were facilitated through data exchange platforms. Whole-transcriptome sequencing was performed on RNA from patient- and control-derived fibroblasts.

Results: We identified heterozygous missense variants in TRAF7 as the cause of a developmental delay–malformation syndrome in 45 patients. Major features include a recognizable facial gestalt (characterized in particular by blepharophimosis), short neck, pectus carinatum, digital deviations, and patent ductus arteriosus. Almost all variants occur in the WD40 repeats and most are recurrent. Several differentially expressed genes were identified in patient fibroblasts.

Conclusion: We provide the first large-scale analysis of the clinical and mutational spectrum associated with the TRAF7 developmental syndrome, and we shed light on its molecular etiology through transcriptome studies.

Reference:

Castilla-Vallmanya L, Selmer KK, Dimartino C, et al. Phenotypic spectrum and transcriptomic profile associated with germline variants in TRAF7. *Genet Med.* 2020;22(7):1215-1226. doi:10.1038/s41436-020-0792-7



Phenotypic spectrum and transcriptomic profile associated with germline variants in *TRAF7*

A full list of authors and affiliations appears at the end of the paper.

Purpose: Somatic variants in tumor necrosis factor receptor-associated factor 7 (*TRAF7*) cause meningioma, while germline variants have recently been identified in seven patients with developmental delay and cardiac, facial, and digital anomalies. We aimed to define the clinical and mutational spectrum associated with *TRAF7* germline variants in a large series of patients, and to determine the molecular effects of the variants through transcriptomic analysis of patient fibroblasts.

Methods: We performed exome, targeted capture, and Sanger sequencing of patients with undiagnosed developmental disorders, in multiple independent diagnostic or research centers. Phenotypic and mutational comparisons were facilitated through data exchange platforms. Whole-transcriptome sequencing was performed on RNA from patient- and control-derived fibroblasts.

Results: We identified heterozygous missense variants in *TRAF7* as the cause of a developmental delay-malformation syndrome in 45

patients. Major features include a recognizable facial gestalt (characterized in particular by blepharophimosis), short neck, pectus carinatum, digital deviations, and patent ductus arteriosus. Almost all variants occur in the WD40 repeats and most are recurrent. Several differentially expressed genes were identified in patient fibroblasts.

Conclusion: We provide the first large-scale analysis of the clinical and mutational spectrum associated with the *TRAF7* developmental syndrome, and we shed light on its molecular etiology through transcriptome studies.

Genetics in Medicine (2020) 22:1215–1226; <https://doi.org/10.1038/s41436-020-0792-7>

Keywords: *TRAF7*; craniofacial development; intellectual disability; blepharophimosis; patent ductus arteriosus

INTRODUCTION

The tumor necrosis factor receptor (TNF-R)–associated factor (TRAF) family contains seven members defined by shared protein domains and their involvement in mediating signal transduction from TNF-R superfamily members.¹ *TRAF7* contains an N-terminal RING finger domain, an adjacent TRAF-type zinc finger domain, a coiled-coil domain, and seven C-terminal WD40 repeats (Fig. 1). The WD40 repeats are unique to *TRAF7* within the TRAF family, with all other members instead containing a C-terminal TRAF domain. In vitro studies have suggested that *TRAF7* plays a role in the regulation of several transcription factors through various mechanisms. It participates in the signal transduction of cellular stress stimuli, such as TNF α stimulation, by activating pathways leading to increased transcriptional activity of AP1 and CHOP/gadd153.^{2–4} These effects are thought to be mediated by synergy between *TRAF7* and the MAP3 kinase MEKK3, leading to the phosphorylation of JNK and p38 (regulators of AP1 and CHOP), with interaction of *TRAF7* and MEKK3 occurring via the *TRAF7* WD40 repeats.^{2,3} Depending on the context, *TRAF7* can positively or negatively regulate the activity of NF- κ B, through ubiquitination of pathway components p65 and NEMO.^{2,5,6} It also

ubiquitinates p53,⁷ and the activity of the proto-oncogene c-Myb is negatively regulated by *TRAF7* through sumoylation and consequent sequestering in the cytosol.⁸ In endothelial cells, *TRAF7* interacts with the C-terminus of ROBO4 to suppress hyperpermeability during inflammation.⁹

Somatic missense variants in *TRAF7*, concentrated within the WD40 domains and frequently recurrent, have been identified in meningiomas, mesotheliomas, intraneural perineuromas, and adenomatoid tumors of the genital tract.^{10–17} Heterozygous germline variants in *TRAF7* have recently been reported in seven patients with a developmental disorder involving cardiac, facial, and digital anomalies and developmental delay (OMIM 618164).¹⁸ Here, we refine our understanding of the *TRAF7* mutational and phenotypic spectrum through the identification of 45 previously undescribed patients, and thereby define a syndrome with a recognizable facial gestalt, specific skeletal and cardiac defects, and developmental delay/intellectual disability, which we propose to name the *TRAF7* syndrome. Almost all identified variants fall in the WD40 repeats, most are recurrent, and all are missense, suggestive of a gain-of-function or dominant negative mechanism, rather than haploinsufficiency. Intriguingly, somatic and germline variants do not overlap. We also

Correspondence: Christopher T. Gordon (chris.gordon@inserm.fr)

These authors jointly supervised this work: Roser Urreiziti, Christopher T. Gordon deceased; Antonie J. van Essen, MD, PhD

Submitted 13 November 2019; revised 22 March 2020; accepted: 23 March 2020
Published online: 7 May 2020

ARTICLE

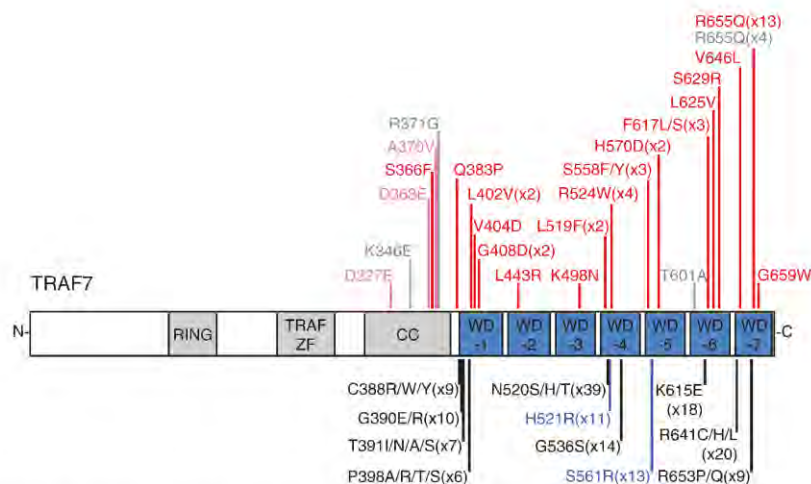
CASTILLA-VALLMANYA *et al*

Fig. 1 *TRAF7* variants. Domain boundaries drawn approximately to scale, based on ref. ⁶ Variants causing the *TRAF7* syndrome are indicated in red (reported here) or gray (previously reported¹⁵). In pink, variants of unknown significance reported here. Beneath the protein, the most recurrent somatic variants (i.e., in greater than five samples) are indicated; in black, those reported in meningiomas^{11,12} and in blue, those in adenomatoid tumors of the genital tract.¹⁶ CC coiled-coil.

present a transcriptomic analysis of fibroblasts from several patients, thereby providing insights into the pathways perturbed by *TRAF7* alteration.

MATERIALS AND METHODS

Variant identification

Genetic testing was performed according to approved ethical guidelines of the relevant institutions (Imagine Institute, University of Barcelona, GeneDx, ASST Papa Giovanni XXIII, Oslo University Hospital, Johns Hopkins University, Haukeland University Hospital, Centogene, Broad Institute, Radboud University Medical Center, University of California–San Francisco [UCSF] Genomic Medicine Laboratory, Baylor College of Medicine, Victorian Clinical Genetics Services, Institut de Génétique Médicale [CHU Lille]) and consent was obtained from all families (including written consent to publish photographs, where applicable). Exome sequencing was performed in various independent research or diagnostic laboratories worldwide, using standard approaches (details available upon request). Targeted capture sequencing of *TRAF7*, in a panel of genes implicated in craniofacial malformations, was performed during clinical diagnostic screening at the Necker Hospital, using a SureSelect kit (Agilent) for capture followed by sequencing on a HiSeq machine (Illumina). PolyPhen-2¹⁹ was used for predicting the pathogenicity of missense variants.

Cell culture

Fibroblasts were obtained from skin biopsies of four patients (age at biopsy range: 8 to 19 years) and six controls (age at biopsy range: 17 years to adult). Corresponding informed consent and institutional ethics approval were obtained (Ethics Committee of the Universitat de Barcelona, IRB00003099), and all methods were performed in accordance with the relevant

guidelines and regulations. Fibroblasts were cultured in Dulbecco's modified eagle medium (DMEM) supplemented with 10% FBS (Gibco, LifeTechnologies) and 1% penicillin–streptomycin (Gibco, LifeTechnologies) and were maintained at 37 °C and 5% CO₂. When appropriate, cells were treated with 10 ng/μl recombinant human TNFα protein (R&D systems) for 6, 24, or 48 hours.

Cell viability assay

Fibroblasts were plated in 96-well plates and synchronized through serum deprivation for 24 hours. Cell viability was tested using an MTT assay, with a solution of 0.5 mg/ml thiazolyl blue tetrazolium bromide (Sigma-Aldrich) in DMEM (Gibco, LifeTechnologies). After 4 hours, formazan crystals were dissolved using dimethyl sulfoxide (DMSO) (Merck Millipore) and absorbance was read at 560 nm.

Total RNA isolation and cDNA retrotranscription

RNA was extracted from fibroblasts using the High Pure RNA Isolation Kit (Roche), following the manufacturer's instructions. Integrity and purity of the RNA was tested by agarose gel electrophoresis and 260/230 and 260/280 absorbance ratios using an ND-1000 Spectrophotometer (Nanodrop Technologies). All samples reached the quality and integrity standards for quantitative reverse transcription polymerase chain reaction (qRT-PCR). For RNA-Sequencing (RNA-Seq) analysis, the quality standards of half of the samples were tested on an Agilent Bioanalyzer 2100 (Agilent Technologies). RNA was retrotranscribed using the High-capacity complementary DNA (cDNA) Reverse Transcription Kit (Applied Biosystems).

RNA-sequencing and data analysis

RNA-Seq was performed by LEXOGEN, Inc. using the QuantSeq 3' messenger RNA (mRNA)-Seq FWD kit for

CASTILLA-VALLMANYA *et al*

library preparation. Single-end reads were aligned to the human reference genome (GRCh37/hg19) and transcriptome using the STAR aligner. Quality metrics were obtained with tools of the RSEQC Quality Control package. Differential expression analysis was performed using the R package DESeq2. The threshold to be considered as a differentially expressed gene (DEG) was set at a false discovery rate (FDR) ≤ 0.05 and a $|\log_2$ fold change $|\geq 1$.

Real-time PCR

qPCR was performed using UPL probes (Roche), according to the manufacturer's instructions. For every assay, the efficiency (E) of the reaction was calculated from a 7-point standard curve. Genomic DNA contamination was assessed and not detected in the samples. Amplification was done using the thermocycler Light Cycler 480 (Roche). Each sample was run in triplicate and the relative transcription level was quantified with the Crossing Point cycle calculation using the Light Cycler® 480 Software (release 1.5.0) (Roche). The *GAPDH* and *PPIA* genes were used as reference genes as they displayed the minimum coefficient of variation. The primer sequences and UPL probes used are available on request.

Ingenuity Pathway Analysis

Ingenuity Pathway Analysis (IPA, Qiagen) was performed on genes that showed an FDR ≤ 0.1 and $|\log_2$ fold change $|\geq 0.38$. Separate runs were performed for each treatment condition. IPA uses Fisher's exact test to calculate statistical significance, considering associations between DEGs and annotated sets of molecules, with a *p* value < 0.05 ($-\log_{10}$ *p* value > 1.3) considered to be nonrandom.

RESULTS

Identification of pathogenic variants in *TRAF7*

We performed exome sequencing, targeted capture sequencing, and Sanger sequencing on individuals with undiagnosed, syndromic developmental delay/intellectual disability and dysmorphic facial features, in several independent clinical or research centers. Comparison of phenotypes and variants was facilitated by the data exchange platforms GeneMatcher²⁰ and DECIPHER.²¹ We identified 45 individuals harboring missense variants in *TRAF7* (Table S1). The cohort includes 36 sporadic cases in which the *TRAF7* variant was de novo, 1 patient with low level maternal mosaicism for the *TRAF7* variant, 5 cases with unknown inheritance, and 1 familial case (patients 24–26) in which affected dizygotic twins inherited a *TRAF7* variant from their affected mother, in whom the variant arose de novo (Fig. S1). Almost all variants occurred in the WD40 repeats (Fig. 1). Patients 1, 2, and 4 are sporadic cases carrying *TRAF7* variants of unknown inheritance in the coiled-coil domain, and display phenotypes only partly overlapping those frequently observed in the rest of the cohort (further details below). We therefore consider these three individuals as having *TRAF7* variants of unknown significance. None of the variants present in patients 1–45 have been reported in the Genome Aggregation Database

(gnomAD, data set v2.1). All affect highly conserved amino acids (based on Multiz alignments of 100 vertebrates at the University of California–Santa Cruz [UCSC] Genome Browser) and all (except one coiled-coil variant) are predicted possibly or probably damaging by PolyPhen-2 (Table S2). The variants in the 45 patients occur at 20 amino acid positions (Fig. 1); recurrent variants occur on eight of these, with the most recurrent by far being p.(Arg655Gln) (13 index cases). The remaining recurrent variants each occur in two to four index cases, and different variants of the same residue are observed at two positions (p.[Ser558Phe] or p.[Ser558Tyr]; p.[Phe617Leu] or p.[Phe617Ser]). The finding of recurrent missense variants largely restricted to the WD40 repeats suggests a disease mechanism involving specific functional changes to the mutant TRAF7 protein, rather than haploinsufficiency. In gnomAD, *TRAF7* has a low probability of being loss-of-function intolerant (pLI = 0.02), further suggesting haploinsufficiency of *TRAF7* does not cause severe pediatric disease.

Phenotype associated with *TRAF7* variants

Clinical details of all patients are provided in Table S1, and a summary of the phenotypes in the core cohort of 42 patients (i.e., excluding the three patients with coiled-coil variants of unknown significance) is provided in Table S3. Many patients presented with feeding difficulties ($n = 24$), often requiring tube feeding in infancy. Short stature was noted in 12 cases, low weight in 5, and microcephaly or macrocephaly in a total of 10. All patients had some form of developmental delay; intellectual disability ($n = 23$) and/or speech delay ($n = 29$) occurred in all but a small minority, while motor delay occurred in the majority ($n = 30$). Hypotonia was noted in 17 patients. Autism spectrum disorder was observed in six cases and epilepsy in seven. There was a range of nonspecific anomalies on brain magnetic resonance imaging (MRI; most frequently, enlarged ventricles). Almost all patients presented with anomalies of the palpebral fissures; most frequently blepharophimosis ($n = 33$), along with epicanthus ($n = 20$), telecanthus ($n = 14$), ptosis ($n = 19$), and up- or downslanting palpebral fissures ($n = 11$) (Fig. 2). Hypertelorism was reported in 17 cases. Ear anomalies ($n = 27$) most frequently consisted of low-set, posteriorly rotated, and/or protruding ears. Other frequent facial features include a bulbous nasal tip ($n = 17$); wide or flat nasal bridge ($n = 11$); micro- or retrognathia, albeit typically mild ($n = 13$); and a high or prominent forehead ($n = 11$). A computational composite from multiple patient photos further highlights the facial gestalt of the syndrome (Fig. S2). Other skull shape anomalies, such as trigonocephaly, dolicocephaly, plagiocephaly, brachycephaly, or bitemporal narrowing, occurred in 18 cases, and craniosynostosis in 3. Palatal anomalies ($n = 15$) included submucous cleft and velopharyngeal insufficiency. Most patients presented with abnormalities of the extremities (Fig. 3a). Although highly variable in nature, major anomalies of the hands were finger deviations ($n = 10$), camptodactyly ($n = 10$), brachydactyly ($n = 6$), and syndactyly ($n = 5$), and

ARTICLE



Fig. 2 Facial features of patients with variants in *TRAF7*. Patient numbers are indicated at the top of each panel. See text for description of the major features.

of the feet, overlapping toes ($n = 10$), pes planus ($n = 10$), varus or valgus abnormalities ($n = 10$), and sandal gap ($n = 5$). Joint limitation in the limbs, hypermobility, and dislocations were occasionally present. Anomalies of the axial skeleton were frequent: short neck ($n = 24$), pectus carinatum ($n = 17$), and other chest shape anomalies ($n = 10$, including barrel-shaped or narrow chest), rib anomalies ($n = 5$), deviations of the vertebral column ($n = 7$), and vertebral anomalies ($n = 14$). Regarding the latter, cervical stenosis or spinal cord compression was of clinical concern in several cases. Congenital cardiac defects were also frequent: 24 patients had patent ductus arteriosus (many of which required surgical repair), 9 had atrial and 6 had ventricular septal defects, and 10 had anomalies of valves. Conductive and/or sensorineural hearing loss occurred in 21 cases. Anomalies of the eyes included refractive errors ($n = 10$) and strabismus ($n = 10$). Infrequent phenotypes included a range of kidney anomalies ($n = 10$), cryptorchidism ($n = 7$), hernias ($n = 11$),

inverted nipples ($n = 6$), and lower limb edema ($n = 3$). In addition to a similar facial appearance among many of the patients, other features contributed to an upper-body gestalt in several, i.e., short neck with sloping shoulders, pectus carinatum, and relative macrocephaly (Fig. 3b). Finally, among the few adult patients in our cohort (seven over 18 years), clinical signs of premature aging²² were noted—two women (20 years and 44 years) had progressive hair loss, with the latter also having premature atherosclerosis, and a 26-year-old male had premature osteoporosis and hair loss.

Among the differential diagnoses in our cohort, an Ohdo-related syndrome (OMIM 249620) was suspected in several patients, with *KAT6B* sequencing performed for five individuals prior to exome, highlighting that the *TRAF7* syndrome overlaps with the group of blepharophimosis–mental retardation syndromes.²³ Also, Noonan/RAS-MAPK pathway gene panels were tested in eight patients, suggesting similarities to rasopathies. Although almost all *TRAF7*



Fig. 3 Anomalies of the extremities and upper-body appearance of patients with variants in *TRAF7*. (a) Extremities. (b) Full- or upper-body images. Patient numbers are indicated at the top of each panel. See text for description of the major features.

variants were identified through trio exome sequencing, inclusion of *TRAF7* on a next-generation sequencing (NGS) panel of genes mutated in neurocristopathy and craniofacial malformation syndromes led to the identification of two further individuals through diagnostic screening (patients 5 and 29). In patients 38 and 42, a strong clinical suspicion of *TRAF7* syndrome, based on comparison with our cohort at the time, led to identification of a *TRAF7* variant through Sanger sequencing or reanalysis of a previously unresolved singleton exome, respectively, highlighting the recognizability of this syndrome.

As noted above, three individuals (1, 2, and 4) harbored variants of unknown inheritance in the coiled-coil domain of *TRAF7* (pink variants in Fig. 1). These patients presented with neurodevelopmental defects, with seizures in two. Their facial features were not reminiscent of those of patients with variants in the WD40 repeats. Interestingly, patient 3, the only case with a *de novo* coiled-coil variant, had typical *TRAF7* syndrome facial features (photographs were reviewed but

permission to publish was denied). Of note, patient 4 had an endometrioid adenocarcinoma, diagnosed at 36 years.

Syndromic *TRAF7* missense variants affect gene expression

As a first approach to begin to explore the effects of syndromic *TRAF7* missense variants, the expression of 17 candidate target genes was assessed by qRT-PCR using skin fibroblast RNA from three patients bearing different variants in the WD40 repeats (p.[Leu402Val], p.[Leu519Phe], p.[Arg655Gln]; patient numbers 6, 13, 33, respectively) versus fibroblast RNA from six control individuals. Of these, nine genes (*EEF1A2*, *FLNB*, *IGFBP4*, *IGFBP7*, *LASS2*, *MMP2*, *NFKBIA*, *NOTCH3*, *SQSTM1*) were selected because their expression appeared to be altered in a previous global transcriptome analysis performed in *TRAF7*-silenced cells,⁶ and because of their known involvement in human developmental disorders or putative role in developmental events relevant to the *TRAF7* syndrome. The expression of *JUN* (encoding a subunit of the AP1 transcription factor) was

ARTICLE

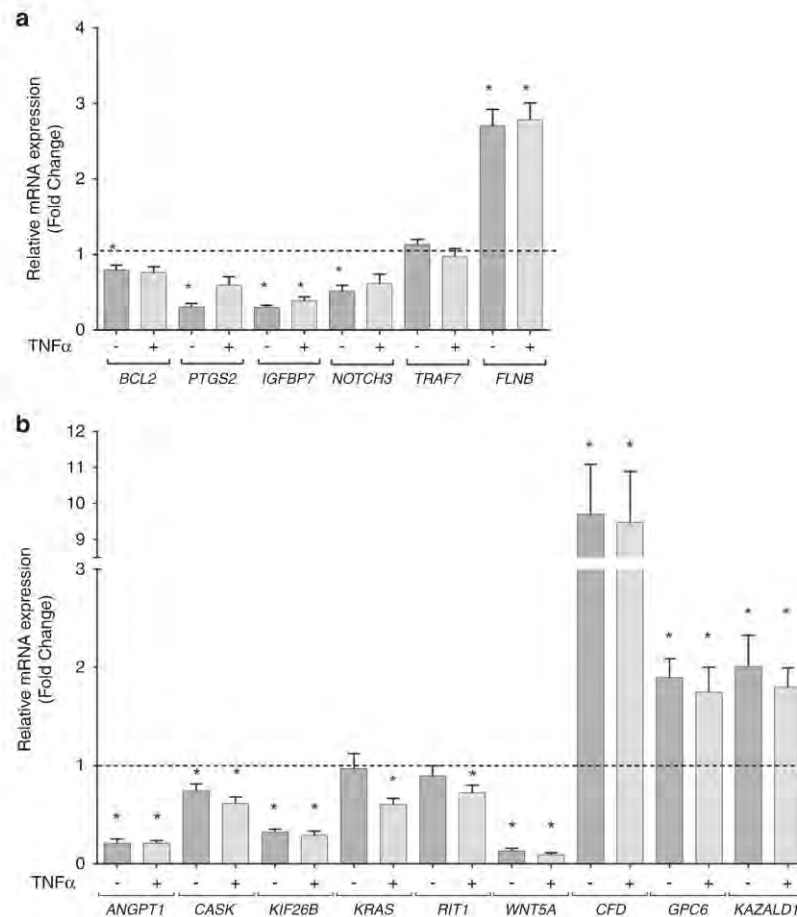
CASTILLA-VALLMANYA *et al*

Fig. 4 Quantitative reverse transcription polymerase chain reaction (qRT-PCR) quantification of messenger RNA (mRNA) levels in *TRAF7* syndrome patient fibroblasts. **(a)** qRT-PCR of *BCL2*, *PTGS2*, *IGFBP7*, *NOTCH3*, *TRAF7*, and *FLNB* in fibroblasts from three patients, with or without TNF α treatment. Relative mRNA level was normalized to the mean of six controls in each treatment condition (dotted line). *GAPDH* was used as a reference gene (the use of *PPIA* gave similar results). Data shown represents the mean \pm SEM of the three patients, in six independent experiments. Asterisks indicate significant differences ($p < 0.05$) between patients and controls in the corresponding condition (treated or untreated). **(b)** qRT-PCR validation of differentially expressed genes (DEGs) identified by RNA-Seq: *ANGPT1*, *CASK*, *KIF26B*, *KRAS*, *RIT1*, *WNT5A*, *CFD*, *GPC6*, and *KAZALD1*. Relative mRNA level was normalized to the mean of six controls in each treatment condition (dotted line). *GAPDH* was used as a reference gene (the use of *PPIA* gave similar results). Data shown represents the mean \pm SEM of the four patients, in two independent experiments. Asterisks indicate significant differences ($p < 0.05$) between patients and controls in the corresponding condition (treated or untreated).

tested because although AP1 activity can be stimulated by TRAF7, the effect of TRAF7 on transcription of AP1 components is unknown. *TRAF7* itself was tested for autoregulation. The rest are known NF- κ B target genes (*CFLAR* [*cFLIP*], *CCL2* [*MCPI*], *VEGFA*, *MYC*, *BCL2*, *PTGS2* [*COX2*]).²⁴ The above genes were also tested after TNF α stimulation.

We found *NOTCH3* (ENSG00000074181) expression decreased by half in untreated patient cells (Fig. 4), matching the direction of differential expression reported in *TRAF7*-silenced cells. In contrast, two other genes displayed an expression profile in patients opposite to that observed in *TRAF7*-silenced cells: *FLNB* (ENSG00000136068) expression levels in patients were over twofold higher than in controls, whereas *IGFBP7* (ENSG00000163453) RNA was fourfold

lower in patients. We also found differences in *BCL2* (ENSG00000171791), with lower expression levels in untreated patient cells than in controls, and *PTGS2* (ENSG00000073756), whose expression was reduced to one third in untreated patient cells. Regarding *TRAF7* itself, none of the three heterozygous missense variants tested altered its expression levels. In the same way, *JUN*, *EEF1A2*, *IGFBP4*, *NFKBIA*, *LASS2*, *MMP2*, *SQSTM1*, *CFLAR*, *CCL2*, *VEGFA*, and *MYC* did not show any variation in their expression levels between patients and controls (data not shown).

To further characterize the effects that syndromic *TRAF7* missense variants could have on gene expression levels in a more unbiased fashion, we performed an mRNA whole-transcriptomic analysis of skin fibroblasts. We used samples from the three patients and the six controls, with and without

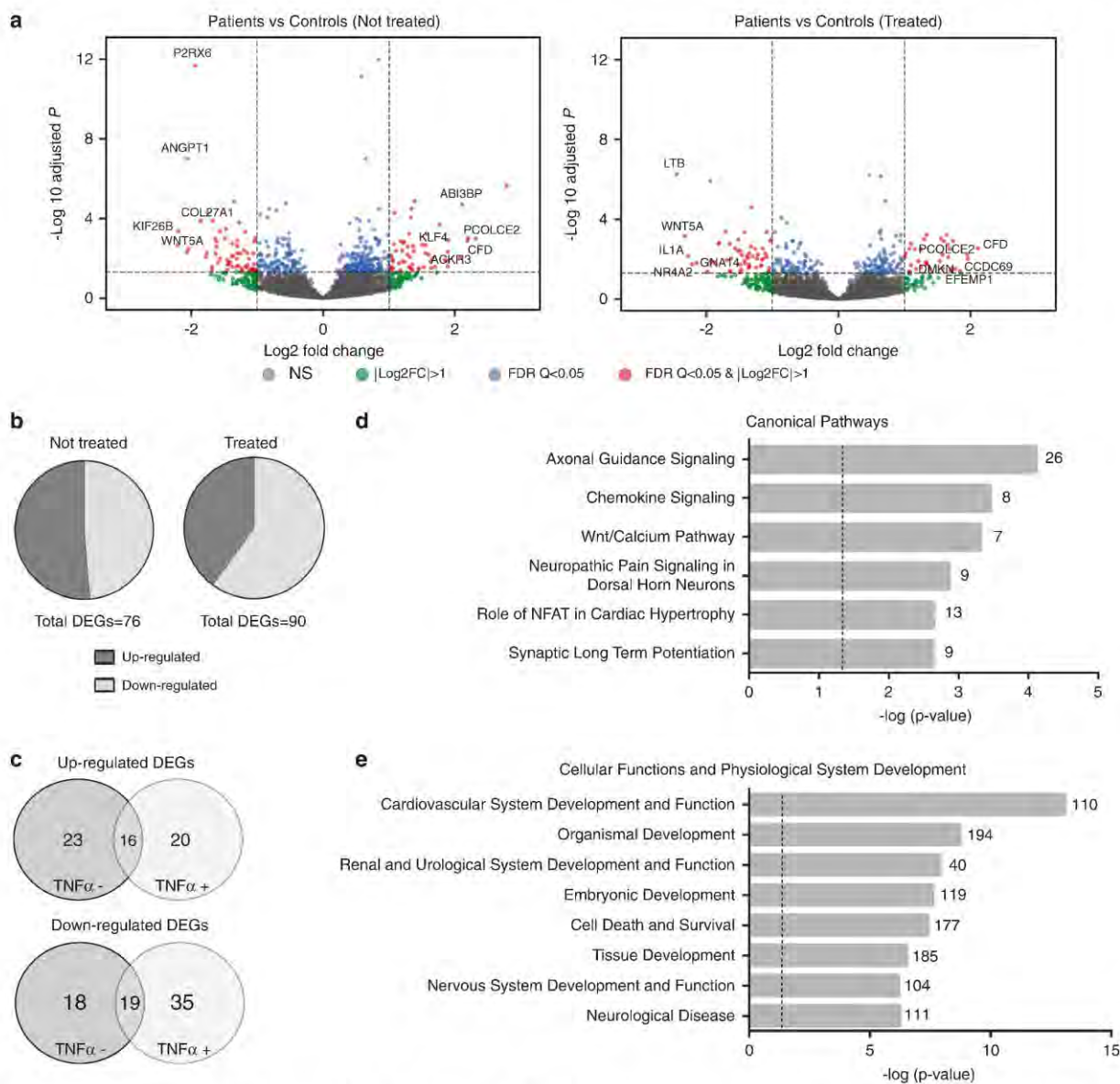
CASTILLA-VALLMANYA *et al*


Fig. 5 Transcriptome analysis of fibroblasts bearing missense *TRAF7* variants. (a) Volcano plots representing differentially expressed genes (DEGs) in each condition (untreated or treated with TNF α [10 ng/ml] for 6 hours), measuring changes in expression (\log_2 fold change) and their significance (false discovery rate [FDR]; $-\log_{10}$ adjusted p value). (b) Proportions of up- and downregulated transcripts in untreated or treated patient fibroblasts. (c) Venn diagrams representing overlapping up- and downregulated DEGs. (d, e) Ingenuity Pathway Analysis of DEGs in *TRAF7* syndrome patient fibroblasts. (d) Selected overrepresented canonical pathways. The number of DEGs included in each pathway is specified and a $-\log_{10} p$ value > 1.3 was considered significant. (e) Selected overrepresented categories of cellular functions and physiological system development. The number of DEGs associated with each category is specified and a $-\log_{10} p$ value > 1.3 was considered significant.

TNF α treatment. We considered DEGs as presenting an adjusted p value < 0.05 and $|\log_2$ fold change| in expression ≥ 1 (Table S4). We identified 76 DEGs in basal conditions (51.31% upregulated and 48.68% downregulated) and 90 DEGs after TNF α treatment (40% upregulated and 60% downregulated) (Fig. 5a, b). A substantial overlap in several DEGs was detected between the untreated and treated conditions, as 16 DEGs were upregulated and 19

downregulated independently of treatment (Fig. 5c). In addition, 55 DEGs were identified only in the treatment condition, suggesting that *TRAF7* syndromic variants may cause an alteration of the signaling pathway that is activated as a response to TNF α ligand.

Twelve DEGs from the RNA-Seq data were selected for qRT-PCR validation based on their high \log_2 fold change and/or functional criteria (i.e., for most, involvement in a human

ARTICLE

CASTILLA-VALLMANYA *et al*

developmental disorder or relevant phenotype in an animal model—see Supplementary Discussion for details) (Table S5). For this step, an additional patient (number 36, bearing the variant p.[Arg655Gln]) was included. Results for 7 of the 12 were confirmatory (*ANGPT1*, *CASK*, *KIF26B*, *WNT5A*, *CFD*, *GPC6*, *KAZALD1*) (Fig. 4b). *KRAS*, which was slightly upregulated in the RNA-Seq analysis, appeared downregulated in treated patient cells by qRT-PCR, while *RIT1* was slightly downregulated only in untreated cells by RNA-Seq and only in treated cells by qRT-PCR. Finally, three genes (*FOXP1*, *SPTAN1*, *MAPK11*) whose log₂ fold changes and significance values were below the general threshold to be considered as DEGs, but which had been selected based on functional criteria, were not validated.

To explore the different pathways and biological functions that might be affected, we performed IPA on the 726 DEGs identified under basal conditions using less stringent criteria than the preceding analyses (Table S6). The axonal guidance signaling canonical pathway was significantly enriched, as 26 genes within this pathway showed alterations in transcript levels between patients and controls. Other significantly enriched canonical pathways included the Wnt/Ca²⁺ pathway and the role of NFAT in cardiac hypertrophy (Fig. 5d). IPA results also showed significant enrichment among the DEGs for genes involved in the development and function of the cardiovascular and nervous systems (Fig. 5e). Similar results were obtained under TNF α -treated conditions (data not shown).

Syndromic TRAF7 missense variants have mild effects on cell viability

Putative differences in cell viability between patient and control fibroblasts were assessed, both in untreated and TNF α -treated conditions, during 24 or 48 hours. Although a slight tendency for increased cell viability was observed in patient fibroblasts under all conditions, significant differences were only observed at 24 hours of treatment with TNF α (Fig. S3).

DISCUSSION

In the present study, we have characterized the clinical features associated with germline variants in *TRAF7*, through analysis of 45 patients. In a cohort of seven patients, Tokita *et al.* reported speech and motor delay, a range of dysmorphic facial features (including epicanthal folds, ptosis, and dysmorphic ears), variable cardiac defects, and anomalies of the extremities (digit deviations and variant creases) as principal phenotypes associated with *TRAF7* variants.¹⁸ The large size of the cohort described here allowed us to further refine the phenotypic spectrum and to highlight several major phenotypes that were not emphasized previously: blepharophimosis, short neck, pectus carinatum and other thoracic defects, vertebral anomalies, patent ductus arteriosus, and hearing loss. All the *TRAF7* variants in our cohort are missense and several are recurrent, with one major mutational hotspot: p.(Arg655Gln). Previously, Tokita *et al.* reported

TRAF7 variants at only four positions (also missense); two in the coiled-coil domain and two in the WD40 repeats (including p.[Arg655Gln]).¹⁸ Our results reveal a highly skewed variant distribution along the protein, which was not evident in the prior study (Fig. 1), and strongly implicate alteration of the WD40 repeats as the central disease mechanism.

The germline *TRAF7* variants reported here are strikingly mutually exclusive to the somatic variants previously identified in tumors (lower part of Fig. 1). This is underscored by the presence of recurrent variants restricted to each disease: p.(Arg655Gln) identified in 13 index cases here but never previously reported in a tumor, and variants at Asn520 reported 39 times in meningioma^{11,12} but not in syndromic patients. This suggests differences in activity of the mutant protein in each disease (for example, disruption of different protein–protein interactions or differences in degree of the same activity). It is possible that when present in the germline, the somatic variants may have a more severe phenotypic effect, perhaps not compatible with life. Interestingly, even among somatic variants, there may also be a trend for certain variants to be more frequent in particular tumor types; p.(His521Arg) and p.(Ser561Arg) (in blue in Fig. 1) are highly recurrent in adenomatoid tumors of the genital tract,¹⁶ but have not been reported in meningiomas.^{10–13} In a few cases, the same amino acid is mutated to a different residue in each disease; for example, the syndromic variant p.(Leu519Phe) and the meningioma variants p.(Leu519Pro) and p.(Leu519Arg) (the latter two are not included in Fig. 1). To the best of our knowledge, there is only one syndromic variant, p.(Arg524Trp) (*de novo* or maternal mosaic in four unrelated cases here), that has also been reported in a tumor sample.¹¹ However, this meningioma also harbored a *SMO* variant, p.(Ala459Val), known to cause increased activity of *SMO*;²⁵ the oncogenicity of the *TRAF7* variant in this case is therefore unclear. One patient in our series with a variant of unknown significance in the coiled-coil domain had an endometrioid adenocarcinoma, while no tumors were reported in the patients with variants in the WD40 domain (although only a few are adults). One patient (43 years of age) in the cohort of Tokita *et al.*¹⁸ had a meningioma. Meningiomas harboring a *TRAF7* variant typically also contain a variant in *KLF4*, *AKT1*, or *PIK3CA*,^{10–13} suggesting a second hit may be required for development of *TRAF7*-associated tumors. Careful monitoring of aging syndromic patients will be required to determine whether they have a greater risk of developing tumors.

WD40 repeats are typically protein or nucleic acid interaction surfaces,²⁶ and the WD40 domain of *TRAF7* is known to interact with *MEKK3*^{2,3} and with the DNA-binding domain of *c-Myb*.⁸ Whether alteration of these or other interactions underlies *TRAF7* syndrome is unknown. Interestingly, *Mekk3* is required for early cardiovascular development in mice.²⁷ Also, phosphorylation of ERK1/2, which are MAP kinases downstream of *MEKK3*, is reduced in cells overexpressing *TRAF7* syndromic variants,¹⁸ and loss of *Erk2*

CASTILLA-VALLMANYA *et al*

in mice causes craniofacial and cardiac malformations and neurogenesis defects.^{28,29} In vitro overexpression of *TRAF7* harboring WD40 domain variants identified in adenomatoid tumors of the genital tract leads to activation of the NF- κ B pathway,¹⁶ and although dysregulation of this pathway has not typically been associated with congenital malformations in humans,³⁰ knockout of *Ikka* (a central component of the NF- κ B pathway) in mice results in craniofacial and skeletal defects.³¹ The *TRAF7* variant distribution identified here, with clustering of recurrent missense variants in the WD40 repeats, is more consistent with a gain-of-function or dominant negative effect rather than haploinsufficiency. Structural studies suggest TRAF proteins can form trimers via the coiled-coil domain,³² and coimmunoprecipitation experiments have shown that TRAF7 can interact with itself² and with TRAF6.³³ An interesting possibility is that TRAF7 harboring syndromic variants could dominantly interfere not only with wild-type TRAF7 molecules but also with other TRAF proteins during development. *TRAF7* loss-of-function animal models have not been reported. Among *TRAF* family members, *Traf4* knockout mice have congenital malformation phenotypes, including tracheal ring disruption, spina bifida, and axial skeletal defects,^{34,35} the latter is of particular interest given the high frequency of costosternal and vertebral anomalies in *TRAF7* syndrome patients.

Tokita *et al.* reported two *TRAF7* syndrome patients with variants in the coiled-coil domain (p.[Lys346Glu] and p.[Arg371Gly]), although these had no or less negative effect on ERK1/2 phosphorylation compared with the two WD40 repeat variants they identified (p.[Thr601Ala] and p.[Arg655Gln]). We report four individuals with coiled-coil domain variants, of which only one was confirmed to have a facial gestalt similar to patients with WD40 repeat variants. This suggests that some coiled-coil domain variants can have a similar molecular effect as those that perturb the WD40 domain. On the other hand, it has been reported that the coiled-coil domain of TRAF7 is required for interaction with NEMO,⁶ and in combination with the zinc finger domain for homodimerization and subcellular localization,² raising the possibility that the molecular consequences of some coiled-coil domain variants may be different from those in the WD40 repeats. Note that none of the fibroblast samples used here for transcriptomic studies were from patients with coiled-coil variants, but comparison of transcriptomes from patients with WD40 versus coiled-coil domain variants may be informative. Confirmation of the causality of all *TRAF7* coiled-coil domain variants, and the associated phenotypic spectrum, will require further functional studies and analysis of a larger number of individuals in this mutational subset.

To gain a better understanding of the pathogenic role of syndromic *TRAF7* variants, patient fibroblasts were compared with controls at a transcriptomic level. This initially involved directly testing the expression of a small number of candidate genes previously found to be altered in *TRAF7*-silenced cells, and subsequently a global analysis of the gene expression landscape by RNA-Seq. Several of the identified DEGs are

especially interesting due to the effects that their alteration is known to produce in human disease or animal models, and their dysregulation therefore plausibly contributes to the pathogenesis of the *TRAF7* syndrome. In this context, the following DEGs are discussed further in the Supplementary Discussion: *FLNB*, *IGFBP7*, *NOTCH3*, *BCL2*, *PTGS2*, *ANGPT1*, *WNT5A*, *KIF26B*, *CASK*, *GPC6*, *KAZALD1*, and *CFD*.

In conclusion, through analysis of a large series of patients, we have defined the phenotypic spectrum associated with germline *TRAF7* variants. The major features in our series are intellectual disability, motor delay, a recognizable facial gestalt including blepharophimosis, short neck, pectus carinatum, digital deviations, hearing loss, and patent ductus arteriosus. *TRAF7* syndrome patients typically require assisted learning and may be at risk of cervical stenosis. Older patients may benefit from monitoring for development of premature aging phenotypes and tumors, although at this stage we cannot conclude whether there is an increased risk of the latter. We have shown there is a strong bias for *TRAF7* syndrome-associated variants to occur in the WD40 repeats, and a major avenue for future investigation will involve determining whether there are different consequences on direction or strength of downstream signaling between these germline variants versus those previously reported in various cancers. Our transcriptomic studies of *TRAF7* syndrome patient fibroblasts revealed a large number of DEGs. The fact that the expression of some genes (but not all) is only affected after TNF α treatment indicates that TRAF7 function in this pathway is disturbed, but that this is not the only pathway affected by the syndromic variants. Several identified DEGs are involved in cardiovascular, skeletal, or nervous system development or function, and are therefore relevant to the phenotypes observed in the patients. Further exploration of the link between *TRAF7* and these putative transcriptional targets is warranted in an animal model of the *TRAF7* syndrome.

SUPPLEMENTARY INFORMATION

The online version of this article (<https://doi.org/10.1038/s41436-020-0792-7>) contains supplementary material, which is available to authorized users.

ACKNOWLEDGEMENTS

We thank the families for their participation. This work was supported by the Agence Nationale de la Recherche (CranioRespiro and ANR-10-IAHU-01), MSD Avenir (Devo-Decode), Spanish Ministerio de Ciencia e Innovación (SAF2016-75946R), CIBERER (ACCI2018-15), Associació Síndrome Opitz C, the Morton S. and Henrietta K. Sellner Professorship in Human Genetics (J.W.I.), JPB Foundation and the Simons Foundation SFARI program (W.K.C.), German Research Foundation (DFG; LE 4223/1; to D.L.), BC Children's Hospital Foundation and Genome BC (CAUSES Study), PG23/FROM 2017 Call for Independent Research as part of the Rapid Analysis for Rapid care project (M.I., A.C.), the Victorian Government's Operational Infrastructure

ARTICLE

CASTILLA-VALLMANYA *et al*

Support Program, the National Human Genome Research Institute (NHGRI) (UM1 HG008900, U01HG009599, UM1 HG006542), a National Institutes of Health (NIH) Common Fund grant (U01HG00769) and the Health Innovation Challenge Fund (DDD study; grant number HICF-1009-003). See Table S7 for supplementary acknowledgements.

DISCLOSURE

M.T.C. and S.Y. are employees of GeneDx, Inc. The other authors declare no conflicts of interest.

Publisher's note Springer Nature remains neutral with regard to jurisdictional claims in published maps and institutional affiliations.

REFERENCES

- Zotti T, Scudiero I, Vito P, Stilo R. The emerging role of TRAF7 in tumor development. *J Cell Physiol.* 2017;232:1233–1238.
- Bouwmeester T, Bauch A, Ruffner H, et al. A physical and functional map of the human TNF- α /NF- κ B signal transduction pathway. *Nat Cell Biol.* 2004;6:97–105.
- Xu L-G, Li L-Y, Shu H-B. TRAF7 potentiates MEKK3-induced AP1 and CHOP activation and induces apoptosis. *J Biol Chem.* 2004;279:17278–17282.
- Scudiero I, Zotti T, Ferravante A, et al. Tumor necrosis factor (TNF) receptor-associated factor 7 is required for TNF α -induced Jun NH2-terminal kinase activation and promotes cell death by regulating polyubiquitination and lysosomal degradation of c-FLIP protein. *J Biol Chem.* 2012;287:6053–6061.
- Tsikitis M, Acosta-Alvarez D, Blais A, et al. Traf7, a MyoD1 transcriptional target, regulates nuclear factor- κ B activity during myogenesis. *EMBO Rep.* 2010;11:969–976.
- Zotti T, Uva A, Ferravante A, et al. TRAF7 protein promotes Lys-29-linked polyubiquitination of I κ B kinase (IKK γ)/NF- κ B essential modulator (NEMO) and p65/RelA protein and represses NF- κ B activation. *J Biol Chem.* 2011;286:22924–22933.
- Wang L, Wang L, Zhang S, et al. Downregulation of ubiquitin E3 ligase TNF receptor-associated factor 7 leads to stabilization of p53 in breast cancer. *Oncol Rep.* 2013;29:283–287.
- Morita Y, Kanei-Ishii C, Nomura T, Ishii S. TRAF7 sequesters c-Myb to the cytoplasm by stimulating its sumoylation. *Mol Biol Cell.* 2005;16:5433–5444.
- Shirakura K, Ishiba R, Kashio T, et al. The Robo4-TRAF7 complex suppresses endothelial hyperpermeability in inflammation. *J Cell Sci.* 2019;132:jcs220228.
- Clark VE, Erson-Omay EZ, Serin A, et al. Genomic analysis of non-NF2 meningiomas reveals mutations in TRAF7, KLF4, AKT1, and SMO. *Science.* 2013;339:1077–1080.
- Clark VE, Harmanci AS, Bai H, et al. Recurrent somatic mutations in POLR2A define a distinct subset of meningiomas. *Nat Genet.* 2016;48:1253–1259.
- Reuss DE, Piro RM, Jones DTW, et al. Secretory meningiomas are defined by combined KLF4 K409Q and TRAF7 mutations. *Acta Neuropathol.* 2013;125:351–358.
- Abedalthagafi M, Bi WL, Aizer AA, et al. Oncogenic PI3K mutations are as common as AKT1 and SMO mutations in meningioma. *Neuro-oncology.* 2016;18:649–655.
- Bueno R, Stawiski EW, Goldstein LD, et al. Comprehensive genomic analysis of malignant pleural mesothelioma identifies recurrent mutations, gene fusions and splicing alterations. *Nat Genet.* 2016;48:407–416.
- Klein CJ, Wu Y, Jentoft ME, et al. Genomic analysis reveals frequent TRAF7 mutations in intraneural perineuriomas. *Ann Neurol.* 2017;81:316–321.
- Goode B, Joseph NM, Stevers M, et al. Adenomatoid tumors of the male and female genital tract are defined by TRAF7 mutations that drive aberrant NF- κ B pathway activation. *Mod Pathol.* 2018;31:660–673.
- Stevens M, Rabban JT, Garg K, et al. Well-differentiated papillary mesothelioma of the peritoneum is genetically defined by mutually exclusive mutations in TRAF7 and CDC42. *Mod Pathol.* 2019;32:88–99.
- Tokita MJ, Chen C-A, Chitayat D, et al. De novo missense variants in TRAF7 cause developmental delay, congenital anomalies, and dysmorphic features. *Am J Hum Genet.* 2018;103:154–162.
- Adzhubei IA, Schmidt S, Peshkin L, et al. A method and server for predicting damaging missense mutations. *Nat Methods.* 2010;7:248–249.
- Sobreira N, Schietecatte F, Valle D, Hamosh A. GeneMatcher: a matching tool for connecting investigators with an interest in the same gene. *Hum Mutat.* 2015;36:928–930.
- Firth HV, Richards SM, Bevan AP, et al. DECIPHER: Database of Chromosomal Imbalance and Phenotype in Humans Using Ensembl Resources. *Am J Hum Genet.* 2009;84:524–533.
- Lesell D, Kubisch C. Hereditary syndromes with signs of premature aging. *Dtsch Arztebl Int.* 2019;116:489–496.
- Verloes A, Bremond-Gignac D, Isidor B, et al. Blepharophimosis-mental retardation (BMR) syndromes: a proposed clinical classification of the so-called Ohdo syndrome, and delineation of two new BMR syndromes, one X-linked and one autosomal recessive. *Am J Med Genet A.* 2006;140:1285–1296.
- Li J, Ma J, Wang KS, et al. Baicalein inhibits TNF- α -induced NF- κ B activation and expression of NF- κ B-regulated target gene products. *Oncol Rep.* 2016;36:2771–2776.
- Sharpe HJ, Pau G, Dijkgraaf GJ, et al. Genomic analysis of smoothened inhibitor resistance in basal cell carcinoma. *Cancer Cell.* 2015;27:327–341.
- Schapiira M, Tyers M, Torrent M, Arrowsmith CH. WD40 repeat domain proteins: a novel target class? *Nat Rev Drug Discov.* 2017;16:773–786.
- Yang J, Boerm M, McCarty M, et al. Mekk3 is essential for early embryonic cardiovascular development. *Nat Genet.* 2000;24:309–313.
- Newbern J, Zhong J, Wickramasinghe RS, et al. Mouse and human phenotypes indicate a critical conserved role for ERK2 signaling in neural crest development. *Proc Natl Acad Sci USA.* 2008;105:17115–17120.
- Samuels IS, Karlo JC, Faruzzi AN, et al. Deletion of ERK2 mitogen-activated protein kinase identifies its key roles in cortical neurogenesis and cognitive function. *J Neurosci.* 2008;28:6983–6995.
- Zhang Q, Lenardo MJ, Baltimore D. 30 years of NF- κ B: a blossoming of relevance to human pathobiology. *Cell.* 2017;168:37–57.
- Sil AK, Maeda S, Sano Y, et al. I κ B kinase- α acts in the epidermis to control skeletal and craniofacial morphogenesis. *Nature.* 2004;428:660–664.
- Park YC, Burkitt V, Villa AR, et al. Structural basis for self-association and receptor recognition of human TRAF2. *Nature.* 1999;398:533–538.
- Yoshida H, Jono H, Kai H, Li J-D. The tumor suppressor cylindromatosis (CYLD) acts as a negative regulator for toll-like receptor 2 signaling via negative cross-talk with TRAF6 AND TRAF7. *J Biol Chem.* 2005;280:41111–41121.
- Régner CH, Masson R, Keding V, et al. Impaired neural tube closure, axial skeleton malformations, and tracheal ring disruption in TRAF4-deficient mice. *Proc Natl Acad Sci U S A.* 2002;99:5585–5590.
- Shiels H, Li X, Schumacker PT, et al. TRAF4 deficiency leads to tracheal malformation with resulting alterations in air flow to the lungs. *Am J Pathol.* 2000;157:679–688.

Laura Castilla-Vallmanya, MSc¹, Kaja K. Selmer, MD, PhD^{2,3}, Clémantine Dimartino, MSc^{4,5}, Raquel Rabionet, PhD¹, Bernardo Blanco-Sánchez, PhD^{4,5}, Sandra Yang, MS, CGC⁶, Margot R. F. Reijnders, MD, PhD⁷, Antonie J. van Essen, MD, PhD⁸, Myriam Oufadem, MSc^{4,5},

Magnus D. Vigeland, PhD^{9,10}, Barbro Stadheim, MD⁹, Gunnar Houge, MD, PhD¹¹, Helen Cox, MD¹², Helen Kingston, MD^{13,14}, Jill Clayton-Smith, MD^{13,14}, Jeffrey W. Innis, MD, PhD¹⁵, Maria Iascone, PhD¹⁶, Anna Cereda, MD¹⁶, Sara Gabbiadini, MD¹⁶, Wendy K. Chung, MD, PhD¹⁷, Victoria Sanders, MS, CGC^{18,19}, Joel Charrow, MD¹⁸, Emily Bryant, MS, CGC¹⁸, John Millichap, MD¹⁸, Antonio Vitobello, PhD^{20,21}, Christel Thauvin, MD, PhD^{20,22}, Frederic Tran Mau-Them, MD^{20,21}, Laurence Faivre, MD, PhD^{21,22}, Gaetan Lesca, MD^{23,24}, Audrey Labalme, MSc²³, Christelle Rougeot, MD²⁵, Nicolas Chatron, MD^{23,24}, Damien Sanlaville, MD, PhD^{23,24}, Katherine M. Christensen, MS, CGC²⁶, Amelia Kirby, MD²⁶, Raymond Lewandowski, MD²⁷, Rachel Gannaway, MS, CGC²⁷, Maha Aly, MSc^{4,5}, Anna Lehman, MD²⁸, Lorne Clarke, MD²⁸, Luitgard Graul-Neumann, MD²⁹, Christiane Zweier, MD, PhD³⁰, Davor Lessel, MD³¹, Bernarda Lozic, MD, PhD³², Ingvild Aukrust, PhD¹¹, Ryan Peretz, MD³³, Robert Stratton, MD³³, Thomas Smol, MD^{34,35}, Anne Dieux-Coëslier, MD³⁴, Joanna Meira, MD, MSc³⁶, Elizabeth Wohler, MS³⁷, Nara Sobreira, MD, PhD³⁷, Erin M. Beaver, MS, CGC³⁸, Jennifer Heeley, MD³⁸, Lauren C. Briere, MS, CGC³⁹, Frances A. High, MD, PhD³⁹, David A. Sweetser, MD, PhD³⁹, Melissa A. Walker, MD, PhD⁴⁰, Catherine E. Keegan, MD, PhD¹⁵, Parul Jayakar, MD⁴¹, Marwan Shinawi, MD⁴², Wilhelmina S. Kerstjens-Frederikse, MD, PhD⁸, Dawn L. Earl, ARNP⁴³, Victoria M. Siu, MD⁴⁴, Emma Reesor, BSc⁴⁴, Tony Yao, BMSc⁴⁴, Robert A. Hegele, MD⁴⁴, Olena M. Vaske, PhD⁴⁵, Shannon Rego, MS⁴⁶, Undiagnosed Diseases Network, Care4Rare Canada Consortium, Kevin A. Shapiro, MD, PhD⁴⁷, Brian Wong, MD⁴⁷, Michael J. Gambello, MD, PhD⁴⁸, Marie McDonald, MD⁴⁹, Danielle Karłowicz, CGC⁴⁹, Roberto Colombo, PhD^{50,51}, Alessandro Serretti, MD⁵², Lynn Pais, MS⁵³, Anne O'Donnell-Luria, MD, PhD⁵³, Alison Wray, MD⁵⁴, Simon Sadedin, PhD⁵⁵, Belinda Chong, PhD⁵⁵, Tiong Y. Tan, MBBS, PhD^{55,56}, John Christodoulou, MD, PhD^{55,56}, Susan M. White, MD^{55,56}, Anne Slavotinek, MBBS, PhD⁵⁷, Deborah Barbouth, MD⁵⁸, Dayna Morel Swols, MS, CGC⁵⁸, Mélanie Parisot, BTS^{59,60}, Christine Bole-Feysot, PhD^{59,60}, Patrick Nitschké, PhD^{5,61}, Véronique Pingault, PhD^{4,5,62}, Arnold Munnich, MD, PhD^{5,62}, Megan T. Cho, MSc, CGC⁶, Valérie Cormier-Daire, MD, PhD^{5,62,63}, Susanna Balcells, PhD¹, Stanislas Lyonnet, MD, PhD^{4,5,62}, Daniel Grinberg, PhD¹, Jeanne Amiel, MD, PhD^{4,5,62}, Roser Urreiziti, PhD¹ and Christopher T. Gordon, PhD^{4,5}

¹Department of Genetics, Microbiology and Statistics, Faculty of Biology, IBUB, Universitat de Barcelona; CIBERER, IRSJD, Barcelona, Spain; ²Department of Research and Innovation, Division of Clinical Neuroscience, Oslo University Hospital and the University of Oslo, Oslo, Norway; ³The National Center for Epilepsy, Oslo University Hospital, Oslo, Norway; ⁴Laboratory of embryology and genetics of human malformations, Institut National de la Santé et de la Recherche Médicale (INSERM) UMR 1163, Institut Imagine, Paris, France; ⁵Paris Descartes-Sorbonne Paris Cité University, Institut Imagine, Paris, France; ⁶GeneDx, Gaithersburg, MD, USA; ⁷Department of Clinical Genetics, Maastricht University Medical Center, Maastricht, The Netherlands; ⁸Department of Genetics, University Medical Center Groningen, Groningen, The Netherlands; ⁹Department of Medical Genetics, Oslo University Hospital, Oslo, Norway; ¹⁰Institute of Clinical Medicine, University of Oslo, Oslo, Norway; ¹¹Department of Medical Genetics, Haukeland University Hospital, Bergen, Norway; ¹²West Midlands Regional Genetics Service, Birmingham Women's NHS Foundation Trust, Birmingham Women's Hospital, Edgbaston, Birmingham, UK; ¹³Manchester Centre for Genomic Medicine, Central Manchester University Hospitals NHS Foundation Trust, Academic Health Sciences Centre, Manchester, UK; ¹⁴Division of Evolution and Genomic Sciences, University of Manchester, School of Biological Sciences, Manchester, UK; ¹⁵Departments of Human Genetics, Pediatrics and Internal Medicine, University of Michigan, Ann Arbor, MI, USA; ¹⁶Department of Pediatrics, ASST Papa Giovanni XXIII, Bergamo, Italy; ¹⁷Departments of Pediatrics and Medicine, Columbia University Medical Center, New York, NY, USA; ¹⁸Ann & Robert H Lurie Children's Hospital of Chicago, Chicago, IL, USA; ¹⁹Northwestern University Feinberg School of Medicine, Chicago, IL, USA; ²⁰UF Innovation en diagnostic genomique des maladies rares, CHU Dijon Bourgogne, Dijon, France; ²¹INSERM UMR1231 GAD, Dijon, France; ²²Centre de Reference maladies rares "Anomalies du Developpement et syndrome malformatifs" de l'Est, Centre de Genetique, Hopital d'Enfants, FHU TRANSLAD, CHU Dijon Bourgogne, Dijon, France; ²³Department of Medical Genetics, Lyon Hospices Civils, Lyon, France; ²⁴Institut NeuroMyoGène, CNRS UMR 5310 - INSERM U1217, Université de Lyon, Lyon, France; ²⁵Hôpital Femme Mère Enfant, Service de Neuropédiatrie, Bron, France; ²⁶Saint Louis University School of Medicine, St. Louis, MO, USA; ²⁷Department of Human and Molecular Genetics, Virginia Commonwealth University, Richmond, VA, USA; ²⁸Department of Medical Genetics, The University of British Columbia, Vancouver, BC, Canada; ²⁹Institute of Human Genetics, Charité, Universitätsmedizin Berlin, Berlin, Germany; ³⁰Institute of Human Genetics, Friedrich-Alexander-Universität Erlangen-Nürnberg, Erlangen, Germany; ³¹Institute of Human Genetics, University Medical Center Hamburg-Eppendorf, Hamburg, Germany; ³²Department of Pediatrics, University Hospital Centre Split; University of Split, School of medicine, Split, Croatia; ³³Driscoll Children's Hospital, Corpus Christi, TX, USA; ³⁴Institut de Génétique Médicale, CHU Lille, Lille, France; ³⁵Université de Lille, EA 7364 - RADEME - Maladies RAres du DEveloppement embryonnaire et du MEtabolisme, Lille, France; ³⁶Division of Medical Genetics, University Hospital Professor Edgard Santos/ Federal University of Bahia (UFBA), Salvador, Bahia, Brazil; ³⁷McKusick-Nathans Department of Genetic Medicine, Johns Hopkins University, Baltimore, MD, USA; ³⁸Mercy Kids Genetics, Mercy Children's Hospital, St. Louis, MO, USA; ³⁹Division of Medical Genetics & Metabolism, Massachusetts General Hospital for Children, Boston, MA, USA;

ARTICLE

CASTILLA-VALLMANYA *et al*

⁴⁰Department of Pediatric Neurology, Massachusetts General Hospital for Children, Boston, MA, USA; ⁴¹Division of Genetics and Metabolism, Nicklaus Children's Hospital, Miami, FL, USA; ⁴²Department of Pediatrics, Division of Genetics and Genomic Medicine, Washington University School of Medicine, St. Louis, MO, USA; ⁴³Seattle Children's Hospital, Seattle, WA, USA; ⁴⁴University of Western Ontario, London, ON, Canada; ⁴⁵Department of Molecular, Cell and Developmental Biology, University of California Santa Cruz, Santa Cruz, CA, USA; ⁴⁶Institute for Human Genetics, University of California San Francisco, San Francisco, CA, USA; ⁴⁷Cortica Healthcare, San Diego, CA, USA; ⁴⁸Department of Human Genetics, Division of Medical Genetics, Emory University School of Medicine, Atlanta, GA, USA; ⁴⁹Division of Medical Genetics, Department of Pediatrics, Duke University Medical Center, Durham, NC, USA; ⁵⁰Faculty of Medicine, Catholic University, IRCCS Policlinico Gemelli, Rome, Italy; ⁵¹Center for the Study of Rare Hereditary Diseases (CeSMER), Niguarda Ca' Granda Metropolitan Hospital, Milan, Italy; ⁵²Department of Biomedical and Neuromotor Sciences, University of Bologna, Bologna, Italy; ⁵³Broad Center for Mendelian Genomics, Program in Medical and Population Genetics, Broad Institute of Massachusetts Institute of Technology and Harvard, Cambridge, MA, USA; ⁵⁴Royal Children's Hospital, Melbourne, Australia; ⁵⁵Victorian Clinical Genetics Services, Murdoch Children's Research Institute, Melbourne, Australia; ⁵⁶Department of Paediatrics, University of Melbourne, Melbourne, Australia; ⁵⁷Department of Pediatrics, University of California San Francisco, San Francisco, CA, USA; ⁵⁸Dr John T. Macdonald Foundation Department of Human Genetics, University of Miami, Miller School of Medicine, Miami, FL, USA; ⁵⁹Genomics Core Facility, Institut Imagine-Structure Fédérative de Recherche Necker INSERM UMR1163, Paris, France; ⁶⁰INSERM US24/CNRS UMS3633, Paris Descartes-Sorbonne Paris Cité University, Paris, France; ⁶¹Bioinformatics Platform, INSERM UMR 1163, Institut Imagine, Paris, France; ⁶²Département de Génétique, Hôpital Necker-Enfants Malades, Assistance Publique Hôpitaux de Paris, Paris, France; ⁶³Laboratory of Molecular and Physiopathological Bases of Osteochondrodysplasia, INSERM UMR 1163, Institut Imagine, Paris, France.

Supplementary information for:

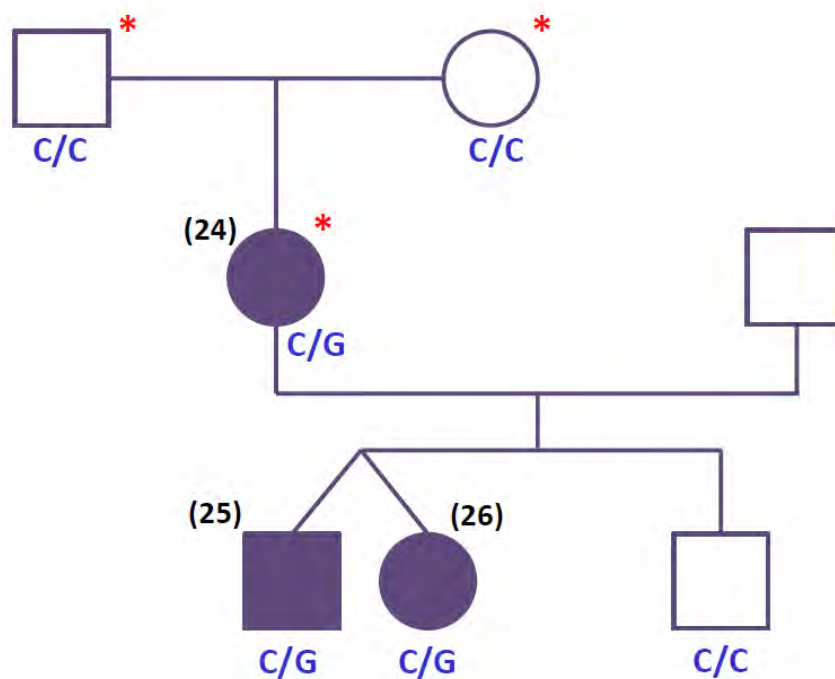
Phenotypic spectrum and transcriptomic profile associated with germline variants in *TRAF7*

Laura Castilla-Vallmanya, Kaja K. Selmer, Clémantine Dimartino, Raquel Rabionet (...), Susanna Balcells, Stanislas Lyonnet, Daniel Grinberg, Jeanne Amiel, Roser Urreizti & Christopher T. Gordon

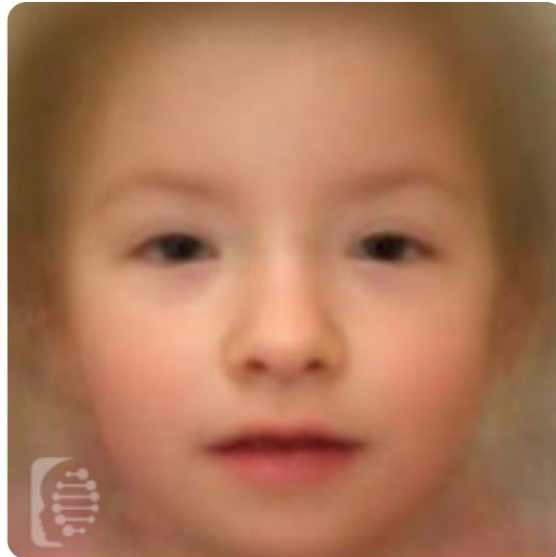
TRAF7; NM_032271.2; c.1851C>G; p.Phe617Leu

* whole exome sequencing

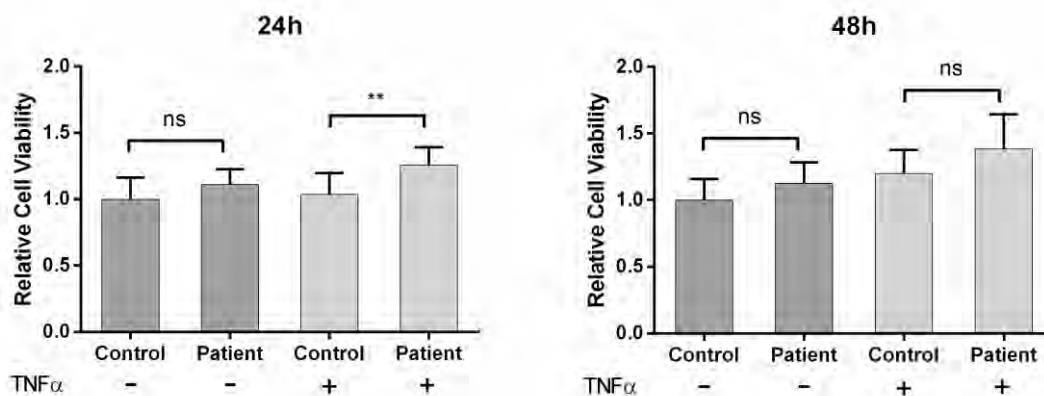
Affected individuals: 24, 25, 26



Supplementary Figure S1. Pedigree of the familial case (patients 24-26).



Supplementary Figure S2. *TRAF7* syndrome facial composite. The image was generated at Face2gene (<https://www.face2gene.com>) using one photo from each of 19 children with *TRAF7* syndrome.



Supplementary Figure S3. MTT viability assay. Fibroblasts from four patients and six controls were exposed to $TNF\alpha$ (10 ng/ml) for 24 hours or 48 hours. Data represent the relative cell viability (mean \pm SD) of three independent experiments (in triplicate). Significant differences are indicated by * (p-value <0.05, One Way ANOVA test).

Supplementary Table S1. Detailed clinical features of patients studied in this report. ABR=auditory brainstem response; CMA=chromosomal microarray analysis; EEG=electroencephalogram; GERD= gastroesophageal reflux disease; ID=intellectual disability; IPS=integrated prenatal screening; MEP=motor evoked potential; NA=not available; NAP=not applicable; ND=not done; PPV=positive pressure ventilation; SGA=small for gestational age; SSEP=somatosensory evoked potential; VEEG=video electroencephalogram; VER=visual evoked response; VUS=variant of unknown significance; ES=exome sequencing.

Characterization of TRAF7 germline variants at a phenotypic and molecular level

Patient no. (ordered by variant, N- to C-terminal. Light blue rows = patients with TRAF7 variants of unknown significance)	Year of birth	Gender	Variant (cDNA, with reference to NM_032271.2)	Variant (protein). Recurrent variants are color-coded.	Inheritance	Pregnancy/Birth	Feeding difficulties	Growth	Cognitive development, speech	Motor development	Epilepsy	Brain MRI	Dysmorphic craniofacial features	Oral cavity, teeth, pharynx, upper respiratory tract
1	2010	F	c.981C>A	p.Asp327Glu	Unknown (mother was negative for the TRAF7 variant)	Born at 39 wks	No	H and W = 90thile	Autism spectrum disorder, speech delay, learning difficulties	Normal	Staring episodes, EEG in 2016 - sharp waves, no seizures	Normal in 2013	No	Normal
2	2018	M	c.1089C>A	p.Asp363Glu	Unknown (mother was negative for the TRAF7 variant, father unavailable for testing)	Born at 36 wks. Delivery was complicated by nuchal cord, patient required resuscitation and oxygen.	Yes - required NICU stay for feeding difficulty and to regulate medication. Dysphagic	At 7 mos, H = 10th %ile, W = 58th %ile, HC = 13th %ile	Global developmental delay reportedly did not cry until 2 mos; at 8 mos he had a social smile; laughed, cooed, but did not babble	At 8 mos he was starting to roll over, but unable to sit independently. He was able to push himself around on his back. He was just beginning to reach for objects with both hands. Diffuse hypocalcaemia	Multifocal seizures with onset on first day postnatally, treated with phenobarbital. Breakthrough seizures occurred at 2 mos and were treated with higher doses of phenobarbital. Developed infantile spasms (with hypsarrhythmia) at 3 mos, they were successfully treated with ACTH and vigabatrin. Ketogenic diet was started due to high risk of recurrence	At 6 mos: Within normal limits for age	Stork bites on back of the neck and forehead	Normal
3	2016	M	c.1047C>T	p.Ser316Phe	De novo	Born to GSP2 mother, natural conception, uncomplicated pregnancy, vaginal delivery at 38 wks. Apgar scores: 8, 9.	No	At birth, W = 2940 kg, L = 48 cm. Failure to thrive. At 9 mos, W and L = 3-10th %ile.	Psychomotor delay	Delayed motor skills	No	At 11 mos: thin corpus callosum, ventriculomegaly, cyst of septum pellucidum and cavum vergae, periventricular leukomalacia, myelination delayed	Slight trigonocephaly, ptosis, short palpebral fissures, right ptosis, short nose, long philtrum, thin upper lip, low set ears	NA
4	1990	F	c.1176C>T	p.Ala370Val	Unknown (mother and father were negative for the TRAF7 variant, father was not available for testing)	Born full term, uncomplicated pregnancy and delivery	No	Short stature	Learning disability, bipolar disorder	Started walking at 3 yrs	Seizures since the age of 10 yrs. Mainly grand mal seizures, rarely petit mal episodes. Now well controlled with Carbamazepine and Gabapentin.	NA	Synophrys, round face, prominent nasal bridge, smooth philtrum, hypoplastic alar nas, overbite	Widely spaced teeth on lower jaw
5	1988	F	c.1148A>C	p.Gln383Pro	De novo	Term born	NA	At birth, W = 3370 g, L = 48 cm, HC = 33.5 cm. At 2.5 yrs, W = -1.5 SD, L = 0.5 SD, OFC = 49 cm. At 10 yrs, L = -1.8 SD, W = +0.5 SD, OFC = +2 SD	Special needs at school	Hypotonia. Sat at 13 mos, walked at 30 mos.	No	NA	Blepharophimosis, epicanthus, telecanthus, bulbous nasal tip, over-folded helices, lacertil flaring of eyebrows	Agenesis of premolar teeth. Nasal speech.
6 (= patient DDD4K.01.139 in DDD study, Nature, 2017)	2008	F	c.1204C>G	Unknown (mother)	De novo	Polypneumonia. Anemic, fluid leaking from 26/40 wks. Induced at 37/40 wks by dexam, assessed at 35/40 wks after delivery. No resuscitation required. Then ventilated for 48 hrs, CPAP for further 12 days. In neonatal period, prominent abdomen, hypotonia with very few spontaneous movements. Isolated for 4 wks.	Poor feeding with reflux all feeds by nasogastric tube from 6 wks. Thickened oral feeds from 6 mos.	Birth weight: 2.22 kg. At 10 mos, OFC at 50th %ile. At 9 yrs 11 mos, H = 136.0 cm, W = 25.75 kg.	Signing by 2 yrs 3 mos, very low words. 1:1 help needed at school. Poor social skills.	Sat at 12 mos, crawled at 18 mos. Walking supported at 1 yr 6 mos and walking just after 7 yrs.	Reflux. Reflux anoxic seizures at 10 yrs.	ND	Neonatal large anterior fontanelle, slightly low set ears, arched eyebrows, puffy eyes, epicanthic folds. At 10 mos: prominent forehead, brachycephaly, blepharophimosis, bilateral ptosis, epicanthic folds, short upturned nose, carp shaped mouth, small jaw.	Submucous cleft palate (open cleft). Left vocal cord paresis.
7	2016	F	c.1204C>G	Unknown (mother)	De novo	Pregnancy uncomplicated. Vaginal delivery at 39+6/7 wks to 37 yo G4P2 mother. Apgar scores: 8, 9. Blue in face at birth. Floppy. Admitted at 4 days of life for lethargy, poor feeding, sepsis, respiratory failure - intubated.	Yes, needed nasogastric gavage feeds in newborn period for 5 days - received therapies. Eats normally at 12 mos.	Weight: at birth = 3.969 kg, at 2 mos = 5 kg (40%), at 5 mos = 6.4 kg (32%), at 9 mos = 8.07 kg (28%), at 12 mos = 8.62 kg (12 %). OFC: L 2 mos = 38.8 cm (39%), at 9 mos = 44.7 cm (69%), Length: at 9 mos = 68.4 cm (25%), at 12 mos = 73.5 cm (36%).	At 12 mos says "Dada". Very alert, interactive and social. Smiles a lot	Hypotonic at birth. Sat at 9 mos. Pulled to stand at 10 mos. Cruising at 11 mos. Still receives physical therapy - twice per week at 12 mos.	No	Mild degree of presumed birth related hemorrhage posteriorly. Small eye: in each caudothalamia groove and along the lateral margin of left frontal horn. Unilateral subependymoma cysts or evidence of prior germinal matrix hemorrhages. Evidence of atypical but likely developmental tortuosity of vessels near the junction of the vein of Galen and straight sinus. The findings are of uncertain clinical significance.	Upturned and short palpebral fissures. Probable telecanthus. Wide nasal bridge and tip. Lowest, posteriorly rotated ears. Mild tentaculis in newborn period.	Normal
8 (= patient DDD4K.03.113 in DDD study, Nature, 2017)	2007	M	c.1211T>A	p.Val404Asp	De novo	Increased nuchal translucency	No	OFC = 50th-75th %ile, H = 50th %ile, W = 25th %ile	Moderate developmental delay. Communicates with simple speech and sign language. Major anxiety issues. Severe ID, no language	Global delay. Walked at 2 yrs 2 mos.	No	Periventricular leukomalacia	Prosis, epicanthic folds, blepharophimosis, small, upturned nose, toried upper lip	Normal
9	2011	M	c.1223G>A	p.Gly408Asp	De novo	Born prematurely (29+5/7 wks), neonatal cerebral bleeding and subsequent hydrocephalus	Yes, particularly in infancy	NA	Global delay, non-ambulant. Truncal hypotonia.	Global delay, non-ambulant. Truncal hypotonia.	West syndrome/infantile spasms, onset at 12 mos	Somewhat thin corpus callosum, otherwise normal (at 6 mos)	Hyper-tony, epicanthic folds, low set ears, lateral flaring of eyebrows, blepharophimosis	Normal ears, lateral flaring of eyebrows, blepharophimosis
10	2011	M	c.1223G>A	p.Gly408Asp	De novo	No complications, born full term, vaginal delivery	No	At birth, W = 3.9 kg, AL 4 yrs, W = 16.6 kg (57.7th %ile), H = 95.5 cm (5.37th %ile), HC = 53 cm (85.58th %ile).	Developmental delay. At 19 mos had 3 words. At 25 mos had 15-20 words, could count to 3-4 and could follow two-step commands. At 4 yrs could put 3 words together and still followed two-step commands; counted to 2 then skipped numbers.	Started walking at 17 mos	No	At ~20 mos, bilateral subdural hematomas, left side larger than right, suggestive of subacute to early chronic in age. Also evidence of chronic subarachnoid hemorrhage overlying the left cerebral hemisphere surface. Brain parenchyma within normal limits for age.	Exam at 19 mos: bilateral epicanthic folds, telecanthus, borderline low-set ears, posteriorly rotated pinnae. Exam at 4 yrs: brachycephaly, short palpebral fissures, posteriorly rotated ears.	NA
11	2010	F	c.1328T>G	p.Leu443Arg	De novo	Uneventful pregnancy. Born prematurely (29 wks). Mother was 38 yrs and father 40 yrs at birth.	Poor sucking at birth and failure to thrive	At birth, L = 38 cm, W = 1380 g, OFC = 27 cm (each <10th %ile for gestational age). Failure to thrive. At 7 yrs, short stature, low weight. Microcephaly.	Developmental delay. Severe ID (IQ 20-35). Delayed receptive and expressive speech; speaks few words at 7 yrs.	Muscle hypotonia. Delayed gross and fine motor development. Began to walk without support at 4.5 yrs.	No	Cerebellar vermis hypoplasia	Dolichocephaly, expressionless face, narrow forehead, retrognathia, narrow palpebral fissures, hyper-telony, telecanthus, blepharophimosis. Low-set, protruding ears with bilateral post-auricular pits.	High-arched palate
12	2008	F	c.1484G>T	p.Lys498Asn	De novo	Positive IPS with T21 risk of 1:140 - no amniocentesis. Apgar spells in neonatal period.	GERD, chokes or gags occasionally. Occasional gastroenteritis.	At 6 mos, HC = 41.2 cm (10th %ile), W = 7.17 kg (50th %ile), L = 67 cm (50th %ile). At 7 yrs, H = 122 cm (50th %ile), W = 26.4 kg (75th %ile), HC = 50.8 cm (25th %ile).	Moderate ID. At 3 yrs, 10 words. At 8.5 years, >100 words, recognizing some sign words, using 2 to 3 word phrases, can answer some simple questions	Sat at 6 mos, walked with support and feeding with fingers at 10 mos, walked independently at 2 yrs, toilet trained at 4 yrs	Occasional episodes of eyes rolling up with head drop and staring. EEG 2015 - grade 2 dybrhythmia, maximum occipitally, no medication	Chorioid plexus cysts on neonatal ultrasound, resolved (normal brain MRI in grade 2 dybrhythmia, maximum occipitally, 2013)	Short, widely-spaced teeth. Velopharyngeal insufficiency until 2.5 yrs.	
13	2008	F	c.1555C>T	p.Asp519Glu	De novo	Born prematurely (27 wks), intensive care treatment for bronchopulmonary dysplasia, neonatal feeding problems.	Yes, major in infancy. PLE at 1 yr	Skar t: at age 8 yrs: 10 cm below the 2.5th %ile, normal HC (80th %ile). Under growth hormone therapy, responding well.	Normal	Weak voice, delayed motor development the first 1-2 yrs	No	Normal (at 6 mos)	Blepharophimosis, hypertelorism, telecanthus, frontal bossing, low-set ears with protruding helices	Bronchopulmonary dysplasia neonatally, associated with premature birth

RESULTS: Chapter 2

14	2003	M	C1555C-T	p16p13del	De novo	Born at 40 wks following a normal pregnancy with no known teratogenic exposures to a 22 yr GI mother and 22 yr father	Unable to independently self-feed	At birth, W = 3.75 kg. Tracked along the 75th %ile for weight. Tracked along the 25th %ile for length until age 13 yrs 9 mos when he started to steadily drop off to the 3rd %ile %ile.	Autism, global developmental delay	Needed therapy in the past for help with fine motor skills such as self feeding. At 14 yrs: gait: walks independently with forward flexion of the trunk at hips but can get more upright when prompted.	No	At 14 yrs, small focus of FAIR. Hyperintensity in the right frontal lobe is nonspecific but unchanged compared to 2012. Age advanced cerebral volume loss with ventricles and sulci enlarged for age, unchanged compared to 2012. Slightly anomalous course of the internal auditory canals bilaterally, possibly due to posterior fossa dysplasia. Mastoid sinuses: bilateral effusions.	Widow's peak, tall and broad forehead, Small teeth		
15	2012	M	C1570C-T	p16p13del	De novo	Uncomplicated pregnancy, no teratogenic exposures. Birth at 38 wks, uncomplicated delivery. Apgar scores: 9, 9. Neonatal course: stayed 5 days in hospital primarily for hyperbilirubinemia, but had increasing respiratory issues noted after discharge and re-admitted within a few days.	No	At birth, HC = 33.5 cm, W = 3173 g, L = 51 cm. At 4 yrs 0 months, H = 92 cm (1.42 SD), W = 13.05 kg (1.54 SD). Steadily developing (macrocephaly over first 12 mos (>97th %ile), and at 15 mos = 50.1 cm (+2 > SD).	10-15 spoken, single words at 2.5 yrs. Diagnosed with autism at 4 yrs. No significant behavioural problems.	Delayed ambulatory development. Hypotonia (decreased muscle tone in both upper and lower limbs).	No	Mildly dilated lateral and 3rd ventricles with abnormality in the positioning of the trigonous bilaterally. Brain MRI: normal.	Trigonocephaly, ocular hypertelorism, bilateral ptosis, down-sloping palpebral fissures, epicanthus, menibular hypoplasia. Simple, low-set and posteriorly rotated ears. Two hair whorls.	Hypoplastic dental enamel and peg-shaped canines, both upper and lower.	
16	2009	M	C1570C-T	p16p13del	De novo	Pregnancy not complicated, vaginal delivery at 39 wks. Large anterior fontanelle. Apgar scores: 10, 10.	No	At birth, W = 3550 g (50th %ile), L = 49 cm (25th %ile), OFC = 37 cm (97th %ile). At 7 yrs, OFC = 56 cm (-2.3 SD), H = 101th %ile, W = 73th %ile.	Normal. First words at 12 mos, first sentences and singing with 2 yrs. No behavioural problems.	Delayed motor skills. Walked at 18 mos.	No	Normal.	Microcephaly and dolichocephaly, delayed closure of anterior fontanelle, depressed nasal bridge, large forehead with prominent metopic ridge, shallow orbits, small palpebral fissures, ptosis, epicanthal folds, small jaw, low set ears	Small conical tooth with supernumerary teeth in the primary dentition.	
17	2012	M	C1570C-T	p16p13del	De novo	Normal vaginal delivery at 36+4 wks. Foetal monitoring due to single umbilical artery and hydromphrosis.	Yes early on; since improved	At birth, W = 2330 g, HC = 33 cm, L = 50 cm. In 2012, L = 77 cm (<<1SD), W = 9.56 kg (<3SD), HC = 49.7 cm (50th).	Developmental delay, especially expressive language	Hypotonia. At 28 mos, pulling to stand, cruising. Excellent fine motor skills.	No	Chori malformation, congenital obstructive hydrocephalus.	Blepharophimosis, low set and posteriorly rotated ears, broad forehead, flat nasal bridge, thin lips.	Normal	
18	2013	M	C1570C-T	p16p13del	De novo	Maternal mosaicism variant present in 1.52% of 66 NGS reads (from blood)	Suspected congenital heart defect on prenatal ultrasound. Fetal echocardiogram at 30+4/7 wks showed hypoplastic aortic arch, small left ventricle, small mitral and aortic valves. Indicated at 39+1/7 wks.	Swallowing study showing oral phase dysphagia, improved.	At birth, W = 3.525 kg, L = 40.5 cm, HC = 35.5 cm. Poor growth, followed by Pediatric Endocrinology. At 5 yrs, W = 14.5 kg (Z = -3.00), H = 98.6 cm (Z = -3.07).	Mildly delayed with articulation difficulties. Age appropriate language skills.	Hypotonia, head lag at 6 mos, walked at 20 mos	No	Ventriculomegaly involving lateral and third ventricles. Asymmetric decreased caliber of the cerebral peduncle at the level of inferior rostral pons. s/p ventriculoperitoneal shunt.	Sparsely eyebrows, short palpebral fissures, narrow pointed nose, flat philtrum, thin upper lip, low set ears	High-arched palate
19	2006	M	C1673C-T	p16p13del	De novo	39+1/7 wks, no complications, normal amniocentesis, normal spontaneous vaginal delivery. Haecid and required PPV and 100% FIO2 for 1 minute. Apgar scores: 2, 5, 6.	GERD, gastrostomy tube, fundoplication, panulose esophagus, USI demonstrated no malrotation, poor GI motility of stomach and small bowel, vomiting, constipation. Feeding difficulties due to reduced coordination, lower muscle tone and strength and oral aversion.	At birth, W = 2136 g, OFC = 31.5 cm, L = 47 cm (5GA). Early growth short stature and failure to thrive. At 10 yrs, W at 23.1%ile, H at 9.5th %ile, OFC at 5th %ile.	Speech delay, first began speaking (with babbling consonants) at 24 mos and used two words other than mama/dada, poor articulation	Gross motor delay: script 14 mos, was able to crawl, cruise and pull to a stand at 24 mos but could only walk with assistance	No	Normal	Prominent metopic suture, small palpebral fissures, ptosis, shallow orbits, male faciem, relative hyperchlorism by comparison to head size with normal interpupillary distance for age, high-arched eyebrows, protruding low set ears with cupped earlobes, prominent nasal bridge with long nose, bulbous nasal tip.	Glottis surgery and supraorbital craniotomy for trachostoma, hypersusibility	
20	2011	F	C1673C-T	p16p13del	De novo	Born vaginally at 41 wks to G5T1P0A3.135 yr mother. Positive UPT (1H 4 for T2), no amniocentesis. Discharged from hospital with mother.	Neonatal feeding difficulties, improved by day 3	At birth, W = 3.88 kg (> 90th %ile), L = 56 cm (>97th %ile), OFC = 33.8 cm (10th %ile). At 13 mos, L = 77 cm (75th %ile), W = 8.2 kg (10th %ile), OFC = 39.8 cm (3rd %ile). At 2 yrs, L = 84.4 cm (10th %ile), W = 10.9 kg (10-25th %ile). At 5 yrs, W = 16.7 kg (10-25th %ile), H = 107 cm (10th %ile).	At 13 mos: three words with meaning, waves hi and bye, normal speech, language and social skills. At 2 yrs: many single words, putting 2 words together, >10 signs. Receiving speech-language therapy.	Gross and fine motor skill delay: sitting at 10 mos; at 13 mos, standing with support, no crawling, and difficulty with pincer grasp due to finger deformities. Walking at 2.5 yrs, receiving OT and PT. Mild early hypotonic.	No	Bicoronal craniosynostosis, absent left and minimal right internal jugular veins with prominent and serpiginous scalp vasculature, high, periorbital (pro)ventriculostomy tube. At 2.5 yrs: bilateral frontal region subdural hygromas.	Bicoronal craniosynostosis requiring cranial vault reconstruction surgeries (frontocephalic and brachycephalic), prominent brow, hyperchloric, blepharophimosis, downslanting palpebral fissures, inverted nasus, wide nasal bridge. External drainage of intracranial vessels.	High arched palate, midline groove in uvula, dentition abnormalities	
21	2009	M	C1673C-A	p16p13del	De novo	Uncomplicated	Yes (neonatal)	Normal. At 5 yrs, HC = 61 cm (+0.32 SD). At 5 yrs 10 mos, H = 148.5 cm (0<H<+1 SD), W = 50 yrs. (12.5 SD).	Mild-moderate ID (IQ 65). Language delay first words at 3 yrs, 3-4 word sentences at 4 yrs.	Delayed independent walking at 2 yrs.	No	NA	Blepharophimosis, short palpebral fissures, telecanthus, epicanthic folds, abnormally left ear duct, pleurocephaly, flat occiput, slight trigonocephaly, impressions in the skull above the lateral eyebrows, broad nasal septum, ruscognathia	Normal	
22	2007	M	C1708C-G	p16p13del	De novo	Uncomplicated pregnancy, mother 35 yrs and father 41 yrs at time of delivery. Decreased fetal movement compared to previous pregnancy. Full term NSVD. Breathing and feeding issues as newborn.	Nasal regurgitation as a baby due to submucous cleft palate, aversion to some foods, milk allergy. Reflux managed with prochlor.	At birth, W = 4.00 kg, L = 56 cm. At 2.73 yrs, W = 17.2 kg (78.19th %ile), L = 107 cm (56.66th %ile). At 8.01 yrs, W = 25.9 kg (52.33th %ile), L = 128.9 cm (56.68th %ile). At 9.26 yrs, W = 38 kg (90.17th %ile), L = 135 cm (50.88th %ile). At 10.06 yrs, W = 42.9 kg (91.29th %ile), L = 138.6 cm (48.06th %ile). Macrocephalic.	At 13 mos: three words with meaning, waves hi and bye, normal speech, language and social skills. At 2 yrs: many single words, putting 2 words together, >10 signs. Receiving speech-language therapy.	Roller at 6 mos, sat by self at 7 mos, crawled at 9 mos, walked unassisted at 17 mos	No	Normal (myoclonus) normal EEG	Chloroid cysts	Macrocephaly, short and down slanting palpebral fissures, widely spaced eyes, proclavertic, and low set ears, simplified helices, narrow nasal bridge, mild micrognathia	Submucous cleft palate
23	2003	M	C1708C-G	p16p13del	De novo	Born at 35 wks by normal vaginal delivery. NICU for difficulty breathing, no suck or swallow reflex, marked hypotonic.	Gastrostomy tube at 4 wks	At birth, W = 2.6 kg, L = 48 cm	Global developmental delay	Hypotonia. Cerebral palsy, with seizures, two abnormal EEGs good response to benzofen. Wheelchair bound.	No	Periventricular leukomalacia, prominence of lateral ventricles, small arched sulci in left temporal fossa	Hypertelorism, epicanthic folds, prominent nasal bridge and glabella, bulbous nasal tip, ridging of sutures	Tracheostomy at 4 wks	

Characterization of TRAF7 germline variants at a phenotypic and molecular level

Case ID	Year	Sex	Variant	Origin	Parental Origin	Birth	Neonatal	Developmental	Speech	Motor	Seizures	Brain	Facial	Other	
24 (mother of patient 25 and 26)	1974	F	c.1851C>G	De novo	NA	NA	NA	Short stature	Learning difficulties in primary school	NA	No	NA	At 38 yrs, mild cerebellar atrophy, dysmorphic corpus callosum, mild ventricular dilation, petri and interventricular white matter hyperintensities, dilated Virchow Robin spaces	Blepharophimosis, small cleft between tragus and auricle, bulbous nasal tip	Cleft palate (operated)
25	2004	M	c.1851C>G	Maternal	Born 36 wks	Yes (infancy), nasogastric tube feeding for 4 wks	At birth, W = 2 kg, At 7.5 yrs, W = 11.5 SD, H = -1 SD, HC = -2 SD. At 12 yrs, W = -2 SD, H = -10.5 SD.	Difficulties writing and drawing. Special needs at school.	Walked at 26 mos. Oral motoricity problems. Synkinesis. Dyspraxia.	No	No	Normal at 8 yrs	Blepharophimosis, bulbous nasal tip, thin upper lip	Velopharyngeal insufficiency	
26 (sister of patient 25)	2004	F	c.1851C>G	Maternal	Born 36 wks	No	At 7.5 yrs, W = -0.5 SD, H = +0.5 SD, HC = -2 SD. At 12 yrs, W = +1 SD, H = +1 SD, HC = -1.5 SD.	Language delay. Difficulties drawing. Special needs at school.	Walked at 22 mos. Synkinesis.	No	No	At 8 yrs, mild vermian atrophy, mild ventricular dilation	Blepharophimosis, bulbous nasal tip, thin upper lip	Velopharyngeal insufficiency	
27	2010	M	c.1849T>C	De novo	Normal gestational course. Born full term via vaginal delivery.	No	At birth, W = 2.86 kg, At 20 mos, W = 8.9 kg (0.15th %ile), HC = 46.5 cm (10.38th %ile). At 4 yrs 2 mos, H = 89 cm (0.9th %ile, Z = -3.11), W = 13.6 kg (3rd %ile, Z = 1.87), HC = 50 cm.	At 20 mos had 4-5 words. At 31 mos had 20 words, no phrases and would point. At 2 mos, delayed development, can say colors and numbers and can communicate his needs, plays make believe and plays well with other children.	First sat independently at 1 yr. Walked at 15 mos. At 31 mos able to run, jump, climb stairs and kick a ball. At 4 yrs 2 mos: delayed development, can hop or stand on 1 foot, uses scissors.	No	No	Normal	Hyper telorism, flat nasal bridge, prominent forehead, blepharophimosis, telecanthus, low-set posteriorly rotated ears with abnormal helices, microstrabismic, mild sagittal synostosis.	Delayed tooth eruption first tooth at 14 mos	
28	2001	F	c.1850T>C	De novo	Born as term. Apparent score 5, 9.	No	At birth, W = 3030 g, L = 48 cm, OFC = 33 cm. Subcutaneous growth normal.	Moderate difficulties at school (dysgraphia)	Sitting at 7.8 mos, walking at 18 mos	No	No	Normal	Narrow upslanting palpebral fissures, micrognathia	Nasal speech due to insubstantiality of the palate	
29	1998	F	c.1873C>G	De novo	Uncomplicated pregnancy, full term	Neonatal feeding difficulties	At birth, W = 3150 g, L = 51 cm, HC = 33 cm. At 4 yrs, W = 13 kg (-2 SD), H = 95 cm (-1.5 SD), HC = 48 cm (-2 SD). At 13 yrs, W = 37 kg (-2.8 SD), H = 149 cm (-1.8 SD), HC = 55 cm.	Major language delay, non verbal	Walked unassisted at 15 mos	No	No	Normal	Hyper telorism, ptosis, bilateral epicanthal folds, short palpebral fissures, posteriorly rotated ears, small jaw	Submucous cleft palate, velopharyngeal insufficiency	
30	2002	F	c.1885A>C	Not inherited from mother; father unavailable for testing	Full term, natural conception. 18 wk ultrasound showed fetal ascites and dysplastic kidney. At birth, respiratory distress, in NICU for 7 mos (was intubated for 2 wks). Passed newborn metabolic and hearing screen.	Yes was on gastrostomy tube- feeds until age 6 yrs	At birth, W = 3175 g. Short stature post neonatally.	Autism and ID, no spoken words, but uses signs and an assisted communication device, does work at 4th grade level (USA) using a computer	Currently in wheelchair, walked at 4 yrs, has trouble with balance, wears AFOs on both ankles, does not run unassisted, uses walker for running, feeds herself, can write but it is difficult.	Yes, from birth to 18 mos and was treated with phenobarbital until age 4 yrs, no seizures since 18 mos of age	Normal	Macrocephaly with bilateral narrowing. Prominence of midline forehead. Midface retraction with hypoplastic maxilla and prognathia, upturned nose with long philtrum. Macrognathia. Small deep-set eyes with upslanting narrow palpebral fissures. Hypertelorism. Bilateral residual ptosis even after surgical repair. Lung scars.	Micro		
31	2012	M	c.1036G>C	De novo	30-67 wk gestation via cesarean section secondary to failure to progress. Two vesical cords identified. Observed in NICU for tachypnea after birth. Discharged at 3 days of life.	GERD, severe oral inefficiency with liquids and solids, mild pharyngeal phase dysphagia with oral aversion, gastrostomy tube placement at 6 mos. Ongoing feeding issues at 4 yrs 4 mos but improved with treatment through intensive feeding program.	At birth, W = 4045 g, L = 53 cm, HC = 36 cm. Postnatal onset growth deficiency. Linear growth tracking at -1.5 to -2 Z-scores since 2-3 mos of age.	Mild to moderate degree of ID. Delayed speech and language skills. At 4 yrs he was signing 3 to 4 word sentences and demonstrated improved verbalizations: Atanda's Clout and Hand of Hacking. Preschool Program. Provided with early intervention services beginning in infancy with occupational and physical therapy. Speech therapy initiated at 14-15 mos. No concerns with social engagement.	Global delays. Walked at 22-23 mos	No	No	Brain MRI at 2 yrs revealed subtle nonspecific findings including cerebral asymmetry, lower signal on the right versus the left, smallish rostrum of the corpus callosum and borderline small cerebellar vermis for age.	Hypertelorism, bilateral epicanthal folds. Small teeth with telecanthus, micropenis, posteriorly rotated ears		
32	2005	M	c.1064G>A	De novo	Increased nuchal translucency, delivered at 38 wks	NA	At birth, W = 3.1 kg, L = 47 cm, OFC = 33.7 cm. Relative microcephaly.	Developmental delay, first word at 18 mos. Licked at 3 yrs. Behavioral issues including acting out.	Sat at 7 mos, walked at 14 mos	No	No	NA	Trigonocephaly, hyper telorism	NA	
33 (also see Urrutia et al /JMG 2016, patient P6, for phenotypic description)	1996	F	c.1064G>A	De novo	Intrauterine growth retardation. Early infancy, anoxia and hypoxic.	Failure to thrive	Short stature, microcephaly	Developmental delay. Poor articulation but communicates by simple speech and some sign language. Behavioral issues including acting out.	hypertonia. Motor delay. Sat at 16 mos, stood with help at 24 mos. Walked unassisted at 4 yrs. Oral motoricity problems.	Yes (last convulsion at 10 yrs)	No	Prominence of the ventricular system	Trigonocephaly, broad and depressed nasal bridge, hypoplastic orbital ridges, upslanting palpebral fissures, prominent eyes, low-set ears, epicanthal folds, micrognathia, bulbous nasal tip. Oxycephalic features more prominent in early childhood.	Buccal-avolar frenula	
34	2004	M	c.1064G>A	De novo	Single umbilical artery and short femur found at US scan. Term birth.	No	At birth, W = 3220 g (43.6th %ile), L = 49 cm (30.96th %ile), HC = 33 cm (10.46th %ile). At 7 mos, W = 8.540 kg (+0.24 SD), L = 67.5 cm (-0.77 SD). At 6 yrs, W = 23.7 kg (-1.06 SD), L = 113.7 cm (0.46 SD), HC = 51.3 cm. At 10 yrs 4 mos, W = 45.4 kg (1.74 SD), L = 160 cm (-0.07 SD).	Moderate ID, most difficulties in speaking. No associated behavioral disorders.	Walked at 18 mos	No	No	Small occipital defect on the right side	Congenital bilateral ptosis and blepharophimosis, bilateral epicanthal folds, brow ridge narrowing, prominent ears, long philtrum, small mouth, broad nasal tip, microstrabismic, downslanting palpebral fissures	NA	
35	2015	M	c.1064G>A	De novo	Birth at 38 weeks 4 days. To 30 yo	Q473013, GBS+ (treated) mother by vaginal delivery. Appr scores 5, 9.	At 21 mos, W = 21.96(-1), L = 37.9th %ile	Developmental delays, receiving early intervention. At 8 mos understands "no", does not point, says "mama /"dada" (non-specific), stranger anxiety, does not wave bye. At 12 mos. puts objects in container and takes them out. At 15 mos. does not use spoon/forking a knife.	hypotonia. At 9 mos: unclear grasp, pulls to stand, stands holding on, crawls, pulls self to sitting position. At 14 mos: begins cruising.	No	No	Normal	Trigonocephaly, brachycephaly, bilateral ptosis, blepharophimosis, telecanthus, hypoplastic nasal alae, hypertelorism, broad nasal root, anteverted nares	NA	
36	2002	M	c.1064G>A	De novo	Cesarean section at 36 wks	Neonatal feeding difficulties, tube feeding for three months	At birth, W = 2360 g, L = 47 cm, OFC 35 cm. At 13 yrs, H = 142 cm (-3rd %ile), W = 34.8 kg (3-10th %ile), HC = 54.8 cm (50-75th %ile)	Mild to moderate ID. Delayed speech at 13 yrs, dyspraxia, can write a few words, at special school.	Muscular hypotonia. Walking at 11 mos.	No	No	Mildly enlarged ventricles, venous anomaly	Triangular skull shape, several hair whorls, prominent veins, sparse eyebrows and lashes, blepharophimosis, retrognathia, small nasal bridge with prominent nasal tip	Malpositioned teeth and diastema between upper incisors	

RESULTS: Chapter 2

37	2015	M	L1964G>A	L1A16559G	De novo	Positive nuchal translucency screen, fetal hydronephrosis, ossification section delivery. Born at 38.5 wks (full term)	No	At birth, W = 3856 g. At 7 yrs, W = 9.5 kg (<3rd %ile)	Developmental delay. At 6 mos babbling; at 10 mos two syllable words ("mama"), at 20 mos follows commands, imitates actions, socializes with children, laughs; at 2 yrs still only says two syllable words. He does not have aggression.	At 8 mos: sitting with support; 9 mos: sitting unsupported, rolling over; 12 mos: sat alone; 20 mos: attempting to pull to stand. At 2 yrs still unable to crawl or walk on his own.	No	Chiri1 malformation (cerebellar tonsils 7.2 mm below foramen magnum) with hydrocephalus. Bilateral middle ear and mastoid effusions. Underwent repeat MRI status post right frontal burr hole for third ventriculostomy	Telecanthus (27 mm from medial to lateral canthus of each eye; 32 mm between medial canthi)	NA
38	2015	M	L1964G>A	L1A16559G	De novo	Increased nuchal translucency, 16,X1 on amniocentesis, born at 35 wks.	Swallowing difficulties	At birth, W = 3300 g, L = 47 cm, OFC = 33.5 cm. At 3.5 yrs, W = 0 SD, H = -2 SD, OFC = +0.5 SD.	Language delay, Drooling.	Walked at 28 mos	No	ND	Blepharophimosis, epicanthus, telecanthus, ptosis, high forehead, cupped and low set ears with anteverted lobes, bilious nasal tip	Velopharyngeal insufficiency, nasal valve
39	2017	F	L1964G>A	L1A16559G	De novo	Born to a 66yr mother. Uncomplicated pregnancy, vaginal delivery at 36 wks 5 days. Apgars 7 and 9 at 1 and 5 minutes. Went home on day 2. noted to have a small head. Maternal UTOX negative.	No	At birth, L = 48 cm, W = 2.7 kg, OFC = 30.5 cm. At 3 mos, OFC = 40.7 cm. At 10 mos, OFC = 45 cm (69th centile), Z = 0.49, H = 68.1 cm (8th centile), Z = -1.4, W = 6.69 kg (1.77th centile), Z = -2.1.	At 5 mos, responds to sounds, no cooing, smiles but not responsively. At 10 mos, developmental delays.	At 5 mos, fine motor development in the 2-3.5 mos range and gross motor skills in the 2-3 mos range. At 8 mos, not sitting, just crawling to roll over. Reduced trunk tone with increased limb tone.	No	At 5 mos: simplified gyral pattern, globally diminished white matter, delayed myelination, mild ventriculomegaly of lateral ventricles, mild to moderate expansion of the extra axial spaces surrounding the convexities. No midline shift or mass effect. Long echo time magnetic resonance spectroscopy within normal limits.	Bilateral ptosis (slight surgery), interrupted eyebrows, sparse eyelashes laterally. Palpebral fissures small and not well formed medially (telecanthus), broad nasal bridge and tip, lipodulcous folds, low set, posteriorly rotated ears, relatively thin lips. Mildly downturned corners of mouth. Small anterior fontanelle at 5 mos. Prominent forehead.	Normal
40	1992	M	L1964G>A	L1A16559G	De novo	Born as full term; NICU stay for 7 days for underdeveloped lung, patent ductus arteriosus, failure to thrive, jaundice, and dysmorphic features.	Yes early on, then improved. Later started to have difficulty swallowing certain textures.	Febrile on thrive. At birth, W = 2.7 kg, L = 48 cm. At 25 yrs, H = 160 cm (short stature), W = 68 kg.	Developmental delay. At 25 yrs, IQ in the 60s. Ability to work in department store in processing and shipping. Able to engage in meaningful conversations.	Developmental delay	No	ND	Prominent nose, asymmetric facies, small philtrum, downslanting palpebral fissures, mild hyperlordosis, ptosis (surgery)	High arched palate
41	2005	F	L1964G>A	L1A16559G	De novo	Fetal US findings - right pelvic kidney, premature arial contractions. Uncomplicated term delivery, did well in the neonatal period.	No initial feeding concerns, decreased appetite & frequent gagging at 12 yrs.	At 13 yrs, H = 1st %ile, W = 15th %ile, HC = 95th %ile	Initially had good language development and was starting to use two-word phrases by 18-24 mos, subsequent loss of language skills, eye contact and pointing contributed her diagnosis of autism spectrum disorder. At 12 yrs could speak in sentences but used language mainly to label and request and was very prompt-dependent, expressive-receptive language skills were at ~1.5 yrs equivalent, but written language skills were significantly better. Intellectual disability of unspecified severity. Changes in health and behavior noted at 12 yrs - fatigue, inconsolable crying, self injurious behaviors.	Delayed motor development, walked at 19 months. At 12 yrs gross motor skills were at the level of a 4 yo and fine motor skills at the level of a 9 yo.	No. EEG at 12 yrs - abnormal due to lack of well-developed awake features, suggestive of mild encephalopathy, no epileptiform features.	At 12 yrs, mild basilar invagination	Somewhat prominent forehead, wide nasal bridge, visible vein across nasal bridge, prominent nose tip, epicanthic folds, telecanthus, mild bilateral ptosis, distichiasis. Features noted in infancy: small chin, low set and posteriorly-rotated ears.	History of narrow palate (w/ palate expander)
42	1999	M	L1964G>A	L1A16559G	Unknown (mother unavailable for testing)	Born by elective C-section at 39 wks	NA	At birth, W = 3.45 kg, L = 48 cm, HC = 34 cm. At 4 yrs 9 mos, H = 87.5 cm (<3rd %ile), W = 15.85 kg (10th %ile), HC = 48 cm (10th %ile).	Moderate ID. Had little speech at 4 yrs. Attended special school for education and works in a supported work environment.	Walked at 15 mos	NA	Normal scan (circular canals), pituitary mass which resolved	Blepharophimosis, epicanthus, downslanting palpebral fissures, ptosis, facial asymmetry, broad nasal tip, large, anteverted ears, left preauricular ear tag, small mouth, synophrys, bi-temporal narrowing	Chromosomal
43	2004	M	L1964G>A	L1A16559G	De novo	Born at 37 wks, emittic liquid in excess	Yes, mild in neonatal period	H = 1.5 SD, W = 1 SD	Developmental delay, delayed speech (ID). Calm, sociable, no behavioral problems.	Hypotonic in infancy, walked at 17 mos	No	Severe congenital (hydrocephalus, variant venous anatomy, falxine sinus, sinus pericranii), tentorium cerebelli dysplasia, Chiri type I malformation	Micropic ridge, craniosynostosis (lamboid and sagittal), epicanthic folds, telecanthus, blepharophimosis, mild ptosis, high arched eyebrows, low set ears, low posterior hairline, low columella, small mouth	Velopharyngeal insufficiency (surgery)
44	2016	M	L1964G>A	L1A16559G	De novo	Delivered by cesarean section at 41 wks to a 32 yr old G2P0x1 mother; little desire to eat but will eat if fed; for the most part parents date, emergency cesarean section indicated for prolonged decelerations	Significant feeding difficulties; little desire to eat but will eat if fed; for the most part parents feed him formula by syringe; tends to regurgitate food up to a few times per day; tried lansoprazole and cyproheptadine to little effect.	At birth, W = 3.37 kg. Failure to thrive at 26 mos, W = 10 kg (Z = -2.5); at 34 mos, H = 89 cm, HC = 49 cm.	Began babbling at 9 mos but no words at 26 mos; meets criteria for autism spectrum disorder	Mildly delayed gross motor milestones; more significant delays in fine motor milestones (pincer grasp at 18 mos)	No	MRI at 6 mos with mild under-opercularization bilaterally	Brachycephaly	NA
45	1986	M	L1975G>T	L1A16559G	De novo	Uncomplicated pregnancy. Born at 41 wks by cesarean section. Healthy parents.	Mild neonatal feeding difficulties	At birth, W = 3200 g (10-25th %ile), L = 48 cm (9th 10th %ile), OFC = not recorded at birth. At 6 mos, OFC = 42 cm (about 10th %ile). At 18 yrs, H = 165 cm (3rd 10th %ile), W = 65 kg (25th 50th %ile), OFC = 53 cm (-> 5 SD).	At 7 yrs, IQ of 58 (mild ID). Delayed speech and language skills: first words at 37-38 mos. Attended special Preschool and School programs. Provided with early intervention services in infancy (physical and occupational therapy). Speech therapy initiated at 18-24 mos. No major social problems. At 10 yrs language skills were significantly better. Changes in behavior were observed at 13-14 yrs: fatigue, loneliness, poor interest in surroundings.	Sitting at 8-9 mos, independent walking at 18 mos. Muscular hypotonia.	No	ND	Blepharophimosis, mild hyperlordosis, small nasal bridge with prominent nasal tip, thin lips	Normal

Characterization of *TRAF7* germline variants at a phenotypic and molecular level

Limbs, extremities	Other skeletal	Cardiac	Hearing	Eyes, vision	Urogenital	Other phenotypes	Previous molecular or metabolic investigations	Method used for <i>TRAF7</i> variant identification	<i>TRAF7</i> variant validated by Sanger sequencing
Normal	Normal	Normal	Normal	Exotropia	Renal US - normal		CMA showed a maternally-inherited 16p13.11 353kb deletion; this variant may be associated with neurodevelopmental disorders with incomplete penetrance. Metabolic testing normal. By ES, VUS: R1F1A, c.2927T>C, p.Val976Ile, heterozygous, inheritance unknown.	ES	Yes
Bilateral clubfoot (appears to be familial; maternal grandfather and maternal aunt both with bilateral clubfoot.)	Normal	Normal	Normal	Normal	Normal		Comprehensive epilepsy gene panel: negative, heterozygous PGLG c.3428A>G (p.Glu1143Gly) variant present - possible association with valproate-induced liver toxicity - not known to cause mitochondrial disorder; newborn screen (2018): abnormal, concerning for cystic fibrosis, subsequent sweat test normal; array CGH: normal male, exome sequencing/mitochondrial genome sequencing/deletion analysis; homoplasmic MT-ATP6 VUS: m.B133G>A (p.E208K), mother is also homoplasmic with no signs of mitochondrial disease; normal miz/metabolic labs	ES	Yes
Normal	Short neck, pectus carinatum	Normal echocardiogram	Normal	Normal	Normal renal ultrasound	Inguinal hernia	FISH Tq11.23 negative	ES	Yes
Congenital hip dysplasia requiring hip replacement bilaterally	Short neck	Echocardiogram was not done but normal cardiac exam	Normal	Myopia	Well-differentiated endometrioid adenocarcinoma 35 yrs	Obesity (BMI=39), hirsutism on face and arms, long history of migraines, Carpal tunnel syndrome at the age of 30 yrs.	By ES, likely pathogenic variant in PIK3R1 (NM_181523.2): c.1519G>T, p.Glu507Cys; inheritance unknown - father was not available for testing but mother and unaffected brother were negative; variants in this gene cause SHOR1 syndrome but the patient's features are atypical for this disorder	ES	Yes
Clino-dactyly Vth fingers, subluxation of patella	Pectus carinatum	Atrioventricular canal defect (surgically repaired)	Conductive deafness, chronic otitis media	NA	NA	Progressive alopecia of the vertex at 18 yrs	Normal karyotype on blood and skin, array-CGH 60k anti in-house intellectual disability NGS gene panel (hypothesis of Ohdo syndrome)	Targeted NGS of a panel of candidate neurocristopathy genes	Yes, candidate neurocristopathy genes
Wide sandal gap, toes II and long, occluded. Marked palmar creases with wrinkled skin. Lateral deviation of right II. Digit V clinodactyly. Prominent proximal interphalangeal joints. Overlapping toes.	Short neck. Neonatal small chest. Slim build.	Patent ductus arteriosus (ligated) and aortic septal defect. A later echocardiogram showed intact septum.	Conductive hearing loss with hearing aids	Four vision in high eye due to dense amblyopia, left partial 3rd nerve palsy with limited upgaze	Right kidney lies in low oblique position in right lower abdomen and has a duplex appearance. No pelvic/ureter dilatation.	Cutis marmorata. Keratosis pilaris.	Array CGH, RAS/MAPK pathway genes, KAT5B	ES	Yes
Bilateral mild talipes equinovarus	Short neck	Normal echocardiogram	Normal	Normal	Normal	No	CMA normal. Congenital hypocalcemia (panel through Lmory Genetics Lab: 1) tests for SMAA (deletion of SMN1), 2) DNA methylation of SNRPN associated with Prader-Willi syndrome, 3) CTG repeat analysis of DMPK and 4) methylation abnormalities associated with UPD 14; all normal. Patient has two VUS in Utrns in NLM (can cause Normalis myopathy): p.R880H maternal and p.V628I paternal, however EMG was normal therefore the variants are assumed benign. Acyl Carnitine and carnitine profile - normal. Plasma amino acid profile - normal. Urine organic acids - normal. Ammonia (u, 4 days): 39 micromol/L.	ES	Yes
Normal	Short neck	Patent ductus arteriosus	Bilateral hearing loss	Hypermetropia	Undescended testis	Umbilical hernia	Array-CGH, KAT5B, EHMT1	ES	ND (identified from high quality calls from ES)
Spartic extremities	Normal	Patent ductus arteriosus, no surgery	Normal	Cerebral visual impairment, Linnegar, strabismus, nystagmus	Unilateral undescended testis	Inguinal hernia	Karyotyping normal, normal array-CGH and normal metabolic screening	Trio ES	Yes
Appear normal. No restriction of joint motion	NA	Echocardiogram: tiny inferior muscular ventricular septal defect with left to right shunt, non-obstructive muscle band seen in the left ventricular cavity, otherwise normal.	Failed newborn and subsequent hearing screens. Middle ear effusion diagnosed and hearing deemed normal after placement of pressure equalizing tubes. Chronic otitis media. Bilateral nasoid opacification could be clinically correlated.	Normal	NA	Anemia, low ferritin.	ES additional findings: TGA2B, c.2133T>G, heterozygous; maternal, VUS: FBML, c.4270C>G, heterozygous; maternal, VUS (family has no features of Marfan syndrome); ALA52, c.47G>A, hemizygous; maternal, VUS. Fragile X testing - normal. CMA - normal. Urine organic acids - non-diagnostic. Carbohydrate deficient transferrin - normal. N-glycan - normal. O-glycan - normal. VLCFA - normal. Plasma amino acids - multiple modest elevations, possibly post-prandial. Von Willebrand testing - normal. Factor XIII - normal. Coagulation Factor VIII activity - normal. Plasminogen Co-factor 32 - (48-175%). CBC - RBC disc width 17.5 (12.5-16%), platelets 613 (150-450) /mm ³ ; MPV 6.8 (7.4-10.4 fL); rest WNL. Ferritin, plasma - 16 (24-354 ng/ml).	ES	Yes
Toe II overlaps III, flat feet	Short neck	At 6 yrs, echocardiogram showed persistent ductus arteriosus with no hemodynamically significant pulmonary stenosis	Mild to moderate conductive loss in the left ear	Strabismus, amblyopia	Hypoplastic tibia minima	high myopia	Normal karyotyping of blood and array-CGH	Trio ES	Yes
Toeing out; gait very low tone. Hyperextension at knees, hyperext joints, tendency to roll into plantar/valgus position of ankles	Neonatal narrow chest (circumference 34 cm)	Persistent small patent ductus arteriosus	Normal. Small external auditory canals.	Normal	Normal abdominal ultrasound	In neonatal period, excess nuchal skin, intertrippable distance 8 cm	Normal karyotype (G banded), multitelomere FISH, KAT5B sequencing (suspected Ohdo syndrome), CMA, FMR1, TSH	ES	Yes
Normal	Short neck	Normal	Subtle hearing loss (sensorineural), bilateral hearing aids.	Normal	Normal	Prominent scalp veins, probably due to lipodystrophy	ATM/mtxix 6.0 SNP array; normal, normal metabolic screening	Trio ES	ND (ES technically confirming with 56 T and 65 C reads)

RESULTS: Chapter 2

Large hands. Syndactyly, most prominent between fingers II and III and between III and IV. Has severe out-toeing bilaterally (right greater than left) which comes from the hip retroversion and severe pes planus with tight heelcords.	Hospitalized for cervical spinal compression in 2012. Pectus abnormality. Short, webbed neck. Exaggerated lumbar lordosis. Grade 2 spondylolisthesis L5/S1.	Bicuspid aortic valve with mild ascending aorta dilation	Bilateral congenital hearing loss, wears hearing aids	Normal	Undescended testes, s/p orchiopexy at 13 yrs	Hypoplastic, wide-spaced nipples. Bilateral lower extremity edema at 13 yrs, with the left being worse than the right.	Normal SNP array	ES	Yes
Camptodactyly of all digits with limited extension of the 1st phalangeal joint on all digits, but more prominent on II and III bilaterally. Limitation of elbow extension bilaterally. Congenital Bilateral radial head dislocations. Lower limb X-rays: mildly abnormal epiphyses.	Spine X-ray: relatively small C3 and C4 vertebral bodies	At birth, large patent ductus arteriosus with a left to right shunt, underwent uncomplicated surgery at 10 days. Anomalous origin of the right coronary artery.	Moderate-severe bilateral conductive hearing impairment (chain dysfunction; wears aids.	Myelinated nerve fibres (right side only), elevated optic discs, absent optic cup	Normal renal ultrasound	Recurrent pneumonia. Chest X-ray: suspected eventration of the diaphragm.	Normal CMA	Trio ES	Yes
Restriction of joint motion and flexion deformity in upper limbs and knee. Flexion deformity with radial deviation of the fingers. Partial cutaneous II-III syndactyly of both hands. Bilateral clinodactyly of finger V. Bilateral brachyphalangy of finger II; confirmed hypoplasia of the middle phalanx by X-ray. Wide sandal gap I-II toes. Metatarsus adductus. Adducted thumbs, deep palmar creases	Spine: congenital progressive thoracolumbar kyphosis (Th12-L1) associated with hemivertebra L1. Operated twice (at 4 and 6 yrs); spondylodesis performed. J-shaped sella turcica. Short neck. Small chest with pectus carinatum, clavicle hypoplasia, slightly curved ribs. Delayed bone age: estimated to be 4 yrs at chronological age 6 yrs.	Atrial septal defect detected at birth and at 7 yrs is still persistent with diameter of 2 mm	Normal	Normal	Right hydrocelestis	Prominent abdomen with umbilical hernia. Localized skin pigmentation disorder with hypopigmentation and hyperpigmentation (abdomen and back). Fine hairs.	Array-CGH: partial trisomy of 17q21.31 paternally inherited, FMRI1, CDG, VLCA, blood amino acid chromatography, urinary organic acid chromatography, urinary oligosaccharides and mucopolysaccharides were normal.	Trio ES	Yes
Leg length discrepancy (R > L), long fingers, webbing between digits II-IV, long toes I, deeply set toenails	Craniocervical junction stenosis with secondary hydrocephalus, T11-T12 hemivertebrae, 11 pairs ribs, short neck	Patent ductus arteriosus causing cardiac compromise and requiring surgical ligation, small atrial septal defect, bicuspid aortic valve	Normal	Normal	Hypospadias. Fetal hydronephrosis.		Normal Illumina HumanCytoSNP-12 array, normal chromosome breakage studies (hypothesis of Fanconi anemia or VACTERL-H)	ES (Nextera Rapid Capture exome kit) - clinical exome negative. Moved to research trio exome via Broad Institute USA	ND (good quality ES, with coverage of 102 reads at the variant site and allele balance of 0.52. Parents: 72 and 73 reads, with zero alternate allele.) Yes
Bilateral radial clinodactyly of digit II of the hands, middle phalanges of digits II-V delta shaped, mild bowing of proximal ulnas, mild bowing and shortening of tibiae, patellar dimples, bilateral pes planus, syndactyly of fingers. Bone age delayed by 2 yrs at 5.5 yrs chronological.	Pointed, protruding sternum (possibly due to sternotomy). Delayed bone age.	Prenatal anomalies (see Pregnancy/Birth). Shone complex, with mild to moderately hypoplastic transverse arch, large patent ductus arteriosus, hypoplastic aortic and mitral valves and bicuspid aortic valve.	Chronic fluid due to eustachian tube dysfunction. Required four sets of tympanostomy tubes. Audiogram at 5 yrs: mild conductive hearing loss rising to within normal limits in R ear and moderate conductive hearing loss rising to within normal limits in L ear.	Had exotropia secondary to bilateral moderate to bilateral hydrocephalus. Resolved. Hyperopia.	Normal		Normal CMA (Illumina HumanCytoSNP-12), Russell-Silver syndrome methylation normal (11p15, 6q24.2, 7p12.1, 7q32.2)	ES	Yes
Upper: bilateral shortened index fingers with delta phalanges and ulnar deviation, requiring surgical correction. Hypoplastic proximal phalanx of the thumb and middle phalanx of the middle fingers. Bilateral camptodactyly and brachydactyly of middle fingers. Altered palmar creases and broad nails on thumb. Lower: bilateral pes planus, fat pads on medial surface of the soles of the feet, and hallux valgus deformities of the toes. Curly right third toe, mild left third toe curl. II-III syndactyly on right foot, with second toe overlapped third. Bilateral dysplastic great toe proximal phalanges and dysplastic middle and distal phalanges in toes II-V. Hypermobile somewhat broad thumbs, interphalangeal contractures, hind toes overriding third, uplifted nails of halluces, pedes planovalgi	Narrow thorax and pectus carinatum, broad posterior ribs, flattened acetabular angles, normal pelvis, posterior ossification defect of sacrum with slightly widening interpediculate distance	Patent ductus arteriosus surgically closed, patent foramen ovale, aberrant right subclavian artery	Bilateral myringotomy tube placement, bilateral mild to moderate conductive hearing loss rising to normal with hearing aids	Minor myopia in one eye; other normal refraction. Strabismus surgery.	Early renal ultrasound showed bilateral small cortical renal cysts that later resolved. Normal renal corticomedullary differentiation, mild left pelviectasis.	Inverted nipples. Pseudotumor cerebri s/p lumboperitoneal shunt placement. Keratosis pilaris on his back with eczema of fingers and near the tips. Enuresis.	Normal array-CGH, SNP array, cardiofaciocutaneous gene panel, ZEB2 and KAT6B sequencing, carbohydrate deficiency glycoprotein syndrome testing, 7 dihydrocholesterol; also has an inherited FLG pathogenic variant; normal newborn screen. TSH, T4, IGF-1, IGFBP3, cortisol all normal.	ES	Yes
Bilateral mild camptodactyly of fingers II-NA V, persistent fetal fingertip pads	52 degree kyphosis and 14 degree right convexity scoliosis at the thoracolumbar junction. Narrow asymmetrical chest with prominence of right ribs. Short neck.	Small ventricular septal defect (closed spontaneously), small-moderate patent ductus arteriosus requiring interventional closure at 2.5 yrs	Normal	Bilateral optic disc pallor, cortical visual impairment (R 20/80, L 10/80), large angle left exotropia (secondary to craniosynostosis). Brushfield spots	Normal abdominal/pelvis ultrasound	At birth: excess nuchal skin posteriorly, loose skin	Normal 180K oligonucleotide CGH array. Negative FGFR1, FGFR2 and FGFR3 mutation analysis. Normal TWIST gene dosage study.	ES	Yes
	Broad thorax, mild scoliosis	No anomalies by ultrasound	Normal	Vision is good. Strabismus.	Bilateral undescended testes (operated)	Hypoglycemia. Inverted nipples.	By ES also has a de novo htz PTPRN mutation (c.2767G>A; p.Asp923Asn). Array CGH: a paternal deletion at 2p12 (863 kb), a maternal deletion at 15q13.3 (389 kb) and a maternal duplication at 16p11.2p11.1 (881 kb). Sanger testing: MED12, KAT6B, CREBBP, EP300; no mutations.	ES	Yes
		Patient had a patent ductus arteriosus and bicuspid aortic valve, but is asymptomatic (no cardiac surgery)	Failed newborn hearing screen. Bilateral mild falling to moderate sensorineural hearing loss; hearing aids recommended.	Strabismus. Normal vision.	NA	Inguinal hernia s/p repair	CMA - normal, PTEN - normal, karyotype - 46,XY, FISH Prader-Willi/Angelman - normal, Fragile X - negative, CREBBP gene analysis - normal, metabolic workup - normal	ES	Yes
Bilateral hamstring contractures, adductor and ankle spasticity, metatarsus adductus	Thoracic scoliosis, pectus carinatum	Normal	Two failed ABRs	Abnormal VER	NA	Curtis marmorata, diastasis recti, hyperreflexia, hiatal hernia	180K oligonucleotide CGH array: normal	ES	Yes

Characterization of *TRAF7* germline variants at a phenotypic and molecular level

Progressive brachymetatarsy of IVth toes, brachydactyly of fingers, unilateral camptodactyly of Vth finger	Short neck	Premature atherosclerosis, ischemic cardiopathy at 41 yrs	Normal	Normal	NA	Premature balding. Inverted nipples. Edema of lower limbs.	Normal CGH. FLNA gene testing (no mutation).	ES	Yes
Metatarsus varus	NA	Atrial septal defect	Normal	Normal	NA	Poor sweating. Dry skin. Keratosis pilaris.	ND	Sanger	NAP
Normal	NA	Normal	Normal	Normal	NA	Poor sweating	ND	Sanger	NAP
Appear normal. No restriction of joint motion.	Skeletal survey (4 yrs 2 mos): diminished height of the posterior aspect of the lower thoracic and lumbar vertebral bodies, with irregularity of the anterior margin of these vertebral bodies; anterior protrusion of the lower margin of the sternum compatible with a pectus carinatum deformity. Delayed bone age: bone age is estimated to be 3 yrs at chronologic age 5 yrs 6 mos; bone mineralization and appearance of the growth plates is normal. Short neck.	At 15 mos, echocardiogram identified a patent ductus arteriosus (subsequently repaired) with mild left atrial and ventricular dilation without evidence of coarctation of the aorta; his EEG was normal.	Failed newborn hearing screen. Pressure equalizing tubes placed and subsequently thought normal.	Normal	Right undescended testicle	Hypothyroidism, on treatment.	Fragile X – normal. CMA – normal. Noonan panel (BRAF, CBL, HRAS, KRAS, MAP2K1, MAP2K2, NRAS, PTPN11, RAF1, SHOC2, SOS1) – normal.	ES	Yes
Long and slender fingers. Clinodactyly.	Barrel-shaped thorax. Spondylolisthesis L5-S1 with pain, paraparesis and urinary incontinence at 10 yrs. Operated at 12 yrs: decompression and osteosynthesis, posterior fixation of L4-L5 and S1. Kyphosis with narrow cervical canal (C2-C3). Altered MEP and SSEP, with improvement after surgery.	Heart echography: mild mitral insufficiency	Normal	Normal	NA	Inverted nipples	Array-CGH, FMR1, CDG, VICFA, blood amino acid chromatography, urinary organic acid chromatography, urinary oligosaccharides and mucopolysaccharides	ES	Yes
Camptodactyly of toes II and fingers II and V with limited joint motion. Sandal gap. Pes planus.	Short and broad neck, pectus carinatum	Patent ductus arteriosus	Normal	Normal	Left pelvic kidney		Array CGH	Targeted NGS of a panel of candidate neurocristopathy genes	Yes
Very flat and narrow feet. Feet rotated laterally. Long first toes.	Short neck with webbing both laterally and anteriorly. Barrel shaped chest. Scoliosis. Compressed cervical spinal cord.	Ventricular septal defect with cleft mitral valve, patent ductus arteriosus	Hearing loss with hearing aids until age 5 yrs	NA	Multicystic dysplastic kidney with compensatory hypertrophy of opposite kidney	Hypertrichosis lower back. Restrictive lung disease due to left hemidiaphragm elevation and scoliosis. Poor sleep.	Negative CMA, negative Noonan panel, negative Jacobsen syndrome testing. Autism ID Xpanded panel: no mutation in 2300+ genes apart from TRAF7.	Autism/ID Xpanded panel	Yes
Some laxity to the knees and a skew foot appearance. Hockey stick palmar crease pattern.	Pectus carinatum, short neck	History of patent ductus arteriosus that closed spontaneously. Persistent left superior vena cava with drainage to the coronary sinus. Echocardiogram at 2 yrs revealed increased trabeculations in left ventricular apex and lateral wall. Most recent echocardiogram at 4 yrs 4 mos: stable increased trabeculations in left ventricular apex and lateral wall. Left ventricular size and systolic function are normal. Subjectively, the aortic sinus seemed dilated but imaging suboptimal due to patient activity.	Severe rising to mild hearing loss bilaterally. Unmasked bone conduction testing suggests a mixed component for at least one ear. Wears binaural behind-the-ear hearing aids.	Normal ophthalmologic examinations.	Bilateral mild hydronephrosis, possible stage I chronic renal disease versus renal dysplasia, malrotated right kidney.	Fair complexion for his family with an ongoing mottled appearance to the skin. Wide and low-placed nipples.	Normal CMA using the Affymetrix CytoScan HD array. Noonan syndrome testing: BRAF, HRAF, ES KRAS, MEK1, MAK2, NRAS, PTPN11, RAF1, SOS1, CBL, SPRED1, the recurrent variant in SHOC2 and RIT1. Normal methylation analysis for Prader-Willi syndrome. Urine organic and plasma amino acid analyses were unrevealing. Normal lactate, pyruvate and creatine kinase. Isoelectric transferrin testing was not considered to be consistent with a congenital disorder of glycosylation. He has had normal N-glycan profile. He has had normal connexin 26 testing. He has an elevated cholesterol level.	ES	Yes
NA	J shaped sella turcica, beaking of the L1 vertebral body, pectus carinatum	Atrial septal defect that closed spontaneously	Hearing loss requiring hearing aids	Incomplete coloboma of the right optic nerve, exotropia	NA	Lymphedema in the legs	Karyotype, CMA, Noonan syndrome panel, craniosynostosis gene panel, metabolic screening	ES	Yes
Flexion deformity in upper limbs with ulnar deviation of the fingers, camptodactyly, pes valgus, left foot and ankle deformity, overlapping toes	Short neck, slender ribs with prominent sternum. By MRI, the atlas is dysmorphic and displaced anteriorly.	NA	NA	Divergent strabismus	Clitoris hypertrophy	Only needs to sleep for a few hours	Normal karyotype. By ES, a de novo VUS in TM9SF1; c.638T>C; p.Val213Ala.	Trio ES	Yes
Bilateral brachyphalangy of digits II and V	Narrow spinal canal	Patent ductus arteriosus	Hearing loss of 30 dB at mean, predominant on low frequencies without need for hearing devices	Myopia and astigmatism	NA	Muscular look, supernumerary nipple, inverted nipples	CMA : microdeletion 2p13 inherited from father	ES	Yes
Digit III brachydactyly	Prominent lower ribs, bell shaped thorax, short neck, bifid sacral bone	Patent ductus arteriosus, atrial septal defect	Normal. Bilateral eustachian tube dysfunction; corrected with surgery.	Normal	NA	Inverted nipples	FISH for chr 13, 18, 21, X, Y: normal. CMA: normal. ID Next gene panel: negative. ES: CELSR1 (VUS, c.8807C>T, p.Pro2936Leu), TGFβ2 (VUS, c.101G>A, p.Arg34His).	ES	Yes
Slender fingers, unilateral radial deviation of distal phalanx of finger II, unilateral camptodactyly of finger V, leg length asymmetry, broad toes with mild camptodactyly, sandal gaps, luxation of left elbow twice	Short and broad neck, fusion of 4th and 5th left ribs, pectus carinatum	Normal echocardiogram	Hearing loss, hearing devices. Cholesteatoma removed.	Mild myopia	Normal	Recurrent infections, CT scan: apical dysteleclases	Karyotyping of blood and fibroblasts, chromosome instability testing, array-CGH (paternally inherited 387 bp deletion at 12p12.2p12.2), NGS panel (2741 HPO genes)	Trio ES	Yes

RESULTS: Chapter 2

Normal (upper arm length is 14 cm, forearm length is 11 cm, hands are 85 mm long with a 52 mm palm length)	Mild pectus carinatum	Patent ductus arteriosus requiring surgical coiling to close, with subsequent difficulty to remove the coil and thus requiring open heart surgery. The patent ductus arteriosus is currently (at 2 yrs) patent at about 1 mm.	Normal	Normal	Fetal hydronephrosis	Right inguinal hernia	Oligo-SNP array without copy number variation identified, but there were three areas of homozygosity identified (via GRCH37/hg 19 Genome assembly): 3q26.2q27.1 (169,004,818-184,474,305) hnz, 7q11.21q11.22 (62,461,703-70,031,272) hnz, 11q14.1q14.2 (82,312,013-87,858,362) hnz	Trio ES	Yes
Overriding toes. Brachymesophalangy of fingers II and V.	Short neck, pectus carinatum, anteverted shoulders	Patent ductus arteriosus requiring surgery	ND	Astigmatism	Unilateral pelvic kidney	Inguinal hernia	Normal array-CGH 60k	Sanger sequencing of WD40 repeats	Yes
Anomalous palmar creases with additional creases bilaterally. Overlapping toes (IV on III) and shorter toes IV and V. Limbs are hard to flex, but no contractures	Conus medullaris terminates at the level of the inferior endplate of L3	Isolated left-sided superior vena cava, small patent ductus arteriosus	Failed newborn hearing screen. ABR NA results suggest normal hearing for 2000-4000 Hz in right ear and mild to moderate hearing loss for speech spectrum in left ear.		Tanner 1 female	Weak cry, Small umbilical hernia.	Negative SNP microarray, 46,XX, passed newborn metabolic screening	Clinical trio ES	Yes
Webbing of finger joints, pes planus, overlapping toes (II III), limited rotation of elbows, contractures of distal phalanges	Pectus carinatum. Short, webbed neck. Severe osteoporosis discovered after broken femur in 20s. Spinal fusion of L4-L5.	Patent ductus arteriosus, atrial septal defect, ventricular septal defect, aortic aneurysm	Mixed hearing loss, bilaterally diagnosed at age 2 yrs. Wears hearing aids. History of pressure equalizing tubes.	Astigmatism, wears glasses for myopia	Cryptorchidism	Frequent upper respiratory infections, some requiring hospitalization. Thinning hair.	Noonan panel - normal	ES	Yes
Long and slightly broad toes I, slightly shallow palmar creases, sandal gaps	Cranio-cervical junction anomaly noted at 12 yrs: marked stenosis at the level of the foramen magnum, with obliteration of the subarachnoid space, structurally abnormal C1 and C2 vertebral bodies. At 13 yrs, C1 laminectomy and C2 occipital spine fusion. Short neck.	Patent ductus arteriosus, primum atrial septal defect, cleft mitral valve - s/p repair	Normal	Mild myopia bilaterally, slightly anomalous optic nerves	Pelvic right kidney, normal left kidney	High pain threshold versus doesn't communicate pain	Karyotype; 22q11.2 FISH; microarray; fragile X; MECP2 sequencing and deletion/duplication testing; sequencing of PTPN11, KRAS, SOS1, FOXC1; Noonan spectrum chip (BRAF, HRAS, MEK1, MEK2, NRAS, PTPN11, RAF1, SOS1 and common SHOC2 mutation testing)	Quad ES (with parents and unaffected sibling)	Yes
Progressive contractures of digits and toes, lateral deviation of fingers, left single palmar crease, adducted left thumb (requiring surgery), restricted supination at the left elbow, syndactyly of fingers II-III, pes planus, overlapping toes	Pectus carinatum, short neck, cervical stenosis, thoracic syrinx. At 12 years, developed clinical signs of myelopathy and underwent cervical spine decompression.	Ventricular septal defects, bicuspid aortic valve	Conductive hearing loss requiring hearing aids	Convergent right strabismus	Hypospadias, pelvic kidney	Inguinal hernia (requiring surgery)	SNP microarray, chromosome breakage analysis, karyotype on skin cells and blood, 7 dehydrocholesterol	Singleton ES	Yes
Thumb laxity (metacarpophalangeal joint), overlapping toes, joint contractures of elbow and lower limbs	Short neck	Patent ductus arteriosus (surgery at 9 yrs)	Normal	Optic atrophy	Hypospadias (mild), unilateral cryptorchidism	Cervical syringomyelic cavity	Karyotype, array-CGH, NGS ID panel (285 genes), craniosynostosis panel	ES	Yes
NA	NA	Patent ductus arteriosus (s/p ligation at 7 mos), bicuspid aortic valve	Suspected hearing loss, several audiology evaluations were inconclusive	NA	NA	Frequent infections, atopic dermatitis	CMA normal	Trio ES	Yes
Pes planus	Mild pectus carinatum, short neck	Normal echocardiogram	Normal	Mild myopia bilaterally	Varicocele on the left side of scrotum	Inguinal hernia	Normal male karyotype (46,XY). No microdeletions or translocations. Fragile X - normal.	Trio ES	Yes

Supplementary Table S2. Characteristics of the *TRAF7* variants identified in the 43 index cases.

¹Parentheses around patients 1, 2 and 4 indicate that their variants should be considered of unknown significance. ²cDNA coordinates refer to NM_032271.2.

Patient number ¹	Mutation (cDNA) ²	Mutation (protein)	gnomAD	PolyPhen2 (score)
(1)	c.981C>A	p.(Asp327Glu)	absent	Pos.Dam (0.56)
(2)	c.1089C>A	p.(Asp363Glu)	absent	benign (0.008)
3	c.1097C>T	p.(Ser366Phe)	absent	Prob.Dam (0.976)
(4)	c.1109C>T	p.(Ala370Val)	absent	Pos.Dam (0.913)
5	c.1148A>C	p.(Gln383Pro)	absent	Prob.Dam (0.999)
6, 7	c.1204C>G	p.(Leu402Val)	absent	Prob.Dam (1)
8	c.1211T>A	p.(Val404Asp)	absent	Prob.Dam (0.999)
9, 10	c.1223G>A	p.(Gly408Asp)	absent	Prob.Dam (0.999)
11	c.1328T>G	p.(Leu443Arg)	absent	Pos.Dam (0.942)
12	c.1494G>T	p.(Lys498Asn)	absent	Prob.Dam (1)
13, 14	c.1555C>T	p.(Leu519Phe)	absent	Prob.Dam (0.998)
15-18	c.1570C>T	p.(Arg524Trp)	absent	Prob.Dam (1)
19, 20	c.1673C>T	p.(Ser558Phe)	absent	Prob.Dam (0.998)
21	c.1673C>A	p.(Ser558Tyr)	absent	Prob.Dam (0.999)
22, 23	c.1708C>G	p.(His570Asp)	absent	Pos.Dam (0.921)
24	c.1851C>G	p.(Phe617Leu)	absent	Prob.Dam (1)
27	c.1849T>C	p.(Phe617Leu)	absent	Prob.Dam (1)
28	c.1850T>C	p.(Phe617Ser)	absent	Prob.Dam (1)
29	c.1873C>G	p.(Leu625Val)	absent	Prob.Dam (0.998)
30	c.1885A>C	p.(Ser629Arg)	absent	Pos.Dam (0.606)
31	c.1936G>C	p.(Val646Leu)	absent	Prob.Dam (1)
32-44	c.1964G>A	p.(Arg655Gln)	absent	Prob.Dam (0.997)
45	c.1975G>T	p.(Gly659Trp)	absent	Prob.Dam (1)

Supplementary Table S3. Summary of phenotypes associated with *TRAF7* variants in the core cohort of 42 cases (patients 3 and 5-45). *, three patients born significantly prematurely are included within the total number of cases with patent ductus arteriosus.

	Total (n=42)
Pregnancy/Birth	
Preterm born	10
Fluid accumulation	8
Feeding difficulties	
Short stature	12
Low weight	5
Microcephaly, macrocephaly	5, 5
Cognitive development, speech	
Speech delay	29
Intellectual disability	23
Autism spectrum disorder	6
Motor development	
Motor delay	30
Hypotonia	17
Epilepsy	
	7
Brain MRI	
Prominence of ventricles	10
Cysts	5
Hemorrhaging, hematoma or hygroma	3
Cerebellar anomalies	3
Corpus callosum anomalies	4
Periventricular white matter anomalies	4
Dysmorphic craniofacial features	
Blepharophimosis	33
Epicanthus	20
Telecanthus	14
Ptosis	19

Hypertelorism	17
Up- or downslanting palpebral fissures	11
Ear anomalies	27
Bulbous nasal tip	17
Anteverted nares	7
Wide and/or flat nasal bridge	11
Micro- and/or retrognathia	13
Skull shape anomalies	18
Craniosynostosis	3
Tall, wide or prominent forehead	11
Oral cavity, teeth, pharynx, upper respiratory tract	
Palatal anomalies	15
Dental anomalies	9
Limbs, extremities	
Contractures or joint limitation (other than fingers/toes)	8
Hypermobility	4
Dislocation or subluxation	3
Deviation of fingers (radial, ulnar)	10 (6, 4)
Camptodactyly	10
Brachydactyly	6
Syndactyly	5
Palmar crease abnormalities	7
Overlapping toes	10
Pes planus	10
Varus anomalies	5
Valgus anomalies	5
Sandal gap	5
Long first toes	4
Other skeletal	
Short neck	24
Pectus carinatum	17

Other chest shape anomalies	10
Vertebral anomalies	14
Scoliosis, kyphosis, lordosis	7
Rib anomalies	5
Delayed bone age	4
Cardiac	
Patent ductus arteriosus	24*
Atrial septal defect	9
Ventricular septal defect	6
Valvular defects (bicuspid aortic, mitral defects)	10 (6, 4)
Hearing	
Hearing loss (conductive, sensorineural, mixed, unknown)	21 (9, 2, 2, 8)
Eyes, vision	
Refractive errors	10
Strabismus	10
Optic disc or nerve anomalies	5
Urogenital	
Kidney abnormalities	10
Cryptorchidism	7
External genitalia abnormalities (male, female)	5 (3, 2)
Other phenotypes	
Hernias (inguinal, umbilical, hiatal)	11 (7, 3, 1)
Progressive thinning of scalp hair (female, male)	3 (2, 1)
Inverted nipples	6
Keratosis pilaris	3
Lower limb edema	3
Recurrent infections	4

Supplementary Table S4. Detailed list of DEGs identified in *TRAF7* syndrome patient fibroblasts by RNA-Seq. Only those DEGs with an adjusted p-value <0.05 and |log₂ fold change| in expression ≥1 are listed.

TNF α -				
Gene	Ensembl Gene ID	Log2 FC	FC	FDR
<i>PCOLCE2</i>	ENSG00000163710	2,20	4,60	9,76E-04
<i>CFD</i>	ENSG00000197766	2,19	4,56	1,34E-03
<i>ABI3BP</i>	ENSG00000154175	2,11	4,31	1,98E-05
<i>KLF4</i>	ENSG00000136826	1,90	3,74	1,26E-03
<i>ACKR3</i>	ENSG00000144476	1,89	3,71	4,74E-03
<i>DMKN</i>	ENSG00000161249	1,89	3,71	1,40E-02
<i>GPC6</i>	ENSG00000183098	1,85	3,60	1,24E-02
<i>PIM1</i>	ENSG00000137193	1,77	3,41	2,00E-04
<i>RARRES3</i>	ENSG00000133321	1,64	3,11	3,19E-02
<i>RHOB</i>	ENSG00000143878	1,64	3,11	1,52E-02
<i>ADA</i>	ENSG00000196839	1,60	3,03	6,67E-03
<i>MCUB</i>	ENSG00000005059	1,57	2,98	5,62E-04
<i>ATOH8</i>	ENSG00000168874	1,55	2,94	5,61E-03
<i>ANK2</i>	ENSG00000145362	1,51	2,84	2,16E-03
<i>SCCPDH</i>	ENSG00000143653	1,39	2,62	1,39E-05
<i>DCLK1</i>	ENSG00000133083	1,38	2,60	4,43E-03
<i>HRH1</i>	ENSG00000196639	1,37	2,58	2,47E-03
<i>C6orf132</i>	ENSG00000188112	1,36	2,56	4,30E-14
<i>TCF7</i>	ENSG00000081059	1,35	2,55	3,83E-02
<i>METRNL</i>	ENSG00000176845	1,34	2,54	3,29E-05
<i>GPCPD1</i>	ENSG00000125772	1,33	2,52	9,03E-05
<i>EBF1</i>	ENSG00000164330	1,33	2,51	3,19E-02
<i>DENND3</i>	ENSG00000105339	1,32	2,50	9,14E-03
<i>HSD3B7</i>	ENSG00000099377	1,31	2,47	5,84E-04
<i>NFIA</i>	ENSG00000162599	1,30	2,47	2,76E-02
<i>ARHGAP26</i>	ENSG00000145819	1,29	2,44	2,61E-03
<i>KAZALD1</i>	ENSG00000107821	1,24	2,36	1,50E-02
<i>LAMC1</i>	ENSG00000135862	1,23	2,35	1,48E-03
<i>STS</i>	ENSG00000101846	1,22	2,32	1,73E-03
<i>S100A10</i>	ENSG00000197747	1,20	2,30	1,47E-02
<i>BASP1</i>	ENSG00000176788	1,18	2,26	1,40E-03
<i>ZNF703</i>	ENSG00000183779	1,15	2,22	1,79E-02
<i>VIM</i>	ENSG00000026025	1,09	2,13	5,31E-05
<i>C15orf39</i>	ENSG00000167173	1,08	2,11	2,04E-03
<i>MCM2</i>	ENSG00000073111	1,07	2,10	3,21E-02
<i>ARNTL2</i>	ENSG00000029153	1,05	2,08	1,22E-02
<i>FYCO1</i>	ENSG00000163820	1,04	2,05	8,46E-03
<i>AFAP1L1</i>	ENSG00000157510	1,03	2,04	3,62E-02
<i>FOXP1</i>	ENSG00000114861	1,02	2,03	7,08E-03
<i>PIDD1</i>	ENSG00000177595	-1,03	0,49	9,87E-04

<i>RFX3</i>	ENSG00000080298	-1,04	0,49	1,46E-03
<i>ARMC9</i>	ENSG00000135931	-1,05	0,48	2,03E-02
<i>C14orf37</i>	ENSG00000139971	-1,06	0,48	5,84E-03
<i>TMEM2</i>	ENSG00000135048	-1,06	0,48	3,31E-02
<i>PGM2L1</i>	ENSG00000165434	-1,10	0,47	3,54E-02
<i>STC2</i>	ENSG00000113739	-1,15	0,45	5,68E-03
<i>FRK</i>	ENSG00000111816	-1,18	0,44	2,67E-02
<i>UAP1L1</i>	ENSG00000197355	-1,18	0,44	4,77E-04
<i>PTK7</i>	ENSG00000112655	-1,20	0,43	4,07E-03
<i>BACE2</i>	ENSG00000182240	-1,25	0,42	5,95E-03
<i>BDH1</i>	ENSG00000161267	-1,27	0,41	1,65E-04
<i>SRPX2</i>	ENSG00000102359	-1,30	0,41	5,61E-03
<i>ARHGEF28</i>	ENSG00000214944	-1,30	0,41	1,29E-03
<i>KIAA1549</i>	ENSG00000122778	-1,30	0,41	1,07E-02
<i>MSI2</i>	ENSG00000153944	-1,34	0,39	1,42E-05
<i>ENPP1</i>	ENSG00000197594	-1,36	0,39	7,75E-03
<i>MDGA1</i>	ENSG00000112139	-1,37	0,39	2,76E-02
<i>HLA-B</i>	ENSG00000234745	-1,38	0,39	1,84E-03
<i>SLC22A17</i>	ENSG00000092096	-1,38	0,38	7,92E-03
<i>EHD3</i>	ENSG00000013016	-1,40	0,38	1,50E-02
<i>EDN1</i>	ENSG00000078401	-1,44	0,37	2,19E-02
<i>KHDRBS3</i>	ENSG00000131773	-1,45	0,36	1,27E-02
<i>SYNGR2</i>	ENSG00000108639	-1,47	0,36	3,38E-04
<i>MMP16</i>	ENSG00000156103	-1,49	0,36	9,87E-04
<i>DNAJC6</i>	ENSG00000116675	-1,56	0,34	4,40E-04
<i>PARD6G</i>	ENSG00000178184	-1,61	0,33	1,46E-03
<i>TLE4</i>	ENSG00000106829	-1,62	0,33	2,61E-03
<i>PIK3CD</i>	ENSG00000171608	-1,63	0,32	6,06E-03
<i>TRIM16L</i>	ENSG00000108448	-1,64	0,32	1,07E-03
<i>FIGN</i>	ENSG00000182263	-1,75	0,30	5,31E-05
<i>IFI6</i>	ENSG00000126709	-1,77	0,29	8,49E-03
<i>COL27A1</i>	ENSG00000196739	-1,85	0,28	1,35E-04
<i>P2RX6</i>	ENSG00000099957	-1,94	0,26	2,11E-12
<i>WNT5A</i>	ENSG00000114251	-2,04	0,24	3,42E-03
<i>ANGPT1</i>	ENSG00000154188	-2,07	0,24	9,95E-08
<i>KIF26B</i>	ENSG00000162849	-2,20	0,22	4,32E-04

TNF α +

Gene	Ensembl Gene ID	Log2 FC	FC	FDR
CFD	ENSG00000197766	2,12	4,34	2,89E-03
CCDC69	ENSG00000198624	1,96	3,89	1,00E-02
PCOLCE2	ENSG00000163710	1,96	3,88	5,86E-03
EFEMP1	ENSG00000115380	1,85	3,59	4,07E-02
DMKN	ENSG00000161249	1,77	3,41	3,18E-02
ABI3BP	ENSG00000154175	1,74	3,33	1,21E-03
GPC6	ENSG00000183098	1,72	3,30	3,01E-02
SYPL2	ENSG00000143028	1,70	3,25	3,91E-02

MITF	ENSG00000187098	1,68	3,21	3,10E-03
TCF7	ENSG00000081059	1,67	3,17	8,02E-03
NR1H3	ENSG00000025434	1,65	3,14	1,97E-03
KAZALD1	ENSG00000107821	1,64	3,12	6,09E-04
ANK2	ENSG00000145362	1,60	3,03	1,26E-03
NFIA	ENSG00000162599	1,58	2,99	5,87E-03
CAMK1D	ENSG00000183049	1,58	2,99	2,95E-02
MCUB	ENSG00000005059	1,56	2,94	9,56E-04
ADA	ENSG00000196839	1,54	2,90	1,33E-02
EBF1	ENSG00000164330	1,39	2,61	2,95E-02
AC009549.1	ENSG00000270607	1,34	2,52	1,75E-02
STS	ENSG00000101846	1,33	2,52	6,09E-04
MTMR9LP	ENSG00000220785	1,33	2,52	1,69E-02
ADTRP	ENSG00000111863	1,33	2,51	1,45E-02
HSD3B7	ENSG00000099377	1,30	2,46	1,04E-03
SMAP2	ENSG00000084070	1,25	2,38	3,21E-03
C8orf48	ENSG00000164743	1,25	2,38	2,69E-02
SUOX	ENSG00000139531	1,21	2,32	1,30E-02
ABCA6	ENSG00000154262	1,18	2,26	3,18E-02
FYCO1	ENSG00000163820	1,16	2,24	3,21E-03
RNF150	ENSG00000170153	1,10	2,15	2,01E-02
SCCPDH	ENSG00000143653	1,10	2,14	1,72E-03
HELLS	ENSG00000119969	1,09	2,13	4,42E-02
CEP120	ENSG00000168944	1,08	2,12	3,01E-03
LARGE1	ENSG00000133424	1,07	2,10	4,58E-02
PARP16	ENSG00000138617	1,02	2,03	5,36E-03
ADGRL2	ENSG00000117114	1,01	2,01	8,47E-03
CARMIL1	ENSG00000079691	1,01	2,01	6,94E-03
NDRG1	ENSG00000104419	-1,01	0,50	1,06E-03
KIF21A	ENSG00000139116	-1,03	0,49	1,21E-03
PRKCA	ENSG00000154229	-1,04	0,48	2,85E-02
FRMD6-AS1	ENSG00000273888	-1,05	0,48	4,36E-02
DNAJC6	ENSG00000116675	-1,05	0,48	4,15E-02
MALT1	ENSG00000172175	-1,09	0,47	4,40E-04
TANC1	ENSG00000115183	-1,09	0,47	8,06E-03
STARD13	ENSG00000133121	-1,10	0,46	5,52E-03
CCDC102A	ENSG00000135736	-1,14	0,45	1,00E-02
ARHGAP29	ENSG00000137962	-1,14	0,45	3,01E-03
ADAMTS12	ENSG00000151388	-1,16	0,45	1,11E-02
SRPX2	ENSG00000102359	-1,17	0,45	2,05E-02
ARHGEF19	ENSG00000142632	-1,17	0,44	2,18E-02
GADD45A	ENSG00000116717	-1,22	0,43	5,86E-03
BACE2	ENSG00000182240	-1,23	0,43	9,57E-03
MARCH9	ENSG00000139266	-1,24	0,42	2,69E-02
PTK7	ENSG00000112655	-1,26	0,42	3,10E-03
ITM2C	ENSG00000135916	-1,29	0,41	7,41E-03

MSI2	ENSG00000153944	-1,31	0,40	2,53E-05
SYNGR2	ENSG00000108639	-1,32	0,40	2,38E-03
TLE4	ENSG00000106829	-1,34	0,39	2,43E-02
MMP16	ENSG00000156103	-1,35	0,39	5,44E-03
ABCC3	ENSG00000108846	-1,35	0,39	1,90E-02
PLOD2	ENSG00000152952	-1,36	0,39	2,82E-02
WNT5B	ENSG00000111186	-1,37	0,39	9,06E-03
FRK	ENSG00000111816	-1,38	0,38	7,40E-03
RRAD	ENSG00000166592	-1,41	0,38	1,66E-02
STC2	ENSG00000113739	-1,42	0,37	4,40E-04
SNHG26	ENSG00000228649	-1,42	0,37	1,24E-02
TRIM16L	ENSG00000108448	-1,46	0,36	6,06E-03
RCAN1	ENSG00000159200	-1,47	0,36	3,48E-02
ENPP1	ENSG00000197594	-1,49	0,36	3,82E-03
PIK3CD	ENSG00000171608	-1,49	0,36	1,90E-02
SGIP1	ENSG00000118473	-1,49	0,36	4,59E-02
AC037198.2	ENSG00000276107	-1,51	0,35	1,07E-03
SLC22A17	ENSG00000092096	-1,51	0,35	3,99E-03
SNORA12	ENSG00000212175	-1,56	0,34	2,89E-03
EDN1	ENSG00000078401	-1,62	0,33	9,09E-03
S1PR3	ENSG00000213694	-1,64	0,32	4,24E-02
LBH	ENSG00000213626	-1,64	0,32	4,21E-02
PARD6G	ENSG00000178184	-1,64	0,32	1,73E-03
COL7A1	ENSG00000114270	-1,69	0,31	1,15E-02
GAS6	ENSG00000183087	-1,71	0,31	4,40E-04
KHDRBS3	ENSG00000131773	-1,80	0,29	1,53E-03
CYR61	ENSG00000142871	-1,82	0,28	1,78E-03
LRRN3	ENSG00000173114	-1,88	0,27	1,51E-02
CPXM2	ENSG00000121898	-1,93	0,26	1,28E-02
ANGPT1	ENSG00000154188	-1,94	0,26	1,22E-06
IL6	ENSG00000136244	-1,98	0,25	4,59E-02
GNA14	ENSG00000156049	-2,14	0,23	1,56E-02
NR4A2	ENSG00000153234	-2,21	0,22	1,82E-02
IL1A	ENSG00000115008	-2,28	0,21	6,99E-03
WNT5A	ENSG00000114251	-2,32	0,20	6,98E-04
LTB	ENSG00000227507	-2,45	0,18	5,57E-07

Supplementary Table S5. Genes selected for qPCR validation. T = transcriptomic criteria, i.e., high differential expression in the RNA-Seq data; F = functional criteria, i.e., for most, alteration in a relevant human disease or animal model. Note that *KRAS*, *SPTAN1*, *CASK*, *MAPK11* and *RIT1* did not meet the log₂ fold change threshold for inclusion in the detailed DEG list in Supplementary Table S4.

Gene	Ensembl Gene ID	- TNF α			+ TNF α			Validated	Selection Criteria
		Log ₂ FC	FC	FDR	Log ₂ FC	FC	FDR		
<i>CFD</i>	<i>ENSG00000197766</i>	2.19	4.56	1.34E-03	2.12	4.34	2.89E-03	Yes	T
<i>GPC6</i>	<i>ENSG00000183098</i>	1.85	3.6	1.24E-02	1.72	3.3	3.01E-02	Yes	T/F
<i>KAZALD1</i>	<i>ENSG00000107821</i>	1.24	2.36	1.50E-02	1.64	3.12	6.09E-04	Yes	T
<i>FOXP1</i>	<i>ENSG00000114861</i>	1.02	2.03	7.08E-03	-	-	-	No	F
<i>KRAS</i>	<i>ENSG00000133703</i>	0.85	1.8	1.07E-12	0.64	1.56	7.22E-07	No	F
<i>SPTAN1</i>	<i>ENSG00000197694</i>	0.51	1.43	3.67E-02	-	-	-	No	F
<i>KIF26B</i>	<i>ENSG00000162849</i>	-2.2	0.22	4.32E-04	-	-	-	Yes	T
<i>ANGPT1</i>	<i>ENSG00000154188</i>	-2.07	0.24	9.95E-08	-1.94	0.26	1.22E-06	Yes	T
<i>WNT5A</i>	<i>ENSG00000114251</i>	-2.04	0.24	3.42E-03	-2.32	0.2	6.98E-04	Yes	T
<i>CASK</i>	<i>ENSG00000147044</i>	-	-	-	-0.84	0.56	3.12E-02	Yes	F
<i>MAPK11</i>	<i>ENSG00000185386</i>	-0.68	0.62	1.02E-03	-0.69	0.62	1.21E-03	No	F
<i>RIT1</i>	<i>ENSG00000143622</i>	-0.49	0.71	4.41E-02	-	-	-	No	F

Supplementary Table S6. Complete list of significant IPA pathways and functions. Categories are ordered according to their p-values. A cutoff of 0.05 was chosen.

Enriched signaling and metabolic canonical pathways

Adipogenesis pathway
 Axonal Guidance Signaling
 UDP-N-acetyl-D-glucosamine Biosynthesis II
 Chemokine Signaling
 Wnt/Ca⁺ Pathway
 Renin-Angiotensin Signaling
 Thrombin Signaling
 Neuropathic Pain Signaling In Dorsal Horn Neurons
 Role of NFAT in Cardiac Hypertrophy
 Synaptic long term potentiation
 GP6 Signaling Pathway
 Mouse Embryonic Stem cell Pluripotency
 Regulation of The Epithelial-Mesenchymal Transition Pathway
 GNRH Signaling
 Basal Cell Carcinoma Signaling
 Endothelin-1 Signaling
 Human Embryonic Stem Cell Pluripotency
 RAN Signaling
 Role of Macrophages, Fibroblasts and Endothelial Cells in Rheumatoid Arthritis
 Ovarian Cancer Signaling
 Adrenomedullin signaling pathway
 Role of Wnt/GSK-3 β Signaling in the Pathogenesis of Influenza
 Apelin Endothelial Signaling Pathway
 Sperm motility
 Molecular Mechanisms of Cancer
 Role of NANOG in Mammalian Embryonic Stem Cell Pluripotency
 Protein Kinase A Signaling
 PPAR α /RXR α Activation
 Hepatic Fibrosis/Hepatic Stellate Cell Activation
 Role of Tissue Factor in Cancer
 PCP Pathway
 Polyamine Regulation in Colon Cancer
 Colorectal Cancer Metastasis Signaling
 UVA-Induced MAPK Signaling
 Glioblastoma Multiforme Signaling
 Aldosterone Signaling in Epithelial Cells
 Role of Osteoblasts, Osteoclasts and Chondrocytes in Rheumatoid Arthritis
 Neuroprotective Role of THOP1 in Alzheimer's Disease
 LXR/RXR Activation
 Paxillin Signaling
 Glioma Signaling
 Cardiac Hypertrophy Signaling
 Breast Cancer Regulation by Stathmin1
 Melatonin Signaling
 UDP-N-acetyl-D-galactosamine Biosynthesis II
 IL-15 Production
 GPCR-Mediated Integration of Enteroendocrine Signaling Exemplified by an L Cell
 fMLP Signaling in Neutrophils
 CREB Signaling in Neurons
 G-Protein Coupled Receptor Signaling
 Integrin Signaling

Sonic Hedgehog Signaling
 RANK Signaling in Osteoclasts
 Gαq Signaling
 Glioma Invasiveness Signaling
 CD28 Signaling in T Helper Cells
 B Cell Receptor Signaling
 Glycogen Degradation II
 Bile Acid Biosynthesis, Neural Pathway
 EIF2 Signaling
 PKCθ Signaling in T Lymphocytes
 PI3K Signaling in B Lymphocytes
 14-3-3-mediated Signaling
 P2Y Purigenic Receptor Signaling Pathway
 VEGF Signaling
 Inhibition of Angiogenesis by TSP1
 Tec Kinase Signaling
 GPCR-Mediated Nutrient Sensing by Enteroendocrine
 Glycogen Degradation III
 UDP-D-xylose and UDP-D-glucuronate Biosynthesis
 Putrescine Biosynthesis III
 Regulation of IL-2 Expression in Activated and Anergic T Lymphocytes
 Apelin Cardiomyocyte Signaling Pathway
 Gap Junction Signaling
 Clathrin-mediated Endocytosis Signaling

Enriched Cellular Functions and Physiological System Development

Cancer
 Organismal Injury and Abnormalities
 Endocrine System Disorders
 Cellular Movement
 Gastrointestinal Disease
 Cardiovascular System Development and Function
 Reproductive System Disease
 Organismal Development
 Renal and urological system development and function
 Embryonic development
 Organismal Survival
 Cell Death and Survival
 Organ Morphology
 Renal and Urological Disease
 Tissue Development
 Cell-To-Cell Signaling and Interaction
 Cellular Assembly and Organization
 Organ Development
 Hematological Disease
 Immunological Disease
 Cellular Development
 Cellular Growth and Proliferation
 Nervous System Development and Function
 Respiratory Disease
 Carbohydrate Metabolism
 Neurological Disease
 Cell Morphology
 Hepatic System Disease
 Tissue Morphology

Gene Expression
Hair and Skin Development and Function
Developmental Disorder
Dermatological Diseases and Conditions
Lipid Metabolism
Small Molecule Biochemistry
Cardiovascular Disease
Connective Tissue Disorders
Inflammatory Response
Skeletal and Muscular Disorders
Hereditary Disorder
Metabolic Disease
Connective Tissue Development and Function
Skeletal and Muscular System Development and Function
Hematological System Development and Function
Immune Cell Trafficking
Cellular Compromise
Nucleic Acid Metabolism
Molecular Transport
Cell Signaling
Tumor Morphology
Amino Acid Metabolism
Post-Translational Modification
Organismal Functions
Auditory and Vestibular System Development and Function
Lymphoid Tissue Structure and Development
Visual System Development and Function
Ophthalmic Disease
Hematopoiesis
Humoral Immune Response
Auditory Disease

Phenotypic spectrum and transcriptomic profile associated with germline variants in *TRAF7*

Castilla-Vallmanya et al.

Supplementary Discussion:

Differentially expressed genes in *TRAF7* syndrome patient fibroblasts.

To gain a better understanding of the pathogenic role of syndromic *TRAF7* variants, patient fibroblasts were compared with controls at a transcriptomic level. As a first approach, 17 genes were selected and analyzed by qPCR. Nine of these genes had been found to be altered in *TRAF7*-silenced cells in previous studies.¹ From these nine, only three showed differential expression in fibroblasts bearing *TRAF7* syndromic variants compared to controls. In particular, *FLNB* was significantly increased in patients compared to controls (over 2-fold) independently of the treatment, as opposed to *TRAF7* knock-down, which has been shown to lead to a reduction of *FLNB* expression.¹ *FLNB* is an actin-binding protein that regulates dynamic changes of the cytoskeleton and has essential scaffolding functions. Given the skeletal malformations present in patients with *TRAF7* variants, it is interesting that alterations in *FLNB* cause several skeletal dysplasias, including spondylocarpotarsal synostosis syndrome (OMIM #272460), Larsen syndrome (OMIM #150250), atelosteogenesis types I (OMIM #108720) and III (OMIM #108721) and boomerang dysplasia (OMIM #112310).² *IGFBP7* (also known as angiomodulin) was, on the other hand, underexpressed in patient fibroblasts independently of the treatment, while it was found overexpressed in *TRAF7*-depleted cells.¹ It is a matrix-bound factor, with knockdown causing vascular patterning defects in zebrafish³ or inhibition of cardiogenesis in embryonic stem cells.⁴ A homozygous variant in humans causes retinal arterial macroaneurysm with supra-aortic stenosis (OMIM #614224).⁵ Reduced expression of *IGFBP7* may contribute to the cardiovascular defects in *TRAF7* syndrome patients. *TRAF7* syndrome patient fibroblasts also expressed lower levels of *NOTCH3*. *Notch3* knockout mice have defects in arterial differentiation and vascular smooth muscle cell maturation.⁶ Toxic neomorphic variants in *NOTCH3* cause the cerebral arteriopathy CADASIL (OMIM #125310),⁷ while C-terminal truncating variants cause lateral meningocele syndrome (OMIM #130720), which includes craniofacial, skeletal and cardiac defects that partly overlap with those of the *TRAF7* syndrome.⁸ Given that the direction of gene expression changes in patient cells versus *TRAF7*-silenced cells can be divergent (*FLNB*, *IGFBP7*), the same (*NOTCH3*) or unchanged in patients, it is difficult to conclude on the basis of these experiments whether the *TRAF7* variants are more likely gain or loss of function. The

differences could stem from the cell types studied; previous studies on *TRAF7*-silencing were performed in an immortalized cell line¹ while we have analyzed primary fibroblasts.

Six other genes tested are downstream targets of NF- κ B and are involved in processes such as inflammation, tumorigenesis and negative regulation of apoptosis.⁹ From these, two genes showed significantly reduced expression in patient fibroblasts, namely *BCL2* and *PTGS2*. *BCL2* is an anti-apoptotic factor that is deregulated in several human cancers.¹⁰ *PTGS2* encodes COX2, which catalyzes the formation of the prostaglandin precursor PGH2 and is generally considered as an inflammation mediator.¹¹ The expression of *PTGS2* was reduced to one third in the patient fibroblasts without TNF α treatment. Interestingly, COX2 deficiency has been associated with inefficient closure of the ductus arteriosus in mice¹² and we observed patent ductus arteriosus in the majority of *TRAF7* syndrome patients, suggesting a pathogenic effect of COX2 deficiency in this context.

To further characterize the gene expression landscape in patients bearing syndromic *TRAF7* variants, we performed RNA-Seq of skin fibroblasts. Consistent with previous data suggesting that *TRAF7* modulates the activity of several transcription factors, the expression of many genes was affected in patient cells. Pathway enrichment analysis of the identified DEGs highlighted pathways involved in the development and function of the nervous system, which could partly explain the intellectual disability present in patients harboring *TRAF7* variants. Interestingly, the cardiovascular system category was also enriched for DEGs; congenital heart defects are frequent in *TRAF7* syndrome patients. Several DEGs are especially interesting due to the role they play in specific cellular processes and the effects that their alteration can produce. *ANGPT1*, *WNT5A* and *KIF26B* were the most downregulated genes in patient fibroblasts under basal conditions. *ANGPT1* encodes angiotensinogen 1 and homozygous knock-out in mice leads to severe vascular malformations and embryonic lethality.¹³ Conditional knock-outs in mice have shown roles for *Angpt1* in cardiac morphogenesis^{14,15} and its deregulation may contribute to the cardiovascular anomalies observed in our cohort. *Wnt5a* is required for the outgrowth of limbs and craniofacial and genital structures in mice,¹⁶ and variants in *WNT5A* cause autosomal dominant Robinow syndrome (OMIM #180700), a condition which shares some skeletal features with the patients we report here.¹⁷ *KIF26B* encodes a kinesin required for kidney development in mice,¹⁸ and interestingly, together with *WNT5A* and *ROR*, it shapes a crucial noncanonical WNT pathway, especially relevant in cell migration events during embryogenesis.¹⁹ *CASK*, mildly downregulated in the patients, encodes a synaptic scaffolding protein. Loss of function variants in this gene are responsible for an X-linked syndrome associating intellectual disability, microcephaly and pontine and cerebellar hypoplasia (OMIM #300749).²⁰ *GPC6*, *KAZALD1* and *CFD* were among the most

upregulated genes in *TRAF7* syndrome patient fibroblasts. *GPC6* encodes a member of the glypican family of cell-surface heparan sulfate proteoglycans, and *GPC6* variants are responsible for a rare autosomal recessive condition defined by proximally shortened limbs; omodysplasia (OMIM #258315).²¹ *KAZALD1* (also known as *IGFPB-rP10*) is expressed specifically in ossification regions of the head in mice and can promote osteoblast proliferation;^{22,23} *KAZALD1* overexpression could therefore play a role in the craniofacial shape anomalies observed in *TRAF7* syndrome patients. *CFD*, by far the most upregulated gene, encodes the complement factor D, a serine protease that acts in the alternative complement pathway. In humans, factor D deficiency leads to an immunologic condition with susceptibility to bacterial infections.²⁴ The significance of *CFD* upregulation in *TRAF7* syndrome patient cells is unclear.

References

1. Zotti T, Uva A, Ferravante A, et al. TRAF7 protein promotes Lys-29-linked polyubiquitination of IkappaB kinase (IKKgamma)/NF-kappaB essential modulator (NEMO) and p65/RelA protein and represses NF-kappaB activation. *J Biol Chem.* 2011;286(26):22924-22933.
2. Krakow D, Robertson SP, King LM, et al. Mutations in the gene encoding filamin B disrupt vertebral segmentation, joint formation and skeletogenesis. *Nat Genet.* 2004;36(4):405-410.
3. Hooper AT, Shmelkov SV, Gupta S, et al. Angiomodulin is a specific marker of vasculature and regulates vascular endothelial growth factor-A-dependent neoangiogenesis. *Circ Res.* 2009;105(2):201-208.
4. Wolchinsky Z, Shivtiel S, Kouwenhoven EN, et al. Angiomodulin is required for cardiogenesis of embryonic stem cells and is maintained by a feedback loop network of p63 and Activin-A. *Stem Cell Res.* 2014;12(1):49-59.
5. Abu-Safieh L, Abboud EB, Alkuraya H, et al. Mutation of IGFBP7 causes upregulation of BRAF/MEK/ERK pathway and familial retinal arterial macroaneurysms. *Am J Hum Genet.* 2011;89(2):313-319.
6. Domenga V, Fardoux P, Lacombe P, et al. Notch3 is required for arterial identity and maturation of vascular smooth muscle cells. *Genes Dev.* 2004;18(22):2730-2735.
7. Mašek J, Andersson ER. The developmental biology of genetic Notch disorders. *Dev Camb Engl.* 2017;144(10):1743-1763.
8. Gripp KW, Robbins KM, Sobreira NL, et al. Truncating mutations in the last exon of NOTCH3 cause lateral meningocele syndrome. *Am J Med Genet A.* 2015;167A(2):271-281.

9. Li J, Ma J, Wang KS, et al. Baicalein inhibits TNF- α -induced NF- κ B activation and expression of NF- κ B-regulated target gene products. *Oncol Rep.* 2016;36(5):2771-2776.
10. Delbridge ARD, Grabow S, Strasser A, Vaux DL. Thirty years of BCL-2: translating cell death discoveries into novel cancer therapies. *Nat Rev Cancer.* 2016;16(2):99-109.
11. Smith WL, Garavito RM, DeWitt DL. Prostaglandin endoperoxide H synthases (cyclooxygenases)-1 and -2. *J Biol Chem.* 1996;271(52):33157-33160.
12. Loftin CD, Trivedi DB, Tiano HF, et al. Failure of ductus arteriosus closure and remodeling in neonatal mice deficient in cyclooxygenase-1 and cyclooxygenase-2. *Proc Natl Acad Sci U S A.* 2001;98(3):1059-1064.
13. Suri C, Jones PF, Patan S, et al. Requisite role of angiopoietin-1, a ligand for the TIE2 receptor, during embryonic angiogenesis. *Cell.* 1996;87(7):1171-1180.
14. Jeansson M, Gawlik A, Anderson G, et al. Angiopoietin-1 is essential in mouse vasculature during development and in response to injury. *J Clin Invest.* 2011;121(6):2278-2289.
15. Kim KH, Nakaoka Y, Augustin HG, Koh GY. Myocardial Angiopoietin-1 Controls Atrial Chamber Morphogenesis by Spatiotemporal Degradation of Cardiac Jelly. *Cell Rep.* 2018;23(8):2455-2466.
16. Yamaguchi TP, Bradley A, McMahon AP, Jones S. A Wnt5a pathway underlies outgrowth of multiple structures in the vertebrate embryo. *Development.* 1999;126(6):1211-1223.
17. Roifman M, Marcelis CLM, Paton T, et al. De novo WNT5A-associated autosomal dominant Robinow syndrome suggests specificity of genotype and phenotype. *Clin Genet.* 2015;87(1):34-41.
18. Uchiyama Y, Sakaguchi M, Terabayashi T, et al. Kif26b, a kinesin family gene, regulates adhesion of the embryonic kidney mesenchyme. *Proc Natl Acad Sci U S A.* 2010;107(20):9240-9245.
19. Susman MW, Karuna EP, Kunz RC, et al. Kinesin superfamily protein Kif26b links Wnt5a-Ror signaling to the control of cell and tissue behaviors in vertebrates. *eLife.* 2017;6.
20. Najm J, Horn D, Wimplinger I, et al. Mutations of CASK cause an X-linked brain malformation phenotype with microcephaly and hypoplasia of the brainstem and cerebellum. *Nat Genet.* 2008;40(9):1065-1067.
21. Campos-Xavier AB, Martinet D, Bateman J, et al. Mutations in the heparan-sulfate proteoglycan glypican 6 (GPC6) impair endochondral ossification and cause recessive omodysplasia. *Am J Hum Genet.* 2009;84(6):760-770.
22. James MJ, Järvinen E, Thesleff I. Bono1: a gene associated with regions of deposition of bone and dentine. *Gene Expr Patterns GEP.* 2004;4(5):595-599.

23. Shibata Y, Tsukazaki T, Hirata K, Xin C, Yamaguchi A. Role of a new member of IGFBP superfamily, IGFBP-rP10, in proliferation and differentiation of osteoblastic cells. *Biochem Biophys Res Commun.* 2004;325(4):1194-1200.
24. Biesma DH, Hannema AJ, van Velzen-Blad H, et al. A family with complement factor D deficiency. *J Clin Invest.* 2001;108(2):233-240.

CHAPTER 3: Functional characterization of *MAGEL2* truncating mutations and generation of an *in vitro* model for Schaaf-Yang syndrome

Article 9: Advancing in Schaaf-Yang syndrome pathophysiology: from bedside to subcellular analyses of truncated *MAGEL2* in patients' fibroblasts

Summary:

Background: The ultra-rare neurodevelopmental disorder Schaaf-Yang syndrome is caused by truncating mutations in *MAGEL2*, a gene mapping to the Prader-Willi region (15q11-q13). The phenotype observed in SYS patients partially overlaps the one typically observed in patients with Prader-Willi syndrome. *MAGEL2* is known for playing a role in retrograde transport and protein recycling regulation. Our aim is to contribute to the characterization of SYS pathophysiology at clinical, genetic and molecular levels.

Methods: We performed an extensive phenotypic and genetic literature revision of previously reported SYS subjects. We analysed the excretion levels of amyloid- β 1-40 peptide, the metabolomic profile and gene expression (by mRNAseq) in SYS patient's fibroblasts compared to controls. We also transfected cell lines with vectors encoding wild-type or mutated *MAGEL2* to assess its protein stability and subcellular localization.

Results: Based on updated knowledge we offer the first guidelines for clinical management of SYS patients. Functional studies show that A β ₁₋₄₀ levels in the extracellular media of SYS fibroblasts were significantly decreased compared to wild-type. We also found altered expression of 132 genes, many of them related to developmental processes and mitotic mechanisms. The truncated form of *MAGEL2* shows a similar degradation pattern to the WT. However, it was significantly switched to the nucleus, compared to a clear cytoplasmic distribution of the WT.

Conclusion: Our guidelines are a useful tool to improve SYS clinical management. A β ₁₋₄₀ excretion level is a promising biomarker for SYS and further experiments are needed to understand the implication of mutated *MAGEL2* in gene expression and cellular localization changes, which suggest a dominant negative or a gain-of function effect of the truncating variants.

Reference: Laura Castilla-Vallmanya, Mercedes Serrano, Mónica Centeno-Pla, Héctor Franco-Valls, Raúl Martínez-Cabrera, Aina Prat-Planas, Elena Rojano, Pedro Seoane, Miriam Navarro, Clara Oliva, Rafael Artuch, Raquel Rabionet, Daniel Grinberg, Susanna Balcells, Roser Urreizti. Advancing in Schaaf-Yang syndrome pathophysiology: from bedside to subcellular analyses of truncated *MAGEL2* in patients' fibroblasts. To be submitted to Journal of Medical Genetics.

Advancing in Schaaf-Yang syndrome pathophysiology: from bedside to subcellular analyses of truncated *MAGEL2* in patients' fibroblasts

Laura Castilla-Vallmanya^{1,2}, Mercedes Serrano^{2,5}, Mónica Centeno-Pla^{1,2}, Héctor Franco-Valls^{1,2}, Raúl Martínez-Cabrera^{1,2}, Aina Prat-Planas^{1,2}, Elena Rojano³, Pedro Seoane^{2,3}, Miriam Navarro^{2,5}, Clara Oliva⁵, Rafael Artuch^{2,5}, Raquel Rabionet^{1,2}, Daniel Grinberg^{1,2}, Susanna Balcells^{1,2}, Roser Urreiziti^{1,2,5}

1) Department of Genetics, Microbiology and Statistics, Faculty of Biology, University of Barcelona, IBUB, IRSJD, Barcelona, Spain.

2) Centro de Investigación Biomédica en Red de Enfermedades Raras (CIBERER)- Instituto de Salud Carlos III, Spain.

3) Department of Molecular Biology and Biochemistry, University of Malaga, Malaga, Spain.

4) Institute of Biomedical Research in Malaga (IBIMA), Málaga, Spain.

5) Clinical Biochemistry Department, Hospital Sant Joan de Déu, Esplugues de Llobregat, Spain.

ABSTRACT:

Background: The ultra-rare neurodevelopmental disorder Schaaf-Yang syndrome is caused by truncating mutations in *MAGEL2*, a gene mapping to the Prader-Willi region (15q11-q13). The phenotype observed in SYS patients partially overlaps the one typically observed in patients with Prader-Willi syndrome. *MAGEL2* is known for playing a role in retrograde transport and protein recycling regulation. Our aim is to contribute to the characterization of SYS pathophysiology at clinical, genetic and molecular levels.

Methods: We performed an extensive phenotypic and genetic literature revision of previously reported SYS subjects. We analysed the excretion levels of amyloid- β 1-40 peptide, the metabolomic profile and gene expression (by mRNAseq) in SYS patient's fibroblasts compared to controls. We also transfected cell lines with vectors encoding wild-type or mutated *MAGEL2* to assess its protein stability and subcellular localization.

Results: Based on updated knowledge we offer the first guidelines for clinical management of SYS patients. Functional studies show that A β ₁₋₄₀ levels in the extracellular media of SYS fibroblasts were significantly decreased compared to wild-type. We also found altered expression of 132 genes, many of them related to developmental processes and mitotic mechanisms. The truncated form of *MAGEL2* shows a similar degradation pattern to the WT. However, it was significantly switched to the nucleus, compared to a clear cytoplasmic distribution of the WT.

Conclusion: Our guidelines are a useful tool to improve SYS clinical management. A β ₁₋₄₀ excretion level is a promising biomarker for SYS and further experiments are needed to understand the implication of mutated *MAGEL2* in gene expression and cellular localization changes, which suggest a dominant negative or a gain-of function effect of the truncating variants.

INTRODUCTION

In 2013, truncating mutations in *MAGEL2* (OMIM* 605283) were associated with a new clinical entity (1), first described as a Prader-Willi like syndrome and lately named Schaaf-Yang syndrome (SYS; OMIM #615547). *MAGEL2* is a single-exon gene that encodes one of the largest proteins of the Type II MAGE protein family (1249 amino acids long). At a structural level, a proline-rich domain is found at the N-terminal region of *MAGEL2*, whose function remains unclear (Figure 1). At the C-terminus, from amino acid 1027–1195, there is a MAGE Homology Domain (MHD): a highly conserved 170-amino acid sequence, present in both type I and type II MAGEs, crucial for protein-protein interactions (2). Through it, *MAGEL2* recognizes and binds the coiled-coil domain of the E3 ubiquitin ligase, TRIM27. The MHD is also crucial for binding VPS35, a subunit of the retromer cargo-selective complex (3). *MAGEL2*, TRIM27 and USP7 form the MUST complex that is recruited to endosomes through direct binding of *MAGEL2* to VPS35 and plays a role in retrograde endosomal transport (3,4). These specialized endosomes participate in endosomal export pathways that deliver membrane protein cargoes either to the trans-Golgi network through retrograde pathways or to the plasma membrane through recycling pathways (5). *MAGEL2* shows a wider expression in human fetal tissues than in adult tissues, where it is predominantly present in the brain (according to GTEx data (6)). In adult mice, it also becomes mostly restricted to the central nervous system (CNS), specifically to the amygdala and the hypothalamus, and predominantly in the suprachiasmatic, the paraventricular and the supraoptic nuclei (7–9).

A dysfunction of the retrograde transport mechanism could be disturbing for many cellular processes. Loss of *MAGEL2* expression causes a reduction in SG protein levels due to impaired endosomal protein trafficking and subsequent lysosomal degradation, resulting in a reduction of circulating bioactive hypothalamic hormones (9). A well-coordinated trafficking network is also key for the correct regulation of amyloid precursor protein (APP) cleavage (10). APP family members are relevant for neuronal differentiation and migration during cortical development (11,12) and proper neuromuscular junction formation and neurotransmission (13). Many studies support a model where retromer deficiency leads to increased APP cleavage, A β peptides production and exocytosis (14–16). In addition, protein levels of the glucose transporter GLUT1 in the cell membrane are reduced after VPS35 and SNX27 inhibition, showing that they are also tightly regulated by the retromer (17).

MAGEL2 is one of the five maternally imprinted protein-coding genes contained in the Prader-Willi region (15q11-q13). Lack of expression of the paternal alleles in this region causes Prader-Willi syndrome (PWS; OMIM #176270) (18). In contrast, point nonsense or frameshift mutations in the paternal allele of *MAGEL2* are predicted to encode a truncated protein lacking

the MHD domain and have been associated with SYS (1). More than a hundred of SYS patients have been reported and phenotypically described in the literature (1,19–37). SYS and PWS patients show overlapping clinical phenotypes: neonatal hypotonia, intellectual disability (ID), developmental delay (DD), feeding difficulties, and other more specific symptoms such as endocrinologic disturbances /hypogonadism and other hormonal imbalances) and sleep disorders. However, SYS patients generally do not present some of the clinical criteria for PWS diagnosis, such as hypopigmentation, characteristic facial dysmorphisms, small hand and feet, hyperphagia, obesity and obsessive-compulsive behaviours, while severe ID, ASD typical behaviours and joint contractures are more frequently present in SYS than in PWS (38–40). Truncating variants in *MAGEL2* have also been associated with Chitayat-Hall syndrome (CHS; OMIM 208080) in 6 patients (41). However, a systematic review of all SYS and CHS patients showed that there is no discernible difference between both syndromes, either at a clinical or genetic level (34). In contrast, two particular *MAGEL2* truncating mutations have been recurrently identified in patients affected by lethal arthrogryposis multiplex congenita (AMC), a much more severe phenotype (21,27,42–44). At the end, there is no specific constellation of symptoms pathognomonic or specific for any of these clinical syndromes; furthermore, they probably conform to a clinical continuum, therefore denoting the need to address clinical denomination according to molecular findings.

Here, we present a standardized set of guidelines for SYS clinical management based on an extensive literature revision, also expanding the clinical and genetic delineation of this rare neurodevelopmental condition. We also contribute to the knowledge of the cellular phenotype, assessing the effect that a recurrent truncating variant has on *MAGEL2* protein stability and subcellular localization using heterologous expression vectors. Finally, we characterized fibroblasts derived from SYS patients through transcriptomic and metabolomic approaches, interpreting the results in the context of molecular and clinical findings.

METHODS

Literature review: A Cochrane Library search and a PubMed database search was performed from the date of the first clinical description of pathology associated with variants in *MAGEL2* till June 30, 2021, using the following terms: *MAGEL2*, *SYS*, Schaaf-Yang syndrome, and different combinations of these terms. Concerning the data extraction, it included first author, publication year, molecular data (identified mutation and residues changes, de novo or inherited condition), pregnancy and perinatal information, multiorganic clinical data, complementary exams information, neuroimaging, and age and cause of death. Unfortunately, in some clinical series, much clinical information is not detailed.

RNA-sequencing and data analysis: Whole RNA was extracted from fibroblasts using the High Pure RNA Isolation Kit (Roche). RNA-Seq was performed by LEXOGEN, Inc. using the QuantSeq 3' messenger RNA (mRNA)-Seq FWD kit for library preparation. ExpHunter Suite was used to analyse the expression data and perform functional enrichment analyses.

Cell culture: Fibroblasts were obtained from skin biopsies of seven *SYS* patients, nine *PWS* patients and eleven controls. Corresponding informed consent and institutional ethics approval were obtained (Ethics Committee of the Universitat de Barcelona, IRB00003099). Fibroblasts were cultured in Dulbecco's modified eagle medium (DMEM) (Sigma-Aldrich, Merck) supplemented with 10% FBS (Gibco, LifeTechnologies), 1% penicillin–streptomycin (Gibco, LifeTechnologies) and 1% GlutaMAX (Gibco, LifeTechnologies). Conditioned medium for ELISA was only supplemented with 1% penicillin–streptomycin (Gibco, LifeTechnologies) and was collected after 72h. HEK293T cells were cultured in DMEM (Sigma-Aldrich, Merck) supplemented with 10% FBS (Gibco, LifeTechnologies) and 1% penicillin–streptomycin (Gibco, LifeTechnologies). The cDNA sequences of interest (ENST00000650528.1) were cloned in the the mammalian expression vector pcDNATM3.1⁽⁺⁾ (Invitrogen, ThermoFisher Scientific) including a hemagglutinin (HA) tag at the C-terminal end (courtesy of the CRG). The vectors were transfected into 60% confluent HEK293T cells using LipofectamineTM 3000 (Invitrogen, ThermoFisher Scientific) and Opti-MEMTM (Gibco, LifeTechnologies). Cells were treated with 10 μ M MG132 (Calbiochem) or 1 μ M Bafilomycin (Sigma-Aldrich, Merck) for 16 hours or 150 μ M Cycloheximide (Sigma-Aldrich, Merck) for 2, 4, 8 or 12 hours prior to total protein extraction.

Protein extraction and western blotting: Total protein extraction was performed using RIPA buffer supplemented with protease inhibitors (04693159001, Roche, Merck) and N-ethylmaleimide (Sigma-Aldrich, Merck) and quantified using the PierceTM BCA Protein Assay kit (ThermoFisher Scientific). Twenty μ g of total protein per lane were run in 10%

Acrylamide/Bis-Acrylamide gels, transferred to a PVDF membrane (Millipore, Merck) and blocked with 5% skimmed milk in TBS-Tween 1X. Different antibodies were used: Anti-HA tag antibody (ab18181, Abcam), Anti- α -Tubulin antibody (T5168, Sigma-Aldrich), Anti-GAPDH Antibody (sc-47724, Santa cruz Biotechnology), Anti-Mouse IgG (Fc specific)–Peroxidase antibody (A0168, Sigma-Aldrich). Results were visualized using the LAS-4000 Luminescent Image Analyzer (Fujifilm) and the Luminata™ Forte Western HRP Substrate (WBLUF0100, Millipore). The detected bands were quantified using ImageJ(68).

Immunocytochemistry: Cells were fixed in 4% PFA, permeabilized with 0,1M Glycine and 0,1% Triton X-100 in PBS and blocked with 0,3M Glycine, 0,05% Triton X-100 and 10% Normal Donkey Serum (#S30-100M, Merck Millipore) in PBS. Coverslips were incubated with anti-HA primary antibody (ab18181, Abcam), Donkey Anti-Mouse Cy2 antibody (#715-225-150, Jackson Immunoresearch) and DAPI (#D1306, Invitrogen,) and mounted with MOWIOL (#475904, Millipore). Images were acquired using a Zeiss confocal microscope LSM 880 and analysed with ImageJ(68).

ELISA analysis: The supernatant of the conditioned medium was obtained after short centrifugation. Total protein concentration was quantified using the Pierce™ BCA Protein Assay kit (ThermoFisher Scientific) and A β ₁₋₄₀ and A β ₁₋₄₂ amyloid peptide using the Amyloid-beta (1-40) High Sensitive ELISA and Amyloid-beta (1-42) High Sensitive ELISA (IBL International GmbH).

Metabolomics analyses: Amino acid analysis was performed through ultra-high-performance liquid chromatography–tandem mass spectrometry as previously described (72). Gas chromatographic/mass spectrometric analyses were used to identify organic acids as described in (73).

Ethical issues: For the three patients whose fibroblasts have been studied, parents gave their written informed consent. Their samples and data were obtained in accordance with the Helsinki Declaration of 1964, as revised in October 2013 (Fortaleza, Brazil). The study was approved by the Institutional Review Board (IRB00003099) of the Bioethical Commission of the University of Barcelona (October 5, 2020).

RESULTS

Clinical management of SYS patients

We performed a systematic revision of all the published patients with SYS (Supplementary Table 1) including molecular and phenotypic data, all of them bearing mutations in *MAGEL2*, with the aim of creating a standardized and useful set of guidelines for SYS clinical management.

The literature-based recommendations have been divided into two life periods: perinatal period (first 28 days of life) and childhood/adolescence. It includes the most relevant medical problems associated with each period and the specific concerns or interventions advisable for each of them. A schematic summarized version of the different clinical areas and tests included in the guidelines are represented in Figure 1 and a detailed, printable version is supplied as Suppl. Table 2.

For the majority of cases pregnancy was uneventful (only polyhydramnios has been reported in some cases), but a high rate of C-sections has been detailed (more than a half of the described patients with delivery information available). Clinical symptoms appear early in life showing a complex phenotype that includes neuromuscular symptoms, respiratory and endocrinological problems, feeding difficulties, and dysmorphic traits. Other clinical issues can appear later and may affect almost all the organs and systems, requiring a coordinated multidisciplinary approach.

Genetic characterization of SYS variants

To date, 51 different variants have been associated with SYS (Figure 2), being p.(Gln666Profs*47) a recurrent mutational hotspot present in 79 cases (in bold in Figure 2). They are mostly truncating mutations and predominantly located in the C-terminal region of the protein, meaning that there is a partial or a total lack of the MHD, potentially compromising the functions that *MAGEL2* carries out through this domain. Three different missense mutations and a small deletion, resulting in a form of the protein lacking 7 residues, have also been associated with SYS phenotypes. These atypical mutations are not predicted to encode a truncated form of the protein, and functional studies have not been performed to support the variant pathogenicity, thus their clinical implications remain to be proven (in green in Figure 2).

The truncated form of *MAGEL2* caused by variant p.Gln638* remains stable in the cell

To evaluate the stability and recycling of the truncated form of the *MAGEL2* protein, HEK293T cells were transfected with an expression vector containing either the WT cDNA sequence of

MAGEL2 (*MAGEL2*-WT) or including the pathogenic truncating variant c.1912C>T; p.Gln638* (*MAGEL2*-Gln638*), which encodes a protein 611 amino acids shorter than the WT form and has been reported in six patients (20,21,23,33,45). The WT and *MAGEL2* cDNAs were tagged with an HA epitope at C-terminus. Blocking of the proteasomal degradation pathway with MG132 (Figure 3A) or the lysosomal pathway with Bafilomycin (Baf) (Figure 3B) showed that *MAGEL2* is mostly degraded via proteasome. Of note, the truncated *MAGEL2*-Gln638* variant is equally expressed in transfected cells and does not present a higher proteasomal degradation rate than the WT form (Figure 3, A&B). Additionally, cells were treated with Cycloheximide (Cx) to block protein synthesis during 2, 4, 6 and 12 hours to evaluate protein stability and half-life of the truncated protein compared to the WT form. Similar stability was observed in both forms (Figure 3, C&D), supporting the idea that the truncated form *MAGEL2*-Gln638* is not degraded and remains stable in the cell.

Presence of variant p.Gln638* affects protein subcellular localization

To determine the subcellular localization of this truncated form of the *MAGEL2* protein, HEK293T, SAOS-2 and HeLa cells were transfected with the expression vectors *MAGEL2*-WT or *MAGEL2*-Gln638*. Immunocytochemistry assays detecting HA showed that in cells transfected with the *MAGEL2*-Gln638* construct, there was a shift of the protein towards the nucleus, while the *MAGEL2*-WT form was mainly located in the cytoplasm (Figure 3 E&F). A similar localization pattern was observed in HEK293T, SAOS-2 and HeLa cells, supporting the idea that presence of variant p.Gln638*, which leads to the lack of part of the C-terminal sequence, affects protein subcellular localization.

SYS fibroblasts show decreased A β ₁₋₄₀ peptide excretion levels

As alterations in *MAGEL2* could be affecting APP cleavage and A β ₁₋₄₀ peptide production rates, levels of A β ₁₋₄₀ peptide were measured by ELISA in extracellular medium from SYS, PWS and control fibroblasts after 72h. SYS fibroblasts showed significantly decreased excretion levels of the processed peptide, both compared to PWS and control fibroblasts. However, no differences were observed in the PWS group compared to the control (Figure 4). A β ₁₋₄₂ peptide was also measured; however, the levels were very low and no differences were observed between conditions (data not shown).

Fibroblasts from SYS patients show altered gene expression patterns

To better understand the effect that MAGEL2 truncating mutations may have in gene expression patterns, we performed an mRNA whole transcriptomic analysis of skin fibroblasts. We used samples from three SYS patients (one of them carrying the nonsense variant p.Gln638* and the other two the highly recurrent frameshift variant p.(Gln666Profs*47)) and six healthy donors. Using the ExpHunter Suite, we identified 132 differentially expressed genes (DEGs), 76 up-regulated and 56 down-regulated (Supplementary Table 3). The top ten up- and down-regulated showing the most significant changes in the expression fold can be found in Table 1.

To explore the different pathways and biological functions that may be affected, we used the same software to perform an enrichment analysis on the 132 identified DEGs. Different REACTOME categories related to mitosis, such as “Resolution of Sister Chromatid Cohesion” and “Mitotic Spindle Checkpoint” were significantly enriched. Consistently, the majority of those genes were also enriched in the “Kinetochores” and “Chromosome, centromeric region” according to GO cellular components enrichment. Another cluster including 5 genes related to “Collagen formation” also appeared in the REACTOME enrichment analysis (Supplementary Table 4).

SYS fibroblasts show altered levels of organic acids and amino acids

Mass spectrometry analysis of metabolites including several organic acids and amino acids in SYS, PWS and control fibroblasts showed increased levels of suberic, sebacic, adipic and malic organic acids in SYS compared to the other two groups (Figure 5). Regarding amino acids, only glutamine showed a robust significant decrease in the SYS group (Figure 5).

We investigated if any of the genes involved in these metabolite’s pathways were differentially expressed in SYS fibroblasts using our transcriptomic data. *ME1* (ENSG00000065833), coding the NADP-dependent malic enzyme protein, was found to be significantly upregulated. No additional genes involved in glutamine (GO:0006541) or other organic acids (GO:0006082) metabolic processes were differentially expressed in SYS fibroblasts.

DISCUSSION

SYS is an ultra-rare neurodevelopmental syndrome caused by variants in the paternal allele of the *MAGEL2* gene that lead to the production of a truncated form of the protein. More than a hundred cases have been published since it was first described in 2013 (1). However, given its low prevalence, the majority of them have been reported as case reports of a single or a very reduced group of patients, making it difficult to establish the general clinical and genetic picture that defines SYS. Moreover, added to the solitude and burden of having a very rare condition, families suffer the lack of clinical guidelines for treatment and follow-up. Evidence-based recommendations help to reduce inequity in health care and empower both families and clinicians facing such a rare disease. To develop the recommendations, we performed an extensive revision of all the SYS cases published so far at both phenotypic (Supplementary Table 1) and genetic level (Figure 2) and elaborated a comprehensive and detailed follow-up programme (reduced version in Figure 1 and printable extended version in Supplementary Table 2). Despite the comprehensive revision, to date, no clear underlying phenotype-genotype correlation is observed with the exception of two particular variants that associate with the much more severe phenotype of CMA.

Genetically, SYS is caused by nonsense or frameshift mutations in the non-silenced paternal allele of *MAGEL2* that lead to the production of a truncated protein that partially or totally lacks the MHD, compromising the functions that *MAGEL2* carries out through this domain. Only one *MAGEL2* missense variant had been previously described as potentially disease-associated (34). The patient carried the paternally inherited variant c.1613C>A (p.Ala538Glu), at the moment of the study, this change was predicted to be deleterious and disease-causing by *in silico* predictors. But it has to be taken into account that *MAGEL2* has been poorly annotated and studied until recently. In the new gnomAD release (v 3.1.1), this particular variant has been identified in 33 individuals with a highest MAF of 0.03 in Amish and at this moment, a majority of *in silico* predictors consider this variant as “tolerated” (including SIFT, FATHMM-MKL...) while other are unable to score it (Polyphen 2, PROVEAN), in general, this variant will be classified as Likely Benign according to ACMG classification (46). Clinically, the patient bearing this variant presents with DD, ASD, and dysmorphic traits. While her presentation shares some traits with SYS, the high frequency of this variant in the Amish populations (and among gnomAD controls) would suggest that this is not the main cause of the disease. At this point, functional analysis of this particular variant could help to improve her diagnosis as this variant could also be modifying her main clinical presentation. After revision of the disease-associated variants published so far, we found two missense mutations that have been identified in two different SYS patients: p.Pro564Ala and p.Ala997Thr (with 2 and 4 carriers in gnomAD v3.1.1)

and an in-frame deletion that leads to a reduction of the protein length of 7 amino acids (p.Ile600_Gln607del). However, their potential causality is not further discussed and the detailed individual clinical evaluations of these patients are not published (27). Functional validation of these atypical variants is essential before considering them as disease-causing and offering genetic counseling, among other consequences. At this point it is worthy to mention that, for years, hg19 genome build had included as “canonical” a shorter version of the gene (lacking the N-terminal half), leading to missannotation of multiple variants. This has been the reference annotation for gnomAD v 2.1.1, explaining that variants present in the general population were considered as “likely pathogenic”. In this work, we have made an effort to improve the *MAGEL2* mutation annotation to avoid further errors. In this sense, mutations p.Thr76Hisfs*23 and p.Glu131Serfs*17 were previously reported as p.Thr679Hisfs*23 and p.Glu734Serfs*17 by McCarthy et al. (27). A thorough revision of these changes revealed that they were, indeed, an error. This is relevant since, as will be discussed later, our results suggest that the presence of a fragment of the N-terminal domain is relevant in the development of the pathology.

The phenotypic overlap between SYS and PWS suggests that the alteration of *MAGEL2* could contribute to different aspects of the PWS phenotype. Of note, two patients carrying atypical deletions involving *MAGEL2*, *NDN* and *MKRN3*, but not the whole PWS region, did not show a full PWS phenotype. One of them only showed mild delayed motor skills and the others displayed obesity, developmental delay and high pain threshold (47,48). These cases point out that the lack of these three genes alone do not cause the full spectrum of PWS symptoms, questioning the causal implications that the loss of *MAGEL2* expression may have in the PWS phenotype. The more severe phenotype frequently observed in SYS compared to PWS cases states a paradoxical situation where the deletion of a whole gene causes a milder phenotype than that caused by the presence of a truncated form of the protein. To evaluate if the truncated form of the protein is degraded or remains stable in the cell, we compared possible differences in the degradation pathways and half-life of the *MAGEL2*-WT and the *MAGEL2*-Gln638* protein forms. Blocking of the proteasomal and lysosomal degradation pathways showed that both forms were degraded via proteasome and the mutant did not show a higher degradation rate than the wild-type form (Figure 3 A&B). Also, no differences between the two forms were observed regarding protein stability and half-life, supporting the hypothesis that the truncated form is expressed and stable and may have a toxic effect (Figure 3 C&D). Immunocytochemistry assays in transfected cell lines showed that, while *MAGEL2*-WT was found in the cytoplasm as previously reported (3,4), the *MAGEL2*-Gln638* was predominantly located inside the nucleus (Figure 3 E&F) in different cell lines. This new localization of the protein suggests that, in addition to the loss of the *MAGEL2* normal functions, SYS-associated

mutations could couple new functions, whose consequences are still unknown, opening a full new field of research.

In *Magel2*^{Δ/m+} mice and PWS patient-derived neuronal cell models, loss of parental *MAGEL2* expression leads to the decreased levels of secretory-granule proteins that lead to reduced levels of mature SGs in neurons and circulating bioactive hormones (9), consistent with its known role in the regulation of endosomal protein trafficking and recycling (3,4,49). They also observed impaired trafficking of M6PR in DPSC-derived neurons from several PWS patients and only one SYS patient, indicating impaired endosome-mediated retrograde transport (9). Under the hypothesis that this impaired trafficking can also be reflected in an aberrant A β peptide production and exocytosis (14–16), A β ₁₋₄₀ peptide excretion levels of SYS, PWS and control fibroblasts were measured. We observed significantly decreased levels of excreted A β ₁₋₄₀ peptide in SYS fibroblasts compared to PWS and control groups, which showed no difference between them (Figure 4). This result supports the idea that the truncated form of the protein may have a different effect on protein trafficking than the complete loss of the protein itself. Dysfunctions in this pathway lead to a dysregulation of A β ₁₋₄₀ levels, stating the reduction of such levels in fibroblasts from SYS patients as a potential biomarker for the disease.

Despite being its most deeply studied function, dysregulation of protein trafficking and recycling is not the only consequence of *MAGEL2* malfunction. In *Magel2* null mice brains and cultured fibroblasts from SYS patients, mTOR and downstream targets of the mTORC1 complex have been found to be upregulated and showed autophagy impairment and increased lipid droplet formation (50). To explore if the truncated form of *MAGEL2* could also be affecting the expression of other genes, we applied an unbiased transcriptomic approach in fibroblasts from 3 SYS patients and 6 controls. In our analysis we did not observe altered expression patterns of mTOR or the downstream targets previously reported (50). However, we identified 132 DEGs between the two groups. Some of the identified DEGs have a role in developmental and neurologic processes, consistent with the features usually present in SYS patients. The most clearly overexpressed DEG was *HOTAIR*, a lncRNA that mediates transcriptional silencing in trans. It promotes H3K27 trimethylation and transcriptional silencing of the *HOXD* locus (51,52). During development, expression of *HOX* genes must be tightly regulated in a spatiotemporal manner to determine body axes and orchestrate organ formation in vertebrates. They are also relevant for the guidance of other prenatal and postnatal differentiation events and postnatal homeostasis (53,54). Of note, primary fibroblasts conserve many features of the embryonic *HOX* gene expression pattern *in vitro* and *in vivo* and reflect their position along the axes during development (55). Other DEGs also play an important role during development, being involved in core limb development and left-right asymmetry (*PITX1*)

(56), embryonic morphogenesis and hindbrain segmentation (*RARB*) (57), specification of limb identity and heart development (*TBX5*) (58) and development of the neural plate (*VANGL2*) (59). Another group of DEGs are implicated in the central nervous system homeostasis, participating in the regulation of neurogenesis (*PTPRD* (60); *SLITRK4* (61)), white matter maintenance (*ASPA*) (62) and in promoting the survival of neuronal cells (*CRLF1*). Interestingly, mutations in *CRLF1* cause an autosomal recessive disease called Crisponi/cold-induced sweating syndrome (CS, MIM#601378), which shows phenotypic overlap with SYS, especially in the neonatal period, as patients also show congenital contractures of the limbs, hypotonia and developmental delay (63). Loss of function mutations in the *KY* gene, significantly underexpressed in SYS patients' fibroblasts, have been recently identified in a few cases showing myopathic, neurogenic or spastic paraplegia phenotypes (64), an emergent and growing disease that may share some clinical features with the neuromuscular affectation observed in SYS.

Different REACTOME categories related to mitosis are enriched within the identified DEGs (Supplementary Table 3). The majority of these selected genes are present in the kinetochore, according to GO cellular components enrichment. However, further experiments should be performed to try to confirm the implication of *MAGEL2* in mitosis, and the alteration of these genes could be a consequence of the nuclear localization of the truncated protein

Endocrine and metabolic alterations in PWS have been widely studied (18). However, little is known regarding metabolic impairment in SYS. A study including 5 female and 4 male SYS patients showed that they present some but not all the endocrine alterations also observed in PWS, like GH deficiency and increased ghrelin levels, and a high prevalence of diabetes mellitus (28). A recently published review of the literature on endocrine abnormalities in *MAGEL2*-related syndromes (45), showed that the most common hormonal deficiencies involve growth hormone (GH), thyroid stimulating hormone (TSH), adrenocorticotrophic hormone (ACTH), antidiuretic hormone (ADH) and gonadotropins, probably caused by hypothalamic impairment and which might contribute to hypoglycemia. The metabolomics analysis of SYS and PWS patients was aimed at finding biomarkers that evaluate the lysosomal, peroxisomal, mitochondrial, and cytosolic metabolic pathways. Although there is no clear evidence of metabolic dysfunctions at the cellular level, the key role of Golgi transport in cell metabolism makes it possible for seemingly unrelated metabolic pathways to be affected.

We detected increased levels of malic, sebacic, adipic and suberic organic acids in SYS fibroblasts compared both to PWS and control groups (Figure 5). Loss-of-function mutations in the mitochondrial malate dehydrogenase, an enzyme that catalyzes the conversion of

malate to oxaloacetate within the Krebs cycle, lead to the accumulation of malate and a phenotype including early-onset generalized hypotonia, psychomotor delay and epilepsy (65). Patients suffering from diabetes show increased urinary excretion of adipic, suberic and sebacic acids. These increased levels of dicarboxylic acids could be related to oxidation of cis-polyunsaturated fatty acids via glucose-induced oxidative stress (66). These alterations in energetic balance are consistent with some metabolic alterations observed in SYS patients, such as frequent hypoglycemic episodes.

We also observed that glutamine levels were significantly decreased in SYS in comparison with the two other groups (Figure 5), while glutamate levels remained unaltered. Glutamine acts as a nucleic acid and nucleotide precursor in certain cell types. However, it seems that in many contexts its key role relies on providing glutamate, which has a wider range of metabolic functions than glutamine itself (67), an example of that is the glutamate/GABA-glutamine cycle in neurons (68). In fact, it has been stated that alterations of the GABAergic system may play an important role in aspects of the pathophysiology of PWS (69). The reason why glutamine levels may be decreased in SYS patients is unknown. One hypothesis could be a dysregulation in retrieval and recycling of a glutamine transporter, such as SLC1A5. In fact, the retromer promotes the retrieval and recycling of SLC1A5 and the transporter's degradation is enhanced upon retromer knockout (70), suggesting that further studies on that transporter in SYS patients derived cell lines could be of interest.

In conclusion, the increasing number of diagnosed SYS patients has allowed the performance of an exhaustive phenotypical delineation of the syndrome and the establishment of a standardized set of guidelines, which we think will help to improve their clinical management. Also, the revision and correction of the mutations causing SYS has provided a clearer picture of their distribution along *MAGEL2*. The subtle changes in gene expression patterns and certain metabolites levels in fibroblasts suggest undescribed effects of the truncated *MAGEL2* form that should further be explored. The overexpression *in vitro* system could be used to improve diagnosis and test the pathogenicity of doubtful missense mutations. Finally, our results support the idea that the SYS phenotype might be explained by a dominant negative or a gain-of function effect of the truncated protein, rather than by a haploinsufficiency situation.

REFERENCES

1. Schaaf CP, Gonzalez-Garay ML, Xia F, Potocki L, Gripp KW, Zhang B, et al. Truncating mutations of MAGEL2 cause Prader-Willi phenotypes and autism. *Nat Genet.* 2013 Nov;45(11):1405–8.
2. Tacer KF, Potts PR. Cellular and disease functions of the Prader-Willi Syndrome gene MAGEL2. *Biochem J.* 2017 Jun 16;474(13):2177–90.
3. Hao Y-H, Doyle JM, Ramanathan S, Gomez TS, Jia D, Xu M, et al. Regulation of WASH-dependent actin polymerization and protein trafficking by ubiquitination. *Cell.* 2013 Feb 28;152(5):1051–64.
4. Hao Y-H, Fountain MD Jr, Fon Tacer K, Xia F, Bi W, Kang S-HL, et al. USP7 Acts as a Molecular Rheostat to Promote WASH-Dependent Endosomal Protein Recycling and Is Mutated in a Human Neurodevelopmental Disorder. *Mol Cell.* 2015 Sep 17;59(6):956–69.
5. Burd C, Cullen PJ. Retromer: a master conductor of endosome sorting. *Cold Spring Harb Perspect Biol.* 2014 Feb 1;6(2).
6. Lonsdale J, Thomas J, Salvatore M, Phillips R, Lo E, Shad S, et al. The Genotype-Tissue Expression (GTEx) project. *Nat Genet.* 2013 May 29;45(6):580–5.
7. Lee S, Kozlov S, Hernandez L, Chamberlain SJ, Brannan CI, Stewart CL, et al. Expression and imprinting of MAGEL2 suggest a role in Prader-willli syndrome and the homologous murine imprinting phenotype. *Hum Mol Genet.* 2000 Jul 22;9(12):1813–9.
8. Kozlov SV, Bogenpohl JW, Howell MP, Wevrick R, Panda S, Hogenesch JB, et al. The imprinted gene *Magel2* regulates normal circadian output. *Nat Genet.* 2007 Oct;39(10):1266–72.
9. Chen H, Victor AK, Klein J, Tacer KF, Tai DJ, de Esch C, et al. Loss of MAGEL2 in Prader-Willi syndrome leads to decreased secretory granule and neuropeptide production. *JCI Insight.* 2020 Sep 3;5(17).
10. Tan JZA, Gleeson PA. The role of membrane trafficking in the processing of amyloid precursor protein and production of amyloid peptides in Alzheimer’s disease. *Biochim Biophys Acta Biomembr.* 2019 Apr 1;1861(4):697–712.
11. Herms J, Anliker B, Heber S, Ring S, Fuhrmann M, Kretschmar H, et al. Cortical dysplasia resembling human type 2 lissencephaly in mice lacking all three APP family members. *EMBO J.* 2004 Oct 13;23(20):4106–15.
12. López-Sánchez N, Müller U, Frade JM. Lengthening of G2/mitosis in cortical precursors from mice lacking β -amyloid precursor protein. *Vol. 130, Neuroscience.* 2005. p. 51–60.
13. Wang P, Yang G, Mosier DR, Chang P, Zaidi T, Gong Y-D, et al. Defective neuromuscular synapses in mice lacking amyloid precursor protein (APP) and APP-Like protein 2. *J Neurosci.* 2005 Feb 2;25(5):1219–25.
14. Small SA, Kent K, Pierce A, Leung C, Kang MS, Okada H, et al. Model-guided microarray implicates the retromer complex in Alzheimer’s disease. *Ann Neurol.* 2005 Dec;58(6):909–19.
15. Muhammad A, Flores I, Zhang H, Yu R, Staniszewski A, Planel E, et al. Retromer deficiency observed in Alzheimer’s disease causes hippocampal dysfunction, neurodegeneration, and A β accumulation. *Proc Natl Acad Sci U S A.* 2008 May 20;105(20):7327–32.

16. Mecozzi VJ, Berman DE, Simoes S, Vetanovetz C, Awal MR, Patel VM, et al. Pharmacological chaperones stabilize retromer to limit APP processing. *Nat Chem Biol.* 2014 Jun;10(6):443–9.
17. Kvainickas A, Jimenez-Orgaz A, Nägele H, Hu Z, Dengjel J, Steinberg F. Cargo-selective SNX-BAR proteins mediate retromer trimer independent retrograde transport. *J Cell Biol.* 2017 Nov 6;216(11):3677 LP – 3693.
18. Cassidy SB, Schwartz S, Miller JL, Driscoll DJ. Prader-Willi syndrome. *Genet Med.* 2012 Jan;14(1):10–26.
19. Soden SE, Saunders CJ, Willig LK, Farrow EG, Smith LD, Petrikin JE, et al. Effectiveness of exome and genome sequencing guided by acuity of illness for diagnosis of neurodevelopmental disorders. *Sci Transl Med.* 2014 Dec 3;6(265):265ra168.
20. Urreiziti R, Cueto-Gonzalez AM, Franco-Valls H, Mort-Farre S, Roca-Ayats N, Ponomarenko J, et al. A De Novo Nonsense Mutation in *MAGEL2* in a Patient Initially Diagnosed as Opitz-C: Similarities Between Schaaf-Yang and Opitz-C Syndromes. *Sci Rep.* 2017 Mar 10;7:44138.
21. Fountain MD, Aten E, Cho MT, Juusola J, Walkiewicz MA, Ray JW, et al. The phenotypic spectrum of Schaaf-Yang syndrome: 18 new affected individuals from 14 families. *Genet Med.* 2017 Jan;19(1):45–52.
22. Palomares-Bralo M, Vallespín E, Del Pozo Á, Ibañez K, Silla JC, Galán E, et al. Pitfalls of trio-based exome sequencing: imprinted genes and parental mosaicism-*MAGEL2* as an example. *Genet Med.* 2017 Nov;19(11):1285–6.
23. Enya T, Okamoto N, Iba Y, Miyazawa T, Okada M, Ida S, et al. Three patients with Schaaf-Yang syndrome exhibiting arthrogryposis and endocrinological abnormalities. *Am J Med Genet A.* 2018 Mar;176(3):707–11.
24. D Hidalgo-Santos A, Del Carmen DeMingo-Aleman M, Moreno-Macián F, Roselló M, Orellana C, Martínez F, et al. A Novel Mutation of in a Patient with Schaaf-Yang Syndrome and Hypopituitarism. *Int J Endocrinol Metab.* 2018 Jul;16(3):e67329.
25. Kleinendorst L, Pi Castán G, Caro-Llopis A, Boon EMJ, van Haelst MM. The role of obesity in the fatal outcome of Schaaf-Yang syndrome: Early onset morbid obesity in a patient with a *MAGEL2* mutation. *Am J Med Genet A.* 2018 Nov;176(11):2456–9.
26. Matuszewska KE, Badura-Stronka M, Śmigiel R, Cabała M, Biernacka A, Kosinska J, et al. Phenotype of two Polish patients with Schaaf–Yang syndrome confirmed by identifying mutation in *MAGEL2* gene. Vol. 27, *Clinical Dysmorphology.* 2018. p. 49–52.
27. McCarthy J, Lupo PJ, Kovar E, Rech M, Bostwick B, Scott D, et al. Schaaf-Yang syndrome overview: Report of 78 individuals. *Am J Med Genet A.* 2018 Dec;176(12):2564–74.
28. McCarthy JM, McCann-Crosby BM, Rech ME, Yin J, Chen C-A, Ali MA, et al. Hormonal, metabolic and skeletal phenotype of Schaaf-Yang syndrome: a comparison to Prader-Willi syndrome. *J Med Genet.* 2018 May;55(5):307–15.
29. Bayat A, Bayat M, Lozoya R, Schaaf CP. Chronic intestinal pseudo-obstruction syndrome and gastrointestinal malrotation in an infant with schaaf-yang syndrome - Expanding the phenotypic spectrum. *Eur J Med Genet.* 2018 Oct;61(10):627–30.

30. Poliak N. Magel2 Gene Mutation and Its Associated Phenotypic Features in A Five-Month-Old Female. Vol. 8, *Journal of Pediatrics & Neonatal Care*. 2018.
31. Tong W, Wang Y, Lu Y, Ye T, Song C, Xu Y, et al. Whole-exome Sequencing Helps the Diagnosis and Treatment in Children with Neurodevelopmental Delay Accompanied Unexplained Dyspnea. *Sci Rep*. 2018 Mar 26;8(1):5214.
32. Gregory LC, Shah P, Sanner JRF, Arancibia M, Hurst J, Jones WD, et al. Mutations in MAGEL2 and L1CAM Are Associated With Congenital Hypopituitarism and Arthrogyposis. *J Clin Endocrinol Metab*. 2019 Dec 1;104(12):5737–50.
33. Negishi Y, Ieda D, Hori I, Nozaki Y, Yamagata T, Komaki H, et al. Schaaf-Yang syndrome shows a Prader-Willi syndrome-like phenotype during infancy. *Orphanet J Rare Dis*. 2019 Dec 2;14(1):277.
34. Patak J, Gilfert J, Byler M, Neerukonda V, Thiffault I, Cross L, et al. MAGEL2-related disorders: A study and case series. *Clin Genet*. 2019 Dec;96(6):493–505.
35. de Andrade GALR, de Oliveira Silva TB, do Nascimento IJB, Boath A, da Costa Cunha K, Chermont AG. Schaaf-Yang syndrome: A novel variant in MAGEL2 gene in the first Brazilian preterm neonate . Vol. 11, *International Journal of Case Reports and Images*. 2020. p. 1.
36. Chen XF, Song YM, Zou CC. Schaaf-Yang syndrome caused by the new variation of MAGEL2 gene in a case. *Zhonghua Er Ke Za Zhi*. 2019 Feb 2;57(2):155–7.
37. Ahn H, Seo GH, Oh A, Lee Y, Keum C, Heo SH, et al. Diagnosis of Schaaf-Yang syndrome in Korean children with developmental delay and hypotonia. *Medicine* . 2020 Dec 18;99(51):e23864.
38. Costa RA, Ferreira IR, Cintra HA, Gomes LHF, Guida L da C. Genotype-Phenotype Relationships and Endocrine Findings in Prader-Willi Syndrome. *Front Endocrinol* . 2019 Dec 13;10:864.
39. Fountain MD, Schaaf CP. Prader-Willi Syndrome and Schaaf-Yang Syndrome: Neurodevelopmental Diseases Intersecting at the Gene. *Diseases*. 2016 Jan 13;4(1).
40. Thomason MM, McCarthy J, Goin-Kochel RP, Dowell LR, Schaaf CP, Berry LN. Neurocognitive and Neurobehavioral Phenotype of Youth with Schaaf-Yang Syndrome. *J Autism Dev Disord*. 2020 Jul;50(7):2491–500.
41. Jobling R, Stavropoulos DJ, Marshall CR, Cytrynbaum C, Axford MM, Londero V, et al. Chitayat-Hall and Schaaf-Yang syndromes: a common aetiology: expanding the phenotype of -related disorders. *J Med Genet*. 2018 May;55(5):316–21.
42. Mejlachowicz D, Nolent F, Maluenda J, Ranjatoelina-Randrianaivo H, Giuliano F, Gut I, et al. Truncating Mutations of MAGEL2, a Gene within the Prader-Willi Locus, Are Responsible for Severe Arthrogyposis. *Am J Hum Genet*. 2015 Oct 1;97(4):616–20.
43. Guo W, Nie Y, Yan Z, Zhu X, Wang Y, Guan S, et al. Genetic testing and PGD for unexplained recurrent fetal malformations with MAGEL2 gene mutation. *Sci China Life Sci*. 2019 Jul;62(7):886–94.
44. Laquerriere A, Jaber D, Abiusi E, Maluenda J, Mejlachowicz D, Vivanti A, et al. Phenotypic spectrum and genomics of undiagnosed arthrogyposis multiplex congenita. *J Med Genet*. 2021 Apr 5;
45. Halloun R, Habib C, Ekhilevitch N, Weiss R, Tiosano D, Cohen M. Expanding the spectrum of endocrinopathies identified in Schaaf-Yang syndrome - a case report and review of the literature. *Eur J Med Genet*. 2021 May 26;104252.

46. Richards S, Aziz N, Bale S, Bick D, Das S, Gastier-Foster J, et al. Standards and guidelines for the interpretation of sequence variants: a joint consensus recommendation of the American College of Medical Genetics and Genomics and the Association for Molecular Pathology. *Genet Med*. 2015 May;17(5):405–24.
47. Buiting K, Di Donato N, Beygo J, Bens S, von der Hagen M, Hackmann K, et al. Clinical phenotypes of *MAGEL2* mutations and deletions. *Orphanet J Rare Dis*. 2014 Mar 25;9:40.
48. Kanber D, Giltay J, Wieczorek D, Zogel C, Hochstenbach R, Caliebe A, et al. A paternal deletion of *MKRN3*, *MAGEL2* and *NDN* does not result in Prader–Willi syndrome. Vol. 17, *European Journal of Human Genetics*. 2009. p. 582–90.
49. Doyle JM, Gao J, Wang J, Yang M, Potts PR. MAGE-RING protein complexes comprise a family of E3 ubiquitin ligases. *Mol Cell*. 2010 Sep 24;39(6):963–74.
50. Crutcher E, Pal R, Naini F, Zhang P, Laugsch M, Kim J, et al. mTOR and autophagy pathways are dysregulated in murine and human models of Schaaf-Yang syndrome. *Sci Rep*. 2019 Nov 4;9(1):15935.
51. Rinn JL, Kertesz M, Wang JK, Squazzo SL, Xu X, Brugmann SA, et al. Functional demarcation of active and silent chromatin domains in human *HOX* loci by noncoding RNAs. *Cell*. 2007 Jun 29;129(7):1311–23.
52. Tsumagari K, Baribault C, Terragni J, Chandra S, Renshaw C, Sun Z, et al. DNA methylation and differentiation: *HOX* genes in muscle cells. *Epigenetics Chromatin*. 2013 Aug 2;6(1):25.
53. Foronda D, de Navas LF, Garaulet DL, Sánchez-Herrero E. Function and specificity of *Hox* genes. *Int J Dev Biol*. 2009;53(8-10):1404–19.
54. Mallo M, Wellik DM, Deschamps J. *Hox* genes and regional patterning of the vertebrate body plan. *Dev Biol*. 2010 Aug 1;344(1):7–15.
55. Rinn JL, Bondre C, Gladstone HB, Brown PO, Chang HY. Anatomic demarcation by positional variation in fibroblast gene expression programs. *PLoS Genet*. 2006 Jul;2(7):e119.
56. Nemeč S, Luxey M, Jain D, Huang Sung A, Pastinen T, Drouin J. *Pitx1* directly modulates the core limb development program to implement hindlimb identity. *Development*. 2017 Sep 15;144(18):3325–35.
57. Serpente P, Tümpel S, Ghyselincq NB, Niederreither K, Wiedemann LM, Dollé P, et al. Direct crossregulation between retinoic acid receptor {beta} and *Hox* genes during hindbrain segmentation. *Development*. 2005 Feb;132(3):503–13.
58. Steimle JD, Moskowitz IP. *TBX5*: A Key Regulator of Heart Development. *Curr Top Dev Biol*. 2017;122:195–221.
59. Ossipova O, Kim K, Sokol SY. Planar polarization of *Vangl2* in the vertebrate neural plate is controlled by Wnt and Myosin II signaling. *Biol Open*. 2015 Apr 24;4(6):722–30.
60. Tomita H, Cornejo F, Aranda-Pino B, Woodard CL, Rioseco CC, Neel BG, et al. The Protein Tyrosine Phosphatase Receptor Delta Regulates Developmental Neurogenesis. Vol. 30, *Cell Reports*. 2020. p. 215–28.e5.
61. Proenca CC, Gao KP, Shmelkov SV, Rafii S, Lee FS. *Slitrks* as emerging candidate genes involved in neuropsychiatric disorders. *Trends Neurosci*. 2011 Mar;34(3):143–53.

62. Kumar S, Mattan NS, de Vellis J. Canavan disease: a white matter disorder. *Ment Retard Dev Disabil Res Rev.* 2006;12(2):157–65.
63. Buers I, Persico I, Schöning L, Nitschke Y, Di Rocco M, Loi A, et al. Crisponi/cold-induced sweating syndrome: Differential diagnosis, pathogenesis and treatment concepts. *Clin Genet.* 2020 Jan;97(1):209–21.
64. Arif B, Rasheed A, Kumar KR, Fatima A, Abbas G, Wohler E, et al. A novel homozygous KY variant causing a complex neurological disorder. *Eur J Med Genet.* 2020 Nov;63(11):104031.
65. Ait-El-Mkadem S, Dayem-Quere M, Gusic M, Chaussenot A, Bannwarth S, François B, et al. Mutations in MDH2, Encoding a Krebs Cycle Enzyme, Cause Early-Onset Severe Encephalopathy. *Am J Hum Genet.* 2017 Jan 5;100(1):151–9.
66. Inouye M, Mio T, Sumino K. Dicarboxylic acids as markers of fatty acid peroxidation in diabetes. *Atherosclerosis.* 2000 Jan;148(1):197–202.
67. Newsholme P, Procopio J, Lima MMR, Pithon-Curi TC, Curi R. Glutamine and glutamate--their central role in cell metabolism and function. *Cell Biochem Funct.* 2003 Mar;21(1):1–9.
68. Bak LK, Schousboe A, Waagepetersen HS. The glutamate/GABA-glutamine cycle: aspects of transport, neurotransmitter homeostasis and ammonia transfer. Vol. 98, *Journal of Neurochemistry.* 2006. p. 641–53.
69. Rice LJ, Lagopoulos J, Brammer M, Einfeld SL. Reduced gamma-aminobutyric acid is associated with emotional and behavioral problems in Prader-Willi syndrome. *Am J Med Genet B Neuropsychiatr Genet.* 2016 Dec;171(8):1041–8.
70. Curnock R, Calcagni A, Ballabio A, Cullen PJ. TFEB controls retromer expression in response to nutrient availability. *J Cell Biol.* 2019 Dec 2;218(12):3954–66.
71. Rueden CT, Schindelin J, Hiner MC, DeZonia BE, Walter AE, Arena ET, et al. ImageJ2: ImageJ for the next generation of scientific image data. *BMC Bioinformatics.* 2017 Nov 29;18(1):529.
72. Casado M, Sierra C, Batllori M, Artuch R, Ormazabal A. A targeted metabolomic procedure for amino acid analysis in different biological specimens by ultra-high-performance liquid chromatography–tandem mass spectrometry. Vol. 14, *Metabolomics.* 2018.
73. Divry P, Vianey-Liaud C, Cotte J. Routine gas chromatographic/mass spectrometric analysis of urinary organic acids. Results over a three-year period. Vol. 14, *Biological Mass Spectrometry.* 1987. p. 663–8.

FIGURES

Schaaf-Yang Syndrome Clinical Management

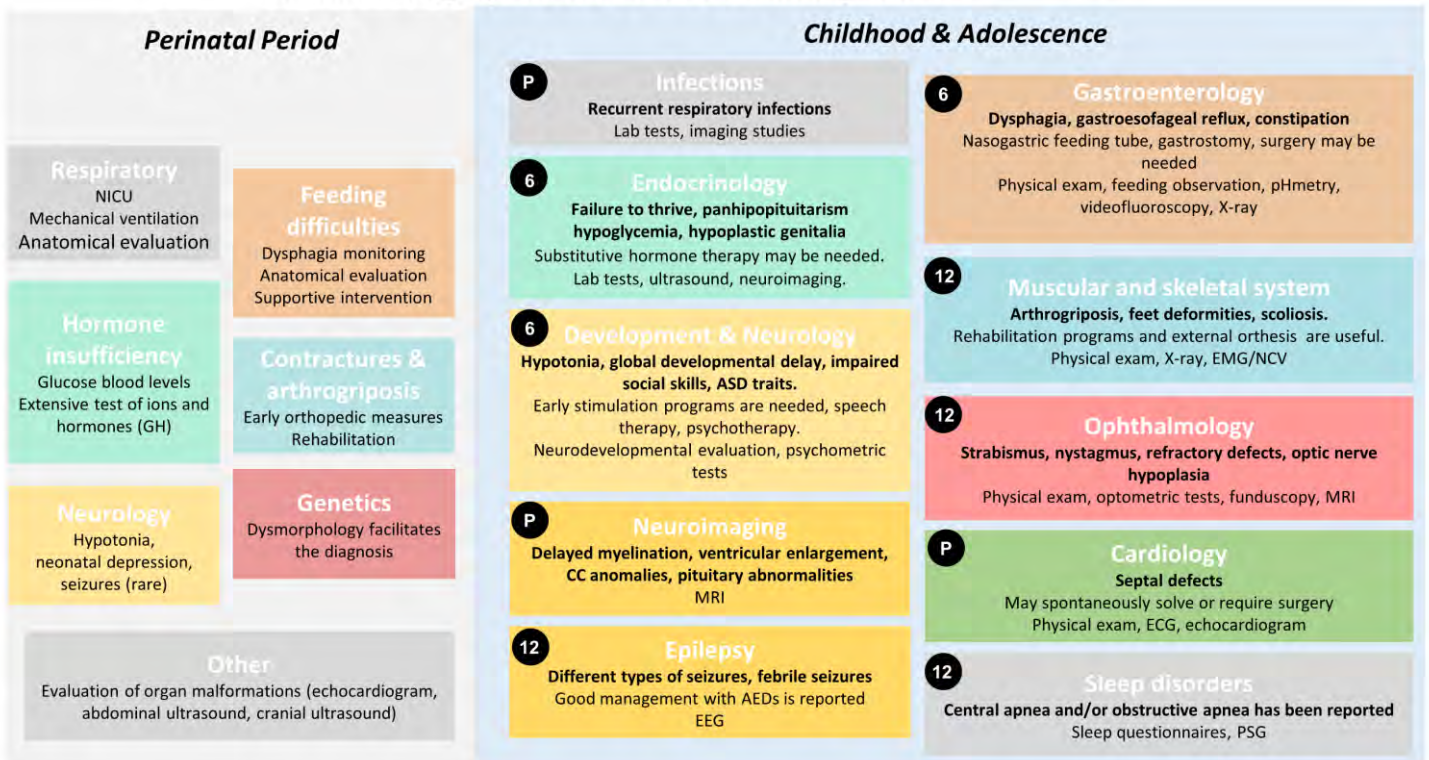


Figure 1. Schaaf-Yang syndrome clinical management schematic guidelines. In bold, the recommended follow-up time for each area.

Legend: ASD: Autism spectrum disorder; ECG: electrocardiogram; EEG: Electroencephalogram; EMG/NCV: electromyogram/nerve conduction velocity; MRI: Magnetic resonance imaging; PSG: Polysomnography Perinatal period: Boxes include the medical area of disease. Medical problems and management requirements are detailed below. Childhood and adolescence: Boxes include medical area of disease. Medical problems and diagnosis are detailed below in bold. Management recommendations and complementary exams are below, not in bold letters. Numbers in black dots state the recommended periodicity for clinical evaluation in months for every specialty. P means personalized, for instance Neuroimaging and cardiology, for many patients is recommended at diagnosis/birth for all patients, but follow-up depends on comorbidities. Please see Supplementary Table 2 for details.

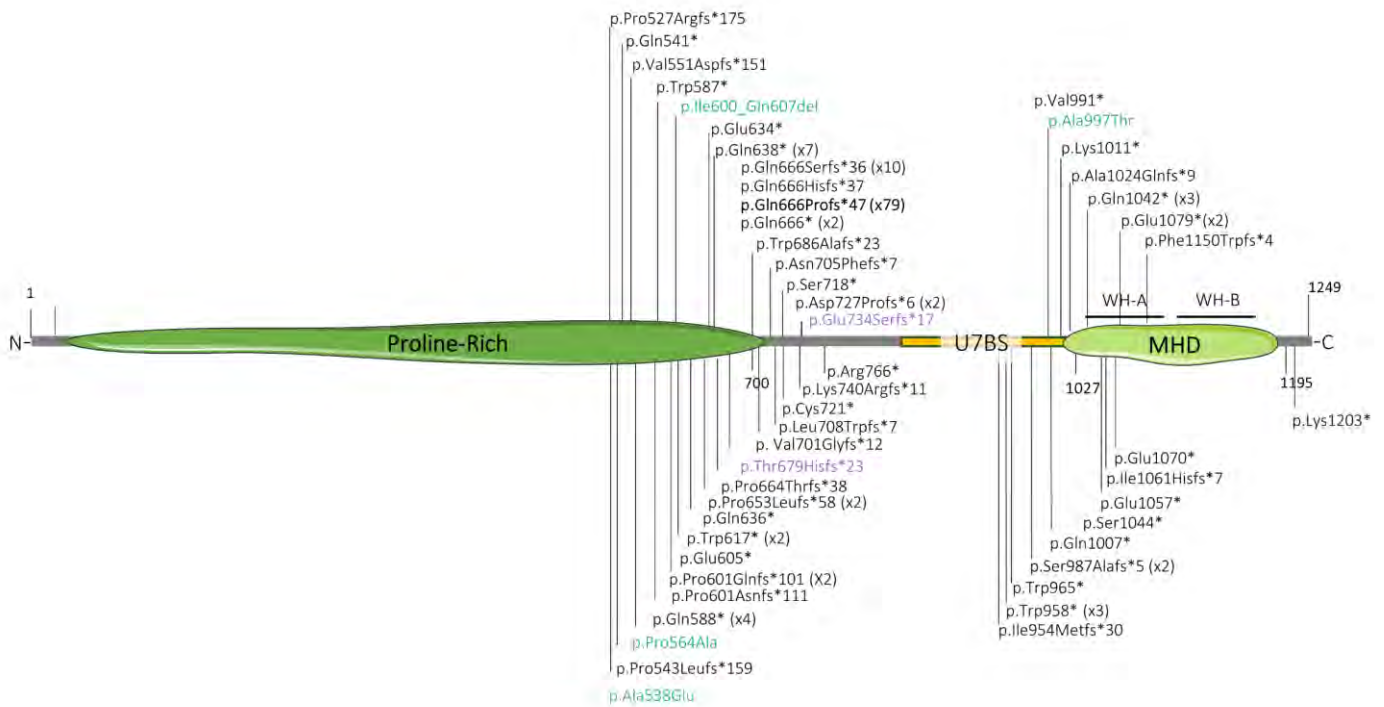


Figure 2. Schematic representation of the position within MAGEL2 of all the variants associated with SYS. The number of cases identified carrying each mutation is specified in brackets. In green, atypical variants that are not predicted to cause a truncated form of the protein. In purple, variants p.Thyr679Hisfs*23 (c.2033delC) and p.Glu734Serfs*17 (c.2199delA), previously misreported as c.224delC and c.390delA in (27).

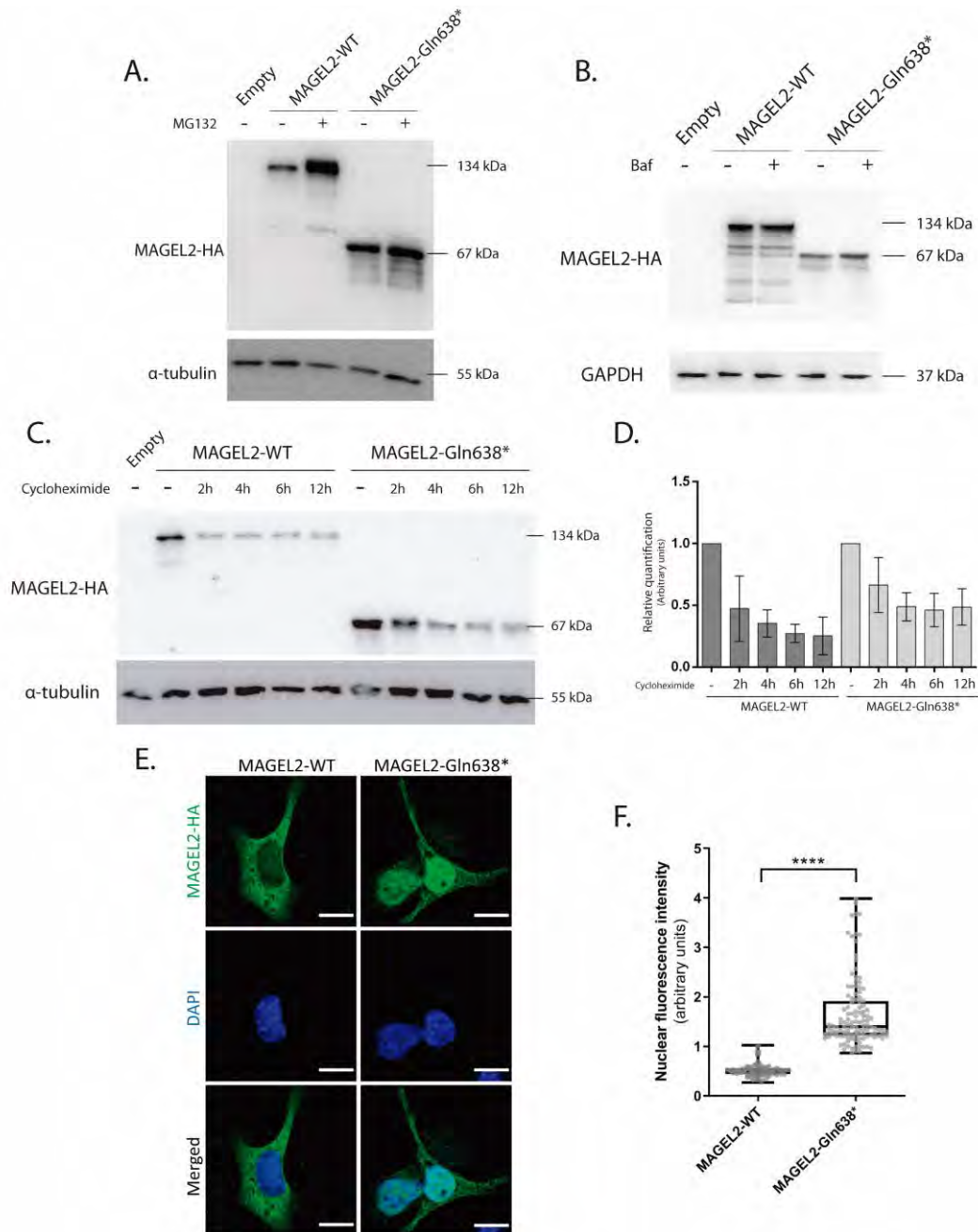


Figure 3. Degradation rate, stability and cellular localization of MAGEL2-WT and MAGEL2-Gln638* proteins. A) Representative Western Blot of heterologously expressed MAGEL2 proteins with or without MG132 treatment (10 μ M for 16 hours) (n=3). B) Representative Western Blot of heterologously expressed MAGEL2 proteins with or without Baf treatment (1 μ M for 16 hours) (n=3). C) Representative Western Blot of heterologously expressed MAGEL2 proteins with or without Cx treatment (150 μ M) during 2, 4, 6 or 12 hours (n=3). D) Quantification of three independent experiments normalized to the expression levels of MAGEL2-WT or MAGEL2-Gln638* without Cx treatment. E) Representative confocal 63X images of SAOS-2 cells transfected with MAGEL2-WT and MAGEL2-Gln638* plasmids. Cells were stained for MAGEL2-HA (green) to determine protein localization. F) Quantification of the MAGEL2-HA nuclear signal in MAGEL2-WT transfected cells versus MAGEL2-Gln638* transfected cells. Nuclear fluorescence intensities were normalized against cytoplasmic fluorescence intensities. Scale bar represents 15 μ m. $n = 221$ to 6 independent experiments. **** $p < 0.00001$.

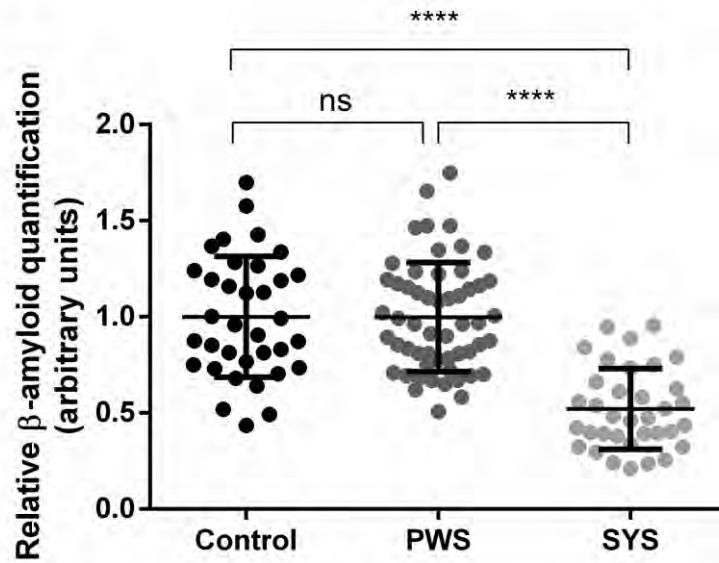


Figure 4. $A\beta_{1-40}$ peptide levels in SYS, PWS and control fibroblasts extracellular medium. Data obtained from at least 3 independent experiments (SYS fibroblasts: n=5; PWS fibroblasts: n=9; Control fibroblasts: n=5). Horizontal lines represent mean values and error bars represent the SD. **** p < 0.00001.

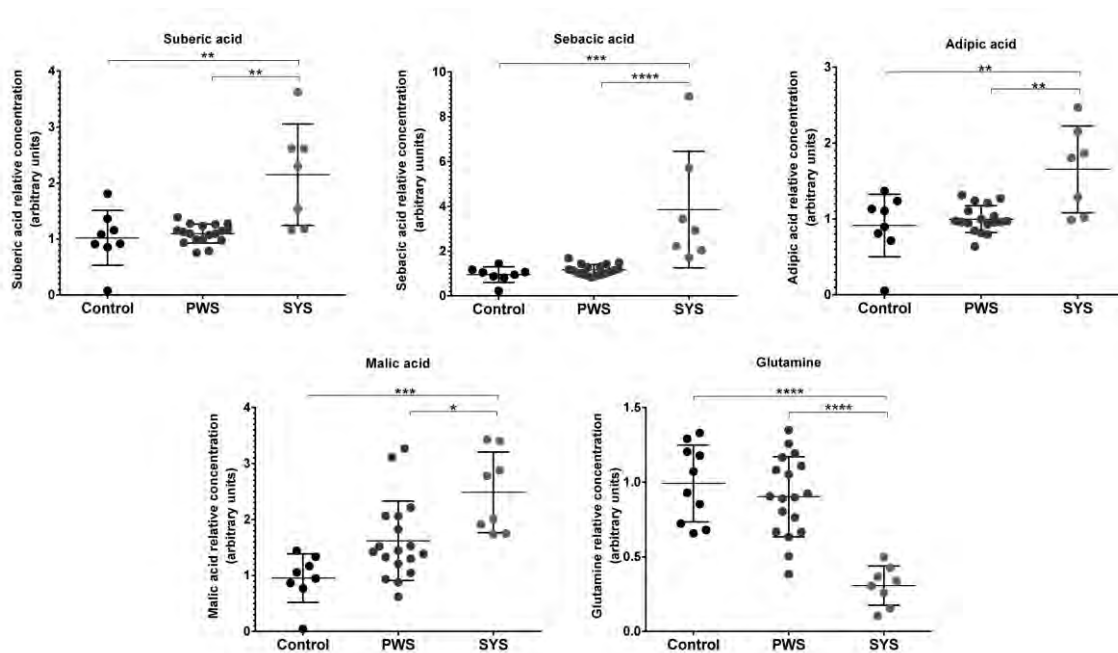


Figure 5. SYS fibroblasts show altered levels of glutamine and different organic acids. Values from 2 replicates have been normalized to the mean of the control group. Horizontal lines represent mean values and error bars represent the SD. **** p < 0.00001.

Table 1. Top ten up- and down-regulated DEGs

	Gene	ID	Log ₂ FC	FDR
Up-regulated	<i>HOTAIR</i>	ENSG00000228630	7.470	8.02E-30
	<i>MTRNR2L1</i>	ENSG00000256618	5.523	1.14E-05
	<i>PTPRD</i>	ENSG00000153707	4.625	1.23E-06
	<i>SLITRK4</i>	ENSG00000179542	4.524	8.81E-03
	<i>GATA2-AS1</i>	ENSG00000244300	4.304	1.41E-18
	<i>PITX1</i>	ENSG00000069011	4.234	8.16E-03
	<i>CLDN1</i>	ENSG00000163347	4.145	1.12E-06
	<i>ISL2</i>	ENSG00000159556	4.088	1.93E-03
	<i>RARB</i>	ENSG00000077092	4.000	1.49E-02
	<i>VANGL2</i>	ENSG00000162738	3.975	8.09E-07
Down-regulated	<i>ANGPTL1</i>	ENSG00000116194	-7.084	3.66E-06
	<i>TBX5</i>	ENSG00000089225	-6.982	9.18E-39
	<i>PI16</i>	ENSG00000164530	-6.385	1.29E-03
	<i>TBX5-AS1</i>	ENSG00000255399	-5.457	5.44E-12
	<i>INMT</i>	ENSG00000241644	-5.041	2.56E-03
	<i>CRLF1</i>	ENSG00000006016	-5.029	6.80E-04
	<i>ASPA</i>	ENSG00000108381	-4.813	1.02E-03
	<i>WISP2</i>	ENSG00000064205	-4.420	3.87E-08
	<i>KY</i>	ENSG00000174611	-4.248	1.30E-11
	<i>APOD</i>	ENSG00000189058	-4.213	6.00E-05

Supplementary information for:

Advancing in Schaaf-Yang syndrome pathophysiology: from bedside to subcellular analyses of truncated MAGEL2 in patients' fibroblasts

Laura Castilla-Vallmanya, Mercedes Serrano, Mónica Centeno-Pla, Héctor Franco-Valls, Raúl Martínez-Cabrera, Aina Prat-Planas, Elena Rojano, Pedro Seoane, Miriam Navarro, Clara Oliva, Rafael Artuch, Raquel Rabionet, Daniel Grinberg, Susanna Balcells, Roser Urreiziti

Supplementary Table 1. Clinical overview of MAGEL2-related disorders patients

		21 publications	Mejlachowicz 2015	Guo 2019	TOTAL
Clinical diagnosis		SYS/CHS	Lethal AMC	(SYS)	
Described cases		103	4	1	108
Protein change		See Figure 2	p.Gln666Serfs*36 (x3); p.Leu708Trpfs*7	p.Gln666Serfs*36	
Phenotype (HPO term)	HPO term identifier				
Pregnancy complications					
Decreased fetal movement	HP:0001558	10/28	4/4		14/32
Polyhydramnios	HP:0001561	5/10	4/4	1/1	10/16
Development & Intellectual disability					
Intellectual disability	HP:0001249	82/82			82/82
Autistic behaviour	HP:0000729	48/64			48/64
Abnormality of brain morphology	HP:0012443	18/27		1/1	19/26
Infantile lethargy/Weak cry	HP:0001254 HP:0001612	14/23			13/21
Neurodevelopmental delay	HP:0012758	93/93	-	-	91/91
Respiratory difficulties					
Respiratory failure requiring mechanical ventilation	HP:0002098	52/72	1/1		51/71
Apnea	HP:0002104	9/14			9/14
Sleep apnea	HP:0010535	47/68			47/68
Respiratory distress requiring endotracheal intubation	HP:0004887	37/59			35/58
Recurrent respiratory infections	HP:0004887	16/50			16/50
	HP:0002205	5/6			5/6
Feeding difficulties					
Poor suck	HP:0011968	89/101		1/1	88/100
Dysphagia	HP:0002033	68/76			66/74
Nasogastric tube feeding in infancy	HP:0002015	34/49			34/49
Gastrostomy tube feeding in infancy	HP:0011470	33/50			33/50
Hyperphagia	HP:0011471	26/52			25/50
	HP:0002591	13/53			13/53

Increased body weight/Obesity	HP:0004324 HP:0001513	19/66			19/66
Gastroesophageal Reflux	HP:0002020	36/70			35/68
Chronic constipation	HP:0012450	38/63			38/63
Physical characteristics					
Neonatal hypotonia	HP:0001319	50/56	1/1	1/1	50/56
Congenital contractures	HP:0002803	84/93		1/1	83/92
Arthrogryposis multiplex congenita	HP:0002804	13/29	4/4		17/33
Scoliosis	HP:0002650	31/55			31/55
Short stature	HP:0004322	31/44			31/44
Abnormality of the eye	HP:0000478	33/44			33/44
Small hands	HP:0200055	26/42			25/40
Camptodactyly of finger	HP:0100490	21/50	4/4		24/52
Tapered fingers	HP:0001182	14/43			12/41
Small feet	HP:0001773	13/34			13/34
Bilateral club foot	HP:0001776	7/19	4/4		10/21
Facial dysmorphism	HP:0001999	60/66	4/4		64/70
Endocrinology					
Hypopituitarism	HP:0040075	4/10			4/10
Growth hormone deficiency	HP:0000824	16/22			16/22
Hypothyroidism	HP:0000821	5/15			5/15
Hypoglycemia	HP:0001943	13/18			13/18
Temperature instability	HP:0005968	36/52			36/52
Diabetes insipidus	HP:0000873	3/7			3/7
Hypogonadism	HP:0000135	35/70		1/1	36/71
Cryptorchidism	HP:0000028	8/12			8/12
Other alterations					
Congenital heart defect	HP:0001627	7/18			5/16
Bradycardia	HP:0001662	3/4			3/4
Epilepsy	HP:0001250	23/75			22/73
Sleep disturbance	HP:0002360	5/5			5 cases
Death in infancy/childhood	HP:0001522 HP:0003819	12 cases	4 cases	1 case	17 cases

Supplementary Table 2. Standardized guidelines for SYS clinical management.

Perinatal period		
Medical problem	Description	Specific concerns or management
Respiratory difficulties	NICU frequently needed, mainly due to neonatal depression. The need of ventilatory assistance during the perinatal period varies from oxygenotherapy to invasive mechanical ventilation, from some hours of support to some months. Laryngeal stridor, glossoptosis, tracheomalacia and pulmonary hypoplasia have also been reported	NICU. Mechanical ventilation. Evaluation by otorhinolaryngologists and pneumologists to rule out anatomical abnormalities. Respiratory support from oxygenotherapy to invasive mechanical ventilation & tracheostomy
Feeding difficulties	Feeding difficulties with frequent choking episodes or inefficient sucking is very frequent. Hypotonia, lethargy, dysphagia and a high palate, all together may hinder oral nutrition.	Nutritionist and specialists in dysphagia are needed. Anatomical evaluation to rule out malformations. Supportive nutritional intervention, from nasogastric tube to permanent gastrostomy or parenteral nutrition may be required.
Contractures	Club feet, arthrogriposis, contractures and other movement restrictions are frequently present at birth. Fetal akinesia may lead to severe arthrogriposis.	Early intervention with orthopedic measures may prove essential to get a better prognosis. Refer to rehabilitation and orthopedic specialists.
Hormone insufficiency	Several endocrinology disturbances have been detected during the perinatal period, such as hypernatremia, diabetes insipidus, growth hormone deficiency (GH), hypoglycemia and hypocalcemia (see Endocrinology section).	Check glucose blood levels during the perinatal period. Laboratory test at this age should include extensive work-up on ions, glucose and hormones to rule out prevalent disturbances. Consult with child endocrinologist.
Other	Evaluation by a geneticist and dysmorphologist is recommended. A detailed physical exam and a standardized protocol to rule out organ malformations including echocardiogram, abdominal ultrasound, cranial ultrasound... is recommended.	
Childhood and adolescence		
Assessment	Follow-up / Studies	Specific concerns or interventions
Endocrinology (E)	6 mo/ Physical exam Lab tests Ultrasound Neuroimaging	E1→Failure to thrive during infancy and childhood, but also early overweight, obesity and hyperphagia beginning after infancy. Diet intervention may be required. E2→Short stature is prevalent (from -1.5 SD to -5SD), sometimes needing GH (consider obstructive apnea when prescribing GH) E3→Diabetes insipidus has been described presenting with polyuria, low urine specific gravity, hyposthenuria, and hypernatremia. Substitutive hormone therapy. E4→Panhypopituitarism caused by hypoplasia of pituitary gland, but also with normal MRI, has been described. Thyroid function, somatomedine C, GH, adrenal hormones, testosterone, LH and FSH need to be checked. Hyperprolactinemia has been detected. Treatment with hormones, including GH, levothyroxine and hydrocortisone, may be needed. Substitutive hormone therapy. During the adolescence consider estrogens. E5→Hypoglycemia. Guarantee glucose intake. E6→Temperature instability. Supportive measures. E6→Hypoplastic genitalia, micropenis and cryptorchidism. Testosterone, surgery.

<p>Gastro- enterology (G)</p>	<p>6 mo/ Physical exam, Feeding observation pHmetry Videofluoroscopy X-ray Lab tests</p>	<p>G1→Feeding problems are almost constant. Initial feeding difficulties are due to dysphagia, recurrent respiratory aspiration and sometimes nasogastric tube and gastrostomy is required. G2→Early onset chronic constipation and gastroesophageal reflux are frequent, too. G3→Rarely reported: intestinal pseudoobstruction, velopharyngeal insufficiency, eosinophilic esophagitis, and food allergies.</p>
<p>Muscular and skeletal system (MS)</p>	<p>12 mo/ Physical exam X-ray Electromyogram Nerve conduction</p>	<p>MS1→Arthrogriposis is very frequent: contractures shortening of the extremities, elbows, knees, hips. Camptodactily, clinodactily, brachydactily of fingers, adducted thumbs. MS2→Club feet and equinovaru feet have been repeatedly described. MS3→Scoliosis, kyphosis, lordosis and asymmetric thorax. Early rehabilitation programs and external orthosis may be needed. Periodical X-ray control of hips in non-ambulant children and spine in all, is recommended. Surgery when needed. MS4→Less frequently reported: mesomelic and rhizomelic shortening of limbs, hip dysplasia, and distal limb muscle atrophy.</p>
<p>Development & Intellectual disability (ND)</p>	<p>6 mo/12 mo Physical exam Developmental scales Parent-reported functional scales</p>	<p>ND1→Abnormal muscle tone and arthrogryposis are very frequent. Hypotonia is the most prevalent, with a probable central origin but, in some cases peripheral nerve conduction is abnormal. ND2→ Gross Motor development may be severely affected with delay in the acquisition of head control, sedestation, and walk (not achieved by many patients). ND3→ Fine Motor development is also abnormal due to motor abnormalities, arthrogryposis and camptodactily. Propositional use of hands, that rely on cognition and social skills, may be altered. Rehabilitation programs, early stimulation, and, later, occupational programs are essential. ND4→ Social skills and communication are frequently severely affected. Only some patients are able to develop scarce language. ND5 → ASD traits and behavioral disturbances are very prevalent. ASD trait may interfere with communication skills. Speech therapists evaluation is recommended for those patients with speech intention initiating vocabulary. Alternatives to speak communication such as signs or electronic devices may be of help. Psychotherapy may be needed for ASD, to treat not only the communicative sphere but also rigidity, reiterative behaviors, hypersensoriality,...</p>
<p>Epilepsy (E)</p>	<p>12 mo/ EEG</p>	<p>E1→ Febrile seizures have been reported. E2→ Epilepsy in less than 50% of patients, different typology (partial, generalized), different AEDs used with success.</p>
<p>Neuroimaging (NI)</p>	<p>At diagnosis & if new symptoms/ MRI</p>	<p>NI1→ Delayed myelination, ventricular enlargement, corpus callosum anomalies (thin, dysplasia or agenesis). NI2 → Normal or hypoplastic pituitary gland are frequently reported. NI3 → Seldom reported: global brain atrophy, increased T2 signal in caudate nucleus or in putamen, globus pallidus, hypoplastic vermis, punctate cerebellar haemorrhages.</p>
<p>Sleep disorders (SD)</p>	<p>12 mo/ Sleep questionnaires PSG</p>	<p>SD1→ Central apnea and/or obstructive apnea has been reported and may worsen cognitive and behavioural problems as well as be the cause of premature death. PSG is recommended</p>
<p>Infections (I)</p>	<p>12 mo/ Lab tests Imaging studies</p>	<p>I1→ Recurrent respiratory infections have been reported in those patients needing ventilatory support and in those without support. Chronic lung disease due to repeated broncopneumonia or recurrent aspirations has been reported. Imaging studies may be required to check lung parenchyma and rule out anatomical malformations. Invasive studies may rarely be necessary. I2→A predisposition to infections in other organs or systems is not reported.</p>

Cardiology (C)	At diagnosis & if new symptoms/ Physical exam, ECG, Echocardiogram	C1→Septal defects have been reported as structural heart anomalies, sometime spontaneously solved (ASD) C2→Bradycardia in a 1-month-old baby was reported.
Ophthalmology (O)	12 mo/ Physical exam Optometric tests Funduscopy MRI	O1→Strabismus and nystagmus, as oculomotor disorder have been described. O2→Refractory defects, and optic nerve hypoplasia or atrophy have been described. O3→Rare: Xerophthalmia, due to sleeping with eyes open. Sight is normally difficult to evaluate in SYS patients. Pediatric ophthalmologists are required. Lack of following with eyes has been described, probably ASD traits underlie this symptom.
Premature death		Reported causes of death (n=3) were severe sleep apnea, cardiac arrest in the context of epilepsy (SUDEP) and unknown causes

Supplementary Table 3. Complete list of DEGs

Gene ID	Gene symbol	Combined FDR	Mean LogFCs
ENSG00000228630	HOTAIR	0.00000000	7.4697
ENSG00000256618	MTRNR2L1	0.00001135	5.5233
ENSG00000153707	PTPRD	0.00000123	4.6245
ENSG00000179542	SLITRK4	0.00880923	4.5239
ENSG00000244300	GATA2-AS1	0.00000000	4.3041
ENSG00000069011	PITX1	0.00816110	4.2342
ENSG00000163347	CLDN1	0.00000112	4.1450
ENSG00000159556	ISL2	0.00193059	4.0878
ENSG00000077092	RARB	0.01493986	4.0001
ENSG00000162738	VANGL2	0.00000081	3.9748
ENSG00000250133	HOXC-AS2	0.00000000	3.7501
ENSG00000114115	RBP1	0.00010963	3.6565
ENSG00000251151	HOXC-AS3	0.00002460	3.5799
ENSG00000170412	GPRC5C	0.00318874	3.5355
ENSG00000158258	CLSTN2	0.00001884	3.2582
ENSG00000205403	CFI	0.00481319	3.2156
ENSG00000176887	SOX11	0.00617501	3.1216
ENSG00000050344	NFE2L3	0.00406723	3.0615
ENSG00000118785	SPP1	0.00001245	2.9987
ENSG00000179348	GATA2	0.00002887	2.8457
ENSG00000165194	PCDH19	0.00016182	2.8371
ENSG00000189120	SP6	0.00048115	2.8068
ENSG00000110328	GALNT18	0.01328474	2.7797
ENSG00000145794	MEGF10	0.00006520	2.7100
ENSG00000145569	FAM105A	0.00486515	2.6858
ENSG00000158164	TMSB15A	0.00000078	2.6185
ENSG00000213190	MLLT11	0.00000008	2.5159
ENSG00000116741	RGS2	0.00007873	2.5044
ENSG00000144355	DLX1	0.00483280	2.5016
ENSG00000139364	TMEM132B	0.00011399	2.4618
ENSG00000122378	FAM213A	0.00287714	2.4111
ENSG00000146250	PRSS35	0.00561639	2.3849
ENSG00000260549	MT1L	0.00000992	2.1904
ENSG00000273038	AL365203.3	0.00000000	1.9057
ENSG00000151725	CENPU	0.00000002	1.8965

ENSG00000090530	P3H2	0.00086613	1.8937
ENSG00000149948	HMGA2	0.00670181	1.8504
ENSG00000131203	IDO1	0.00013629	1.8327
ENSG00000138135	CH25H	0.00008401	1.7432
ENSG00000156970	BUB1B	0.00373261	1.7240
ENSG00000104368	PLAT	0.00860139	1.7015
ENSG00000143228	NUF2	0.00632092	1.6711
ENSG00000114268	PFKFB4	0.00014643	1.6596
ENSG00000121621	KIF18A	0.00034690	1.6581
ENSG00000170312	CDK1	0.00213696	1.5856
ENSG00000115163	CENPA	0.00279515	1.5844
ENSG00000164687	FABP5	0.00080168	1.5778
ENSG00000111110	PPM1H	0.00645193	1.5669
ENSG00000197632	SERPINB2	0.01326318	1.4831
ENSG00000150995	ITPR1	0.00769409	1.4761
ENSG00000124813	RUNX2	0.00001473	1.4757
ENSG00000176971	FIBIN	0.01272529	1.4381
ENSG00000254726	MEX3A	0.00017300	1.4358
ENSG00000102096	PIM2	0.00093743	1.4035
ENSG00000197646	PDCD1LG2	0.01170811	1.3984
ENSG00000259207	ITGB3	0.00648175	1.3957
ENSG00000118193	KIF14	0.00636966	1.3816
ENSG00000152952	PLOD2	0.00006319	1.3715
ENSG00000050730	TNIP3	0.00404054	1.3498
ENSG00000168679	SLC16A4	0.00212062	1.3118
ENSG00000150051	MKX	0.00001061	1.2801
ENSG00000171812	COL8A2	0.01530689	1.2742
ENSG00000135048	TMEM2	0.00436512	1.2558
ENSG00000171502	COL24A1	0.00000125	1.2508
ENSG00000140263	SORD	0.01645580	1.2443
ENSG00000188342	GTF2F2	0.00000000	1.2364
ENSG00000137269	LRRC1	0.00543204	1.2269
ENSG00000135916	ITM2C	0.00288275	1.2159
ENSG00000057019	DCBLD2	0.00000000	1.2142
ENSG00000140945	CDH13	0.00007483	1.1570
ENSG00000176697	BDNF	0.00008341	1.1214
ENSG00000067177	PHKA1	0.00188460	1.1207
ENSG00000154188	ANGPT1	0.00002689	1.1025
ENSG00000130066	SAT1	0.00760640	1.0727
ENSG00000103187	COTL1	0.00983754	1.0350
ENSG00000132429	POPDC3	0.00001490	1.0274
ENSG00000178695	KCTD12	0.00106130	-1.0194
ENSG00000188112	C6orf132	0.00000368	-1.0303
ENSG00000099377	HSD3B7	0.00134145	-1.0580
ENSG00000176658	MYO1D	0.00404705	-1.1198
ENSG00000173517	PEAK1	0.00000101	-1.1545
ENSG00000182179	UBA7	0.00009340	-1.1594
ENSG00000189320	FAM180A	0.00180989	-1.2136
ENSG00000138131	LOXL4	0.00469257	-1.2375
ENSG00000138744	NAAA	0.00357893	-1.2792
ENSG00000239653	PSMD6-AS2	0.00185430	-1.3232
ENSG00000138356	AOX1	0.00195770	-1.3434
ENSG00000157404	KIT	0.00002769	-1.3879
ENSG00000176928	GCNT4	0.00415318	-1.4183

ENSG00000229847	EMX2OS	0.00241163	-1.4284
ENSG00000266094	RASSF5	0.00012660	-1.4698
ENSG00000116667	C1orf21	0.00005050	-1.5643
ENSG00000139132	FGD4	0.00322221	-1.7180
ENSG00000152117	AC073869.1	0.00144781	-1.7284
ENSG00000228784	LINC00954	0.00041045	-1.7334
ENSG00000153993	SEMA3D	0.00004346	-1.7822
ENSG00000206538	VGLL3	0.00000000	-1.8117
ENSG00000196935	SRGAP1	0.00000972	-1.9512
ENSG00000204682	CASC10	0.00032805	-2.0733
ENSG00000035664	DAPK2	0.00001064	-2.0752
ENSG00000149292	TTC12	0.00930174	-2.1262
ENSG00000172348	RCAN2	0.00062630	-2.1702
ENSG00000287733	novel transcript (lncRNA)	0.00002544	-2.1759
ENSG00000235505	AP002004.1	0.00073579	-2.1960
ENSG00000107738	VSIR	0.00000000	-2.2341
ENSG00000215386	MIR99AHG	0.00000168	-2.2998
ENSG00000130038	CRACR2A	0.00001310	-2.3839

Supplementary Table 3. Significantly enriched REACTOME categories

ID	Description	pvalue	p.adjust	qvalue	Gene symbol	Gene Count
REACTOME						
R-HSA-2500257	Resolution of Sister Chromatid Cohesion	0.0000927	0.0223995	0.0212078	<i>CENPA,KIF18A,NUF2,CENPU,BUB1B,CDK1</i>	6
R-HSA-141424	Amplification of signal from the kinetochores	0.0002435	0.0223995	0.0212078	<i>CENPA,KIF18A,NUF2,CENPU,BUB1B</i>	5
R-HSA-69618	Mitotic Spindle Checkpoint	0.0005179	0.0332646	0.0314948	<i>CENPA,KIF18A,NUF2,CENPU,BUB1B</i>	5
R-HSA-1474290	Collagen formation	0.0001799	0.0223995	0.0212078	<i>P3H2, LOXL4,PLOD2,COL24A1,COL8A2</i>	5
R-HSA-1474244	Extracellular matrix organization	0.0018623	0.0623008	0.0589862	<i>P3H2,SPP1,LOXL4,PLOD2,COL24A1,COL8A2,ITGB3</i>	7
GO Biological Process						
GO:0007517	Muscle organ development	0.0000987	0.0661964	0.0577844	<i>PITX1,TBX5,RGS2,POPDC3,MEGF10,MKX,VANGL2,PI16,CDK1,SOX11</i>	10
GO:0050769	Positive regulation of neurogenesis	0.0016499	0.0818553	0.0714535	<i>RARB,ASPA,RGS2,DLX1,PTPRD,KIT,BDNF,SOX11,GATA2</i>	9
GO Cellular Components						
GO:0000776	Kinetochores	0.0001378	0.0130901	0.0123286	<i>RASSF2,CENPA,KIF18A,NUF2,CENPU,BUB1B</i>	6
GO:0000775	Chromosome, centromeric region	0.0009309	0.0294791	0.0277642	<i>RASSF2,CENPA,KIF18A,NUF2,CENPU,BUB1B</i>	6

Article 10: Generation of human iPSC lines from two Schaaf-Yang Syndrome (SYS) patients

Summary:

Truncating heterozygous mutations in *MAGEL2* cause Schaaf-Yang syndrome (#OMIM 6615547; SYS), a rare neurodevelopmental disorder with a high phenotypic overlap with Prader-Willi syndrome (#OMIM 176270; PWS). Here, we generated two iPSC lines with mRNA reprogramming from fibroblasts obtained from two SYS patients with the heterozygous c.1912C>T variant (SYS1) or the highly recurrent variant c.1996dupC (SYS2). We confirmed that the reprogrammed iPSC lines have a normal karyotype, express pluripotency markers and have the potential to differentiate to the three germ layers. These lines are a valuable resource for the generation of relevant *in vitro* models of SYS.

Reference:

Laura Castilla-Vallmanya, Daniel Grinberg, Susanna Balcells, Roser Urreizti & Isaac Canals. Generation of human iPSC lines from two Schaaf-Yang Syndrome (SYS) patients. To be submitted to Stem Cell Research.

Lab Resource: Multiple Cell Lines - template

Title: Generation of human iPSC lines from two Schaaf-Yang Syndrome (SYS) patients

Authors: Laura Castilla-Vallmanya^{1,2}, Daniel Grinberg^{1,2}, Susanna Balcells^{1,2}, Roser Urreiziti^{1,2,3}, Isaac Canals⁴

Affiliations:

1) Department of Genetics, Microbiology and Statistics, Faculty of Biology, University of Barcelona, IBUB, IRSJD, 08028 Barcelona, Spain.

2) Centro de Investigación Biomédica en Red de Enfermedades Raras (CIBERER)- Instituto de Salud Carlos III, Spain.

3) Clinical Biochemistry Department, Hospital Sant Joan de Déu, 08950, Barcelona, Esplugues de Llobregat, Spain.

4) Neurodevelopment and Neurodegeneration Group, Faculty of Medicine, Lund University, Lund, Sweden.

Abstract: Truncating heterozygous mutations in *MAGEL2* cause Schaaf-Yang syndrome (#OMIM 6615547; SYS), a rare neurodevelopmental disorder with a high phenotypic overlap with Prader-Willi syndrome (#OMIM 176270; PWS). Here, we generated two iPSC lines with mRNA reprogramming from fibroblasts obtained from two SYS patients with the heterozygous c.1912C>T variant (SYS1) or the highly recurrent variant c.1996dupC (SYS2). We confirmed that the reprogrammed iPSC lines have a normal karyotype, express pluripotency markers and have the potential to differentiate to the three germ layers. These lines are a valuable resource for the generation of relevant *in vitro* models of SYS.

Resource Table:

Alternative name(s) of stem cell lines	SYS1	
(Used by researchers)	SYS2	
Institution	Lund University, University of Barcelona	
Contact information of distributor	Isaac Canals (isaac.canals@med.lu.se) Susanna Balcells (sbalcells@ub.edu)	
Type of cell lines	Induced pluripotent stem cells	
Origin	Human	
Additional origin info required	SYS1 Age: 20 years old Sex: Female Ethnicity: European	SYS2 Age: 6 years old Sex: Male Ethnicity: European

Cell Source	Fibroblasts
Clonality	Clonal
Method of reprogramming	Non-modified RNA and microRNA transfection
Genetic Modification	NO
Type of Genetic Modification	Non genetically modified
Evidence of the reprogramming transgene loss (including genomic copy if applicable)	Non-applicable (mRNA reprogramming)
Associated disease	Schaaf-Yang syndrome (SYS)
Gene/locus	SYS1: <i>MAGEL2</i> : Chr15: 23643549-23647867, NM_019066.5: c.1912C>T (p.Q638*) SYS2 <i>MAGEL2</i> : Chr15: 23643549-23647867, NM_019066.5: c.1996dupC (p.Q666Pfs*47)
Date archived/stock date	Not available yet
Cell line repository/bank	Lines have not been registered
Ethical approval	Institutional Review Board (IRB00003099) of the Bioethical Commission of the University of Barcelona (October 5, 2020)

Resource utility

Truncating mutations in *MAGEL2* cause a multisystemic disorder called Schaaf-Yang syndrome. Given their capacity to differentiate to different cell types, iPSCs are a powerful tool to study multisystemic diseases. We generated two iPSC lines from patients with two different mutations in *MAGEL2* that could be used to generate SYS models.

Resource Details

Schaaf-Yang syndrome (#OMIM 6615547; SYS) is a rare developmental disorder, which was first considered to be a Prader-Willi-like syndrome due to high phenotypic overlap. However, some recurrent and exclusive clinical features such as distal joint contractures, autistic traits and more severe intellectual disability and developmental delay, led to its statement as an independent condition (1). *MAGEL2* is a single-exon gene that maps to 15q11-q13, also known as the Prader-Willi region, which encodes a protein consisting of 1249 amino acids. Almost all identified mutations are predicted to

cause the translation of a truncated form of the protein lacking the MHD functional domain, located at the C-terminal end of *MAGEL2* (2).

Both iPSC lines have been generated from patients that have already been clinically and genetically described elsewhere: SYS1 (3) and SYS2 (4).

We successfully generated and characterized two iPSC lines from fibroblasts obtained from two SYS patients, each carrying a recurrent disease-causing mutation in *MAGEL2* in heterozygosis (SYS1: c.1912C>T and SYS2: c.1996dupC). The StemRNA 3rd Gen Reprogramming Kit (Stemgent®) was used to establish the iPSCs lines by transfecting an RNA cocktail containing non-modified reprogramming mRNAs (OCT4, SOX2, KLF4, cMYC, NANOG and LIN28 (OSKMNL)), immune evasion mRNAs (E3, K3, B18) and double-stranded microRNAs from the 302/367 cluster into fibroblasts.

Approximately 10-12 days after transfection, iPSC colonies emerged and 6 clones for each line were picked and passaged for expansion. One clone of each cell line was selected for further characterization and validation. Both lines presented normal growing and iPSC colony morphology (Figure 1A, Table1) and were mycoplasma free (Table 1). Both SYS1 and SYS2 were confirmed to be positive for the pluripotency stem cell markers OCT4, NANOG and SOX2 through immunofluorescence and microscopy (Figure 1B, Table 1). Consistently, expression of pluripotency-associated genes *OCT4*, *NANOG* and *SOX2* was highly increased in iPSCs compared to fibroblasts, while expression of a fibroblast gene, *DCN*, could only be detected in fibroblasts but not iPSCs, confirming successful reprogramming of the clones towards a pluripotent state (Figure 1C, Table 1). To ensure genome integrity of SYS1 and SYS2, we performed a Giemsa-banded karyotyping analysis, which showed normal diploid 46, XX karyotype for SYS1 and 46, XY for SYS2 (Figure 1D, Table 1). Moreover, to confirm that the origin of each iPSC line was the corresponding fibroblastic line, a microsatellite PCR analysis was performed (available with the authors). To further prove the parental origin of the lines, the maintenance of the disease-associated genotype in the iPSCs was checked by Sanger sequencing (Figure 1E, Table 1) using specific primers (Table 2), confirming the presence of the patient-specific mutation. Finally, to demonstrate the pluripotent capacity of the cells, we differentiated them into the three germ layers and identify cells from each germ layer using immunofluorescence microscopy to detect specific markers (Figure 1F, Table 1).

Materials and Methods

1) Fibroblasts reprogramming

Fibroblasts were plated in 4-well plated coated with Laminin-521 (Stem Cell Technologies) and maintained in DMEM (ThermoFisher Scientific) supplemented with GlutaMAX (ThermoFisher Scientific) at 37°C and 5% CO₂ in a humidified atmosphere. The day after, medium was replaced with Essential 8™ medium (ThermoFisher Scientific) and cells were transfected with the StemRNA 3rd Gen Reprogramming Kit (Stemgent®) RNA cocktail using lipofectamine RNAiMAX (ThermoFisher Scientific) for 4 consecutive days. Media was changed daily until ES-like appearing colonies emerge around days 10-12 after transfection, then colonies were picked and plated in laminin-coated 4-well plates in Essential 8™ medium. Cells were passaged using TrypLE™ Select Enzyme (ThermoFisher Scientific) to 6-well plated coated with Matrigel (Corning, Inc.) for expansion, medium was supplemented with Rock inhibitor (Y-27632) (StemCell Technologies) for 24 hours after every passage.

2) Embryonic body (EB) formation and in vitro differentiation

For EB formation, iPSCs were detached and distributed in a V-bottom 96-well plate, where were maintained in Essential 8™ medium supplemented with Rock inhibitor for 24 hours. Then, the EBs were transferred to Matrigel-coated chamber-flasks and the differentiation protocol to the tree germ layers was performed as in (5).

3) Immunofluorescence staining

Cells were fixed with 4% paraformaldehyde (PFA) for 15 minutes and blocked in potassium-phosphate-buffered saline with 0.25% Triton X-100 (TKPBS) and 5% Normal Donkey Serum (NDS; Merck Millipore) for 1 hour at room temperature. Primary antibodies (Table 2) were incubated at 4°C in the same solution overnight. Secondary antibodies (Table 2) were incubated at room temperature for 2 hours. For nuclear staining, 0,5 µg/ml DAPI (Invitrogen) in TKPBS was incubated for 5 minutes. Slides were mounted with polyvinyl alcohol mounting medium with DABCO® (Sigma-Aldrich) and left to dry overnight. All images were captured with a fluorescence microscope using 20x or 40x objectives and analysed with the ImageJ software.

4) Gene expression

RNA was isolated with the RNeasy Mini Kit (Qiagen) following manufacturer's instructions. RNA was treated with DNase I (Qiagen) to avoid DNA contamination. A Nanodrop ND-1000 spectrophotometer

(Saveen & Werner) was used to quantify the obtained RNA. Then, 1 µg of RNA was reverse transcribed using the qScript cDNA Synthesis Kit (Quantabio). RT-qPCRs were performed using TaqMan Universal PCR Master Mix and gene-specific TaqMan assays (Table 2) with an iQ5 Real-Time PCR detection system (Bio-Rad).

5) Karyotyping

SYS1 and SYS2 at passage 8 and 9 after transfection were prepared for karyotyping. Cells were incubated with 2ng/ml KaryoMAX™ Colcemid™ (Gibco) in Essential 8™ medium for 45 minutes at 37°C in the CO2 incubator. Then, cells were harvested using StemPro Accutase and fixed with Carnoy's fixative. Twenty metaphases for each cell line were analysed by Servicio de Medicina Genética y Molecular (Hospital Sant Joan de Déu, Barcelona)

6) Mutation analysis, microsatellites analysis and mycoplasma contamination test

DNA was extracted using the DNeasy Mini Kit (Qiagen) following manufacturer's instructions. Mutation analysis was performed by PCR amplification using specific primers (Table 2), followed by Sanger sequencing performed at the Scientific and Technological Center of the University of Barcelona (CCiTUB). Four specific microsatellites primers (Table 2) labelled with 6FAM were used for PCR and subsequent capillary electrophoresis analysis, using GeneScan™ 600 LIZ™ (Applied Biosystems) as size standard, was also performed at CCiTUB. Cell culture supernatants were tested using the Mycoplasma Detection Kit (Biotools).

References

1. Schaaf CP, Gonzalez-Garay ML, Xia F, Potocki L, Gripp KW, Zhang B, et al. Truncating mutations of *MAGEL2* cause Prader-Willi phenotypes and autism. *Nat Genet.* 2013 Nov;45(11):1405-8.
2. Patak J, Gilfert J, Byler M, Neerukonda V, Thiffault I, Cross L, et al. *MAGEL2*-related disorders: A study and case series. *Clin Genet.* 2019 Dec 1;96(6):493–505.
3. Urreiziti R, Cueto-Gonzalez AM, Franco-Valls H, Mort-Farre S, Roca-Ayats N, Ponomarenko J, et al. A de Novo Nonsense Mutation in *MAGEL2* in a Patient Initially Diagnosed as Opitz-C: Similarities between Schaaf-Yang and Opitz-C Syndromes. *Sci Rep.* 2017 Mar 10;7:44138
4. Palomares-Bralo M, Vallespín E, Del Pozo Á, Ibañez K, Silla JC, Galán E, et al. Pitfalls of trio-based exome sequencing: Imprinted genes and parental mosaicism - *MAGEL2* as an example. *Genet Med.* 2017 Nov;19(11):1285–6.
5. Canals I, Soriano J, Orlandi JG, Torrent R, Richaud-Patin Y, Jiménez-Delgado S, et al. Activity and High-Order Effective Connectivity Alterations in Sanfilippo C Patient-Specific Neuronal Networks. *Stem Cell Reports.* 2015 Oct 13;5(4):546–57

Additional files:

Figure 1

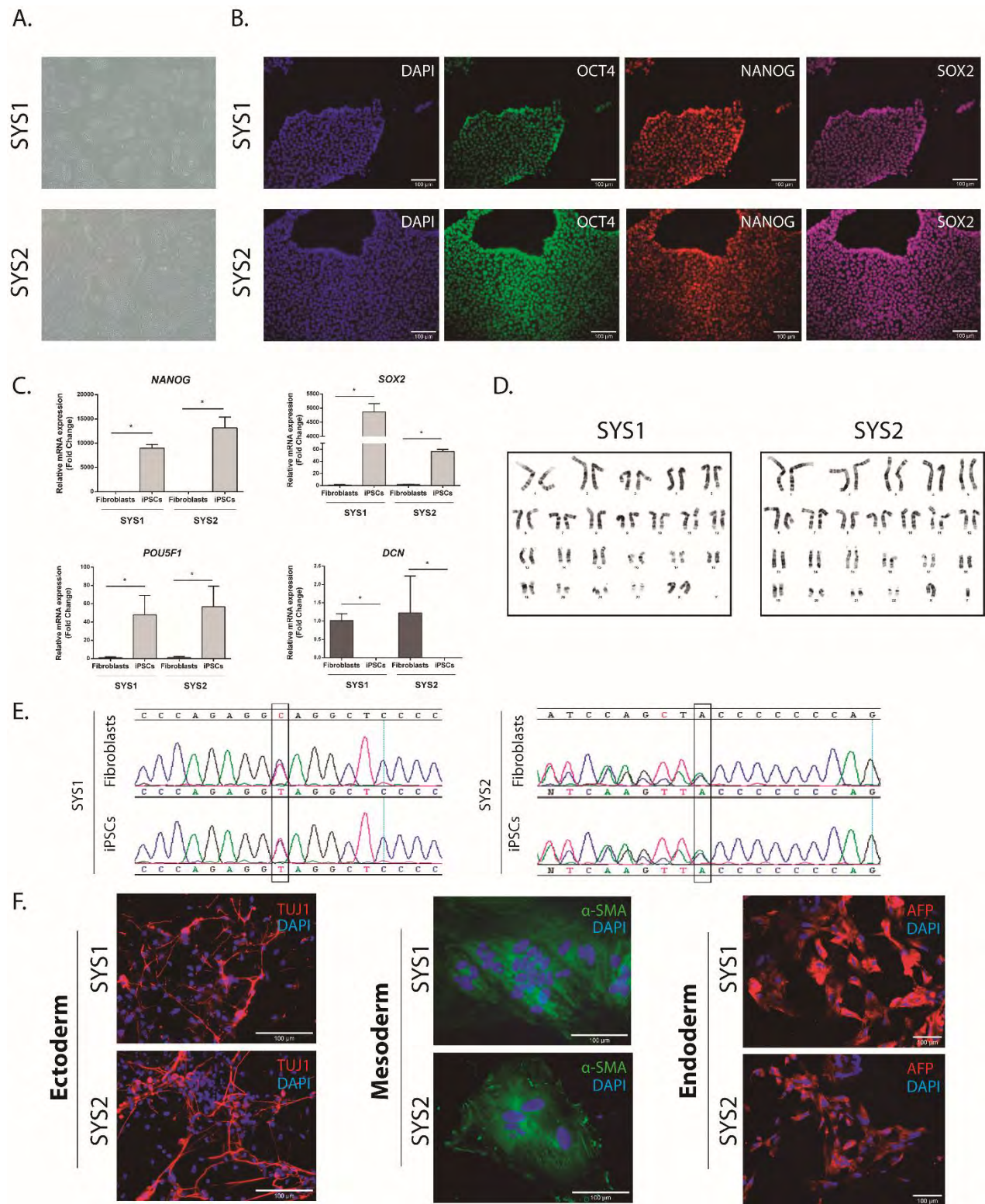


Figure 1. Characterization of the generated SYS1 and SYS2 lines from SYS patients.

Table 1: Characterization and validation

Classification	Test	Result	Data
Morphology	Photography Bright field	Normal morphology of iPSC colony	Fig. 1A
Phenotype	Immunocytochemistry Qualitative analysis	Positive staining of pluripotency markers: OCT3/4, NANOG and SOX2	Fig. 1B
	RT-qPCR Quantitative analysis	Relative expression of pluripotency markers: positive for <i>OCT3/4</i> , <i>NANOG</i> and <i>SOX2</i> and negative for <i>DCN</i>	Fig. 1C
Genotype	Karyotype (G-banding) and resolution	46, XX and 46XY, Resolution 300-500	Fig. 1D
Identity	Microsatellite PCR (mPCR) OR	Performed, 7 loci tested, 100% matched	Available with the authors
	STR analysis	N/A	N/A
Mutation analysis (IF APPLICABLE)	Sequencing	Heterozygous nonsense (<i>SYS1</i>) and frameshift (<i>SYS2</i>) mutations	Fig. 1E
	Southern Blot OR WGS	N/A	N/A
Microbiology and virology	Mycoplasma	Negative	Available with the authors
Differentiation potential	Embryoid body formation and differentiation	Endoderm: α -fetoprotein (AFP); Mesoderm: α -smooth muscle actin (α -SMA); Ectoderm: β -III-tubulin (TUJ1)	Fig. 1F
Donor screening (OPTIONAL)	HIV 1 + 2 Hepatitis B, Hepatitis C	N/A	N/A
Genotype additional info (OPTIONAL)	Blood group genotyping	N/A	N/A
	HLA tissue typing	N/A	N/A

Table 2: Reagents details

Antibodies used for immunocytochemistry				
	Antibody	Dilution	Company Cat #	RRID
Pluripotency markers	Mouse anti-OCT3/4	1:100	Santa Cruz Biotechnology #sc-5279	AB_628051
	Rabbit anti-NANOG	1:100	Abcam #ab21624	AB_446437
	Goat anti-SOX2	1:50	R&D Systems #AF2018	AB_355110
Differentiation Markers	Rabbit anti-AFP	1:100	Dako #A0008	AB_2650473
	Mouse anti- α SMA	1:100	Sigma Aldrich #A5228	AB_262054
	Rabbit anti-TUJ1	1:500	Biolegend #802001	AB_2564645
Secondary antibodies	Donkey anti-mouse Alexa-488	1:500	Invitrogen #A21202	AB_141607
	Donkey anti-rabbit Alexa-568	1:500	Invitrogen #A10042	AB_2534017
	Donkey anti-goat Alexa-647	1:500	Invitrogen #A21447	AB_141844
Primers				
	Target	Size of band	Forward/Reverse primer (5'-3')	
Targeted mutation sequencing	<i>MAGEL2</i>	717bp	CATCCGACCTGCCCCACA / GAGGTCCTGCGCTCTTTAGA	
	Target	Assay ID (TaqMan)		
Pluripotency markers	<i>POUF51 (OCT3/4)</i>	Hs01654807_s1		
	<i>NANOG</i>	Hs02387400_g1		
	<i>SOX2</i>	Hs04234836_s1		
Fibroblast marker	<i>DCN</i>	Hs00754870_s1		
Housekeeping gene	<i>YWHAZ</i>	Hs01122445_g1		



DISCUSSION

This thesis started as part of a collaborative translational project that was set up in 2011 with the aim of identifying the genetic cause underlying Opitz C syndrome. To fulfill this objective, a cohort of 19 patients from 15 families diagnosed with OCS, or BOS, from all over the world was gathered in order to identify the molecular origin of the syndrome. The chosen methodology was whole exome sequencing, preferably trio-WES. Of note, all the patients of the Opitz C cohort were tested through karyotype and the majority by SNP array or aCGH to exclude bigger genetic aberrations that would not be detectable by WES. The diagnostic success rate achieved was 93.3% (14/15 families) for the “Opitz C cohort”, as the only cases that still remain unsolved are the OC10 siblings. The genetic diagnosis of nine of these patients was performed as part of the work presented in this thesis (highlighted in orange in **Figure 13**).

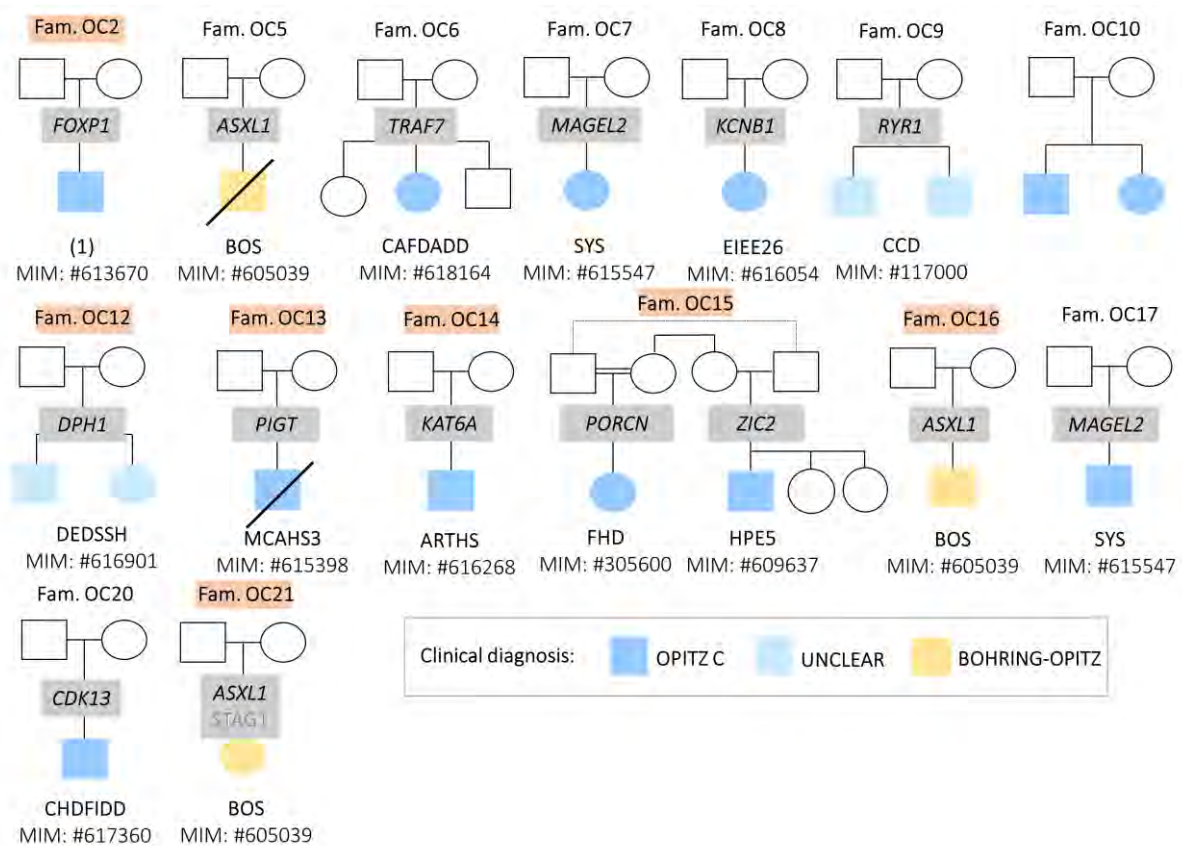


Figure 13. Pedigrees of the 15 families included in the Opitz C cohort, the identified causal gene and the final genetic diagnosis. Different colours represent the initial clinical diagnosis.

(1): Mental retardation with language impairment and with or without autistic features; BOS: Bohring-Opitz Syndrome; CAFDADD: Cardiac, facial, and digital anomalies with developmental delay; SYS: Schaaf-Yang syndrome; EIEE26: Early Infantile Epileptic Encephalopathy 26; CCD: Central Core Disease of muscle; DEDSSH: Developmental Delay with Short stature, Dysmorphic features and Sparse Hair; MCAHS3: Multiple Congenital Anomalies-Hypotonia-Seizures syndrome 3; ARTHS: Arboleda-Tham Syndrome; FHD: Focal dermal hypoplasia; HPE5: Holoprosencephaly 5; CHDFIDD: Congenital heart defects, dysmorphic facial features, and intellectual developmental disorder.

What we observed was that most of the patients carried mutations in different genes, many of them already associated with other ultra-rare NDDs, very usually, of recent description (**Figure 13**). This scenario is a clear example of the effect that NGS techniques are having on the diagnosis of syndromic neurodevelopmental disorders. Our overall results confirm that OCS is a very heterogeneous entity without a common genetic cause and could be declared as extinct, as already proposed by other authors (152). However, we think that OCS is still a useful clinical description that can help clinicians and geneticists to better delineate the clinical spectrum of severe NDD patients and potentially accelerate the diagnosis process, as thoroughly discussed in Urreizti et al. (28). Also, from a social perspective, OCS can be useful as a clinical “label” for families and patients in their first years of life, as stress and uncertainty of being undiagnosed can really affect their mental health and wellness until a final molecular diagnosis is reached.

These results also prove that WES is a powerful tool to identify the molecular basis of ultra-rare NDDs, as it has allowed each patient to be re-diagnosed according to the particular molecular cause of his/her disease. Although it is true that genetic testing greatly helps to overcome the difficulties encountered in clinical diagnosis, mostly caused by the variable phenotypes shown by patients of the same syndrome, it cannot be considered as a substitute. In the first instance, a deep and thorough clinical characterization of the patient can orientate the genetic testing to be performed in each particular case. Also, in difficult cases where genetic testing results are inconclusive or ambiguous, a revision of the clinical description can lead to a successful re-analysis of the genetic data and the establishment of the molecular diagnosis. Approximately 25-68% of NDD patients studied with NGS techniques obtain a clear genetic diagnosis (45). The higher diagnostic yield reached in the Opitz C cohort can be explained by deep analysis of the sequencing data followed by functional analyses that have been carried out for each particular case. Below, I will discuss the main difficulties that we have encountered when establishing a genetic diagnosis for each patient and the tools, strategies and considerations that have been crucial to reach such a successful diagnostic rate.

1. INTERPRETATION OF THE IDENTIFIED VARIANTS

One of the biggest challenges and time-consuming steps of genetic diagnosis through NGS is the **interpretation of the identified variants**. Even after the application of different bioinformatic and quality filters, thousands of variants per exome remain as potential candidates. To obtain a manageable number of candidates, the resulting variants are filtered considering their prevalence in the general population, functional predictors scores and

additional published data on functional studies and segregation within the family, as advised by the ACMG guidelines (35). On average, each exome presents around 500 rare coding variants that are present in less than 1% of the population (153). When prioritizing the variants, it is highly advisable to follow the ACMG nomenclature, including 5 categories ranging from “benign” to “pathogenic” (35), as it is used on the majority of sequencing reports allowing standardization across different laboratories. There are several user-friendly web tools that perform automatic classification of the variants based on the ACMG guidelines criteria, like Varsome (154) and wInterVar (155). It is undeniable that they have a strong potential to facilitate the understanding of the functional consequences of the filtered variants, smoothing the path for their interpretation by clinicians and researchers. However, it is highly advisable to perform a careful manual revision of the *in silico* predictions and previously published functional data of the best candidates before taking them as definitive.

1.1 VUS interpretation and IF reporting

Some of those filtered mutations can be considered as **variants of unknown significance** (VUS) when the evidences supporting pathogenicity or neutrality are not enough to tip the balance against one direction or the other. The implementation of NGS-based testing involves the appearance of more VUS than other methods, such as gene-panels, as a larger portion of the genome is sequenced and a larger number of variants is identified. VUS are normally included in the patient’s final report, although its clinical utility is limited. It may be useful in some cases when such variants could be modifying the phenotype of the patient or potentially explaining part of it, especially in complex cases. Also, new information could appear over the years and allow reclassification of a certain VUS to “likely pathogenic” or “pathogenic”.

It is very important to consider the impact that the reporting of the genetic findings may have on the family. It is crucial that they are informed by trained clinicians or genetic counselors that can explain the information rigorously and solve all their doubts. The more variants are reported to the family, even if they are considered as VUS, the more stress and uncertainty they might feel. Reason why it is crucial that geneticists make an extra effort to manually classify the most relevant identified variants and avoid total reliance on automatic classification systems.

An illustrative example of the importance of careful variant interpretation and the utility of reporting VUS is the case presented in Article 1. In patient OC21, WES showed three *de novo* heterozygous variants: a frameshift mutation in *BACH1*, a missense mutation in *STAG1* and a

splicing mutation in *ASXL1*. As a result of the identification of the *STAG1* variant, patient OC21 was initially reported with a possible Cornelia De Lange-like phenotype in a large cohort of patients with cohesinopathies (156). However, the characteristics of the variant did not match the rest of previously reported disease-causing *STAG1* mutations (157) and *in silico* predictors classified it as benign, questioning its pathogenicity. We think that this variant should be considered as a VUS, which is not the main cause of the disease and probably benign, although the possibility of it acting as a modifier of the patient's phenotype cannot be discarded. Regarding the variant in *ASXL1*, it was a *de novo* mutation affecting the acceptor splice site at intron 12 of the gene, predicted to lead to the appearance of a premature STOP codon and the production of a truncated form of the protein, similarly to the variants that had been previously associated with Bohring-Opitz syndrome (65,69,158). The fact that the clinical presentation of patient OC21 did not strictly meet the clinical criteria for BOS did not totally support this hypothesis. However, results from functional studies, which will be discussed below, confirmed the effect on splicing of the *ASXL1* variant, identifying it as the most probable cause of the disease.

Another challenge related to variant reporting when performing NGS techniques is the identification of what is known as **incidental findings (IFs)**, that are those findings unrelated to the original purpose of the sequencing test but that have medical relevance for patient care. Obviously, IFs are not restricted to the proband when including unaffected family members to the analysis, as they may have direct implications for all the sequenced individuals. The ACMG published a list including highly penetrant and medically actionable variants in 59 pre-selected genes, which is reviewed and updated over time (159). When identified, these variants are recommended to be returned to the patient. The genes included in this list are mostly related to late-onset medical conditions whose prognosis may improve with frequent monitoring or lifestyle changes, such as several cardiovascular conditions or different types of cancers (159). Determining which IFs and how should be reported back to the patients is still a highly controversial issue (160). Little is known about how people who are not familiar with these disorders would react with these findings and deal with the options they would have regarding prevention and reproductive choice (161). For this reason, the family should be properly informed about the possibility of the identification of IFs, their possible associated consequences and that they have the right to decide to get them reported back or not. This information has to be provided and discussed during the informed consent process and **before** the performance of the initial genetic diagnostic test. The documents linked to this informed consent include the informed decision that the family makes related IFs and that the final relevant clinical information should be assessed and reported according to the criteria of experts in the field.

1.2 Advantages of using trio-WES

Choosing the **optimal experimental design** is one of the ways to significantly increase the diagnostic power of WES. Although analyzing the genomic data of the patient as a singleton helps to reduce the economic costs of the sequencing, it results in a significantly increased number of detected variants that need to be classified, adding complexity and slowing down the diagnostic process. Many studies of big cohorts have demonstrated a variable improvement in the diagnostic outcomes when using **trio-WES** (including the proband and both parents) or family-based exome sequencing compared to singletons (162,163). Trio-WES reduces the number of uncertain findings and the consequent analytic cost, helps to prioritize *de novo* changes in sporadic cases, drastically reduces the number of required low-throughput Sanger cosegregation testing and reduces the overall time to establish a final diagnosis. For these reasons, we established trio-WES as the gold standard strategy within the Opitz C project.

In Article 2 we presented a familiar case with two related patients from a highly consanguineous family (family OC15), one of them was analyzed as a singleton (Patient 1) and the other as a trio (Patient 2). This resulted in the identification of variants in 52 selected genes in the first patient and only 12 in the second, showing how the performance of trio-WES can lead to a significant reduction in the number of identified uncertain variants. To validate these results, we performed the segregation analysis through Sanger sequencing of 16 heterozygous variants in Patient 1 and only 6 variants in Patient 2, which supposed a decrease in the time needed to establish the disease-causing mutation in the second case.

Despite the familial relationship between the patients, the screening for shared pathogenic variants was negative. Instead, each patient carried a *de novo* variant in an already known ID/DD gene; *PORCN* associated with Focal dermal hypoplasia (FDH; MIM #305600) and *ZIC2* associated with Holoprosencephaly 5 (HPE5; MIM #609637). This demonstrates that, while the cost advantage of singleton WES is evident and it yields acceptable diagnostic results in highly consanguineous populations, *de novo* mutations also have a significant prevalence in such populations and can be underdiagnosed if this possibility is not taken into consideration. *De novo* mutations represent up to 27.8% of the ID mutations in families from near and Great Middle East populations, which show high consanguinity rates and ID is commonly caused by recessive mutations (164,165). We strongly recommend trio-WES as a preferred choice to avoid misdiagnosis, even in consanguineous families, or, if unavailable, a thorough analysis of putative dominant variants and the following study of the segregation pattern of a high number of candidates.

1.3 Interpretation of public reference databases

It is generally assumed that when diagnosing patients suffering from severe dominant disorders with pediatric-onset, the variant causing the disease has to be absent or extremely rare in **public reference databases**. Following the ACMG guidelines for variant interpretation, absence from reference populations should be considered as moderate evidence for pathogenicity. Thus, if the observed frequency of a variant in the general population is higher than the incidence of the associated condition, it should be considered as benign or weakly penetrant (35). The rationale behind the significant weight of this criterion in variant interpretation is partly based on the assumption that the tested individuals belong to North European and North American populations, which are highly represented in reference databases. However, this is not the case in other ethnicities and populations that appear to be considerably underrepresented in the most used databases, such as gnomAD (39). Although other more ethnic-specific databases can be incorporated, such as Iranome (166) and Greater Middle East Variome (167), their potential is limited due to a much smaller sample size. Considering the ethnicity of the analysed patient is very important in this sense, as some variants that are considered rare in some populations can be more frequently found in others.

We found this was the case for one patient carrying a variant in the *ASXL1* gene. As reported in Article 3, patient OC16 presented a clinical phenotype meeting all the criteria for BOS diagnosis. Under such clear clinical suspicion, we performed manual Sanger sequencing of the *ASXL1* gene and identified a *de novo* heterozygous frameshift mutation (p.Gly646Trpfs*12), which was similar to other variants identified as disease-causing in BOS patients. However, the putative pathogenicity of the identified mutation was questioned due to its presence in 132 carriers from the ExAC database (168) (accessed at the moment of the study). A revision of the literature showed that it was not the first time that mutations causing BOS were present in ExAC (70). This could be explained because *ASXL1* is one of the most commonly mutated genes during hematopoietic clonal expansion of cells with aging, approximately 10% of individuals over 65 years old show pathogenic variants in this gene (169,170). The p.Gly646Trpfs*12 identified in our patient is one of the two most frequent LoF mutations in ExAC and it is located in a eight-nucleotide G-homopolymer tract, which could lead to overrepresentation caused by sequencing errors. Of note, 66% of the carriers of this variant in ExAC belong to the Cancer Genome Atlas population and it is considered the most commonly associated *ASXL1* variant to myeloid malignancies (171). This variant does not appear in the gnomAD v.2.1.1 release (39), as it did not pass the quality control filters due to the presence of allelic imbalance in many of the carriers. Showing that databases are constantly trying to improve their algorithms and criteria to avoid this kind of situation.

This example highlights the importance of performing a careful interpretation of the data included in reference population databases, considering factors as potential **allelic imbalance**, **age and origin of the sequenced cohorts**, that could include patients diagnosed with cancer (70). This kind of phenomenon is more frequently considered when testing genes with known susceptibility to the accumulation of age-related somatic variants, but it could be frequently overlooked in genes lacking a good functional characterization. To avoid misdiagnosis caused by automated variant assessment, the process should also involve a revision of the already existing criteria and consideration of the unique biology of each gene to avoid over-dependence on variant frequencies.

1.4 Utility of matchmaking tools

Another way to improve diagnostic rates is using **matchmaking tools**, such as Genematcher (172). They are platforms that promote the establishment of connections between different research or diagnostic teams with patients bearing mutations in a gene, usually with none or very few precedents in the literature. The collaborations between groups from all over the world that might arise from these connections are extremely useful in ultra-rare disorders to be able to gather cohorts with a significant number of patients and increase the diagnostic yield (**Figure 14**).

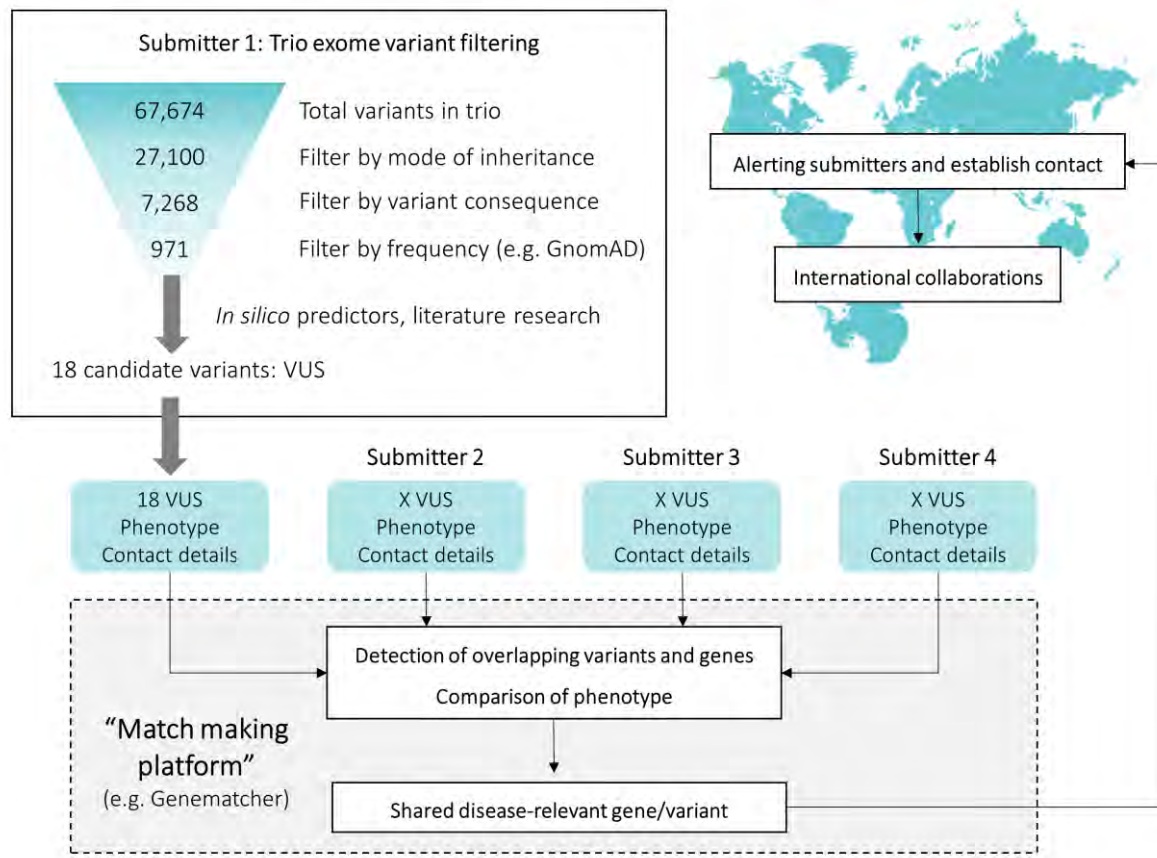


Figure 14. Representative pipeline of a typical trio-WES data analysis resulting in the identification of several VUS and use of matchmaking tools as a criteria for final selection of the disease-causing mutation. Adapted from (173).

The possibility of **studying larger groups of patients** has the potential to significantly improve the delineation of a certain syndrome both at a clinical and genetic level, even if it has been already described, as shown in Article 4 of this thesis. In this work, we provide a detailed clinical and genetic description of patient OC14 (Patient 1 in Article 4), who was molecularly re-diagnosed with KAT6A or Arboleda-Tham syndrome (ARTHS; OMIM #616268), together with 4 other patients diagnosed by our collaborators. We also performed an extensive revision of the almost 80 cases previously published in the literature and presented a clinical overview of KAT6A syndromic patients. We think this expansion of the clinical delineation of the KAT6A syndrome can contribute to its establishment as a distinctive entity that could be diagnosable at a clinical level, increasing the chance of early diagnosis and potentially improving patients' prognosis. From a genetic perspective, four of the patients carried novel *de novo* heterozygous nonsense or frameshift mutations, that clustered with many of the variants already reported in the literature, and only one of them presented a missense mutation. As the rest of the missense mutation carriers, our patient did not show cardiac alterations. However, congenital heart

defects were present in 70% of patients with truncating mutations, suggesting a genotype-phenotype correlation regarding cardiac features.

Sharing information with other groups becomes even more crucial when the identified mutation is located in a gene that has never been associated with any NDD. In these cases, even if all the *in silico* evidences suggest an association of a certain mutation with the disease, more evidence is needed to be stated as disease-causing. Highly reliable evidence would be finding a group of other patients carrying equivalent mutations and showing a similar phenotype. Needless to say, matchmaking tools are a very efficient tool to gather cohorts of patients with undescribed mutations, allowing deep study of the phenotype and delineation of **novel neurodevelopmental syndromes**.

This was the case for patient OC6 of our cohort who carried a missense mutation in *TRAF7*, a gene that until that moment had only been associated with tumorigenesis (76). Thanks to Genematcher, we could establish an active collaboration with several research groups from all over the world and gather a cohort of 45 patients. While we were gathering the cohort of patients with germline variants in *TRAF7* described in Article 8, seven unrelated individuals bearing missense variants in *TRAF7* and overlapping phenotypes were reported (174), leading to the delineation of a new developmental disorder (CAFDADD; OMIM #618164). However, the larger size of our cohort allowed further delineation of the phenotypic spectrum of this recently identified syndrome, highlighting some major traits that could not be seen in the first group of patients.

Such a large number of patients also allowed us to use the Face2gene platform (<https://www.face2gene.com/>) that uses deep learning algorithms to build computational-based classifiers (syndrome gestalts) for each syndrome from a series of facial pictures of the patients. Then, when a picture from a new patient is introduced, it will be compared to all the syndrome gestalts, generating a list of prioritized syndromes with similar morphology that could guide clinicians during the diagnostic process. **Deep learning-based platforms** of this kind are still in their early days; thus, it is crucial that we all collaborate to train the algorithms to be able to benefit from their potential in the future.

1.5 Interpreting phenotypic heterogeneity

In disorders with such a low prevalence, gathering a cohort of patients is usually a challenging and long process. It might take several years until a group of patients is large enough to perform an accurate and exhaustive delineation of the syndrome, that could be used later on

in clinical diagnosis. The increase of the number of published cases of a certain disease normally implies a better characterization of its phenotype, but it also brings to light the **phenotypic heterogeneity** observed between different patients. Even in patients with the same causal mutation, the disease manifestations may be variable, complicating diagnostic and patient management. These differences add a layer of complexity to the diagnostic process, especially when trying to solve cases with milder and less clear affectations.

The advantage of using HPOs as a **standardized language to describe phenotypic traits** is quite evident and especially relevant in cases presenting high phenotypic heterogeneity. A recent study in a cohort of neuromuscular disease patients showed that the cases where the confirmed variant ranked in the first position increased from 62% to 90% when including seven HPO terms to the analysis, compared to using variant data alone (175). Although restricted to a specific cohort, it provides a solid example of the utility and potential of using standardized phenotypic annotation to improve variant interpretation and prioritization analyses. Also, the use of phenotype-driven custom HPO gene panels to filter exome variants generates a shorter list of variants to assess that lead to increased success rate, compared with other available datasets such as OMIM and Orphanet (153).

Even in monogenic disorders, identifying the genetic origin of a certain phenotype is not so straightforward, as genotype-phenotype correlations are not that clear. Different factors can contribute to this non-linear correlation: environmental ones, such as diet, pathogens or temperature; or stochastic processes that lead to fluctuations and errors in gene expression (176). Additional genetic variation may also have a substantial contribution to phenotype variation across individuals, highlighting the importance of the specific genetic background of each individual. Genetic variants that can modify the phenotypic consequences of a certain primary disease-causing variant are known as **genetic modifiers**. Usually, genetic modifier variants are not disease-causing themselves, but they can increase (enhancer) or decrease (suppressor) the severity of disease presentation (**Figure 15**). The relevance of their effects is also variable and might result in significant phenotypic and penetrance variability (14).

WGS is the most suitable and promising NGS tool to perform studies on modifier variants, as it allows a more comprehensive view of the genetic variants present across the whole genome of the individual, together with the identification of structural variants. However, the identification, prioritization and interpretation of modifier variants is still very challenging. To date, there is not any established computational method to improve candidate modifier identification but it is an open area for research (14). Nowadays, the experimental approaches to detect modifier variants mainly rely on the use of model organisms like yeast and *C.elegans*, which allow high-throughput reverse and forward genetic screenings (177).

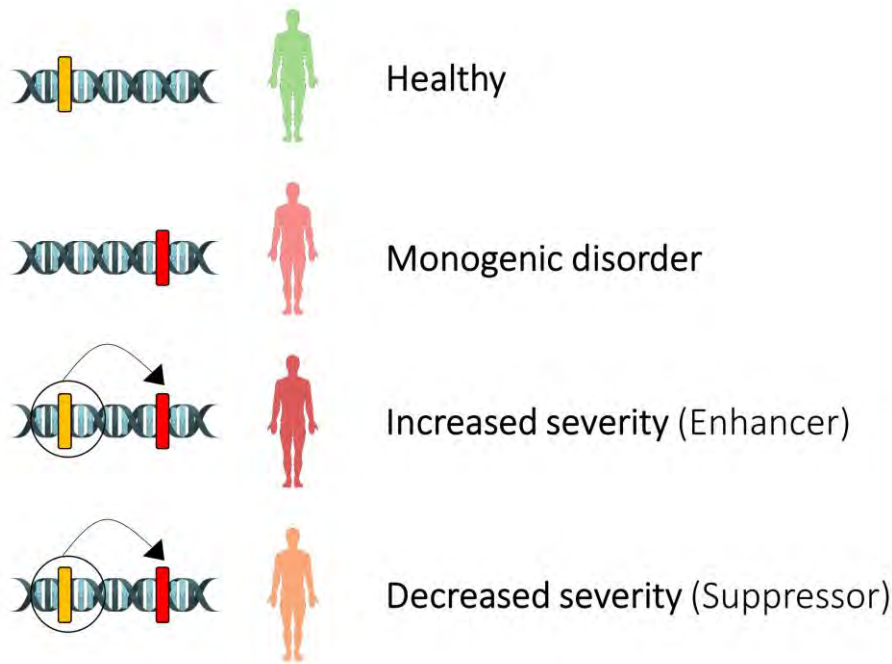


Figure 15. Representation of how the presence of a genetic modifier variant (in yellow) can modulate the severity of a disease-causing variant (in red) in a monogenic disorder, complicating its characterization. Image created with Servier Medical Art. (Adapted from (14)).

1.6 Dealing with unsolved cases

Despite the broad range of tools and strategies that can be used to try to identify the disease-causing variant, there are many cases in which it cannot be identified, which are considered as **unsolved cases**. When dealing with an unsolved case, the periodical reanalysis of the existing sequencing data is very important to increase the chances of identifying the disease-causing mutation. This is due to the rapid improvement of annotation algorithms and the constant discovery of novel disease-associated genes. Repeating the annotation process after some time including new information from different databases may lead to an increase in the diagnostic yield of around 6-10% compared to the initial rates (178,179). Also, the revision of the clinical history of the patient can also shed some light as more detailed delineations of the phenotypes associated with certain genes may have been published.

During these years, we have performed several reanalysis of the WES data of the four members of the OC10 family, the only one that remains undiagnosed in the Opitz C cohort, together with a thorough revision of the clinical phenotype. We also performed WGS in one of the index cases. Unfortunately, no suitable new candidates that could explain the phenotype observed in the siblings have arisen from these analyses.

Apart from reanalysing the already existing data, another option to try to solve the negative cases would be using other techniques. A first approximation could be WGS as it allows the analysis of deep intronic or CNV variants not detected by WES. Other techniques that can complement WES in unsolved cases are RNA-seq and proteomics, included in the “multi-omics” approach to the diagnosis of monogenic diseases proposed by Stenton et al. (36). They propose a model in which WES/WGS data from inconclusive cases is analysed together with transcriptomic and proteomic data. Transcriptomics allows the detection of aberrant transcript expression levels, aberrant splicing patterns and mono-allelic expression events and proteomics can detect aberrant protein expression. The integration of the results of these techniques will help to localize causative variants on the gene-level. For instance, the incorporation of RNA-seq in a cohort of undiagnosed patients with muscle disorders increased the diagnostic yield by 35%(180). The main limitation of these techniques is tissue selection and availability, as there are significant differences on mRNA and protein expression of different genes across sample tissues (36). Nonetheless, it is clear that the application of this “multi-omics” approach has a great potential to identify more rapidly and precisely the molecular cause of monogenic diseases, hence it is an expanding and promising field nowadays.

2. VALIDATION AND FUNCTIONAL CHARACTERIZATION OF THE VARIANTS

After identifying a group of patients with common phenotypes and carrying similar mutations, the irrefutable proof that such mutations are the cause of a certain disease is to **functionally demonstrate their pathogenicity**. To do so, different functional studies can be performed as an indispensable complement to understand the impact that a certain genetic variant may have on the expression levels or the function of the encoded protein. However, the performance of functional studies is not only important to test the pathogenicity, but also to better understand the cellular mechanisms underlying a certain disease that will allow the design of novel therapeutic strategies. These studies normally need an interdisciplinary approach using different techniques complementing one to the other to reach a deep and accurate understanding of the pathophysiology of the studied disorder. These techniques include *in silico*, *in vitro* and *in vivo* strategies. In this thesis, different *in silico* and *in vitro* approaches have been used to functionally confirm the pathogenicity of different variants (Articles 1, 4 and 6) or to try to better understand the underlying mechanisms (Articles 7, 8 and 9).

2.1 Validation of splicing variants

Different approaches can be used to test the effect that a mutation may have on the **mRNA splicing pattern** and the expression of the different gene transcripts. There are some *in silico* tools, like the Human Splicing Finder (181), that use different algorithms to predict the functional impact of a certain sequence variation on splicing motifs (**Figure 16**), including donor and acceptor splice sites, branch points and exonic splicing enhancers (ESE) or silencers (ESS). Even though they facilitate the filtering of variants when analyzing WES data, their results must be taken with caution and an experimental validation of the effect in splicing is highly advisable. The experimental approach used mostly depends on whether a cellular biological sample of the patient, either fibroblasts from a skin biopsy or lymphoblasts from a blood sample, is available for testing or not (**Figure 16**). Alternatively, mini gene splicing assays using exon trapping vectors, such as pSPL3, can be used to experimentally confirm the effects on splicing when RNA from the patient is not available. It mainly involves the cloning of the reference and variant-containing region into the mini-gene construct, its transfection into mammalian cells and the analysis of the resultant RNA products as if it was coming directly from the patient (**Figure 16**).

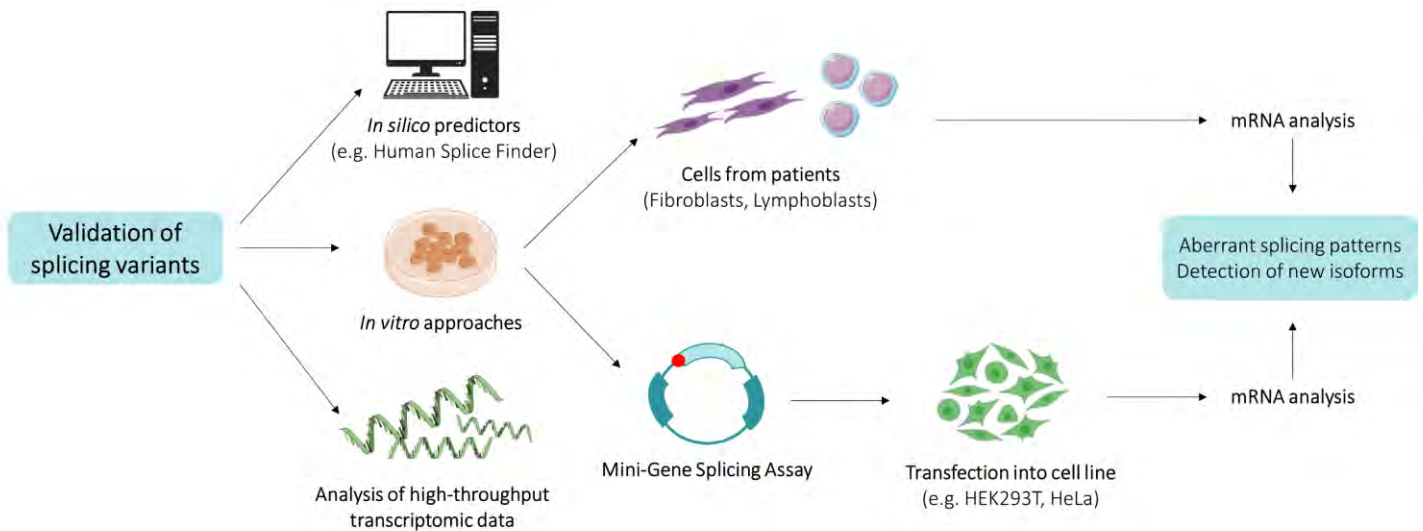


Figure 16. Strategies for functional validation of splicing variants. Image created with Servier Medical Art.

In Article 5, we identified two mutations in the *PIGT* gene in compound heterozygosity in patient OC13. The patient carried a previously reported missense mutation inherited from his father and a novel mutation that affected the canonical splice acceptor site of intron 3, of maternal origin. To verify the pathogenicity of the novel splicing variant, the effect of the mutation was studied in the **patient's fibroblasts** by Sanger sequencing analysing the different expressed cDNA amplicon lengths and comparing them to a control line. Through this functional approach, we could verify that the novel mutation had an effect on the normal *PIGT* splicing pattern that leads to the skipping of exon 4. After the functional validation of this novel variant, patient OC13 could be re-diagnosed with multiple congenital anomalies-hypotonia-seizures syndrome 3 (MCAHS3, OMIM #615398).

The same approach was used to confirm the pathogenicity of the *ASXL1* splicing variant identified in patient OC21 in Article 1, that caused the retention of intron 12. This result was a key evidence to consider the variant as disease-causing and diagnose the patient as a mild BOS case, extending the phenotypic spectrum of this syndrome. This particular case was also discussed with Dr. Bianca Russell, who is in charge of the patient repository and confirmed that during the last years more BOS cases have been identified presenting a milder phenotype than the one typically associated with this disorder (personal communication). The increasing phenotypic heterogeneity observed among BOS patients, highlights the need of finding a suitable biomarker that could be tested in cases where pathogenicity of the variant is not clear and/or the clinical manifestations are mild or unclear. A biomarker is defined as a measurable characteristic that can be objectively evaluated as an indicator of normal biological processes, pathogenic processes or pharmacological response to a therapeutic intervention (182). Our

group has established different international collaborations to start a project to identify a suitable biomarker for BOS, which will hopefully help to shed some light on the pathophysiologic mechanisms underlying this syndrome during the upcoming years.

A **mini-gene splicing assay** had to be used to test the effect on splicing of the *de novo* mutation in *FOXP1* identified in patient OC2 (Article 4), as cells from the patient were unavailable. This approach allowed us to confirm the pathogenicity of the variant, which caused the skipping of exon 16 and encoded a truncated form of FOXP1 lacking the FOX domain, crucial for its transcriptional repression activity (183).

2.2 Effects on protein function of *DPH1* variants

When the identified variant cannot be directly associated with decreased protein levels, the functional test to check its pathogenicity can become much more complex. In the best case scenario, the affected protein would have a clearly described function and its activity would be linked to a parameter that could be more or less easily measured. For instance, this is sometimes the case in genetic disorders that compromise the function of an enzyme involved in the synthesis or degradation pathway of a certain substrate. Then, the levels of such substrates may be directly measured to assess if protein function is impaired due to a certain genotype. However, in some cases it is not so straightforward and indirect approaches need to be used to **evaluate abnormal protein function**.

In Article 7, we used the indirect DT-mediated ADPR assay to **test the effect on DPH1 functionality** of 7 pathogenic variants (2 novel and 5 previously described). We observed a decrease in protein activity that generally correlated with the severity of the corresponding patients' clinical phenotype. Modeling of the DPH1-DPH2 heterodimer containing the different variants and its molecular dynamics simulations also showed an effect on DPH1 structure. Therefore, we were able to establish a correlation between the DPH1 loss of activity in an *in vitro* ADPR assay, the *in silico* modeling and the severity of the phenotype observed in the patients.

Variants p.(Met6Lys) and p.(Pro382Ser), which cause a milder phenotype, showed similar activity levels to the wild-type (WT). These results showed that the DT-mediated ADPR assay is not suitable to functionally confirm the pathogenicity of these two variants, probably due to technical limitations to detect subtle *in vitro* activity reductions. However, different *in silico* results suggest that these variants could be pathogenic. This brings to light how a particular test can be adequate for testing certain mutations but not others, for example due to limited

detection range. Pathogenicity testing through one single technique can lead to misinterpretation and rejection of a suitable candidate as cause of the disease, especially when trying to evaluate subtle effects.

It should be emphasized that the diagnostic success reached in the case of family OC12 strongly relied on the collaboration of interdisciplinary groups from all over the world, both at the clinical and experimental level. In this case, it was key finding additional cases of this ultra-rare syndrome to improve its clinical delineation and also a biochemical group with solid experience in the performance of a functional assay suitable to test DPH1 function in an *in vitro* model.

2.3 Molecular characterization of *TRAF7* germline mutations

We also wanted to **functionally characterize germline mutations in *TRAF7*** to better understand the cellular mechanisms behind this novel syndrome. All the variants described so far, in Article 8 and 2 additional publications (174,184), are missense and cluster to the C-terminus region of the protein, three of them located in the coiled-coil domain and the rest in the WD40 repeats. The nature of the mutations suggest that they most likely cause a GoF or dominant negative situation, rather than haploinsufficiency. Also, according to gnomAD, *TRAF7* is predicted to be tolerant to LoF mutations, supporting this hypothesis.

Despite being of the same kind and affecting the same domains, neurodevelopmental mutations are mutually exclusive to the somatic mutations identified in adenomatoid tumors, mesotheliomas, meningiomas and perineuriomas (**Figure 17**). This is particularly striking for the variants present in syndromic cases (p.Arg655Gln) and in meningiomas (p.Asn520Ser), which are highly recurrent and private within each condition (**Figure 17**). There are a few exceptions to this observation in which the mutation occurs in the same position but the amino acid change is different. The fact that, in general, the mutations are not coincident could imply that the different *TRAF7* variants may have a diverse effect in the activity of mutated protein specific to one disease or the other. They could maybe affect in a different manner the interactions with its partners or only one of the mutation types may lead to a neomorphic effect. One possibility could be that the somatic mutations are not compatible with life when present in the germline due to a stronger phenotypic effect. Or it could just be a stocastical artifact.

It is noteworthy that the eldest patient of the cohort was diagnosed with a meningioma (174), thus long-term follow-up of the younger cases is highly recommended to ascertain if germline *TRAF7* variants increase predisposition to formation of meningiomas or other tumour types. The case of *TRAF7* is not unique, instead there is a large number of disorders that show

diverse levels of developmental defects and cancer predisposition (185), as further discussed below.

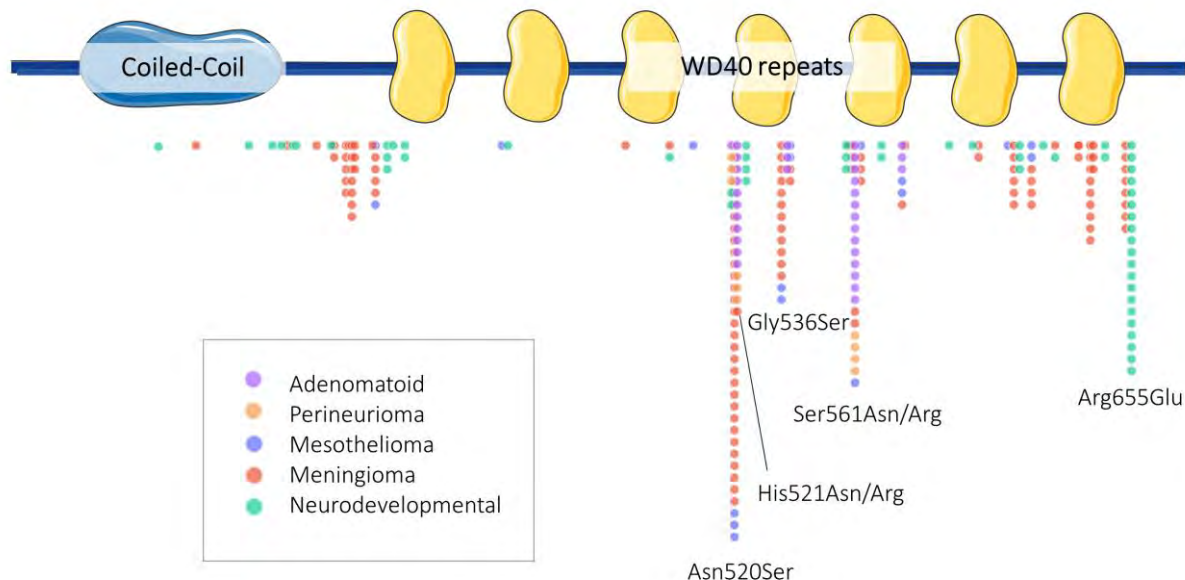


Figure 17. Described somatic and germline missense mutations in the C-terminal end of TRAF7. Different colours represent the different associated tumours/diseases (see legend). A label with the specific change is shown for those positions mutated in more than 10 cases. Image created with Servier Medical Art.

Little is known about why missense mutations in *TRAF7* cause such a severe developmental phenotype. As TRAF7 is involved in signal transduction of several cellular pathways that control transcription, our approach to better understand the pathogenic role of germline variants was to analyse gene expression levels in skin fibroblasts from patients and controls through qPCR and mRNA-seq. The latter is a hypothesis-free approach that has an expanded discovery power compared to qPCR, which is restricted to the analysis of a small set of pre-selected candidate genes.

Our transcriptomic studies on syndromic variants open the door to further exploration of the link between TRAF7 and its putative transcriptional targets that may help to better understand TRAF7-syndrome molecular mechanisms. For instance, in our lab we are now analyzing of the expression of some of the identified DEGs in TRAF7-silenced fibroblasts trying to elucidate if germinal missense mutations are LoF, if the results match those obtained in patient's fibroblasts, or GoF, if they are in the opposite direction. Preliminary results suggest a gain-of-function effect, but further replicates are still needed.

However, the presented transcriptomic analyses also have some limitations that are worth mentioning: i) Cell type: Gene expression patterns are very specific and highly variable among different tissues and cell types (97). Thus, the potential of using skin fibroblasts to understand the phenotype-genotype correlation of a disease without skin affectation can be questioned, as further discussed below. It could be more representative to study these patterns in cell types from tissues related to the phenotype of the patients, such as neurons, astrocytes or cardiomyocytes. ii) Sample size: The limited number of included lines (3 patients and 6 controls) could have had an effect on the discovery power and the reproducibility of our results. As a result of the international collaboration established thanks to the Genematcher platform, we received fibroblasts from two patients that could be tested together with our patient OC6 (patients 6,13 & 33 in Article 8). Two additional lines were received from other groups after the mRNAseq was performed, which were included in the subsequent qPCR validation. Despite that only 3 lines were included in the NGS experiment, the fact that the two other lines showed similar alterations in the selected genes when tested through qPCR, reinforces the validity and reproducibility of our results. iii) Sample heterogeneity: Another important factor regarding the sample is the age differences of the donors when the skin biopsy was obtained. Patients' ages ranged from 8 to 19 years old, while all the controls were adults except for two of them that were 17-19 years old. It has been proven that gene expression levels change with age in skin, adipose tissue, blood and brain (186). These changes caused by aging can lead to the appearance of false positive or false negative results when comparing gene expression levels between the two groups.

2.4 Functional characterization of *MAGEL2* truncating variants

A truncating mutation was previously identified in the paternal allele of the *MAGEL2* gene of patient OC7 (115). Mutations of this kind had already been associated with Schaaf-Yang syndrome (113), evidence that was considered as strong criteria to establish the variant as disease-causing. However, not much was known about *MAGEL2* and even less about its role in the pathogenesis of SYS. For this reason, we were interested in the **functional characterization of disease-causing variants in *MAGEL2***.

In Article 9, we performed an extensive revision of all the SYS cases published so far, aiming to improve the general picture of the clinical and genetic landscape of this syndrome. This kind of compilation can be very useful especially in ultra-rare disorders, as the majority of cases are published as single case reports and the publication of large case series, where the syndrome can be more consistently delineated, are not that common.

At a genetic level, we saw that the vast majority of mutations reported in SYS cases were point nonsense or frameshift mutations in the paternal allele of *MAGEL2*. These variants are predicted to encode a truncated protein that partially or totally lacks the MHD domain, which is crucial for the majority of known functions of *MAGEL2*. Only four variants of other types have been identified in SYS patients, three missense mutations and one in-frame deletion that results in a protein form lacking seven residues (122,129). Few or none individual clinical details of these patients were reported. Thus, the pathogenicity of mutations that do not cause a loss of the C-terminal end of the *MAGEL2* protein remains to be proven.

We also created a set of standardized guidelines aiming to orientate clinicians and improve the management of SYS cases. Management guidelines are considered a good tool to increase care consistency and efficiency, while closing the gap between scientific evidence and what clinicians do. However, they may involve different limitations and opinions about their utility are quite diverse across clinicians [discussed in Woolf et al. (187)].

A relevant question regarding *MAGEL2*-related syndromes is why the deletion of the whole gene (PWS) causes a milder phenotype than the variants that lead to the production of a truncated form of the protein (SYS). A similar situation is also observed in patients carrying a whole gene deletion of *MAGEL2*, who present milder phenotypes than typical SYS patients (188,189), and in *Magel2*-KO models that do not recapitulate the whole SYS phenotype, lacking characteristic distal joint contractures (140,146).

A possible explanation could be that the deletion of the complete *MAGEL2* paternal copy, including the promoter of the gene, may lead to **leaky expression of the maternal allele** in patients with paternal deletion, but not in patients with truncating mutations as the paternal allele is mutated but expressed (**Figure 18**). There is a precedent of epigenetic flexibility on the *Ndn* gene, also included in the PWS region and maternally imprinted, as the maternal allele of *Ndn* was found to be expressed at extremely low levels in absence of the paternal allele in a mouse model. Although a high degree of non-genetic heterogeneity was observed, this residual expression in some subsets of neurons reduced birth lethality and breathing deficiency in about half of the mutant mice (190). This theory is also backed up by the detection of *MAGEL2* transcripts on brain sections of both PWS patients and a mouse model bearing the complete deletion of the paternal copy of the gene and the promoter (191).

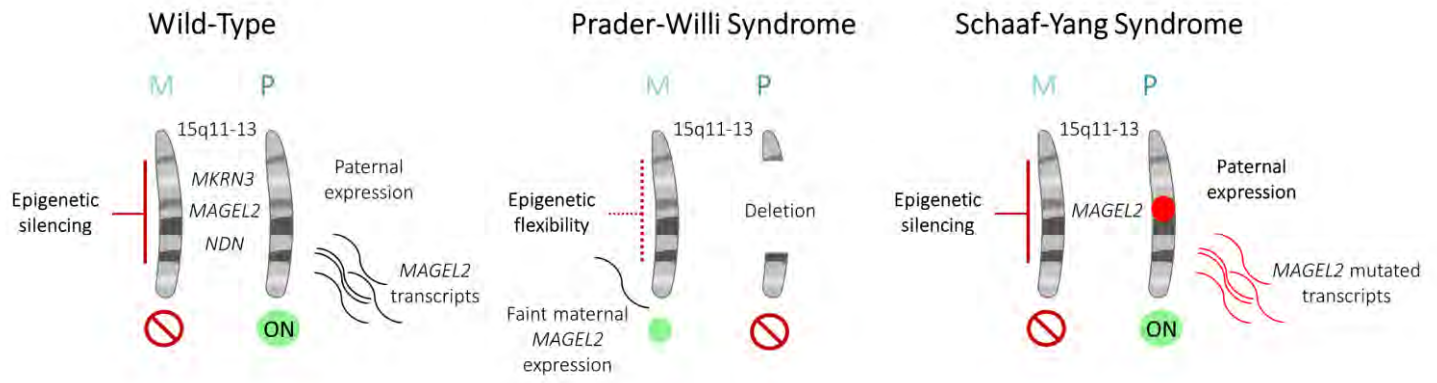


Figure 18. Schematic representation of the hypothetic leaky maternal expression of *MAGEL2* in PWS and the expression of a normal amount of *MAGEL2* mutated transcripts in SYS, that could contribute to differences in severity of the phenotypes. Image created with Servier Medical Art.

The second possible explanation, which can coexist with the first one, is related to the fact that *MAGEL2* is a single-exon gene, thus truncating mutations would not be expected to activate the NMD mechanism. Then, the truncated protein product would be present in the cell and may, potentially, have **neomorphic effects** that increase the severity of the phenotype in SYS patients. Aiming to prove this hypothesis, we heterologously overexpressed the *MAGEL2*-WT and the *MAGEL2*-Gln638* (variant present in patient OC7) protein forms in a cell line. We saw that both isoforms are mainly degraded via proteasome and at similar rates, supporting the idea that the truncated form is stable inside the cell and might have a toxic effect. At a cellular localization level, we also observed differences, as the *MAGEL2*-WT presence was mainly cytosolic, while *MAGEL2*-Gln638* location was drastically switched to the nucleus.

The next steps would be overexpressing other truncating and missense variants reported in SYS patients to confirm the reproducibility of the results and the utility of our in vitro system to test the pathogenicity of *MAGEL2* mutations. It would also be interesting to verify if the endogenous truncated form is stable and this switch also happens in fibroblasts from patients and not only in our artificial system. But, unfortunately, a suitable commercial antibody for direct *MAGEL2* detection is not available nowadays. Further research is needed to validate and understand the implications of this change of location and to understand the contribution it may have on the pathophysiologic mechanism underlying SYS.

Supporting a higher impact on protein trafficking dysregulation of the truncated form than the total lack of *MAGEL2* protein. We measured $A\beta_{1-40}$ peptide excretion levels of SYS, PWS and control fibroblasts and observed significantly decreased levels in SYS fibroblasts compared to PWS and control groups, which showed similar expression levels.

Using fibroblasts from SYS patients, we also performed an unbiased mRNA-seq analysis to investigate if the presence of the truncated MAGEL2 protein could also be affecting the expression patterns of other genes. Our analysis did not replicate the results obtained by Crutcher et al. (192), showing increased alteration in genes of the mTOR pathway, but identified 132 DEGs between the SYS and the control groups. Some of the most affected genes are known to play a role during development or in neurological homeostasis. Pathway enrichment analysis highlighted some functions related to mitosis among the identified DEGs. All these results are preliminary and further experiments are needed to validate them in other cellular models and understand the real effect of these changes on expression detected on SYS fibroblasts. Nevertheless, they are a good starting point to potentially define novel roles of MAGEL2 in mitosis and other cellular processes.

The limitations of these experiments are mainly the same ones discussed for Article 8, regarding the relevance of the cell type used (skin fibroblasts), sample size and sample heterogeneity. Regarding the mRNA-seq experiments, the sample size and its heterogeneity was equivalent to the one discussed in Article 8, three SYS patients and six controls, who were mostly adults. However, for the A β ₁₋₄₀ peptide measurements we could increase the sample size, including six SYS patients, nine PWS patients and six age-matched controls. This increase in the number of tested individuals gives additional robustness to our results, nevertheless replication in a bigger cohort is highly advisable.

3. *IN VITRO* AND *IN VIVO* DISEASE MODELS

One of the limitations that are often encountered when studying a rare syndromic neurodevelopmental disorder is the establishment of **suitable and relevant disease models**. An ideal model of a human disorder needs to meet certain requirements (193): i) Construct validity, it mimics the genetic aberration responsible for the disease in humans; ii) Face validity, its phenotype resembles the one observed in patients; iii) Predictive validity, the model and the patient have a similar response to a certain treatment. Using a specific disease model is crucial, not only to expand the knowledge about the cellular processes underlying its pathophysiology, but also to test safety and efficacy of potential therapeutic approaches. There are different strategies that could be used to obtain more reliable results, which mainly involve cellular or animal models.

As said before, the different functional studies performed along this thesis have been mainly focused on the use of **skin fibroblasts from patients** as a model of disease. There are some arguments in favour and against their utility as a cellular model. Some of the arguments for the use of primary skin fibroblasts are their availability, as they can be isolated from a punch skin biopsy that very rarely leads to complications, and robustness in culture, storage and transport. They also reflect the genetic background of each specific patient, which can be useful for the identification and characterization of modifier variants. Fibroblasts can be genetically manipulated through relatively complex but feasible techniques, such as electroporation, lentiviral constructs or CRISPR/Cas9 genome editing. Also, different studies have proven their usefulness as cellular models for the investigation of the pathogenic mechanisms underlying different neurological diseases and potential therapies (194,195). However, some limitations of using primary skin fibroblasts as a disease model need to be highlighted and discussed. Fibroblasts reflect the chronological and biological aging of the donors (196), meaning that selection of age and sex matched patients and controls is very important, which can sometimes be difficult to achieve. Cell growth is generally slow, especially in cells from aged individuals, implying that sometimes several weeks in culture are needed to get sufficient amounts of biological material to perform biochemical tests. Last but not least, fibroblasts expression profile, genomic signatures and signaling can be significantly different to the characteristic features of the most relevant cell type for each disease (e.g. neurons for neurodevelopmental disorders).

Animal models, such as rodents and zebrafish, are widely used as a tool to study neurodevelopmental disorders. They have shown a strong potential to achieve identification of novel disease-causing genes, understanding of the molecular and biological mechanisms underlying a disease and development of new therapeutic strategies. However, fundamental differences between humans and animal models regarding neural development, genetics and disease mechanisms have emerged as a result of the advancement of imaging, genomic and genetic technologies (197). These differences may explain why there are cases in which the animal model carrying a certain mutation only recapitulates some of the phenotypic manifestations, but does not show the full-phenotype observed in patients. However, their utility in genetic diagnosis is undeniable, especially when trying to prioritize a variant in a gene that has never been associated with disease before. For instance, the existence of a KO model exhibiting a similar phenotype, despite only recreating part of the clinical traits, can be considered as strong evidence of pathogenicity (35).

Given the advantages and limitations of using patients' fibroblasts and animals as disease models, the utilization of **human neural cellular models** is an interesting middle ground approach. Being specific and relevant human cell types, they can provide useful and complementary information that in primary fibroblasts or animal models would be very difficult to obtain.

With the final aim of generating suitable cellular models for the study of SYS, in Article 10 we reprogrammed 2 fibroblastic cell lines to iPSCs, obtained from 2 different SYS patients bearing the p.Gln638* (SYS1) and the p.Gln666Profs*47 (SYS2) mutations in *MAGEL2*. The used reprogramming approach led to the emergence of iPSCs colonies in only 10-12 days after the last transfection, a significantly shorter time than other methods. This method is non-integrative, which avoids the need of integrating exogenous pluripotency factors into the target cell genome, which could potentially be transcriptionally reactivated giving tumorigenic characteristics to iPS-derived differentiated cells (198). Once the iPSC clones were isolated and expanded, we performed several characterization experiments to ensure complete reprogramming [(reviewed in Tiscornia et al. (199))].

In parallel, we also reprogrammed 4 additional fibroblastic cell lines: 2 from control individuals and 2 from additional SYS patients, one of them also carrying the recurrent mutation p.Gln666Profs*47 and the other the p.Gln1007*. However, the validation experiments to confirm all the parameters commented above will be performed during the following months.

When all the lines are properly characterized, the next step will be differentiating them to relevant neural cell types (**Figure 19**). In the case of SYS, we propose excitatory/inhibitory

cortical neurons, hypothalamic neurons and astrocytes as the cell types of greatest interest, which could be differentiated following already established protocols based on fully chemically defined media (200) or forced expression of transcription factors (201–203). These models would help to assess putative impairment in synaptic network formation and in excitatory/inhibitory synaptic transmission, effects at a hypothalamic neuron level and the putative role of astrocytes in the pathophysiologic mechanisms of SYS.

Together with the iPSCs from SYS patients, we also reprogrammed fibroblasts from 2 controls of a similar age. These patient and control lines may be differentiated in parallel to help uncover putative differences that define SYS neural models, like differences in electrophysiology or gene expression patterns. However, it is important to highlight that some of these differences might be subtle, making it difficult to be sure whether they are related to *MAGEL2* variants or to intrinsic variability among individuals.

To overcome this limitation, a complementary approach could be the generation of isogenic controls by correcting the mutation of each specific iPSC line using CRISPR/Cas9 (**Figure 19**). This would lead to the obtention of a control line with the exact same genetic background and observed differences could be attributed to the specific disease-causing variant. Nevertheless, it is important to consider that using a specific isogenic control for each patient line will rapidly increase the number of experimental conditions included in every experiment and thus, the handling complexity and economic cost derived from it.

Another option could be using iPSC from a WT individual as the starting material and generate the different mutations through CRISPR/Cas9 genome editing. This approach would significantly reduce economic and time costs at the expense of not including the genetic background of the patients in the cellular model.

Organoids are another type of cellular model that can be generated from iPSCs and could be of great relevance to study the role of *MAGEL2* in the brain during development (**Figure 19**). Brain organoids are 3D *in vitro* models that auto organize themselves recapitulating the typical architecture of the developing brain. There are several well-established protocols that could be used to generate cortical organoids (204) and hypothalamic arcuate organoids (205) and study impairments caused by *MAGEL2* variants. It has been proven that cortical organoids contain different cell populations in different maturation stages (206). Thus, single-cell RNAseq (scRNAseq) could be an interesting approach to obtain information about the different neuronal subtypes and evaluate possible alterations in the developmental process in patients compared to controls.

The generated *in vitro* models could also be used to test potential therapeutic strategies. Given that the maternal allele of *MAGEL2* in SYS patients is silenced by methylation, an interesting approach that could be considered is the activation of the expression of this healthy allele using a CRISPR/Cas9-mediated epigenetic editing system. As previously done in mice with the Oct4 gene, whose transcription is normally inhibited through hypermethylation at the promoter region in NIH3T3 cells (207).

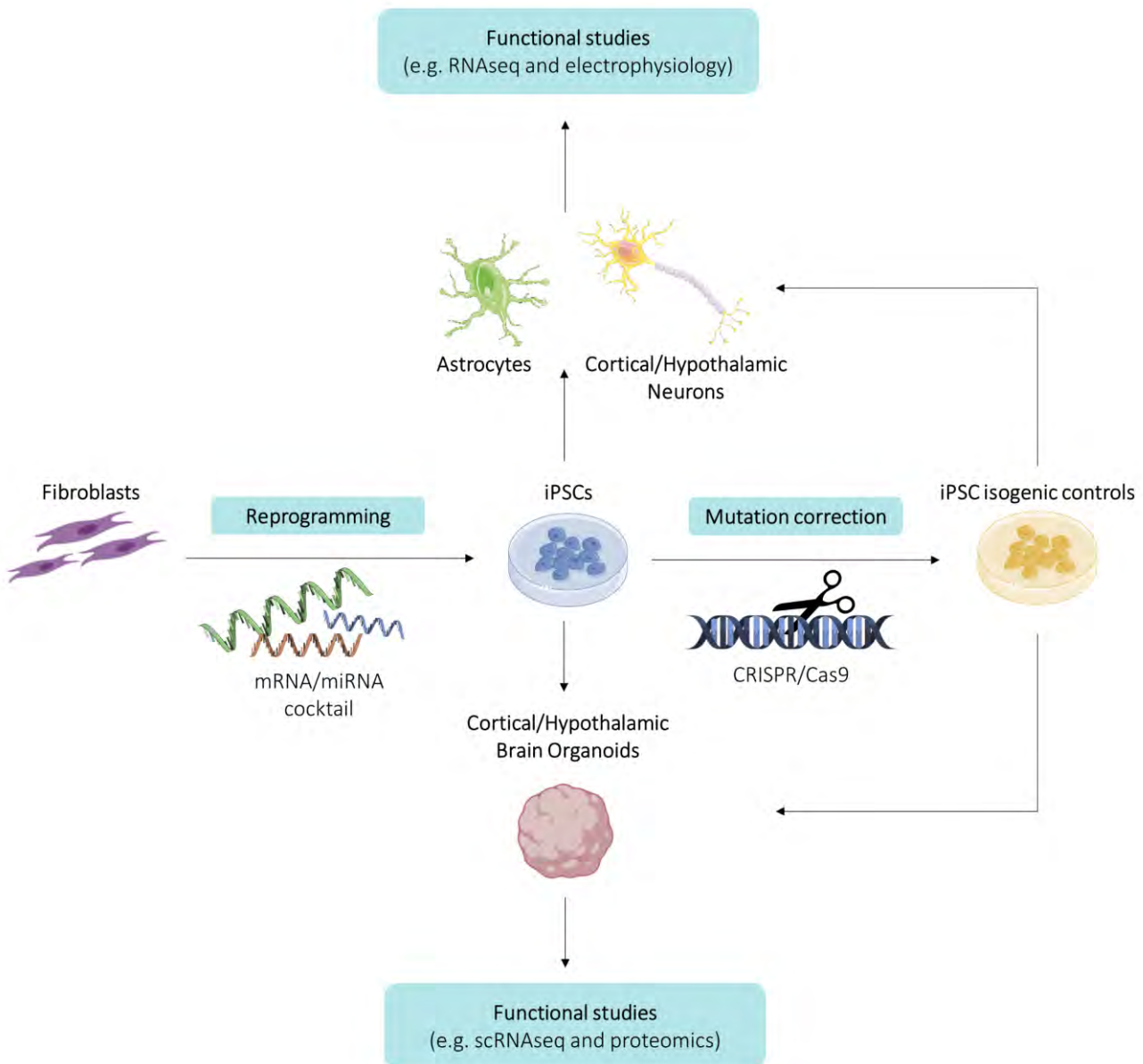


Figure 19. Schematic representation of the outline of the project to obtain *in vitro* models of SYS using fibroblasts from patients as starting material. Image created with Servier Medical Art and BioRender.com.

4. DEVELOPMENT AND CANCER

The advancements in epigenetic regulation knowledge are bringing to light the similarities between development and cancer. In Ref. (185), Bellacosa reviews the founding concepts of this idea and the current understanding of this connection. He states that normal development and cancer are in general two opposing processes (**Figure 20**). During development, highly coordinated and specific epigenetic instructions promote the generation of all the differentiated cell types from an undifferentiated cell, the fertilized egg. While in cancer, aberrant epigenetic instructions lead to a progressive decrease in differentiation during tumorigenesis that results in the acquisition of undifferentiated features. He also highlights how signaling pathways that play a role in normal morphogenesis during development promoting a wide variety of processes (e.g. invaginations, angiogenesis and patterning at a tissular level and proliferation, differentiation and apoptosis in the cell) are acquired and unbalanced in cancer initiation, progression, invasion and metastasis (185). A good example of this phenomenon is that alterations in all the genes identified and studied along this thesis (**Figure 20**) can potentially lead either to malformation syndromes or tumorigenesis.

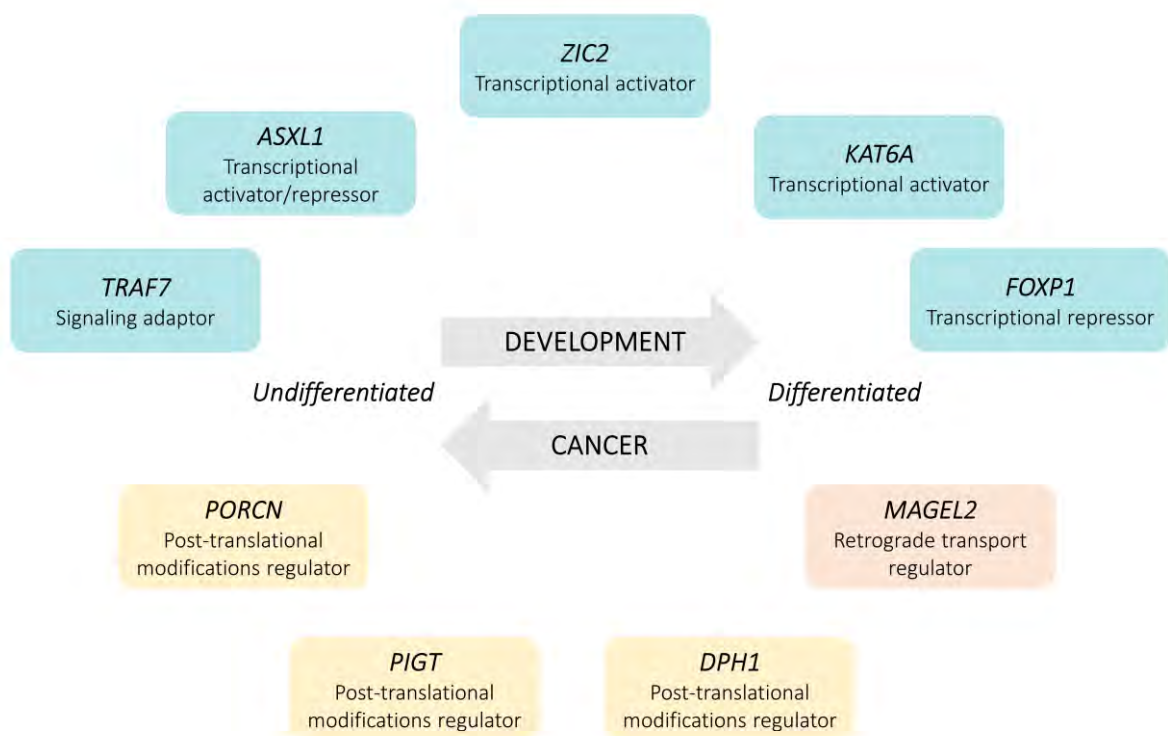


Figure 20. The different functions of the genes identified as disease-causing in the Opitz C cohort patients are crucial for normal developmental differentiation and can promote loss of differentiation when altered in a tumorigenic context. In general, their functions are related to gene expression modulation (in blue), different post-translational modifications (in yellow) and regulation of the retrograde transport mechanism (in orange).

Transcription plays crucial roles in neoplasia, for instance its dysregulation can lead to decreased expression of genes that promote cellular differentiation or increased expression of genes that promote cell division (208). Some of the identified genes act as gene expression modulators by activating or repressing transcription (in blue in **Figure 20**): *ASXL1*, *FOXP1*, *ZIC2* and *KAT6A* have been reported to be oncogenes in different cancer types as a result of GoF variants (58,59,209–211) or expression of chimeric transcripts resulting from chromosomal translocations (212); *TRAF7* does not directly modulate transcription, but is a signaling adaptor of different pathways that regulate transcriptional events (78,79) and missense mutations drive different types of neoplasms through poorly known mechanisms (89).

Post-translational modifications tightly regulate the activity of downstream effectors and dysregulation can potentially play a role in different human cancers (213). The subgroup of genes (in yellow in **Figure 20**), including *PORCN*, *PIGT* and *DPH1*, are implicated in the synthesis of post-translational modifications of different nature and have been positively related to oncogenic mechanisms (214–216).

Finally, retrograde trafficking is not only important for protein homeostasis, thus its dysregulation can lead to retrotranslocation of activated transmembrane proteins (e.g. receptor tyrosine kinases) to the nucleus promoting enhanced transcription of cancer metastasis drivers (217). To date, *MAGEL2* (in orange in **Figure 20**) has not been directly linked to tumorigenesis, however *MAGE* family members are normally expressed by gametes and trophoblasts and many of them are aberrantly expressed in various types of human cancer, mediating the malignant phenotype (218).

The dual role in development and cancer is the connecting link between all the genes studied in this thesis. This connection might partially explain the phenotypic similarities observed among the patients that led to their diagnosis within the same clinical entity, but further research is needed before we can settle this question. Either way, close follow-up of patients affected by these ultra-rare NDDs is highly advisable, as the effect that developmental mutations may have in cancer predisposition and progression is unclear. Further investigation of the molecular mechanisms underlying these NDDs would not only provide deeper knowledge of their molecular and clinical features, but also could contribute to the development of new therapeutic strategies tackling the overlapping features between development impairment and cancer. Using cancer drugs for developmental conditions and vice versa will hopefully be a feasible strategy in the future (185). This situation would be extremely beneficial for patients suffering from rare developmental disorders, given the limited economic resources invested in the development of therapeutic approaches to treat them.

5. FINAL REMARKS AND FUTURE PERSPECTIVES

Advances in the genetic diagnosis field have led to the identification and delineation of a significant number of new disorders. To give some numbers, over 2500 new monogenic conditions have been added to OMIM during the last decade (219). This huge amount of novel phenotypes has led to a new challenge: **naming novel genetic disorders**. Unlike human genes, whose official name and symbol is designated by the HUGO Gene Nomenclature Committee (HGNC) (220), there is not a standard way to name genetic conditions. Genetic conditions names can be derived from different sources, like the basic genetic or biochemical cause of the conditions, the gene which contains the variant that causes the condition, one or more major signs of the disorder, the parts of the body affected by the condition or the name of a specific physician or researcher, (eponyms). Deciding which is the best criteria to name genetic conditions is a very controversial issue that has not been addressed yet.

On the one hand, from the perspective of a geneticist, it could be argued that naming a phenotype after the symbol for the causative gene is the most suitable approach. This seems especially logical for those phenotypes that have been identified by reverse phenotyping, meaning that a pathogenic gene variant is first identified in a group of patients and then the associated phenotype is described. On the other hand, it is true that it gets more complicated for disorders with genetic heterogeneity and genes that cause more than one phenotype, which account for more than one-third of the known disease genes (219). In these cases, naming the disease after the gene symbol could be misleading to the families and their health-care providers. There is not an ideal formula to solve this issue, however it would be very useful to establish a standardized way of naming emerging genetic conditions to facilitate communication between geneticists, clinicians and patients.

Future perspectives of ultra-rare neurodevelopmental disorders diagnosis involve further improvements on NGS techniques and interpretation of the sequencing data, coupled with refinements of clinical delineation of each particular disorder. In fact, during the last decade we have already seen huge advances in NGS technologies, including better sequencing coverage, shorter times to get results, application of automated pipelines and a large decrease in economic costs, among others. These advances have already positioned WES as a front-row diagnostic option in NDD cases. In the upcoming years, if costs keep decreasing following the same trend and interpretation of non-coding variants is further optimized, WGS could also be included as a routine analysis in clinics. Including RNA-seq and proteomics as part of a “multi-omics” approach, in cases where tissue collection is possible, would definitely improve diagnostic yields.

Improvement in diagnosis will not only result in the identification of novel disease-causing genes, but also in the implementation of improved genetic counseling and design of personalised therapeutic strategies. Due to the very complex nature of NDDs, the success of potential treatments will depend on the combination of multidisciplinary approaches, including genetics, functional genomics, reliable disease models and the identification of measurable biomarkers.

Lastly, I would like to emphasize the impact that being diagnosed has on the life of the patients and their families. **Receiving an accurate diagnosis** helps to avoid additional unnecessary clinical investigations or interventions, to choose the best management and therapy options for the patient and to improve the prognosis of the disease, especially in cases where early intervention can make a big difference. The results of genetic testing might also be crucial for genetic counseling and future family planning.

Nowadays, that the vast majority of NDDs do not have a cure, our aims should be focused on providing ways to improve the quality of life of these patients. This includes a reduction of the time needed to establish a diagnosis, so that the families can get the answer that they have been looking for as soon as possible. Knowing the precise cause and the expected progress of the disease is great relief for patients and families. Also, being able to join the patient association of a particular disease can be a good opportunity to share different ways to handle daily life situations and useful symptomatic treatments.

This work constitutes a humble contribution to the research of ultra-rare neurodevelopmental disorders. However, there is still a long road ahead of us and research efforts should be put into taking the next steps towards improved diagnostic methods and personalised therapy.



CONCLUSIONS

- The combination of whole-exome sequencing and functional studies has allowed the establishment of the molecular diagnosis of all but one of the families investigated, resulting in a diagnostic yield of 93.3%.
- Recessive inheritance should not be automatically assumed in cases of developmental disorders from highly consanguineous families.
- Careful interpretation of reference population data considering possible allelic imbalance, ethnicity, age and origin of the sequenced cohorts is crucial to avoid misdiagnosis.
- Functional studies based on mRNA have been useful to prove the pathogenicity of three novel splicing variants in the *ASXL1*, *PIGT* and *FOXP1* genes.
- Variants in *DPH1* cause a variable decrease in protein functionally and different structural alterations that correlate with the severity of the phenotype.
- The establishment of a cohort including 45 TRAF7-syndrome patients has allowed the delineation of a novel clinically recognizable syndrome caused by germline missense mutations in *TRAF7*. Patients' fibroblasts show specific alterations in their transcriptomic profile.
- Almost all mutations reported in Schaaf-Yang syndrome patients are nonsense or frameshift mutations in *MAGEL2* and encode truncated forms of the protein lacking the MHD functional domain. A possible toxic neomorphic effect of these truncated forms is suggested by experiments performed in fibroblasts and transfected cells.
- In rare diseases, matchmaking platforms are invaluable tools to establish national and international collaborations among clinicians, researchers and families. Collaborative work is key to reduce the time needed to receive a robust diagnosis, improve phenotypic delineations and unravel their pathophysiological molecular mechanisms.



REFERENCES

1. Stiles J, Jernigan TL. The basics of brain development. *Neuropsychol Rev*. 2010 Dec;20(4):327–48.
2. Ismail FY, Shapiro BK. What are neurodevelopmental disorders? *Curr Opin Neurol*. 2019 Aug;32(4):611–6.
3. American Psychiatric Association. *Diagnostic and Statistical Manual of Mental Disorders (DSM-5®)*. American Psychiatric Pub; 2013. 991 p.
4. Accardo PJ, Capute AJ. *Capute & Accardo's Neurodevelopmental Disabilities in Infancy and Childhood: The spectrum of neurodevelopmental disabilities*. Paul H Brookes Publishing; 2008. 721 p.
5. Shevell M, Ashwal S, Donley D, Flint J, Gingold M, Hirtz D, et al. Practice parameter: evaluation of the child with global developmental delay: report of the Quality Standards Subcommittee of the American Academy of Neurology and The Practice Committee of the Child Neurology Society. *Neurology*. 2003 Feb 11;60(3):367–80.
6. Marrus N, Hall L. Intellectual Disability and Language Disorder. *Child Adolesc Psychiatr Clin N Am*. 2017 Jul;26(3):539–54.
7. Newschaffer CJ, Croen LA, Daniels J, Giarelli E, Grether JK, Levy SE, et al. The epidemiology of autism spectrum disorders. *Annu Rev Public Health*. 2007;28:235–58.
8. Corsello G, Giuffrè M. Congenital malformations. *J Matern Fetal Neonatal Med*. 2012 Apr;25 Suppl 1:25–9.
9. REGULATION (EU) No 536/2014 [Internet]. REGULATION (EU) No 536/2014 OF THE EUROPEAN PARLIAMENT AND OF THE COUNCIL of 16 April 2014 on clinical trials on medicinal products for human use, and repealing Directive 2001/20/ EC. [cited 2021 May 5]. Available from: <http://eur-lex.europa.eu/legal-content/EN/TXT/PDF/?uri=CELEX:32014R0536&qid=1421232837997&from=EN>
10. Rode J. Rare diseases: understanding this public health priority. Paris: EURORDIS [Internet]. 2005; Available from: http://beta.eurordis.org/IMG/pdf/princeps_document-EN.pdf
11. Wright CF, FitzPatrick DR, Firth HV. Paediatric genomics: diagnosing rare disease in children. *Nat Rev Genet*. 2018 May;19(5):325.
12. Boycott KM, Rath A, Chong JX, Hartley T, Alkuraya FS, Baynam G, et al. International Cooperation to Enable the Diagnosis of All Rare Genetic Diseases. *Am J Hum Genet*. 2017 May 4;100(5):695–705.
13. Seaby EG, Rehm HL, O'Donnell-Luria A. Strategies to uplift novel Mendelian gene discovery for improved clinical outcomes. *Front Genet*. 2021 Jun 17;12:674295.
14. Rahit KMT, Tarailo-Graovac M. Genetic Modifiers and Rare Mendelian Disease. *Genes*. 2020 Feb 25;11(3).
15. Austin CP, Cutillo CM, Lau LPL, Jonker AH, Rath A, Julkowska D, et al. Future of Rare Diseases Research 2017-2027: An IRDiRC Perspective. *Clin Transl Sci*. 2018 Jan;11(1):21–7.
16. Saul RA. *Medical Genetics in Pediatric Practice*. 2013. 503 p.

17. Vickers RR, Gibson JS. A Review of the Genomic Analysis of Children Presenting with Developmental Delay/Intellectual Disability and Associated Dysmorphic Features. *Cureus*. 2019 Jan 12;11(1):e3873.
18. Boat TF, Wu JT, Committee to Evaluate the Supplemental Security Income Disability Program for Children with Mental Disorders, Board on the Health of Select Populations, Board on Children, Youth, and Families, Institute of Medicine, et al. *Clinical Characteristics of Intellectual Disabilities*. National Academies Press (US); 2015.
19. D'Arrigo S, Gavazzi F, Alfei E, Zuffardi O, Montomoli C, Corso B, et al. The Diagnostic Yield of Array Comparative Genomic Hybridization Is High Regardless of Severity of Intellectual Disability/Developmental Delay in Children. *J Child Neurol*. 2016 May;31(6):691–9.
20. Flore LA, Milunsky JM. Updates in the genetic evaluation of the child with global developmental delay or intellectual disability. *Semin Pediatr Neurol*. 2012 Dec;19(4):173–80.
21. Bélanger SA, Caron J. Evaluation of the child with global developmental delay and intellectual disability. *Paediatr Child Health*. 2018 Sep;23(6):403–19.
22. Köhler S, Gargano M, Matentzoglou N, Carmody LC, Lewis-Smith D, Vasilevsky NA, et al. The Human Phenotype Ontology in 2021. *Nucleic Acids Res*. 2021 Jan 8;49(D1):D1207–17.
23. Köhler S, Doelken SC, Mungall CJ, Bauer S, Firth HV, Bailleul-Forestier I, et al. The Human Phenotype Ontology project: linking molecular biology and disease through phenotype data. *Nucleic Acids Res*. 2014 Jan;42(Database issue):D966–74.
24. Castells-Sarret N, Cueto-González AM, Borregan M, López-Grondona F, Miró R, Tizzano E, et al. Comparative genomic hybridisation as a first option in genetic diagnosis: 1000 cases and a cost–benefit analysis. *Anales de Pediatría (English Edition)*. 2018 Jul 1;89(1):3–11.
25. Kirchhoff M, Bisgaard A-M, Bryndorf T, Gerdes T. MLPA analysis for a panel of syndromes with mental retardation reveals imbalances in 5.8% of patients with mental retardation and dysmorphic features, including duplications of the Sotos syndrome and Williams-Beuren syndrome regions. *Eur J Med Genet*. 2007 Jan;50(1):33–42.
26. Miller DT, Adam MP, Aradhya S, Biesecker LG, Brothman AR, Carter NP, et al. Consensus statement: chromosomal microarray is a first-tier clinical diagnostic test for individuals with developmental disabilities or congenital anomalies. *Am J Hum Genet*. 2010 May 14;86(5):749–64.
27. Opitz JM, Johnson RC, McCreadie SR, Smith DW. The C syndrome of multiple congenital anomalies. *Birth Defects Orig Artic Ser*. 1969;2:161–6.
28. Urreiziti R, Grinberg D, Balcells S. C syndrome - what do we know and what could the future hold? *Expert Opinion on Orphan Drugs*. 2019 Mar 4;7(3):91–4.
29. Amberger JS, Bocchini CA, Schiettecatte F, Scott AF, Hamosh A. OMIM.org: Online Mendelian Inheritance in Man (OMIM®), an online catalog of human genes and genetic disorders. *Nucleic Acids Res*. 2014 Nov 26;43(D1):D789–98.
30. Gilissen C, Hoischen A, Brunner HG, Veltman JA. Disease gene identification strategies for exome sequencing. *Eur J Hum Genet*. 2012 May;20(5):490–7.

31. Dillon OJ, Lunke S, Stark Z, Yeung A, Thorne N, Melbourne Genomics Health Alliance, et al. Exome sequencing has higher diagnostic yield compared to simulated disease-specific panels in children with suspected monogenic disorders. *Eur J Hum Genet.* 2018 May;26(5):644–51.
32. Lionel AC, Costain G, Monfared N, Walker S, Reuter MS, Hosseini SM, et al. Improved diagnostic yield compared with targeted gene sequencing panels suggests a role for whole-genome sequencing as a first-tier genetic test. *Genet Med.* 2018 Apr;20(4):435–43.
33. Dewey FE, Murray MF, Overton JD, Habegger L, Leader JB, Fetterolf SN, et al. Distribution and clinical impact of functional variants in 50,726 whole-exome sequences from the DiscovEHR study. *Science.* 2016 Dec 23;354(6319).
34. Taliun D, Harris DN, Kessler MD, Carlson J, Szpiech ZA, Torres R, et al. Sequencing of 53,831 diverse genomes from the NHLBI TOPMed Program. *Nature.* 2021 Feb;590(7845):290–9.
35. Richards S, Aziz N, Bale S, Bick D, Das S, Gastier-Foster J, et al. Standards and guidelines for the interpretation of sequence variants: a joint consensus recommendation of the American College of Medical Genetics and Genomics and the Association for Molecular Pathology. *Genet Med.* 2015 May;17(5):405–24.
36. Stenton SL, Kremer LS, Kopajtich R, Ludwig C, Prokisch H. The diagnosis of inborn errors of metabolism by an integrative ‘multi-omics’ approach: A perspective encompassing genomics, transcriptomics, and proteomics. *J Inherit Metab Dis.* 2020 Jan;43(1):25–35.
37. Landrum MJ, Lee JM, Benson M, Brown GR, Chao C, Chitipiralla S, et al. ClinVar: improving access to variant interpretations and supporting evidence. *Nucleic Acids Res.* 2018 Jan 4;46(D1):D1062–7.
38. Stenson PD, Mort M, Ball EV, Evans K, Hayden M, Heywood S, et al. The Human Gene Mutation Database: towards a comprehensive repository of inherited mutation data for medical research, genetic diagnosis and next-generation sequencing studies. Vol. 136, *Human Genetics.* 2017. p. 665–77.
39. Karczewski KJ, Francioli LC, Tiao G, Cummings BB, Alföldi J, Wang Q, et al. The mutational constraint spectrum quantified from variation in 141,456 humans. *Nature.* 2020 May;581(7809):434–43.
40. Rentzsch P, Witten D, Cooper GM, Shendure J, Kircher M. CADD: predicting the deleteriousness of variants throughout the human genome. *Nucleic Acids Res.* 2019 Jan 8;47(D1):D886–94.
41. Vaser R, Adusumalli S, Leng SN, Sikic M, Ng PC. SIFT missense predictions for genomes. *Nat Protoc.* 2016 Jan;11(1):1–9.
42. Schwarz JM, Cooper DN, Schuelke M, Seelow D. MutationTaster2: mutation prediction for the deep-sequencing age. *Nat Methods.* 2014 Apr;11(4):361–2.
43. Adzhubei IA, Schmidt S, Peshkin L, Ramensky VE, Gerasimova A, Bork P, et al. A method and server for predicting damaging missense mutations. *Nat Methods.* 2010 Apr;7(4):248–9.
44. Choi Y, Sims GE, Murphy S, Miller JR, Chan AP. Predicting the functional effect of amino acid substitutions and indels. *PLoS One.* 2012 Oct 8;7(10):e46688.

45. Evers C, Staufner C, Granzow M, Paramasivam N, Hinderhofer K, Kaufmann L, et al. Impact of clinical exomes in neurodevelopmental and neurometabolic disorders. *Mol Genet Metab.* 2017 Aug;121(4):297–307.
46. Coban-Akdemir Z, White JJ, Song X, Jhangiani SN, Fatih JM, Gambin T, et al. Identifying Genes Whose Mutant Transcripts Cause Dominant Disease Traits by Potential Gain-of-Function Alleles. *Am J Hum Genet.* 2018 Aug 2;103(2):171–87.
47. Ghosh R, Oak N, Plon SE. Evaluation of in silico algorithms for use with ACMG/AMP clinical variant interpretation guidelines. *Genome Biol.* 2017 Nov 28;18(1):225.
48. Gearhart J. New potential for human embryonic stem cells. *Science.* 1998 Nov 6;282(5391):1061–2.
49. Takahashi K, Yamanaka S. Induction of pluripotent stem cells from mouse embryonic and adult fibroblast cultures by defined factors. *Cell.* 2006 Aug 25;126(4):663–76.
50. Takahashi K, Tanabe K, Ohnuki M, Narita M, Ichisaka T, Tomoda K, et al. Induction of pluripotent stem cells from adult human fibroblasts by defined factors. *Cell.* 2007 Nov 30;131(5):861–72.
51. Kavyasudha C, Macrin D, ArulJothi KN, Joseph JP, Harishankar MK, Devi A. Clinical Applications of Induced Pluripotent Stem Cells - Stato Attuale. *Adv Exp Med Biol.* 2018;1079:127–49.
52. Hockemeyer D, Jaenisch R. Induced Pluripotent Stem Cells Meet Genome Editing. *Cell Stem Cell.* 2016 May 5;18(5):573–86.
53. Opitz JM, Putnam AR, Comstock JM, Chin S, Byrne JLB, Kennedy A, et al. Mortality and pathological findings in C (opitz trigonocephaly) syndrome. *Fetal Pediatr Pathol.* 2006 Jan 1;25(4):211–31.
54. Travan L, Pecile V, Fertz M, Fabretto A, Brovedani P, Demarini S, et al. Opitz trigonocephaly syndrome presenting with sudden unexplained death in the operating room: a case report. *J Med Case Rep.* 2011 Jun 21;5:222.
55. Abdel-Wahab O, Adli M, LaFave LM, Gao J, Hricik T, Shih AH, et al. ASXL1 mutations promote myeloid transformation through loss of PRC2-mediated gene repression. *Cancer Cell.* 2012 Aug 14;22(2):180–93.
56. Sahtoe DD, van Dijk WJ, Ekkebus R, Ovaa H, Sixma TK. BAP1/ASXL1 recruitment and activation for H2A deubiquitination. *Nat Commun.* 2016 Jan 7;7:10292.
57. Fisher CL, Lee I, Bloyer S, Bozza S, Chevalier J, Dahl A, et al. Additional sex combs-like 1 belongs to the enhancer of trithorax and polycomb group and genetically interacts with Cbx2 in mice. Vol. 337, *Developmental Biology.* 2010. p. 9–15.
58. Strefford JC, An Q, Wright SL, Konn ZJ, Matherson E, Minto L, et al. Variable Breakpoints Target PAX5 in Patients with Dicentric Chromosomes: A Model for the Basis of Unbalanced Translocations in Cancer. Vol. 112, *Blood.* 2008. p. 790–790.
59. Gelsi-Boyer V, Trouplin V, Adélaïde J, Bonansea J, Cervera N, Carbuccia N, et al. Mutations of polycomb-associated gene ASXL1 in myelodysplastic syndromes and chronic myelomonocytic leukaemia. *Br J Haematol.* 2009 Jun;145(6):788–800.
60. Bohring A, Silengo M, Lerone M, Superneau DW, Spaich C, Braddock SR, et al. Severe

- end of Opitz trigonocephaly (C) syndrome or new syndrome?. Vol. 85, American Journal of Medical Genetics. 1999. p. 438–46.
61. Bohring A, Oudesluijs GG, Grange DK, Zampino G, Thierry P. New cases of Bohring-Opitz syndrome, update, and critical review of the literature. *Am J Med Genet A*. 2006 Jun 15;140(12):1257–63.
 62. Russell B, Johnston JJ, Biesecker LG, Kramer N, Pickart A, Rhead W, et al. Clinical management of patients with ASXL1 mutations and Bohring-Opitz syndrome, emphasizing the need for Wilms tumor surveillance. *Am J Med Genet A*. 2015 Sep;167A(9):2122–31.
 63. Kaname T, Yanagi K, Chinen Y, Makita Y, Okamoto N, Maehara H, et al. Mutations in CD96, a member of the immunoglobulin superfamily, cause a form of the C (Opitz trigonocephaly) syndrome. *Am J Hum Genet*. 2007 Oct;81(4):835–41.
 64. Hastings R, Cobben J-M, Gillessen-Kaesbach G, Goodship J, Hove H, Kjaergaard S, et al. Bohring-Opitz (Oberklaid-Danks) syndrome: clinical study, review of the literature, and discussion of possible pathogenesis. *Eur J Hum Genet*. 2011 May;19(5):513–9.
 65. Hoischen A, van Bon BWM, Rodríguez-Santiago B, Gilissen C, Vissers LELM, de Vries P, et al. De novo nonsense mutations in ASXL1 cause Bohring-Opitz syndrome. *Nat Genet*. 2011 Jun 26;43(8):729–31.
 66. Magini P, Della Monica M, Uzielli MLG, Mongelli P, Scarselli G, Gambineri E, et al. Two novel patients with Bohring-Opitz syndrome caused by de novo ASXL1 mutations. *Am J Med Genet A*. 2012 Apr;158A(4):917–21.
 67. Dangiolo SB, Wilson A, Jobanputra V, Anyane-Yeboa K. Bohring-Opitz syndrome (BOS) with a new ASXL1 pathogenic variant: Review of the most prevalent molecular and phenotypic features of the syndrome. *Am J Med Genet A*. 2015 Dec;167A(12):3161–6.
 68. Arunachal G, Danda S, Omprakash S, Kumar S. A novel de-novo frameshift mutation of the ASXL1 gene in a classic case of Bohring-Opitz syndrome. *Clin Dysmorphol*. 2016 Jul;25(3):101–5.
 69. Urreiziti R, Roca-Ayats N, Trepas J, Garcia-Garcia F, Aleman A, Orteschi D, et al. Screening of CD96 and ASXL1 in 11 patients with Opitz C or Bohring-Opitz syndromes. *Am J Med Genet A*. 2016 Jan;170A(1):24–31.
 70. Carlston CM, O'Donnell-Luria AH, Underhill HR, Cummings BB, Weisburd B, Minikel EV, et al. Pathogenic ASXL1 somatic variants in reference databases complicate germline variant interpretation for Bohring-Opitz Syndrome. *Hum Mutat*. 2017 May;38(5):517–23.
 71. Bedoukian E, Copenheaver D, Bale S, Deardorff M. Bohring-Opitz syndrome caused by an ASXL1 mutation inherited from a germline mosaic mother. *Am J Med Genet A*. 2018 May;176(5):1249–52.
 72. Cuddapah VA, Dubbs HA, Adang L, Kugler SL, McCormick EM, Zolkipli-Cunningham Z, et al. Understanding the phenotypic spectrum of ASXL -related disease: Ten cases and a review of the literature. *American Journal of Medical Genetics Part A*. 2021;185(6):1700-1711.
 73. Zhao J, Hou Y, Fang F, Ding C, Yang X, Li J, et al. Novel truncating mutations in ASXL1 identified in two boys with Bohring-Opitz syndrome. *Eur J Med Genet*. 2021

- Mar;64(3):104155.
74. Xie P. TRAF molecules in cell signaling and in human diseases. *Journal of Molecular Signaling*. Ubiquity Press Ltd; 2013;8(1):7.
 75. Ha H, Han D, Choi Y. TRAF-mediated TNFR-family signaling. *Curr Protoc Immunol*. 2009 Nov;Chapter 11:Unit11.9D.
 76. Zotti T, Scudiero I, Vito P, Stilo R. The Emerging Role of TRAF7 in Tumor Development. *J Cell Physiol*. 2017 Jun 6;232(6):1233–8.
 77. Bouwmeester T, Bauch A, Ruffner H, Angrand P-O, Bergamini G, Croughton K, et al. A physical and functional map of the human TNF-alpha/NF-kappa B signal transduction pathway. *Nat Cell Biol*. 2004 Feb;6(2):97–105.
 78. Xu L-G, Li L-Y, Shu H-B. TRAF7 Potentiates MEKK3-induced AP1 and CHOP Activation and Induces Apoptosis. *J Biol Chem*. 2004 Apr 23;279 (17):17278–82.
 79. Scudiero I, Zotti T, Ferravante A, Vessichelli M, Reale C, Masone MC, et al. Tumor Necrosis Factor (TNF) Receptor-associated Factor 7 Is Required for TNF α -induced Jun NH(2)-terminal Kinase Activation and Promotes Cell Death by Regulating Polyubiquitination and Lysosomal Degradation of c-FLIP Protein. *J Biol Chem*. 2012 Feb 17;287(8):6053–61.
 80. Morita Y, Kanei-Ishii C, Nomura T, Ishii S. TRAF7 Sequesters c-Myb to the Cytoplasm by Stimulating Its Sumoylation. *Tansey W, editor. Mol Biol Cell*. 2005 Nov 8;16(11):5433–44.
 81. Xu D, Zhao W, Wang C, Zhu H, He M, Zhu X, et al. Up-regulation of TNF Receptor-associated Factor 7 after spinal cord injury in rats may have implication for neuronal apoptosis. *Neuropeptides*. 2018 Oct;71:81–9.
 82. Tsikitis M, Acosta-Alvear D, Blais A, Campos EI, Lane WS, Sánchez I, et al. Traf7, a MyoD1 transcriptional target, regulates nuclear factor- κ B activity during myogenesis. *EMBO Rep*. 2010 Dec 15;11(12):969–76.
 83. Yoshida H, Jono H, Kai H, Li J-D. The Tumor Suppressor Cylindromatosis (CYLD) Acts as a Negative Regulator for Toll-like Receptor 2 Signaling via Negative Cross-talk with TRAF6 and TRAF7. *J Biol Chem*. 2005 Dec 9;280 (49):41111–21.
 84. Clark VE, Erson-Omay EZ, Serin A, Yin J, Cotney J, Ozduman K, et al. Genomic analysis of non-NF2 meningiomas reveals mutations in TRAF7, KLF4, AKT1, and SMO. *Science*. 2013 Mar 1;339(6123):1077–80.
 85. Reuss DE, Piro RM, Jones DTW, Simon M, Ketter R, Kool M, et al. Secretory meningiomas are defined by combined KLF4 K409Q and TRAF7 mutations. *Acta Neuropathol*. 2013 Mar;125(3):351–8.
 86. Clark VE, Harmancı AS, Bai H, Youngblood MW, Lee TI, Baranoski JF, et al. Recurrent somatic mutations in POLR2A define a distinct subset of meningiomas. *Nat Genet*. 2016 Oct;48(10):1253–9.
 87. Yuzawa S, Nishihara H, Yamaguchi S, Mohri H, Wang L, Kimura T, et al. Clinical impact of targeted amplicon sequencing for meningioma as a practical clinical-sequencing system. *Mod Pathol*. 2016 Jul;29(7):708–16.

88. Georgescu M-M, Nanda A, Li Y, Mobley BC, Faust PL, Raisanen JM, et al. Mutation Status and Epithelial Differentiation Stratify Recurrence Risk in Chordoid Meningioma-A Multicenter Study with High Prognostic Relevance. *Cancers*. 2020 Jan 17;12(1).
89. Goode B, Joseph NM, Stevers M, Van Ziffle J, Onodera C, Talevich E, et al. Adenomatoid tumors of the male and female genital tract are defined by TRAF7 mutations that drive aberrant NF-kB pathway activation. *Mod Pathol*. 2018 Apr;31(4):660–73.
90. Tamura D, Maeda D, Halimi SA, Okimura M, Kudo-Asabe Y, Ito S, et al. Adenomatoid tumour of the uterus is frequently associated with iatrogenic immunosuppression. *Histopathology*. 2018 Dec;73(6):1013–22.
91. Stevers M, Rabban JT, Garg K, Van Ziffle J, Onodera C, Grenert JP, et al. Well-differentiated papillary mesothelioma of the peritoneum is genetically defined by mutually exclusive mutations in TRAF7 and CDC42. *Mod Pathol*. 2019 Jan;32(1):88–99.
92. Bueno R, Stawiski EW, Goldstein LD, Durinck S, De Rienzo A, Modrusan Z, et al. Comprehensive genomic analysis of malignant pleural mesothelioma identifies recurrent mutations, gene fusions and splicing alterations. *Nat Genet*. 2016 Apr;48(4):407–16.
93. Hung YP, Dong F, Dubuc AM, Dal Cin P, Bueno R, Chirieac LR. Molecular characterization of localized pleural mesothelioma. *Mod Pathol*. 2020 Feb;33(2):271–80.
94. Najm P, Zhao P, Steklov M, Sewduth RN, Baietti MF, Pandolfi S, et al. Loss-of-function mutations in TRAF7 and KLF4 cooperatively activate RAS-like GTPase signaling and promote meningioma development. *Cancer Res*. 2021 Jul 2.
95. Schapira M, Tyers M, Torrent M, Arrowsmith CH. WD40 repeat domain proteins: a novel target class? *Nat Rev Drug Discov*. 2017 Oct 13;16(11):773–86.
96. Zotti T, Vito P, Stilo R. The seventh ring: Exploring TRAF7 functions. *J Cell Physiol*. 2012 Mar 1;227(3):1280–4.
97. Lonsdale J, Thomas J, Salvatore M, Phillips R, Lo E, Shad S, et al. The Genotype-Tissue Expression (GTEx) project. *Nat Genet*. 2013 May 29;45(6):580–5.
98. Kamaludin AA, Smolarchuk C, Bischof JM, Eggert R, Greer JJ, Ren J, et al. Muscle dysfunction caused by loss of Magel2 in a mouse model of Prader-Willi and Schaaf-Yang syndromes. *Hum Mol Genet*. 2016 Jul 19;25(17):3798–809.
99. Chen H, Victor AK, Klein J, Tacer KF, Tai DJ, de Esch C, et al. Loss of MAGEL2 in Prader-Willi syndrome leads to decreased secretory granule and neuropeptide production. *JCI Insight*. 2020 Sep 3;5(17).
100. Hao Y-H, Fountain MD Jr, Fon Tacer K, Xia F, Bi W, Kang S-HL, et al. USP7 Acts as a Molecular Rheostat to Promote WASH-Dependent Endosomal Protein Recycling and Is Mutated in a Human Neurodevelopmental Disorder. *Mol Cell*. 2015 Sep 17;59(6):956–69.
101. Doyle JM, Gao J, Wang J, Yang M, Potts PR. MAGE-RING protein complexes comprise a family of E3 ubiquitin ligases. *Mol Cell*. 2010 Sep 24;39(6):963–74.
102. Lee AK, Potts PR. A Comprehensive Guide to the MAGE Family of Ubiquitin Ligases. Vol. 429, *Journal of Molecular Biology*. 2017. p. 1114–42.
103. Hao Y-H, Doyle JM, Ramanathan S, Gomez TS, Jia D, Xu M, et al. Regulation of WASH-dependent actin polymerization and protein trafficking by ubiquitination. *Cell*. 2013

- Feb 28;152(5):1051–64.
104. Burd C, Cullen PJ. Retromer: a master conductor of endosome sorting. *Cold Spring Harb Perspect Biol.* 2014 Feb 1;6(2).
 105. Lee S, Walker CL, Karten B, Kuny SL, Tennese AA, O'Neill MA, et al. Essential role for the Prader-Willi syndrome protein *necdin* in axonal outgrowth. *Hum Mol Genet.* 2005 Mar 1;14(5):627–37.
 106. Panda S, Antoch MP, Miller BH, Su AI, Schook AB, Straume M, et al. Coordinated Transcription of Key Pathways in the Mouse by the Circadian Clock. *Cell.* 2002 May;109(3):307–20.
 107. Carias KV, Zoeteman M, Seewald A, Sanderson MR, Bischof JM, Wevrick R. A MAGEL2-deubiquitinase complex modulates the ubiquitination of circadian rhythm protein CRY1. *PLoS One.* 2020 Apr 21;15(4):e0230874.
 108. Kozlov SV, Bogenpohl JW, Howell MP, Wevrick R, Panda S, Hogenesch JB, et al. The imprinted gene *Magel2* regulates normal circadian output. *Nat Genet.* 2007 Oct;39(10):1266–72.
 109. Cheon CK. Genetics of Prader-Willi syndrome and Prader-Will-Like syndrome. *Ann Pediatr Endocrinol Metab.* 2016 Sep;21(3):126–35.
 110. Costa RA, Ferreira IR, Cintra HA, Gomes LHF, Guida L da C. Genotype-Phenotype Relationships and Endocrine Findings in Prader-Willi Syndrome. *Front Endocrinol .* 2019 Dec 13;10:864.
 111. Cassidy SB, Schwartz S, Miller JL, Driscoll DJ. Prader-Willi syndrome. *Genet Med.* 2012 Jan;14(1):10–26.
 112. Holm VA, Cassidy SB, Butler MC, Hanchett JM, Greenswag LR, Whitman BY, et al. Prader-Willi Syndrome: Consensus Diagnostic Criteria. Vol. 91. 1993.
 113. Schaaf CP, Gonzalez-Garay ML, Xia F, Potocki L, Gripp KW, Zhang B, et al. Truncating mutations of *MAGEL2* cause Prader-Willi phenotypes and autism. *Nat Genet.* 2013 Nov;45(11):1405–8.
 114. Soden SE, Saunders CJ, Willig LK, Farrow EG, Smith LD, Petrikin JE, et al. Effectiveness of exome and genome sequencing guided by acuity of illness for diagnosis of neurodevelopmental disorders. *Sci Transl Med.* 2014 Dec 3;6(265):265ra168.
 115. Urreizti R, Cueto-Gonzalez AM, Franco-Valls H, Mort-Farre S, Roca-Ayats N, Ponomarenko J, et al. A De Novo Nonsense Mutation in *MAGEL2* in a Patient Initially Diagnosed as Opitz-C: Similarities Between Schaaf-Yang and Opitz-C Syndromes. *Sci Rep.* 2017 Mar 10;7:44138.
 116. Fountain MD, Aten E, Cho MT, Juusola J, Walkiewicz MA, Ray JW, et al. The phenotypic spectrum of Schaaf-Yang syndrome: 18 new affected individuals from 14 families. *Genet Med.* 2017 Jan;19(1):45–52.
 117. Palomares-Bralo M, Vallespín E, Del Pozo Á, Ibañez K, Silla JC, Galán E, et al. Pitfalls of trio-based exome sequencing: imprinted genes and parental mosaicism-MAGEL2 as an example. *Genet Med.* 2017 Nov;19(11):1285–6.
 118. Enya T, Okamoto N, Iba Y, Miyazawa T, Okada M, Ida S, et al. Three patients with

- Schaaf-Yang syndrome exhibiting arthrogryposis and endocrinological abnormalities. *Am J Med Genet A*. 2018 Mar;176(3):707–11.
119. D Hidalgo-Santos A, Del Carmen DeMingo-Aleman M, Moreno-Macián F, Roselló M, Orellana C, Martínez F, et al. A Novel Mutation of in a Patient with Schaaf-Yang Syndrome and Hypopituitarism. *Int J Endocrinol Metab*. 2018 Jul;16(3):e67329.
 120. Kleinendorst L, Pi Castán G, Caro-Llopis A, Boon EMJ, van Haelst MM. The role of obesity in the fatal outcome of Schaaf-Yang syndrome: Early onset morbid obesity in a patient with a MAGEL2 mutation. *Am J Med Genet A*. 2018 Nov;176(11):2456–9.
 121. Matuszewska KE, Badura-Stronka M, Śmigiel R, Cabała M, Biernacka A, Kosinska J, et al. Phenotype of two Polish patients with Schaaf–Yang syndrome confirmed by identifying mutation in MAGEL2 gene. Vol. 27, *Clinical Dysmorphology*. 2018. p. 49–52.
 122. McCarthy J, Lupo PJ, Kovar E, Rech M, Bostwick B, Scott D, et al. Schaaf-Yang syndrome overview: Report of 78 individuals. *Am J Med Genet A*. 2018 Dec;176(12):2564–74.
 123. McCarthy JM, McCann-Crosby BM, Rech ME, Yin J, Chen C-A, Ali MA, et al. Hormonal, metabolic and skeletal phenotype of Schaaf-Yang syndrome: a comparison to Prader-Willi syndrome. *J Med Genet*. 2018 May;55(5):307–15.
 124. Bayat A, Bayat M, Lozoya R, Schaaf CP. Chronic intestinal pseudo-obstruction syndrome and gastrointestinal malrotation in an infant with schaaf-yang syndrome - Expanding the phenotypic spectrum. *Eur J Med Genet*. 2018 Oct;61(10):627–30.
 125. Poliak N. Magel2 Gene Mutation and Its Associated Phenotypic Features in A Five-Month-Old Female. Vol. 8, *Journal of Pediatrics & Neonatal Care*. 2018.
 126. Tong W, Wang Y, Lu Y, Ye T, Song C, Xu Y, et al. Whole-exome Sequencing Helps the Diagnosis and Treatment in Children with Neurodevelopmental Delay Accompanied Unexplained Dyspnea. *Sci Rep*. 2018 Mar 26;8(1):5214.
 127. Gregory LC, Shah P, Sanner JRF, Arancibia M, Hurst J, Jones WD, et al. Mutations in MAGEL2 and L1CAM Are Associated With Congenital Hypopituitarism and Arthrogryposis. *J Clin Endocrinol Metab*. 2019 Dec 1;104(12):5737–50.
 128. Negishi Y, Ieda D, Hori I, Nozaki Y, Yamagata T, Komaki H, et al. Schaaf-Yang syndrome shows a Prader-Willi syndrome-like phenotype during infancy. *Orphanet J Rare Dis*. 2019 Dec 2;14(1):277.
 129. Patak J, Gilfert J, Byler M, Neerukonda V, Thiffault I, Cross L, et al. MAGEL2-related disorders: A study and case series. *Clin Genet*. 2019 Dec;96(6):493–505.
 130. de Andrade GALR, de Oliveira Silva TB, do Nascimento IJB, Boath A, da Costa Cunha K, Chermont AG. Schaaf-Yang syndrome: A novel variant in MAGEL2 gene in the first Brazilian preterm neonate. Vol. 11, *International Journal of Case Reports and Images*. 2020.
 131. Chen XF, Song YM, Zou CC. [Schaaf-Yang syndrome caused by the new variation of MAGEL2 gene in a case]. *Zhonghua Er Ke Za Zhi*. 2019 Feb 2;57(2):155–7.
 132. Ahn H, Seo GH, Oh A, Lee Y, Keum C, Heo SH, et al. Diagnosis of Schaaf-Yang syndrome in Korean children with developmental delay and hypotonia. *Medicine*. 2020 Dec 18;99(51):e23864.

133. Halloun R, Habib C, Ekhilevitch N, Weiss R, Tiosano D, Cohen M. Expanding the spectrum of endocrinopathies identified in Schaaf-Yang syndrome - a case report and review of the literature. *Eur J Med Genet.* 2021 May 26;104252.
134. Fountain MD, Schaaf CP. Prader-Willi Syndrome and Schaaf-Yang Syndrome: Neurodevelopmental Diseases Intersecting at the Gene. *Diseases.* 2016 Jan 13;4(1).
135. Thomason MM, McCarthy J, Goin-Kochel RP, Dowell LR, Schaaf CP, Berry LN. Neurocognitive and Neurobehavioral Phenotype of Youth with Schaaf-Yang Syndrome. *J Autism Dev Disord.* 2020 Jul;50(7):2491–500.
136. Marbach F, Elgizouli M, Rech M, Beygo J, Erger F, Velmans C, et al. The adult phenotype of Schaaf-Yang syndrome. *Orphanet J Rare Dis.* 2020 Oct 19;15(1):294.
137. Wolfgram PM, Carrel AL, Allen DB. Long-term effects of recombinant human growth hormone therapy in children with Prader–Willi syndrome. Vol. 25, *Current Opinion in Pediatrics.* 2013. p. 509–14.
138. Burman P, Ritzén EM, Lindgren AC. Endocrine dysfunction in Prader-Willi syndrome: a review with special reference to GH. *Endocr Rev.* 2001 Dec;22(6):787–99.
139. Boccaccio I, Glatt-Deeley H, Watrin F, Roëckel N, Lalande M, Muscatelli F. The human MAGEL2 gene and its mouse homologue are paternally expressed and mapped to the Prader-Willi region. *Hum Mol Genet.* 1999 Dec;8(13):2497–505.
140. Bischof JM, Stewart CL, Wevrick R. Inactivation of the mouse Magel2 gene results in growth abnormalities similar to Prader-Willi syndrome. *Hum Mol Genet.* 2007 Nov 15;16(22):2713–9.
141. Mercer RE, Wevrick R. Loss of Magel2, a candidate gene for features of Prader-Willi syndrome, impairs reproductive function in mice. *PLoS One.* 2009 Jan 27;4(1).
142. Tennesse AA, Wevrick R. Impaired hypothalamic regulation of endocrine function and delayed counterregulatory response to hypoglycemia in Magel2-null mice. *Endocrinology.* 2011 Mar;152(3):967–78.
143. Luck C, Vitaterna MH, Wevrick R. Dopamine pathway imbalance in mice lacking Magel2, a Prader-Willi syndrome candidate gene. *Behav Neurosci.* 2016 Aug 1;130(4):448–59.
144. Bonnemaïson ML, Eipper BA, Mains RE. Role of adaptor proteins in secretory granule biogenesis and maturation. *Front Endocrinol .* 2013 Aug 14;4:101.
145. Tacer KF, Potts PR. Cellular and disease functions of the Prader–Willi Syndrome gene MAGEL2. *Biochem J.* 2017 Jul 1;474(13):2177–90.
146. Schaller F, Watrin F, Sturny R, Massacrier A, Szepetowski P, Muscatelli F. A single postnatal injection of oxytocin rescues the lethal feeding behaviour in mouse newborns deficient for the imprinted Magel2 gene. *Hum Mol Genet.* 2010 Dec 15;19(24):4895–905.
147. Meziane H, Schaller F, Bauer S, Villard C, Matarazzo V, Riet F, et al. An Early Postnatal Oxytocin Treatment Prevents Social and Learning Deficits in Adult Mice Deficient for Magel2, a Gene Involved in Prader-Willi Syndrome and Autism. *Biol Psychiatry.* 2015 Jul 15;78(2):85–94.
148. Bertoni A, Schaller F, Tyzio R, Gaillard S, Santini F, Xolin M, et al. Oxytocin

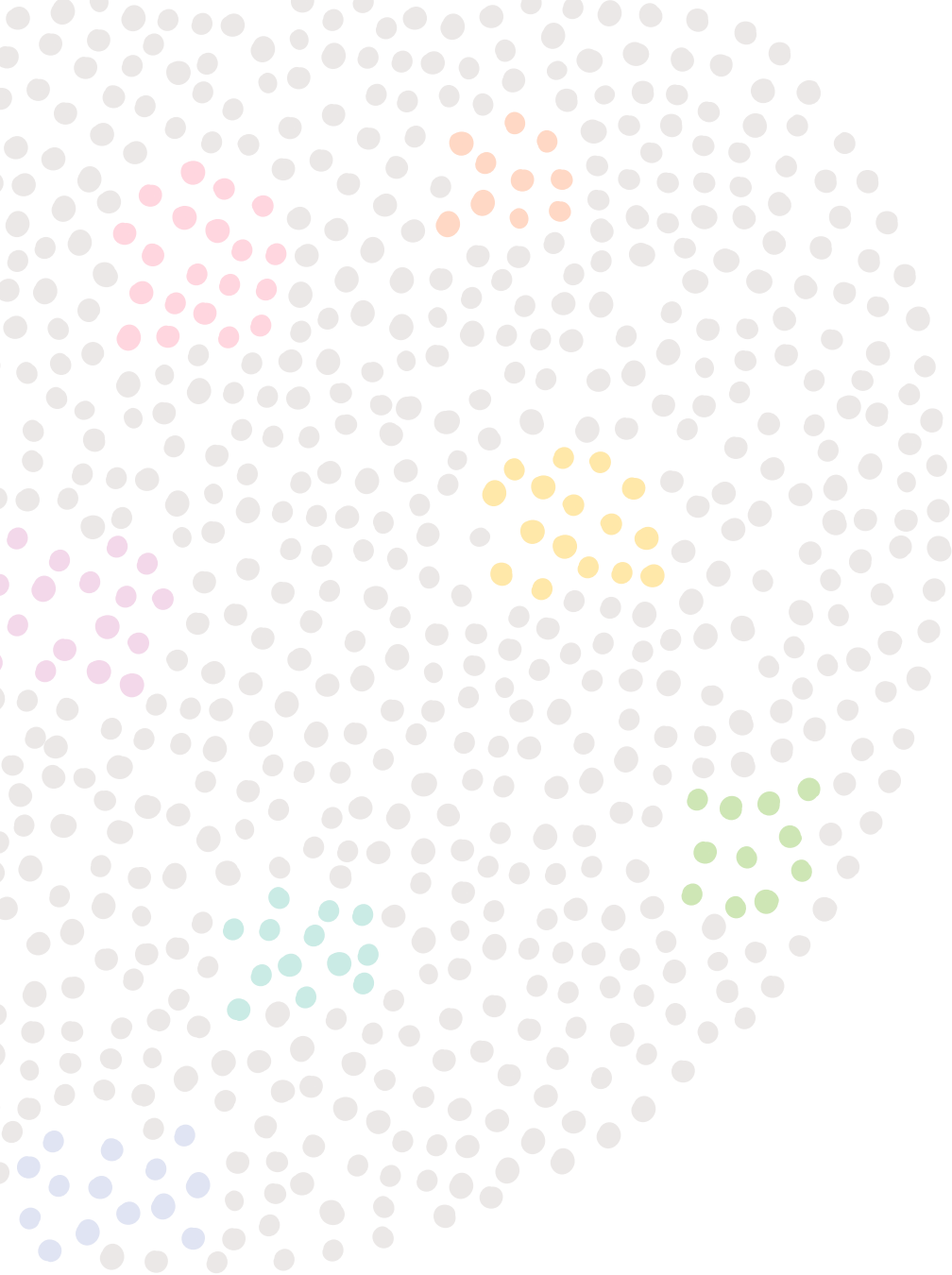
- administration in neonates shapes the hippocampal circuitry and restores social behavior in a mouse model of autism. *BioRxiv* (doi: 10.1101/2020.09.21.306217)
149. Reichova A, Schaller F, Bukatova S, Bacova Z, Muscatelli F, Bakos J. The Impact of Oxytocin on Neurite Outgrowth and Synaptic Proteins in *Magel2*-Deficient Mice. *Dev Neurobiol.* 2021 Feb 20;
 150. Tauber M, Boulanouar K, Diene G, Çabal-Berthoumieu S, Ehlinger V, Fichaux-Bourin P, et al. The Use of Oxytocin to Improve Feeding and Social Skills in Infants With Prader-Willi Syndrome. *Pediatrics.* 2017 Feb;139(2).
 151. Ieda D, Negishi Y, Miyamoto T, Johmura Y, Kumamoto N, Kato K, et al. Two mouse models carrying truncating mutations in *Magel2* show distinct phenotypes. *PLoS One.* 2020 Aug 17;15(8):e0237814.
 152. Toriello HV, Colley C, Bamshad M. Update on the Toriello-Carey syndrome. *Am J Med Genet A.* 2016 Oct;170(10):2551–8.
 153. Kernohan KD, Hartley T, Alirezaie N, Care4Rare Canada Consortium, Robinson PN, Dymont DA, et al. Evaluation of exome filtering techniques for the analysis of clinically relevant genes. *Hum Mutat.* 2018 Feb;39(2):197–201.
 154. Kopanos C, Tsiolkas V, Kouris A, Chapple CE, Aguilera MA, Meyer R, et al. VarSome: the human genomic variant search engine. *Bioinformatics.* 2019 Jun 1;35(11):1978.
 155. Li Q, Wang K. InterVar: Clinical Interpretation of Genetic Variants by the 2015 ACMG-AMP Guidelines. *Am J Hum Genet.* 2017 Feb 2;100(2):267–80.
 156. Yuan B, Neira J, Pehlivan D, Santiago-Sim T, Song X, Rosenfeld J, et al. Clinical exome sequencing reveals locus heterogeneity and phenotypic variability of cohesinopathies. *Genet Med.* 2019 Mar;21(3):663–75.
 157. Lehalle D, Mosca-Boidron A-L, Begtrup A, Boute-Benejean O, Charles P, Cho MT, et al. *STAG1* mutations cause a novel cohesinopathy characterised by unspecific syndromic intellectual disability. Vol. 54, *Journal of Medical Genetics.* 2017. p. 479–88.
 158. Russell B, Tan W-H, Graham JM Jr. Bohring-Opitz Syndrome. In: Adam MP, Ardinger HH, Pagon RA, Wallace SE, Bean LJH, Mirzaa G, et al., editors. *GeneReviews.* Seattle (WA): University of Washington, Seattle; 2018.
 159. Kalia SS, Adelman K, Bale SJ, Chung WK, Eng C, Evans JP, et al. Recommendations for reporting of secondary findings in clinical exome and genome sequencing, 2016 update (ACMG SF v2.0): a policy statement of the American College of Medical Genetics and Genomics. *Genet Med.* 2017 Feb;19(2):249–55.
 160. de Wert G, Dondorp W, Clarke A, Dequeker EMC, Cordier C, Deans Z, et al. Opportunistic genomic screening. Recommendations of the European Society of Human Genetics. *Eur J Hum Genet.* 2021 Mar;29(3):365–77.
 161. Isidor B, Julia S, Saugier-Verber P, Weil-Dubuc P-L, Bézieau S, Bieth E, et al. Searching for secondary findings: considering actionability and preserving the right not to know. Vol. 27, *European Journal of Human Genetics.* 2019. p. 1481–4.
 162. Farwell KD, Shahmirzadi L, El-Khechen D, Powis Z, Chao EC, Tippin Davis B, et al. Enhanced utility of family-centered diagnostic exome sequencing with inheritance model-based analysis: results from 500 unselected families with undiagnosed genetic conditions.

- Genet Med. 2015 Jul;17(7):578–86.
163. Retterer K, Juusola J, Cho MT, Vitazka P, Millan F, Gibellini F, et al. Clinical application of whole-exome sequencing across clinical indications. *Genet Med.* 2016 Jul;18(7):696–704.
 164. Monies D, Abouelhoda M, Assoum M, Moghrabi N, Rafiullah R, Almontashiri N, et al. Lessons Learned from Large-Scale, First-Tier Clinical Exome Sequencing in a Highly Consanguineous Population. *Am J Hum Genet.* 2019 Oct 3;105(4):879.
 165. Shalev SA. Characteristics of genetic diseases in consanguineous populations in the genomic era: Lessons from Arab communities in North Israel. *Clin Genet.* 2019 Jan;95(1):3–9.
 166. Fattahi Z, Beheshtian M, Mohseni M, Poustchi H, Sellars E, Nezhadi SH, et al. Iranome: A catalog of genomic variations in the Iranian population. *Hum Mutat.* 2019 Nov;40(11):1968–84.
 167. Scott EM, Halees A, Itan Y, Spencer EG, He Y, Azab MA, et al. Characterization of Greater Middle Eastern genetic variation for enhanced disease gene discovery. *Nat Genet.* 2016 Sep;48(9):1071–6.
 168. Karczewski KJ, Weisburd B, Thomas B. The ExAC browser: displaying reference data information from over 60 000 exomes. *Nucleic acids.* 2017.
 169. Xie M, Lu C, Wang J, McLellan MD, Johnson KJ, Wendl MC, et al. Age-related mutations associated with clonal hematopoietic expansion and malignancies. *Nat Med.* 2014 Dec;20(12):1472–8.
 170. Jaiswal S, Fontanillas P, Flannick J, Manning A, Grauman PV, Mar BG, et al. Age-related clonal hematopoiesis associated with adverse outcomes. *N Engl J Med.* 2014 Dec 25;371(26):2488–98.
 171. Van Ness M, Szankasi P, Frizzell K, Shen W, Kelley TW. Analysis of ASXL1 mutations in a large series of myeloid malignancies. *Laboratory investigation.* nature publishing group; 2016. p. 381A – 381A.
 172. Sobreira N, Schiettecatte F, Valle D, Hamosh A. GeneMatcher: a matching tool for connecting investigators with an interest in the same gene. *Hum Mutat.* 2015 Oct;36(10):928–30.
 173. Petersen B-S, Fredrich B, Hoepfner MP, Ellinghaus D, Franke A. Opportunities and challenges of whole-genome and -exome sequencing. *BMC Genet.* 2017 Feb 14;18(1):14.
 174. Tokita MJ, Chen C-A, Chitayat D, Macnamara E, Rosenfeld JA, Hanchard N, et al. De Novo Missense Variants in TRAF7 Cause Developmental Delay, Congenital Anomalies, and Dysmorphic Features. *Am J Hum Genet.* 2018 Jul 5;103(1):154–62.
 175. Thompson R, Papakonstantinou Ntalis A, Beltran S, Töpf A, de Paula Estephan E, Polavarapu K, et al. Increasing phenotypic annotation improves the diagnostic rate of exome sequencing in a rare neuromuscular disorder. *Hum Mutat.* 2019 Oct;40(10):1797–812.
 176. Domingo J, Baeza-Centurion P, Lehner B. The Causes and Consequences of Genetic Interactions (Epistasis). *Annu Rev Genomics Hum Genet.* 2019 Aug 31;20:433–60.

177. van Leeuwen J, Pons C, Mellor JC, Yamaguchi TN, Friesen H, Koschwanez J, et al. Exploring genetic suppression interactions on a global scale. *Science*. 2016 Nov 4;354(6312).
178. Costain G, Jobling R, Walker S, Reuter MS, Snell M, Bowdin S, et al. Periodic reanalysis of whole-genome sequencing data enhances the diagnostic advantage over standard clinical genetic testing. *Eur J Hum Genet*. 2018 May;26(5):740–4.
179. Salfati EL, Spencer EG, Topol SE, Muse ED, Rueda M, Lucas JR, et al. Re-analysis of whole-exome sequencing data uncovers novel diagnostic variants and improves molecular diagnostic yields for sudden death and idiopathic diseases. *Genome Med*. 2019 Dec 17;11(1):83.
180. Cummings BB, Marshall JL, Tukiainen T, Lek M, Donkervoort S, Foley AR, et al. Improving genetic diagnosis in Mendelian disease with transcriptome sequencing. *Sci Transl Med*. 2017 Apr 19;9(386).
181. Desmet F-O, Hamroun D, Lalande M, Collod-Bérout G, Claustres M, Bérout C. Human Splicing Finder: an online bioinformatics tool to predict splicing signals. *Nucleic Acids Res*. 2009 May;37(9):e67.
182. Strimbu K, Tavel JA. What are biomarkers? *Curr Opin HIV AIDS*. 2010 Nov;5(6):463–6.
183. Sollis E, Graham SA, Vino A, Froehlich H, Vreeburg M, Dimitropoulou D, et al. Identification and functional characterization of de novo FOXP1 variants provides novel insights into the etiology of neurodevelopmental disorder. *Hum Mol Genet*. 2016 Feb 1;25(3):546–57.
184. Accogli A, Scala M, Pavanello M, Severino M, Gandolfo C, De Marco P, et al. Sinus pericranii, skull defects, and structural brain anomalies in TRAF7-related disorder. *Birth Defects Res*. 2020 Aug;112(14):1085–92.
185. Bellacosa A. Developmental disease and cancer: biological and clinical overlaps. *Am J Med Genet A*. 2013 Nov;161A(11):2788–96.
186. Glass D, Viñuela A, Davies MN, Ramasamy A, Parts L, Knowles D, et al. Gene expression changes with age in skin, adipose tissue, blood and brain. *Genome Biol*. 2013 Jul 26;14(7):R75.
187. Woolf SH, Grol R, Hutchinson A, Eccles M, Grimshaw J. Potential benefits, limitations, and harms of clinical guidelines. *BMJ*. 1999 Feb 20;318(7182):527–30.
188. Kanber D, Giltay J, Wiczorek D, Zogel C, Hochstenbach R, Caliebe A, et al. A paternal deletion of MKRN3, MAGEL2 and NDN does not result in Prader–Willi syndrome. Vol. 17, *European Journal of Human Genetics*. 2009. p. 582–90.
189. Buiting K, Di Donato N, Beygo J, Bens S, von der Hagen M, Hackmann K, et al. Clinical phenotypes of MAGEL2 mutations and deletions. *Orphanet J Rare Dis*. 2014 Mar 25;9:40.
190. Rieusset A, Schaller F, Unmehopa U, Matarazzo V, Watrin F, Linke M, et al. Stochastic loss of silencing of the imprinted Ndn/NDN allele, in a mouse model and humans with prader-willi syndrome, has functional consequences. *PLoS Genet*. 2013 Sep 5;9(9):e1003752.
191. Matarazzo V, Muscatelli F. Natural breaking of the maternal silence at the mouse and

- human imprinted Prader-Willi locus: A whisper with functional consequences. *Rare Dis.* 2013;1:e27228.
192. Crutcher E, Pal R, Naini F, Zhang P, Laugsch M, Kim J, et al. mTOR and autophagy pathways are dysregulated in murine and human models of Schaaf-Yang syndrome. *Sci Rep.* 2019 Nov 4;9(1):15935.
193. Tărlungeanu DC, Novarino G. Genomics in neurodevelopmental disorders: an avenue to personalized medicine. *Exp Mol Med.* 2018 Aug 7;50(8):1–7.
194. Auburger G, Klinkenberg M, Drost J, Marcus K, Morales-Gordo B, Kunz WS, et al. Primary skin fibroblasts as a model of Parkinson's disease. *Mol Neurobiol.* 2012 Aug;46(1):20–7.
195. Canals I, Benetó N, Cozar M, Vilageliu L, Grinberg D. EXTL2 and EXTL3 inhibition with siRNAs as a promising substrate reduction therapy for Sanfilippo C syndrome. *Sci Rep.* 2015 Sep 8;5:13654.
196. Tigges J, Krutmann J, Fritsche E, Haendeler J. The hallmarks of fibroblast ageing. *Mech Ageing Dev.* 2014;138:26-44.
197. Zhao X, Bhattacharyya A. Human Models Are Needed for Studying Human Neurodevelopmental Disorders. *Am J Hum Genet.* 2018 Dec 6;103(6):829–57.
198. Ben-David U, Benvenisty N. The tumorigenicity of human embryonic and induced pluripotent stem cells. *Nat Rev Cancer.* 2011 Apr;11(4):268–77.
199. Tiscornia G, Vivas EL, Izpisua Belmonte JC. Diseases in a dish: modeling human genetic disorders using induced pluripotent cells. *Nat Med.* 2011 Dec;17(12):1570–6.
200. Rajamani U, Gross AR, Hjelm BE, Sequeira A, Vawter MP, Tang J, et al. Super-Obese Patient-Derived iPSC Hypothalamic Neurons Exhibit Obesogenic Signatures and Hormone Responses. *Cell Stem Cell.* 2018 May 3;22(5):698–712.e9.
201. Zhang Y, Pak C, Han Y, Ahlenius H, Zhang Z, Chanda S, et al. Rapid single-step induction of functional neurons from human pluripotent stem cells. *Neuron.* 2013 Jun 5;78(5):785–98.
202. Yang N, Yang N, Chanda S, Südhof T, Wernig M. Generation of pure GABAergic neurons by transcription factor programming. *Nat Methods.* 2017;14(6):621-628
203. Canals I, Canals I, Ginisty A, Quist E, Timmerman R, Fritze J, et al. Rapid and Efficient Induction of Functional Astrocytes from Human Pluripotent Stem Cells. *Nat Methods* 15, 693–696 (2018).
204. Sloan SA, Andersen J, Paşca AM, Birey F, Paşca SP. Generation and assembly of human brain region-specific three-dimensional cultures. *Nat Protoc.* 2018 Sep;13(9):2062–85.
205. Huang W-K, Wong SZH, Pather SR, Nguyen PTT, Zhang F, Zhang DY, et al. Generation of hypothalamic arcuate organoids from human induced pluripotent stem cells. *Cell Stem Cell.* 2021;S1934-5909(21)00163-6.
206. Yoon S-J, Elahi LS, Paşca AM, Marton RM, Gordon A, Revah O, et al. Reliability of human cortical organoid generation. *Nat Methods.* 2018 Dec 20;16(1):75–8.

207. Kang JG, Park JS, Ko J-H, Kim Y-S. Regulation of gene expression by altered promoter methylation using a CRISPR/Cas9-mediated epigenetic editing system. *Sci Rep.* 2019. 9(11960).
208. Darnell JE Jr. Transcription factors as targets for cancer therapy. *Nat Rev Cancer.* 2002 Oct;2(10):740–9.
209. Banham AH, Connors JM, Brown PJ, Cordell JL, Ott G, Sreenivasan G, et al. Expression of the FOXP1 transcription factor is strongly associated with inferior survival in patients with diffuse large B-cell lymphoma. *Clin Cancer Res.* 2005 Feb 1;11(3):1065–72.
210. Inaguma S, Ito H, Riku M, Ikeda H, Kasai K. Addiction of pancreatic cancer cells to zinc-finger transcription factor ZIC2. Vol. 6, *Oncotarget.* 2015. p. 28257–68.
211. Kong Q, Li W, Hu P, Zeng H, Pan Y, Zhou T, et al. The expression status of ZIC2 is an independent prognostic marker of hepatocellular carcinoma. *Liver Res.* 2020 Mar;4(1):40–6.
212. Rozman M, Camós M, Colomer D, Villamor N, Esteve J, Costa D, et al. Type I MOZ/CBP (MYST3/CREBBP) is the most common chimeric transcript in acute myeloid leukemia with t(8;16)(p11;p13) translocation. *Genes Chromosomes Cancer.* 2004 Jun;40(2):140–5.
213. Sharma BS, Prabhakaran V, Desai AP, Bajpai J, Verma RJ, Swain PK. Post-translational modifications (PTMs), from a cancer perspective: An overview. *Oncogene.* 2019 May 8;2(3).
214. Wu G, Guo Z, Chatterjee A, Huang X, Rubin E, Wu F, et al. Overexpression of Glycosylphosphatidylinositol (GPI) Transamidase Subunits Phosphatidylinositol Glycan Class T and/or GPI Anchor Attachment 1 Induces Tumorigenesis and Contributes to Invasion in Human Breast Cancer. Vol. 66, *Cancer Research.* 2006. p. 9829–36.
215. Liu M, Yin K, Guo X, Feng H, Yuan M, Liu Y, et al. Diphthamide Biosynthesis 1 is a Novel Oncogene in Colorectal Cancer Cells and is Regulated by MiR-218-5p. *Cell Physiol Biochem.* 2017 Nov 17;44(2):505–14.
216. Zhong Z, Sepramaniam S, Chew XH, Wood K, Lee MA, Madan B, et al. PORCN inhibition synergizes with PI3K/mTOR inhibition in Wnt-addicted cancers. *Oncogene.* 2019 Oct;38(40):6662–77.
217. Maisel SA, Schroeder J. Wrong place at the wrong time: how retrograde trafficking drives cancer metastasis through receptor mislocalization. *J Cancer Metastasis Treat.* 2019 Feb 13; 2019; 5:7.
218. Simpson AJG, Caballero OL, Jungbluth A, Chen Y-T, Old LJ. Cancer/testis antigens, gametogenesis and cancer. *Nat Rev Cancer.* 2005 Aug;5(8):615–25.
219. Rasmussen SA, for the OMIM curators, Hamosh A. What's in a name? Issues to consider when naming Mendelian disorders. Vol. 22, *Genetics in Medicine.* 2020. p. 1573–5.
220. Bruford EA, Braschi B, Denny P, Jones TEM, Seal RL, Tweedie S. Guidelines for human gene nomenclature. *Nat Genet.* 2020 Aug;52(8):754–8.



Combining exome sequencing
and functional studies to identify causal genes
of ultra-rare neurodevelopmental disorders

Laura Castilla Vallmanya

2021

Tesi Doctoral

Universitat de Barcelona

Combining exome sequencing and functional studies to identify causal genes of ultra-rare neurodevelopmental disorders

Memòria presentada per

Laura Castilla-Vallmanya

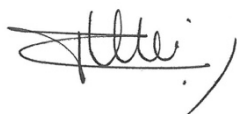
Per optar al grau de

Doctora per la Universitat de Barcelona

Programa de Genètica

Departament de Genètica, Microbiologia i Estadística

Tesi dirigida per la Dra. Roser Urreizti Frexedas (codirectora) i la Dra. Susanna Balcells Comas (codirectora i tutora)



Dra. Roser Urreizti Frexedas
(codirectora)



Dra. Susanna Balcells Comas
(codirectora i tutora)



Laura Castilla-Vallmanya

Barcelona, Juliol del 2021



UNIVERSITAT DE
BARCELONA

L'autora de la tesi doctoral, Laura Castilla Vallmanya, i les seves directores, la Dra. Susanna Balcells Comas i la Dra. Roser Urreizti Frexedas, volen deixar constància de que el present treball ha sigut dirigit també pel Dr. Daniel Grinberg Vaisman, en igualtat de condicions que les altres dues directores. Per raons administratives, el seu nom no ha pogut constar oficialment.

Barcelona, Juliol de 2021



Laura Castilla Vallmanya
(Estudiant)



Dr. Daniel Grinberg Vaisman
(Professor emèrit)



Dra. Susanna Balcells Comas
(Codirectora i tutora)



Dra. Roser Urreizti Frexedas
(Codirectora)

1. NEURODEVELOPMENTAL DISORDERS

During the development of the human brain, many different cell types have to proliferate, differentiate into specialized cell types, migrate to specific locations and form connections between them. It is a highly complex and tightly regulated process that will form an organ capable of complex language, cognition and emotion (1).

Neurodevelopmental disorders (NDD) encompass a series of chronic diseases in which the development of the central nervous system (CNS) is perturbed. These disorders, with onset in the developmental period, affect a large and heterogeneous group of patients who may present disability at the neuropsychiatric, motor and/or intellectual level, impairing normal functioning. Many different causes can be the origin of the functional limitations that define NDDs, which can have genetic, metabolic, nutritional, structural and/or immunological origin (2). According to the Diagnostic and Statistical Manual of Mental Disorders (DSM-5), neurodevelopmental disorders include (**Figure 1**): intellectual developmental disorders, communication disorders, autism spectrum disorder (ASD), attention deficit/hyperactivity disorder (ADHD), specific learning disorder, and motor disorders (3). However, NDDs can rarely be treated as independent entities, as the co-occurrence of different neurodevelopmental disorders in one single individual is more frequent than it would be expected by chance (4), making them difficult to diagnose in some cases.

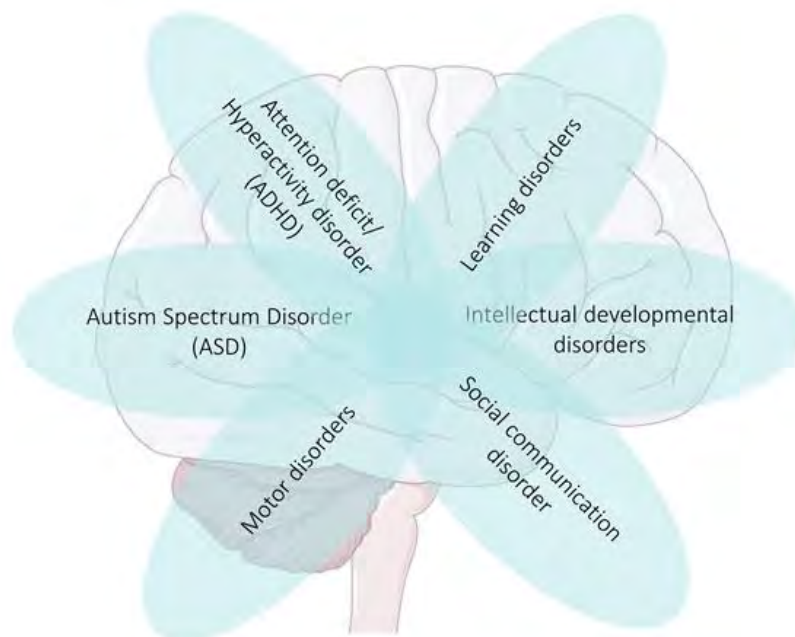


Figure 1. Neurodevelopmental disorders based on Diagnostic and Statistical Manual for Mental Disorders, 5th Edition (DSM-5) (3).

The prevalence of intellectual disability (ID) and developmental delay (DD) in the general population is 1-3% (5) and approximately 50% of the DD/ID cases have a genetic origin (6) (**Figure 2**). ASD phenotypes are present in 0,7% of people (7) while congenital malformations (not always associated with cognitive dysfunction) are observed in 2-3% of the general population (8).

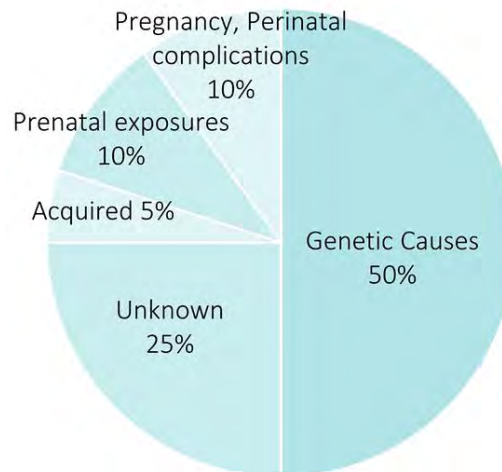


Figure 2. Causes of ID and their respective percentages. [Adapted from Marrus & Hall (6)].

There is a wide range of syndromes that cause ID/DD phenotypes coupled with different kinds of congenital malformations. However, their prevalence in the general population is very low, reason why the majority of them are classified as rare disorders. A certain disorder is considered as rare when it affects less than 1 in 2000 individuals and as ultra-rare if it affects no more than one person in 50000 (9). To date, almost 7000 different rare disorders have been described. Despite the low prevalence of each single disorder, as a group they have a big impact on society, as it is estimated that 6-8% of the EU population are rare disease patients (10). These percentages show how, as a whole, rare diseases represent a serious global issue both at a health and social levels.

Around 80% of rare diseases have a genetic origin (10) and the majority of them are monogenic (11). In 2017 it was estimated that the molecular origin of more than half of the identified rare genetic diseases was still unknown (12), but this percentage has been decreasing over the last years and the same tendency is expected to be maintained in the future (13). Nevertheless, even for those rare genetic diseases which have a clearly identified disease-causing gene, diagnosis and patient management can be very challenging due to the frequently observed phenotypic variability among different mutations (14).

2. DIAGNOSIS OF ULTRA-RARE NEURODEVELOPMENTAL DISORDERS

It is estimated that approximately half of the patients suffering from rare diseases are undiagnosed, while the waiting time for those who have been diagnosed is 5-6 years on average, reaching several decades in some cases of ultra-rare diseases (15). During this time, commonly called “**diagnostic odyssey**”, patients and their families face a long journey, usually full of uncertainty, hope and perseverance. The key to success of the diagnostic odyssey of ultra-rare NDDs is close collaboration of multidisciplinary teams, including clinical, bioinformatic and genetic experts.

2.1 Clinical diagnosis

In clinics, developmental delay is described in patients when two or more features of the developmental process are substantially delayed. These aspects include gross and fine movement, cognitive function, language/speech, social skills and activities of daily life related to personal care. The presence of DD becomes evident when a child fails to reach the developmental milestones associated with his/her specific age group. The concept “developmental delay” is reserved for children under five years old, while “intellectual disability” is used for older patients when IQ can be more accurately tested (16,17).

It is estimated that DD/ID occurs can be classified in four groups depending on its severity: mild, moderate, severe and profound. Approximately 95% of the DD/ID cases account for phenotypes ranging from mild to moderate. These patients require limited assistance and can live independently in an environment providing moderate aid and are normally diagnosed during early educational years due to low academic performance. Severe ID affects about 3.5% of patients, who show obvious delay related to development. They do need daily assistance and supervision but are generally able to learn simple routines and comprehend speech, although their communication skills are usually impaired. Finally, the remaining 1.5% of the cases are considered to present profound ID. They normally present several physical limitations and extremely limited oral communication, which make them completely dependent on a caretaker figure. Both severe and profound ID are identified within the first two years of life and frequently present comorbid conditions (18).

Between 30% and 40% of the ID cases are associated with other conditions that can be syndromic or not. The syndromic DD/ID cases also present with additional neurological

conditions, associated dysmorphic features or both (17,19). A particular feature is considered as dysmorphic when it is present in less than 5% of the population and it has been developed through malformation, deformation or disruption mechanisms. They can be divided into major and minor anomalies depending on the degree of alteration of the physical appearance and normal function. Some of the most frequent major dysmorphic features are orofacial clefts, neural tube defects and limb anomalies. Minor anomalies mostly occur in the head, face and hands. Usually, patients display a distinctive constellation of anomalies that constitutes a specific phenotype that differs from the standard (20). In DD/ID cases it is crucial to perform an exhaustive clinical assessment of these dysmorphic features that should include the description of the following anatomical regions: head shape, eyes, hair, nose, ears, mouth, jaw, neck, trunk area, genitalia and upper and lower limbs. Examination of other internal organ abnormalities, like the heart or the brain, caused by anomalous development should also be performed to develop a complete phenotypic description of the patient (21).

Given the intrinsic phenotypic heterogeneity present in the majority of ultra-rare NDDs, it is essential to try to use standardized terms to describe the observed clinical traits. They help to reduce ambiguity and misinterpretation across the scientific community and improve the implementation of automated analyses and classification, reducing time and errors. With this aim, the Human Phenotype Ontology (HPO) (22) was launched in 2008 and has been actively revised and updated since then. The HPO is a “comprehensive resource that systematically defines and logically organizes human phenotypes” functioning as a translational bridge between genomic data and the disease (**Figure 3**). It has different translational and research applications, such as the interpretation of sequencing data in diagnostics, discovery of novel gene-disease associations and cohort analytics to improve disease phenotypic delineation. Nowadays, the great majority of phenotype-driven genomic diagnostics software use HPO-based computational disease models (22).

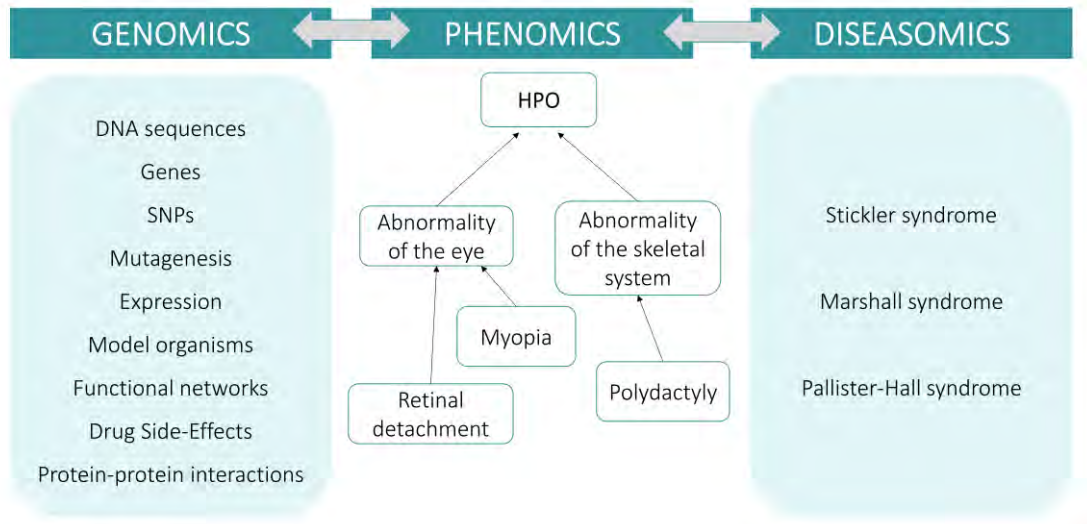


Figure 3. The HPO as a central resource to connect genomic and diseasome data through standardized phenomic descriptions. It facilitates data integration between molecular biology and human disease. [Adapted from Kölher et al. (23)].

While it is essential to perform a deep and systematic clinical phenotyping of the patient, it is important to highlight that the phenotype can be incomplete at the moment of the first clinical evaluation. For this reason, the performance of additional examinations (periodical follow-ups) looking for new traits is highly advisable and might guide the diagnostic process. Also, an exhaustive clinical description can help in a retrospective manner when genetic laboratory results are ambiguous (16).

2.2 Genetic diagnosis

There are cases in which an exhaustive phenotyping leads to a directed clinical suspicion, then the appropriate test according to the associated genetic alteration is performed. In the case that a chromosomal or genomic alteration is suspected, different molecular cytogenetic techniques can be used. Traditionally, the most used one has been the karyotype that allows the detection of large gains or losses of genetic material and large structural reorganizations, present in about 3-5% of DD/ID patients and/or congenital malformations (24). Aiming to improve the diagnosis rates, other techniques have been implemented, for example fluorescent in-situ hybridization (FISH), that allow the precise detection of translocations, and multiplex ligation-dependent probe amplification (MLPA), that allows the detection of microdeletions and microduplications in specific genomic regions (25). Then, the use of whole genome arrays including single nucleotide polymorphisms (SNP) and compared genomic hybridization arrays (aCGH) significantly increased the diagnostic rates of patients with DD/ID, ASD or congenital malformations (26).

If the clinical features can be clearly associated with a specific disease linked to variants in a specific gene, the faster and most cost-effective approach would be performing a screening of the whole candidate gene through Sanger sequencing. This sequencing technique allows the generation of very high quality long reads, however a starting hypothesis is needed as its discovery power is very limited.

When there is not a clear clinical suspicion the strategy to follow usually consists of performing some molecular cytogenetic techniques, such as karyotype and aCGH, to discard the possibility of chromosomal or genomic rearrangements. If the result is negative, an hypothesis-free NGS analysis should be carried out aiming to identify a point mutation or small deletion/insertion.

2.2.1 Next-generation sequencing techniques

Not much more than a decade ago, the diagnostic process of patients suffering from rare NDDs mainly involved many years of documentation of the clinical phenotype and performance of biochemical and imaging tests. In some cases, these investigations led to a suspected particular clinical disorder and different genetic studies were performed using a set of laboratory techniques with low individual efficiency. As could be expected, the success rates were considerably low. The appearance of next generation sequencing

(NGS) technologies represented a before and an after in the NDDs diagnostic field. During their early years they were mostly restricted to particular cases and frequently used by diagnosis research groups due to its low performance and high prices. However, the dramatic technical improvements and cost decrease during the last decade has made their inclusion possible as routine genetics diagnostic tools.

The incorporation of these novel genetic diagnostic tests, together with the improvement of the bioinformatic tools necessary for the analysis of the output data, had led to a significant decrease of the average time needed for rare NDDs patients to get a diagnosis. This has also led to a rapid increase in the identification of novel genes linked to neurodevelopmental disorders. These tools have also shown that, in some particular clinically defined syndromes, there is no common molecular cause. However, in some cases, these clinical entities are still useful as clinical or phenotypical “labels”. The Opitz C syndrome (OCS; OMIM # 211750) is an example of such situations. OCS is an ultra-rare syndromic neurodevelopmental disorder that was first clinically described by Opitz et al in 1969 (27). After deep genetic study, Opitz C syndrome has been redefined as a clinical entity without a common molecular basis, as thoroughly discussed in Urreizti et al. (28).

There are several different NGS platforms ranging from gene panels, which include some key candidate genes, to the sequencing of the whole genome (WGS). In research, the most commonly used strategies are sequencing of the whole exome (WES) and WGS. In the clinical environment, custom **gene panels** for specific groups of disorders are still frequently used, together with the clinical exome. The clinical exome is a gene panel including around 6000 different genes previously associated with disease according to data from different Mendelian disorders databases, such as OMIM (29). Gene panels are an intermediate approach between the screening of one single gene and the analysis of the whole exome. They are still a popular tool in clinics as they present a high sensitivity detecting variants in several candidate genes while reducing the complexity of the analysis and data interpretation. The main limitation of gene panels is that the analysis is restricted to a particular group of genes, meaning that the posterior re-analysis of newly described genes is not possible.

WES is a very powerful approach to identify the disease-causing mutation. Even though the 20000 protein-coding genes contained in the human exome only represent 1-2% of the whole genome, it is estimated that approximately 85% of the described monogenic disorders are associated with variants in coding regions (30). Compared to gene panels, it has the advantage of being a much less restrictive approach, as it is hypothesis-free

and has a much higher discovery potential. Thus, it allows the discovery of variants in genes that have never been associated with disease and the posterior reanalysis of recently described genes in unsolved cases. This advantage is particularly relevant in highly heterogeneous disorders, like NDDs, where new associated genes are frequently identified. However, WES presents disadvantages compared to gene panels as the volume of output data is significantly larger, adding complexity to the processing and interpretation steps. Also, the probability of finding variants with unknown significance (VUS) and incidental findings (IFs) increases, hindering the variant interpretation process (31).

WGS covers the entire genome of an individual. Although the coverage (number of reads of a certain region) is lower than in WES, it is more uniform (32). WGS provides the possibility of detecting deep intronic variants and copy number variants (CNV), overcoming the limitation that WES presents for the detection of large indels or CNVs. It is well known that some deep intronic variants can affect normal splicing patterns and/or interfere with regulatory domains or non-coding RNAs normal function that control the expression patterns of other genes. Like the data obtained from WES, WGS data can also be reanalysed over time. Apart from a relatively higher economic cost compared to WES, the identification of a huge amount of VUS in poorly known genome regions is one of the main limitations of WGS, as it leads to an increase in the time and resources needed for the analysis of the data.

2.2.2 Variant interpretation

A crucial part of the genomic approach to the diagnosis of genetic diseases is the interpretation of the variants identified through NGS. Thousands of variants are identified per exome (33) and millions when performing a WGS (34) (**Figure 4**). The identified single-nucleotide variants (SNVs) and indels are filtered according to different criteria related to mutation type, minor allele frequency in the general population (MAF) and associated clinical phenotype. To systematically prioritize and classify such numbers of variants according to their putative pathogenic consequences, in 2015 the American College of Medical Genetics (ACMG) published the “ACMG Standards and Guidelines” as a resource for clinical geneticists (35) (**Figure 4**).

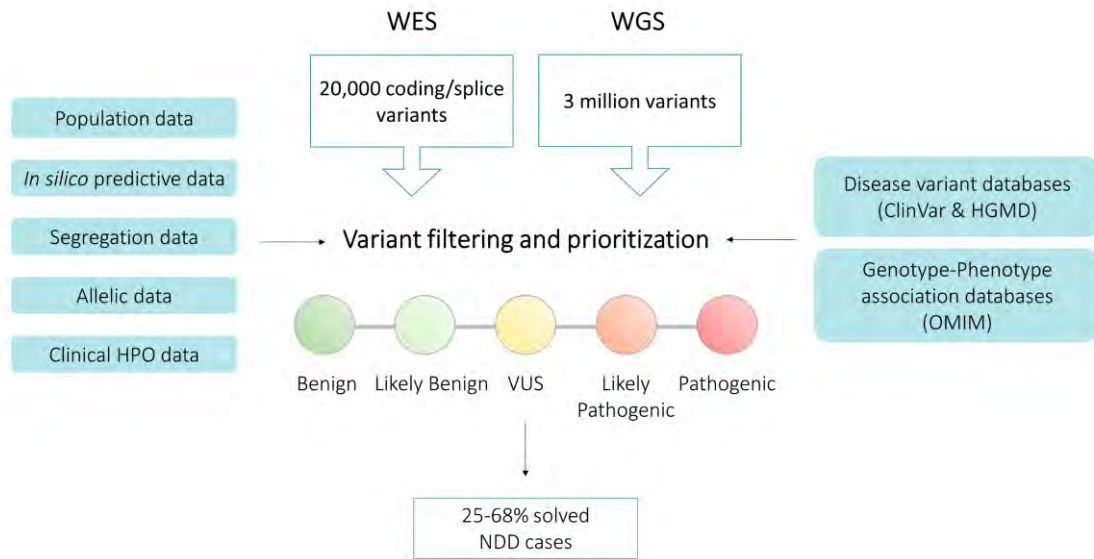


Figure 4. Genomic approach to the diagnosis of rare monogenic neurodevelopmental disorders following the ACMG guidelines. [Adapted from Stenton et al. (36)].

One of the criteria proposed by the ACMG is based on population data, so that the presence of the same variant or other variants with similar consequences in databases such as ClinVar (37), HGMD (38) and OMIM (29), that contain disease-associated mutations, would lean the scale to the pathogenic side. Similarly, its frequency and the number of homozygous individuals in control population databases, such as gnomAD (39), is also considered.

Then, computational and predictive data should also be carefully considered. There are many different *in silico* predictors that allow variant classification according to pathogenicity based on the type of amino acid change, the conservation of the specific residue across different species and possible alterations of the splicing pattern. The ones that are more frequently used are CADD (40), SIFT (41), Mutation Taster (42), PolyPhen-2 (43) and PROVEAN (44). Apart from predictive data, well-established functional studies that show deleterious effects are considered as strong evidence. Unfortunately, strong and robust functional evidence supporting the pathogenicity is not always available. Part of the work presented in this thesis has been carried out aiming to fill this knowledge gap in different particular ultra-rare neurodevelopmental disorders.

Another important evidence is segregation data, which allows the validation of the inheritance pattern of the identified variants. It provides strong evidence in inherited disease cases where the variant cosegregates with the disease in multiple affected family members or, in the case of *de novo* variants, if it is absent in both parents.

Segregation analyses are also key to elucidate if compound heterozygous mutations are in *cis* or in *trans*.

Finally, as mentioned before, adding the clinical description of the patient using HPO terms can reinforce the association of a particular variant, especially when the patient's phenotype is characteristic of mutations in a specific gene.

Consideration of all these criteria recommended by the ACMG guidelines leads to the classification of each variant into one of the following categories: "Benign", "Likely Benign", "VUS", "Likely Pathogenic" and "Pathogenic" (**Figure 4**). It is estimated that the use of NGS techniques coupled with careful variant interpretation lead to the establishment of a clear genetic diagnosis for approximately 25-68% of tested NDD patients (45).

2.2.3 Functional validation studies

The interpretation of the specific contribution that a novel variant may have to the patient's phenotype could be challenging. For instance, nonsense or frameshift variants are usually assumed to be loss-of-function (LoF) alleles as the encoded transcript would lead to the production of a peptide lacking functionally relevant domains or the nonsense-mediated decay (NMD) mechanism could be triggered. Nevertheless, truncating mutations in last exons escape this process and, in some cases, may behave as benign or gain-of-function (GoF) alleles (46). In the case of missense mutations, the complexity is even higher as they can result in many different possible scenarios (e.g., hypomorphic, hypermorphic, neomorphic, antimorphic...). As said before, functional *in silico* predictors can be useful tools to predict the pathogenicity of the identified variants. However, their results should be taken cautiously as they can return incorrect predictions, depending on the algorithms, previous knowledge on the protein structure, function and binding to other partners, etc. (47). These incorrect predictions can lead not to wrong clinical interpretation of variants.

Functional studies constitute essential tools to complement *in silico* predictions, as they provide experimental data that can help to elucidate and understand the effect of a variant at an *in vitro*, *ex vivo* and/or *in vivo* level. These functional validation studies (**Figure 5**) can be performed using a wide range of approaches, such as study of splicing patterns, mutation correction and phenotype rescue, detection of relevant biomarkers levels, generation of knockout (KO) cellular or animal models, etc. It is worth mentioning

that the performance of experiments to check the functionality and pathogenicity of a variant not only benefits that specific patient who will receive an accurate molecular diagnosis, but they may also help to elucidate the molecular mechanisms of the disease, crucial for posterior design and development of therapeutic strategies.

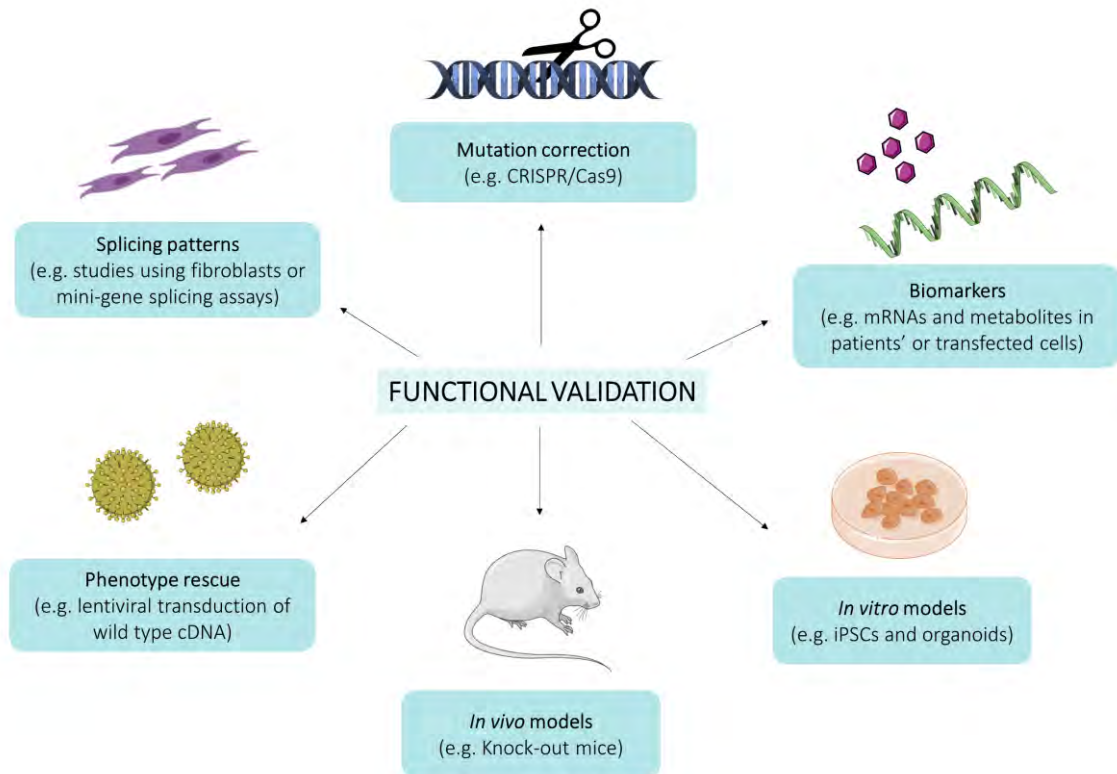


Figure 5. Examples of functional validation approaches frequently used to investigate the pathogenicity of VUS. Image created with Servier Medical Art.

2.2.3.1 Cellular models of disease: iPSCs

Cellular models constitute an effective tool to study the molecular mechanisms of genetic diseases, as well as to perform preliminary tests of different therapeutic strategies. Obviously, they present several limitations, like an incomplete representation of the whole organism reaction to certain compounds. Traditionally, human cell cultures have been limited to immortalized cell lines obtained from tumour biopsies (HeLa, HEK297, SaOs cells, etc) and primary cell lines obtained directly from patients (mainly, but not limited to, lymphoblasts and fibroblasts, due to their accessibility). Despite being useful tools, it is noteworthy that immortalized cell lines may present genetic and epigenetic aberrations and oncogene expression and that it can be difficult to obtain primary cells from patients, especially the relevant cell type for each specific disease (e.g. cells from the CNS in neurodevelopmental disorders).

In 1998, a new and promising path was opened for disease modeling with the derivation of human embryonic stem cells (hESCs) (48). However, this model presented several barriers, including strong ethical concerns regarding the use of hESCs in research. The discovery of methodologies that allow direct reprogramming of somatic cells to induced pluripotent stem cells (iPSCs) (49,50) has reshaped the approach to disease modelling and therapeutic strategy design of many diseases (51), overcoming hESCs limitations. The high potential of iPSCs resides in their capacity to be differentiated to many different cell types (**Figure 6**). Also, iPSCs present the exact same genomic background that the cells they have been differentiated from, usually fibroblasts from patients and controls. In this sense, it is important to consider that different individual iPSC lines may show variability in their potential to differentiate into other cell types, which might be caused by differences in the genetic background and the reprogramming history of each line (52).

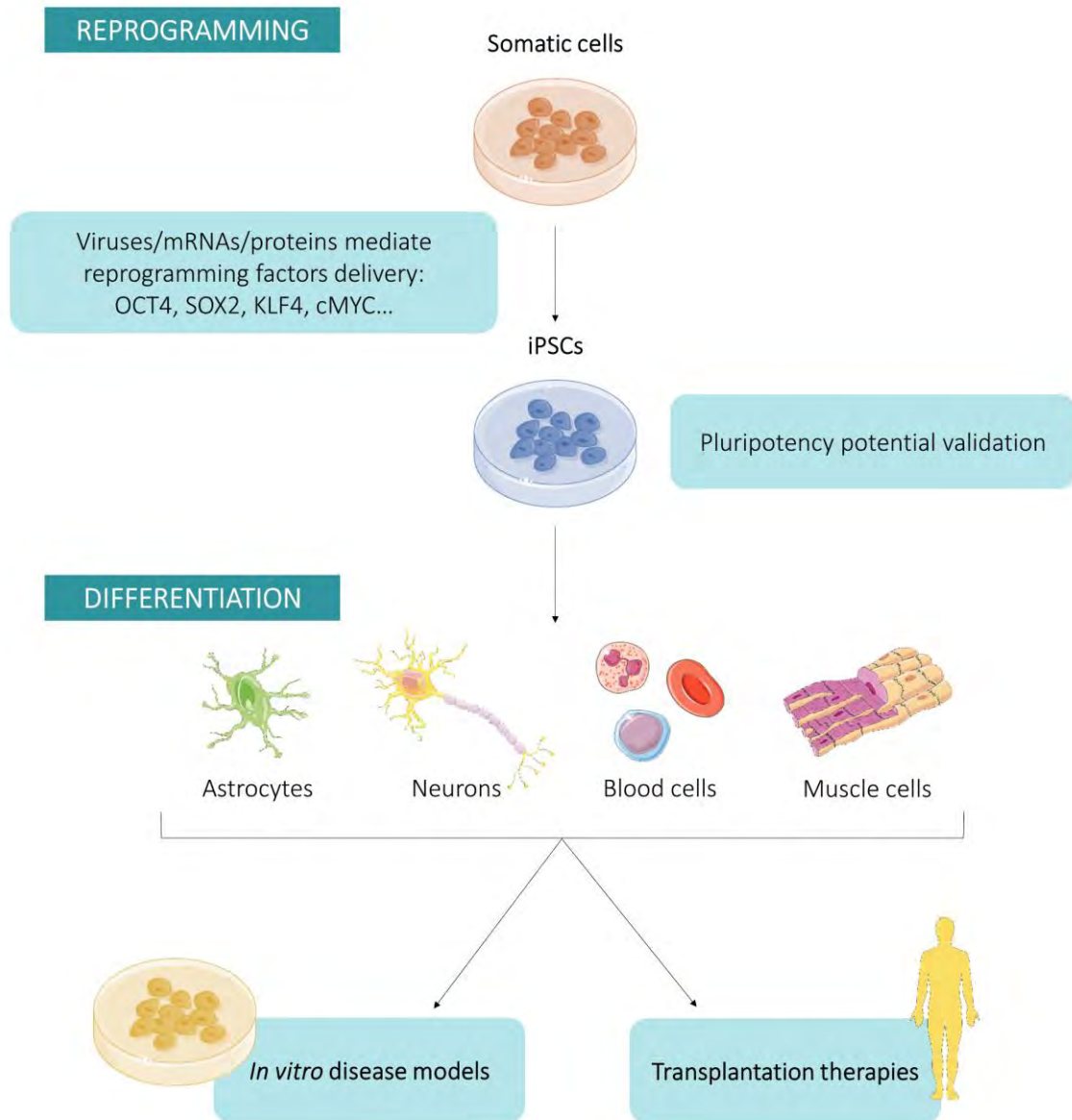


Figure 6. General picture of iPSCs reprogramming and differentiation processes and their main applications: *in vitro* disease modelling and cellular therapy. Image created with Servier Medical Art. [Adapted from Hockemeyer & Jaenisch (52)].

3. GENES RELATED TO THE OPITZ C CLINICAL ENTITY

In this thesis different patients that were clinically diagnosed with Opitz C syndrome were genetically diagnosed using WES aiming to identify the genetic origin of this ultra-rare neurodevelopmental condition. Since its description, more than 60 patients have been diagnosed with OCS, all of them showing highly variable multi-systemic manifestations, including developmental delay, trigonocephaly due to premature fusion of the metopic suture, midline dysmorphologies, hypotonia, seizures, limb malformations and congenital anomalies (53,54). Our group started to gather a cohort of OCS patients in 2011 in collaboration with Dr. G. Neri and Dr. J. Opitz himself, and genetically diagnosed seven of them before the start of the present work in 2017. The identified variants were located in different genes, namely *ASXL1*, *TRAF7*, *MAGEL2*, *KCNB1*, *RYR1* and *CDK13*. Below, the genes that were previously identified and have been more deeply studied at a functional level in this thesis and their preliminar associations with disease are described.

3.1 *ASXL1* and Bohring-Opitz syndrome

The *ASXL1* gene (Additional sex combs like transcriptional regulator 1; OMIM * 612990) is located in the chromosomal region 20q11.21 and belongs to the Enhancer of trithorax and Polycomb gene family. It encodes the ASXL1 protein, which is 1543 amino acids long and plays a crucial role in **chromatin remodelling**, by promoting histone methylation (55) and deubiquitination (56). It acts as a transcriptional activator or repressor depending on the cellular context and regulates *HOX* genes during axial patterning (57). GoF variants have been associated with acute lymphoblastic leukemia (58), myelodysplastic syndromes and chronic myelomonocytic leukemia (59). On the other hand, LoF variants disrupt normal hematopoiesis, but are not associated with tumorigenesis (57).

Germinal mutations in the *ASXL1* gene are the genetic cause of Bohring-Opitz syndrome (BOS, OMIM # 605039). BOS is a severe neurodevelopmental syndrome characterized by intrauterine growth retardation (IUGR), failure to thrive, nevus flammeus, deep psychomotor delay, seizures, severe hypotonia and flexion deformities of the upper limbs. These deformities lead to a clinically recognizable feature known as the “Bohring-Opitz syndrome posture” (60–62). The patients show trigonocephaly, characteristic dysmorphologies and congenital anomalies, resembling other syndromic forms of DD

like the Opitz C syndrome (63,64). In fact, due to the high degree of overlapping, it was proposed that both pathologies were the same syndrome with a very wide severity spectrum, going from mild phenotype (OCS) to a more severe one (BOS) (63).

More than 50 cases of BOS have been reported in the literature and approximately half of them harboured *de novo* mutations in the *ASXL1* gene (62,65–73). The identified germline disease-causing variants are heterozygous nonsense or frameshift mutations and mostly clustered to the centre of the protein (**Figure 7**), however the exact molecular mechanisms underlying these variants are still poorly known.

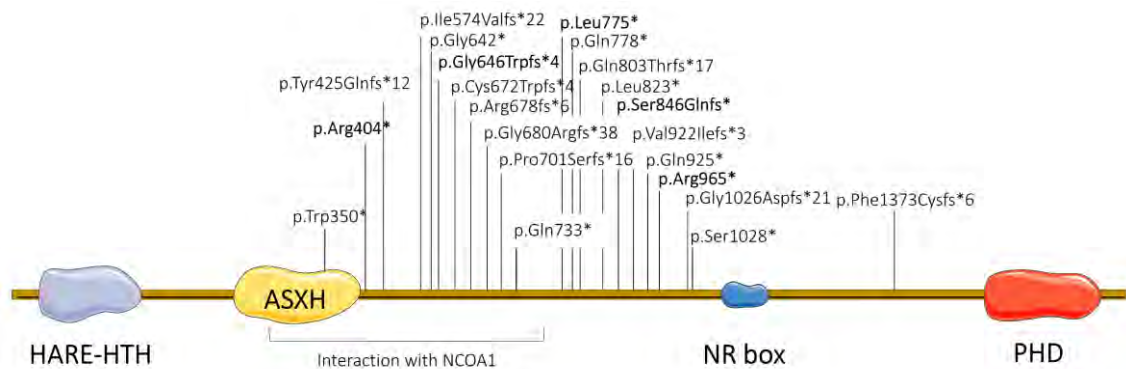


Figure 7. Representation of ASXL1 with mutations reported in Bohring–Opitz syndrome patients. Mutations in bold have been reported more than once. HARE-HTH: HB1, ASXL, restriction endonuclease HTH domain (aa 11–86); ASXH: ASX homology domain (aa 255–364); NR box: nuclear receptor box (aa 1107–1112); PHD: plant homeodomain (aa 1503–1540). Image created with Servier Medical Art.

Although the BOS phenotype appears to be well-defined, some patients have been clinically diagnosed with BOS but tested negative for *ASXL1* mutations. This situation could be explained by genetic heterogeneity of the syndrome (65), somatic mosaicism or a need to improve the actual clinical diagnostic criteria for BOS (62).

3.2 TRAF7 and role in tumorigenesis

The *TRAF7* gene (TNF receptor associated factor 7; OMIM * 606692) maps to the 16p13.3 chromosomal region, has 21 coding exons and only 1 known protein-coding transcript which translates to the TRAF7 protein (Ensembl data). TRAF7 is one of the seven members of the tumour necrosis factor receptor-associated factor (TRAF) protein family. TRAF proteins act as **signalling adaptors** directly binding to the cytoplasmatic domain of receptors of several families. In addition, most of them have E3 ubiquitin ligase activity that can activate downstream signalling events. The signalling pathways in which these proteins participate are involved in a wide range of cellular processes, such as cell survival, proliferation, migration, differentiation, cytokine production and autophagy. Tumour necrosis factor (TNF) family ligands lead to the transduction of these cellular signals through activation of different effectors, such as nuclear factor- κ Bs (NF- κ Bs), mitogen-activated protein kinases (MAPKs), or interferon-regulatory factors (IRFs) (74,75). At a structural level, TRAF proteins share several conserved domains (**Figure 8**). A RING finger domain is present at the N-terminus in all of them, except for TRAF1, and constitutes the core of the ubiquitin ligase catalytic domain. At the C-terminus, there is a TRAF domain, crucial for oligomerization and interaction with their partners (74,75). However, this characteristic TRAF domain is not present in TRAF7; instead, seven repeats of the WD40 domain are found (76).

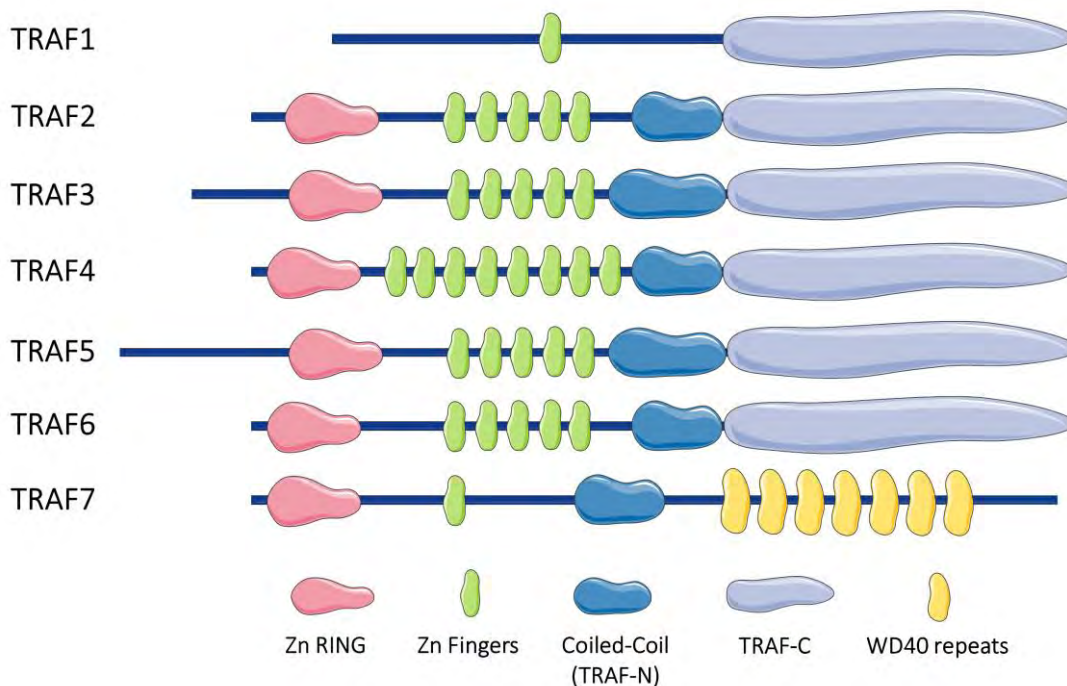


Figure 8. The different members of the TRAF family and their protein domains. Image created with Servier Medical Art.

TRAF7 activation involves homodimerization through its Zn fingers and coiled-coil domains (77). In a Tumour necrosis factor- α (TNF α) induced response (**Figure 9**), the WD40 repeats domain is crucial for the interaction of TRAF7 with MEKK3, which in turn promotes TRAF7 stabilization through phosphorylation and subsequent self-ubiquitination (77). This interaction also promotes the activation of several cellular components such as JNK, p38 and NF- κ B (78,79). Additionally, this domain is essential for the negative regulation of the proto-oncogene c-Myb by sumoylation (80). The Zn RING and Zn fingers domains promote caspase-mediated apoptosis and ubiquitination of NEMO and the NF- κ B subunit p65, leading to lysosomal degradation and a decrease of NF- κ B pathway activity (78). Knocking-down *TRAF7* in primary neuronal cells led to increased active caspase-3 protein levels and a decreased number of apoptotic primary neurons (81). Through the regulation of NEMO, TRAF7 is also involved in MyoD1 regulation, promoting a decrease in myogenesis (82).

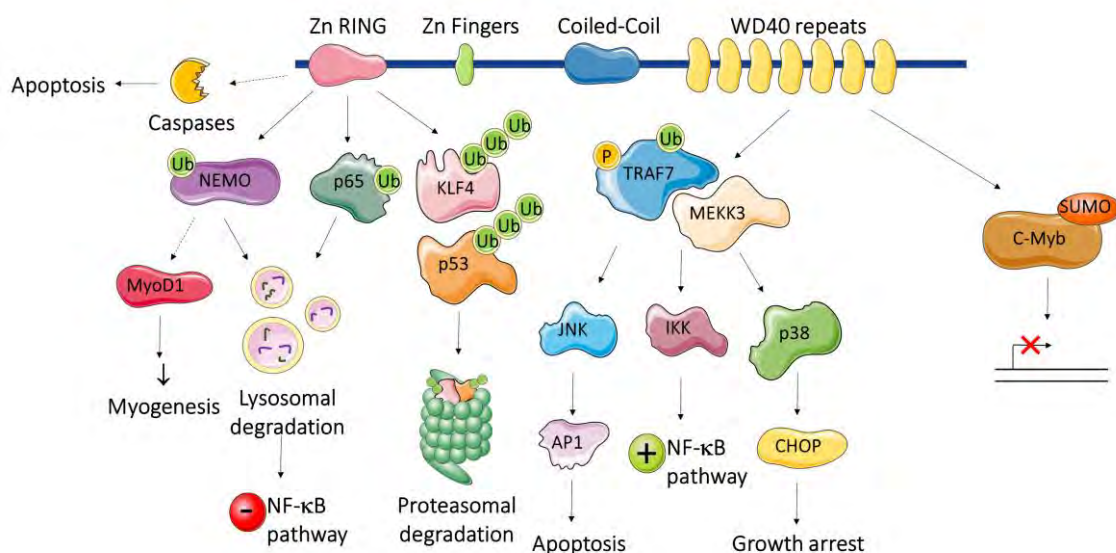


Figure 9. TRAF7 protein roles and functions in TNF α induced response. Image created with Servier Medical Art.

TRAF7 also plays an important role in the Toll Like Receptor 2 (TLR2) signalling pathway. Together with TRAF6, they promote the activation of NF- κ B due to the recognition of pathogen-associated molecular patterns, being of great relevance in innate immunity pathways (83).

Somatic point mutations in *TRAF7* have been linked to the development of different tumour types. So far, more than 70 different mutations have been identified in different types of meningioma (84–88). Mutations in *TRAF7* have been also identified in

intra-neural perineuriomas, adenomatoid tumours of the male and female genital tract, well-differentiated papillary mesothelioma of the peritoneum (89–91), diffuse pleural mesothelioma (92) and localized pleural mesothelioma (93). *TRAF7* mutations seem to genetically characterize a group of neoplasms that develop from cells that wrap vital organs such as the brain, the peripheral nerves, the testis, the uterus and the fallopian tube (89). The great majority of the tumour-related mutations in *TRAF7* reported so far are heterozygous, mostly missense and 88% of them are restricted to the WD40 repeats domain at the C-terminus of the protein. The molecular mechanisms by which *TRAF7* somatic missense variants promote tumorigenesis in the different cancer types are nowadays an open research topic. For instance, a recently published study (94) showed that *TRAF7* loss-of-function leads to proteostasis dysregulation and hyperactivation of RAS-related GTPases, causing aberrant actin cytoskeletal organization and promoting oncogenic transformation in meningiomas. This new proposed mechanism put the focus on the function of the WD40 domain as a scaffolding structure important for the interaction with small GTPases (95), instead of the most extensively described one as a modulator of the NF- κ B pathway (96), at least in tumorigenesis.

3.3 *MAGEL2* and *MAGEL2*-related disorders

The *MAGEL2* gene (MAGE family member L2; OMIM * 605283) is a maternally silenced single-exon protein-coding gene contained in the Prader-Willi region (15q11-q13). In adult humans, its expression is mostly restricted to the CNS [according to GTEx data (97)], but it is also present in cells of mesodermal origin, involved in muscle, bone and fat tissues development (98). In adult animal mice, *Mage12* expression is enriched in the hypothalamus and the amygdala, especially enriched in the ventromedial, arcuate, tuberal, lateral, anterior and paraventricular hypothalamic nuclei (99). The *MAGEL2* gene encodes the MAGEL2 protein, one of the largest proteins of the Type II MAGE protein family.

MAGEL2 has three relevant structural and functional elements (**Figure 10**): a highly proline-rich with an unknown function, a U7BS domain, which is a binding site for USP7 (100,101), and a MAGE Homology Domain (MHD). The MHD is the characteristic domain of the MAGE protein family and it confers high specificity to their protein-protein interactions (102). In particular, *MAGEL2* recognizes and binds to its partners TRIM27 and VPS35 through this domain (103).

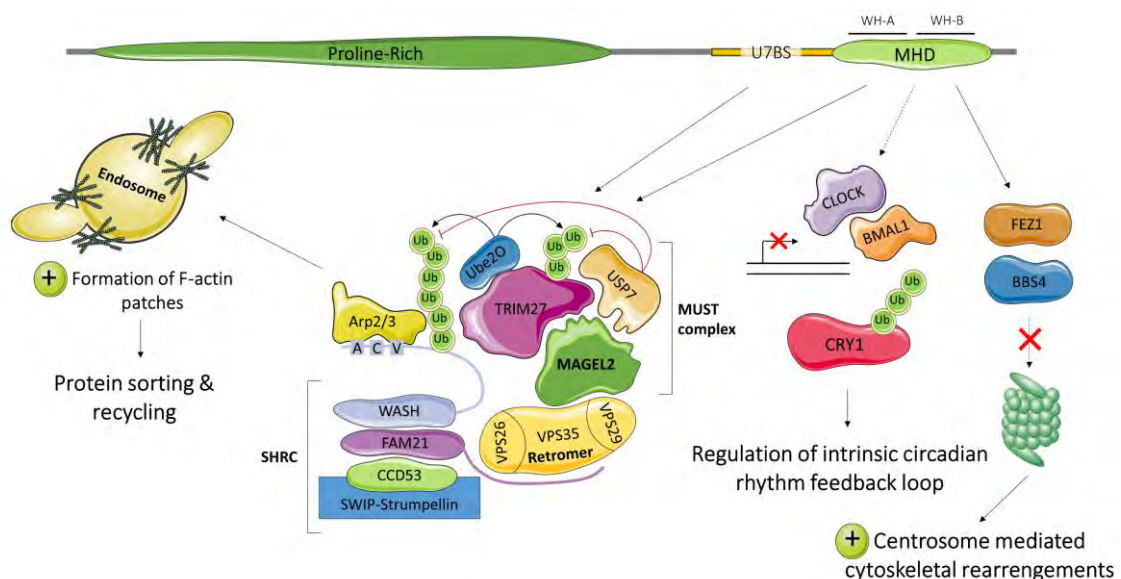


Figure 10. *MAGEL2* protein described roles and functions. Image created with Servier Medical Art.

The role of *MAGEL2* in the retrograde endosomal transport is its most extensively studied cellular function (**Figure 10**). *MAGEL2*, TRIM27 and USP7, form the MUST complex that is recruited to endosomes (100,103), which participate in the sorting of protein cargoes through retrograde and recycling pathways (104). The retromer complex

recruits the MUST complex, via MAGEL2-VPS35 binding, and the WASH regulatory complex (SHRC) to the endosomal membrane. Then, TRIM27 activates the SHRC complex, through WASH polyubiquitination, promoting the formation of endosomal F-actin patches. These localized branched patches are crucial for endosomal protein sorting, as they demarcate discrete domains within the endosome where specific proteins are segregated and sorted to their respective destinations (100,103). A well-coordinated trafficking network is key to ensure an appropriate cell distribution and a correct function of a wide variety of proteins.

It has also been proposed that MAGEL2 is involved in the centrosome-related cytoskeletal rearrangements during neurite outgrowth driven by Fez proteins and BBS4 (**Figure 10**), by protecting them from proteasomal degradation (105).

MAGEL2 shows a highly circadian expression pattern in humans and mice, being one of many clock-controlled genes (106,107). Consistent with *Magel2* expression in the hypothalamus and the role of the suprachiasmatic nucleus of the hypothalamus as a central pacemaker in mammals, *Magel2*-deficient mice showed reduced amplitude of activity and increased daytime activity, together with progressive infertility in males and other endocrine alterations (108). Also, *MAGEL2* contributes to the regulation of the ubiquitination balance of CRY1, crucial in the circadian rhythm feedback loop (107) (**Figure 10**).

3.3.1 Prader-Willi syndrome

The Prader-Willi locus is a complex chromosomal region that contains genes that are differentially expressed depending on their parental origin (**Figure 11A**). The PWS region comprises 6Mb on the long arm of chromosome 15, 2.5Mb of which contain five protein-coding genes and more than 80 non-coding RNA genes of exclusive paternal expression and two maternally expressed protein-coding genes (109,110).

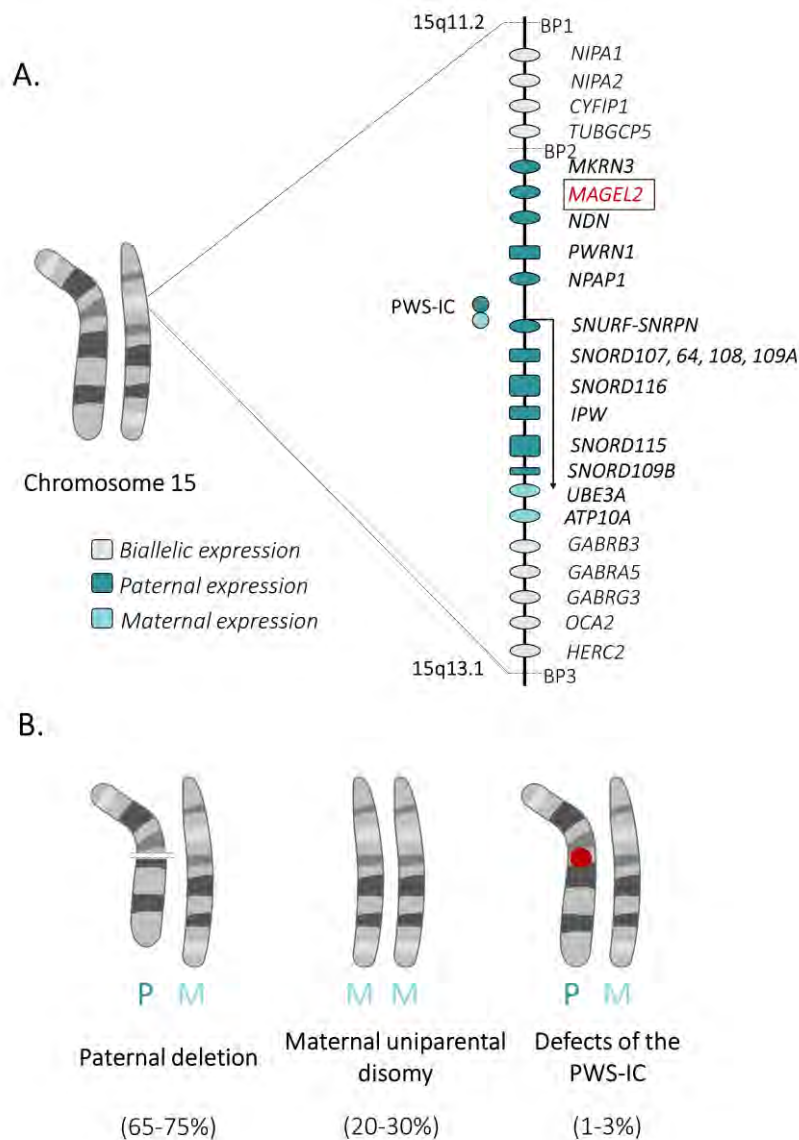


Figure 11. A) Chromosome map of PWS region (15q11-q13). Protein-coding genes are represented as ovals and RNA genes as rectangles. B) Possible genetic causes of Prader-Willi syndrome. In brackets, the frequency in which each phenomenon is observed in PWS patients. Image created with Servier Medical Art.

When the paternal alleles of these maternally silenced genes are not expressed, it causes an haploinsufficiency situation that results in Prader-Willi syndrome (PWS; OMIM # 176270). This lack of expression of the paternal allele can be caused by several molecular causes (**Figure 11B**) with different prevalence: deletion of paternal 15q11-q13 (65-75%), maternal uniparental disomy of chromosome 15 (mUPD) (20-30%) and defects of the PWS-IC (PWS imprinting centre) (1-3%) (111). The individual contribution that the loss of expression of each gene contained in the PWS region has on the typical phenotype observed in patients remains unclear.

Prader-Willi syndrome was described almost 70 years ago, and nowadays, it is still under extensive characterization and study. It is a complex imprinting disorder that causes major alterations in the endocrine, cognitive and neurologic systems, behaviour and metabolism of the affected individuals. PWS is a rare genetic disease that shows a prevalence of 1 in 10,000-30,000 live births, equally affecting both sexes and all ethnic populations (111). Children with PWS show severe hypotonia, feeding difficulties, failure to thrive and developmental delays during early infancy. Older children and adults present other clinical traits such as early-onset obesity, characteristic facial features, hypogonadism, hyperphagia/ obsession with food, obsessive/compulsive behaviour, mild mental retardation, sleep disturbances, high pain threshold, short stature related to growth hormone (GH) deficiency, hypopigmentation and small hands and feet (112). The obesity that these patients tend to develop can become one of the leading life-threatening conditions in this genetic condition (111).

3.3.2 Schaaf-Yang syndrome

Truncating mutations in the paternal allele of *MAGEL2* were first described as disease-causing in four patients with a PWS-like phenotype, but normal methylation patterns at 15q11-q13 (113). The phenotypic differences observed in the patients compared to typical PWS cases led to the delineation of a new disease named Schaaf-Yang syndrome (SYS; OMIM # 615547). Since then, more than 150 cases of SYS carrying more than 50 different variants have been reported in the literature (113–132). These variants are mostly nonsense or frameshift mutations and predominantly located at the C-terminal end of the protein, meaning that there is a partial or a total lack of the MHD, compromising the functions that *MAGEL2* carries out through this domain.

SYS was initially considered a PWS-like phenotype as the patients manifest overlapping clinical phenotypes with PWS patients (**Figure 12**). But there are some characteristics that support that SYS should be considered a differential diagnosis of PWS, especially during the early life period. Overlapping phenotypes include neonatal hypotonia, ID, DD, feeding difficulties, different hormonal disbalances and sleep disorders. However, some of the standardized criteria considered for PWS (e.g., hypopigmentation, characteristic facial dysmorphisms, small hand and feet, hyperphagia, obesity and obsessive-compulsive behaviour) are not frequent in SYS patients. For instance, childhood hyperphagia and increased weight gain present in 67% of PWS patients, are only present in 22% of SYS patients (133). In contrast, SYS cases show more severe ID and DD,

ASD typical behaviours and joint contractures more frequently than PWS patients (110,134,135). In adulthood the differences in the phenotypes of these two syndromes might become less apparent than in childhood, making them more difficult to discern at a clinical level (136).

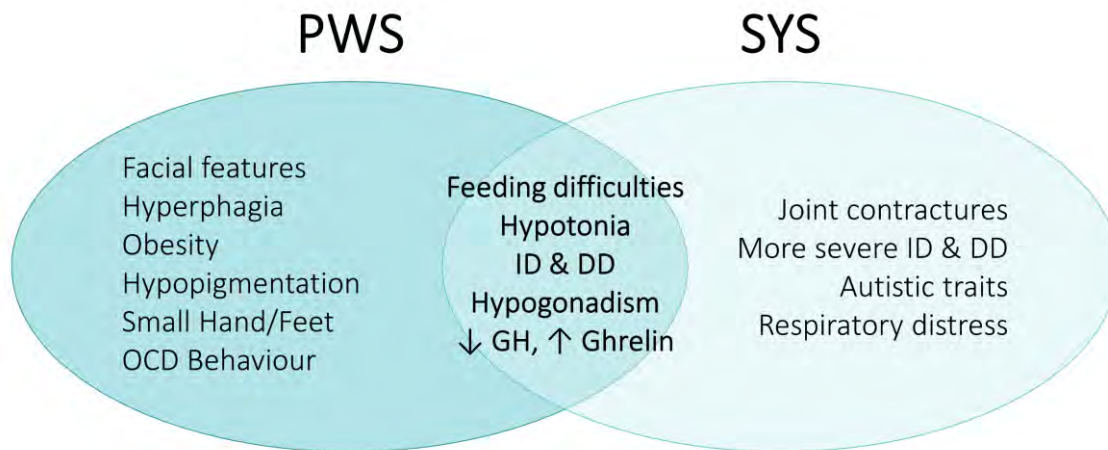


Figure 12. Phenotypic overlap between *MAGEL2*-related syndromes: PWS and SYS.

Endocrine and metabolic alterations in PWS have been widely studied, being hypogonadism and GH deficiency the most prevalent (111). The last one had been reported in more than 300 patients and GH therapy is recommended as an early intervention for PWS (137,138). A review of the literature on endocrine abnormalities in *MAGEL2*-related syndromes has been recently published (133) highlighting GH, thyroid-stimulating hormone (TSH), adrenocorticotrophic hormone (ACTH), antidiuretic hormone (ADH) and gonadotropins as the most common hormonal deficiencies in SYS. These endocrine alterations are thought to be caused by hypothalamic impairment and might lead to hypoglycemia.

An update of the clinical and genetic data of all the published SYS cases have been conducted as part of this thesis in close collaboration with the clinical expert Dr Serrano from Hospital Sant Joan de Déu.

3.3.3 *In vitro* and *in vivo* models of *MAGEL2*-related syndromes

Human *MAGEL2* gene and its murine homologue have a similar genomic organization. The gene in mice is located in chromosome 7, in a syntenic region to the human PWS cluster and it is also expressed only from the paternal allele. Moreover, both *MAGEL2* forms are intronless and contain a CpG island that can be found in its 5'-UTR. The

proteins encoded by the human and the mouse genes have a 77% similarity (139). Two different KO mouse models have been generated to study *Magel2* loss.

In the first mouse model, generated by Dr. Wevrick team in 2007, the coding sequence of the gene was replaced by a LacZ reporter leaving the original promoter intact (140). Several publications report extensive phenotyping of this KO mouse (98,108,140–143), the most relevant observed phenotypes are summarized in **Table 1**. Quantitative proteomics of the hypothalamus of these mice showed several components of the dense secretory granules (SG) to be downregulated (99). SG are exocytic organelles involved in the processing and release of hormones and neuropeptides in neuroendocrine cells (144). Decreased SG protein levels were also observed in different PWS *in vitro* models caused by impaired endosomal protein trafficking and subsequent lysosomal degradation, resulting in a reduction of circulating bioactive hypothalamic hormones (99).

Table 1. Relevant phenotypes observed in *MAGEL2*-related syndromes mouse models.

Phenotype	Magel2 Knock-out		Truncated Magel2
	Wevrick et al	Muscatelli et al	Ieda et al
Neonatal mortality	10%	50%	-
Suckling defects	NA	+	NA
Neonatal failure to thrive and pre-wean growth retardation	+	+	+
Increased leptin plasma levels, reduced leptin sensitivity	+	NA	NA
Weight gain, decreased lean mass with increased adiposity	+	NA	-
Abnormal behaviour in novel environments	+	+	NA
Progressive infertility and decreased olfactory discrimination	+	NA	NA
Decreased locomotor activity, muscle dysfunction and decreases bone mineral content	+	NA	NA
Growth hormone axis impairment	+	+	NA
Decreased oxytocin	+	+	NA
Decreased serotonin	+	NA	NA
Blunted circadian rhythm, decreased orexin levels	+	NA	NA

A second mouse model was generated in 2010 by deleting the promoter and the majority of the coding sequence of *Mage12* (146). This model has not been so deeply characterized as the previously mentioned, a comparison of the observed phenotypes in both models can be found in **Table 1**. Impaired oxytocin (OXT) production in the hypothalamus was one of the highlights of the model, being the prohormone maturation the main issue (146). A daily dosage regimen of subcutaneous injections of OXT for 7 days after birth restored suckling activity, prevented the appearance of abnormal social behaviour and spatial learning deficits and led to partial anatomical and functional restoration of the central OXT system in the animals throughout adulthood (147), suggesting that it should be considered as a potential therapeutic approach for SYS and PWS (148,149). In fact, a phase 2 clinical trial has already been carried out in PWS patients, who after a short course of repeated intranasal OXT administration showed improved oral feeding and social skills (150).

More recently, Ieda et al. (151) generated two additional mouse models to study *Mage12*. In an attempt to model the putative toxic effects of the truncated form of the protein, they generated a transgenic mouse overexpressing the N-terminal region of *Mage12*, including part of the Proline-Rich protein domain. They observed a high rate of fetal and neonatal death, probably caused by the strong ubiquitous overexpression of the truncated form in various organs. They also generated a genome-edited mouse carrying a 234 bp deletion on *Mage12* (c.1690_1924del) that encodes a truncated form of the protein [p.(Glu564Serfs*130)], mimicking an equivalent situation to that observed in SYS patients. They could detect the presence of a shorter transcript in the brain at cDNA levels and maintenance of the normal imprinting pattern. However, the model failed to recapitulate the SYS phenotype (**Table 1**), as no obvious abnormal traits were observed in the *Mage12*^{P:fs} individuals, except for mild neonatal growth retardation.

3.4 Other genes identified in Opitz C patients

Six other genes had been identified as disease-causing in the OCS patients that were diagnosed along this thesis. All of them play crucial roles within the cell and have already been associated with different ultra-rare neurodevelopmental disorders. In principle, all these genes do not belong to the same functional pathway nor present a clear functional connection between them. Making it difficult to find a plausible explanation for the many phenotypic similarities found in those patients that led to their categorization within the same clinical diagnosis.

The main aim of this thesis is to genetically diagnose a group of patients affected by severe syndromic neurodevelopmental disorders and contribute to the elucidation of the underlying pathophysiological molecular mechanisms.

To address this general aim, the following specific objectives were defined:

1) Identification of causal genes of patients clinically diagnosed as Opitz C syndrome and functional validation of some of the identified disease-causing variants.

- To perform whole exome sequencing analysis in eight affected families to identify and validate the molecular cause of the disease.
- To functionally evaluate the effects of the variants predicted to affect splicing in *KAT6A*, *PIGT*, *ASXL1* and *FOXP1* genes, using fibroblasts from patients or mini-gene splicing assays.
- To test the effects on protein activity caused by recessive variants in *DPH1*.

2) Characterization of heterozygous *TRAF7* germline variants at phenotypic and molecular levels.

- To gather a cohort of patients carrying *TRAF7* germline missense mutations to improve the clinical delineation of the novel TRAF7-syndrome.
- To perform an analysis of the transcriptomic profile in TRAF7 patients' fibroblasts to elucidate the pathways that may be affected by the mutations.

3) Functional characterization of *MAGEL2* truncating mutations and generation of an *in vitro* model for SYS.

- To investigate putative changes in transcriptomic and metabolomic profiles and A β ₁₋₄₀ peptide excretion levels that might contribute to the molecular definition of the SYS phenotype in fibroblasts.
- To explore the effects of a truncating MAGEL2 variant in protein stability and subcellular localization.
- To reprogram fibroblasts to iPSCs and characterize its pluripotency as a first step to generate relevant *in vitro* neural models for SYS.

